S&G 3726

S&G 3726

3726

Victoria
UNIVERSITY OF WELLINGTON
Te Whare Wānanga o te Ūpoko o te Ika a Māui

MECHANISMS OF LATE QUATERNARY COASTAL UPLIFT ALONG THE RAUKUMARA PENINSULA SEGMENT OF THE HIKURANGI MARGIN, NORTH ISLAND, NEW ZEALAND.

Kate Wilson[1*], Kelvin Berryman[2], Tim Little[1], Ursula Cochran[2], Nicola Litchfield[2].

[1] School of Earth Sciences, Victoria University of Wellington, PO Box 600, Wellington, New Zealand.

[2] GNS Science, PO Box 30-368, Lower Hutt, New Zealand.

* Present address: GNS Science, PO Box 30-368, Lower Hutt, New Zealand.

REPORT PREPARED FOR THE EARTHQUAKE COMMISSION

Project Number 6UNI/501

June, 2007.

GNS SCIENCE
TE PŪ AO

S+G
3726

Victoria
UNIVERSITY OF WELLINGTON
Te Whare Wānanga
o te Ūpoko o te Ika a Māui

MECHANISMS OF LATE QUATERNARY COASTAL UPLIFT ALONG THE RAUKUMARA PENINSULA SEGMENT OF THE HIKURANGI MARGIN, NORTH ISLAND, NEW ZEALAND.

Kate Wilson[1*], Kelvin Berryman[2], Tim Little[1], Ursula Cochran[2], Nicola Litchfield[2].

[1] School of Earth Sciences, Victoria University of Wellington, PO Box 600, Wellington, New Zealand.

[2] GNS Science, PO Box 30-368, Lower Hutt, New Zealand.

* Present address: GNS Science, PO Box 30-368, Lower Hutt, New Zealand.

REPORT PREPARED FOR THE EARTHQUAKE COMMISSION

Project Number 6UNI/501

June, 2007.

GNS
SCIENCE
TE PŪ AO

STG 3726

ELSEVIER

Available online at www.sciencedirect.com

ScienceDirect

Sedimentary Geology 197 (2007) 333–354

Sedimentary Geology

www.elsevier.com/locate/sedgeo

A Holocene incised valley infill sequence developed on a tectonically active coast: Pakarae River, New Zealand

Kate Wilson [a,*,1], Kelvin Berryman [b], Ursula Cochran [b], Tim Little [a]

[a] *School of Earth Sciences, Victoria University of Wellington, PO Box 600, Wellington, New Zealand*
[b] *GNS Science, PO Box 30368, Lower Hutt, New Zealand*

Received 1 May 2006; received in revised form 19 October 2006; accepted 23 October 2006

Abstract

A sequence of fluvio-estuarine sediments exposed beneath the highest Holocene marine terrace at Pakarae, North Island, New Zealand, records the early-mid Holocene infilling of the Pakarae valley. This sequence was developed on an active, coseismically uplifting coastline and provides a valuable comparison to widely used facies models for estuaries, which were developed exclusively from stable coastal settings. We describe eight sedimentary sections, distributed along a 220 m stretch of riverbank and present twelve new radiocarbon ages. Sedimentology and benthic foraminifera are used to divide the sequence into eight bio-lithofacies. These units are grouped into four paleoenvironmental facies associations: barrier, estuarine, estuary-head delta and floodplain. We compare the distribution of the Pakarae paleoenvironmental facies associations to those in models of incised valley infill sequence models and case studies of infilled valleys. These data allow us to present new contributions to the development of a facies model for the sedimentary infilling of an incised valley system that was experiencing coseismic uplift synchronous with deposition. We suggest the distinctive characteristics of such a model would include (1) part, or all, of the transgressive and lowstand sequences may now lie above modern sea level, (2) the transgressive sedimentary sequence is typically condensed relative to the coeval amount of eustatic sea level (SL) rise that occurred during that period, and (3) evidence of relative SL falls, such as transitions from estuarine to fluvial environments, despite conditions of rapid and continuous eustatic SL rise.
© 2006 Elsevier B.V. All rights reserved.

Keywords: Facies models; Estuary; Tectonic uplift; Incised valley fill; New Zealand

1. Introduction

A common feature to studies of sedimentary sequences that have accumulated as fill deposits in formerly incised valleys is their location on stable coastlines. Here we study a sedimentary sequence at Pakarae, North Island, New Zealand, to develop a facies architecture model for incised valley infill sequences that is applicable to active coseismically uplifting coastlines. Several conceptual models have been developed to explain the distribution of facies within drowned valleys (Roy, 1984; Dalrymple et al., 1992; Allen and Posamentier, 1994; Heap et al., 2004). These models have been useful for assessing the petroleum potential of ancient transgressive estuarine sediments and the significance of these as sequence boundaries in oil exploration, and, more recently, to reconstruct Holocene post-glacial sea level (SL) changes, as is important for climate change studies. These models are now widely

* Corresponding author. Tel.: +64 4 570 4530; fax: +64 4 570 4600. *E-mail address:* K.Wilson@gns.cri.nz (K. Wilson).

1 Present address: GNS Science, PO Box 30368, Lower Hutt, New Zealand.

0037-0738/$ - see front matter © 2006 Elsevier B.V. All rights reserved.
doi:10.1016/j.sedgeo.2006.10.007

accepted and cited. However, taking into account that a large proportion of the world's coastlines are in regions of active tectonics, it is timely to consider how incised valley infill sequences differ according to tectonic setting. Results from this study show that past tectonic movements significantly influence sequences of incised valleys; recognition of this can improve interpretations of infill sequences for the purposes of petroleum research and the reconstruction of Holocene SL change.

At the Pakarae River mouth a raised sequence of marine terraces attest to late Holocene coseismic uplift events with a recurrence interval of ca. 850 yr (Fig. 1, Ota et al., 1991). The highest terrace, which corresponds with the maximum Holocene flooding surface, is underlain by a sequence of estuarine, fluvial and marine sediments that were deposited under conditions of rising sea level (SL). These are now exposed above sea level due to continuing tectonic uplift (Berryman et al., 1992). These sediments provide an opportunity to study the stratigraphic development of incised valleys under conditions of rising eustatic SL and coseismic uplift. Our approach uses sedimentology, macropaleontology and micropaleontology (benthic foraminifera) to reconstruct the paleoenvironments that accompanied infilling of the Pakarae incised valley, on the East Coast of the North Island, New Zealand. In comparison with previous work on the incised valley infill sequences our study is unique as we are able to observe outcrop exposure of the Holocene sequences rather than making reconstructions based on cores and, or, seismic images.

1.1. Models of incised valley infilling

Three widely recognised models of incised valley infill have been developed by Roy (1984), Dalrymple et al. (1992) and Allen and Posamentier (1993, 1994). As mentioned above, these were all developed for stable coastlines. Here we summarise these models and compare their settings to that of Pakarae valley.

The three incised valley infill models are similar to one another in their recognition of three to four main sedimentary environments. All models recognise a fluvial/floodplain environment, a central estuary basin and a barrier environment. Dalrymple et al. (1992) also includes a fluvial delta environment at the head of the estuary and Allen and Posamentier (1993, 1994) include a shoreface environment. The models of valley infilling predict that these environments will translate landward under rising SL. Once the SL highstand (maximum flooding surface) is attained the estuary is subsequently infilled by fluvial sediments that prograde seaward.

Based on the Roy (1984) classification the Pakarae valley is comparable to the drowned river valley estuary. According to the Dalrymple et al. (1992) model the Pakarae River valley would be classified as a wave-dominated estuary (as opposed to tide-dominated). The case studies of individual Holocene estuarine infill sequences, upon which the models are based, have commonly been of large estuaries at the mouths of major rivers that have extensive catchment areas [for example, Hawkesbury River estuary: 109 km length (Roy et al., 1980); Miramichi River estuary: >40 km length (Dalrymple et al., 1992); Gironde estuary, 100 km length (Allen and Posamentier, 1993)]. In contrast, the paleo-Pakarae estuary was <0.5 km wide at the location of the studied sections (Fig. 1), and based on the distribution of estuarine sediments along the riverbank, we estimate the estuary would have been <1 km in length. For this reason we must consider whether the facies models of Roy (1984), Dalrymple et al. (1992) and Allen and Posamentier (1993), based on studies of larger estuaries, are still applicable when scaled down to this extent. We begin by assuming that scaling is at least approximately valid as we can find no evidence presented in the literature to the contrary. Small estuaries are potentially more suitable for comparison to simplified facies models because multiple tributaries, as found in large estuaries, do not exist.

1.2. Tectonic setting of the Pakarae valley

Moderate to high late Quaternary coastal uplift rates have been recorded at many locations along the East Coast of the North Island, an active continental margin inboard of the Hikurangi subduction zone (Fig. 1). The Pakarae locality has the highest Holocene uplift rate identified along this segment of the Australia–Pacific plate boundary at 3.2 ± 0.8 mm/yr (Ota et al., 1988; Yoshikawa, 1988; Berryman et al., 1989; Ota et al., 1991; Ota et al., 1992; Wilson et al., 2006). The high uplift rate, and evidence for a coseismic uplift process on this coast make Pakarae an ideal location for studying incised valley architecture on a tectonically active coast.

Uplifted forearc basin clastic sediments of Miocene to Pliocene age dominate the eastern region of the Raukumara Peninsula, East Coast, North Island (Fig. 1, Mazengarb and Speden, 2000). In the vicinity of Pakarae, Oligocene and Miocene marine siltstones and mudstones are juxtaposed across the Pakarae Fault, a normal fault, uplifted to the east and striking almost perpendicular to the trend of the subduction zone (Kingma, 1964; Mazengarb and Speden, 2000). This fault offsets the

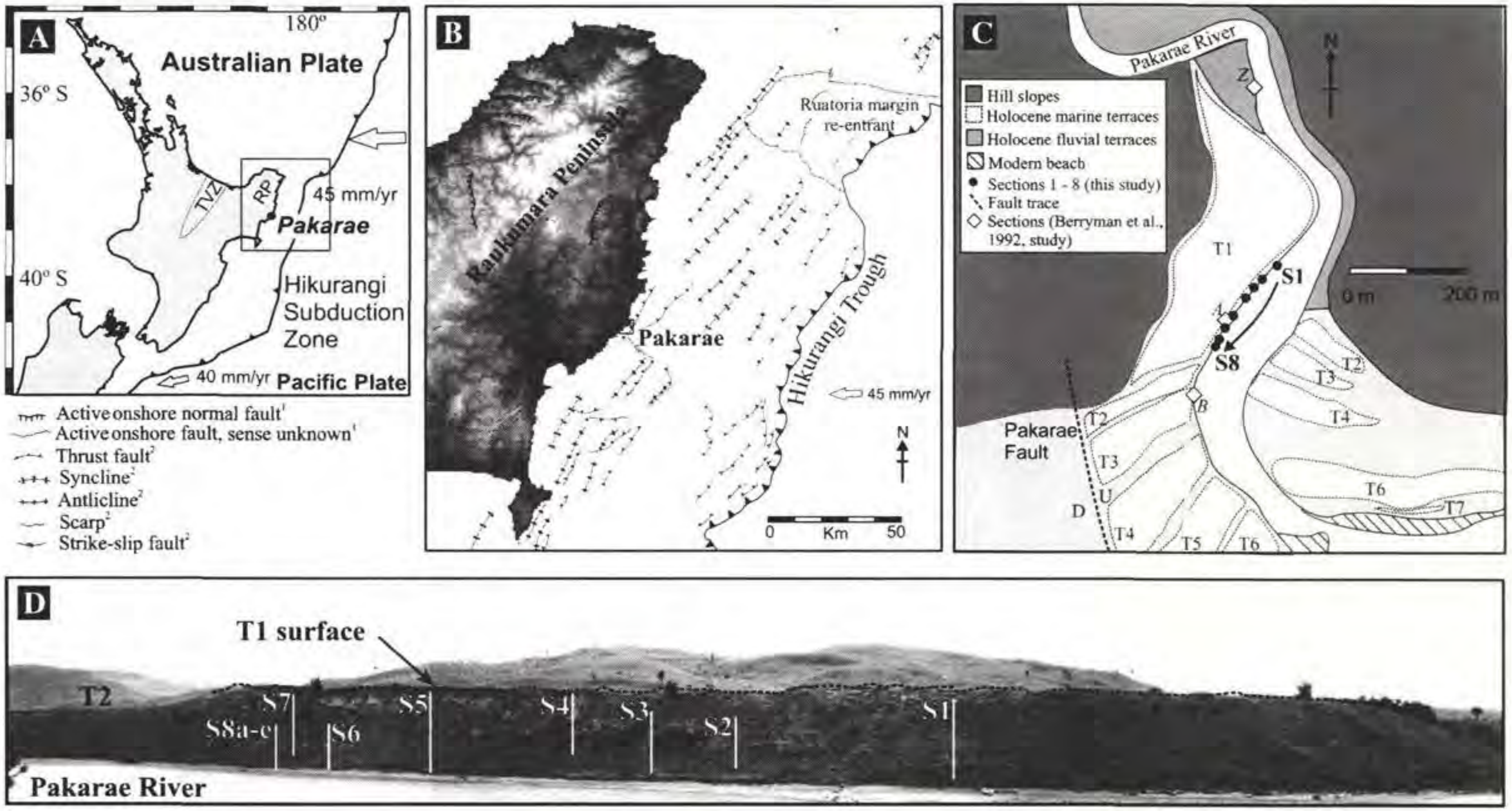

Fig. 1. (A) North Island, New Zealand with major tectonic features. TVZ: Taupo volcanic zone, RP: Raukumara Peninsula. Continental-oceanic convergence at the latitude of the Raukumara Peninsula is oblique; the Pacific Plate has a velocity of 45 mm/yr relative to the Australian Plate (Beavan and Haines, 2001; De Mets et al., 1994). Hikurangi subduction deformation front after Collot et al. (1996). (B) Topography and tectonic features of the Raukumara Peninsula. [1]Onshore active faults from the GNS Science Active Faults Database (http://data.gns.cri.nz/af/). [2] Offshore structures from Lewis et al. (1997). (C) Pakarae River mouth with major geomorphic elements, marine terraces (after Wilson et al., 2006) and stratigraphic section locations (S1–S8). (D) The Pakarae riverbank, transgressive sedimentary sequence exposures beneath TI (highest Holocene marine transgression surface) with Sections 1–8e. The riverbank is 25 m high.

Holocene marine terraces but is not believed to be causing any significant coastal uplift. Rather, an unmapped offshore reverse fault is thought to be responsible for most of the coastal uplift (Ota et al., 1991; Wilson et al., 2006). The Pakarae River has a catchment area of ca. 230 km^2. The modern river mouth has a small sand bar across the mouth, the prevailing longshore current is northerly and the spring tidal range is 1.7 m.

The Pakarae marine terraces were first mapped, correlated, and dated by Ota et al. (1991). They recognised seven terraces, naming them T1–T7 from oldest and highest to youngest and lowest. T1 was recognised as corresponding with the maximum Holocene marine transgression. Wilson et al. (2006) have revised the distribution of these terraces and their age. These data indicate that uplift over the past 7000 yr has been achieved by sudden uplift events during which 2–2.5 m of coastal uplift has taken place every 850±450 yr.

Radiocarbon ages from the fluvio-estuarine sedimentary sequence underlying T1 were presented by Ota et al. (1988). These authors summarised the stratigraphy, but they did not make interpretations concerning the identification and timing of individual uplift events. The sequence was later studied in more detail by Berryman et al. (1992). They used stratigraphy, radiocarbon ages and tephrochronology from three riverbank sections to produce paleogeomorphological maps showing the evolution of the river valley from ca. 9000 to 1000 yr B.P. A relative sea level curve for the period from 11,000 yr B.P. to present was constructed for this site. Importantly these data showed that during the period 11,000–7000 calibrated years before present (cal. years B.P.), when eustatic SL in the New Zealand region was consistently rising, there were fluctuations in relative SL at Pakarae, including an apparent 4 m fall in relative SL between 10,500 and 9500 cal. yr B.P. This short-term fall was attributed to tectonic and eustatic causes, the eustatic component being based upon correlations to other East Coast locations where trees in growth position aged ca. 10,000 cal. yr B.P. are buried by marine sediments thus indicating a possible hiatus in SL rise at this time (Berryman et al., 1992). A comparison between the amount of eustatic SL rise inferred to have taken place in New Zealand (ca. 34±2 m, Gibb, 1986) from 11,000–7000 cal. yr B.P. versus the amount of sediment deposited during that same period in the Pakarae valley (12 m) suggested that as much as 22±2 m of tectonic uplift may have taken place at Pakarae during this period.

Of the three sections (Location A, B and Z) targeted by Berryman et al. (1992), only Location A is in common with the sections that we will examine here (Fig. 1). Their Location Z was revisited by us but will not be used in this study, as there was a lack of recognised marine or estuarine deposits. The approximate site of their Location B was also revisited and again new sites were considered preferable because of uncertainty as to whether the riverbank section was in place or slumped. We believe that most of the section of their Location A has been encompassed by our new sections. However, we cannot exactly correlate our new data with the measured section of Berryman et al. (1992), at Location A, because that section was a composite of several nearby sections.

2. Methodology

To construct a facies architecture model from the Pakarae sedimentary sequence we require information on the age and depositional environments of the sediments. To do this we use the radiocarbon dating, tephrochronology, sedimentology, benthic foraminifera and shell assemblages.

2.1. Chronology

Radiocarbon ages were collected at significant sedimentary unit contacts to estimate the timing of paleoenvironmental change at Pakarae and to compare these changes with eustatic SL movements. Three conventional radiocarbon ages were obtained on wood (2 small wood branches, one concentration of wood chips). Nine accelerated mass spectrometry (AMS) radiocarbon ages were obtained on marine shells, principally *Austrovenus stutchburyi* or *Paphies australis*. Well-preserved shells were preferentially selected for dating (particularly bivalves with articulated valves) in order to have samples that have undergone as little reworking or transportation as possible. All radiocarbon ages are presented at the 2-sigma age range (95% probability) and in units of calibrated radiocarbon years before present (cal. years B.P.), unless otherwise stated.

A tephra unit correlated within four sections (Sections 5–7, and 8d) provided further age control. This tephra was identified on the basis of its glass chemistry and heavy mineralogy and in the context of its bounding radiocarbon ages. Glass shards of 63–250 μm size were mounted in epoxy blocks, these were polished and carbon coated. Ten glass shards from the tephra were analysed with a JEOL-733 microprobe using a 10-μm-diameter beam of 8 nA at 15 kV accelerating voltage in the Analytical Facility of Victoria University of Wellington. Heavy mineral identification was done on selected grains using the electron microprobe.

2.2. Stratigraphy and sedimentology

Sections were chosen for study along the Pakarae riverbank on the basis of the quality and extent of their exposure and to maximise coverage along the strike of the river. A total of 90 m of vertical section was measured over eight sections (1–8). Section 1 is the furthest upstream, with ascending numbers corresponding to sections that are located progressively further downstream. Section 8 is subdivided into 5 small sections (8a–8e, Fig. 2B). Horizontal bedding was used as the main criterion that a section was in place. At the base of Section 5 we used an auger to retrieve sediments from 1 m deeper than the naturally exposed base of the section. We generally had near-continuous exposure vertically down the riverbank though in some cases (Section 1, 3 and 5) we shifted horizontally along the bedding. The amount of horizontal offset was recorded in each case and it was everywhere <10 m.

Each section was photographed, measured, described and sampled. Estimates of sediment sorting were made by visual comparison to the charts of Anstey and Chase (1974). Estimates of clast angularity were made by visual comparison with the charts of Powers (1953). Samples of approximately 80 cm^3 were taken from almost every sedimentary unit that we described, larger samples were collected from gravely units. Grain size was estimated in the field and the fraction >63 μm was measured for samples that underwent micropaleontological processing. Where the beds were greater than 2 cm thick samples were taken 4–10 vertical cm apart, if the sediment was particularly homogenous samples were taken at up to 50 cm apart vertically.

The vertical distance of every sedimentary unit contact was measured relative to a reference datum fixed to the top of the exposed section. All heights were later calibrated to elevations in metres above mean sea level (m AMSL) by their relationship to one or more of the 58 elevation control points we had spanning all the sections. On sloping sections all measurements were converted to elevations by taking two points where the elevation was measured (by level or RTK-GPS) and proportionally adjusting the elevation of every depth measurement in between. Elevation uncertainties at the 95% confidence interval range from ±0.22–0.31 m.

2.3. Micropaleontological processing

Selected sediment samples were processed for microfossil content to assist with paleoenvironmental interpretation. Microfossils have been demonstrated to be useful in differentiating coastal waterbody types (for example: Darienzo et al., 1994; Hemphill-Haley, 1995; Shennan et al., 1999; Hayward et al., 1999b; Patterson et al., 2000; Hayward et al., 2004). The preservation of diatom and pollen microfossils within the Pakarae sediments was very poor and the results did not contribute to paleoenvironmental interpretation. Benthic foraminifera are common in the Pakarae sediments and these were used in interpretation of the sediment depositional environment.

In total 199 samples were processed for the foraminiferal study, an average of one sample per 0.45 m of section. However, sampling was concentrated around significant stratigraphic contacts and in parts with high unit variability. Samples were processed using the standard techniques of Hayward et al. (1999a). Where possible 100–200 benthic foraminifera were picked, 100 tests being considered adequate for environmental assessment using brackish foraminifera (Hayward et al., 1996, 1999b, 2004). In some cases when well-preserved benthic foraminifera were very rare we used a floating technique to concentrate the foraminifera. In total 29 samples were floated. Approximately 5 g of the > 0.063 mm sediment fraction was stirred into sodium polytungstate with a specific gravity of 1.6; the fraction that floated contained the concentrated foraminifera. Identification of the well-preserved foraminifera was made with reference to Hayward et al. (1999a) and Hayward et al. (1997). For each sample the relative amounts of macro shell fragments and wood or plant matter were estimated and noted as either absent, scattered or abundant. The abundance of planktic foraminifera was noted for each sample, but we did not identify or count them as they yield no information about the paleo-elevation of the sediment.

3. Results

3.1. Chronology

Ages of the infill sediment range from ca. 10,230 cal. yr B.P. at 1.1 m AMSL to ca. 7400 cal. yr B.P. at 18.3–18.7 m AMSL (Table 1). The ages young upwards with the exception of two samples that occur out of chronological order at the >2 sigma level. In Section 5 the sample at 14.5 m AMSL is a large piece of wood that is not in growth position (Fig. 2). Because this is detrital material it must be older than the sediment that it is preserved within hence the reversed chronology is not a significant concern. A shell sample from Section 4 at 18.9 m AMSL yielded an age of 8350–8170 cal. yr B.P. and is older than the next sample below it (Section 5 at 18.3 m AMSL). This lower sample has an age of 7530–

7280 cal. yr B.P. It is likely that the higher sample may have been re-deposited.

The tephra layer that occurs at ca. 7 m AMSL in Sections, 5, 6, 7, and 8d has a major element glass chemistry characteristic of the Okataina volcanic centre and it contains the diagnostic heavy mineral cummingtonite (referenced to datasets in Lowe, 1988; Stokes and Lowe, 1988; Froggatt and Rogers, 1990, Table 2). Cummingtonite is a heavy mineral present in only three Okataina volcanic centre tephras: the Rotoehu (ca.

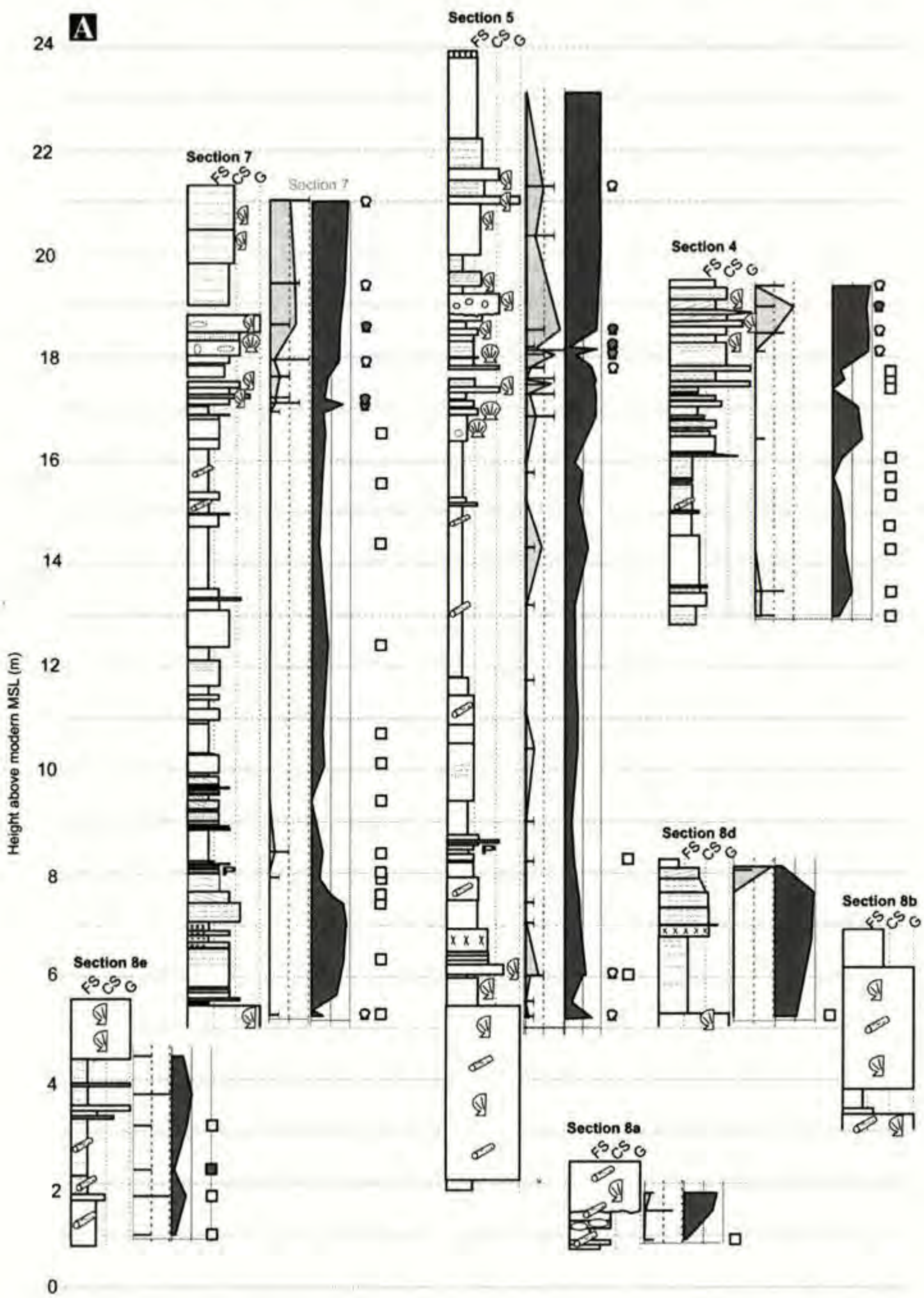

Fig. 2. (A) Sedimentology of the Pakarae River incised valley infill sequence. Sedimentary units, grain size, bedding structures and presence of shells and wood are shown. The graphs alongside show the abundance of benthic foraminifera (columns), the percentage of intertidal foraminifera (light grey-shaded line graph), and the percentage of sediment >63 μm in each sample collected for foraminifera analysis (dark grey-shaded line graph). (B) Location of sections along the Pakarae riverbank, note the vertical exaggeration. Shaded boxes encompass sections belonging to the same section number.

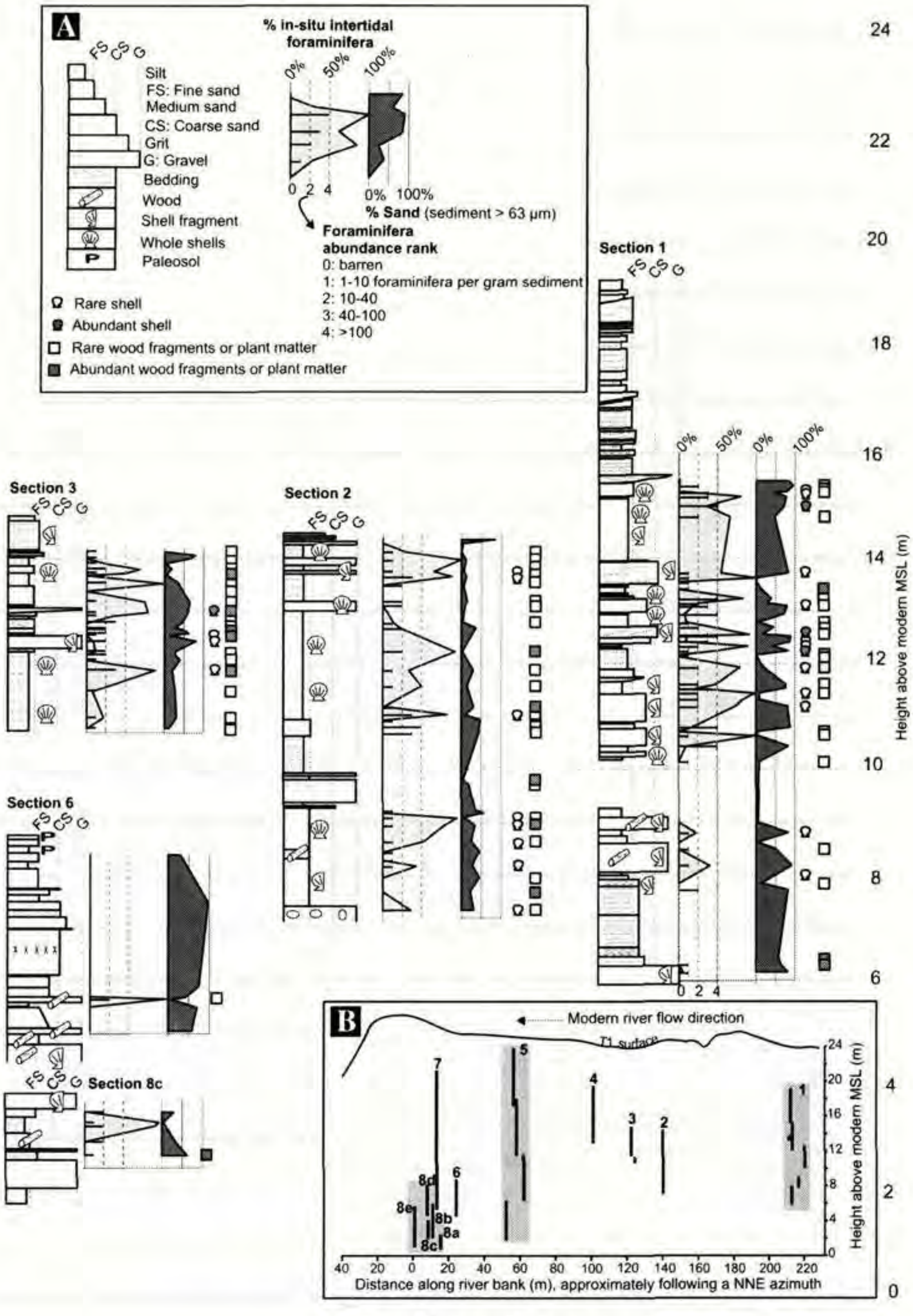

Fig. 2 (*continued*).

50,000 cal. yr B.P.), the Rotoma (9464–9531 cal. yr B.P.) and the Whakatane (5465–5590 cal. yr B.P. (Froggatt and Lowe, 1990). The bounding radiocarbon ages indicate this is the Rotoma tephra. Berryman et al. (1992) also identified this tephra as Rotoma, although their assignment was based only on bracketing radiocarbon ages. Our geochemical analyses confirm that tephra preserved in the riverbank sections is the Rotoma. Tephra isopach maps of Vucetich and Pullar (1964), suggest the Rotoma ash should be <7.5 cm thick in the Pakarae region and this is compatible with our observations of the outcrop where the tephra appears to

Table 1
Radiocarbon ages obtained from the Pakarae incised valley infill sequence

Section	Sample height (m)	Lab number[a]	Sample material[b]	Dating technique	^{13}C (‰)	Radiocarbon age[c] (radiocarbon years BP)	Calibrated age[d] 2 sigma (cal. years BP)
1	15.2±0.22	NZA 21854	A	AMS	−1.27	8056±30	8590–8410
1	10.05±0.22	NZA 22529	A	AMS	1.05	8458±35	9210–8980
1	6.3±0.22	WK 16864	Wood	Standard	−28.2	8420±59	9530–9240
1	6±0.22	NZA 21961	A	AMS	−0.91	8868±30	9600–9450
2	14.15±0.22	NZA 22528	A	AMS	1.42	8082±35	8640–8420
2	7.5±0.22	NZA 21852	A, B	AMS	−3.71	8338±30	9010–8770
4	18.9±0.22	NZA 22526	A, B	AMS	0.98	7791±35	8350–8170
5	18.3–18.7±0.22	NZA 21851	A, B. C	AMS	−0.49	6847±30	7430–7280
5	14.5±0.22	Wk 16454	Wood	Standard	−27.2	8219±52	9290–9000
7	17.15±0.22	NZA 22527	A	AMS	0.39	7981±35	8540–8360
8a	1.1±0.31	Wk 16453	Wood	Standard	−28	9158±52	10420–10180
8b	4.4±0.31	NZA 21853	A	AMS	−2.9	9266±30	10200–9990

[a] Wk: The University of Waikato Radiocarbon Dating Laboratory; NZA: Institute of Geological and Nuclear Sciences Rafter Radiocarbon Laboratory.

[b] Shell: A: *Austrovenus stutchburyi*, B: *Paphies australis*, C: *Melagraphia aethiops*.

[c] Conventional radiocarbon age before present (1950 AD) after Stuiver and Polach, 1977.

[d] Calibrated age in calendar years. Wood ages calibrated using Southern Hemisphere atmospheric data of McCormac et al. (2004) marine ages calibrated using data from Hughen et al. (2004). Radiocarbon ages calibrated using OxCal v3.10.

be largely reworked with only the thin fining-upwards layers at the base being a primary airfall deposit.

3.2. Foraminifera

Of the 199 samples analysed, 56 were barren of foraminifera (either benthic and planktic) and only 36 samples had sufficient foraminifera for >100 benthic specimens to be counted (Fig. 2). Two populations of foraminifers were recognised: one poorly-preserved and one well-preserved. The presence or absence of foraminifera and relative proportions of poorly-to well-preserved foraminifera formed the basis for four foraminiferal assemblages to be distinguished. The assemblages are (1) barren, (2) reworked, (3) marginal-estuarine and (4) intertidal (Fig. 3). The spatial distribution and composition of each assemblage are described in Fig. 3.

The poorly-preserved tests are typically fragmented and encrusted, some are infilled with sediment or a chemical precipitate such as pyrite. Most specimens were unidentifiable but those that could be identified included *Bolivina* spp, *Bulimina* spp, *Fissurina* spp, *Globocassidulina* spp, *Laevidentalina* spp, *Notorotalia* spp, *Trifarina* spp, and *Uvigerina* spp. Many of these species are typical of fully marine conditions in outer harbours and on the mid to inner shelf, some are known to have been extinct before the Holocene (Hayward et al., 1999a). We conclude the poorly preserved specimens were probably reworked from the Miocene–Pleistocene sedimentary bedrock of the Pakarae River catchment (Mazengarb and Speden, 2000). For this reason we group them in an "Other" category of foraminifera in the census and in foraminifera assemblage descriptions (Fig. 3).

The well-preserved benthic foraminifera are characterised by whole, clear and clean tests, and provide a stark contrast to the reworked specimens (Fig. 3). *Ammonia parkinsonia f. aoetana* is the dominant well-preserved species. Well-preserved *Elphidium excavatum f.*

Table 2
Major element glass chemistry and heavy mineral chemistry of the tephra within Sections 5–8 at 7 m AMSL

Element	Glass (n=10)		Cummingtonite (n=4)	
	Average %	1σ	Average%	1σ
SiO_2	78.37	0.30	52.63	1.41
Al_2O_3	12.44	0.17	0.29	0.08
TiO_2	0.13	0.05	1.32	0.64
FeO	0.96	0.06	21.30	2.79
MnO	0.08	0.03	1.21	0.62
MgO	0.12	0.02	21.62	2.17
CaO	0.81	0.09	1.49	0.38
Na_2O	3.63	0.16	0.12	0.20
K_2O	3.30	0.10	0.03	0.02
Cl	0.17	0.04	–	–

The glass geochemistry is characteristic of an Okataina Volcanic Centre source (referenced to datasets in Stokes and Lowe, 1988; Lowe, 1988). Cummingtonite was also detected in the tephra using the electron microprobe, four grains were analysed and the results closely match the cummingtonite analyses of Froggatt and Rogers (1990).

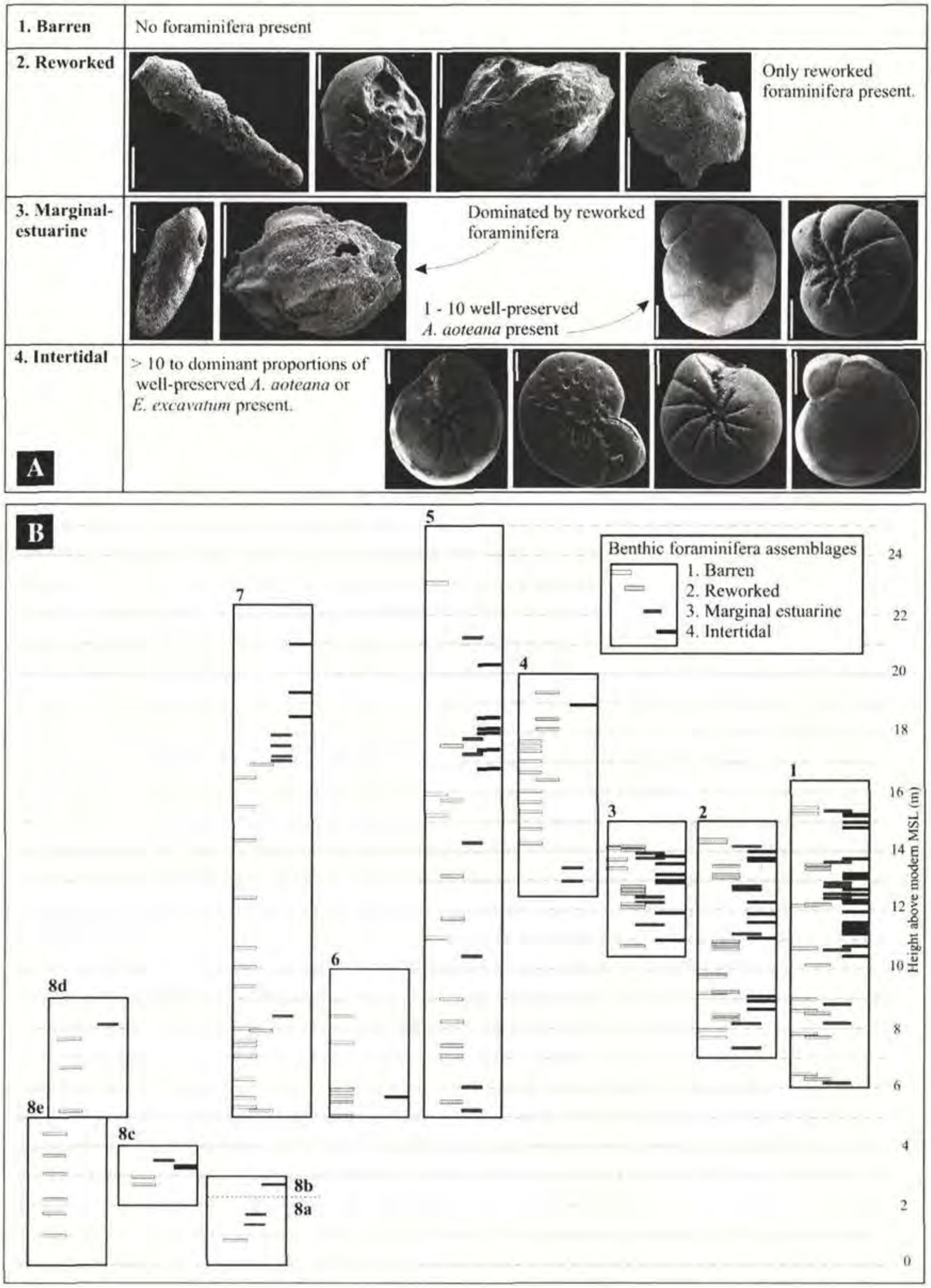

Fig. 3. (A) Benthic foraminifera assemblages, with representative images of the specimens within each group. The white bars in each image represent 100 µm. (B) Distribution of the foraminifera assemblages in the Pakarae sections.

excavatum were rare and only identified in nine samples. *A. aoteana* and *E. excavatum* are common species in brackish to very slightly brackish environments. *A. aoteana* is often a dominant species in the intertidal and subtidal zones of lower estuaries and mid to inner areas of enclosed harbours (Hayward et al., 1999a). The well-preserved nature of these specimens indicates that they are *in situ* fossils.

The difference between the marginal-estuarine and intertidal assemblages is based on the number of well-preserved (≈ *in situ*) foraminifera picked from each sample. We do not use the percentage of *in situ* tests as this can cause an artificial bias in those samples with extremely low abundances. Approximately equal sample sizes were scanned for foraminifera therefore the numbers of foraminifera picked are comparable measures. The foraminiferal assemblages tend to be clustered together at varying elevations within the sections (Fig. 3). Intertidal assemblages are notably clustered between ca.16 and 10 m AMSL in the upstream Sections 1, 2, and 3, and between 17 and 20 m AMSL in the downstream Sections 7 and 5 (Fig. 3).

3.3. Bio-lithofacies

Ten bio-lithofacies (Facies 1–10) are recognised within the studied sedimentary sequences. We define a bio-lithofacies as a sedimentary unit with a characteristic lithology and biological assemblage. The sedimentary and faunal characteristics of each facies, and their distribution, are described in Table 3. Here we interpret the depositional environment of each facies.

3.3.1. Facies 1: non-fossiliferous silt and sand units 0.2–8 m thick

As it is the most widespread unit, the depositional environment of this facies is of critical importance to this study. We infer that the most likely depositional environment is fluvial. Evidence for this includes the complete absence of marine fauna, the silty nature of the sediments, channelling, and its content of scattered detrital wood.

Marine fauna could be absent from this unit for reasons other than the sediment having been deposited in a non-marine environment. For example (i) there could be poor marine fossil preservation because the calcareous shells and foraminifera tests may have been leached out by acidic ground water; (ii) the marine environment may not have suited the specific living preferences of the marine fauna; or (iii) sediment deposition rates could have been so high that the marine fauna are either highly "diluted" or could not survive under such rapid sedimentation. With the available data we suggest that the non-fossiliferous facies was deposited in a fluvial environment.

3.3.2. Facies 2: thick shelly gravel units 0.5–3.5 m thick

We interpret this facies to have been deposited in a fluvial delta environment at the head of a paleo-estuary, henceforth called the estuary-head delta. The very poor sorting and clast angularity suggests short transport distances for the clasts. The marginal-estuarine foraminifera assemblages and juvenile intertidal *A. stutchburyi* shells indicate the sediment must have been deposited within reach of tidal flow. Radiocarbon ages from below and within the facies at the downstream end of the sections suggest rapid deposition of the gravel (*cf.* wood age of 10,200–9990 cal. yr B.P. at 1.1 m AMSL in Section 8a and shell age of 10,200–9990 cal. yr B.P. at 4.4 m AMSL in Section 8b, Fig. 4). The facies displays variable thicknesses along the riverbank; this may be because its distribution was controlled by proximity to the bedrock high (beneath Sections 1 and 2) which was the source of the gravels (Fig. 4).

3.3.3. Facies 3: non-fossiliferous gravel beds 0.2–0.6 m thick

The non-fossiliferous gravel facies is most likely a fluvial channel deposit because of the thin nature of the beds and high-energy currents implied by the presence of large clasts. A non-marine environment is indicated by the absence of shells in the gravel. The range of clast sizes and the angularity of clasts suggest that the gravel has not been transported far, particularly since the clasts consist chiefly of mudstone, a soft lithology that would be quickly rounded during transport. The mudstone clasts are of identical lithology to that of the local outcrops of Neogene bedrock, thus supporting a nearby source. The poor sorting and angularity of clasts might suggest a colluvial depositional environment, but bedding indicates fluvial deposition of this proximally derived gravel.

3.3.4. Facies 4: silt and sand units with abundant marine fauna, 0.1–1.5 m thick

We interpret the depositional environment of this facies to be the central basin of an estuary. The primary evidence of this are abundant whole and *in situ P. australis* and *A. stutchburyi* shells and the intertidal foraminifera assemblages (Table 3). Observed and measured grain size variation between sand and silt and evidence of channelling is consistent with an

Table 3
Distribution and sedimentary characteristics of the bio-lithofacies of the Pakarae infill sequence

Bio-lithofacies	Distribution	Characteristics	Interpretation of depositional environment
Facies 1: non-fossiliferous gravel	S2, ~10 m; S6, 8c, 8e, 2–6 m	Beds <0.6 m thick; clast-supported gravel; angular — subrounded mudstone clasts 2–40 mm diameter. Matrix of silty medium sand to coarse sand. Always have sharp bounding contacts.	Fluvial channel lags
Facies 2: thin shelly gravel	S5, ~22 m; S4, 5, 7, 12–13 m; S1, 8–9 m	Beds <0.5 m thick; rounded — subangular mudstone clasts, 2–150 mm diameter. Clast and matrix supported (matrix of coarse sand). Abundant fragments of *A. stutchburyi* and *P. australis*. Fragmentation degree varies from shell grit to whole bivalve halves. Basal contacts sharp and wavy.	Estuarine tidal channel lags
Facies 3: thick shelly gravel	S1, 2, 5–7, 8a–8e, 7–1 m	Beds 0.5–3.5 m thick. Very poor sorting, clasts vary 2–150 mm diameter. Dominantly subangular clasts, occasional rounded and angular clasts. Clast-supported with a silt matrix. Occasional small twigs and detrital wood. Rare juvenile *A. stutchburyi* shells and micromolluscs. Sharp bounding contacts. Three matrix samples contained marginal-estuarine foram assemblages; one sample contained a reworked assemblage.	Estuary-head delta
Facies 4: shelly well-sorted sands	S4, 5, 7, >20 m	Beds up to 2 m thick. Well-sorted medium to coarse sand. Occasional cm-scale lenticular cross-bedding and mm-scale laminations. Occasional shells, some identified as *A. stutchburyi*. Six samples analysed for foraminifera: one barren, one reworked, one marginal-estuarine and three intertidal assemblages.	Barrier
Facies 5: non-fossiliferous well-sorted sands	S6, 7, 8d, 7–8 m	Well-sorted medium to coarse sand with mm-scale laminations. All bounding contacts sharp. Six foram samples: a mixture of reworked and barren assemblages.	Reworked tephra and fluvial sands
Facies 6: silt and sand with abundant marine fauna	S1, 10–15 m; S2 and S3, 11–14 m; S4, ~19 m, S5, 16–19 m; S6, 8b, 8c, 2–6 m	Silt and silty fine sand, beds are usually massive, some display faint mm to centimetre scale laminae; rare units with centimetre-scale lenticular cross-beds and millimetre-scale flaser bedding. Most bounding contacts are sharp and there are frequent scoured angular unconformities indicating channelling. Abundant whole and *in situ P. australis* and *A. stutchburyi* shells. Foraminifera assemblages dominantly intertidal.	Estuary central basin
Facies 7: Silt and sand with rare marine fauna	S1, rare 10–15.5 m; S2, rare 7–14.5 m; S3, rare 11.5–14 m; S4, 13–13.5 m; S5, rare 6–18 m; S7, 17–18.5 m; S7, 8b, 8d, rare 2.5–8 m	Silt or silty fine to medium sand, occasional detrital wood chips less than 20 mm in length. Beds are usually massive, rare units with millimetre to centimetre-scale horizontal and wavy laminations. Foraminifer assemblages dominantly marginal-estuarine.	Estuarine margins
Facies 8: non-fossiliferous silt and sand	S1, >15 m, 6–8 m, 12–14 m; S2, 9–11 m, 7–8 m, 12–14 m; S3, >14 m, 11–14 m; S4, 13.5–18.5 m; S5, 5.5–16 m, <2 m; S6, 4–9 m; S7, 8.5–17 m; S7, 6.5–5.5 m; S8a–8d, varying elevations; 8e, 0.9–3.4 m	Silt and silty fine to medium sand; detrital wood common with branches up to 200 mm diameter. Units commonly massive; occasional millimetre to centimetre-scale horizontal bedding. Gradational bounding contacts. Occasional coarser-grained units (medium sand to coarse sand) with unconformable wavy basal contacts.	Fluvial

(continued on next page)

Table 3 (*continued*)

Bio-lithofacies	Distribution	Characteristics	Interpretation of depositional environment
		Marine indicators absent. Foraminifera assemblages are either barren or reworked.	
Facies 9: tephra	S5–7, 8d, 6–7 m	Beds 0.85–0.24 m thick. Very sharp bounding contacts. ~150 mm of medium-coarse millimetre-scale shower-bedded grains at the base all units, upper parts very fine grained with massive beds of clay-sized glass particles.	Primary airfall tephra at base, reworked tephra at top
Facies 10: paleosols	S5–7, occasional between 8 and 9 m	Silt units characterised by a dark brown tint in the sediment due to a high organic content and by a crumbly texture and greasy feel due to high clay content.	Period of non-deposition

estuarine environment subject to varying current energies and meandering tidal channels (Fig. 2).

3.3.5. Facies 5: silt and sand units with rare marine fauna 0.1–1.5 m thick

The distinguishing feature of this bio-lithofacies is the occurrence of marginal-estuarine foraminifera assemblages (Fig. 3). The benthic foraminifer *A. aoteana* indicate this unit probably deposited close to an estuary, perhaps between mean high water and extreme high water spring level. However, the abundances are so low it is conceivable that either the depositional site was only inundated during extreme high tides or storm surges, or that the intertidal forams could have been wind-blown up river.

3.3.6. Facies 6: thin shelly gravel units <0.5 m thick

The thin shelly gravel layers are interpreted as estuary tidal channel lags. The scoured bases, abundant fragmented shells and large clast sizes indicate a high-energy depositional environment. The shell species consist of *A. stutchburyi* and *P. australis*, both of which inhabit sheltered, marine to brackish-marine, intertidal environments (Morton and Miller, 1968; Hayward et al., 1999a,b). The foraminifera assemblages are dominantly estuarine to marginal-estuarine therefore both the macro-and mircofauna indicate a brackish-marine, intertidal paleoenvironment.

3.3.7. Facies 7: tephra

The lenticular shape of the tephra (correlations between the units suggests a horizontal top and curved concave-up base, Fig. 4), and the considerable thickness of very fine reworked tephra suggest that the depositional environment may have been an abandoned oxbow or backwater swamp of the Pakarae River. Such a low-energy paleoenvironment would have been required to preserve the tephra, and allow the clay-sized glass particles to settle out of suspension. The lack of marine indicators in the surrounding tephra lense argues against deposition within an estuary.

3.3.8. Facies 8: non-fossiliferous well-sorted sand units 0.4–1 m thick

This sand was probably deposited in a fluvial environment as it contains no shells or foraminifera. Most of the grains consist of volcanic glass, suggesting reworking of the underlying Rotoma tephra, with subordinate amounts of quartz grains.

3.3.9. Facies 9: paleosol

The paleosol units occur within silt, where they are characterised by a dark brown tint signifying a higher organic content and they have a crumbly texture with a greasy feel due to high clay content. Paleosols record a prolonged period during which the sediment surface was above water and not undergoing continuous sedimentation thereby allowing soil to develop.

3.3.10. Facies 10: shelly well-sorted sand units up to 2.5 m thick

We interpret the shelly well-sorted sand to have been deposited near the mouth of an estuary inside a wave-dominated barrier, probably representing the flood tidal delta. The clean, well-sorted nature of the facies is characteristic of sediments sorted by waves and tidal currents (Allen and Posamentier, 1993; Roy et al., 1994). The occasional *A. stutchburyi* shells and dominantly intertidal foraminifera assemblages are consistent with an intertidal environment.

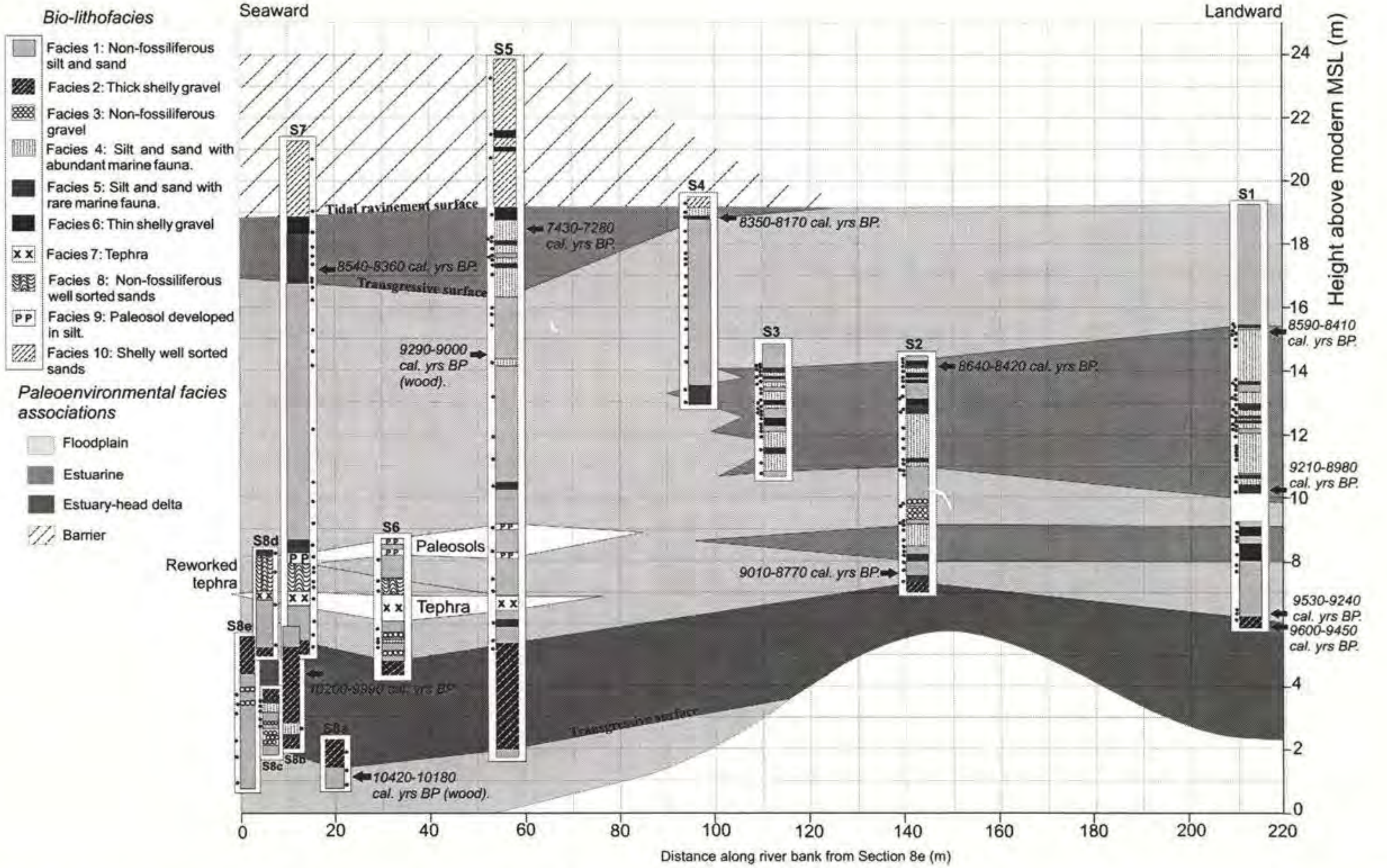

Fig. 4. Bio-lithofacies and paleoenvironmental facies associations of the Pakarae River sections, correlations between the sections based on stratigraphy and paleoenvironmental interpretations. Tidal ravinement surface and transgressive surface after the terminology of Allen and Posamentier (1993).

3.4. Paleoenvironmental facies associations and correlations between sections

With the exception of the paleosols and tephra facies, which can be correlated reliably between sections, the rest of the bio-lithofacies have highly variable distribution and correlation of individual units is not feasible. This is why we simplify the stratigraphy further by adopting four basic paleoenvironmental facies associations to enable correlation between the sections (Fig. 4). We define a paleoenvironmental facies association as a package of bio-lithofacies from a similar depositional paleoenvironment. Four paleoenvironmental facies associations are recognised within the Pakarae sequence: barrier, estuarine, estuary-head delta and floodplain. The composition of each of these is described below:

- The floodplain paleoenvironmental facies association is comprised of Facies 1, non-fossiliferous silts and sand, Facies 3, non-fossiliferous gravel bio-lithofacies and Facies 8, non-fossiliferous well-sorted sands.
- The estuarine paleoenvironmental facies association is composed mainly of Facies 4, silt and sand with abundant marine fauna and Facies 6, thin shelly gravels. Both the floodplain and estuarine paleoenvironmental facies associations include occasional units of Facies 5 (silts and sand with rare marine fauna). Because Facies 5 is interpreted as a marginal-estuarine deposit we package it within the paleoenvironmental facies association of the surrounding bio-lithofacies.
- The estuary-head delta paleoenvironmental facies association consists of Facies 2, thick shelly gravel bio-lithofacies. With increasing distance from the bedrock high these coarse gravel sediments become interfingered with units of Facies 1, non-fossiliferous silts, and Facies 4, silts with abundant marine fauna.
- The barrier paleoenvironmental facies association is dominated by Facies 10, shelly well-sorted sands and also includes some units of Facies 6, thin shelly gravels.

4. Discussion

To characterise the facies architecture of an incised valley on a tectonically active coast we compare the paleoenvironmental facies association distribution profile we have developed from Pakarae (Fig. 4) to facies models for stable coasts (Fig. 5A, B, D Roy, 1984; Dalrymple et al., 1992; Allen and Posamentier, 1993) and case studies of infilled Holocene estuaries on stable coasts (for example, Fletcher et al., 1990; Chappell, 1993; Woodroffe et al., 1993; Nichol et al., 1996; Woodroffe, 1996; Lessa et al., 1998; Long et al., 1998; Dabrio et al., 2000; Sloss et al., 2005, 2006). We then modify these models to better reflect the expected architecture of valley infill on tectonically active coasts.

4.1. Comparisons of Pakarae stratigraphy to stable coast models of incised valley infilling

The paleoenvironmental facies associations we identify have been developed on their own merits, but many do have similarities with the facies divisions of Dalrymple et al. (1992), Roy (1984) and Allen and Posamentier (1993, Fig. 5A, B, D). Our barrier paleoenvironmental facies association is comparable to the barrier-shoreface facies of Dalrymple et al. (1992), the estuary mouth facies of Allen and Posamentier (1993), and the tidal delta sand of Roy (1984). The estuarine paleoenvironmental facies association of this study is similar to the central basin facies of Dalrymple et al. (1992), the tidal estuarine sand and mud facies of Allen and Posamentier (1993), and the estuarine mud facies of Roy (1984). The Pakarae estuarine facies, consisting of silts, sands and occasional thin shelly gravels, is generally coarser and more variable than the equivalent facies described by Roy (1984), Dalrymple et al. (1992), and Allen and Posamentier (1993), which are dominantly or entirely muds or silts. Nevertheless our Pakarae data benefits from micro and macrofossil data to confirm the estuarine paleoenvironment. The coarser sediment and greater variability of this facies at Pakarae is probably due to the relatively restricted space in the Pakarae incised valley, which may have inhibited the development of a deep central basin where fine sediments could uniformly accumulate. The estuary-head delta paleoenvironmental facies association of Pakarae is similar to the bay-head delta facies of Dalrymple et al. (1992). Bay-head and estuary-head are interchangeable terms and refer to the same physiographic location within an estuary; we henceforth use the term "estuary-head". Our floodplain paleoenvironmental facies association corresponds to the alluvial package of Dalrymple et al. (1992), the fluvial or floodplain packages of Allen and Posamentier (1993) and Roy (1984). The recognition of fluvial sediments in these studies is based on an absence of evidence of marine or tidal processes in the sediment deposition, similar to the criteria we have used at Pakarae.

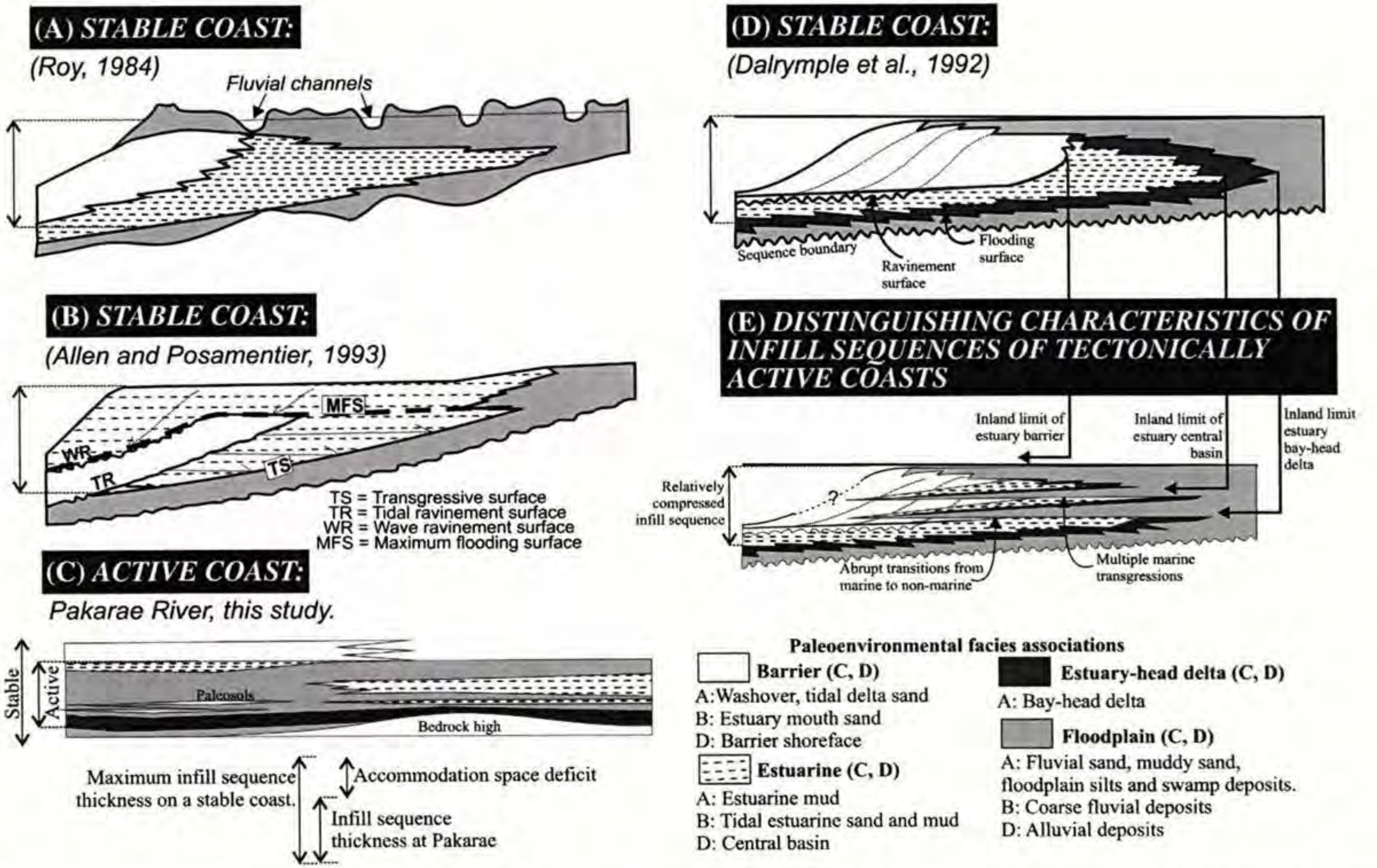

Fig. 5. Comparisons between incised valley facies models of stable coasts (A, B, D), and an active coast (C), and a model for the distinguishing characteristics of an infill sequence on a tectonically active coast (E). All thicknesses (denoted by the vertical arrows) are relative. (A) Stable coast facies model Roy (1984), central estuarine basin mud facies in the middle, thinning landward, underlain and overlain by fluvial sediments. (B) Stable coast facies model Allen and Posamentier (1993), thick estuarine facies in middle thinning landward. (C) Uplifting active coast, Pakarae River (this study), includes three estuarine paleoenvironmental facies associations, two of which pinch out seaward within a floodplain paleoenvironmental facies association. (D) Stable coast facies model Dalrymple et al. (1992), thick central estuarine basin facies in middle thinning landward, underlain and overlain by fluvial sediments. (E) Modification of a stable coast infill model to better reflect the distinguishing characteristics produced by a tectonically active coast.

The stratigraphic framework of Pakarae is simplified by the use of paleoenvironmental facies associations (Fig. 4). This allows correlation of groups of bio-lithofacies from similar depositional environments. The spatial and chronological relationships between the paleoenvironmental facies associations forms the basis of our comparisons with stable coast facies models of incised valley infill. This is also a significant improvement upon the previous data collected from Pakarae by Berryman et al. (1992) which used three widely spaced sections between which unit correlation was not possible and did not utilise paleoenvironmental data from microfossils.

There are two elements of similarity between Pakarae facies distribution and the facies models of Dalrymple et al. (1992), Roy (1984) and Allen and Posamentier (1994, Fig. 5A, B, D): (1) the occurrence of floodplain sediments at the base of the sequence and the immediately overlying estuary-head delta facies; (2) the occurrence of barrier sands at the top of the sequence. The major difference between Pakarae valley sequence and existing stable-coast models is within the middle part of the infill sequence where estuarine and fluvial facies alternate at Pakarae instead of displaying a deepening central estuary basin facies as predicted in the models. We discuss the similarities first and then the important differences.

It is significant that both the basal floodplain and capping barrier package are present at Pakarae because it suggests that the whole sequence of the Holocene valley infill is represented in the outcrop exposures. We infer there is no additional valley infill below the extent of the exposures we have documented at Pakarae. A juvenile *A. stutchburyi* shell from the lowest estuary-head package is dated at 10,200–9990 cal. yr B.P. (Table 1). At this time eustatic SL was ca. 23 m below modern MSL (Gibb, 1986). The present elevation of this shell sample at 4.4 ± 0.31 m indicates an uplift rate of 2.7 ± 0.5 mm/yr since its deposition. This is within the uncertainty range of the late Holocene uplift rate calculated at Pakarae from the elevation of marine terraces (3.2 ± 0.8 mm/yr, Wilson et al., 2006). We infer the incised valley floor that was inundated at ca. 10000 cal. yr B.P. probably now resides close to modern MSL, assuming that the average uplift rate has been constant for the past 10,000 yr. This supports our inference that there is no valley infill below the Pakarae riverbank exposures.

The presence of a laterally continuous layer of the estuary-head delta paleoenvironmental facies (extending the full 220 m length of the sections) deposited on top of the basal fluvial deposits at Pakarae is consistent with the Dalrymple et al. (1992) facies model (Fig. 5D). The base of the estuary head paleoenvironmental facies association is termed the "flooding surface" by Dalrymple et al. (1992), and the "transgressive surface" by Allen and Posamentier (1994). The gravel-rich, carbonate poor nature of the estuary-head delta paleoenvironmental facies does contrast with the transgressive sand sheet described by Sloss et al. (2005, 2006) in their infilling models of two Australian estuaries, Burrill Lake and Lake Illawarra. They noted a basin-wide, carbonate-rich sand sheet as the initial transgressive marine unit in two incised valleys. Lacking in lithic components, they suggested the sand was sourced from the continental shelf rather than the catchment (Sloss et al., 2005) and this may explain why a similar unit is not seen in the Pakarae River incised valley. The more youthful landscape of the eastern North Island has higher erosion rates relative to southeastern Australia therefore the Pakarae River incised valley receives a higher catchment sediment input, most likely masking any contribution of continental shelf sand to the transgressive marine unit. At Pakarae the gravel-rich estuary-head delta paleoenvironmental facies marks the start of the post-glacial marine transgression along this part of the incised valley. Radiocarbon ages from juvenile *A. stutchburyi* shells within this facies indicate that the estuary head shifted landward ca. 200 m between 10,200–9990 cal. yr B.P. and 9600–9450 cal. yr B.P. (Fig. 4, Table 1).

The distribution of paleoenvironmental facies associations in the middle section at Pakarae, between the estuary-head delta package and the barrier sands, does not reconcile with the common stable-coast facies models (Roy, 1984; Dalrymple et al., 1992; Allen and Posamentier, 1994). In this part of the section sediments of the central estuary basin would be expected (Fig. 5A, B, D). In contrast, the sediments at Pakarae between the basal estuary-head delta and capping paleoenvironmental facies associations show a complex alternation and interfingering of floodplain and estuarine paleoenvironmental facies associations (Figs. 4 and 5C). We consider this to be an important characteristic of the facies architecture of incised valley infill sequences on coseismically uplifting coastlines.

There are three units of estuarine paleoenvironmental facies association sediments in the middle stratigraphic section of the Pakarae incised valley infill sequence. The highest and youngest estuarine paleoenvironmental facies association is at the seaward end of the sections. It overlies a floodplain facies, pinches out landward into floodplain sediments and grades upwards into estuary barrier sands. This paleoenvironmental facies association distribution can be likened to a typical transgressive estuarine sequence (Fig. 4). The upper estuarine unit is thickest at the seaward end and its base is erosional above silts of the floodplain paleoenvironmental facies association (Fig. 2). The basal unconformity represents a transgressive surface, after Allen and Posamentier (1994) (Fig. 5B). The estuarine silts and sands contain *in-situ* intertidal foraminifera and the shells of *A. stutchburyi* and *P. australis*, common intertidal brackish-marine species. The estuarine unit coarsens upward into cross-bedded barrier sands. The thin gravel beds at ca. 19 m AMSL in Sections 5 and 7 probably represent tidal channels at the estuary barrier (Fig. 2), corresponding to a tidal ravinement surface (Fig. 4, Fig. 5B, Allen and Posamentier, 1994).

The lower and middle estuarine paleoenvironmental facies associations are located at the landward end of the sections (Fig. 4). Both units appear to either pinch out or gradationally merge seaward into a fluvial facies which lies at the same elevation in the seaward sections, though the contact between the estuarine and floodplain paleoenvironmental facies associations is concealed (Fig. 4). Floodplain sediments overlie both estuarine units. These lower two units of the estuarine paleoenvironmental facies association do not reconcile with existing models of incised valley infilling because in this section the marine environment should, if anything, become deeper due to rising eustatic SL. We have not conclusively resolved why this is so but can propose four possible scenarios:

(1) The non-marine sediments were deposited prior to estuary establishment: For example there may have been alluvial aggradation or colluvial fan deposition at the locations of Sections 5 and 7 before the estuarine sediments of Sections 1–4 were deposited.
(2) Birds-foot estuary-head delta morphology: A splayed fluvial delta front, in which there was switching between distributaries (e.g. a prodelta environment). Localised lobes of rapid sediment deposition that inhibited marine fauna colonisation, may account for the close juxtaposition of non-marine and marine-influenced sediments.
(3) The paleo-estuary was not oriented in the same direction as the modern river mouth: The former river mouth may have been in a different location therefore the paleo-seaward direction could have been different from the modern seaward.
(4) The estuarine paleoenvironmental facies associations were once continuous in the seaward direction, but have been removed by fluvial cut and fill subsequent to tectonic uplift, coastal emergence, and consequent river baselevel fall.

None of these scenarios are completely satisfactory to explain the juxtaposition of seaward non-marine sediments at equivalent elevations to landward estuarine sediments. Colluvial fan deposition (scenario 1) is inconsistent with the silty laminations and cross-bedding displayed by the seaward floodplain unit. A floodplain aggradation mechanism implies ca. 7 m of floodplain sediment was deposited within ca. 400 yr at a location very close to the coastline (*cf.* elevation of the ca. 9500 cal. yr B.P. Rotoma tephra at 7 m and wood aged ca. 9100 cal. yr B.P. at 14 m in Section 5), whilst leaving an area of lower elevation landward into which the middle estuarine paleoenvironmental facies association was deposited after ca. 9100 cal. yr B.P. (indicated by shell age of 9210–8980 cal. yr B.P. at 10 m elevation in Section 1). One might expect a river to grade to a consistent base level, and not form the significant topography implied by this scenario.

A splayed delta-front is possible (scenario 2) but it implies the sediments barren of marine fauna (now identified by us as floodplain sediments) were deposited rapidly in an estuary, seaward of locations inhabited by a rich estuarine fauna, without entraining any marine fauna. Furthermore the restricted space in the Pakarae valley means the development of a splayed delta is unlikely. For the same reason, an alternative river mouth orientation (scenario 3) is improbable. Marine terraces on the east side of the river are underlain by mudstone bedrock. Therefore the paleo-river mouth cannot have flowed east, this only leaves a narrow valley width open to the west.

Scenario 4, post-uplift fluvial cut-and-fill, is the preferred scenario because it is known from the late Holocene marine terraces that tectonic uplift at the Pakarae River mouth occurs at intervals of ca. 850 yr (Ota et al., 1991; Wilson et al., 2006); therefore it most likely also occurred during deposition of the infill sequence. River incision following a sudden base level fall, caused by coastal uplift during an earthquake, is likely. The paleosol layer near the base of the fluvial package at 9 m, approximately the same elevation as the lowest estuarine unit, is interpreted as an unconformity because it indicates a hiatus in sedimentation. An issue with this scenario is that the floodplain paleoenvironmental facies association seaward of the middle estuarine unit is relatively uniform and there are no indications of an unconformity that may be equivalent an incision event following abandonment of the middle landward estuarine unit. The 2.5 m thickness of the floodplain sequence between the middle and upper estuarine units is significant and possibly represents rapid deposition of a large fluvial sediment pulse. The sediment pulse was probably due to catchment destabilisation triggered by an earthquake, probably the same event that caused abandonment of the middle estuarine unit.

The Pakarae stratigraphy is compared with case studies of incised valley infills as an additional check on whether our interpretation of fluvial package in the middle section of the Pakarae stratigraphy is anomalous (for example: Fletcher et al., 1990; Chappell, 1993; Woodroffe et al., 1993; Nichol et al., 1996; Woodroffe, 1996; Heap and Nichol, 1997; Lessa et al., 1998; Long et al., 1998; Dabrio et al., 2000; Heap et al., 2004; Sloss et al., 2005). While there are some details of the stratigraphy that differ between these case studies and the facies models this is probably due to varying sediment supply rates, estuary sizes and tidal ranges. Overall, there is a broad consistency between the examples and the stable coast models. The main signature is of a transgressive sequence of non-marine sediments, followed by estuarine sediments that become progressively increasingly marine-influenced, and then a reversion back to non-marine sediments.

The study of Dabrio et al. (2000) is particularly comparable to our Pakarae study as similar biostratigraphic tools were used at two river valleys in the south of Spain. Within the Guadalete River trangressive sequence the fauna (benthic foraminifera and shells) show a transition from low-diversity, restricted water assemblage to an increasingly diverse, open-water fauna as SL reached maximum flooding. The highstand sediments are represented by a transition back to low-diversity restricted water fauna as a result estuary infilling (Dabrio et al., 2000). A comparable biostratigraphic sequence is not evident at Pakarae. The middle and lower estuarine units of Sections 1–3 show no apparent increase in marine influence or species diversity. The upper estuarine unit of Sections 4, 5 and 7, show some evidence of increasing marine influence: the foraminifera assemblages change from rare intertidal to abundant intertidal species between 16 and 20 m AMSL (Fig. 3), however there is no change in species diversity.

An alternating fluvial-estuarine-fluvial succession was suggested by Dalrymple et al. (1992) to occur if sea level fell before a valley was full. Subsequent sea level rise was predicted to deposit a second valley fill sequence over the incised remnants of the former fill sequence, resulting in a stacked pattern (for example, the three stacked Pleistocene channel fill sequences underlying Chesapeake Bay, Colman and Mixon, 1988). It is not surprising that there are similarities between the Pakarae sequence and that such as Chesapeake Bay as both are related to intermittent marine regressions within an overall trend of rising SL. However, the documentation of alternating fluvial-estuarine facies at Pakarae is the first of its kind to be recognised. Firstly, the Pakarae sedimentary successions are of Holocene age, and secondly, the marine regressions are tectonically-induced rather than eustatic SL change. The extent to which the detailed nature of the estuarine-fluvial transition preserved at Pakarae is analogous to a eustatic SL-related transition is unknown given that the marine regressions at Pakarae were sudden whereas eustatic SL change occurs gradually.

The coseismic marine regressions that appear to have occurred during infilling of the Pakarae incised valley probably had a similar geomorphic effect to sudden infilling of the incised valley. This raises the question of whether a delta ever developed at the mouth of the Pakarae River following uplift events, an evolutionary pathway suggested by Boyd et al. (1992) and Heap et al. (2004) to occur once estuaries infill either under falling or stable eustatic SL conditions. Any early Holocene deltaic deposits of the Pakarae River would have been deposited seaward of the present riverbank outcrops, therefore they would have since been removed by erosion. It is possible that immediately following uplift events the sediment delivery at the Pakarae river mouth was high enough to overwhelm the rates of eustatic SL rise and create a delta. However, the alternating fluvial-estuarine sequence preserved along the riverbank indicates that the rate of eustatic SL rise was eventually sufficient to develop an estuary in the incised valley, which was maintained until the next uplift event.

A recent study by Sakai et al. (2006) addressed a similar question to this study: to interpret the tectonic controls on incised valley infilling on an uplifting coastline in Japan. Evidence for three uplift events of the Isumi River lowlands was found. An early Holocene event at ca. 9000 cal. yr B.P., during the period of eustatic SL rise, was identified by an age gap in landward cores and a correlative period of very rapid sediment progradation within a marine silt sequence in the seaward cores. The rapid sedimentation and associated progradation was interpreted to be the result of increased erosion, probably related to an earthquake (Sakai et al., 2006). Other events younger than the culmination of eustatic SL rise, at 6400 and 3500 cal. yr B.P., were identified by uplifted terraces and were associated with barrier establishment and enclosure of a lagoon. Our resolution of rapid deposition events is constrained by less age control than the Sakai et al. (2006) study, but it is possible that the middle, seaward floodplain paleoenvironmental facies association at Pakarae is an example of the rapid sedimentation and fluvial progradation event demonstrated at the Isumi River.

Comparison between Pakarae and the Isumi River sequence illustrates that the preserved sedimentary signature of an uplift event within a transgressive estuarine sequence depends on the location of the preserved sequence within the incised valley. For example, the preserved Pakarae sequences were probably near the landward edge of the estuary and seaward of this point there were probably pulses of rapidly accumulating sediment corresponding to each coseismic event and associated catchment destabilisation. The more landward parts of estuaries probably record hiatuses or unconformities, while seaward portions may respond with sediment progradation.

4.2. Development of a facies architecture model for an incised valley infill sequence on a coastline undergoing coseismic uplift

Both the Pakarae and Isumi River examples demonstrate that there are significant differences between the incised valley infill sequences of stable and active coasts. Therefore we can begin to develop a modified facies model of the sedimentary infilling of an incised valley system that was experiencing coseismic uplift synchronous with deposition (Fig. 5E). The characteristics of this can be used to recognise similar tectonic settings in the ancient sedimentary record.

On a coastline undergoing uplift synchronously with eustatic SL rise, we predict the transgressive estuarine sequence will be compressed and will not extend as far inland relative to that on a stable coastline (Fig. 5E). If uplift occurred suddenly (i.e. by earthquakes) one might expect abrupt lateral shifts in the paleoenvironment thus sharp facies boundaries. For example, the estuarine central basin sediments might slowly transgress landward during eustatic SL rise, suddenly retreat seaward synchronous with an uplift event, and then subsequently resume gradual landward movement under the continuing eustatic SL rise. This would produce a saw-tooth pattern of interfingering fluvial and estuarine facies at the landward margin (Fig. 5E). If coastal uplift occurred continuously and aseimically this would result in a compressed estuarine sequence with gradational facies transitions. No SL regressions would be recorded if the uplift was always less than the rate of eustatic SL rise rate.

We can demonstrate that the Pakarae valley infill sequence is compressed by comparing the preserved thickness of infill to the eustatic New Zealand SL curve (Gibb, 1986). To do this we have to assume that sedimentation rates in the paleo-valley approximately kept pace with eustatic SL rise. This is indicated by the presence of intertidal foraminifera and bivalves throughout the estuarine paleoenvironmental facies associations. There is 14.1 ± 0.38 m between the oldest and youngest shell radiocarbon samples. An age of 10,200–9990 cal. yr B.P. was obtained from a shell at 4.4 m AMSL, and an age of 7430–7280 cal. yr B.P. was obtained from 18.5 m AMSL (Fig. 4, Table 1). According to the Gibb (1986) eustatic SL curve there was 21 ± 2 m of eustatic SL rise between these two ages. An uncertainty of ± 2 m to this value to reflect the uncertainty of the eustatic SL curve. SL rise creates accommodation space for sedimentation within incised valleys. If sedimentation within the Pakarae incised valley kept pace with the creation of accommodation space by SL rise then 21 ± 2 m of sediment is expected to have been deposited between these two dated shells. The differential between the preserved sediment thickness (14.1 ± 0.38 m) and the accommodation space created during this period (21 ± 2 m) is 6.9 ± 2.04 m (uncertainty calculated as the square root of the sum of the variances, Fig. 4, Table 1). We call this residual the accommodation space deficit (Fig. 5). The substantial deficit between the highest and lowest dated shells is an indicator that the transgressive sequence at Pakarae is compressed relative to that which would be expected on a stable coast. The accommodation space deficit value of 6.9 ± 2.04 m is a significant refinement on the Berryman et al. (1992) study that estimated an accommodation space deficit of ca. 22 m for the Pakarae sequence. Our new estimate benefits from better paleoenvironmental and age control.

We cannot compare the inland extent of the marine sediments at Pakarae to other incised valleys because the geomorphology of Pakarae is unique. The initial depth and slope of the paleo-fluvial valley and rates of fluvial sediment delivery to the coast determine how far inland the maximum Holocene SL transgression reached and these vary with each valley.

Another distinguishing feature we identify for incised valley infills on coseismically uplifting coasts is a distinctive saw-tooth pattern stratigraphy (Fig. 5E). This is created by multiple cycles of sudden SL regressions (earthquakes) followed by gradual SL transgressions (eustatic SL rise). This is in contrast to an aseismic, gradual uplift mechanism, which might instead produce a compressed infill sequence with no reversals in the SL trend. While the paleoenvironmental package distribution of Pakarae has not produced an obvious saw tooth pattern (Fig. 5C), the alternations of fluvial and estuarine paleoenvironmental facies indicates that more than one SL transgression occurred during the valley infilling. The three separate estuarine units indicate at least three periods of marine transgression into the Pakarae paleo-valley. The Pakarae stratigraphy actually indicates that a saw-tooth pattern stratigraphy is perhaps oversimplified and more complex sedimentation patterns are likely because of local circumstance, particularly with rapid fluvial sediment delivery due to catchment destabilisation following earthquakes. The feature of landward estuarine package juxtaposed at the same elevation with a fluvial paleoenvironmental facies in the seaward direction is evidence of this. Evidence of SL reversals in the form of transitions from marine to fluvial environments despite continuous eustatic SL rise, is a remarkable stratigraphic feature at Pakarae and we believe it is an important characteristic of incised valley infills on coseismic tectonically active coasts.

It is possible that fluvial sedimentation pulses rather than uplift could produce saw-tooth stratigraphic patterns and vertical transitions from estuarine to fluvial packages. Both would cause seaward movement of the shoreline and preserve stratigraphic signature of a marine regression stratigraphic signature. However, with SL rising at such fast rates during the early Holocene we believe that it is unlikely that fluvial sedimentation could have been rapid enough to cause seaward movement of the coastline, and this mechanism does not explain the accommodations space deficits recorded at Pakarae. Furthermore, the mostly likely cause of a sediment pulse is destabilisation of the catchment triggered by an earthquake. Offshore sediment cores have shown no evidence of sedimentation pulses during the early Holocene which could be related to earthquakes (Foster and Carter, 1997; Carter et al., 2002; Orpin, 2004), and sediment pulses are unlikely to be climate-related as this is a period of expanding vegetation and slope stabilisation (McGlone et al., 1994).

This discussion shows that some features of the Pakarae sedimentary can be related to the occurrence of coseismic uplift during infilling of the incised valley. We suggest these may be characteristics that can be integrated into a facies model of incised valley infill on active margins. However, the general applicability of these features is yet to be tested. The Pakarae River is an ideal location for this type of study due to the abundant outcrop data, small size and a well-documented history of coseismic uplift events. Conversely, we do not know how the small size of the Pakarae incised valley and the high sediment input rates of the region affect the facies development, hence its value as a representative sequence is not known. Future work on uplifted incised valley infill sequences in other tectonically active regions will help to resolve this and to further refine a facies model for infill sequences on active coasts.

5. Conclusions

The stratigraphy preserved beneath the highest late Holocene marine terrace represents infilling of the Pakarae incised valley during early Holocene post-glacial SL rise. This example of infilling of an incised valley on a tectonically active coast provides a timely comparison with established facies models of incised valley infills, which have been developed exclusively for stable coasts (Roy, 1984; Dalrymple et al., 1992; Allen and Posamentier, 1994). At Pakarae the basal fluvial package, the immediately overlying estuary-head delta package, and the capping barrier package correlate well with models of incised valley infill and indicate that the complete sequence of incised valley infill is present within the Pakarae outcrops. The middle section of the Pakarae stratigraphy displays complex alternations of estuarine and fluvial environments and thus differs from facies architecture models of stable coasts, which display only central estuarine basin sediments in this section. These differences are probably related incision of the fluvial system in response to a fall in base level coupled with rapid delivery of large volumes of earthquake-generated sediment in the catchment following uplift.

Pakarae demonstrates that on coseismic uplifting coastlines distinctive incised valley infill facies architecture is developed and it is timely for a new facies model for such a setting to be developed. The distinguishing characteristics may include: (1) part, or all, of the transgressive and lowstand sequences can be above modern SL, (2) during the period of eustatic SL rise up to the culmination age (c. 7000 cal. yr B.P. in New Zealand) the infill sedimentary sequence is thinner than the amount of eustatic SL rise that occurred during that period, (3) evidence of relative SL falls (tectonic uplift), such as transitions from estuarine to fluvial environments, during periods of time when SL was constantly rising, and (4) periods of rapid fluvial sedimentation that may represent catchment destabilisation following earthquakes.

Acknowledgements

This research was funded by an Earthquake Commission Student Grant (Project 6UNI/501). Kate Wilson was supported by the GNS Science Sarah Beanland Memorial Scholarship. Dr. Rodger Sparks and Dawn Chambers of the Rafter Radiocarbon Laboratory are thanked for their contribution to the radiocarbon dating. Dr. Bruce Hayward and Ashwaq Sabba are gratefully thanked for assistance and advice with foraminifera identification. Hannu Seebeck, Matt Hill and Vicente Perez provided fieldwork assistance. Dr. Craig Sloss, Dr. Andrew Heap and one anonymous reviewer are thanked for their reviews, which significantly improved this manuscript.

References

Allen, G.P., Posamentier, H.W., 1993. Sequence stratigraphy and facies model of an incised valley fill: the Gironde estuary, France. Journal of Sedimentary Petrology 63 (3), 378–391.

Allen, G.P., Posamentier, H.W., 1994. Transgressive facies and sequence architecture in mixed tide-and wave-dominated incised valleys: example from the Gironde estuary, France. In: Dalrymple, R.W., Boyd, R., Zaitlin, B.A. (Eds.), Incised-valley Systems: Origin and Sedimentary Sequences, SEPM Special Publication, vol. 51. SEPM (Society for Sedimentary Geology), Tulsa, OK, United States, pp. 225–241.

Anstey, R.L., Chase, T.L., 1974. Environments Through Time. Burgess Publishing Ltd, Minneapolis. 136 pp.

Beavan, J., Haines, J., 2001. Contemporary horizontal velocity and strain rate fields of the Pacific–Australian plate boundary zone through New Zealand. Journal of Geophysical Research 106 (B1), 741–770.

Berryman, K.R., Ota, Y., Hull, A.G., 1989. Holocene paleoseismicity in the fold and thrust belt of the Hikurangi subduction zone, eastern North Island, New Zealand. Tectonophysics 163, 185–195.

Berryman, K.R., Ota, Y., Hull, A.G., 1992. Holocene evolution of an estuary on a tectonically rising coast: the Pakarae River locality, eastern North Island, New Zealand. Sedimentary Geology 80, 151–162.

Boyd, R., Dalrymple, R.W., Zaitlin, B.A., 1992. Classification of clastic depositional environments. Sedimentary Geology 80, 139–150.

Carter, L., Manighetti, B., Elliot, M., Trustrum, N., Gomez, B., 2002. Source, sea level and circulation effects on the sediment flux to the deep ocean over the past 15 ka off eastern New Zealand. Global and Planetary Change 33, 339–355.

Chappell, J., 1993. Contrasting sedimentary geologies of lower Daly River, northern Australia, and lower Sepik-Ramu, Papua New Guinea. Sedimentary Geology 83, 339–358.

Collot, J.-Y., Delteil, J., Lewis, K., Davy, B., Lamarche, G., Andru, J.-C., Barnes, P., Chanier, F., Chaumillon, E., Lallemand, S., De Lepinay, B.M., Orpin, A., Pelletier, B., Sosson, M., Toussaint, Uruski, C., 1996. From oblique subduction to intra-continental transpression: structures of the southern Kermadec–Hikurangi margin from multibeam bathymetry, side-scan sonar and seismic reflection. Marine Geophysical Researches 18 (2–4), 357–381.

Colman, S.M., Mixon, R.B., 1988. The record of major Quaternary sea-level changes in a large coastal plain estuary, Chesapeake Bay, eastern United States. Palaeogeography, Palaeoclimatology, Palaeoecology 68, 99–116.

Dabrio, C.J., Zazo, C., Goy, J.L., Sierro, F.J., Borja, F., Lario, J., Gonzalez, J.A., Flores, J.A., 2000. Depositional history of estuarine infill during the last postglacial transgression (Gulf of Cadiz, Southern Spain). Marine Geology 162, 381–404.

Dalrymple, R.W., Zaitlin, B.A., Boyd, R., 1992. Estuarine facies models: conceptual basis and stratigraphic implications. Journal of Sedimentary Petrology 62 (6), 1130–1146.

Darienzo, M.E., Peterson, C.D., Clough, C., 1994. Stratigraphic evidence for great subduction-zone earthquakes at four estuaries in Northern Oregon, U. S. A. Journal of Coastal Research 10, 820–876.

De Mets, C., Gordon, R.G., Argus, D.F., Stein, S., 1994. Effect of recent revisions to the geomagnetic reversal timescale on estimates of current plate motions. Geophysical Research Letters 21, 2191–2194.

Fletcher III, C.H., Knebel, H.J., Kraft, J.C., 1990. Holocene evolution of an estuarine coast and tidal wetlands. Geological Society of America Bulletin 102, 283–297.

Foster, G., Carter, L., 1997. Mud sedimentation on the continental shelf at an accretionary margin – Poverty Bay, New Zealand. New Zealand Journal of Geology and Geophysics 40, 157–173.

Froggatt, P.C., Lowe, D.J., 1990. A review of late Quaternary silicic and some other tephra formations from New Zealand: their stratigraphy, nomenclature, distribution, volume and age. New Zealand Journal of Geology and Geophysics 33, 89–109.

Froggatt, P.C., Rogers, G.M., 1990. Tephrostratigraphy of high-altitude peat bogs along the axial ranges, North Island, New Zealand. New Zealand Journal of Geology and Geophysics 33, 111–124.

Gibb, J.G., 1986. A New Zealand regional Holocene eustatic sea-level curve and its application to determination of vertical tectonic movements. In: Reilly, W.I., Harford, B.E. (Eds.), Recent Crustal Movements of the Pacific Region. The Royal Society of New Zealand Bulletin, vol. 24. Royal Society of New Zealand, Wellington, New Zealand, pp. 377–395.

Hayward, B.W., Grenfell, H.R., Cairns, G., Smith, A., 1996. Environmental controls on benthic foraminiferal and thecamoebian associations in a New Zealand tidal inlet. Journal of Foraminiferal Research 26, 150–171.

Hayward, B.W., Hollis, C.J., Grenfell, H.R., 1997. Recent elphidiidae (foraminiferida) of the South-west Pacific and fossil elphidiidae of New Zealand. Institute of Geological and Nuclear Sciences Monograph, vol. 16. Lower Hutt, New Zealand. 170 pp.

Hayward, B.W., Grenfell, H.R., Reid, C., Hayward, K., 1999a. Recent New Zealand shallow-water benthic foraminifera: taxonomy, ecologic dstribution, biogeography, and use in paleoenvironmental assessment. Institute of Geological and Nuclear Sciences Monograph, vol. 21. Lower Hutt, New Zealand. 264 pp.

Hayward, B.W., Grenfell, H.R., Scott, D.B., 1999b. Tidal range of marsh foraminifera for determining former sea-level heights in New Zealand. New Zealand Journal of Geology and Geophysics 42, 395–413.

Hayward, B.W., Scott, G.H., Grenfell, H.R., Carter, R., Lipps, J.H., 2004. Techniques for estimation of tidal elevation and confinement (~ salinity) histories of sheltered harbours and estuaries using benthic foraminifera: examples from New Zealand. The Holocene 14 (2), 218–232.

Heap, A.D., Nichol, S.L., 1997. The influence of limited accommodation space on the stratigraphy of an incised-valley succession: Weiti River estuary, New Zealand. Marine Geology 144 (1–3), 229–252.

Heap, A.D., Bryce, S., Ryan, D.A., 2004. Facies evolution of Holocene estuaries and deptas: a large-sample statistical study from Australia. Sedimentary Geology 168, 1–17.

Hemphill-Haley, E., 1995. Diatom evidence for earthquake-induced subsidence and tsunami 300 yr ago in southern coastal Washington. Geological Society of America Bulletin 107, 367–378.

Hughen, K.A., Baillie, M.G.L., Bard, E., Bayliss, A., Beck, J.W., Bertrand, C., Blackwell, P.G., Buck, C.E., Burr, G., Cutler, K.B., Damon, P.E., Edwards, R.L., Fairbanks, R.G., Friedrich, M., Guilderson, T.P., Kromer, B., McCormac, F.G., Manning, S., Bronk Ramsey, C., Reimer, P.J., Reimer, R.W., Remmele, S., Southon, J.R., Stuiver, M., Talamo, S., Taylor, F.W., van der Plicht, J., Weyhenmeyer, C.E., 2004. Marine04 marine radiocarbon age calibration, 0–26 cal kyr BP. Radiocarbon 46 (3), 1059–1086.

Kingma, J.T., 1964. Sheet 9, Gisborne (1st Ed.) Geological Map of New Zealand 1 : 250 000. Department of Scientific and Industrial Research, Wellington.

Lessa, G.C., Meyers, S.R., Marone, E., 1998. Holocene stratigraphy in the Paranagua Bay estuary, southern Brazil. Journal of Sedimentary Research 68 (6), 1060–1076.

Lewis, K.B., Collot, J.-Y., Davy, B., Delteil, J., Lallemand, S., Uruski, C., 1997. North Hikurangi GeodyNZ swath maps: depths, texture and geological interpretation 1: 500000. National Institute of Water and Atmospheric Research Miscellaneous Series Chart 72. Wellington, New Zealand.

Long, A.J., Innes, J.B., Kirby, J.R., Lloyd, J.M., Rutherford, M.M., Shennan, I., Tooley, M.J., 1998. Holocene sea-level change and coastal evolution in the Humber estuary, eastern England: an assessment of rapid coastal change. The Holocene 8 (2), 229–247.

Lowe, D.J., 1988. Late Quaternary volcanism in New Zealand: towards an integrated record using distal airfall tephras in lakes and bogs. Journal of Quaternary Science 3 (2), 111–120.

Mazengarb, C., Speden, I.G. (compilers), 2000. Geology of the Raukumara area. Institute of Geological and Nuclear Sciences 1:250,000 Geological Map 6. Institute of Geological and Nuclear Sciences Limited, Lower Hutt, New Zealand.

McCormac, F.G., Hogg, A.G., Blackwell, P.G., Buck, C.E., Higham, T.F.G., Reimer, P.J., 2004. SHCal04 southern hemisphere calibration, 0–26 ka cal BP. Radiocarbon 46, 1087–1092.

McGlone, M.S., Anderson, A.J., Holdaway, R.N., 1994. An ecological approach to the Polynesian settlement of New Zealand. In: Sutton, D.G. (Ed.), The Origins of the First New Zealanders. Auckland University Press, Auckland, pp. 136–163.

Morton, J., Miller, M., 1968. The New Zealand Sea Shore. Collins, London. 638 pp.

Nichol, S.L., Boyd, R., Penland, S., 1996. Sequence stratigraphy of a coastal-plain incised valley estuary: Lake Calcasieu, Louisiana. Journal of Sedimentary Research 66 (4), 847–857.

Orpin, A., 2004. Holocene sediment deposition on the Poverty-slope margin by the muddy Waipaoa River, East Coast New Zealand. Marine Geology 209, 69–90.

Ota, Y., Berryman, K.R., Hull, A.G., Miyauchi, T., Iso, N., 1988. Age and height distribution of Holocene transgressive deposits in eastern North Island, New Zealand. Palaeogeography, Palaeoclimatology, Palaeoecology 68, 135–151.

Ota, Y., Hull, A.G., Berryman, K.R., 1991. Coseismic uplift of Holocene marine terraces in the Pakarae River area, eastern North Island, New Zealand. Quaternary Research 35, 331–346.

Ota, Y., Hull, A.G., Iso, N., Ikeda, Y., Moriya, I., Yoshikawa, T., 1992. Holocene marine terraces on the northeast coast of North Island, New Zealand, and their tectonic significance. New Zealand Journal of Geology and Geophysics 35, 273–288.

Patterson, R.T., Hutchinson, I., Guilbault, J.-P., Clague, J.J., 2000. A comparison of the vertical zonation of diatom, foraminifera, and macrophhyte assemblages in a coastal marsh: implications for greater paleo-sea level resolution. Micropaleontology 46 (3), 229–244.

Powers, M.C., 1953. A new roundness scale for sedimentary particles. Journal of Sedimentary Petrology 23, 117–119.

Roy, P.S., 1984. New South Wales Estuaries: their origin and evolution. In: Thom, B.G. (Ed.), Coastal Geomorphology in Australia. Academic Press, Sydney, Australia, pp. 99–121.

Roy, P.S., Thom, B.G., Wright, L.D., 1980. Holocene sequences on an embayed high-energy coast: an evolutionary model. Sedimentary Geology 26, 1–19.

Roy, P.S., Cowell, P.J., Ferland, M.A., Thom, B.G., 1994. Wave-dominated coasts. In: Carter, R.W.G., Woodroffe, C.D. (Eds.), Coastal evolution: Late Quaternary shoreline morphodynamics. Cambridge University Press, Cambridge, pp. 121–186.

Sakai, T., Fujiwara, O., Kamataki, T., 2006. Incised-valley-fill succession affected by rapid tectonic uplifts: an example from the uppermost Pleistocene to Holocene of the Isumi River lowland, central Boso Peninsula, Japan. Sedimentary Geology 185, 21–39.

Shennan, I., Scott, D.B., Rutherford, M., Zong, Y., 1999. Microfossil analysis of sediments representing the 1964 earthquake, exposed at Girdwood Flats, Alaska, USA. Quaternary International 60, 55–73.

Sloss, C.R., Jones, B.G., Murray-Wallace, C.V., McClennen, C.E., 2005. Holocene sea level fluctuations and the sedimentary evolution of a barrier estuary: Lake Illawarra, New South Wales, Australia. Journal of Coastal Research 21 (5), 943–959.

Sloss, C.R., Jones, B.G., McClennen, C.E., de Carli, J., Price, D.M., 2006. The geomorphological evolution of a wave-dominated barrier estuary: Burrill Lake, New South Wales, Australia. Sedimentary Geology 187 (3–4), 229–249.

Stokes, S., Lowe, D.J., 1988. Discriminant function analysis of late Quaternary tephras from five volcanoes in New Zealand using glass shard major element chemistry. Quaternary Research 30, 270–283.

Stuiver, M., Polach, H.A., 1977. Discussion: reporting of C-14 data. Radiocarbon 19 (3), 355–363.

Vucetich, C.G., Pullar, W.A., 1964. Stratigraphy of Holocene ash in the Rotorua and Gisborne districts. Part 2. New Zealand Geological Survey Bulletin 73, 43–63.

Wilson, K., Berryman, K., Litchfield, N., Little, T., 2006. A revision of mid-late Holocene marine terrace distribution and chronology at the Pakarae River mouth, North Island, New Zealand. New Zealand Journal of Geology and Geophysics 49, 477–489.

Woodroffe, C.D., 1996. Late Quaternary infill of macrotidal estuaries in northern Australia. In: Nordstrum, K.F., Roman, C.T. (Eds.), Estuarine Shores: Evolution, Environments and Human Alterations. John Wiley & Sons Ltd, Chichester, pp. 89–114.

Woodroffe, C.D., Mulrennan, M.E., Chappell, J., 1993. Estuarine infill and coastal progradation, southern van Diemen Gulf, northern Australia. Sedimentary Geology 83, 257–275.

Yoshikawa, T., 1988. Pattern and rate of tectonic movement and Late Quaternary geomorphic development in the Raukumara Peninsula, northeastern North Island, New Zealand. Bulletin of the Department of Geography, University of Tokyo 20, 1–28.

R00132006_SEDGEO_3738

ELSEVIER

Quaternary Science Reviews 26 (2007) 1106–1128

QSR

Holocene coastal evolution and uplift mechanisms of the northeastern Raukumara Peninsula, North Island, New Zealand

Kate Wilson[a,*,1], Kelvin Berryman[b], Ursula Cochran[b], Tim Little[a]

[a]*School of Earth Sciences, Victoria University of Wellington, P.O. Box 600, Wellington, New Zealand*
[b]*GNS Science, Victoria University of Wellington, P.O. Box 30368, Lower Hutt 5040, New Zealand*

Received 29 March 2006; received in revised form 4 January 2007; accepted 18 January 2007

ELSEVIER

Quaternary Science Reviews 26 (2007) 1106–1128

QSR

Holocene coastal evolution and uplift mechanisms of the northeastern Raukumara Peninsula, North Island, New Zealand

Kate Wilson[a,*,1], Kelvin Berryman[b], Ursula Cochran[b], Tim Little[a]

[a]*School of Earth Sciences, Victoria University of Wellington, P.O. Box 600, Wellington, New Zealand*
[b]*GNS Science, Victoria University of Wellington, P.O. Box 30368, Lower Hutt 5040, New Zealand*

Received 29 March 2006; received in revised form 4 January 2007; accepted 18 January 2007

Abstract

The coastal geomorphology of the northeastern Raukumara Peninsula, New Zealand, is examined with the aim of determining the mechanisms of Holocene coastal uplift. Elevation and coverbed stratigraphic data from previously interpreted coseismic marine terraces at Horoera and Waipapa indicate that, despite the surface morphology, there is no evidence that these terraces are of marine or coseismic origin. Early Holocene transgressive marine deposits at Hicks Bay indicate significant differences between the thickness of preserved intertidal infill sediments and the amount of space created by eustatic sea level rise, therefore uplift did occur during early Holocene evolution of the estuary. The palaeoecology and stratigraphy of the sequence shows no evidence of sudden land elevation changes. Beach ridge sequences at Te Araroa slope gradually toward the present day coast with no evidence of coseismic steps. The evolution of the beach ridges was probably controlled by sediment supply in the context of a background continuous uplift rate. No individual dataset uniquely resolves the uplift mechanism. However, from the integration of all evidence we conclude that Holocene coastal uplift of this region has been driven by a gradual, aseismic mechanism. An important implication of this is that tectonic uplift mechanisms do vary along the East Coast of the North Island. This contrasts with conclusions of previous studies, which have inferred Holocene coastal uplift along the length of the margin was achieved by coseismic events. This is the first global example of aseismic processes accommodating uplift at rates of $>1\,\mathrm{mm\,yr^{-1}}$ adjacent to a subduction zone and it provides a valuable comparison to subduction zones dominated by great earthquakes.

© 2007 Elsevier Ltd. All rights reserved.

1. Introduction

The interpretation of Holocene coseismic uplift along the East Coast of the North Island, New Zealand, despite changes in upper plate structures and Hikurangi subduction zone dynamics is examined in this study. Early Holocene transgressive marine sediments and mid-late Holocene marine terraces occur extensively along the East Coast adjacent to the Hikurangi subduction zone (Ota, 1987; Ota et al., 1988, 1992). At several localities on the central and southern East Coast detailed studies have produced sound evidence of terrace formation by sudden, episodic uplift processes, that are by inference, coseismic (Berryman, 1993; Hull, 1987; Ota et al., 1991). Other terraces along this margin with similar geomorphology have been presumed to be coseismically uplifted.

This study focuses on the northeastern (NE) tip of the Raukumara Peninsula, at the northern end of the onland Hikurangi margin (Fig. 1A, inset). There, suites of 4–5 marine terraces were recorded by Ota et al. (1992). These terraces are geomorphically similar to those on the southern margin suggesting their origin by a common uplift mechanism. However, in the Raukumara Peninsula region upper plate compressional structures are absent or poorly expressed and there have been no large historical earthquakes. This contrasts with the central and southern Hikurangi margin where upper plate thrust faults are common both on and offshore and where coseismic coastal uplift has taken place in historic time (e.g., the 1931 Napier earthquake and 1855 Wairarapa earthquake).

It is important to determine the mechanism of tectonic uplift along the Raukumara Peninsula particularly due to

*Corresponding author. Tel.: +64 4 570 4530; fax: +64 4 570 4600.
E-mail address: K.Wilson@gns.cri.nz (K. Wilson).
[1]Present address: GNS Science, PO Box 30368, Lower Hutt, New Zealand.

0277-3791/$ - see front matter © 2007 Elsevier Ltd. All rights reserved.
doi:10.1016/j.quascirev.2007.01.005

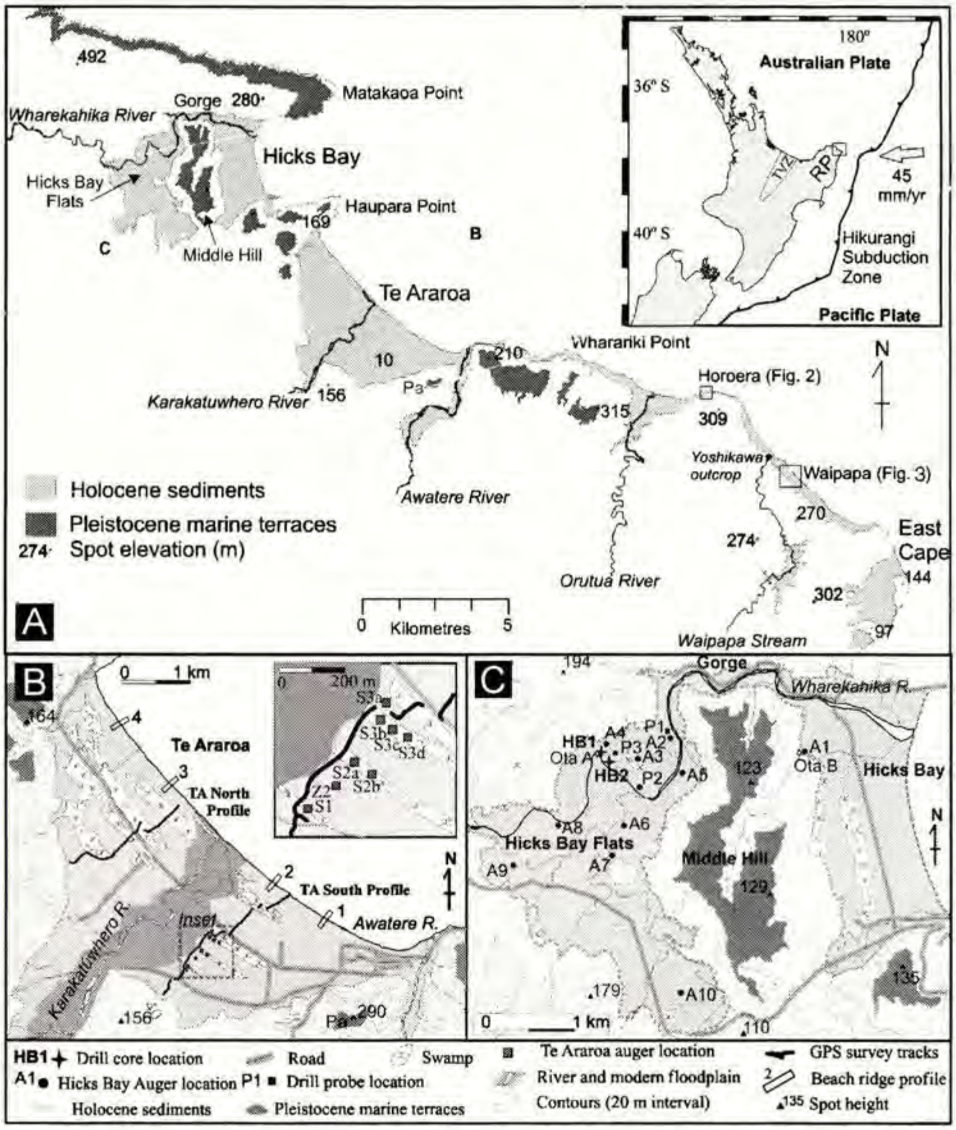

Fig. 1. Location map of the northeastern Raukumara Peninsula region. Inset: Plate tectonic setting of the Raukumara Peninsula (RP: Raukumara Peninsula, TVZ: Taupo Volcanic Zone). (B) Topography of the Te Araroa area with locations auger profiles, GPS survey tracks and locations of modern beach ridge profiles. (C) Topography of the Hicks Bay area with locations of core, probe and auger profiles.

the poorly known hazard of a great subduction earthquake (Stirling et al., 2002). There have been no subduction earthquakes in historic times but the occurrence of uplifted Holocene coastal features along the Raukumara Peninsula raises the question of whether these are related to great palaeo-earthquakes. This sector of the margin is presently estimated to be weakly coupled compared to the southern Hikurangi margin (Reyners, 1998; Wallace et al., 2004. Therefore, this location also provides an interesting study of how upper plate deformation varies with interplate coupling strength—variables that can be rarely tested on other global subduction margins.

We revisit the marine terraces at Horoera and Waipapa (Fig. 1A) to evaluate whether or not they were uplifted coseismically. In addition a geomorphic study of the late Holocene beach ridge sequence at Te Araroa (TA, Fig. 1B) and a palaeoenvironmental study of the early Holocene uplifted transgressive marine deposits in nearby Hicks Bay (HB, Fig. 1C) were undertaken to further assess rates and processes of Holocene tectonic uplift in the NE Raukumara Peninsula. In this paper we present a summary of the regional geology and previous work related to all study sites: Horoera, Waipapa, HB and TA. We then outline the methodology of this study and summarise the results at each location in turn. The data from each site is integrated and analysed in the context of determining the regional Holocene mechanism of uplift and its relationship to the geodynamics of the Hikurangi margin.

2. Tectonic setting

The Raukumara Peninsula is located at the NE end of the East Coast of the North Island; HB, TA and East Cape are located at the NE tip of the peninsula (Fig. 1A). The Hikurangi Trough lies approximately 60 km offshore to the east of HB–TA. Convergence between the Australian and Pacific Plates occurs at ~45 mm yr^{-1} at an azimuth of 266° (De Mets et al., 1990, 1994). The local geology near HB–TA consists of Pliocene forearc basin muddy sandstones of the Mangaheia Group or Early Cretaceous to Eocene igneous rocks (Matakaoa Volcanics) of the Miocene East Coast Allocthon (Mazengarb and Speden, 2000).

In stark contrast with the central to southern parts of the Hikurangi margin, the Raukumara Peninsula contains few known active onshore faults. Mazengarb and Speden (2000) note that mapped active fault segments are typically short and these faults have a normal sense of slip (Ota et al., 1991, Mazengarb, 1984). Inactive faults on the Raukumara Peninsula generally strike northwest, approximately perpendicular to the emplacement direction of the East Coast Allocthon and are primarily Early Miocene-age thrust faults (Mazengarb and Speden, 2000).

3. Previous studies of NE Raukumara Peninsula Quaternary coastal geology

Holocene deposits in the HB–TA regions were first descibed by Henderson and Ongley (1920) and Ongley and MacPherson (1928). Garrick (1979) mapped beach ridges at TA and presented two profiles from the southeastern side of the Karakatuwhero River (Fig. 1B). Three radiocarbon ages of shells collected within 320 m of the modern beach shore, yielded ages of <1068 cal yr BP, establishing the Holocene age of the beach ridges. Projecting the average progradation rate (derived from the oldest of these radiocarbon ages) back to the highest beach ridge inland, Garrick (1979), calculated an average beach ridge uplift rate of 1.5 mm yr^{-1}. Garrick (1979) divided the beach ridges into four zones separated by intervening swamps that he called Coastal Revisions (CRs1–3). Each Revision was proposed to have formed during a period of coastal erosion; although, Garrick (1979) suggested that the oldest zone (CR3) may have formed instead as a result of relatively fast coastal emergence. Ota et al. (1992) subsequently mapped the beach ridges at TA, dividing them into 5 Zones (named I–V). The zones were defined by the continuity of beach ridges. They recognised two, 2 m high, scarps between Zones III–IV and IV–V. The swamps between zones II–V coincide with the Coastal Revisions of Garrick (1979). Ota et al. (1992) did not discuss the formation of the TA beach ridges or mechanisms of their subsequent uplift.

Yoshikawa et al. (1980) included the Holocene terraces of the HB–TA, East Cape and Whangaparoa (on the northwestern side of the Raukumara Peninsula, 25 km west of HB) into a single landform which they referred to as the TA terrace. They noted at least 3–4 sub-levels of terraces within this larger terrace and presented a profile across marine terraces at Waipapa Stream (Fig. 1A). Maps of marine terraces from HB to East Cape, and 26 radiocarbon ages from Holocene deposits in the region were presented by Ota et al. (1992). These authors recognised three marine terraces at HB based on aerial photograph interpretation, with the lowest and highest terraces continuing inland behind Middle Hill. An exposure along the Wharekahika River called "Location A" (henceforth called Ota A) includes abundant *Austrovenus stutchburyi* shells (a common estuarine species); the highest elevation shell bed yielded a radiocarbon age of 7662–7429 cal yr BP. They identified an overlying tephra as the Whakatane tephra (5590–5465 cal yr BP, Froggatt and Lowe, 1990). Ota et al. (1992) mapped marine terraces almost continuously from the Awatere River mouth to East Cape, recognising up to five terraces at the Orutua River mouth and Horoera Point, and three at Waipapa Stream mouth (Fig. 1A). All radiocarbon ages presented by these authors from shells within the terrace cover deposits were <1240–930 cal yr BP. Ota et al. (1992) interpreted all of these late Holocene terraces as having been uplifted suddenly during earthquakes.

4. Methods

4.1. Elevation measurements

All elevations and topographic profiles measured in this study were obtained using a real-time kinematic GPS. In each of the three study areas several datums, such as geodetic benchmarks and tide levels, were measured to provide calibration to the position of mean sea level (MSL). The uncertainty of each calibration point relative to MSL dictates the accuracy of the elevation measurements; hence the overall uncertainty varies between the regions. At Horoera and Waipapa one benchmark, four high-tide points and two mid-tide sea level (SL) points were used as calibration points, elevations in this area have a 95% uncertainty of ±0.22 m. At TA three benchmarks, three estimated high-tide markers and two measurements of the tide level at certain times of the day were used and the elevation measurements here have a 95% uncertainty of ±0.42 m. At HB three benchmarks, and one high-tide measurement resulted yield an uncertainty of ±0.3 m.

4.2. Geomorphic analysis of the Horoera and Waipapa coastal terraces

At Horoera nine topographic profiles were measured normal to the shoreline and strike of the terraces (Fig. 2, P1–P9), and 10 profiles parallel with the shoreline and strike of the terraces were obtained at the front and rear of each terrace (Fig. 2, 1F–5F and 1R–5R). At Waipapa three topographic profiles, all normal to the shoreline and to the strike of the terraces, were obtained. Twenty auger holes were hand-drilled on the Horoera terraces, and eight on the Waipapa terraces, to examine the stratigraphy of their cover sediments.

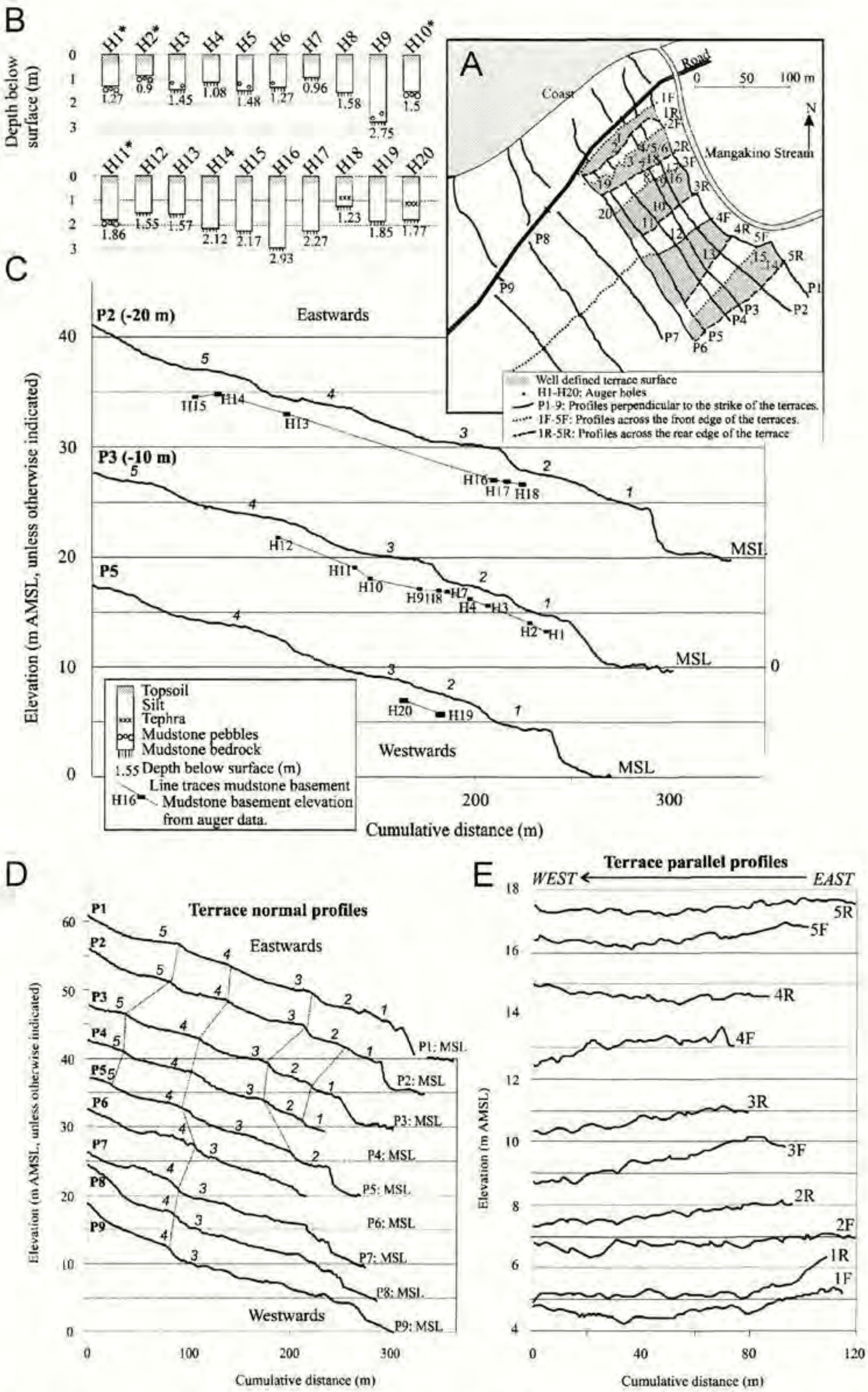

Fig. 2. (A) Location of elevation profiles and auger holes on the Horoera terraces. (B) Stratigraphy of auger profiles H1-H20 on the Horoera terraces. *denotes augers that did not reach the mudstone bedrock. (C) Profiles 1, 3 and 5 (crossing perpendicular to the strike of the terraces) with the bedrock elevations projected onto them. Terraces are numbered 1–5. (D) Profiles 1–9 with terraces 1–5 labelled, dotted lines trace the recognisable risers along the strike of the terraces. (E) Elevation profiles along following the strike of the terraces along the front (1F–5F) and rear (1R–5R) of the terraces.

4.3. TA Beach Ridges

Elevation profiles, TA North and TA South, were taken across the coastal plain either side of the Karakatuwhero River at TA (Fig. 1B). Where swamps could not be crossed (particularly on TA North) several short segments of profile have been joined together with the intervening distance left blank. Seven hand augers were drilled on the

TA plain, most of them within swamps (Fig. 1B inset, named S1–S3a and Z2). The sedimentary characteristics were visually assessed and samples were taken at significant unit boundaries. Three samples were processed for diatom content using the same techniques as will be described for the HB study. Two radiocarbon samples of wood were obtained from auger holes S1 and S3d. All radiocarbon ages are presented at the 2-sigma age range (95% probability) and as calibrated radiocarbon years, unless otherwise stated.

The glass geochemistry of three tephra samples from the augers S1 and S2a were analysed. Glass shards of 63–250 μm size were mounted in epoxy blocks, these were polished and carbon coated. At least 10 glass shards from the tephra were analysed with a JEOL-733 microprobe in the Analytical Facility of Victoria University of Wellington, using a 10-μm-diameter beam of 8 nA at 15 kV accelerating voltage.

4.4. HB palaeo-estuary

Stratigraphic descriptions of sediments infilling the HB Flats were obtained from natural exposures and auger holes at 10 locations (A1–A10, Fig. 1C). These data along with five cone penetrometer probes allowed us to locate suitable places for collecting drill cores. A hydraulic, truck-mounted drill rig collected sediment cores HB1 and 2 (Fig. 1C). Hollow-stem augers, with an inside diameter of 85 mm, were used to simultaneously advance the hole and take "undisturbed" core samples. Core samples were taken in a thin-walled stainless steel liner at intervals of approximately 0.5 m. The cores were extruded into PVC liners. All surfaces of the core were scraped to remove the outer ~5 mm of sediment to reduce the chance of contamination by sediment smearing inside the core liner. In some sections, particularly near the top, there is some compression of the sediment so that when the core was extruded it had a length <0.5 m. The method of coring means that the whole sequence was captured, but we leave a blank space on the corelogs where compression occurred. There was no evidence of core disturbance during drilling. Cores were logged in the field with a visual assessment of the sediment type, grain size, colour and macrofossil content. Sampling was undertaken in the lab with 20 mm slices of sediment removed and the inner portion of the slices processed for microfossils and isotopes. All cores are stored in the coolstore at Victoria University of Wellington.

Five new radiocarbon ages have been obtained from HB: four from the drill cores and one from an auger drilled at the riverbank exposure next to the HB1 drill site. All of these except sample HB1/−0.26 m AMSL were fragments of *A. stutchburyi*; HB1/−0.26 m AMSL was a small twig (~30 mm long, 5 mm diameter).

4.4.1. Micropalaeontology study

- *Foraminifera*: Ninety-one samples were selected from HB1 and 2 for a foraminifera study. Samples were processed using the standard techniques of Hayward et al. (1999a). Where possible 100–200 benthic foraminifera were picked, ~100 tests being adequate for environmental assessment using brackish foraminifera (Hayward et al., 1996, 1999b, 2004a, b). Only well-preserved foraminifera were identified, identification was made with reference to Hayward et al. (1997, 1999a), and personal communication with B. Hayward and A. Sabaa (Geomarine Research, May 2004). The relative amounts of macro shell fragments and wood or plant matter in each sample were estimated and planktic foraminifera were counted but not identified. In some cases when well-preserved benthic foraminifera were very rare we used a floating technique to concentrate the foraminifera. In total, 21 samples were floated. Approximately 5 g of the >0.063 mm sediment fraction was stirred into sodium polytungstate with a specific gravity of 1.6; the fraction that floated contained the concentrated foraminifera.
- *Palynology*: Nine samples from cores HB1 and 2 (Table 1) were processed for spores and pollen following the standard technique of Moore and Webb (1978) and Moore et al. (1991). Bill McLea (VUW) identified the pollen species.
- *Diatoms*: Sixteen samples from HB1 and 2, and five sampled from Ota A, A8 and 10 were analysed for diatom content. Twelve of these samples were fully processed by a standard method as described in Cochran et al. (2006). Diatom species were identified at ×1600 magnification with reference to standard floras (e.g., Krammer and Lange-Bertalot, 1991, 1999a, b, 2000a, b; Hartley, 1996; Witkowski et al., 2000). Where possible the species were assessed for their salinity and habitat preferences taken from van Dam et al. (1994) and Round et al. (1990) and the above floras. The remaining nine samples were assessed by placing a wet smear of sediment on the slide and checking for the presence or absence of diatoms.

4.4.2. Stable isotopes

Thirty-one samples from HBI between 10.3 and 6.2 m AMSL were selected for C and N stable isotope study. Sediment samples of ~10 g were finely ground and homogenised with a mortar and pestle. Samples were run on a Europa Geo 20–20 mass spectrometer in continuous flow with an automatic N and C analyser (ANCA) elemental analyser at the Rafter Stable Isotope Laboratory. Whole sediment samples were run for total carbon and nitrogen content (%C and %N), and carbon and nitrogen isotopes ($\delta^{13}C$ and $\delta^{15}N$). A split of the whole sample was treated with 1N HCl overnight to demineralise the sediment. The split was run on the ANCA again to get total organic carbon and nitrogen content (%TOC and %TON). Inorganic carbon (%$CaCO_3$) contribution was calculated from %C (total)−%TOC (organic).

Table 1
Palynological results from Hicks Bay cores, HB1 and 2

Core	Elevation (m AMSL)	Monolete spore type	*Cyathea* type	*Dicksonia* type	*Cyperaceae* type	Nothofagus	*Brassica* type	Leptospermum	Poaceae	*Dacrydium cupressinum*	*Podocarpus* type	Ascarina	Phyllocladus	Apiaceae	Olea
HB1	9.96		18				1			4					
HB1	9.86	18	32	3	5	4	1	2	2	22	13	3	2		
HB1	9.36		2												
HB1	8.36		11												
HB1	7.96	5	25							8	2			2	1
HB2	8.82														
HB2	6.02	1	20				1				1				
HB2	5.68	5	6							1					
HB2	1.84	10	25			1				6	4			1	

5. Results

5.1. Horoera and Waipapa terrace stratigraphy and geomorphology

All auger profiles on the Horoera terraces revealed a ~0.2–0.3 m interval of sandy topsoil overlying orange-grey mottled silt on bedrock. All but four of the augers reached the mudstone bedrock (Fig. 2A). Mudstone pebbles that could not be drilled through were encountered in Augers H1–2 and H10–11. Shell fragments were found at the base of H1–2. Auger holes H18 and 20 contained a <10 mm thick layer of fine-grained white tephra.

The sharpness of definition of the terrace risers deteriorates to the west, away from the Mangakino Stream (Fig. 2C). Five terraces can be identified in profiles P1–4. From P5 to P9 the only riser that is continuously recognisable is that between terraces 3 and 4 (Fig. 2C). The elevation of the terraces decreases from east to west (Fig. 2D). The average height decrease (measured along the strike of the terrace risers) from east to west over a distance of ~100 m is ~0.5 m (Fig. 2D). The mudstone bedrock increases in elevation landward at approximately the same gradient as the terrace surfaces and the cover sediments are nearly constant in thickness. Repeated augers bounding the ~2 m riser between terraces 2 and 3 however, shows that there is not an equivalent elevation change on the basement surface as there is at the surface (Fig. 2B). For example in P2 there is a well-defined 2.5 m riser between terraces 2 and 3, yet the elevation of the mudstone bedrock on either side of the surface riser changes by only 0.5 m (Fig. 2B).

Only one auger at Waipapa reached the underlying mudstone bedrock at a depth below the surface of 4.6 m (W1a, Fig. 3B). All other augers reached the water table and drilling could not go further; therefore, the measurements record the minimum thickness of coverbed material on the terraces. All augers, except those on terrace 2, recovered homogenous fine-medium well-sorted grey sand. Augers W2a and W2b recovered grey-brown silt.

Waipapa terraces 3 and 4 are relatively narrow with very sharp risers and almost horizontal terrace surfaces (although the landward edge of terrace 3 has been disturbed by the gravel road, Fig. 3A,C). Terrace 4 increases in height along strike towards the south by approximately 1.5 m over 100 m. The riser between terraces 3 and 2 remains very steep along strike increasing in height from 3 m in the north to 6 m in the south (Fig. 3C). Terrace 2 decreases in definition and elevation towards the south. Terrace 1 is very wide with a gentle slope, and the riser between terraces 1 and 2 decreases in definition toward the south. A riser between terrace 1 and the modern beach cannot be distinguished either in the field or on the elevation profiles.

The amount of sand or silt cover on the terraces is generally greater than the height of the adjacent seaward riser. For example, the thickness of sand on terrace 4 is 4.6 m and the riser height between terraces 4 and 3 is 3.5 m.

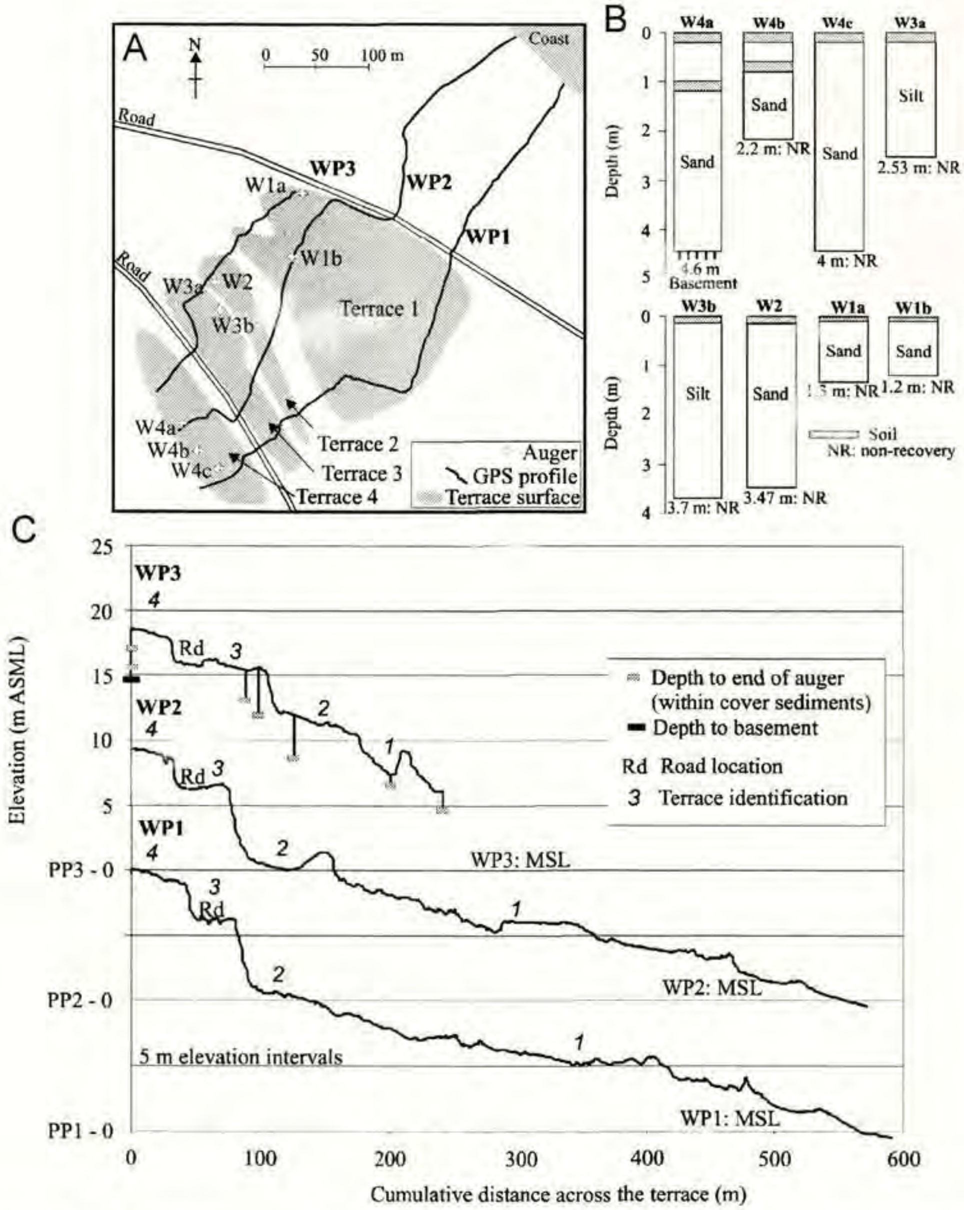

Fig. 3. (A) Location map of the Waipapa terraces, profiles and auger holes, and approximate boundaries of the terraces shown. (B) Auger hole stratigraphy. (C) Elevation profiles, WP1–WP3, with the auger hole depths projected to WP3.

On terrace 3 there is a minimum of 3.7 m of silt, compared with the terrace 3-2 riser height of 3 m. Terrace 2 has a minimum of 3.5 m of sand cover and an adjacent terrace 2-1 riser height of up to 3 m (Fig. 3).

5.2. TA beach ridge sequence

The elevation profiles of TA North and TA South are similar to one another in the section extending from the beach to ~400 m inland (Fig. 4B,C). Both display 6 well-defined beach ridges with an amplitude of ~0.5 m. The average elevation of the ridges over the 400 m increases by 0.8 m in the TA South profile, and 1.2 m in the TA North profile (Fig. 4B,C). The modern storm ridge of TA North is ~0.9 m lower than the equivalent in TA South. We observed a gradual northwards decrease of modern storm ridge elevation along the TA shoreline (Fig. 4D). This is attributed to the dominant sediment source, the Awatere River, being at the south end of the bay.

From ~400 m inland to the back of the coastal plain (to the edge of the colluvial fans at ~2000 m inland) the two profiles are dissimilar. On the inland coastal plain to the north of the river there are numerous swampy areas and several sand dunes (Fig. 1B). The beach ridges on the TA North profile are indistinct at >750 m inland and large steps of 1–2 m in the profile can be seen particularly around the road and sand dune (Fig. 4B). The TA South profile is preferred for geomorphic interpretation because it appears

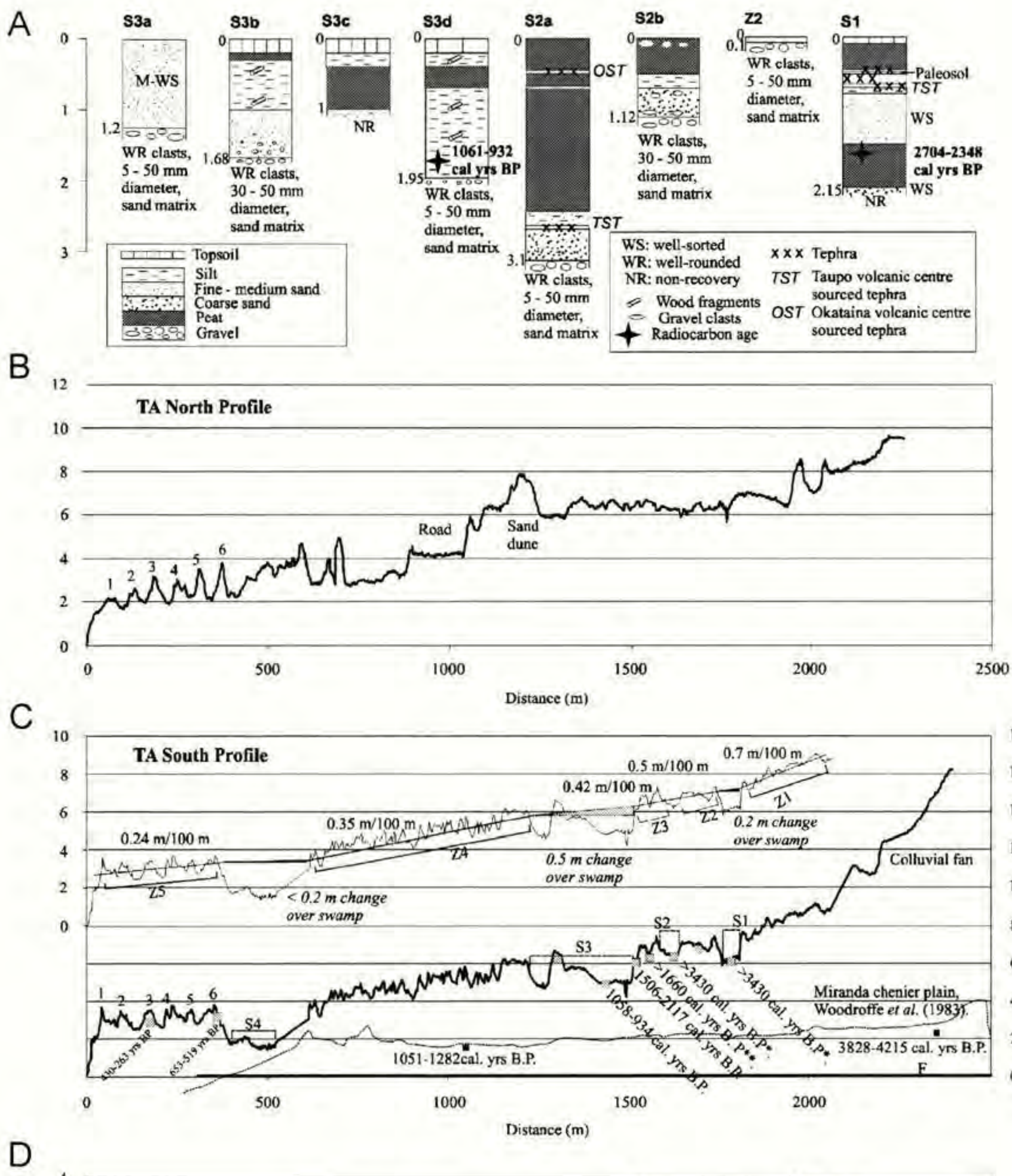

Fig. 4. Te Araroa Beach Ridges. (A) Auger stratigraphy (locations shown on Fig. 1B). (B) TA South elevation profile. Top profile shows the names of the beach ridge zones (Z1–Z5) and the gradient of each zone and the amount of elevation change across the swamps. The middle profile shows the names of each swamp zone (S1–S4), and radiocarbon ages from this study and Garrick (1979), Ota et al. (1992) and this study. (C) TA North elevation profile. (D) Profiles from the intertidal wave zone to the crest of the modern storm beach ridge at four locations along the Te Araroa beach (Profiles 1–4, south to north, respectively, see locations Fig. 1B). Main sediment source is to the south. *Waimihia tephra, 3375–3485 cal yr BP (Froggatt and Lowe, 1990). **Sea-rafted Taupo pumice identified by Ota et al., 1992, eruption age of 1720–1600 cal yr BP (Froggatt and Lowe, 1990).

to have fewer swamps, suggesting less possible fluvial modifications to the beach ridges, and it has no sand dunes (Fig. 4C).

The TA South profile shows beach ridges up to 2100 m inland with ridge definition deteriorating inland (Fig. 4C). Four swamps that can be seen on aerial photos can be distinguished on the elevation profiles (S1–4, Fig. 4C). We identify five zones of beach ridges (Z1–5, Fig. 4C), these are the same zones as Ota et al. (1992) identified except that we divide their Zone II into two separate zones (Z1 and Z2), we do not identify anything equivalent to the Ota et al. (1992) Zone I, which they only locate on the northern side of the river.

Lines projected through the midpoint of all the beach ridges of each zone of TA South show that the average beach ridge elevation increases landward. The gradients vary from 0.24/100 to 0.7/100 m (Fig. 4). Twenty-seven beach ridges have been identified on the TA South profile; the average elevation difference between the successive ridge crests is 0.17 m.

The beach ridges are composed of well-rounded greywacke gravel clasts that are generally 10–50 mm in diameter. On the southern coastal plain there is very little sand cover (auger Z2, ~1700 m inland has only 0.1 m of cover sand, Fig. 4A). The intervening swamps are infilled with silt and peat (S3b–d, S2a–b, and S1, Fig. 4A). Three silt samples were analysed for diatoms (Table 2). The silt from S2b contained abundant, freshwater diatoms indicative of a freshwater, ponded wetland. The other two samples, from S3b and S3d were barren of diatoms; these are interpreted as overbank silts.

Age control on the TA beach ridges comes from previously obtained radiocarbon ages and observations of tephra occurrences (Garrick, 1979; Ota et al., 1992), new radiocarbon ages presented here, and our tephra analyses. Two new radiocarbon samples were collected from the base of auger holes in swamps S1 and S3. Wood fragments within silt at the base of S3d yielded an age of 1058–934 cal yr BP. A wood sample collected by Ota et al. (1992) from the landward side of this swamp had a radiocarbon age of 1506–2117 cal yr BP. Our radiocarbon age from the base of S3 is consistent with the previously collected data and with the absence of tephra in the swamp, it dates the start of infilling of the swamp; therefore, dates the minimum age of the beach ridges immediately landward (in Zone 3). Ota et al. (1992) also observed sea-rafted

Table 2
Diatom results from Hicks Bay cores, HB1 and HB2

Location/core	Elevation (m AMSL)	Depth (m)	Processing method	Diatom observations	Paleoenvironmental interpratation
Hicks Bay					
Ota A	6.3		Smear	Rare brackish marine diatoms	Brackish-marine
Ota A	3.5		Smear	Barren	Possibly overbank silts, or diatoms not preserved
HB1	9.96		Smear	Barren	" "
HB1	9.36		Smear	Barren	" "
HB1	8.36		Full	Sparse well-preserved brackish marine diatoms	Brackish-marine
HB1	7.96		Full	" "	Brackish-marine
HB1	7.46		Full	" "	Brackish-marine
HB1	5.78		Full	" "	Brackish-marine
HB1	3.62		Full	" "	Brackish-marine
HB1	−0.16		Full	" "	Brackish-marine
HB1	−0.26		Full	" "	Brackish-marine
HB2	9.2		Smear	Barren	Possibly overbank silts, or diatoms not preserved
HB2	8.82		Smear	Barren	" "
HB2	8.11		Full	Sparse well-preserved brackish marine diatoms	Brackish-marine
HB2	6.02		Full	" "	Brackish-marine
HB2	5.66		Full	" "	Brackish-marine
HB2	4.84		Full	" "	Brackish-marine
HB2	3.76		Full	" "	Brackish-marine
A8		−4.5	Smear	Abundant well-preserved freshwater diatoms	Freshwater, not overbank silts
A8		−5.8	Smear	Moderate concentrations of well-preserved freshwater diatoms	Freshwater, not overbank silts
A10		−1.35	Smear	Fragments of fresh water diatoms	Probably overbank silts
Te Araroa plain					
S3b		0.98	Smear	Barren	Probably overbank silts
S3d		0.9	Smear	Barren	Probably overbank silts
S2b		0.67	Smear	Abundant freshwater diatoms	Wetland with some ponded open water.

Taupo pumice on beach ridges within Zone 3, implying the beach ridges were formed prior to 1720–1600 cal yr BP. (Froggatt and Lowe, 1990).

Peat from the base of S1 yielded a radiocarbon age of 2701–2351 cal yr BP. The tephra lying approximately 1 m above the radiocarbon sample has a Taupo volcanic centre glass geochemical signature (Supplementary Data B). This tephra was ~50 mm thick and composed of coarse lapilli. It is most likely to be the Waimihia tephra, 3375–3485 cal yr BP (Froggatt and Lowe, 1990), which is typically the only coarse-grained Taupo volcanic centre tephra found in the East Cape region. The alternative is the Taupo tephra (1720–1600 cal yr BP, Froggatt and Lowe, 1990) which has an age consistent with the radiocarbon date but it is usually absent or very fine grained in this region. We infer, based on the grain size characteristics, that the tephra in swamp S1 is the Waimihia. Either it has been redeposited or the radiocarbon age represents younger material (either younger tree roots growing down or contamination during sample collection).

Swamp S2 contains a tephra near the base at −2.6 m depth (auger S2a, Fig. 4A). This is a Taupo volcanic zone sourced tephra (Supplementary Data B) with a coarse lapilli texture, inferred to be the Waimihia tephra. This gives the beach ridges in Zone 2 a minimum age of 3375–3485 cal yr BP. A tephra at −0.5 m in Swamp S2, with an Okataina volcanic centre glass geochemistry, is unidentified. Two shells samples were collected by Garrick (1979) from the beach ridges within Zone 5, these yielded ages of 420–263 and 653–519 cal yr BP (Fig. 4C).

Overall the age control on the oldest beach ridges remains relatively poor, though the start of ridge accretion must be >3375–3485 cal yr BP (the age of the Waimihia tephra which was found in swamp S1). Using the Waimihia tephra as the minimum age of the beach ridges at the front edge of Zones 1 and 2, the maximum uplift rates can be calculated (Table 5). Uplift rates can also be calculated using the radiocarbon ages of Garrick (1979) and Ota et al. (1992) for Zones 3 and 5. We use the modern elevation of the crest of the beach ridge and subtract the elevation of the modern storm beach ridge (4 m) to get a total amount of uplift (Fig. 4D). The calculated uplift rates range between 0.5 and 2 mm yr^{-1} (Table 5).

5.3. HB palaeo-estuary

5.3.1. HB flats stratigraphy

Shells exposed along the banks of the Wharekahika River on the HB Flats attest to an early Holocene estuarine palaeoenvironment in this area (Location Ota A, Fig. 1C, Ota et al., 1992). This transgressive estuarine sequence was targeted for drilling and palaeoenvironmental analysis. For purposes of palaeo-SL studies an ideal place to drill is at the margins of the palaeo-estuary where many species of tidal-wetland microflora and -fauna have restricted salinity or inundation tolerances and are thus sensitive to changes in MSL (Hayward et al., 1999b, 2004b; Patterson et al., 2000). Stratigraphic sections of the HB Flats were studied to provide a guide on the extent of the palaeo-estuary deposits and eliminate areas with gravel layers that would inhibit drilling.

At most locations inland of the Ota A river outcrop, gravels were encountered in augered holes and by the penetrometer resistance probes (A1–10, Fig. 1C, Supplementary Data A). At least the upper 4 m of sedimentary infill everywhere on the HB Flats is a mixture of silt and gravel. Similarity between these silts and gravels and modern river sediments implies that they are fluvial deposits: probably overbank (silt) and flood (gravel) deposits. A diatom sample from silts in A10 contained fragments of freshwater diatoms. The fragmented nature of the specimens supports a depositional environment of overbank silts (Table 2).

Diatoms from A8 (Fig. 1C) at 5.8 m below the surface indicated the enclosing silts were deposited in freshwater (Table 2). This was a lower elevation than where estuarine sediments were found downstream at Ota A and A4. We inferred that the location of A8 is probably upstream of the head of the palaeo-estuary. Therefore, the distribution of gravels and freshwater sediments left only a small area suitable for drilling. HB1 was drilled on the riverbank next to Ota A, and HB2 is located ~100 m downstream. HB1 was drilled at an elevation of 11.76 m above MSL (AMSL) and reached a depth of 12 m. HB2 was drilled at an elevation of 11.81 m AMSL and penetrated to 10 m below the surface. All locations within the cores are henceforth referred to by their elevations in metres AMSL (m AMSL).

5.3.2. Cores HB1 and 2

The sedimentary record preserved in drill cores HB1 and 2 was subjected to a high-resolution palaeoenvironmental study utilising foraminifera, macrofauna, palynology, diatoms and stable isotopes. From the base of both cores (at −0.24 m AMSL in HB1 and 1.9 m AMSL in HB2) up to 3.3 and 4.1 m AMSL in HB1 and HB2, respectively, they are dominated by blue-grey silt with occasional *A. stutchburyi* shells and wood fragments. *A. stutchburyi* is a shallow-burrowing bivalve common, and frequently monospecific, at mid- to low-tide elevations in estuaries and sheltered sand flats (Morton and Miller, 1968; Marsden and Pilkington, 1995; Marsden, 2004; Beu, 2006).

At 3.3–4.7 m AMSL in HB1 and 4.1–4.7 m AMSL in HB2 there is a unit of medium-coarse grey sand bounded by sharp contacts (Fig. 5). This sandy unit contains wood fragments, coarse shell grit and large *A. stutchburyi* fragments. Above the sand unit up to 7.2 m AMSL (HB1) and 5.2 m AMSL (HB2) is blue-grey silt with occasional *A. stutchburyi* shells and wood fragments. From 7.2 m AMSL (HB1) and 5.2 m AMSL (HB2) up to 8.3 m AMSL both cores are composed of massive silt with occasional wood chips. At ~8.3 m in both cores there is a 0.2 m thick silty peat and this is overlain by a fine-grained 10 mm thick tephra. From the tephra up to ~11.6 m AMSL (0.5 m below the surface) there is massive orange-brown

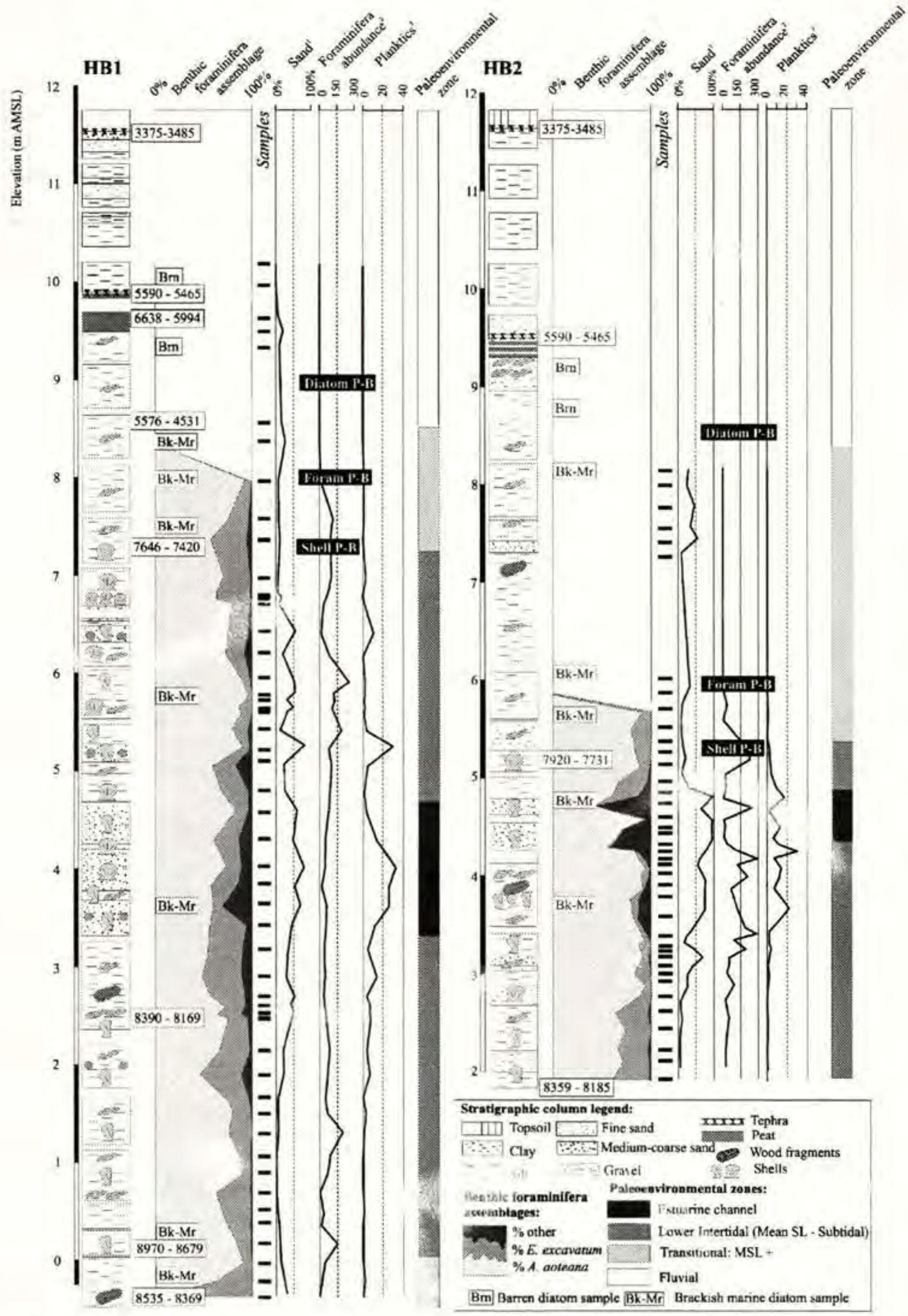

Fig. 5. Cores HB1 and HB2. Stratigraphy, radiocarbon ages, micropalaeontology and palaeoenvironmental zones. [1]sand = percentage of sediment samples greater than 63 microns, [2]foraminifera abundance = number of benthic foraminifera per gram of sediment, [3]planktics = number of planktics picked per sample.

silt. At ~11.6 m AMSL there is a 50 mm-thick coarse-grained orange tephra; this is immediately overlain by topsoil.

Fifty-one samples from HB1 were studied for foraminifera. The samples were selected between 10.54 and −0.38 m AMSL, with an average sampling density of 1 per 0.21 m in this interval. Seven samples from above 7.96 m AMSL were barren of foraminifera, as was one sample from below −0.22 m AMSL. Forty samples were selected from HB2 from between 8.12 and 1.94 m AMSL, a sampling density of one per 0.15 m. Eight samples from above 5.68 m AMSL were barren. In both cores there is a transition from samples containing forams (forams present) to samples barren of forams. We call this the foram present–barren (P–B) transition. Foraminifera census data is available at (GNS Online Data Repository).

All samples from HB1 and 2 containing foraminifera were dominated by *Ammonia parkinsonia f. aoteana* with secondary proportions of *Elphidium excavatum f. excavatum*, and minor amounts of "Other" benthic species (Fig. 5, GNS Data Repository). Common "Other" species included *Haynesina depressula*, *Elphidium charlottense*, *Notorotalia* species, and *Bulimina* species (GNS Data Repository). *A. aoteana* ranges from 46% to 95% of the assemblage in HB1 and 2 with an average of 72% in HB1 and 79% in HB2. *E. excavatum* has a range of 1–43% and averages 23% in HB1 and 13% in HB2. Others range from 1% to 57%, with an average of 5% in HB1 and 8% in HB2.

A. aoteana is a common species in "brackish to very slightly brackish environments". It is often a dominant species in the intertidal and subtidal zones of the seaward parts of estuaries and mid to inner areas of enclosed harbours (Hayward et al., 1999a). *E. excavatum* is restricted to brackish environments and it usually lives at intertidal depths in the inner-mid zones of estuaries and in enclosed tidal inlets (Hayward et al., 1999a). *H. depressula* is an intertidal, brackish-marine species and *E. charlottense* is a slightly more open-water species. *E. charlottense* occurs most commonly at intertidal–subtidal elevations on sheltered sandy beaches (Hayward et al., 1999a). All the samples analysed for foraminifera assemblages are likely to be from the lower intertidal zone of a sheltered, slightly brackish, estuary.

The change in foraminifera assemblage at the foram P–B transition is sudden, and there is no gradual decrease in foraminifera abundance approaching this transition (Fig. 5). This transition occurs at a higher elevation than the Shell P–B transition in both cores (0.75 m higher in HB1 and 0.5 m higher in HB2). There is no visual change in core sedimentology at the Shell or foram P–B transitions. We interpret these transitions to be a gradual environmental change to a less saline or higher elevation setting. It was around this transition that we concentrated sampling for pollen, diatoms, and stable isotopes.

Palynology samples were selected from the HB1 and 2 cores either side of the foraminifera P–B transition. A sample (HB1/9.86 m AMSL) was taken from a peat unit, and one sample (HB2/1.84 m AMSL) was taken from a unit with abundant *A. stutchburyi* fragments. All samples were dominated by *Cyathea* type pollen with minor amounts of *Podocarpus* type and *Dacrydium cupressinum* pollen (Table 1). These pollen types indicate the regional forest was a lowland podocarp forest; however, they yield no information about the environment in the immediate vicinity of the sample location. Pollen from plants such as rushes, sedges, saltwort and mangroves can be indicative of the local environment and have been used elsewhere as corroborative evidence of coastal waterbody and SL change (Shennan et al., 1994; Goff et al., 2000; Cochran et al., 2006). We conclude that palynology is not suitable for palaeoenvironmental interpretation of the HB cores, possibly because the core locations were too far from the estuary margins where saltmarsh plants were growing.

The highest diatom samples (HB1/9.96, 9.36 and HB2/9.2 and 8.82 m AMSL) are barren. A barren result from a smear slide means that the diatoms have a very low abundance or they are not present. All other samples from the HB cores below HB1/8.36 m AMSL and HB2/8.11 m AMSL contain sparse well-preserved brackish diatom assemblages. Abundances were not high enough to warrant full census counts. Above and below the foram P–B transition the diatom assemblages do not change significantly (Table 2). There are several reasons why this could be so: (1) the foraminifera may not be present in the shallow parts of the cores, above the P–B transition, because of dissolution or extremely low abundances, despite the palaeoenvironment remaining the same across the barren–intertidal transition as the diatoms indicate, or (2) there was a small change in salinity across the foram P–B transition that inhibited intertidal foraminifera survival but the environment remained suitable for diatoms.

SEM images of the foraminifera do not provide any strong evidence for poor preservation closer to the foram P–B transition thus suggesting chemical dissolution or mechanical breakage has not been responsible for this transition. This implies the foram P–B transition and the transition from intertidal-shells-present to barren-of-shells is probably a real palaeoenvironmental change.

The 31 samples selected for stable isotope study from HB1 span the peat layer (~9.76 m AMSL), the foram P–B transition at 7.96 m AMSL and the start of the *A. stutchburyi* shells at 7.26 m AMSL (Fig. 6). We selected these samples to test whether C and N isotopic values and ratios showed sensitivity to palaeoenvironmental change in the core and if a more detailed study could assist with detecting small palaeo-salinity changes. Most of the samples are dominated by silt, though there are some sand samples between 6.8 and 5.8 m AMSL. Variation in sand content does not appear to correlate with any significant isotopic excursion in the sandy regions.

Both carbon and nitrogen isotopic values show prominent excursions spanning the peat layer (~−2 m), $\delta^{13}C$ shows an isotopic decrease (Fig. 6A) and C/N increases during this interval (Fig. 6B). The $\delta^{13}C$ plot shows a slight trend toward more negative values below 7.8 m AMSL while the C/N ratio is highly variable below the peat layer but shows an overall increase beneath the foram P–B transition (Fig. 6).

$\delta^{13}C$ and the C/N ratio have previously been the most useful parameters for distinguishing organic matter provenance (Meyers, 1994; Thornton and McManus, 1994; Muller and Mathesius, 1999). Published observations of freshwater and marine $\delta^{13}C$ values vary slightly, but all agree that marine $\delta^{13}C$ values are higher than freshwater values (Fig. 6A) and higher C/N values are indicative of terrestrial organic matter (Fig. 6B). In both of the HB1 plots of $\delta^{13}C$ and C/N we see the values are not within the

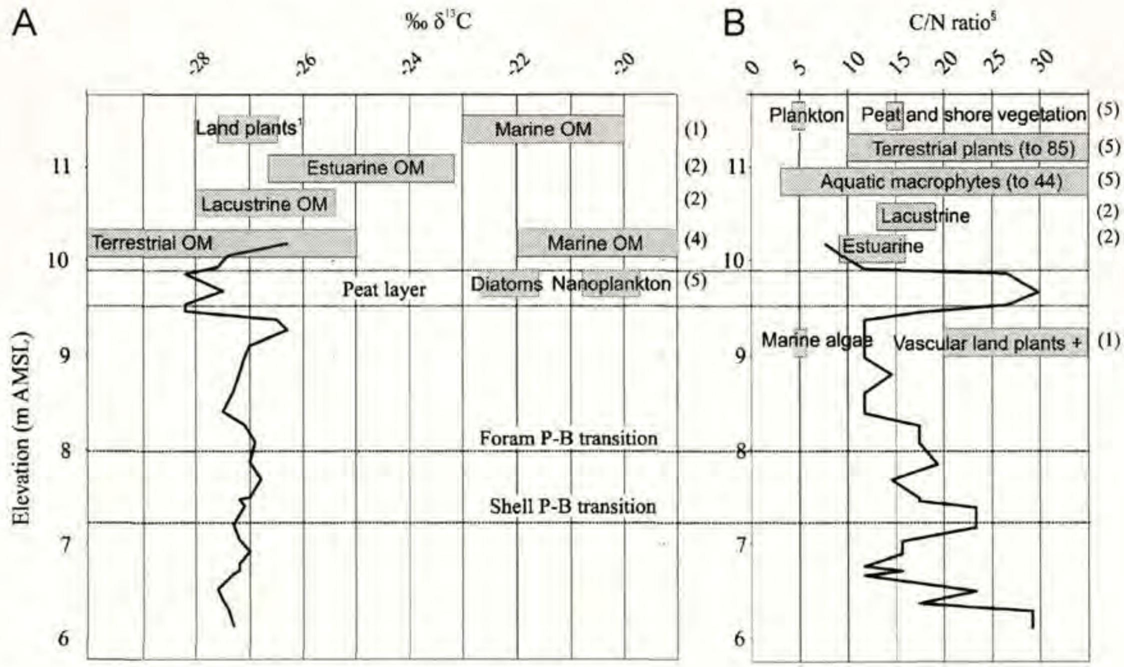

Fig. 6. Stable isotope measurements from the upper 6 m of HB1 with major stratigraphic boundaries marked. (A and B) ‰ $\delta^{13}C$ and C/N ratio of HB1 with superimposed value ranges for terrestrial, estuarine and marine organic matter from several publications. (1) Meyers (1994), (2) Thornton and McManus (1994), (3) Fontugne and Jouanneau (1987), (4) Gearing et al. (1984), (5) Muller and Voss (1999). [1]Land plants with a C4 pathway. [§]C:N ratio is calculated by an atomic ratio where $C{:}N = (\%C^{14})/(\%N^{12})$.

range of typical marine organic matter (Fig. 6A, B). We conclude that for the HB cores this technique is not a viable tool for distinguishing freshwater and marine palaeoenvironments. This is probably because the marine environment at HB was a sheltered intertidal inlet and received a high terrestrial sediment input. We emphasise that this was a test of the technique. Consequently, we have not considered the extent to which the C and N isotopes are affected by factors such as preservation of organic material, transportation, microbial activity, water depth and temperature, water currents, unusual weather events (drought, flood, wind, etc.). The sharp peaks in all isotopic values at the peat layer indicate that the stable isotopes do reflect significant increases in organic matter. However, this is clearly visible in the cores and in this study a quantification of the amount of C (total) is not especially helpful for environmental interpretation and the stable isotopes do not add any higher palaeoenvironmental resolution beyond that attained from the microfossils.

5.3.3. *Age control of Cores HB1 and 2*

Four new radiocarbon dates were collected from the cores, two each from HB1 and 2 (Table 3). One radiocarbon age was collected from an auger hole at Ota A, and three ages previously collected by Ota et al. (1992) at Ota A have been recalibrated. These four ages from Ota A are directly correlated to their equivalent elevations in HB1 as this core was collected <5 m away from the riverbank exposure. The Waimihia tephra (3485–3375 cal yr BP) is at 11.6 m AMSL in both cores and Whakatane tephra (5590–5465 cal yr BP) is at 9.8 m AMSL in HB1 and 9.5 m AMSL in HB2, thus providing additional age control (Fig. 5).

The radiocarbon dates occur in chronological order, younging upwards with increasing elevation, except in two cases (Fig. 5, Table 3). A wood age (5576–4531 cal yr BP) collected by Ota et al. (1992) at Ota A/8.6 m is younger than the radiocarbon age from the peat 1.2 m above (6638–5994 cal yr BP) The wood age partly overlaps with and is younger than the Whakatane tephra whereas the peat age is older than the tephra. Due to the overlap with the higher Whakatane tephra, we suggest that the wood age (Ota A/8.6 m) is unreliable and could be a tree root younger than its surrounding sediment. The wood age at HB1/−0.26 m (8535–8369 cal yr BP) is younger than the shell age at 0.42 m above (HB1/0.16 m: 8970–8679 cal yr BP), and it overlaps by 21 years with the $2-\sigma$ age of the shell 2.76 m higher at HB1/2.5 m: 8390–8169 cal yr BP). Both shell samples are likely to have been in life position but it is possible that the wood fragment was from a tree root.

The *A. stutchburyi* shell ages are used to date the timing of sediment deposition and for tectonic uplift rate calculations because they are *in situ* fossils and can be directly related to the palaeo-MSL. Observations of the riverbank section adjacent to the HB1 and 2 core sites (Ota A) from 6.8 to 7.5 m AMSL are that all the *A. stutchburyi* shells exposed within this section are articulated whole bivalves preserved in growth position. The excellent preservation of the shells in the riverbank, only ~5 m from

Table 3
Radiocarbon ages HB and TA

Sample name[a]	Sample material	Lab number[b]	Dating Technique	^{13}C (‰)	Radiocarbon Age[c] (radiocarbon years BP)	2-sigma calibrated age[d] (cal. years BP)
S3d/1.6–1.8 m depth	Detrital organic matter within silt	NZA 22393	AMS	−26.85	1142±30	1058–934
S1/1.59 m depth	Peat	NZA 22394	AMS	−27.49	2485±30	2701–2351
HB1/0.16 m AMSL	*A. stutchburyi*	NZA 21087	AMS	−1.04	8276±35	8970–8679
HB1/−0.26 m AMSL	Wood	NZA 20754	AMS	−28.66	7678±30	8535–8369
HB2/1.9 m AMSL	*A. stutchburyi*	NZA 22544	AMS	1.26	7812±35	8359–8185
HB2/5.2 m AMSL	*A. stutchburyi*	NZA 20910	AMS	−0.48	7360±35	7920–7731
Ota A 2.5 m AMSL[e]	*A. stutchburyi*	NZA 17348	AMS	−0.06	7824±55	8390–8169
Ota A 7.2 m AMSL[e]	*A. stutchburyi*	NZA 5461	Standard		7046±66	7646–7420
Ota A 8.6 m AMSL[e]	Wood	GaK 10474	Standard		4470±180	5576–4531
Ota A 9.8 m AMSL[e]	Peat	GaK 10473	Standard		5590±140	6638–5994

[a]Elevations within HB1 and HB2 have an uncertainty of ±0.3 m.
[b]NZA: Rafter Radiocarbon Laboratory, GaK: Gakushuin University.
[c]Conventional radiocarbon age before present (1950 AD) after Stuiver and Polach (1977).
[d]Marine dates calibrated using Hughen et al., 2004; terrestrial dates calibrated using McCormac et al. (2004).
[e]Previously published in Ota et al. (1992).

the drill sites allows us to be quite certain that the *A. stutchburyi* fragments retrieved in the cores were formerly whole *in situ* shells but were broken during drilling or core extrusion, the ability to reconstruct whole shells from the fragments in the further cores supports this. Whilst there have been reported occurrences of transported *A. stutchburyi* found at distances >20 km from estuaries (Hayward and Stilwell, 1995) these reported shells occurred in association with open beach shell assemblages and only consisted of disarticulated shells. The coupled occurrence of the articulated *A. stutchburyi* fragments with intertidal foraminifera assemblages also suggests the *A. stutchburyi* are *in situ*. This is further supported by their monospecific occurrence in the cores because *A. stutchburyi* are typically the only species found at intertidal elevations in New Zealand estuaries (Healy, 1980; Beu, 2006). If the *A. stutchburyi* have been reworked then their ages at least represent the maximum age of the enclosing sediment, however for reasons discussed above, we are confident the *A. stutchburyi* are *in situ* and as such do represent the time of sediment deposition.

5.3.4. HB palaeoenvironmental evolution

The sedimentology, foraminifera, macrofauna, and diatom data of the cores is combined to define four palaeoenvironmental zones: (1) Estuarine Channel (or Tsunami), (2) Lower Intertidal Estuarine, (3) Fluvial, and (4) Transitional (Fig. 5). The distribution, characteristics and justification for each zone is discussed below.

Estuarine Channel (or Tsunami). This zone occurs in HB1 at 3.3–4.7 m AMSL and at 4.1–4.7 m AMSL in HB2 (Fig. 5). The characteristics of this unit are medium-coarse sand, fragmented shells, shell grit, and relatively high proportions of "Other" foraminifera and planktic species. The coarser sand and mechanical breakage of the shells indicates a higher-energy depositional environment than the surrounding silts. The high proportion of "Other" foraminifera, such as the open coast species of *Zealfloris parri* and *Trifarina angulosa* and the high proportion of planktic species, indicates increased hydraulic exchange with the open ocean. We interpret this unit as an estuarine channel because of the evidence of higher energy (tidal currents) and increased open coast hydraulic exchange. This layer also displays several characteristics of a tsunami deposit. For example: it is a distinct sedimentary unit of anomalously coarse sand within silt, the lower contact is sharp and possibly erosional, and it contains deeper water marine foraminifera and is relatively shell-rich (Nelson et al., 1996; Shennan et al., 1996; Goff et al., 2001, 2004). However, we have no data on the spatial extent of the sand layer to test the tsunami theory, e.g., tsunami deposits typically fine landward (Goff et al., 2001), and the narrow marine inlet of the HB gorge (Fig. 1C) may restrict the entry of a tsunami into the HB Flats, particularly given eustatic SL was lower than present and the coastline further offshore than present. Future work could focus upon tracing the extent of the sand layer on the HB Flats and correlating the deposit to other coastal locations to resolve this issue. To date no tsunami deposits of ~8 ka age have been detected in the region although few studies have been undertaken.

Lower intertidal. This zone occurs in HB1 at 0–3.3 and 4.7–[illegible] and in HB2 [illegible] and 4.7–5.2 m AMSL (Fig. 5). Sediments of this zone are homogenous blue-grey silts, with scattered *A. stutchburyi* shells (that were probably *in situ* prior to drilling disturbance), and occasional small wood fragments. Foraminifera assemblages are dominated by *A. aoteana* and *E. excavatum* and diatom samples are characteristic of brackish marine environments. Our interpretation is of a lower intertidal estuarine palaeoenvironment because this is the preferred living environment of the foraminifera and shells. The fine sediment is consistent with deposition in the central part of an estuary where currents generated by both tidal and fluvial energy are at a minimum (Dalrymple et al., 1992).

Fluvial. The fluvial zone occurs in both cores above 8.5 m AMSL (HB1) and 8.3 m AMSL (HB2) (Fig. 5). Dominated by orange-brown silt, this zone has scattered wood fragments, and both cores contain a 0.1–0.3 m thick peat, and two tephra layers. This palaeoenvironmental zone is distinguished by a lack of marine indicators: no shells, foraminifera or marine diatoms. The peat layer indicates a fresh water environment existed at least some of the time. The absence of chemical corrosion signals in the foraminifera indicates that groundwater dissolution was not responsible for the absence or calcareous test higher in the cores thus decreased salinity is the most likely reason for their absence. In the cores the silts do not contain any sedimentary structures; however, in the adjacent riverbank outcrop some decimetre-thick horizontal layers with gradational contacts can be seen. This is compatible with an overbank fluvial silt depositional environment.

Transitional. The transitional zone occurs in HB1 between −0.5 to 0 and 7.2–8.5 m AMSL, it is thicker in HB2 where it occurs between 5.2 and 8.3 m AMSL (Fig. 5). Grey-brown silt dominates this zone; there are no shells or foraminifera. However, the diatoms indicate a brackish marine environment. We interpret this as a transitional environment between the intertidal and fluvial environments. Salinity levels probably decreased below the threshold for the foraminifera and shells, but allowed diatoms to persist. Alternatively, the diatoms, which are more readily transported, could have been redeposited in this environment.

The early Holocene palaeogeography and associated sedimentary infilling of the HB Flats can be inferred from the sequence of palaeoenvironmental zones and radiocarbon ages in cores HB1 and HB2 and supplemented by outcrop and auger hole data (Fig. 5, Supplementary Data A). We divide the valley evolution into 8 stages (Fig. 7, 1–8), and this follows a typical incised valley infill sequence of fluvial to estuarine and a return to fluvial conditions following eustatic SL stabilisation (cf. Roy, 1984; Dalrymple et al., 1992; Allen and Posamentier, 1993).

Uplift rates, from five shell samples in HB1, 2 and the riverbank exposure next to HB1, range from 0.9 to 2.2 mm yr^{-1}, with an average of 1.7 mm yr^{-1} (Table 4). We use only the radiocarbon ages from *A. stutchburyi* shells because we are confident these are *in situ* (compared to the wood samples), and for the purposes of calculating accommodation space deficits the *A. stutchburyi* are most likely to have been living at equivalent elevations. *A. stutchburyi* have a living depth range of mid- to low-tide elevations (Healy, 1980; Beu, 2006). In calculating uplift rates we use a living depth of -0.42 ± 0.42 m for the *A. stutchburyi*, which accounts for the shells living at an

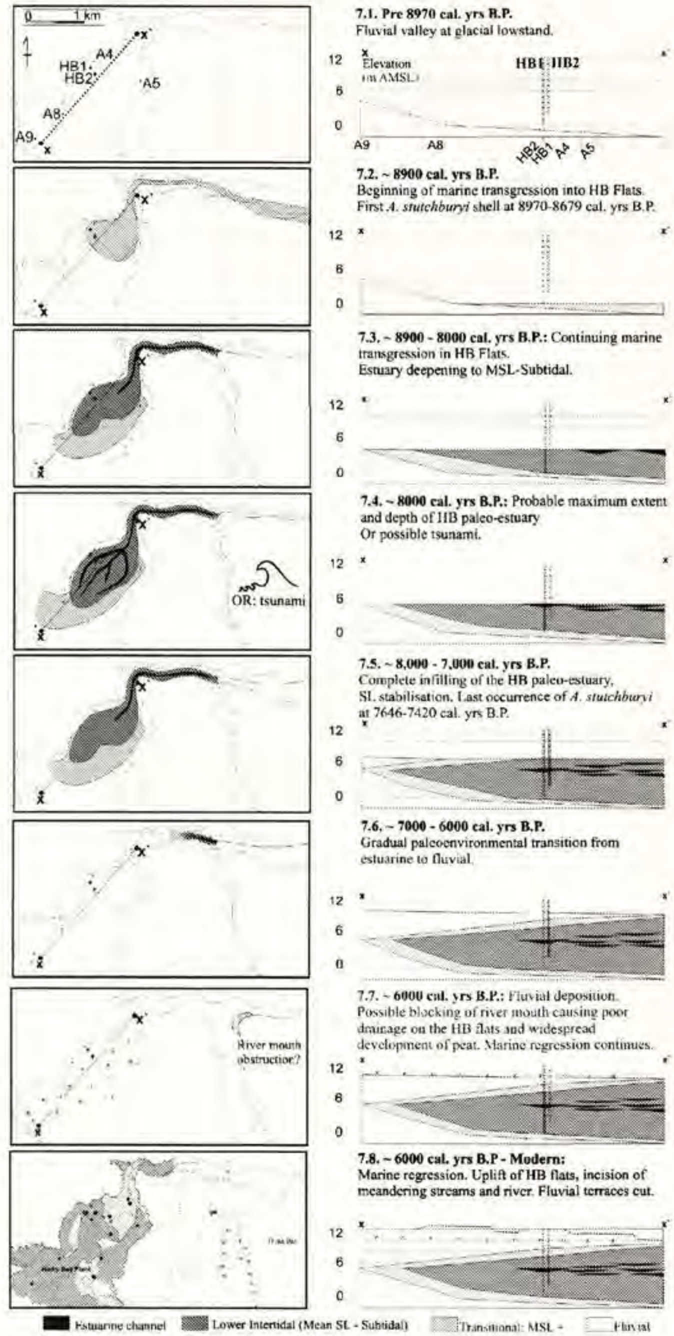

Fig. 7. Palaeogeographic evolution of the Hicks Bay Flats in plan and stratigraphic profile view.

elevation midway between mid and low tide with a 95% uncertainty spanning the mid–low tide range of 0.85 m (the spring tidal range at HB is 1.7 m, therefore mid–low tide elevations are 0 to −0.85 m AMSL). We suggest that the *A. stutchburyi* are *in situ*, however, if they have been transported they are most likely to have been moved to deeper marine environments; therefore, the uplift rates presented here would be minimum rates. The Gibb (1986) eustatic SL curve is used to estimate the position of eustatic SL at the time that the *A. stutchburyi* were living. Whilst subject to relatively large uncertainties, the Gibb (1986)

Table 4
Tectonic uplift rate calculations from HB

Radiocarbon sample	Present elevation (m AMSL)	Living depth (m)	Age (ka)[a]	Eustatic SL change since deposition (m)[b]	Total uplift since deposition (m)[c]	Uplift rate ($mm\,yr^{-1}$)[d]	Uplift rate range[e]
Ota A/7.2 m	7.2 ± 0.3	-0.42 ± 0.42	7646–7420	2.1 ± 2	8.88 ± 2.07	1.18	0.89–1.48
Ota A/2.5 m	2.5 ± 0.3	-0.42 ± 0.42	8390–8169	14.1 ± 2	16.18 ± 2.07	1.95	1.68–2.23
HB1/0.16 m AMSL	0.16 ± 0.3	-0.42 ± 0.42	8970–8679	17.5 ± 2	17.24 ± 2.07	1.95	1.69–[illegible]
HB2/5.2 m AMSL	5.2 ± 0.3	-0.42 ± 0.42	7920–7731	6 ± 2	10.78 ± 2.07	1.38	1.1–1.66
HB2/1.9 m AMSL	1.9 ± 0.3	-0.42 ± 0.42	8359–8185	14.1 ± 2	15.58 ± 2.07	1.88	1.62–2.16

To calculate these uplift rates we estimate the amount of vertical motion, relative to MSL, that each radiocarbon dated sample has been through since its deposition.
We use a living depth of -0.42 ± 0.42 m AMSL for the living depth of the *A. stutchburyi* (this assumes the shells are in-situ which we judge to be true). The Gibb (1986) New Zealand eustatic SL curve is used estimate the position of eustatic SL at the time of sample deposition with an estimated uncertainty of ± 2 m.

[a]2-sigma calibrated radiocarbon age (see Table 3).

[b]Estimated from the Gibb (1986), eustatic SL curve using the midpoint of the 2-sigma calibrated age and projecting this to the middle of the eustatic SL points (see Fig. 9). We estimate an uncertainty of ± 2 m for estimates of the past eustatic SL using this Holocene SL curve.

[c]Total uplift = (present elevation + eustatic SL change) − living depth. Uncertainty = sum of the squares of the errors of sample elevation, living depth and eustatic SL change estimate.

[d]Uplift rate = total uplift/mid-point of the 2-sigma calibrated radiocarbon age.

[e]Uplift rate range = [(total uplift + 2 m)/youngest radiocarbon age] − [(total uplift − 2 m)/oldest radiocarbon age)].

curve is based upon data collected from tectonically stable regions of New Zealand and is preferable for use in this study in contrast to using a global eustatic SL curve.

6. Discussion: uplift mechanisms of the NE Raukumara Peninsula

6.1. *Evidence of coseismic uplift*

Several lines of evidence have been presented to show the NE Raukumara Peninsula has undergone tectonic uplift throughout the Holocene. The critical question we seek to address is how this uplift is achieved? Namely, by sudden, coseismic events, the commonly accepted uplift mechanism for the rest of the Hikurangi margin, or by gradual, aseismic mechanisms?

The most familiar evidence for coseismic coastal uplift along the Hikurangi margin, and globally, are marine terraces whereby the terrace strath is an abandoned surface and the riser approximates the single-event uplift. The terraces at Waipapa and Horoera display a stepped morphology similar to coseismic marine terraces southward along the margin such as at the Pakarae River mouth and Mahia Peninsula (Ota et al., 1991, Berryman, 1993, Wilson et al., 2006); therefore, the same uplift mechanism was assumed by Ota et al. (1992). However, the detailed coverbed sedimentology and topographic data we collected is not compatible with the Waipapa and Horoera terraces having a marine origin.

Marine terraces are typically covered in marine deposits such as well-sorted sands, gravels, shells and/or shell hash, comparable to sediments of the modern beach adjacent to the terraces (e.g., Hull, 1987; Ota et al., 1991; Berryman, 1993; Wilson et al., 2006). In contrast, no marine deposits were found on any of the Horoera terraces except at the base of terrace 1. Terraces 2–5 have coverbeds exclusively of silt. The modern beach at Horoera displays a mixture of exposed mudstone platform with abundant rock-boring shells, and coarse shelly sands. We infer that the silt cover on the Horoera terraces is not of marine origin because: (a) it has no modern analogue on the Horoera coastline; (b) it is poorly sorted and fine grained, not characteristic of wave-deposited sediments; and (c) there are no shells within the silt. In contrast the Waipapa terraces are mantled by thick deposits of homogenous medium fine-grained well-sorted sand, these are most likely to be dune sands as the modern beach consists of medium-coarse sand with scattered shells. Auger W4a was the only one to reach the bedrock platform at Waipapa and no coarse sands or shells were encountered on the strath.

The detailed topography of the Waipapa and Horoera terraces also suggests they are not of marine origin. At Horoera the terrace risers appear to be superficial features that do not involve bedrock incision; across the most distinctive terrace riser (that between terraces 3–2) there is no accompanying step in the bedrock below it (Fig. 2). The silt coverbeds and observation that the terraces increase in elevation eastward toward the current position of the Mangakino Stream suggests an alluvial fan origin, rather than marine. The stepped surface morphology may have been created by intermittent stream flooding rather than coseismic uplift. Augers H1 and H2, and exposures along the beach at Horoera and in the Mangakino Stream show that terrace 1 has ~0.5 m of mudstone gravel with rare whole shells on the bedrock strath. It is from this terrace that a shell radiocarbon age of <250 yr BP was obtained by Ota et al. (1992). A marine environment may have covered the bedrock there at some stage, though the bedrock strath was not necessarily wave cut. Moreover, the shells there could be anthropogenic deposits. The Raukumara Peninsula region was settled by Maori 800–500 yr BP (McGlone et al., 1994). Numerous pas (fortified places) along the coastline attest to Maori occupation of the Horoera area, thus the shells on terrace 1 could be part of midden deposits.

At Waipapa each terrace has a differing coast-parallel slope inconsistent with wave-cut platform creation (Fig. 3). A degree of along-strike tilt on terraces could be anticipated if uplift of the terraces was controlled by a nearby fault causing differential uplift, or if there was preferential deposition of sediment at one end of a terrace due to alongshore drift or prevailing winds. However, opposing directions of tilt on different terraces is difficult to account for. We suggest the Waipapa terraces are probably depositional landforms created by sand dunes that have been shaped into a terrace-like form by either anthropogenic alterations (the site is close to a Maori pa, these are commonly terraced as part of the fortifications or for cultivation) or fluvial processes.

This re-assessment of the Horoera and Waipapa terraces as non-marine means that they do not provide any evidence of coseismic uplift in this part of the Raukumara Peninsula, as was inferred by Ota et al. (1992). Nonetheless, a wood radiocarbon sample, collected by Yoshikawa et al. (1980) from an riverbank exposure along the Waipapa Stream (labelled "Yoshikawa outcrop", Fig. 1A), indicates this area still has a high coastal uplift rate. The sample had an age of 9900–9400 cal yr BP and was collected from silt containing marine and estuarine diatoms at 7 m AMSL. This equates with an uplift rate of 2.7–3.3 mm yr^{-1} (using 22 ± 2 m of eustatic SL rise, Gibb, 1986). The lack of marine terraces indicates that this rapid coastal uplift is either not being accommodated by coseismic movements, or slope and fluvial processes have removed the marine terraces. To further investigate uplift mechanisms of this region this we examine the beach ridge sequence at TA where the wide (>2 km) coastal plain suggests there has been no coastal erosion.

It is most likely that the TA beach ridges have accreted since SL stabilisation at ~7 ka; therefore, the present elevation of the relict beach ridges is the product of tectonic uplift. The decrease in ridge elevation seaward dictates that uplift occurred during accretion of the coastal plain. If the beach ridge sequence was uplifted by discrete coseismic events then, like marine terraces, a step should be present in the sequence. Ota et al. (1992) observed two 2 m scarps at the seaward edge of beach ridge Zones 3 and 4. Their profile was in the same location as our TA South profile. While the equivalent scarps can be seen in the TA South profile, it is important to note that they do not actually equate with a 2 m step in the overall elevation of the beach ridges. Across the width of the swamps adjacent to these scarps (S3 and S4) there is only a slight change in beach ridge elevation (0.5 m across S3 and <0.2 m across S4, Fig. 4C). Three marine terraces on the HB coastal plain were mapped by Ota et al. (1992) based on steps identified in aerial photographs. By comparisons to TA we infer the steps recognised by Ota et al. (1992) are those at the landward edge of swamps and like at TA, there is probably no significant net elevation change across the swamps.

With no evidence of coseismic steps in the terrace and beach ridge sequences of the NE Raukumara Peninsula we finally question whether the palaeo-estuary infill sequence of the HB Flats can be used to elucidate tectonic uplift

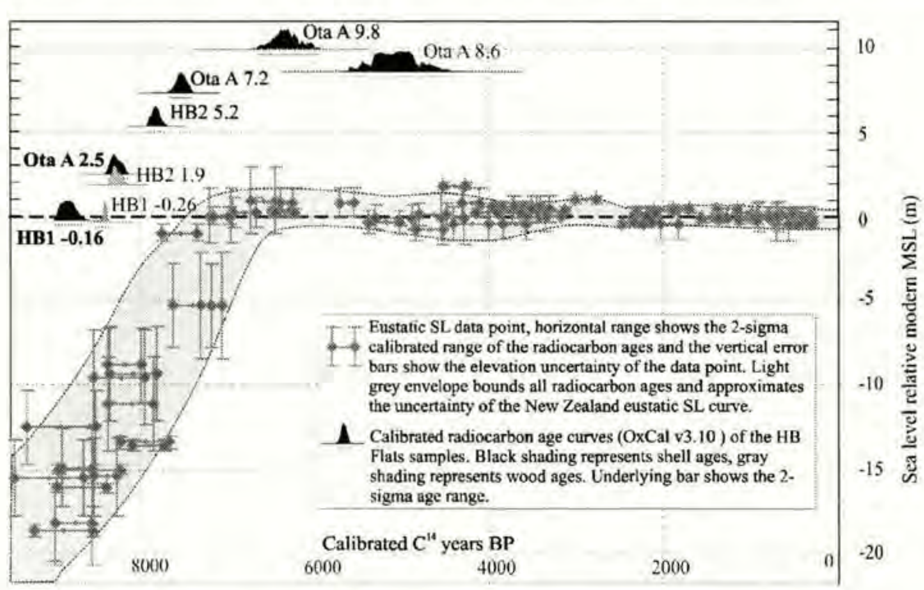

Fig. 8. New Zealand Holocene sea level curve (grey cross-hair data points, after Gibb, 1986) with radiocarbon ages from the HB Flats plotted at their present elevation relative to modern MSL (with an uncertainty of ±0.3 m). The elevation of the HB Flats radiocarbon ages above the eustatic SL curve represents the total amt of tectonic uplift since sample deposition. Radiocarbon ages plotted using OxCal v3.10 Bronk Ramsey (2005), wood samples calibrated using Southern Hemisphere Atmospheric data from McCormac et al. (2004) and shell samples calibrated using Marine data from Hughen et al. (2004).

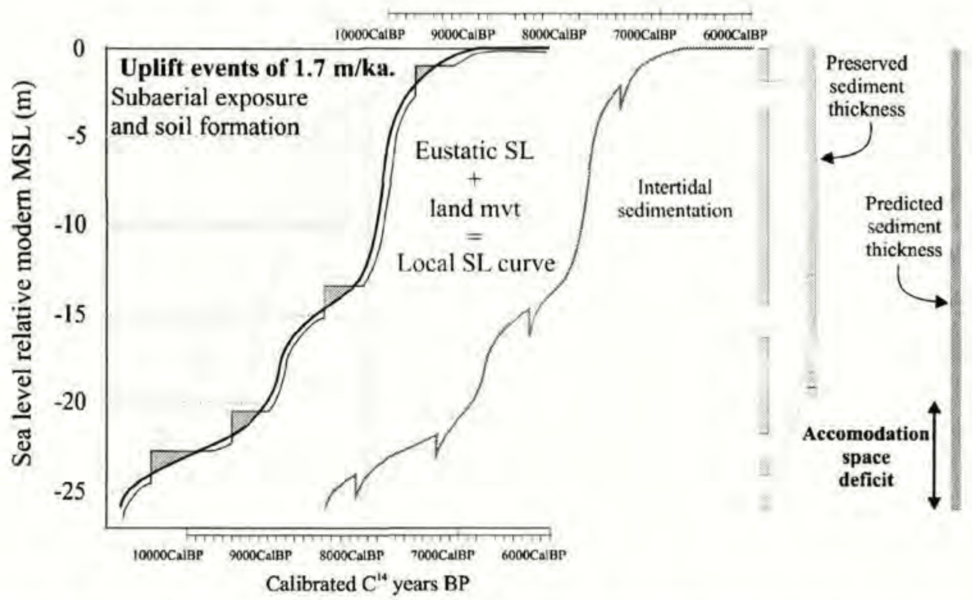

Fig. 9. Cartoon depicting the hypothetical development of a relative SL curve for a site undergoing coseismic uplift during eustatic SL rise. This is based on an uplift rate of $1.7\,\mathrm{mm\,yr^{-1}}$, equating with one uplift event of $1.7\,\mathrm{m\,ka^{-1}}$, it assumes all uplift is accommodated by coseismic movement with no interseismic vertical movement, and that there is no post-uplift erosion of the sequence. This shows how the relative SL curve would have a dominantly positive SL tendency, punctuated by sudden, and short-lived SL falls. If sedimentation kept pace with SL rise then this would result in a lesser thickness of sediment deposited relative to the amount of space created by eustatic SL rise—termed the "accommodation space deficit".

mechanisms. Estuarine, salt marsh and tidal inlet sediments have been used at subduction zone margins globally to document land elevation changes associated with earthquakes (e.g., Atwater, 1987; Darienzo et al., 1994; Nelson et al., 1996; Shennan et al., 1996; Clague, 1997; Sherrod et al., 2000; Hayward et al., 2004a) and on passive coasts to document eustatic SL changes and glacio-isostatic vertical land movements (e.g., Shennan et al., 1994; Shennan et al., 1995; Dawson and Smith, 1997; Dawson et al., 1998; Bratton et al., 2003) (Fig. 8).

The HB palaeo-estuary infill sequence has been uplifted either during or since deposition at rates of $0.9–2.2\,\mathrm{mm\,yr^{-1}}$ (Table 4). If this uplift was caused by coseismic mechanisms, we predict the events would be recorded by (1) a sudden palaeoenvironmental change reflecting an increase in land elevation. For example, a change from subtidal to MSL elevation or higher, and a freshening of the aquatic environment would be expected. Or (2) an unconformity should occur if the uplifted sediments were exposed subaerially and eroded. During deposition of the early Holocene HB Flats sequence eustatic SL was rising. An uplift event would, therefore, be recorded as a negative SL tendency (a marine regression) within a sequence predominantly displaying a positive SL tendency (a marine transgressive sequence; Fig. 9).

Referring back to the record of palaeoenvironmental change from the HB cores and examining the sequence in terms of possible uplift events there is only one significant sharp contact: that between lower intertidal sediments and the subtidal estuarine channel (the coarse sand layer at ~4 m AMSL in HB1 and HB2, Fig. 5). This sharp sedimentary contact is discounted as being an uplift event because (a) the inferred palaeoenvironment goes from lower intertidal to possibly subtidal—a positive SL tendency consistent with rising eustatic SL, and (b) the sharp contact may represent with scouring at the base of a tidal channel, or tsunami deposition. All other palaeoenvironmental zone contacts are gradational.

In the absence of sharp contacts and unconformities in the HB1 and 2 cores we assess whether there are any marine regressions that may indicate an uplift event. There is only one gradational contact during the time period of rising SL where a negative SL tendency is inferred from the palaeoenvironmental data: at ~8–7 ka where the environment changes from possibly subtidal to lower intertidal (Stage 5, Fig. 7). This transition is sustained; therefore, it was unlikely to have been an uplift event (which would cause a relatively short-lived SL regression). The sustained and gradual nature of the palaeoenvironmental transition is more likely to be normal infilling of the estuary. That the subtidal–intertidal transition is followed by a gradual change to a fluvial environment coincident with the stabilisation of SL supports an estuary infilling cause for the marine regression.

6.2. Alternative uplift mechanisms

The Holocene geomorphic and sedimentary data of the NE Raukumara Peninsula coastal region has not yielded evidence of coseismic uplift events; therefore, alternative mechanisms of uplift are now considered. Two alternative scenarios are (1) continuous and gradual aseismic uplift and (2) frequent events causing small amounts of uplift that cannot be individually detected by our study methodology.

The TA beach ridge morphology is consistent with a gradual uplift mechanism. The beach ridge sequence displays a seaward slope, implying uplift during beach ridge accretion and progradation. Under a constant uplift process the each new ridge probably forms when the previous ridge reaches a threshold height above MSL. Frequent, small magnitude uplift events as a cause of beach ridge uplift cannot be discounted, but the large number of ridges implies a frequency of events not supported by the historical seismicity catalogue. For example, in zone Z5 and Z4 of the TA South Profile there are 16 beach ridges, a radiocarbon age from the S3 swamp implies all these ridge are less than 1058–934 cal yr BP This implies a frequency of coastal-uplift causing events of 58–66 years yet the historical record, extending back 150 years records only a maximum earthquake size of M_S 6.7 (East Cape, 1914, Dowrick and Smith, 1990) and there is no record of this event causing coastal uplift.

There are several changes in the mean slope of the beach ridge zones; the gradients vary between 0.24 and 0.7 m per 100 m (Fig. 4C). Such changes in slope could be due to (1) uplift rates varying through time, or (2) sediment supply varying through time. Zone 5 has the lowest gradient of 0.24/100 m and radiocarbon ages suggest this zone is <650 cal yr BP This age is approximately coincident or slightly post-dates the arrival of Maori in the region (McGlone et al., 1994; Wilmshurst, 1997). Sedimentation pulses have been recorded in several lake cores from the eastern North Island associated with the arrival of Maori and land clearance by fires (Wilmshurst, 1997; Eden and Page, 1998). The rapid development of beach ridge Zone 5 at TA could be in response to enhanced sediment supply due to land burning and clearance by the Maori settlers. This correlation between probable increased sediment supply and lower gradient beach ridge zone suggests that sediment supply is the dominant control on the slope of the beach ridge zones, rather than varying uplift rates.

The estuarine sequence underlying the HB Flats contains no distinct stratigraphic changes that one might attribute to a sudden uplift event. However, we need to consider what the minimum amount of uplift is that would be resolvable with the available data in order to distinguish between continuous and punctuated uplift mechanisms. Most of the sediment in the HB1 and 2 cores is from a lower intertidal environment. The spring tidal range of HB is 1.7 m and therefore, most of the sediment was deposited between 0 and −0.85 m relative to MSL. Assuming no post-uplift erosion, >0.85 m of uplift would be needed to completely convert this palaeoenvironmental zone to an elevation greater than MSL. However, our palaeoecological proxies do not resolve a MSL—high-tide foraminiferal assemblage. If an uplift event did change the palaeoenvironment to above MSL then it would probably be recognisable as a section barren of foraminifera within the lower intertidal sequence. Our sampling resolution of 1 sample per 0.21 m (HB1) or 0.15 m (HB2) is sufficiently dense that we do not think we would have missed such an event. An uplift event of >1.7 m would have elevated the sequence above the high spring tide level. An unconformity, a palaeosol or a foraminifera-barren section would probably record subaerial exposure.

This means that uplift of the HB Flats has been accommodated either by constant, gradual uplift, or in intermittent uplift events of <1.7 m, and probably <0.85 m presuming we could recognise a palaeoenvironmental change from lower intertidal to MSL-high tide. We can detect if, and approximately how much, uplift occurred during deposition of the sequence by comparing the thickness of sediment preserved with the amount of accommodation space created by eustatic SL rise during the equivalent time period (the accommodation space concept is illustrated in Fig. 9). If no uplift occurred during deposition of the sequence then the thickness of intertidal sediment should approximately equal the amount of space created in the estuary by eustatic SL rise. This assumes that sedimentation within the palaeo-estuary approximately kept pace with the rising eustatic SL. Our palaeoenvironmental data shows that within the marine-influenced portion of the cores this is a valid assumption because the foraminifera assemblages consistently represent a lower intertidal environment (with the exception of the thin sedimentary unit representing a tidal channel or tsunami, both of which are still consistent with a lower intertidal elevation).

The large uncertainties associated with the eustatic SL curve, and to a lesser degree, with the radiocarbon ages, mean that calculating the exact amount of sediment "missing" within each core is subject to large uncertainties. Post-depositional sediment compaction is not accounted for in the calculations of accommodation space deficits as we consider this to be minor compared with the magnitude of the deficits in question. A study by Paul and Barras (1998) of a sequence of Holocene silty clays with shelly lenses, similar to the HB core sediments, found that over a 20 m thickness of sediment a maximum of 2.5 m of correction was required to approximately recalibrate the sediment depths for the affects of compaction. This equates with a mid-section correction of ~10% of the bed thickness (Paul and Barras, 1998).

The available data suggests a consistent accommodation space deficit of ~30–60%, over five varying time periods (Fig. 10). The most plausible explanation for this is gradual uplift synchronous with sediment deposition. If uplift had occurred intermittently then periods of time where no uplift occurred would be expected. Future work using drill cores at more marginal locations on the HB Flats may capture tidal-wetland microfaunal assemblages more sensitive to the rates of SL changes and provide better resolution to quantify coseismic uplifts less than 0.85 m if they did occur. However, the absence of chaotic or disturbed sedimentary layers within the palaeo-estuary sequence suggests there were no environmental

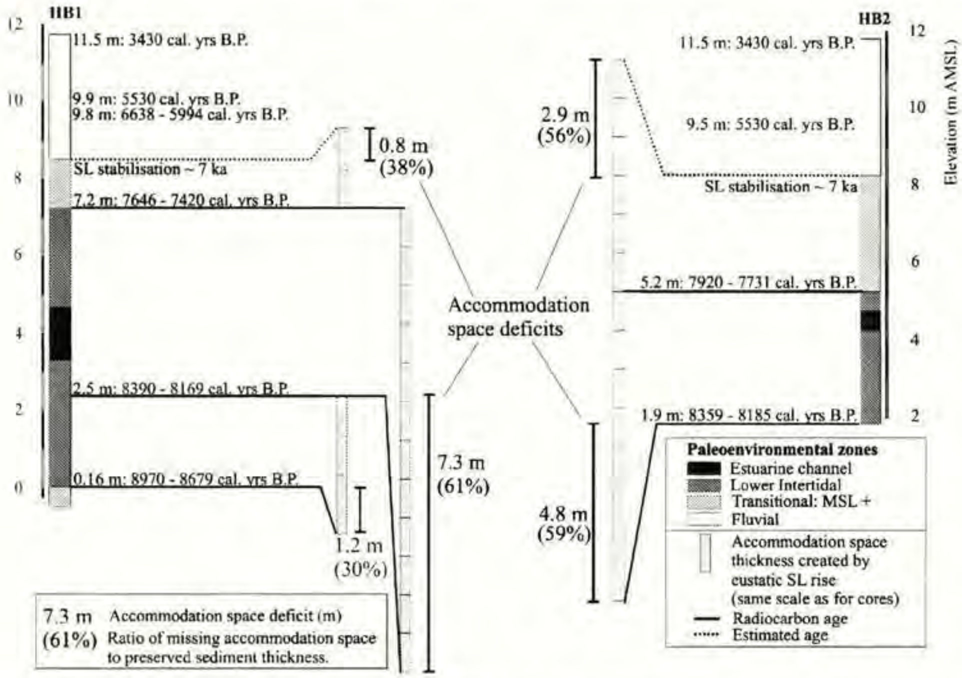

Fig. 10. Thickness of intertidal sediment in HB1 and 2 compared with the thickness of accommodation space created by rising eustatic SL during the same time period. The elevations within cores HB1 and 2 have an uncertainty of 0.3 m, estimates of past eustatic SL have an uncertainty of ± 2 m and are from the Gibb (1986) New Zealand SL curve, shown in Fig. 8.

perturbations during valley infilling as you might expect earthquake shaking to produce.

To re-assess which of the two uplift mechanisms are most likely for the NE Raukumara Peninsula—gradual, aseismic uplift or frequent small events—both the TA beach ridge sequence and the HB palaeo-estuary sequence support an aseismic uplift mechanism. Frequent, small events cannot be discounted given the resolution of our data but this is not supported by the relatively undisturbed HB Flats sedimentary sequence or the historical seismicity record of the region.

6.3. *Global examples of aseismic tectonic uplift and seismic hazard implications*

The recognition of aseismic mechanisms as the most likely driver of tectonic uplift of the NE Raukumara Peninsula is significant in a global context as there are very few examples of this worldwide. This location provides us with a valuable contrast to the comparatively well-documented occurrence of coseismic coastal movements associated with great earthquakes at subduction margins with similar rates of plate convergence (e.g. Cascadia and the Nankai Trough). Glacio-isostatic adjustments at high-latitude locations can produce uplift rates at similar magnitudes to, and higher than, the uplift rates recorded in the NE Raukumara Peninsula (e.g., Ekman and Makinen, 1996; James et al., 2000; Forman et al., 2004; Larsen et al., 2004; Miettinen, 2004; Berglund, 2005). Aseismic and coseismic uplift mechanisms have contributed to coastal uplift at rates up to 10 mm yr^{-1} at Isla Mocha, Chile (Nelson and Manley, 1992). Both mechanisms of uplift were attributed to rupture and creep on an inferred offshore imbricate thrust fault. Aseismic coastal uplift at ~1 mm yr^{-1} has been recorded at eastern Kyushu, Japan, where it has been related to subduction of a buoyant body, the Kyushu–Palau Ridge (Nakada et al., 2002, and references therein). Similar to Kyushu, aseismic uplift of the NE Raukumara Peninsula is probably related to subduction of a buoyant body, namely, the Hikurangi Plateau and associated sediment underplating. The geodynamic significance of this and the relationships between plate coupling and upper plate deformation mechanisms is to be explored further in a following paper (Wilson et al., in preparation).

Identification of aseismic processes accommodating uplift in the NE Raukumara Peninsula region contributes to resolving the seismic hazard of this area. With no large to great subduction zone earthquakes in historical times the Hikurangi subduction zone interface is a significant source of uncertainty in national seismic hazard assessments (Stirling et al., 2002). This study shows there have been no coseismic coastal uplift events, therefore implying no large to great earthquakes have been generated either on the subduction interface or by offshore upper plate faults during the Holocene, along this sector of the Hikurangi margin.

7. Conclusions

In summary, our interpretation of the Horoera and Waipapa terraces is that they do not have a marine origin.

Table 5
Uplift rates from the TA beach ridges

Location	Elevation (m)	Age (ka)	Modern analog elevation (m)	Total uplift (m)	Uplift Rate ($m\,ka^{-1}$)	Uncertainty
Front edge Z1	8.4	>3.43	4	4.4	1.3	Maximum
Front edge Z2	8	>3.43	4	4	1.2	Maximum
Front edge Z3	7.6	1.8115[a]	4	3.6	2.0	(1.7–2.4)[b]
Back edge Z5	4.3	0.586[c]	4	0.3	0.51	(0.46–0.58)[b]

[a]Radiocarbon age of Ota et al. (1992). Midpoint of the 2σ calibrated age BP.
[b]Maximum uplift rate = calculated using the minimum age of the 2σ calibrated age range; minimum uplift rate: calculated using the maximum age of the 2σ calibrated age range.
[c]Radiocarbon age of Garrick (1979). Midpoint of the 2σ calibrated age BP.

Therefore, they do not provide evidence of coseismic coastal uplift. How then, is the rapid uplift (at rates of 0.5–3.3 $mm\,yr^{-1}$) achieved? The TA beach ridge sequence does not display any steps indicative of significant coseismic uplift events. Rather, the gradient of the beach ridge zones is approximately constant with small variations probably related to sediment supply fluctuations superimposed on a background uplift rate. The palaeoecology of the HB transgressive sequence shows no evidence of coseismic uplift events of a magnitude >0.85 m, all palaeoenvironmental transitions appear to be gradational. Accommodation space deficits at varying time intervals indicate that uplift occurred throughout deposition of the HB Flats sedimentary infill sequence.

This combination of different methodologies applied to varying time periods at four different coastal locations leads to our conclusion that a continuous, aseismic process has driven Holocene coastal uplift of the NE Raukumara Peninsula. This is an important outcome for several reasons. Firstly, it is a rare example of aseismic tectonic mechanisms driving coastal uplift in a global context. The second significant implication of these results is that we have shown that Holocene coastal uplift mechanisms do vary along the East Coast of the North Island. This implies that similar coastal geomorphology (e.g., raised terraces, wide coastal plains and uplifted estuaries) can be produced by different tectonic processes. Recognition of this brings some reconciliation to the former inconsistency of similar Holocene coastal tectonic processes along the Hikurangi margin, despite the apparent contrasts in upper plate structures (Table 5).

Acknowledgements

This research was funded by the Earthquake Commission (Project 6UNI/501). KJW was supported by the GNS Science Sarah Beanland Memorial Scholarship. Peter Barker, assisted by Matt Hill, carried out the drilling. Alvaro Gonzalez and Ruth Wightman provided field assistance. John Begg is thanked for providing the calibrated radiocarbon ages of the Gibb, 1986, eustatic SL data. Bill McLea provided the palynology information. Bruce Hayward and Ashwaq Sabaa are thanked for assisting with foraminifera identification and Karyne Rogers is thanked for her assistance and advice with the stable isotope study. The manuscript was improved by reviews by two anonymous reviewers.

Appendix A. Supplementary materials

Supplementary data associated with this article can be found in the online version at doi:10.1016/j.quascirev.2007.01.005.

References

Allen, G.P., Posamentier, H.W., 1993. Sequence stratigraphy and facies model of an incised valley fill: the Gironde estuary, France. Journal of Sedimentary Petrology 63, 378–391.
Atwater, B.F., 1987. Evidence for great Holocene earthquakes along the outer coast of Washington State. Science 236, 942–944.
Berglund, M., 2005. The Holocene shore displacement of Gastrikland, eastern Sweden: a contribution to the knowledge of Scandinavian glacio-isostatic uplift. Journal of Quaternary Science 20, 519–531.
Berryman, K.R., 1993. Age, height, and deformation of Holocene terraces at Mahia Peninsula, Hikurangi subduction margin, New Zealand. 1. Tectonics 12, 1347–1364.
Beu, A.G., 2006. Marine Mollusca of Oxygen Isotope Stages of the last 2 million years in New Zealand. Part 2. Biostratigraphically useful and new Pliocene to Recent bivalves. Journal of the Royal Society of New Zealand 36, 151–338.
Bratton, J.F., Colman, S.M., Thieler, E.R., Seal II, R.R., 2003. Birth of the modern Chesapeake Bay estuary between 7.4 and 8.2 ka and implications for global sea level rise. Geo-Marine Letters 22, 188–197.
Clague, J.J., 1997. Evidence for large earthquakes at the Cascadia subduction zone. Reviews of Geophysics 35, 439–460.
Cochran, U., Berryman, K., Mildenhall, D., Hayward, B., Southall, K., Hollis, C., Barker, P., Wallace, L., Alloway, B., Wilson, K., 2006. Paleoecological insights into subduction zone earthquake occurrence, eastern North Island, New Zealand. Geological Society of America Bulletin 118, 1051–1074.
Dalrymple, R.W., Zaitlin, B.A., Boyd, R., 1992. Estuarine facies models: conceptual basis and stratigraphic implications. Journal of Sedimentary Petrology 62, 1130–1146.
Darienzo, M.E., Peterson, C.D., Clough, C., 1994. Stratigraphic evidence for great subduction-zone earthquakes at four estuaries in Northern Oregon, USA. Journal of Coastal Research 10, 820–876.

Dawson, S., Dawson, A.G., Edwards, K.J., 1998. Rapid Holocene relative sea-level changes in Gruinart, Isle of Islay, Scottish Inner Hebrides. The Holocene 8, 183–195.

Dawson, S., Smith, D.E., 1997. Holocene relative sea-level changes on the margin of a glacio-isostatically uplifted area: an example from northern Caithness, Scotland. The Holocene 7, 59–77.

De Mets, C., Gordon, R.G., Argus, D.F., Stein, S., 1990. Current plate motions. Geophysics Journal International 101, 425–478.

De Mets, C., Gordon, R.G., Argus, D.F., Stein, S., 1994. Effect of recent revisions to the geomagnetic reversal timescale on estimates of current plate motions. Geophysical Research Letters 21, 2191–2194.

Dowrick, D., Smith, E.G., 1990. Surface was magnitudes of some New Zealand earthquakes 1901–1988. Bulletin of the New Zealand National Society for Earthquake Engineering 23, 198–210.

Eden, D.N., Page, M.J., 1998. Palaeoclimatic implications of a storm erosion record from late Holocene lake sediments, North Island, New Zealand. Palaeogeography, Palaeoclimatology, Palaeoecology 139, 37–58.

Ekman, M., Makinen, J., 1996. Recent postgalcial rebound, gravity change and mantle flow in Fennoscandia. Geophysical Journal International 126, 229–234.

Fontugne, M.R., Jouanneau, J.-M., 1987. Modulation of particulate organic carbon flux to the ocean by a macrotidal estuary: evidence from measurements of carbon isotopes on organic matter from the Gironde system. Estuarine, Coastal and Shelf Science 24, 377–387.

Forman, S.L., Lubinski, D.J., Ingolfsson, O., Zeeberg, J.J., Snyder, J.A., Siegert, M.J., Matishov, G.G., 2004. A review of postglacial emergence on Svalbard, Franz Josef Land and Novaya Zemlya, northern Eurasia. Quaternary Science Reviews 23, 1391–1434.

Froggatt, P.C., Lowe, D.J., 1990. A review of late Quaternary silicic and some other tephra formations from New Zealand: their stratigraphy, nomenclature, distribution, volume and age. New Zealand Journal of Geology and Geophysics 33, 89–109.

Garrick, R.A., 1979. Late Holocene uplift at Te Araroa, East Cape, North Island, New Zealand. New Zealand Journal of Geology and Geophysics 22, 131–139.

Gearing, J.N., Gearing, P.J., Rudnick, D.T., Requejo, A.G., Hutchins, M.J., 1984. Isotopic variability of organic carbon in a phytoplankton-based, temperate estuary. Geochimica et Cosmochimica Acta 48, 1089–1098.

Gibb, J.G., 1986. A New Zealand regional Holocene eustatic sea-level curve and its application to determination of vertical tectonic movements, a contribution to IGCP-Project 200. In: Recent Crustal Movements of the pacific Region. Bulletin of the Royal Society of New Zealand, pp. 377–395.

Goff, J.R., Chague-Goff, C., Nichol, S.L., 2001. Paleotsunami deposits: a New Zealand perspective. Sedimentary Geology 143, 1–6.

Goff, J.R., McFadgen, B.G., Chague-Goff, C., 2004. Sedimentary differences between the 2002 Easter Storm and the 15th-century Okoropunga tsunami, southeastern North Island, New Zealand. Marine Geology 204, 235–250.

Goff, J.R., Rouse, H.L., Jones, S.L., Hayward, B.W., Cochran, U., McLea, W., Dickinson, W.W., Morley, M.S., 2000. Evidence for an earthquake and tsunami about 3100–3400 yr ago, and other catastrophic slatwater inundations in a coastal lagoon, New Zealand. Marine Geology 170, 231–249.

Hartley, B., 1996. An Atlas of British Diatoms. Biopress Ltd., Bristol.

Hayward, B., Stilwell, J.D., 1995. Floating cockle shells (*Austrovenus stutchburyi*)—their significance to paleoenvironmental assessments. Tane 35, 143–148.

Hayward, B.W., Grenfell, H.R., Reid, C., Hayward, K., 1999a. Recent New Zealand shallow-water benthic foraminifera: taxonomy, ecologic dstribution, biogeography, and use in paleoenvironmental assessment. Institute of Geological and Nuclear Sciences Monograph 21. Lower Hutt, New Zealand: Institute of Geological and Nuclear Sciences Limited, 264p.

Hayward, B.W., Grenfell, H.R., Scott, D.B., 1999b. Tidal range of marsh foraminifera for determining former sea-level heights in New Zealand. New Zealand Journal of Geology and Geophysics 42, 395–413.

Hayward, B.W., Cochran, U., Southall, K., Wiggins, E., Grenfell, H.R., Sabaa, A., Shane, P.R., Gehrels, R., 2004a. Micropalaeontological evidence for the Holocene earthquake history of the eastern Bay of Plenty, New Zealand, and a new index for determining the land elevation record. Quaternary Science Reviews 23, 1651–1667.

Hayward, B.W., Scott, G.H., Grenfell, H.R., Carter, R., Lipps, J.H., 2004b. Techniques for estimation of tidal elevation and confinement (~salinity) histories of sheltered harbours and estuaries using benthic foraminifera: examples from New Zealand. The Holocene 14, 218–232.

Healy, W.B. (Compiler), 1980. Pauatahanui Inlet—an environmental study. New Zealand Department of Scientific and Industrial Research Information Series 141, 1–198.

Henderson, J., Ongley, M., 1920. The geology of the Gisborne and Whatatutu Subdivisions, Raukumara Division. New Zealand Geological Survey Bulletin 21.

Hughen, K.A., Baillie, M.G.L., Bard, E., Beck, J.W., Bertrand, C.J.H., Blackwell, P.G., Buck, C.E., Burr, G.S., Cutler, K.B., Damon, P.E., Edwards, R.L., Fairbanks, R.G., Friedrich, M., Guilderson, T.P., Kromer, B., McCormac, G., Manning, S., Ramsey, B.B., Reimer, P.J., Reimer, R.W., Remmele Jr., S.S., Stuiver, M., Talamo, S., Taylor, F.W., van der Plicht, J., Weyhenmeyer, C.E., 2004. Marine04 marine radiocarbon age calibration, 0–26 Cal Kyr BP. Radiocarbon 46, 1059–1086.

Hull, A.G., 1987. A late Holocene marine terrace on the Kidnappers Coast, North Island, New Zealand: some implications for shore platform development processes and uplift mechanisms. Quaternary Research 28, 183–195.

James, T.S., Clague, J.J., Wang, K., Hutchinson, I., 2000. Postglacial rebound at the northern Cascadia subduction zone. Quaternary Science Reviews 19, 1527–1541.

Krammer, K., Lange-Bertalot, H., 1991. Bacillariophyceae: Achnanthaceae. Gustav Fischer Verlag, Stuttgart.

Krammer, K., Lange-Bertalot, H., 1999a. Bacillariophyceae: Bacillariaceae, Epithemiaceae, Surirellaceae. Specktrum Akademischer Verlag, Heidelberg.

Krammer, K., Lange-Bertalot, H., 1999b. Bacillariophyceae: Naviculaceae. Specktrum Akademischer Verlag, Heidelberg.

Krammer, K., Lange-Bertalot, H., 2000a. Bacillariophyceae: Centrales, Fragilariaceae, Eunotiaceae. Spektrum Akademischer Verlag, Heidelberg.

Krammer, K., Lange-Bertalot, H., 2000b. Bacillariophyceae: English and French Translation of the Keys. Spektrum Akademischer Verlag, Heidelberg.

Larsen, C.F., Motyka, R.J., Freymueller, J.T., Echelmayer, K.A., Ivins, E.R., 2004. Rapid uplift of southern Alaska caused by recent ice loss. Geophysical Journal International 158, 1118–1133.

Marsden, I.D., 2004. Effects of reduced salinity and seston availability on growth of the New Zealand little-neck clam *Austrovenus stutchburyi*. Marine Ecology Progress Series 266.

Marsden, I.D., Pilkington, R., 1995. Spatial and temporal variations in the condition of *Austrovenus stutchburyi* Finlay, 1927 (Bivalvia: Veneridae) from the Avon-Heathcote estuary, Christchurch. New Zealand Natural Sciences 22, 57–67.

Mazengarb, C., 1984. The Fernside Fault: an active normal fault, Raukumara Peninsula, New Zealand. New Zealand Geological Survey Record 3, 98–103.

Mazengarb, C., Speden, I.G.C., 2000. Geology of the R... Institute of Geological and Nuclear Sciences 1:250,000 geological map 6. Institute of Geological and Nuclear Sciences Limited, Lower Hutt, New Zealand.

McCormac, F.G., Hogg, A.G., Blackwell, P.G., Buck, C.E., Higham, T.F.G., Reimer, P.J., 2004. SHCal04 southern hemisphere calibration, 0–26 ka cal BP. Radiocarbon 46, 1087–1092.

McGlone, M.S., Anderson, A.J., Holdaway, R.N., 1994. An ecological approach to the Polynesian settlement of New Zealand. In: Sutton, D.G. (Ed.), The Origins of the First New Zealanders. Auckland University Press, pp. 136–163.

Meyers, P.A., 1994. Preservation of elemental and isotopic source identification of sedimentary organic matter. Chemical Geology 114, 289–302.

Miettinen, A., 2004. Holocene sea-level changes and glacio-isostasy in the Gulf of Finland, Baltic Sea. Quaternary International 120, 91–104.

Moore, P.D., Webb, J.A., 1978. An illustrated Guide to Pollen Analysis. Hodder and Stoughton, London.

Moore, P.D., Webb, J.A., Collinson, M.E., 1991. Pollen Analysis. Blackwell Scientific Publications, Oxford, Boston.

Morton, J., Miller, M., 1968. The New Zealand Sea Shore. Collins, London.

Muller, A., Mathesius, U., 1999. The paleoenvironments of coastal lagoons in the southern Baltic Sea, I. The application of sedimentary C_{org}/N ratios as source indicators. Palaeogeography, Palaeoclimatology, Palaeoecology 145, 1–16.

Muller, A., Voss, M., 1999. The paleoenvironments of coastal lagoons in the southern Baltic Sea, II. $d^{13}C$ and $d^{15}N$ ratios of organic matter—sources and sediments. Palaeogeography, Palaeoclimatology, Palaeoecology 145, 17–32.

Nakada, M., Tahara, M., Shimizu, H., Nagaoka, S., Uehira, K., Suzuki, S., 2002. Late Pleistocene crustal uplift and gravity anomaly in the eastern part of Kyushu, Japan, and its geophysical implications. Tectonophysics 351, 263–283.

Nelson, A.R., Manley, W.F., 1992. Holocene coseismic and aseismic uplift of Isla Mocha, South-Central Chile. Quaternary International 15/16, 61–76.

Nelson, A.R., Shennan, I., Long, A.J., 1996. Identifying coseismic subsidence in tidal-wetland stratigraphic sequences at the Cascadia subduction zone of western North America. Journal of Geophysical Research 101, 6115–6135.

Ongley, M., MacPherson, E.O., 1928. The geology of the Waiapu Subdivision, Raukumara Division. New Zealand Geological Survey Bulletin 30.

Ota, Y., 1987. Holocene coastal tectonics of eastern North Island, New Zealand. In: A preliminary report on late Quaternary seismo-tectonic movement in the Circum Pacific area, 1st survey (1985/1986).

Ota, Y., Berryman, K.R., Hull, A.G., Miyauchi, T., Iso, N., 1988. Age and height distribution of Holocene transgressive deposits in eastern North Island, New Zealand. Palaeogeography, Palaeoclimatology, Palaeoecology 68, 135–151.

Ota, Y., Hull, A.G., Berryman, K.R., 1991. Coseismic uplift of Holocene marine terraces in the Pakarae River area, eastern North Island, New Zealand. Quaternary Research 35, 331–346.

Ota, Y., Hull, A.G., Iso, N., Ikeda, Y., Moriya, I., Yoshikawa, T., 1992. Holocene marine terraces on the northeast coast of North Island, New Zealand, and their tectonic significance. New Zealand Journal of Geology and Geophysics 35, 273–288.

Patterson, R.T., Hutchinson, I., Guilbault, J.-P., Clague, J.J., 2000. A comparison of the vertical zonation of diatom, foraminifera, and macrophhyte assemblages in a coastal marsh: implications for greater paleo-sea level resolution. Micropaleontology 46, 229–244.

Paul, M.A., Barras, B.F., 1998. A geotechnical correction for post-depositional sediment compression: examples from the Forth valley, Scotland. Journal of Quaternary Science 13, 171–176.

Reyners, M., 1998. Plate coupling and the hazard of large subduction thrust earthquakes at the Hikurangi subduction zone, New Zealand. New Zealand Journal of Geology and Geophysics 41, 343–354.

Round, F.E., Crawford, R.M., Mann, D.G., 1990. The Diatoms: Biology and Morphology of the Genera. Cambridge University Press, Cambridge.

Roy, P.S., 1984. New South Wales Estuaries: Their Origin and Evolution. Coastal Geomorphology in Australia, Academic Press, Australia, pp. 99–121.

Shennan, I., Innes, J.B., Long, A.J., Zong, Y., 1994. Late Devensian and Holocene relative sea-level changes at Loch nan Eala, near Arisaig, northwest Scotland. Journal of Quaternary Science 9, 261–283.

Shennan, I., Innes, J.B., Long, A.J., Zong, Y., 1995. Late Devensian and Holocene relative sea-level changes in Northwestern Scotland: new data to test existing models. Quaternary International 26, 97–123.

Shennan, I., Long, A.J., Rutherford, M.M., Green, F.M., Innes, J.B., Lloyd, J.M., Zong, Y., Walker, K.J., 1996. Tidal marsh stratigraphy, sea-level change and large earthquakes, I: A 5000 year record in Washington, USA Quaternary Science Reviews 15, 1023–1059.

Sherrod, B.L., Bucknam, R.C., Leopold, E.B., 2000. Holocene relative sea level changes along the Seattle Fault at Restoration Point, Washington. Quaternary Research 54, 384–393.

Stirling, M.W., McVerry, G., Berryman, K.R., 2002. A new seismic hazard model for New Zealand. Bulletin of the Seismological Society of America 92, 1878–1903.

Stuiver, M., Polach, H.A., 1977. Discussion: reporting of C-14 data. Radiocarbon 19, 355–363.

Thornton, S.F., McManus, J., 1994. Application of organic carbon and nitrogen stable isotope and C/N ratios as source indicators of organic matter provenance in estuarine systems: evidence from the Tay estuary, Scotland. Estuarine, Coastal and Shelf Science 38, 219–233.

van Dam, H., Mertens, A., Sinkeldam, J., 1994. A coded checklist and ecological indicator values of freshwater diatoms from the Netherlands. Netherlands Journal of Aquatic Ecology 28, 117–133.

Wallace, L.M., Beavan, J., McCaffrey, R., Darby, D., 2004. Subduction zone coupling and tectonic block rotations in the North Island, New Zealand. Journal of Geophysical Research 109, B12406.

Wilmshurst, J.M., 1997. The impact of human settlement on vegetation and soil stability in Hawke's Bay, New Zealand. New Zealand Journal of Botany 35, 97–111.

Wilson, K.J., Berryman, K.R., Litchfield, N.J., Little, T.A., 2006. A revision of Mid to Late Holocene marine terrace distribution and chronology at New Zealand's most tectonically active coastal location, Pakarae River, North Island, New Zealand. New Zealand Journal of Geology and Geophysics 49, 477–489.

Wilson, K., Berryman, K., Little, T., Litchfield, N., Cochran, U., in preparation. Relationship between coastal geomorphology and subduction geodynamics in the Raukumara sector of the Hikurangi subduction zone.

Witkowski, A., Lange-Bertalot, H., Metzeltin, D., 2000. Diatom Flora of Marine Coasts I.A.R.G. Gantner Verlag K.G., Ruggell.

Yoshikawa, T., Ota, Y., Yonekura, N., Okada, A., Iso, N., 1980. Marine terraces and their tectonic deformation on the northeast coast of the North Island, New Zealand. Geographical Review of Japan 53, 238–262.

JQSR_26_7119531

TECTONICS, VOL. 26, TC4013, doi:10.1029/2006TC002021, 2007

Click Here for Full Article

Early Holocene paleoseismic history at the Pakarae locality, eastern North Island, New Zealand, inferred from transgressive marine sequence architecture

Kate Wilson,[1,2] Kelvin Berryman,[3] Ursula Cochran,[3] and Tim Little[1]

Received 18 July 2006; revised 23 March 2007; accepted 23 May 2007; published 16 August 2007.

[1] Early Holocene transgressive marine deposits infilling the Pakarae River paleovalley are used to extend the paleoseismic history of the Pakarae River locality, East Coast, North Island, New Zealand, back in time prior to eustatic sea level stabilization at ~7 calibrated (cal) ka B.P. Paleoenvironmental evolution of the Pakarae River paleovalley from 7 to 10 cal ka B.P is reconstructed using sedimentology and biostratigraphy. Two estuarine units display sudden vertical transitions to floodplain sediments implying significant marine regressions and estuary abandonment. These regressions are attributed to coseismic coastal uplift events at ~9000 and ~8500 cal years B.P. A third uplift between 8500 and ~7350 cal years B.P. is inferred from a significant difference between the amount of sediment preserved and the predicted sediment thickness according to the eustatic sea level curve. This study demonstrates the utility of the analysis of transgressive deposits and their paleoenvironmental characteristics for neotectonic investigations on active coasts. **Citation:** Wilson, K., K. Berryman, U. Cochran, and T. Little (2007), Early Holocene paleoseismic history at the Pakarae locality, eastern North Island, New Zealand, inferred from transgressive marine sequence architecture, *Tectonics*, *26*, TC4013, doi:10.1029/2006TC002021.

1. Introduction

[2] With rising awareness of the devastating effects of subduction zone earthquakes, long-term records of plate interface and upper plate paleoseismicity are becoming increasingly important. Coastal environments are commonly the only places that preserve a record of such events; for example, coseismic subsidence is often documented by drowning of tidal marsh sequences, and uplift recorded by abandonment of marine terraces on parts of the coastline favorable for their preservation [e.g., *Atwater*, 1987; *Clague*, 1997; *Darienzo et al.*, 1994; *Marshall and Anderson*, 1995; *Merritts*, 1996; *Zachariasen et al.*, 1999]. The duration of these records is commonly limited by the time elapsed since stabilization of postglacial eustatic sea level (SL). This is because modern SL can be used as a datum against which to measure noneustatic (i.e., tectonic) effects. Here we extend the paleoseismic history at the Pakarae River mouth (henceforth called the Pakarae locality), New Zealand's most tectonically active coastal location, back beyond the time of eustatic SL stabilization at ~7 ka [*Gibb*, 1986] by unraveling an event history in the transgressive fluviomarine sequence.

[3] Tectonic uplift since ~7 ka, taking place at an average rate of 3.2 ± 0.8 mm/yr, is recorded at the Pakarae River mouth, North Island, New Zealand, by a flight of seven Holocene marine terraces [*Ota et al.*, 1991; *Wilson et al.*, 2006]. Prior to 7 ka the incised valley of the Pakarae River was infilled by a transgressive sedimentary sequence under conditions of rapidly rising eustatic SL [*Berryman et al.*, 1992]. *Wilson et al.* [2007a] have demonstrated that tectonic uplift occurred during deposition of the sequence and was a major control on the facies distribution. Here we further investigate the paleogeographic evolution and tectonic history of the Pakarae paleoestuary by applying two methods to identify the timing of tectonic uplift that has affected the transgressive estuarine sequence. One method is to compare the thickness of the estuarine section with that on a stable coast. On stable coasts the thickness of sediment should approximately equal the amount of eustatic SL rise. If tectonic uplift occurs during transgression, the total thickness of sediment will be less than the amount of eustatic SL rise. The deficit will approximately equal the tectonic uplift component, though this does rely on several assumptions such as sedimentation rates keeping pace with eustatic SL rise and estuary infilling being controlled by eustatic SL rise rather than fluvial aggradation. This technique is most effective where it can be demonstrated, particularly using microfauna, that the infilling sediment is consistently from an intertidal environment, which implies sedimentation rates equal the rate of eustatic SL rise and a lack of fluvial aggradation. The second, and most important, method employed is to use the paleoenvironmental facies architecture to detect sudden marine regressions that identify tectonic event horizons. We use the sedimentological and paleoenvironmental data reported by *Wilson et al.* [2007a] to constrain a paleogeographic model of the Pakarae locality coastal evolution during the early Holocene and discuss evidence for the timing and magnitude of early Holocene uplift events at the Pakarae locality. Transgressive marine sequence analysis is an emerging field of coastal

[1]School of Earth Sciences, Victoria University of Wellington, Wellington, New Zealand.
[2]Now at GNS Science, Lower Hutt, New Zealand.
[3]GNS Science, Lower Hutt, New Zealand.

Copyright 2007 by the American Geophysical Union.
0278-7407/07/2006TC002021$12.00

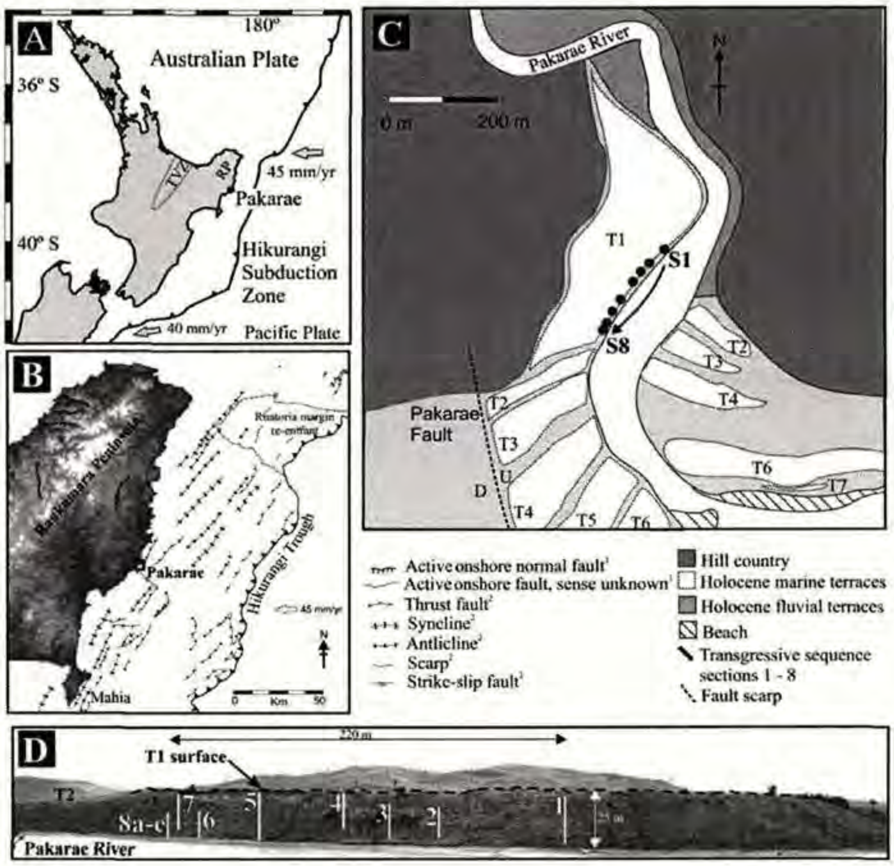

Figure 1. (a) North Island, New Zealand, with major tectonic features. TVZ, Taupo volcanic zone; RP, Raukumara Peninsula. Relative plate motions are after *DeMets et al.* [1990, 1994]; Hikurangi subduction deformation front is after *Collot et al.* [1996]. (b) Topography and tectonic features of the Raukumara Peninsula. Superscript 1 indicates onshore active faults from the GNS Science Active Faults Database (http://data.gns.cri.nz/af/). Superscript 2 indicates offshore structures from *Lewis et al.* [1997]. (c) Pakarae River mouth with major geomorphic elements, marine terraces [after *Wilson et al.*, 2006], and stratigraphic section locations. (d) Pakarae River, transgressive exposures beneath TI (highest Holocene marine transgression surface) with sections 1–8e. Riverbank ~25 m high.

paleoseismology that enables us to extending the paleoseismic history of this significant location adjacent to the Hikurangi subduction zone.

[4] The Pakarae locality is an important site along this sector of the margin because the Holocene record there can be used to place constraints on the boundaries of various upper plate strain domains, and to clarify where episodic (coseismic) versus aseismic tectonic processes may have operated along the Hikurangi margin. The Pakarae River mouth is situated on the southeastern Raukumara Peninsula, ~65 km inboard of the Hikurangi subduction trough on the eastern coast of North Island, New Zealand (Figure 1). No subduction earthquakes have occurred in historic times along this section of the margin. The presence of a stepped sequence of Holocene coseismic marine terraces at the Pakarae River mouth has been interpreted to record permanent uplift and is most likely a consequence of faulting in the upper plate of this subduction zone [*Ota et al.*, 1991; *Wilson et al.*, 2006]. Alternatively, sediment underplating (inferred from seismic velocities which image a weak zone along the plate interface) has been suggested as a cause of long-term uplift of Raukumara Peninsula [*Eberhart-Phillips and Reyners*, 1999; *Litchfield et al.*, 2007; *Reyners et al.*, 1999; *Walcott*, 1987]. Normal faulting is persistent in the Raukumara Range, but reverse faults are inferred in the coastal area and offshore [*Lewis et al.*, 1997; *Mazengarb*, 1984; *Mazengarb and Speden*, 2000].

[5] The Pakarae River mouth marine terraces were first mapped, correlated, and dated by *Ota et al.* [1991]. Seven terraces were recognized and named T1–T7 from oldest to youngest. T1 was recognized by *Berryman et al.* [1992] as corresponding with the maximum Holocene marine

Table 1. Radiocarbon Ages Obtained From the Pakarae River Mouth Transgressive Sedimentary Sequence

Section	Sample Height, m	Lab Number[a]	Sample Material[b]	Dating Technique	^{13}C, ‰	Radiocarbon Age,[c] radiocarbon years B.P.	Calibrated Age 2 Sigma,[d] cal years B.P.	Sample Living Depth[e]
1	15.2 ± 0.22	NZA 21854	A	AMS	−1.27	8056 ± 30	8,590 − 8,410	−0.2
1	10.05 ± 0.22	NZA 22529	A	AMS	1.05	8458 ± 35	9,210 − 8,980	−0.2
1	6.3 ± 0.22	WK 16864	Wood	Standard	−28.2	8420 ± 59	9,530 − 9,240	?
1	6 ± 0.22	NZA 21961	A	AMS	−0.91	8868 ± 30	9,600 − 9,450	−0.2
2	14.15 ± 0.22	NZA 22528	A	AMS	1.42	8082 ± 35	8,640 − 8,420	−0.2
2	7.5 ±0.22	NZA 21852	A, B	AMS	−3.71	8338 ± 30	9,010 − 8,770	−0.2
4	18.9 ± 0.22	NZA 22526	A, B	AMS	0.98	7791 ± 35	8,350 − 8,170	−0.2
5	18.3 − 18.7 ± 0.22	NZA 21851	A, B. C	AMS	−0.49	6847 ± 30	7,430 − 7,280	−0.2
5	14.5 ± 0.22	Wk 16454	Wood	Standard	−27.2	8219 ± 52	9,290 − 9,000	?
7	17.15 ± 0.22	NZA 22527	A	AMS	0.39	7981 ± 35	8,540 − 8,360	−0.2
8a	1.1 ± 0.31	Wk 16453	Wood	Standard	−28	9158 ± 52	10,420 − 10,180	?
8b	4.4 ± 0.31	NZA 21853	A	AMS	−2.9	9266 ± 30	10,200 − 9,990	−0.2

[a]Wk, University of Waikato Radiocarbon Dating Laboratory; NZA, Institute of Geological and Nuclear Sciences Rafter Radiocarbon Laboratory.
[b]Shell. A, *Austrovenus stutchburyi*; B, *Paphies australis*; C, *Melagraphia aethiops*.
[c]Conventional radiocarbon age before present (1950 A.D.) after *Stuiver and Polach* [1977].
[d]Calibrated age in calendar years. Wood ages are calibrated using Southern Hemisphere atmospheric data of *McCormac et al.* [2004], marine ages are calibrated using data from *Hughen et al.* [2004]. Radiocarbon ages are calibrated using OxCal version 3.10.
[e]Estimated based on *Austrovenus stutchburyi* living at mean sea level and burrowing to a depth of 0.2 m below the sediment surface.

transgression, which in the New Zealand region occurred ~7 cal ka B.P. [*Gibb*, 1986]. The age of uplift of each terrace was estimated from radiocarbon dates and tephra distribution by *Ota et al.* [1991]. This chronology has been revised by *Wilson et al.* [2006]. Although the Pakarae Fault, a reactivated Tertiary normal fault near the Pakarae River mouth, was argued to have moved during terrace uplift events, it did not rupture with every terrace-forming event. Rather uplift was inferred to have been driven by slip on an active reverse fault located a few kilometers offshore of the Pakarae River mouth [*Ota et al.*, 1991]. As part of this original study, *Ota et al.* [1988] presented radiocarbon dates from the sedimentary sequence underlying T1 and made summaries of the stratigraphy but no further interpretations were made.

[6] The Pakarae River mouth transgressive sequence was interpreted in more detail by *Berryman et al.* [1992]. Stratigraphy, radiocarbon dates and tephrochronology were used to produce paleogeographic maps showing evolution from 9 to 1 ka B.P. and they constructed a relative SL curve for the Pakarae locality from 11 ka B.P. to present-day. *Berryman et al.* [1992] showed there was a deficit in the amount of sediment preserved when compared to the amount of accommodation space created by eustatic SL rise, as estimated from the *Gibb* [1986] SL curve. They attributed the deficit to tectonic uplift during deposition of the sequence but specific events could not be identified on the basis of their data. Unconformities and weathering horizons within the sequence were mentioned and inferred to be indicative of uplift events. *Berryman et al.* [1992] inferred a regression in the relative SL curve for the Pakarae locality at ~10.5–9.5 cal years B.P. This was attributed to a eustatic SL fall rather than a tectonic uplift event because of (1) correlation to similarly aged trees growing in and overwhelmed by estuarine deposits at several other sites along the East Coast and (2) correlation with a change in the trend of the *Gibb* [1986] eustatic SL curve.

[7] *Wilson et al.* [2007a] recently examined the Pakarae River mouth sedimentary sequence; they remeasured one section in common with the *Berryman et al.* [1992] study and described seven new riverbank sections spanning a 220 m stretch of the riverbank. Twelve new radiocarbon ages were presented (Table 1). Sedimentology and benthic foraminifera assemblages were used to define four broad paleoenvironmental facies associations (Figure 2), the distribution of which was used to develop a facies architecture model for sediment infill of an incised valley in an uplifting tectonic setting. In this paper we combine all the available stratigraphic data and facies model results previously presented (1) to develop models of the paleogeographic evolution of the Pakarae River paleoestuary and (2) to identify and date specific tectonic event horizons.

2. Methodology

2.1. Reconstruction of the Pakarae Locality Paleoenvironments

[8] The facies architecture profile developed from the Pakarae riverbank sections [*Wilson et al.*, 2007a] provides the basis for paleogeographic reconstructions (Figure 2). On the basis of sedimentology and foraminifera data eight biolithofacies were identified in the Pakarae riverbank sequence; these were nonfossiliferous gravels (interpreted as a fluvial channel lag), thin shelly gravels (estuarine tidal channel lags), thick shelly gravels (estuary head delta), shelly well-sorted sands (barrier environment), nonfossiliferous well-sorted sands (reworked tephra and fluvial sand), silt and sand with abundant marine fauna (central estuary basin), silt and sand with rare marine fauna (estuarine margin), and nonfossiliferous silt and sand (fluvial) (Figure 2)

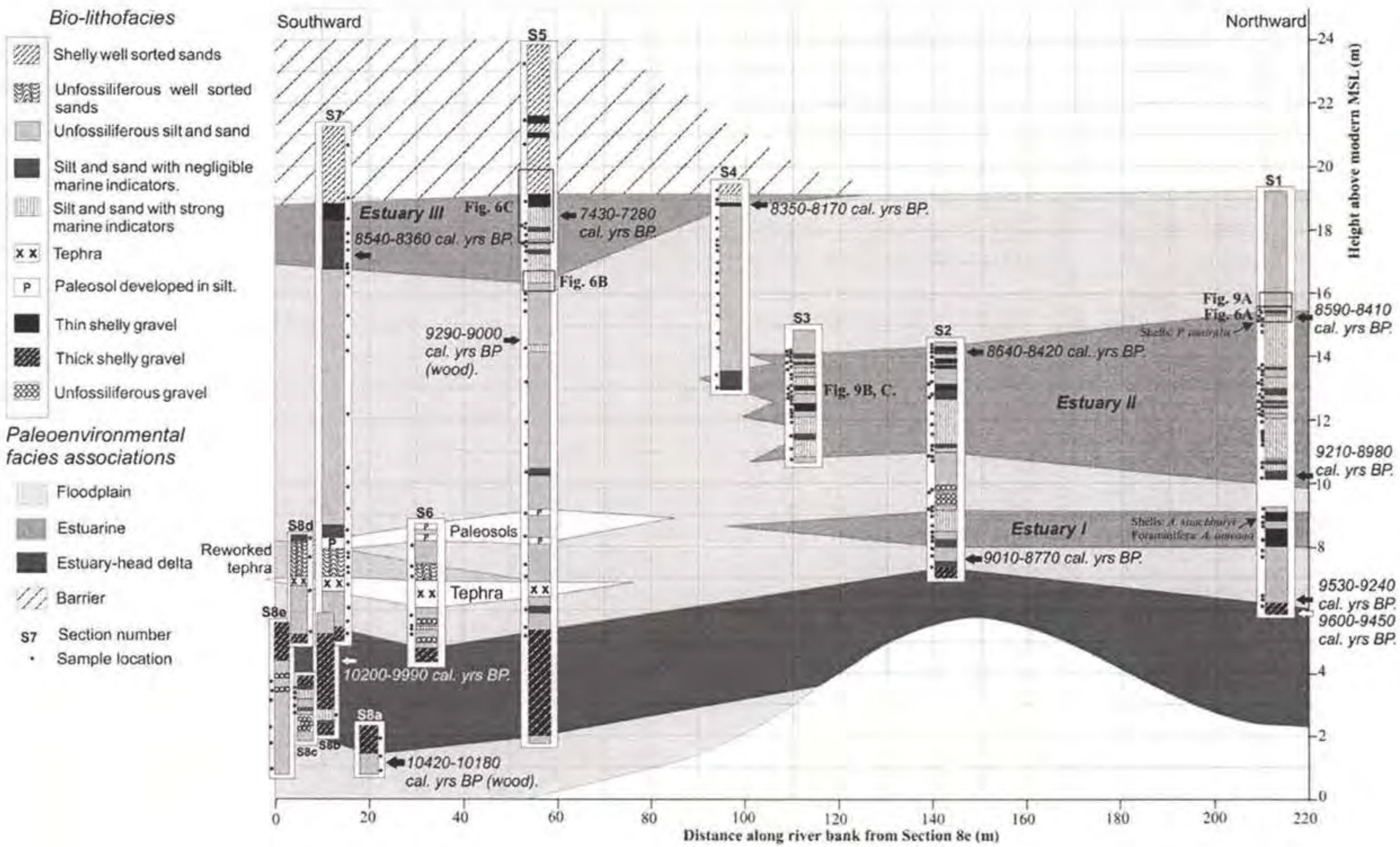

Figure 2. Biolithofacies and paleoenvironmental facies associations of the Pakarae River incised valley infill sedimentary sequence after *Wilson et al.* [2007a]. Locations of section photos in subsequent figures are shown.

[*Wilson et al.*, 2007a]. From these eight biolithofacies, four paleoenvironmental facies associations are distinguished, namely, floodplain, estuary head delta, estuarine, and barrier (Figure 2).

[9] The paleogeographic models of the Pakarae paleoestuary were constructed sequentially with stepwise addition of each sedimentary unit, starting with the basal floodplain deposit resting on a bedrock surface. For each facies or stratigraphic unit we develop an associated plan view of the paleogeography of the Pakarae River valley that satisfies the preserved distribution of the facies. Each of our paleogeographic reconstructions of the Pakarae River valley represents our best fit model, but they are not unique because of the limited exposure available in outcrop. For all paleoenvironmental facies within each time slice we aimed to satisfy the following criteria (in no order of relative importance): (1) the predicted spatial relationships of the Pakarae River mouth paleoenvironments to one another, (2) the temporal relationships between eustatic SL data and the radiocarbon ages within the Pakarae River mouth sedimentary sequence, and (3) the average timing and magnitude of uplift events at the Pakarae locality as inferred by the post-7 ka marine terraces. These criteria are discussed further below.

2.1.1. Predicted Spatial Relationships of the Pakarae River Mouth Paleoenvironments

[10] On the basis of depositional models developed for Holocene infilling of incised valleys [*Roy*, 1984; *Dalrymple et al.*, 1992; *Allen and Posamentier*, 1993] we expect that each of the four depositional environments identified in Pakarae River mouth sedimentary sequence should have a predictable spatial relationship to one another. In a landward to seaward direction, in plan view, the order of the facies should be floodplain, estuary head delta, estuary, and then a estuary mouth barrier. These models are based upon eustatic SL rise being the main parameter controlling the facies relationship, rather than fluvial processes such as river mouth progradation or regression. At the Pakarae River mouth the estuary head delta facies may not always occur between the floodplain and estuarine facies because its distribution appears to be chiefly controlled by proximity to a local gravel supply [*Wilson et al.*, 2007a]. Therefore, in our models we generally show the floodplain facies merging directly into the estuarine facies. No modern estuary exists at the Pakarae River mouth to use as an analogue; hence we use only the outcrop data as a guide to the size and length of the paleoestuary.

[11] The proximity of the river to base level has important implications for the amount of fluvial aggradation that could have occurred while still maintaining the rivers longitudinal profile. However, beyond outcrop data we cannot constrain the position of river mouth relative to the shoreline or the valley paleoslope; thus the possible thickness of fluvial aggradation cannot be estimated. While it would be interesting to know how high the river could have aggraded to this is not critical to our interpretation of uplift events. In all cases where fluvial aggradation is a possibility it occurs stratigraphically above an estuarine unit therefore we suggest the shoreline and river base level must have been nearby.

2.1.2. SL Constraints Imposed Eustatic SL curve and the Radiocarbon Age Control

[12] The eustatic SL curve provides an estimate of the amount of sediment that should be deposited between age control points. As eustatic SL rose, accommodation space within the paleovalley was created. If sedimentation rates within the paleoestuary approximately kept pace with the rate of accommodation space creation (as supported by the presence of intertidal microfauna throughout the sequence [*Wilson et al.*, 2007a]), the sediment thickness between two age control points should approximate the amount of eustatic SL that occurred during that time interval. In our paleoenvironmental reconstructions we compare the present elevations of the radiocarbon dated shells with the eustatic SL at the time of their deposition to assess whether the sediment thickness between the shells is consistent with the estimated amount of eustatic SL rise or if there is a significant difference. For each radiocarbon age we take the midpoint of the 2-sigma calibrated age range and project this across to the midpoint of the SL curve envelope, and use the eustatic SL at this midpoint as the estimate of eustatic SL at that time (Figure 3). The New Zealand eustatic SL curve was developed by *Gibb* [1986] using wood and shell radiocarbon ages selected from tectonically stable parts of the New Zealand coastline (Figure 3). Taking the upper and lower bounds of the eustatic SL curve envelope produces a wide range of eustatic SL elevations; there can be up to 15 m of uncertainty where the curve is very steep (Figure 3). For consistency we take the midpoint eustatic SL and apply an arbitrary uncertainty of ± 2 m at a 95% confidence interval to all paleo-SL estimates. We try to produce paleoenvironmental reconstructions where the eustatic SL change between each age control point is within 2 m of the change predicted by the eustatic SL curve.

[13] When considering preserved sediment thicknesses and relationships to eustatic SL changes we do not account for the affects of postdepositional sediment compaction. A study of Holocene intertidal sediments infilling the Forth Valley, Scotland, by *Paul and Barras* [1998] examined the effects of compaction on silty clays with shelly lenses, similar to the Pakarae River mouth sediments. They found that over a 20 m thickness of sediment a maximum of 2.5 m of correction was required to approximately account for the affects of compaction. This equates with a midsection correction of $\sim$10% of the bed thickness [*Paul and Barras*, 1998]. Therefore it is likely that the Pakarae River mouth sediments have compacted slightly but the correction required to account for this is minor in comparison to the magnitudes of eustatic and tectonic relative SL changes that we will be discussing. Furthermore, the gravel layers within the Pakarae River mouth sequence probably undergo little to no postdepositional compaction. The clast-supported nature of the gravels means that water expulsion has little effect on bed thickness.

2.1.3. Average <7 ka Timing and Magnitude of Tectonic Events at Pakarae

[14] The marine terraces at the Pakarae River mouth record tectonic uplift subsequent to the stabilization of SL at $\sim$7 ka. During that time sudden uplift events have

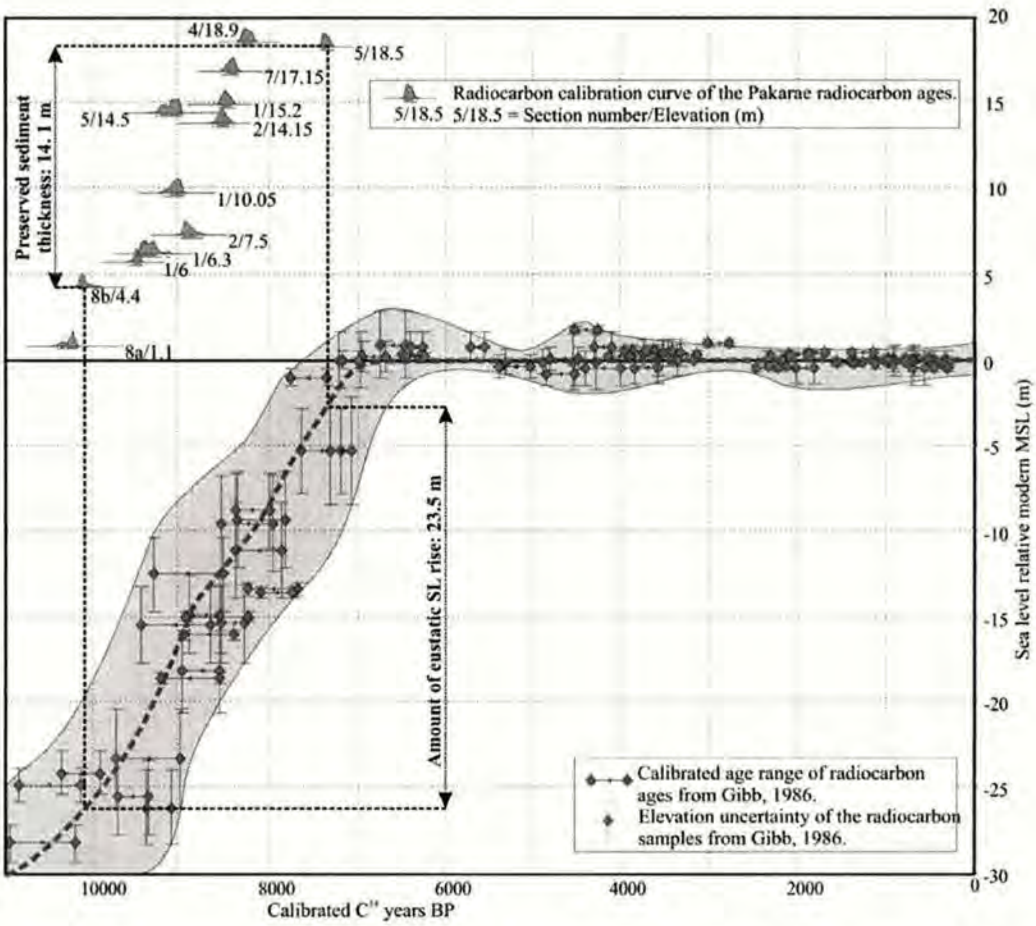

Figure 3. Pakarae transgressive sequence radiocarbon ages plotted at their modern elevation (m AMSL) and the data of *Gibb* [1986] to envelope the New Zealand eustatic SL curve. Radiocarbon ages are calibrated using OxCal v3.10 (B. Ramsey, 2005), marine samples are calibrated using the calibration curve of *Hughen et al.* [2004], and wood samples are calibrated using Southern Hemisphere atmospheric data from *McCormac et al.* [2004]. Dashed lines and arrows show a comparison between the thickness of sediment preserved at Pakarae and the amount of eustatic SL rise that occurred from ~10,100 cal years B.P. to ~7300 cal years B.P. The deficit between these two measurements approximates the net amount of tectonic uplift that occurred during that time interval.

occurred at an average interval of 850 ± 450 years with an average coastal uplift magnitude of 2.7 ± 1.1 m per event [*Ota et al.*, 1991; *Wilson et al.*, 2006]. It is possible that the characteristics of tectonic uplift at the Pakarae locality changed during the Holocene, nevertheless our paleoenvironmental models for the early Holocene attempt to stay within the uncertainties of the post-7 ka single uplift event measurements.

2.2. Age Control

[15] Age control is derived from radiocarbon ages and the tephrochronology presented by *Wilson et al.* [2007a]. Nine estuarine shell radiocarbon ages and three detrital wood radiocarbon ages were obtained from throughout the Pakarae valley infill sedimentary sequence (Figure 3 and Table 1). The tephra at ~7 m above mean sea level (AMSL) in sections 5–8 is identified as the Rotoma (9535–9465 cal years B.P. [*Froggatt and Lowe*, 1990]).

3. Results: Paleogeographic Evolution of the Pakarae River Paleoestuary

3.1. Models of Estuary Evolution

[16] We identify eight stages of paleogeographic evolution of the Pakarae River paleoestuary. There is evidence for at least two significant marine regressions that we suggest are tectonically driven coastal uplift events. A third uplift

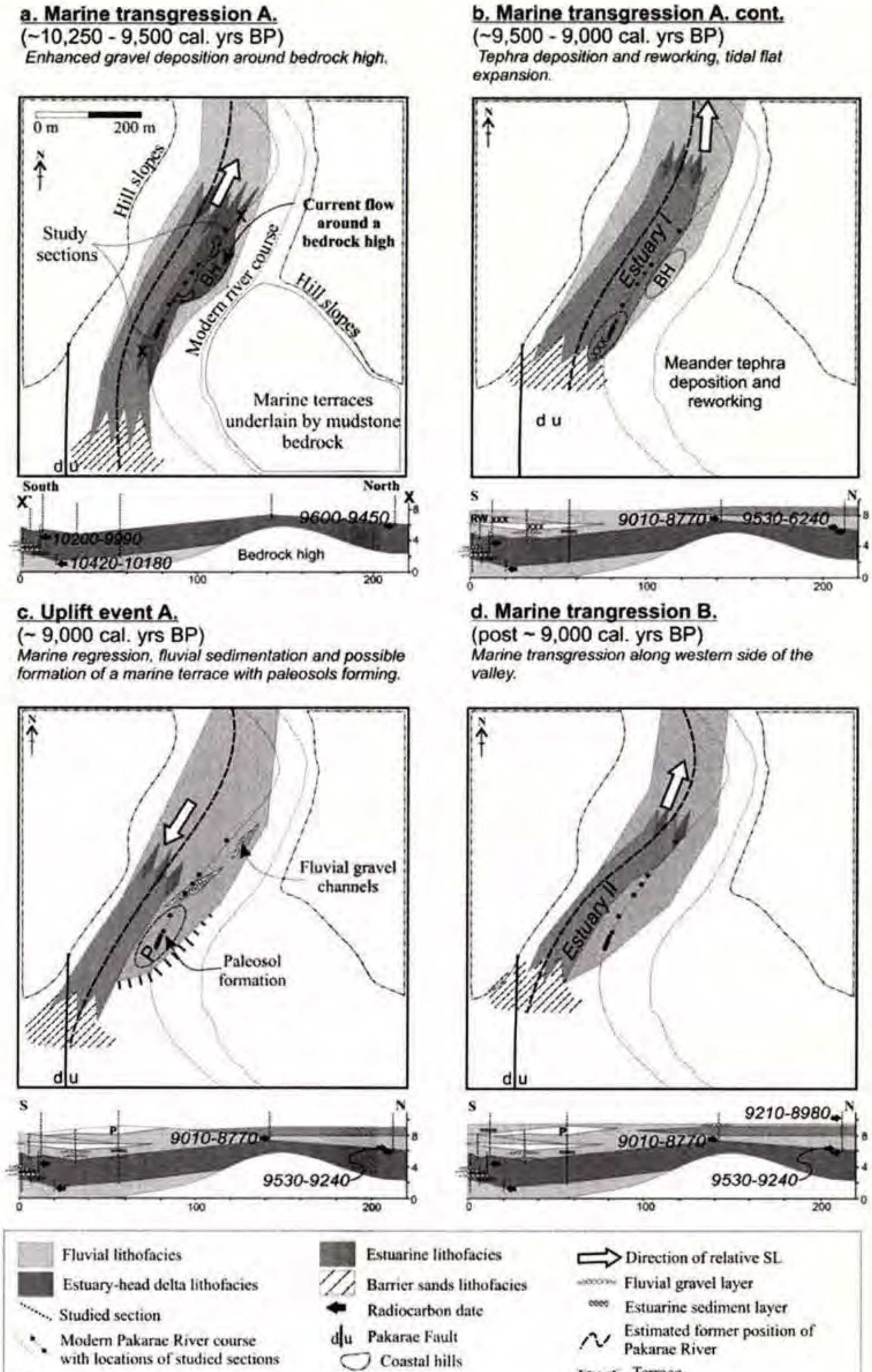

Figure 4. Paleogeographic evolution of the Pakarae River, reconstruction of preserved stratigraphy and relative SL changes from ~10 to 7 ka.

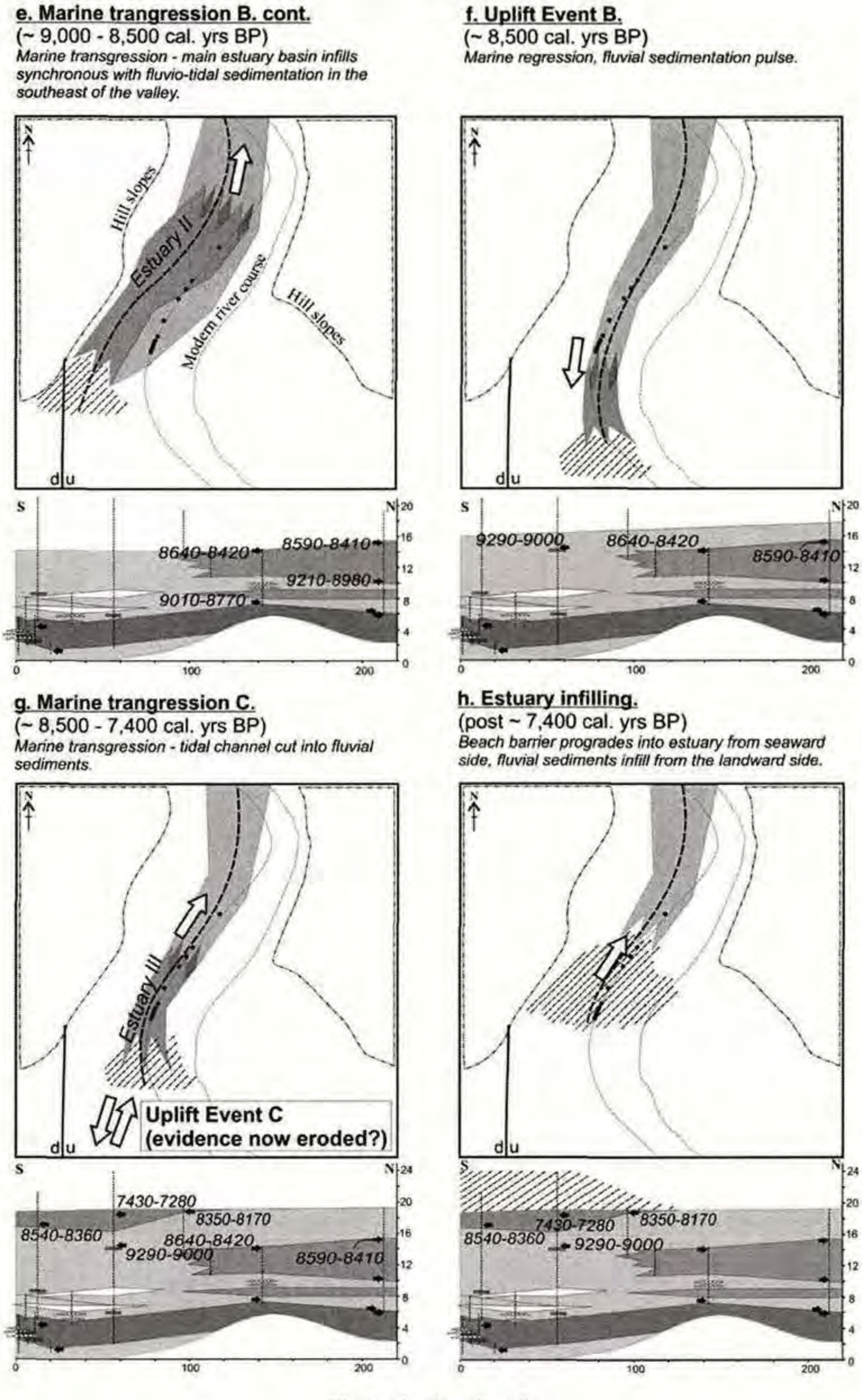

Figure 4. (continued)

event is inferred from a significant accommodation space deficit.

3.1.1. Marine Transgression A: ~10.25–9.5 ka

[17] The oldest sedimentary unit is an alluvial unit that represents SL lowstand deposition. The floodplain facies, consisting of massive silt with occasional gravel beds, forms the basal surface upon which transgressive marine deposits subsequently accumulated. Detrital wood within the basal floodplain facies has a radiocarbon age of 10,420–10,180 cal years B.P. cal years B.P. Estuary head delta deposits overly the floodplain facies. These deltaic deposits appear as a laterally continuous unit of gravel. The poorly sorted nature and clast angularity implies a short transportation distance of the sediments. We infer that the gravel clasts were sourced from the mudstone bedrock high that outcrops at the base of section 1 or from hillsides flanking the Pakarae River valley. Prior to gravel deposition, at ~10,300 cal years B.P., New Zealand eustatic SL was ~−24 ± 2 m and rising at ~7 mm/yr. The estuary head delta sediments probably represent the first incursion of the marine environment into the incised valley that the Pakarae River had cut during the previous glacial lowstand. Two radiocarbon ages from estuarine shells within the estuary head deltaic gravels indicate the sedimentary unit decreases in age toward the north (Figure 2). This is consistent with a transgressive marine sequence. Our paleogeographic reconstruction shows a transgressive estuary with gravel deposition around the bedrock high (Figure 4a).

3.1.2. Marine Transgression A Continued: ~9.5–9 ka

[18] Overlying the estuary head gravels are floodplain and estuarine sediments. The nonmarine sediments may have accumulated around a topographic high created above the basement outcrop at the base of section 2. The Rotoma tephra was deposited and preferentially accumulated in the downstream sections (S5–S8). The overthickening and lenticular shape of the tephra probably represents infilling of an abandoned oxbow of the river. This suggests that the river mouth was located farther to the west than it is at present. Estuarine facies were deposited in the sections S1 and S2 up to ~9 ka. This unit is called estuary I (Figure 4b).

3.1.3. Uplift Event A: ~9 ka

[19] At an elevation of ~9 m AMSL the estuary I facies is overlain by floodplain sediments and, at equivalent elevations in the southern sections, a series of paleosols are present. Both of these transitions provide evidence of a significant, and sudden marine regression. Eustatic SL was rising during this time period and estuarine facies might therefore be expected to be overlain, in a normal stratigraphic order, by increasingly marine-influenced sediment. That estuary I is instead overlain by nonmarine floodplain sediments indicates either that there was a fall in SL due to tectonic uplift or that there was rapid fluvial progradation. The paleosols in sections 5–7 occur within floodplain silts. Paleosols represent a period of time when a surface did not receive sediment, and a soil was allowed to develop. Therefore rapid fluvial progradation is unlikely to have occurred at this time. It is more likely that the river was subject to a fall in its base level, a change that lowered the elevation at which fluvial sediments were deposited. A fall in river base level is consistent with a marine regression. This could have been caused by eustatic SL fall, a change in fluvial discharge or tectonic uplift. The New Zealand eustatic SL curve of *Gibb* [1986] is not of sufficient resolution to discount a eustatic SL fall. *Carter et al.* [1986] used submerged shorelines in the southwest Pacific to infer the ages of several stillstands, or hiatuses, during Holocene SL rise. The ages of the stillstands do not, however, coincide with the estimated ~9 ka environmental change at Pakarae, and a stillstand would not trigger fluvial incision into an already existing estuary. Furthermore, sea level falls can result in fluvial channel readjustments (e.g., changes to sinuosity or bed roughness) rather than incision [*Schumm*, 1993; *Holbrook and Schumm*, 1999; *Wellner and Bartek*, 2003]. Assuming estuary I was close to the shoreline, a change in river discharge or decreased sediment supply would not have caused a significant (if any) incision due to its proximity to the base level. Furthermore, a change in fluvial discharge is most likely to be climatically controlled, hence of regional extent. However, eastern North Island offshore sediment cores do not display any significant changes in sediment flux at this time [*Foster and Carter*, 1997; *Carter et al.*, 2002].

[20] Sharp changes from intertidal foraminifera assemblages to foraminifera-barren ones at the estuary I–floodplain contact suggests that this base level fall was sudden [*Wilson et al.*, 2007a]. The paleogeographic reconstruction shows a southward shift in the marine-floodplain interface (Figure 4c). The floodplain environment moved over sections 1 and 2, at sections 5–7 a fluvial terrace formed upon which the paleosols developed. This terrace is analogous to the fluviotectonic terraces present at the modern Pakarae River mouth. There is no evidence in outcrop of a scour surface that records the river base level fall. This would provide further evidence of fluvial incision but could probably only be located by drilling. Eustatic SL was rising during this period, therefore the most likely cause of a marine regression is tectonic uplift, we call this uplift event A. Uplift must have been of a sufficiently large amount to elevate the more southern sections (sections 5–7) above the depositional height of floodplain sediments (although we cannot quantify this amount) and to raise estuary I out of intertidal range. Estuary I contains foraminifera assemblages dominated by *Ammonia aoteana* (a species dominant at intertidal-subtidal elevations in brackish environments [*Hayward et al.*, 1999]) and fragments of *Austrovenus stutchburyi* (a common estuarine shell that lives between MSL and subtidal elevations, Figure 2 [*Marsden and Pilkington*, 1995; *Morton*, 2004]). The occurrence of these two species together suggests that the sediment of estuary I was deposited at MSL or slightly deeper. The Pakarae River mouth beach has a spring tidal range of 1.7 m. Therefore the only firm constraint we can place on the magnitude of uplift event A is that it was probably >0.85 m. The amount of uplift can also be roughly estimated from the paleosols. If it takes approximately 200–300 years for a soil to develop on a fluvial terrace and eustatic SL was rising at ~7 mm yr^{-1}, then the terrace must have been uplifted by >1.4–2.1 m to allow sufficient elevation before marine inundation resumed.

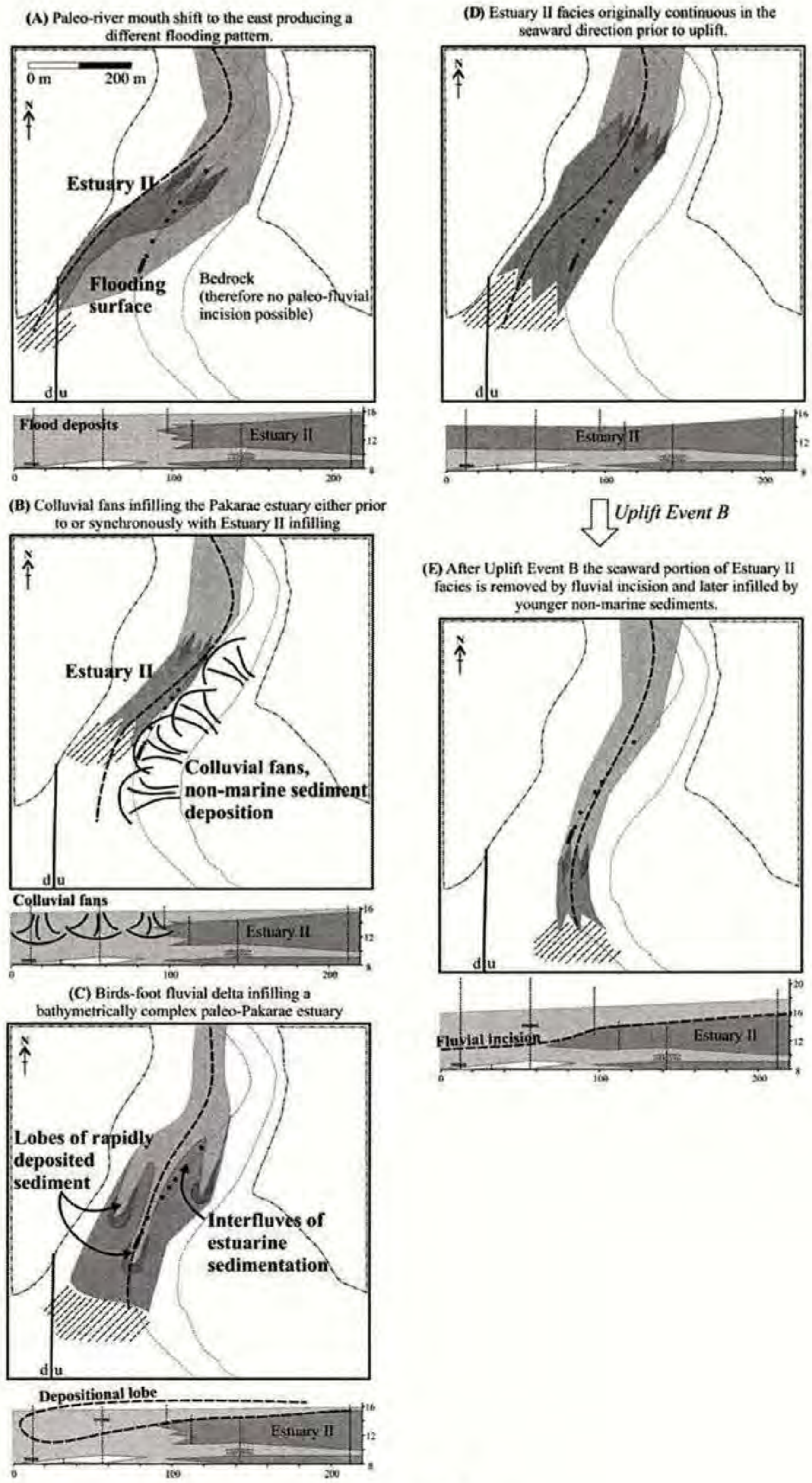
(A) Paleo-river mouth shift to the east producing a different flooding pattern.
0 m
200 m
N
Estuary II
Flooding surface
Bedrock (therefore no paleo-fluvial incision possible)
d u
Flood deposits
Estuary II
(B) Colluvial fans infilling the Pakarae estuary either prior to or synchronously with Estuary II infilling
N
Estuary II
Colluvial fans, non-marine sediment deposition
d u
Colluvial fans
Estuary II
(C) Birds-foot fluvial delta infilling a bathymetrically complex paleo-Pakarae estuary
N
Lobes of rapidly deposited sediment
Interfluves of estuarine sedimentation
d u
Depositional lobe
Estuary II
(D) Estuary II facies originally continuous in the seaward direction prior to uplift.
N
d u
Estuary II
Uplift Event B
(E) After Uplift Event B the seaward portion of Estuary II facies is removed by fluvial incision and later infilled by younger non-marine sediments.
N
d u
Fluvial incision
Estuary II

Figure 5

3.1.4. Marine Transgression B: Post-9 ka

[21] Floodplain sediments were deposited in all sections following the above inferred uplift event. As discussed, the southern sections must have been subaerial for sufficient periods of time to allow paleosols to form. Two to three paleosol units can be distinguished. This shows there may have been intermittent flooding of the surface as the base level of the river increased in elevation with rising eustatic SL before it was completely overwhelmed by fluvial sedimentation. In the northern sequence (in sections 1 and 2) 1–2 m of fluvial silt and gravel was deposited over the silty clay sediments of estuary I. When eustatic SL became high enough following uplift event A, an estuary called estuary II was reestablished in the northern sections. *A. stutchburyi* shells from the base of estuary II have a radiocarbon age of 9210–8980 cal years B.P. This age overlaps (at the 2-sigma interval) with a shell age at the base of estuary I (Figure 4d). We suggest that the shells at the base of estuary II were reworked from deposits at the top of estuary I. No cross-cutting occurs between Estuaries I and II in the outcrop but these radiocarbon ages suggest it does occur elsewhere in the sequence. At the same time that estuary II reestablished in sections 1 and 2, nonmarine sedimentation continued in the southern sections. This apparent anomaly of having nonmarine sedimentation south, or in the possible seaward direction, of a marine environment is discussed further below (section 3.1.5).

3.1.5. Marine Transgression B Continued: 9–8.5 ka

[22] Estuary II was infilled during Marine Transgression B (Figure 4e). The thickness of the intertidal estuarine infill ranges from 3.5 to 5.5 m (decreasing thickness southward, Figure 2). Radiocarbon ages from the top of estuary II range between 8640 and 8410 cal years B.P. (Figure 4e). We therefore estimate that estuary infilling ceased at ~8.5 ka. Infilling of estuary II took place over ~500 years. During the time period of infilling between 9 and 8.5 ka, there was ~5–8 m of eustatic SL rise. Accounting for uplift in event A of ~2–3 m, 1 m of fluvial deposition and the 5.5 m of estuarine sediment in section 1, the thickness of the estuary II facies is consistent with the amount of eustatic SL rise during this time interval (within the uncertainty of the radiocarbon ages and the eustatic SL curve, Figure 3).

[23] Floodplain facies were deposited southward of estuary II. The southward direction is the modern seaward direction. If we assume that the paleoestuary was always aligned approximately north-south (this is reasonable given the valley is bedrock controlled), then it appears that nonmarine sediments accumulated seaward of estuary II. How this sedimentation pattern could have occurred is not fully resolved. We offer four possible paleogeographic scenarios including scenario A in which the paleoriver mouth may have been in a different location therefore producing a different flooding pattern and scenario B for birds foot fluvial delta. The southward nonmarine sediments were deposited as lobes within an estuarine environment in which localized sedimentation rates were too high for marine fauna to survive or they are too heavily diluted to be detected; in scenario C, colluvial fans were depositing sediment above MSL in the southern sections or scenario D is for fluvial cut and fill: Originally, present estuarine sediments were removed from the southern sections by postuplift incision to be replaced by younger floodplain sediments (Figure 5). It is not well determined whether the floodplain facies of the southern sections was emplaced prior to, synchronously with, or after emplacement of estuary II. A detrital wood fragment radiocarbon age of 9290–9000 cal years B.P. from the floodplain facies of section 5 is older than estuarine shell ages from equivalent elevations in sections 1 and 2 (radiocarbon ages of 8640–8420 and 8590–8410 cal years B.P., Figure 2). This supports model B (birds foot delta) or model C (colluvial fan) as both of these scenarios require emplacement of the southern nonmarine sediment prior to estuary establishment in the northern sections. However, because the wood is detrital and could have been reworked, while the shells are in situ, the wood age is a less reliable indicator of sediment depositional age than the shells.

[24] None of these scenarios are entirely consistent with the stratigraphic and age data of the Pakarae River mouth sedimentary sequence. A combination of the above processes may be responsible. The width of the Pakarae River paleovalley (<200 m) is relatively narrow and leaves little room for multiple, or migrating sediment deposition lobes. An alternative river mouth orientation (model A) is unlikely because marine terraces on the east side of the river are underlain by mudstone bedrock. Therefore the paleoriver mouth cannot have been located to the east, this only leaves a narrow valley width open to the west (<140 m). Such a small shift in the river mouth location is not likely to have caused a radically different flooding pattern in the Pakarae valley and the proximity to the paleoshoreline would have limited the elevation to which fluvial sediments may have been deposited. The birds foot delta scenario unrealistically implies that sediment delivered to the estuary by the river bypassed sections 1–3, without entraining any of the inhabitant marine fauna and preferentially settled seaward in sections 5 and 7. To inhibit colonization by marine fauna, we have implied that sedimentation rates must have been very rapid. However, section 1 indicates sedimentation rates here were approximately equal to the rate of eustatic SL rise. By inference, rates in sections 5 and 7 must have been greater than the rate of eustatic SL rise. Therefore sediment would have quickly built up above MSL. Colluvial fan deposition is inconsistent with the presence of horizontal sedimentary bedding structures seen throughout the nonmarine facies. Postuplift fluvial cut and fill is possible, although there are no detectable unconformities evident of an incision horizon within the nonmarine sediments of sections 5 and 7.

Figure 5. Four scenarios to explain the juxtaposition of seaward barren sediments against landward estuarine sediments with a rich marine fauna in the Pakarae paleovalley (see Figure 4d for the map legend). (a) Alternative paleoriver mouth orientation. (b) Colluvial fans entering paleoestuary. (c) Birds foot fluvial delta infilling the paleoestuary. (d and e) Postuplift fluvial incision removing seaward estuary II facies.

3.1.6. Uplift Event B: ~8.5 ka

[25] Abandonment of estuary II occurred ~8.5 ka. Like the abandonment of estuary I, this regressive estuarine-floodplain transition is inconsistent with rising eustatic SL and could represent either a tectonic uplift or fluvial progradation (Figure 4f). The radiocarbon ages of the highest shells in sections 1 and 2 are statistically indistinguishable with ages of 8590–8410 and 8640–8420 cal years B.P., respectively. This synchronicity in paleoenvironmental change at these two locations is consistent with a sudden tectonic uplift event. If fluvial progradation caused estuary abandonment, then the shell ages from the top of the estuarine facies would be expected to get younger seaward. A layer of *Paphies australis* shells characteristically marks the contact between marine and floodplain sediments in sections 1–3 (Figures 2 and 6). The abrupt changes in the foraminifera assemblages (from intertidal to barren), and the presence of life assemblages of *P. australis* indicate marine regression from this site was rapid. Life assemblages are those in which there are a range of shells from juvenile to adult. *Hull* [1987] infers sudden death from the preservation of life assemblages because if the environmental change was gradual, then the smaller, and younger, species component of the assemblage would have moved to more suitable environments. Again, eustatic SL was rising during this time period; therefore a tectonic uplift event is the most likely explanation for the marine regression. We call this uplift event B (Figure 4f).

3.1.7. Marine Transgression C: 8.5–7.4 ka

[26] The highest elevation and youngest estuarine facies, correlated between sections 4, 5, and 7, represents estuary III. This estuary evolved due to eustatic SL transgression (Figure 4g). Three radiocarbon ages have been obtained from this facies (Table 1). Two ages of poorly preserved shells at the base of the facies are 8350–8170 cal years B.P. (section 4, 18.9 m) and 8540–8360 cal years B.P. (section 7, 17.15 m). Well-preserved shells from near the top of the facies have an age of 7430–7280 cal years B.P. (section 5, 18.3–18.7 m). The large age differences and contrasts in shell preservation imply two shell populations within estuary III. We suggest that the older, degraded shells are reworked. They may have been transported from the seaward part of estuary III when it was initially established seaward of its present location or removed from the top of estuary II if it has been incised by estuary III elsewhere in the sequence. The base of the estuarine facies is sharp and probably represents a transgressive surface (in the nomenclature of *Dalrymple et al.* [1992] and *Allen and Posamentier* [1993], Figure 6).

[27] If we assume the shell age of 7430–7280 cal years B.P. is from an in situ sample and representative of the age of infilling of estuary III, then there was an interval of ~1160 years between the occupations of estuary II and estuary III (calculated from the difference between the midpoints of the bounding radiocarbon ages). During this time interval there was ~10 ± 2 m of eustatic SL rise (Figure 3). The elevation difference between the in-place dated shells in estuary II and estuary III is 3.5 m. The calculated accommodation space deficit (the difference between preserved sediment thickness and the amount accommodation space created by eustatic SL rise) is ~6.5 ± 2 m (Figure 7). One uplift event horizon has been identified during this time period: that at the top of estuary II, inferred to represent uplift event B. It is unlikely, however, that a single event could account for the entire accommodation space deficit of ~6.5 m. For example the M_W 7.4 1931 Napier earthquake produced a maximum of 3.5 m of coastal uplift [*Hull*, 1990] and by comparison of the faults rupture areas, *Berryman* [1993] estimated events of M_W 7.5–8 were required to uplift the Mahia Peninsula marine terraces up to 4 m. Average uplift magnitudes at the Pakarae River mouth are 2.7 ± 1.1 m per event [*Ota et al.*, 1991; *Wilson et al.*, 2006]. The accommodation space deficit of ~6.5 m probably represents at least two uplift events: uplift event B as well as an inferred, uplift event C. This scenario would be broadly consistent with the uplift event frequency inferred from the marine terrace data. Marine terraces were formed at intervals of 850 ± 450 years [*Wilson et al.*, 2006], and the accommodation space deficit of 6.5 m accumulated over ~1160 years; therefore two uplift events within this time interval are feasible. Evidence for uplift event C was probably recorded in the sedimentary sequence seaward of section 7. This part of the sequence has been eroded during marine terrace formation.

3.1.8. Estuary Infilling and Marine Regression: Post-7.4 ka

[28] The upper contact between estuary III and the barrier sands is gradational (Figure 6). This unit represents infilling of the paleoestuary during the last several hundred years of eustatic SL rise (~7.4–7 ka, Figure 4h). Some scouring at the base of tidal channel gravels can be seen (Figure 6), consistent with a tidal ravinement surface [after *Dalrymple et al.*, 1992]. The barrier sands grade upward into aeolian sands. After ~7 ka marine regression continued due to repeated tectonic uplift events during the subsequent period of stable eustatic SL, as recorded by the mid to late Holocene marine terraces.

4. Discussion

4.1. Chronology of Relative SL Change

[29] Our paleogeographic reconstructions have been used to identify three previously unrecognized uplift events in the Holocene: Two event horizons are distinguished by abrupt regressions within the Pakarae River sedimentary sequence (uplift events A and B) and a third, younger uplift event is inferred from a significant accommodation space deficit between 8.5 and 7.4 ka B.P. (uplift event C). The oldest event (uplift event A) occurred ~9210–8770 cal years B.P. The magnitude of uplift was >0.85 m and was sufficient enough to cause the river to abandon its bed (creating a fluvial terrace) and grade to a new base level (section 3.1.3). The timing of the second event, uplift event B, is well constrained by two radiocarbon ages dating the death of shells due to estuary abandonment. This occurred at 8640–8410 cal years B.P. The third event, uplift event C, occurred in the time interval between the uplift event B and 7430–7280 cal years B.P. No magnitude constraints can be placed

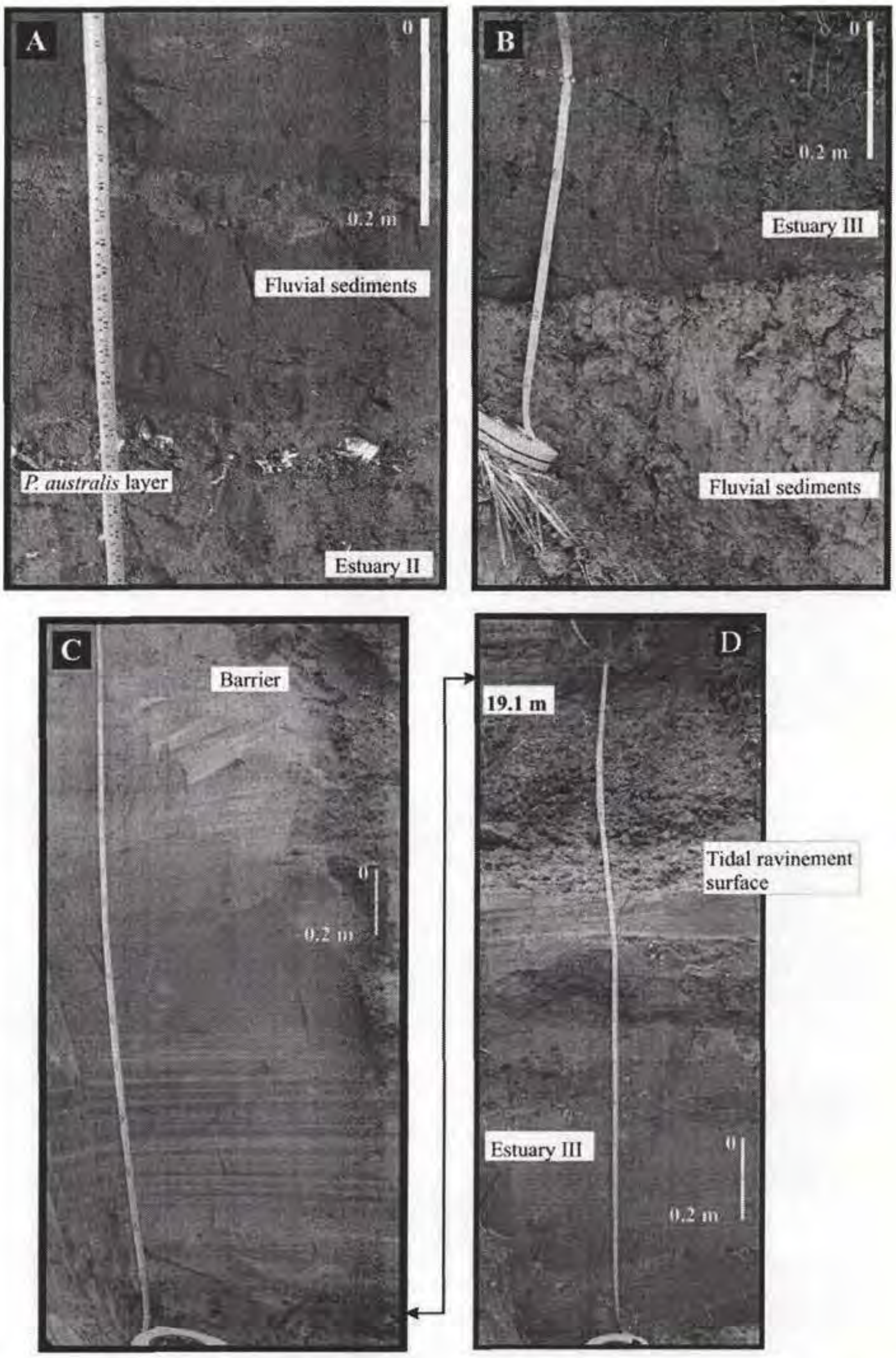

Figure 6. (a) Section 1, facies contact between estuary II and fluvial sediments at ~15.3 m AMSL. Shells are *P. australis*. (b) Sections 5, facies contact between fluvial sediments and the base of estuary III, ~16.2 m AMSL. (c and d) Section 5, facies contact between barrier sands and the top of estuary III: ~19–20 m AMSL (Figure 6c) and ~19–17.5 m AMSL (Figure 6d).

on the uplift events B and C. However, accommodation space deficits suggest a combined vertical movement of 6.5 ± 2 m. A new relative Holocene SL curve for the Pakarae locality has been constructed using data presented here and marine terrace data of *Ota et al.* [1991] and *Wilson et al.* [2006] (Figure 8).

[30] The relative SL curve is a significant revision of the previous curve constructed for the Pakarae locality by

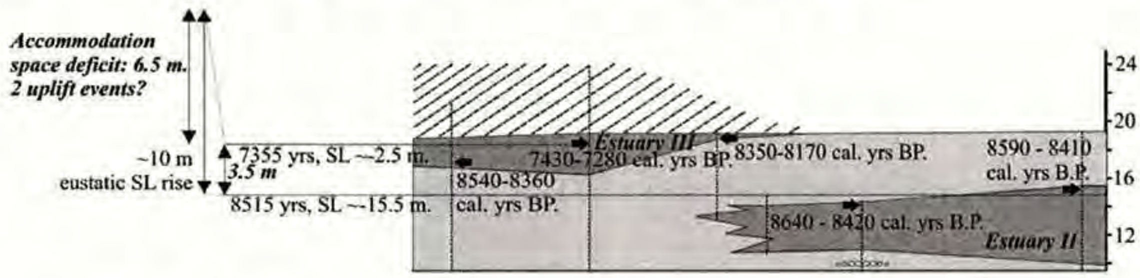

Figure 7. Relationships between preserved sediment thickness and amounts of eustatic SL rise for the time period between the deposition of estuary II and estuary III.

Berryman et al. [1992]. The Berryman et al. curve showed a similar trend but evidence of pre-7 ka uplift was based only on accommodation space deficits, not on specific facies distributions, and individual events were not delineated. As previously discussed, *Berryman et al.* [1992] suggested a relative SL fall at ~10,500–9500 cal years B.P., which they inferred to have been a eustatic regression rather than tectonic one based partly on correlation to the eustatic SL curve. Recent calibration of the *Gibb* [1986] SL curve does not show the equivalent change in trend at ~10.5–9.5 cal years B.P. Our data does not support an uplift event during this time period. However, if one did occur near 10,500 cal years B.P., the Pakarae River mouth sedimentary sequence would have been unlikely to preserve a record of it, as the sequence is younger than ~10,400 cal years B.P. and the location was probably undergoing terrestrial (floodplain) sedimentation at that time.

4.2. Uplift Rates

[31] The radiocarbon ages obtained from the Pakarae River transgressive sequence, in combination with the *Gibb* [1986] eustatic SL data, can be used to calculate average uplift rates over time periods extending back to ~10,000 cal years B. P. (Table 2). We obtain an average uplift rate is 3.15 ± 0.8 mm/yr (excluding the wood radiocarbon ages as the depositional elevation of these samples relative to MSL is uncertain). This rate is of the same as that calculated using the younger Pakarae River mouth marine terrace data [*Wilson et al.*, 2006] and indicates steady average uplift rates of the Pakarae locality since ~10,000 cal years B.P.

4.3. Tsunami Events

[32] With such a high frequency of coastal uplift (i.e., earthquake) events Pakarae River mouth is an obvious

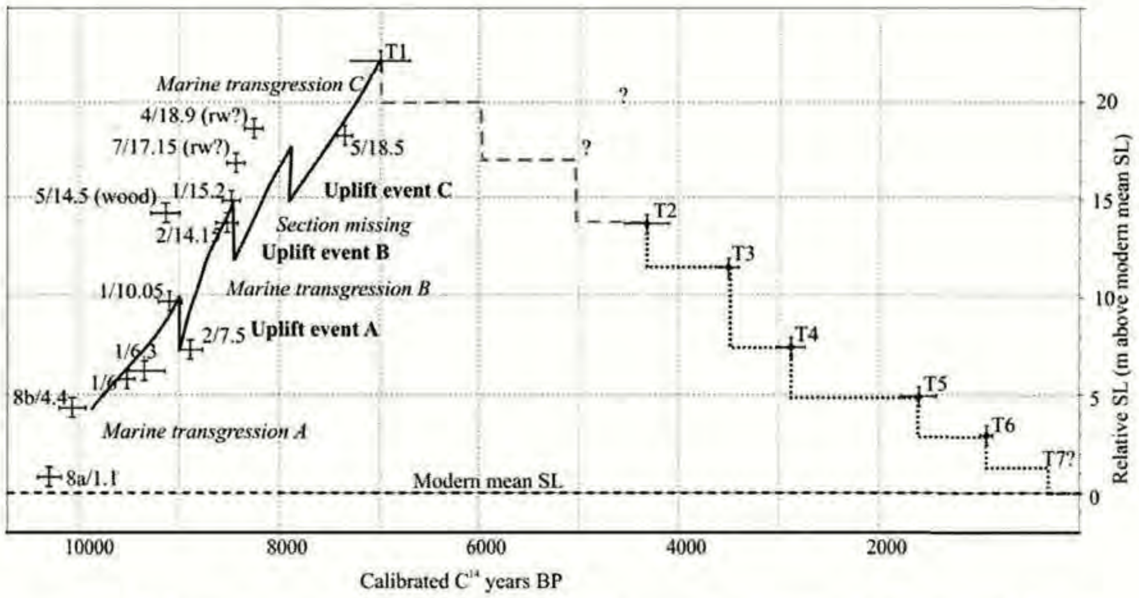

Figure 8. Pakarae locality Holocene relative SL curve. Transgressive sequence data presented in this study and the post-7 ka marine terrace data presented by *Wilson et al.* [2006]; (rw?), probable reworked sample.

Table 2. Calculation of Holocene Uplift Rates as Estimated From Radiocarbon Ages Obtained From the Pakarae River Mouth Transgressive Sedimentary Sequence

Section	Sample Height, m	Calibrated Age 2 sigma, cal years B.P.	Sea Level at Time of Deposition,[a] m	Total Uplift,[b] m	Uplift Rate,[c] mm/yr	Minimum Uplift Rate,[d] mm/yr	Maximum Uplift Rate,[e] mm/yr
1	15.2 ± 0.22	8,590 − 8,410	−12	27	3.2	2.9	3.4
1	10.05 ± 0.22	9,210 − 8,980	−19	28.85	3.2	2.9	3.4
1	6.3 ± 0.22	9,530 − 9,240	−20	26.1	2.8[f]	2.5	3.0
1	6 ± 0.22	9,600 − 9,450	−22	27.8	2.9	2.7	3.2
2	14.15 ± 0.22	8,640 − 8,420	−12.5	26.45	3.1	2.8	3.4
2	7.5 ± 0.22	9,010 − 8,770	−18	25.3	2.8	2.6	3.1
4	18.9 ± 0.22	8,350 − 8,170	−12.5	31.2	3.8	3.5	4.1
5	18.3–18.7 ± 0.22	7,430 − 7,280	−2.5	20.8	2.8	2.5	3.1
5	14.5 ± 0.22	9,290 − 9,000	−19.5	34	3.7[f]	3.4	4.0
7	17.15 ± 0.22	8,540 − 8,360	−14.5	31.45	3.7	3.4	4.0
8a	1.1 ± 0.31	10,420 − 10,180	−27	28.1	2.7[f]	2.5	3.0
8b	4.4 ± 0.31	10,200 − 9,990	−26	30.2	3.0	2.8	3.2

[a]Sea level estimated using *Gibb*'s [1986] New Zealand Holocene sea level curve; the midpoint of the 2σ calibrated radiocarbon age is projected to the SL curve; we estimate an uncertainty of ±2 m using this method.
[b]Total uplift = modern sample elevation − eustatic SL at time of deposition.
[c]Uplift rate = (total uplift)/(midpoint of the 2σ calibrated radiocarbon age). Average is 3.15 and 2 SD is 0.8.
[d]Minimum uplift rate = (total uplift −2 m)/(maximum 2σ calibrated age).
[e]Maximum uplift rate = (total uplift +2 m)/(minimum 2σ calibrated age).
[f]Wood samples, may have been deposited above MSL; therefore these are maximum uplift rates.

candidate for tsunami inundation. Tsunamigenic sources include an offshore thrust fault, the Pakarae normal fault, the Hikurangi subduction interface, trans-Pacific tsunamis (particularly from South America), submarine landslides, and other offshore faults such as the Lachlan Fault. Tsunami deposits can be recognized as anomalous high-energy influxes into low-energy environments [*Cochran*, 2002; *Goff et al.*, 2001]. There are many high-energy sedimentary layers in the Pakarae River sedimentary sequence that could be indicative of tsunamis. However, in general the sequence is too variable to be able to isolate anomalous deposits and unequivocally attribute them to a tsunami. Our facies analysis has shown that this paleoestuary was extremely dynamic. It would be difficult to distinguish tsunami-emplaced layers from other high-energy environments or events such as tidal channels, storm deposits, and flood deposits. For example, Figures 9b and 9c show two shell and gravel layers within laminated estuarine silts. These gravel layers could be tsunami deposits, suggesting a high frequency of events, or they could represent migrating tidal channel lags within the estuary. Mapping the extent of the deposits would be required to differentiate between channel and more extensive flood or tsunami deposits.

[33] One unit that we suggest may be a tsunami deposit is a coarse sand layer within section 1 at ~15.5 m AMSL (Figure 9a). The base of this unit is erosional and it contains entrained silt rip-up clasts; the sand displays unidirectional, high-angle bedding. There are scattered shells even though the unit occurs within floodplain sediments. These features are all indicative of a tsunami deposit. However, the unit occurs 0.23 m above the horizon marking the abandonment of estuary II, a horizon which has been identified as representing uplift event B. The unit cannot be correlated to sections 2 and 3, which also display the uplift event horizon. If the coarse sand influx was a tsunami generated by the uplift event, then we are uncertain what the intervening 0.23 m of silt sediment represents. It may be that sediment was deposited immediately following uplift event B (though it does not display any chaotic or colluvial-type sediments). Alternatively, the tsunami deposit may be unrelated to uplift event B, and may have been from a different tsunamigenic source. This layer has a depositional age of <8600 cal years B.P. A possible tsunami deposit dated at ~8000 cal years B.P. has been identified within a paleoestuary sequence at Hicks Bay, 100 km north of the Pakarae locality [*Wilson et al.*, 2007b]. These tsunami deposits may correlate and be indicative of a regional tsunamigenic source such as the Hikurangi subduction interface or a trans-Pacific Ocean tsunami. These examples demonstrate the complexity of distinguishing tsunami deposits within a dynamic estuary such as Pakarae River mouth.

4.4. Interpretation of Transgressive Sequences for Paleoseismology

[34] We identify three major reasons why transgressive deposits are useful in coastal paleoseismic studies: (1) the ability to extend earthquake records prior to the time of eustatic SL stabilization, (2) potential for application on coastlines that do not preserve marine terraces, and (3) the ability to distinguish mechanisms of uplift on coastlines without historical occurrences of coseismic uplift. These are discussed further.

[35] 1. As previously stated, coastal neotectonic studies are frequently limited by the length of time since eustatic SL stabilization. This study has demonstrated that transgressive fluviomarine deposits can record evidence of tectonic events prior to eustatic SL stabilization for the Holocene. This

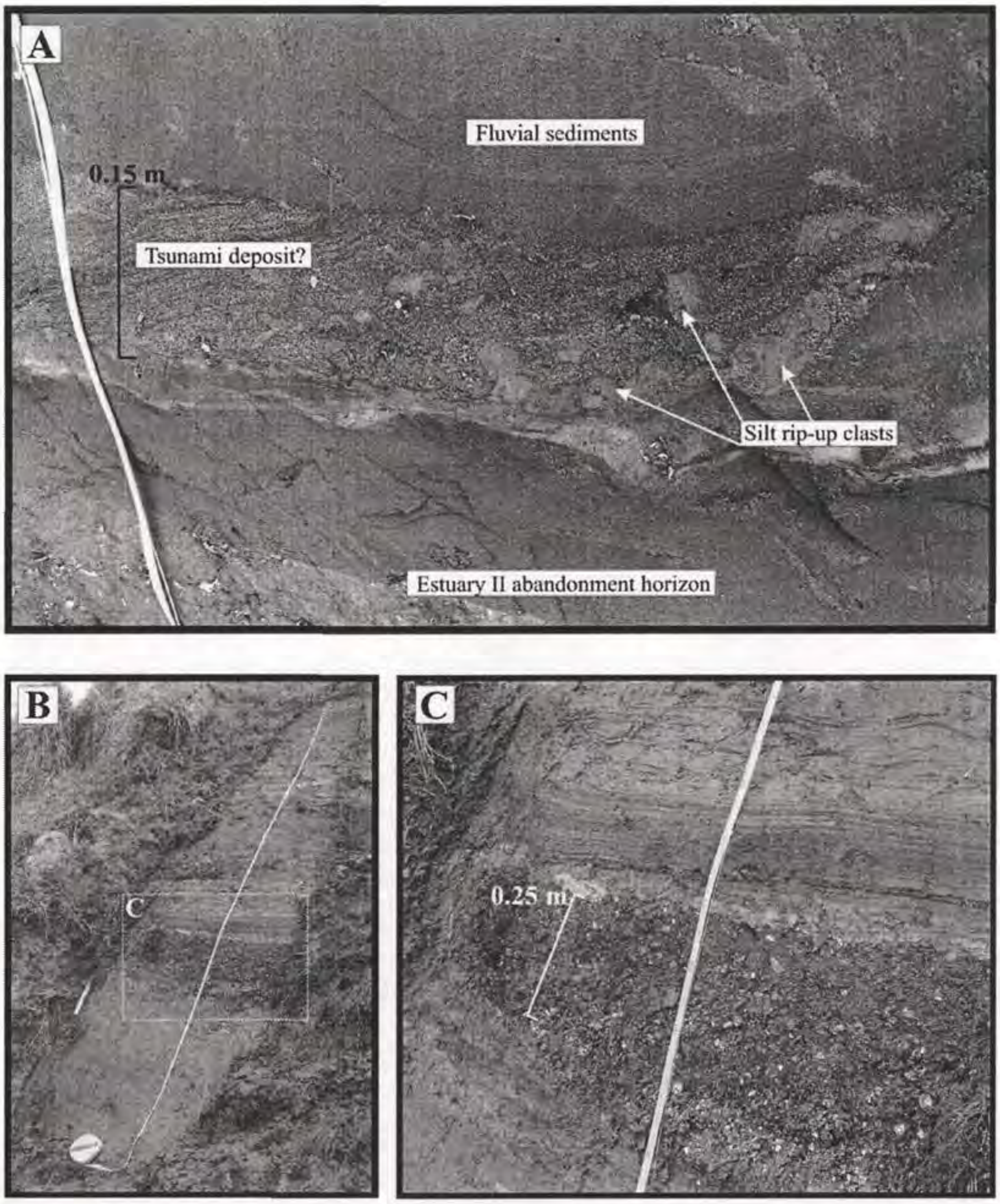

Figure 9. Examples of high-energy sedimentary units within low-energy paleoenvironments. (a) Section 1, ~15–16 m AMSL. (b) Section 3, ~11–15.8 m AMSL. (c) Section 3, 12–13 m AMSL.

technique may therefore be particularly valuable in regions with long recurrence intervals.

[36] 2. During postglacial SL rise estuaries were probably widespread along the New Zealand coastline, as they were globally. These are now largely infilled but the sequences may have untapped potential for coastal neotectonic studies if the locations do not display marine terraces. Many areas of the New Zealand coast are undergoing erosion, therefore where marine terraces are not well formed or have not been preserved, transgressive sequences can be a tool for determining uplift rates and mechanisms.

[37] 3. On some coastlines there may be uncertainty over tectonic uplift mechanisms. Marine terraces are frequently assumed to be coseismic landforms; however terrace morphology can be created by other processes, and on coastlines where there have been no historical occurrences of coseismic uplift this is an important issue. For example, gradual uplift coupled with periods of storminess or varying sediment supply, may create benched coastlines. Usually

these scenarios can be tested by collecting a suite of radiocarbon samples from the same marine terrace to test their coherence [*Berryman*, 1993; *Ota et al.*, 1991], and in rare cases by studying the ecological assemblages on the terrace straths [*Hull*, 1987]. This study has shown that the style of uplift events (sudden or gradual, i.e., coseismic or aseismic) can be estimated from the marine transgression fill deposits. This technique may provide a more accurate determination of uplift mechanisms than marine terraces. At the Pakarae locality the synchronicity of abandonment of estuary II, the apparent estuary-wide nature of the paleoenvironmental change and the very sharp facies contacts at the top of Estuaries I and II, are indicators that uplift was widespread and sudden. The preservation of a life assemblage of *P. australis* at the top of estuary II is a good indicator of sudden environmental changes, as is the sharp transition from intertidal foraminifera assemblages to sediments barren of foraminifera. In locations where there is uncertainty about the uplift mechanism of marine terraces, we suggest transgressive deposits, if accessible, may be useful in resolving this.

4.5. Limitations of Neotectonic Analysis of Transgressive Deposits

[38] While the use of transgressive deposits in detecting uplift events has been successful at the Pakarae locality, there are also several limitations. First, detailed local knowledge of postglacial eustatic SL rise is essential, and in areas undergoing glacioisostatic rebound, tectonic uplift signals may be more difficult to isolate. Second, it is not always possible to quantify the amount of uplift that occurs with each event. Quantification is limited by the accuracy of the eustatic SL curve and by the paleoenvironmental bathymetric control. At the Pakarae locality paleoenvironmental control is relatively weak because only in situ *A. aoteana* foraminifera were preserved. This is a common intertidal species; hence its presence places relatively little control on the position of paleomean SL. Foraminifera with greater SL sensitivity can generally be found at estuary margins. Therefore there is potential to place better constraints of the amounts of uplift if the exposures are in the right location or if drill cores can reach marginal estuarine locations. Third, a wide spatial distribution of exposures (or drill cores) is needed to detect each event. Correlation of events across different sections is needed to understand the paleogeography of the valley. Even at the Pakarae River mouth, a relatively small paleovalley, direct stratigraphic evidence of uplift event C is missing and was probably only recorded further seaward. Availability of age control also potentially limits the interpretation of uplift events from transgressive sequences. Only uplift event B has been accurately dated within the Pakarae River mouth sequence. There appears to be a high degree of shell reworking and this has limited the age constraints we can place on uplift event A. Sediment reworking is probably a common characteristic of uplifting transgressive estuaries; with rapid sediment depocenter changes as a result of alternating eustatic SL rises (causing landward movement) and tectonic uplift events (causing seaward retreat).

5. Conclusions

[39] A fluvioestuarine transgressive sequence has been used to identify tectonic uplift events that occurred during infilling of the Pakarae River incised valley. Stratigraphic evidence suggests there was abandonment of two estuarine units (at ~9000 and 8600 cal years B.P.) and microfaunal evidence suggests the paleoenvironmental change was sudden. We attribute these characteristics to rupture of an offshore reverse fault producing coseismic coastal uplift. A third uplift event at prior to ~7350 cal years B.P. is inferred from a significant accommodation space deficit.

[40] This study has extended the paleoseismic history of the Pakarae locality to cover the past 10,000 years. This is possibly the longest continuous record of coastal paleoseismology in the world. A long record has been attained through the combined use of marine terrace data, postdating the culmination of eustatic SL rise, and by the use of transgressive marine facies architecture, which relies upon constantly rising eustatic SL. The use of biostratigraphy to document the sudden nature of paleoenvironmental change adds robustness to inferences based on the marine terraces that uplift on this part of the Hikurangi margin occurs by coseismic processes.

[41] **Acknowledgments.** This research was funded by an EQC student grant (Project 6UNI/501). K.J.W. was supported by the GNS Science Sarah Beanland Memorial Scholarship. Rodger Sparks and Dawn Chambers of the Rafter Radiocarbon Laboratory are thanked for their contribution to the radiocarbon dating. Hannu Seebeck, Matt Hill, and Vicente Perez provided fieldwork assistance. This manuscript was improved thanks to reviews by John Holbrook and one anonymous reviewer.

References

Allen, G. P., and H. W. Posamentier (1993), Sequence stratigraphy and facies model of an incised valley fill: The Gironde estuary, France, *J. Sediment. Petrol.*, *63*, 378–391.

Atwater, B. F. (1987), Evidence for great Holocene earthquakes along the outer coast of Washington State, *Science*, *236*, 942–944.

Berryman, K. R. (1993), Age, height, and deformation of Holocene terraces at Mahia Peninsula, Hikurangi subduction margin, New Zealand, *Tectonics*, *12*, 1347–1364.

Berryman, K. R., Y. Ota, and A. G. Hull (1992), Holocene evolution of an estuary on a tectonically rising coast: The Pakarae River locality, eastern North Island, New Zealand, *Sediment. Geol.*, *80*, 151–162.

Carter, R. M., L. Carter, and D. P. Johnson (1986), Submergent shorelines in the SW Pacific: Evidence for an episodic post-glacial transgression, *Sedimentology*, *33*, 629–649.

Carter, L., B. Manighetti, M. Elliot, N. Trustrum, and B. Gomez (2002), Source, sea level and circulation effects on the sediment flux to the deep ocean over the past 15 ka off eastern New Zealand, *Global Planet. Change*, *33*, 339–355.

Clague, J. J. (1997), Evidence for large earthquakes at the Cascadia subduction zone, *Rev. Geophys.*, *35*, 439–460.

Cochran, U. (2002), Detection of large Holocene earthquakes in the sedimentary record of Wellington, New Zealand using diatom analysis, Ph.D. thesis, Victoria Univ. of Wellington, Wellington, New Zealand.

Collot, J.-Y., et al. (1996), From oblique subduction to intra-continental transpression: Structures of the southern Kermadec-Hikurangi margin from multibeam bathymetry, side-scan sonar and seismic reflection, *Mar. Geophys. Res.*, *18*, 357–381.

Dalrymple, R. W., B. A. Zaitlin, and R. Boyd (1992), Estuarine facies models: Conceptual basis and stratigraphic implications, *J. Sediment. Petrol.*, *62*, 1130–1146.

Darienzo, M. E., C. D. Peterson, and C. Clough (1994), Stratigraphic evidence for great subduction-zone earthquakes at four estuaries in northern Oregon, U.S.A., *J. Coastal Res.*, *10*, 820–876.

DeMets, C., R. G. Gordon, D. F. Argus, and S. Stein (1990), Current plate motions, *Geophysics J. Int.*, *101*, 425–478.

DeMets, C., R. G. Gordon, D. F. Argus, and S. Stein (1994), Effect of recent revisions to the geomagnetic reversal timescale on estimates of current plate motions, *Geophys. Res. Lett.*, *21*, 2191–2194.

Eberhart-Phillips, D., and M. Reyners (1999), Plate interface properties in the northeast Hikurangi subduction zone, New Zealand, from converted seismic waves, *Geophys. Res. Lett.*, *26*, 2565–2568.

Foster, G., and L. Carter (1997), Mud sedimentation on the continental shelf at an accretionary margin—Poverty Bay, New Zealand, *N. Z. J. Geol. Geophys.*, *40*, 157–173.

Froggatt, P. C., and D. J. Lowe (1990), A review of late Quaternary silicic and some other tephra formations from New Zealand: Their stratigraphy, nomenclature, distribution, volume and age, *N. Z. J. Geol. Geophys.*, *33*, 89–109.

Gibb, J. G. (1986), A New Zealand regional Holocene eustatic sea-level curve and its application to determination of vertical tectonic movements, A contribution to IGCP-Project 200, in *Recent Crustal Movements of the Pacific Region, Bull. R. Soc. N. Z.*, *24*, 377–395.

Goff, J. R., C. Chague-Goff, and S. L. Nichol (2001), Paleotsunami deposits: A New Zealand perspective, *Sediment. Geol.*, *143*, 1–6.

Hayward, B. W., H. R. Grenfell, C. Reid, and K. Hayward (1999), *Recent New Zealand Shallow-Water Benthic Foraminifera: Taxonomy, Ecologic Distribution, Biogeography, and Use in Paleoenvironmental Assessment, Monogr.*, vol. 21, 264 pp., Inst. of Geol. and Nucl. Sci. Lower Hutt, New Zealand.

Holbrook, J., and S. A. Schumm (1999), Geomorphic and sedimentary response of rivers to tectonic deformation: A brief review and critique of a tool for recognizing subtle epeirogenic deformation in modern and ancient settings, *Tectonophysics*, *305*, 287–306.

Hughen, K. A., et al. (2004), Marine04 marine radiocarbon age calibration, 0–26 cal kyr BP, *Radiocarbon*, *46*, 1059–1086.

Hull, A. G. (1987), A late Holocene marine terrace on the Kidnappers Coast, North Island, New Zealand: Some implications for shore platform development processes and uplift mechanisms, *Quat. Res.*, *28*, 183–195.

Hull, A. G. (1990), Tectonics of the 1931 Hawke's Bay earthquake, *N. Z. J. Geol. Geophys.*, *33*, 309–320.

Lewis, K. B., J.-Y. Collot, B. Davy, J. Delteil, S. Lallemand, and C. Uruski (1997), North Hikurangi GeodyNZ swath maps: Depths, texture and geological interpretation 1:500,000, *Misc. Ser. Chart 72*, Natl. Inst. for Water and Atmos. Res., Wellington, New Zealand.

Litchfield, N., S. Ellis, K. Berryman, and A. Nicol (2007), Insights into subduction-related uplift along the Hikurangi Margin, New Zealand, using numerical modeling, *J. Geophys. Res.*, *112*, F02021, doi:10.1029/2006JF000535.

Marsden, I. D., and R. Pilkington (1995), Spatial and temporal variations in the condition of Austrovenus stutchburyi Finlay, 1927 (Bivalvia: Veneridae) from the Avon-Heathcote estuary, Christchurch, *N. Z. Nat. Sci.*, *22*, 57–67.

Marshall, J. S., and R. S. Anderson (1995), Quaternary uplift and seismic cycle deformation, Peninsula de Nicoya, Costa Rica, *Geol. Soc. Am. Bull.*, *107*, 463–473.

Mazengarb, C. (1984), The Fernside Fault: An active normal fault, Raukumara Peninsula, New Zealand, *N. Z. Geol. Surv. Rec.*, *3*, 98–103.

Mazengarb, C., and I. G. Speden, Compilers, (2000), Geology of the Raukumara area, scale 1:250,000, *Geol. Map 6*, Inst. of Geol. and Nucl. Sci., Lower Hutt, New Zealand.

McCormac, F. G., A. G. Hogg, P. G. Blackwell, C. E. Buck, T. F. G. Higham, and P. J. Reimer (2004), SHCal04 Southern Hemisphere calibration, 0–26 ka cal BP, *Radiocarbon*, *46*, 1087–1092.

Merritts, D. J. (1996), The Mendocino triple junction: Active faults, episodic coastal emergence, and rapid uplift, *J. Geophys. Res.*, *101*, 6051–6070.

Morton, J. (2004), *Seashore Ecology of New Zealand and the Pacific*, edited by B. W. Hayward, Bateman, Auckland, New Zealand.

Ota, Y., K. R. Berryman, A. G. Hull, T. Miyauchi, and N. Iso (1988), Age and height distribution of Holocene transgressive deposits in eastern North Island, New Zealand, *Palaeogeogr. Palaeoclimatol. Palaeoecol.*, *68*, 135–151.

Ota, Y., A. G. Hull, and K. R. Berryman (1991), Coseismic uplift of Holocene marine terraces in the Pakarae River area, eastern North Island, New Zealand, *Quat. Res.*, *35*, 331–346.

Paul, M. A., and B. F. Barras (1998), A geotechnical correction for post-depositional sediment compression: Examples from the Forth valley, Scotland, *J. Quat. Sci.*, *13*, 171–176.

Reyners, M., D. Eberhart-Phillips, and G. Stuart (1999), A three-dimensional image of shallow subduction: Crustal structure of the Raukumara Peninsula, *Geophys. J. Int.*, *137*, 873–890.

Roy, P. S., (1984), New South Wales estuaries: Their origin and evolution, in *Coastal Geomorphology in Australia*, pp. 99–121, Academic, Orlando, Fla.

Schumm, S. A. (1993), River response to baselevel change: Implications for sequence stratigraphy, *J. Geol.*, *101*, 279–294.

Stuiver, M., and H. A. Polach (1977), Discussion: Reporting of ^{14}C data, *Radiocarbon*, *19*(3), 355–363.

Walcott, R. I. (1987), Geodetic strain and the deformation history of the North Island, of New Zealand during the late Cainozoic, *Philos. Trans. R. Soc. London, Ser. A*, *321*, 163–181.

Wellner, R. W., and L. R. Bartek (2003), The effect of sea level, climate, and shelf physiography on the development of incised-valley complexes: A modern example from the East China Sea, *J. Sediment. Res.*, *73*, 926–940.

Wilson, K. J., K. R. Berryman, N. J. Litchfield, and T. A. Little (2006), A revision of mid to late Holocene marine terrace distribution and chronology at New Zealand's most tectonically active coastal location, Pakarae River, North Island, New Zealand, *N. Z. J. Geol. Geophys.*, *49*, 477–489.

Wilson, K. J., K. Berryman, U. Cochran, and T. A. Little (2007a), A Holocene incised valley infill sequence developed on a tectonically active coast: Pakarae River, New Zealand, *Sediment. Geol.*, *197*, 333–354, doi:10.1016/j.sedgeo.2006.10.007.

Wilson, K., K. Berryman, U. Cochran, and T. Little (2007b), Holocene coastal evolution and uplift mechanisms of the northeastern Raukumara Peninsula, North Island, New Zealand, *Quat. Sci. Rev.*, *26*, 1106–1128, doi:10.1016/j.quascirev.2007.01.005.

Zachariasen, J., K. Sieh, F. W. Taylor, R. L. Edwards, and W. S. Hantoro (1999), Submergence and uplift associated with the giant 1833 Sumatran subduction zone earthquake: Evidence from coral microatolls, *J. Geophys. Res.*, *104*, 895–919.

K. Berryman, U. Cochran, and K. Wilson, GNS Science, P.O. Box 30368, Lower Hutt, New Zealand. (k.wilson@gns.cri.nz)

T. Little, School of Earth Sciences, Victoria University of Wellington, P.O. Box 600, Wellington, New Zealand.

New Zealand Journal of Geology & Geophysics, 2006, Vol. 49: 477–489
0028–8306/06/4904–0477 © The Royal Society of New Zealand 2006

A revision of mid–late Holocene marine terrace distribution and chronology at the Pakarae River mouth, North Island, New Zealand

KATE WILSON[1*]
KELVIN BERRYMAN[2]
NICOLA LITCHFIELD[2]
TIM LITTLE[1]
[1]School of Earth Sciences
Victoria University of Wellington
PO Box 600
Wellington 6140, New Zealand
[2]GNS Science
PO Box 30368
Lower Hutt 5040, New Zealand
*Present address: GNS Science, PO Box 30368, Lower Hutt 5040, New Zealand.

Abstract A suite of seven marine terraces at the Pakarae River mouth, New Zealand, provide evidence for the highest Holocene coastal uplift rates adjacent to the Hikurangi Subduction Zone. New elevation, coverbed stratigraphy, and age data allow for a timely revision of the distribution, nomenclature, and chronology of these terraces. Terrace correlation primarily is based on the elevation of the wave-cut strath. Terrace preservation either side of the river is more equal than previously proposed. The age of abandonment of each terrace is c. 7 ka (T1), 4.3 ka (T2), 3.5 ka (T3), 2.89 ka (T4), 1.6 ka (T5), 0.91 ka (T6), and <0.91 ka (T7). The average Holocene tectonic uplift rate at Pakarae is 3.2 ± 0.8 mm/yr. The abandonment of each terrace, from T2 to T7, probably took place after a discrete uplift event. The average time interval between these events is 850 ± 450 yr and the average uplift magnitude is 2.7 ± 1.1 m per event. We infer that uplift has been accommodated by slip on an offshore reverse fault. Normal slip on the Pakarae Fault, at right angles to the margin, occurs at a comparatively slower rate and has probably made little contribution to coastal uplift.

Keywords marine terraces; Pakarae River; coastal uplift; neotectonics

INTRODUCTION

The Pakarae River mouth locality (henceforth called Pakarae) has the greatest number of Holocene marine terraces of any location adjacent to the Hikurangi Subduction Zone (Berryman et al. 1989; Ota et al. 1991, 1992). Seven terraces elevated above modern mean sea level (MSL) provide evidence of past sudden coastal uplift since sea level (SL) stabilised in the mid Holocene. The well-preserved record of coastal uplift distinguishes the Pakarae location as one of the most tectonically active coastal areas of the Pacific Rim (Berryman et al. 1992; Ota & Yamaguchi 2004). Accurate knowledge of the timing, frequency, and magnitude of coastal uplift for each event at Pakarae provides a long record of tectonism in the subduction margin. The proximity of the study location to a subduction thrust (that has no historic record of slip during large or great earthquakes), and a normal fault offsetting the terraces locally at Pakarae, begs the question of what fault, or faults, is driving the rapid coastal uplift rates along this part of the Hikurangi margin.

Moderate to high late Quaternary coastal uplift rates (0.5–3 mm/yr) have been recorded by marine terraces at many locations along the Raukumara Peninsula (Fig. 1A–D); the Pakarae region has the highest Holocene uplift rates recorded along this segment of the Hikurangi margin (Ota et al. 1988, 1992; Yoshikawa 1988; Berryman et al. 1989; Berryman 1993). Offshore of Pakarae, directly to the east, is the Hikurangi Subduction Zone (Fig. 1A); the continental shelf has been deformed by strike slip, contractional, and extensional faulting, and several margin indentations may indicate previous seamount collisions (Collot et al. 1996). In the vicinity of Pakarae, Oligocene and Miocene marine siltstones and mudstones are juxtaposed across the Pakarae Fault, a north-striking structure on the western side of the Pakarae River (Kingma 1964; Mazengarb & Speden 2000). Several short segments of active normal faults have been mapped in the Pakarae region, including the Pakarae Fault (Fig. 1D) and the Waihau Bay Fault, located 10 km north of Pakarae (Mazengarb 1984, 1998; Mazengarb & Speden 2000). Walcott (1987) and Thornley (1996) inferred that the Raukumara Peninsula is undergoing margin-normal extension due to uplift driven by sediment underplating. The character of active faulting at Pakarae is therefore of relevance to understanding the geodynamic relationships between onshore normal faults, offshore upper plate compressional structures, and the subduction interface.

The Pakarae Holocene marine terraces were previously mapped, correlated, and dated by Ota et al. (1991). Seven terraces, named T1–T7, from oldest to youngest, were recognised at Pakarae. T1 corresponds to the maximum mid-Holocene marine transgression at c. 7 ka (Gibb 1986). The terraces were correlated across the Pakarae River based on their age and height. Only terraces T4 and T5 were mapped on both sides of the river. Landward tilting of the terraces was indicated by terrace height projections normal to the coast (Ota et al. 1991). The timing of uplift of each terrace was estimated from tephra coverbed distribution and radiocarbon ages of shells that were collected from close to the wave-cut strath. Shells from T1–T6 were collected for radiocarbon dating either from natural river bank exposures of the marine terrace coverbeds on the west bank, or from soil pits excavated on the eastern bank. T7 was dated by correlation to the lowest terrace at Waihau Bay, 15 km north of Pakarae, which is overlain by sea-rafted Loisells Pumice. Originally thought to be uniformly <700 yr BP (McFadgen 1985), this pumice is

G06007; Online publication date 22 November 2006
Received 15 March 2006; accepted 18 October 2006

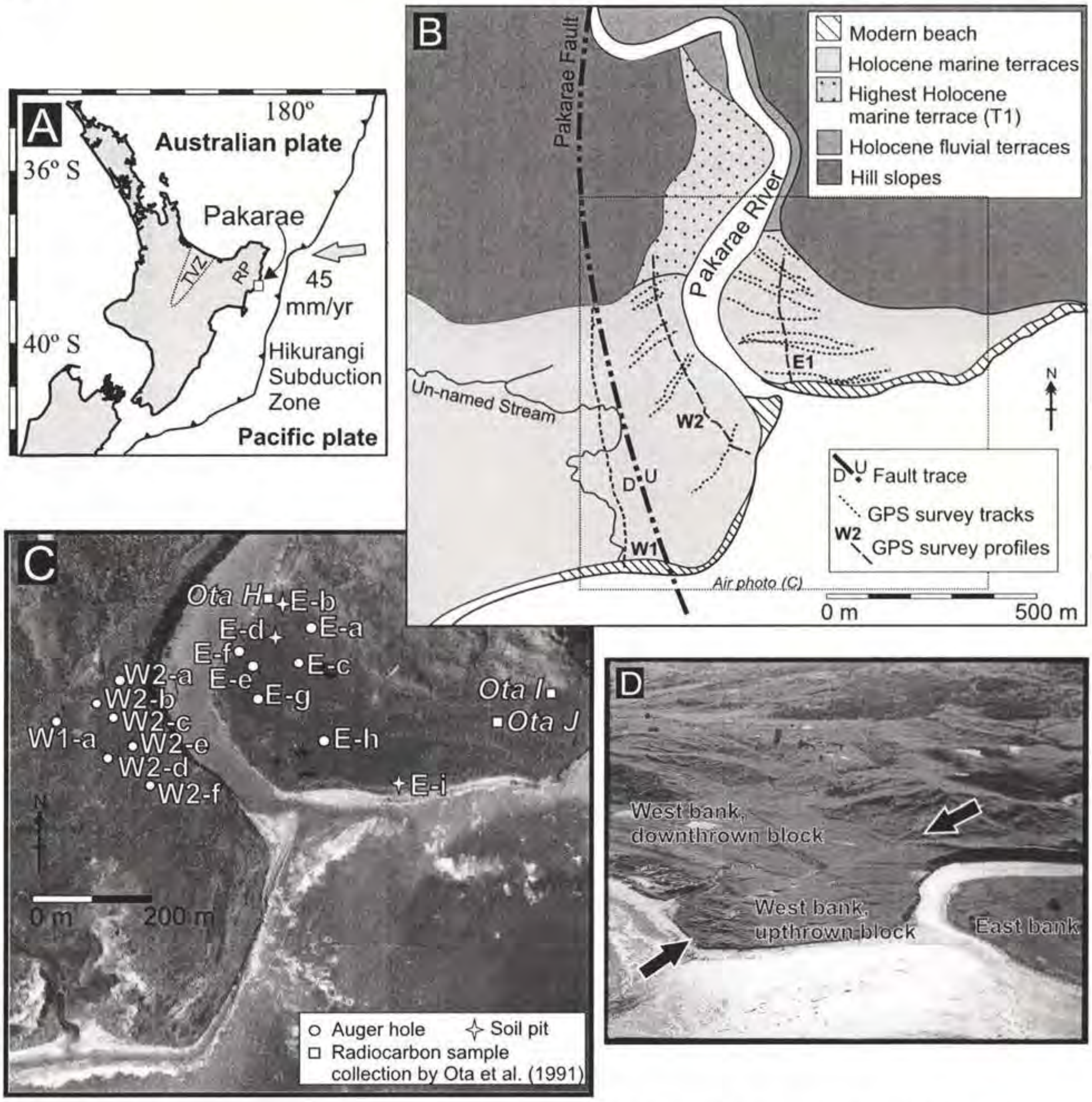

Fig. 1 The Pakarae River mouth locality. **A**, Location map and the Hikurangi Subduction Zone, North Island New Zealand. RP, Raukumara Peninsula; TVZ, Taupo Volcanic Zone. Arrow shows the relative plate motion vector from De Mets et al. (1994). **B**, Major geomorphic features of the Pakarae River mouth and GPS survey lines referred to in text. W1, W2 and E1 refer to elevation profiles shown in Fig. 2. **C**, Locations of cover sediment profiles shown in Fig. 2. Points "Ota ..." are radiocarbon date collection locations of Ota et al. (1991) referred to in text. **D**, Oblique aerial photo of the Pakarae River mouth showing the geomorphology of the Pakarae Fault (arrowed).

now acknowledged to be diachronous in its age at different sites around the New Zealand coastline (Shane et al. 1998).

As part of a broader study at Pakarae we have collected new information on terrace elevation, coverbed stratigraphy, including tephra, and ages of fossils in the terrace deposits. These new data provide the basis for revising the correlation of the terraces across the Pakarae River and for reconsidering the timing and rates of Holocene coastal uplift events. In this study we use 3 GPS elevation profiles across the terraces, 16 terrace cover sediment profiles, and 3 new radiocarbon ages to revise the original terrace distribution and chronology detailed by Ota et al. (1991). The geomorphology and age of the raised terraces allow inferences to be made regarding the types of faults most likely to have played a key role in the uplift of this coast.

METHODS

In this study we use the following terminology: **marine terraces** refer to relict coastal erosion surfaces overlain by marine and non-marine cover sediments; risers separate the

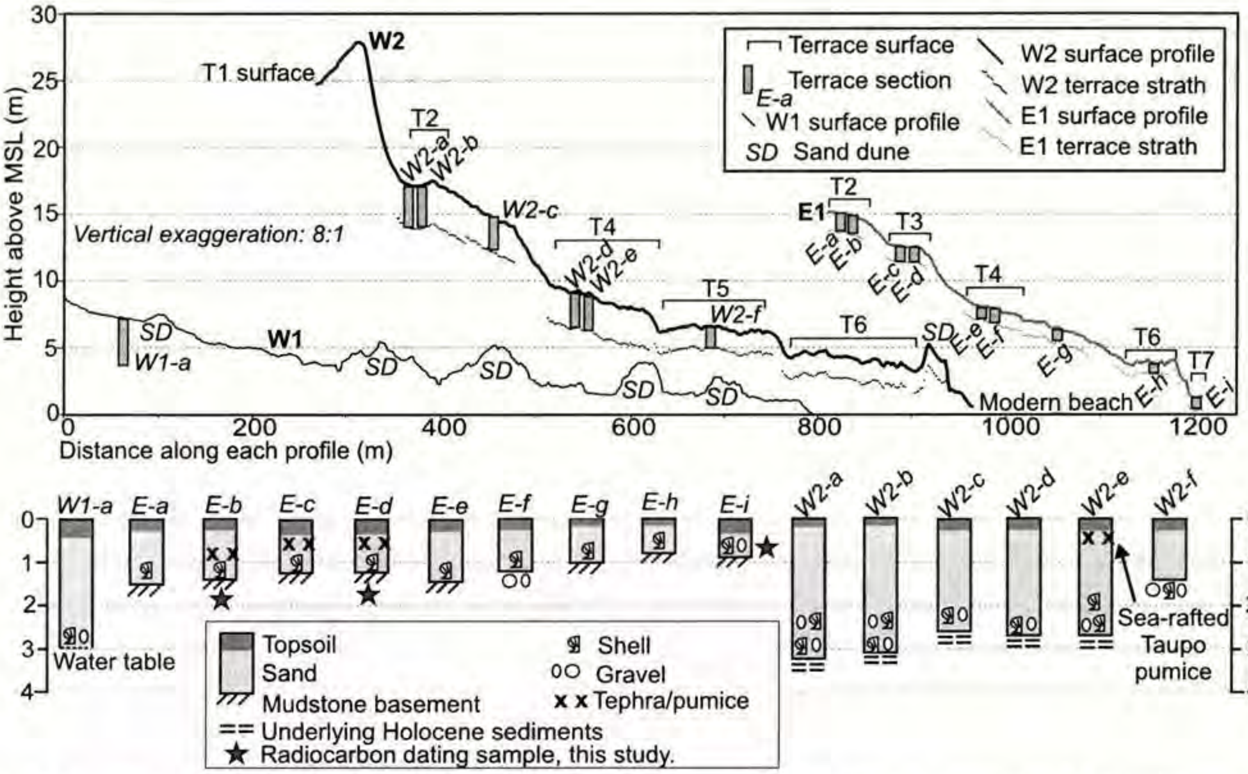

Fig. 2 **(Top)** GPS height profiles across the Pakarae Holocene marine terraces, location of profiles shown on Fig. 1. Profiles W2 and E1 have the terrace straths plotted based on the amount of cover material on each terrace; location of the soil pits and auger holes shown. Profile E2 not shown as it is similar to E1. See text for discussion of the GPS elevation uncertainties. **(Below)** Simplified coverbed stratigraphy on the Holocene marine terraces from soil pits and augering.

terraces. **Wave-cut strath** refers to the surface cut by coastal erosion processes when the surface was approximately at MSL; the **shoreline angle** is the angle formed at the landward edge of a terrace where strath intersects the riser to the higher terrace; the **terrace surface** refers to the modern surface of the terrace, which includes a certain thickness of cover sediments deposited since the sea abandoned the terrace.

A microtopographic survey of the terrace surfaces was carried out using a Real Time Kinematic (RTK) GPS. The elevations have an uncertainty of ±0.16 m at a 95% confidence interval. The perimeter of each terrace on the east bank and on the upthrown side of the fault on the west bank was surveyed. Linear profiles across all terraces were also made: W1 on the west bank on the downthrown side of the fault, and W2 on the west bank, upthrown side of the fault, and E1 on the east bank (Fig. 1B).

The stratigraphy of the terrace sediment cover was determined at 16 locations using a hand auger or soil pits (Fig. 1C). Coverbed sediments were described by a visual assessment of their colour and grain size (Fig. 2).

Our height correlations between the terraces are based on the elevation of the wave-cut straths, which we obtained by subtracting the depth of cover sediment from the terrace surface elevation, as determined from the GPS. On approximately one-half of the terraces we had two measurements of the cover sediment thickness over the wave-cut strath and there was always <0.15 m difference between the two measurements (the av. difference was 0.1 m, Fig. 2). Given that 0.1 m is less than the elevation measurement uncertainty on each terrace, it was not deemed essential to take more than one measurement of cover sediment thickness per terrace. However, we assign a 95% uncertainty of ±0.5 m to the elevations of the wave-cut straths to take account of irregularities created by variable erosion of the platforms. To calculate the elevation of the wave-cut strath of the lowest terrace on the west bank we used the cover sediment thickness from the terrace above it as an approximate measure of the cover sediment thickness (Fig. 2); this assumption may result in a slight underestimation of the wave-cut strath elevation as there is a trend of decreasing cover sediment thickness with decreasing age. Therefore, the lowest terrace probably has slightly less cover sediment than the one above it. Only one auger hole was taken on the downthrown side of the fault: this sampled the highest terrace. The auger hole reached the water table at 3 m and further sediment recovery was not possible. With the surface elevation of the terraces having an uncertainty of ±0.16 m and the cover sediment thickness variation <0.15 m, we believe ±0.5 m is a conservative estimate of the uncertainty at a 95% confidence interval for the elevation of each of the wave-cut straths at the Pakarae River mouth.

Shell material was collected for radiocarbon dating from all auger holes and soil pits (Fig. 2, 3). We always collected shells from as close as possible to the wave-cut strath. These shells occur within coarse sand and mudstone-clast gravels that represent the paleo-beach deposits at the time when the terrace was being cut. Whole shells were collected if present,

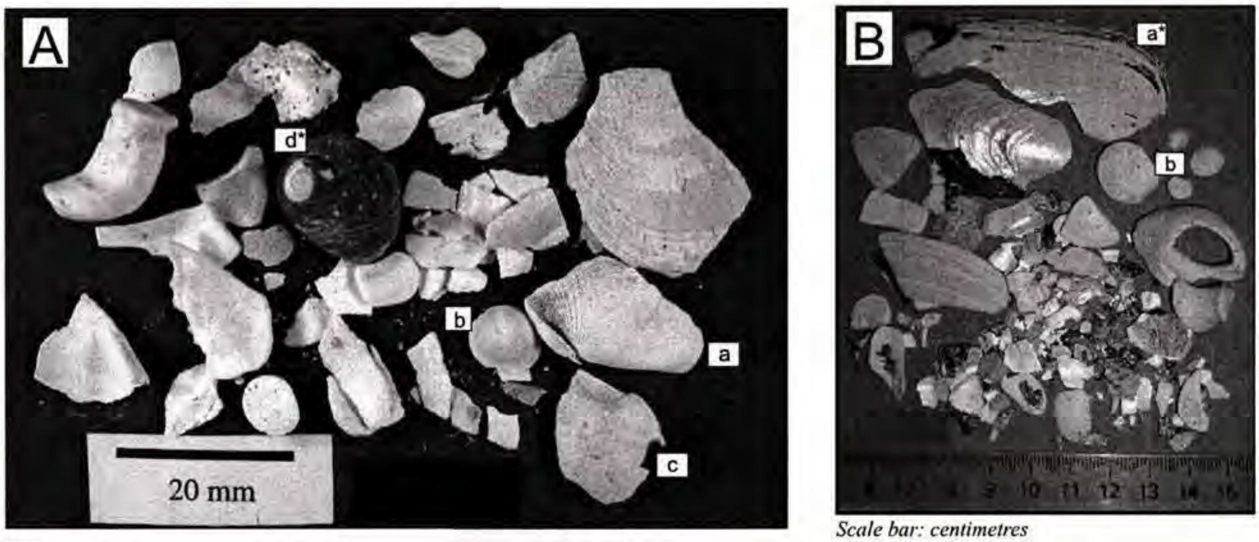

Scale bar: centimetres

Fig. 3 Shell species and radiocarbon samples from the Pakarae marine terraces. * radiocarbon AMS sample. **A**, T2 north bank: (a) fragment of *Pholadidea* spp., (b) fragments of cat's eye (Ataota), *Turbo smaragdus*, (c) fragments of cockle, *Austrovenus stutchburyi*, (d) spotted top shell (Maihi), *Melagraphia aethiops* and unidentified shell fragments. **B**, T6 north bank: (a) scimitar shell (Peraro) *Zenatia acinaces*, (b) fragments of cat's eye (Ataota), *Turbo smaragdus* and unidentified shell fragments. **C**, T3 north bank: (a) blue mussel (Toretore), *Mytilus edulis galloprovincialis*, (b) fragments of cat's eye (Ataota), *Turbo smaragdus*, (c) fragments of cockle, *Austrovenus stutchburyi*, (d) spotted top shell (Maihi), *Melagraphia aethiops* and unidentified shell fragments.

otherwise well-preserved shell fragments were collected; the shell species have been identified where possible (Fig. 3). Accelerator mass spectrometer (AMS) radiocarbon ages of shells were determined at the Rafter Radiocarbon Laboratory, Institute of Geological & Nuclear Sciences Ltd. We chose to date only terraces which had the highest age uncertainty as most of the terraces have been previously dated by Ota et al. (1991). The radiocarbon ages of Ota et al. (1991) have been calibrated for use in this study using the marine calibrations of Hughen et al. (2004). All radiocarbon ages will be presented as the 2 σ age estimate in calibrated years before present (cal. yr BP). Tephra was identified by its physical characteristics, age relationships, and comparison with tephra isopach maps of Vucetich & Pullar (1964).

RESULTS

Marine terrace characterisation

RTK GPS profiles oriented approximately normal to the terraces show distinctive staircase topography with flat to gently sloping surfaces separated by steep risers (Fig. 2). The terrace surfaces are up to 120 m wide and display morphology similar to the modern beach mudstone platform, which is exposed from the beach out to c. 150 m offshore within the intertidal surf zone. From terrace profiles W2 and E1 we can identify six terraces on the west bank and six terraces on the east bank of the Pakarae River. On the downthrown side of the Pakarae Fault (profile W1), separate terraces were not differentiated because they are covered by sand dunes (Fig. 2). Therefore, discussions of the west bank terraces refer to the upthrown side of the fault only.

Cover sediment thickness is greatest on the west bank, while on both sides of the river there is a general decrease in cover sediment thickness with decreasing terrace elevation, possibly reflecting a greater accumulation of aeolian sand over time (Fig. 2). Cover sediment stratigraphy generally fines upwards. The basal deposits sit directly on the wave-cut strath and are everywhere coarse sand with shells (whole shells, and shell hash) and mudstone-clast gravel (Fig. 2). On the east bank all wave-cut straths are incised in mudstone. On the west bank all wave-cut straths, except underlying the most recent two terraces, are incised into hard, mottled fluvial silts (Fig. 2). These silts were deposited by the Pakarae River during the early Holocene when the coastline was farther to the east. Shell species in the beach deposits (Fig. 3) are mostly from rocky shore habitats and all are from intertidal environments (Morton & Miller 1968; Marsden & Pilkington 1995; Marsden 2004; Morton 2004). The beach deposits are overlain by well-sorted, massive medium sand barren of shells. The change from coarse shelly sand to medium unfossiliferous sand represents a transition between shoreface beach sands and aeolian sands. Dark brown topsoil has developed on the aeolian sand on all terraces.

The depths of cover sediment that we measured on the east bank are similar to those of Ota et al. (1991). Both studies included the use of soil pits to measure sediment thickness above the wave-cut strath. On the west bank our measurements of cover sediment thickness are significantly less than those of Ota et al. (1991) (cf. second highest terrace: our study, 3.2 m; Ota et al. 1991, 5 m). The difference is because we obtained sediment thickness in the middle of the terrace surface, whereas Ota et al. (1991) used outcrops along the riverbank. Our recent observations along the riverbank reveal that much of it has slumped and therefore these outcrops overestimate the thickness of sediment and underestimate the elevation of the wave-cut strath.

Terrace ages

Three new shell radiocarbon ages from the east bank were obtained: from the highest (14 m), second highest (11.5 m), and the lowest (1 m) terraces (Fig. 2, Table 1). The two highest terraces on the east bank have a mantle of Waimihia Tephra (3430–3470 cal. yr BP; Froggatt & Lowe 1990). The Waimihia Tephra is identified by its age relationship to the highest terrace (i.e., must be <c. 7 ± 0.5 ka BP, the time of eustatic SL stabilisation; Gibb 1986) and its coarse lapilli texture. The middle terrace of the west bank has a layer of sea-rafted pumice clasts within the sand (section W2-c). We identify this as the Taupo Pumice based on its age relationships to the terraces and other known occurrences of this pumice along the east coast of the North Island. These rounded pumice clasts are up to 5 cm in diameter; they are probably a storm-deposit and indicate that the terrace is older than the age of the Taupo eruption at 1720–1600 cal. yr BP (Froggatt & Lowe 1990).

DISCUSSION

Terrace correlation and chronology

Revised terrace correlations across the Pakarae River are primarily based on new data on the elevation of the shoreline angles and wave-cut straths, and we also use two of the three additional radiocarbon ages (Table 1). We consider that the elevation of the shoreline angle is the most reliable feature for correlating the terraces because this would have been the same on both sides of the river.

One potential problem with correlating shoreline angle elevations across the river is the possible influence of tilting due to movement on the Pakarae or other faults. Projections of the terrace surface elevations to an east–west plane striking approximately normal to the Pakarae Fault show a small gradient (0.19°, 3.4 m/km) of terrace tilt towards the west (Fig. 4A), a gradient not significant enough to affect terrace correlations across the c. 100 m wide Pakarae River. Ota et al. (1991) also documented westward tilt normal to the Pakarae Fault. However, they interpreted this as evidence of landward tilt. We confirm landward tilt by projecting the terrace surface elevations to a plane striking normal to the Pakarae River and approximately normal to the Hikurangi subduction margin (Fig. 4). The projected elevations show a 0.23° landward tilt (a gradient of 4.1 m/km, Fig. 4).

Our terrace correlations indicate the presence of seven distinct terraces (Fig. 5). This is the same number as determined by Ota et al. (1991); however, our terrace distribution and correlation is significantly different (cf. Fig. 5B,C). In several cases there are conflicting radiocarbon ages from what are interpreted to be the same terrace. We resolve this by recognising that tephra occurrence provides an age constraint that can help distinguish which radiocarbon ages are more likely to be correct. We then consider from where the radiocarbon samples were collected. Some samples collected by Ota et al. (1991) are from areas where the terraces are indistinct and difficult to map and correlate. Lastly, we give preference to younger radiocarbon ages. We cannot see a mechanism for transporting young shell into the basal beach deposits of higher terraces, yet there are several mechanisms by which older shells could be recycled onto lower terraces. The following details the nomenclature, correlation, and distribution of each terrace from oldest (T1) to youngest (T7):

T1: The T1 surface is present only on the west bank (Fig. 5B,C). Our interpretation agrees with Ota et al. (1991) that this is the maximum Holocene SL transgression surface of c. 7 ± 500 cal. yr BP (we estimate a 95% uncertainty of 500 yr for the timing of eustatic SL stabilisation based on Gibb 1986). The oldest marine sediments underlying this surface have been dated at 7430–7280 cal. yr BP by Wilson et al. (in press), therefore constraining the timing of uplift to younger than 7430–7280 cal. yr BP.

T2: T2 is the second highest terrace on the west bank and the highest terrace on the east bank (Fig. 5C). It was previously

Table 1 Radiocarbon age data collected during this study from the Pakarae marine terraces.

Sample height (m)	Sample name	Sample material	Dating technique	^{13}C (‰)	Radiocarbon age* (radiocarbon yr BP)	Calibrated age† 2 σ (cal. yr BP)	Lab. number‡
14	East highest terrace	Shell, *Melagraphia aethiops*	AMS	1.33	4148 ± 30	4391–4138	NZA 22657
11.5	East 2nd highest terrace	Shell, *Mytilus edulis galloprovincialis*	AMS	0.52	3582 ± 30	3610–3403	NZA 22659
1	East lowest terrace	Shell, *Zenatia acinaces*	AMS	–8.48	2078 ± 30	1802–1582	NZA 22658

*Conventional radiocarbon age before present (AD1950) after Stuiver & Polach (1977).
†Marine calibration in calendar years after Hughen et al. (2004). 1 σ range (68% probability) and 2 σ range (95% probability) reported.
‡NZA: Institute of Geological & Nuclear Sciences Rafter Radiocarbon Laboratory.

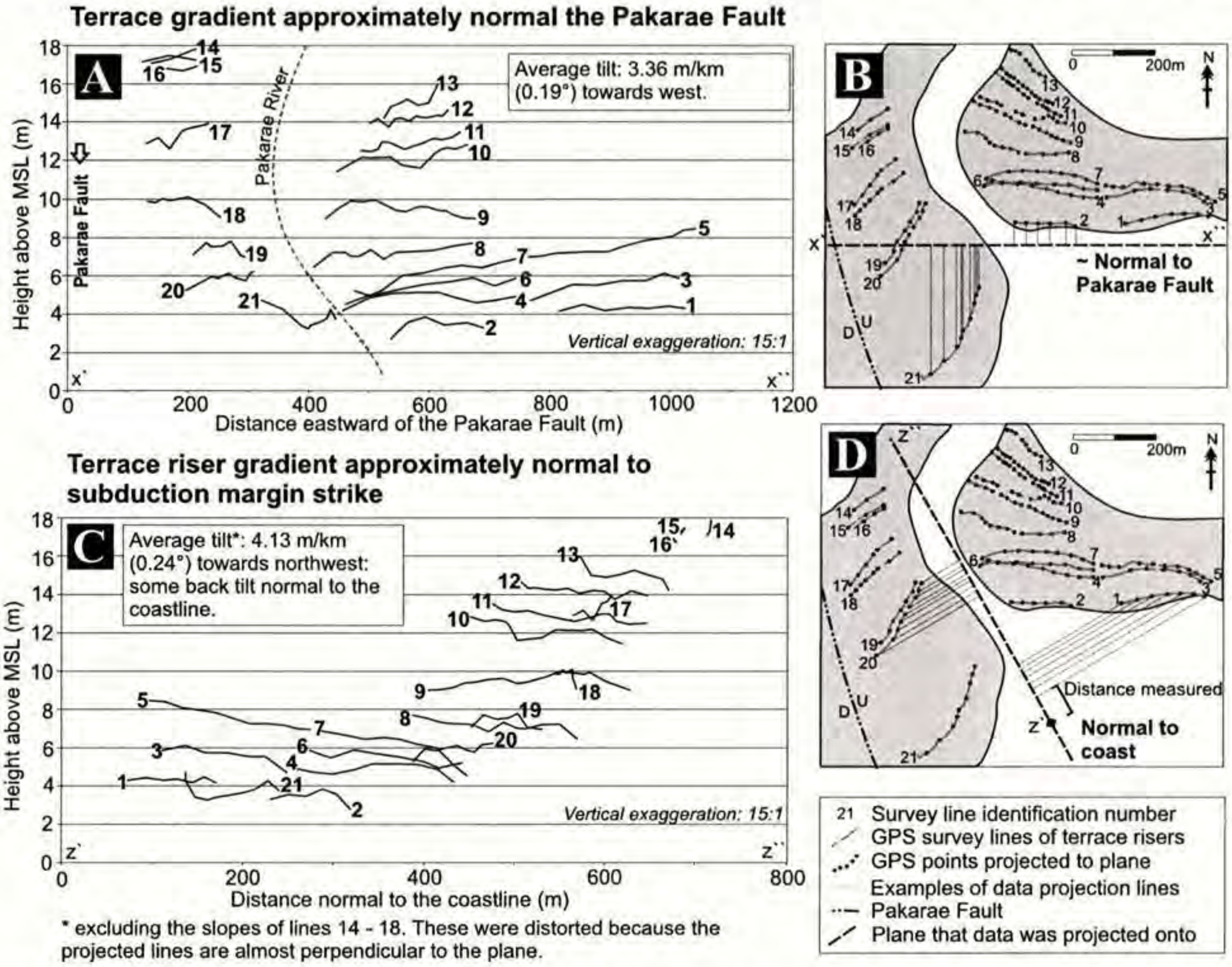

Fig. 4 Height profiles along the Pakarae terrace risers. Riser heights are projected to a plane approximately normal to the Pakarae Fault (A,B) and to a plane approximately normal to the Hikurangi subduction margin (C,D). The profiles test whether the terraces are back tilted relative to the Pakarae Fault or the subduction margin.

mapped as T3 on the east bank by Ota et al. (1991) because it had a younger radiocarbon age than the terrace of similar elevation on the west bank terrace (6410–6138 cal. yr BP on the west bank versus 4602–4130 cal. yr BP on the east bank; Ota et al. 1991). Our radiocarbon age of this terrace of 4391–4138 cal. yr BP on the west bank supports a younger terrace age of c. 4300 cal. yr BP, which is also consistent with the presence of the Waimihia Tephra in the terrace cover sediments. We therefore revise the terrace correlation in spite of the age difference inferred by Ota et al. (1991) because the shoreline angles are almost identical in elevation (c. 14 m AMSL) on both sides of the river. We interpret the older (c. 6.3 ka) radiocarbon age obtained by Ota et al. (1991) from the west bank as a reworked shell.

T3: The T3 terrace is the second highest terrace on the east bank but is less distinct on the west bank (Fig. 2). On the west bank, T3 has a significant surface gradient; however, this gradient is considerably less than that of the other risers, and we infer it to be a modified terrace surface. In the field, the T3 terrace on the west bank is sufficiently clear that its perimeter could be mapped. The seaward edge of the slope of the wave-cut strath on the west bank is the same elevation as the wave-cut strath of T3 on the east bank. The steeper terrace slope observed on the west bank T3 may result from poor wave-cut strath planation or is more likely due to aeolian sand accumulation towards the rear of the terrace, which would also explain why there is no riser separating T2 and T3 on the west bank. On the east bank, T3 is mantled by the Waimihia Tephra (3430–3470 cal. yr BP), and we obtained a radiocarbon age of 3610–3403 cal. yr BP from beneath the tephra; an age of 2714–2338 cal. yr BP was obtained by Ota et al. (1991). We prefer our radiocarbon age as an estimate of the age of the second highest terrace because it is compatible with the presence of the overlying 3430–3470 cal. yr BP Waimihia Tephra. Furthermore, the location of Ota et al.'s sample yielding the 2714–2338 cal. yr BP age is farther away from the river mouth at a location where terrace risers become less distinctive. For this reason, we could not map the terrace distribution in the eastern area (Fig. 5C), and it is possible the young age of Ota et al. (1991) is not from a terrace correlative to the second highest terrace as defined by us close to the river. Ota et al. (1991) previously mapped T3 only on the east bank, where it was their highest terrace (Fig. 5B). We revise this in light of our new age estimates of the terrace and our data on the wave-cut strath elevations (Fig. 5C).

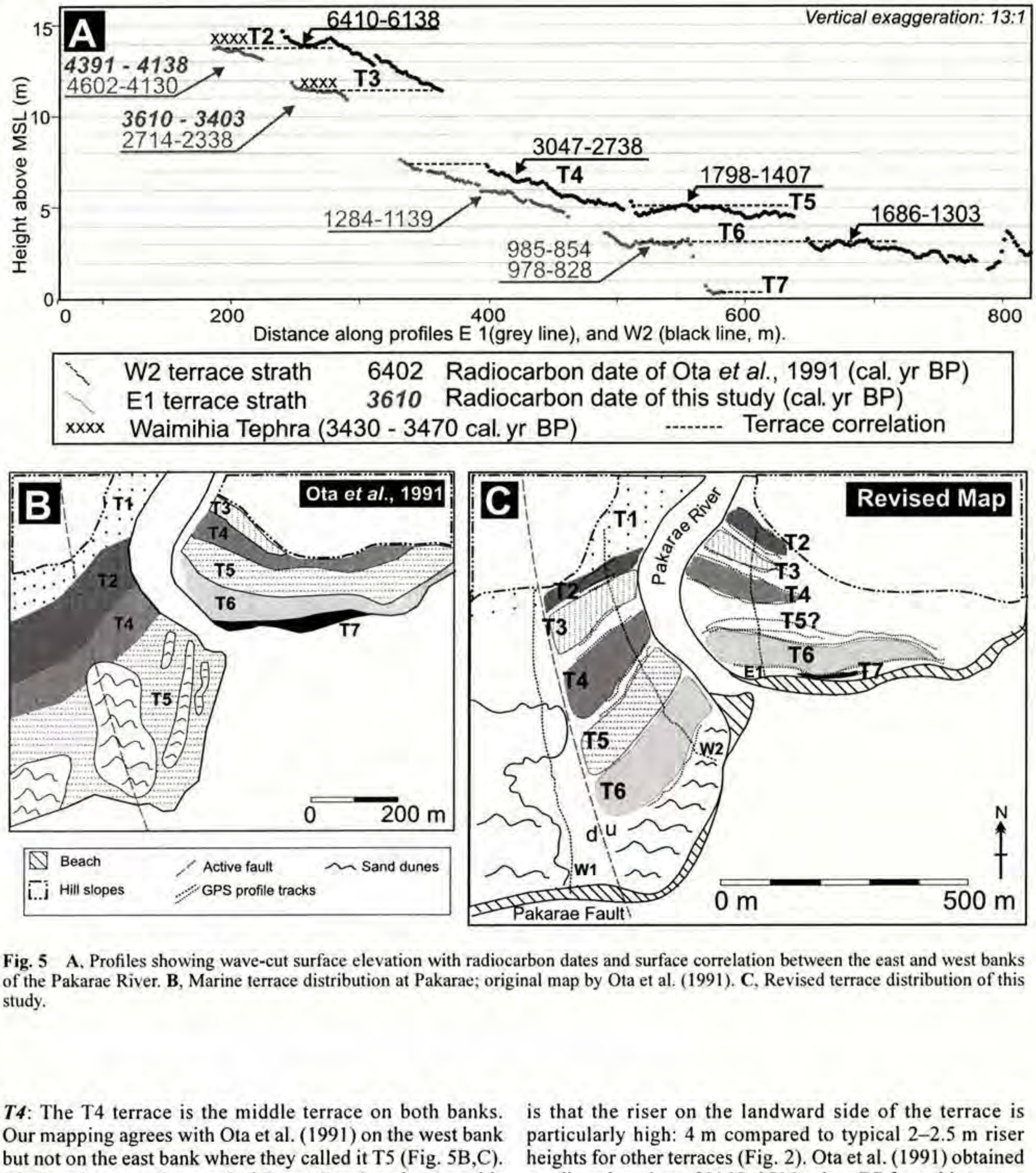

Fig. 5 **A**, Profiles showing wave-cut surface elevation with radiocarbon dates and surface correlation between the east and west banks of the Pakarae River. **B**, Marine terrace distribution at Pakarae; original map by Ota et al. (1991). **C**, Revised terrace distribution of this study.

T4: The T4 terrace is the middle terrace on both banks. Our mapping agrees with Ota et al. (1991) on the west bank but not on the east bank where they called it T5 (Fig. 5B,C). We found scattered sea-rafted Taupo Pumice clasts on this terrace on the west bank, as did Ota et al. (1991). They also found the same clasts on what we are calling T4 on the east bank, but despite this they mapped it as T5 on the east side. The mapping of these as different terraces by Ota et al. (1991) is plausible given that the sea-rafted pumice can be of diachronous age and deposited by storm waves some distance from the shoreface, but the simplest interpretation in our view is that these terraces are the same age. The terrace surface of T4 is relatively wide and gently sloping with the shoreline angles at 7.5 m AMSL and mid points of the wave-cut strath at c. 6 m AMSL on both banks. Another distinctive feature common to the T4 terrace on both sides of the river is that the riser on the landward side of the terrace is particularly high: 4 m compared to typical 2–2.5 m riser heights for other terraces (Fig. 2). Ota et al. (1991) obtained a radiocarbon date of 3047–2738 cal. yr BP from this terrace on the west bank and 1284–1139 cal. yr BP on the east bank. The presence of Taupo Pumice (erupted 1720–1600 cal. yr BP; Froggatt & Lowe 1990) as a storm beach deposit constrains the terrace age to the older date because pumice would not occur as part of the basal beach deposit if the younger age were correct. The east bank radiocarbon sample was collected from a location far to the east of the river mouth (point "Ota-J", Fig. 1C), where the terraces are indistinct, and therefore this sample may date a terrace younger than T3. For these reasons we prefer to use the older radiocarbon age of 3047–2738 cal. yr BP as the age of this terrace.

T5: The T5 terrace is distinctive on the west bank but poorly developed or preserved on the east bank (Fig. 2, 5). On the west bank, T5 is wide and gently sloping with sharp 1–2 m risers above and below. Ota et al. (1991) also mapped this surface as T5 (Fig. 5B); however, their T5 is wider than our definition of T5 (Fig. 5C). The narrowing of T5 between interpretations is because we have subdivided Ota et al.'s T5 into T5 and T6 terraces. Both our profiles and that of Ota et al. (1991) show a step in the surface topography of c. 1.5 m at our T5/T6 riser; however, Ota et al. (1991) did not split the terrace here apparently because the lower section yielded a similar radiocarbon date to the upper one (1783–1418 cal. yr BP upper strath, 1680–1307 cal. yr BP lower strath). We do not have any auger holes from the lower surface to verify that there is a step down in the wave-cut strath elevation, but the surface topography is clearly stepped and therefore we have divided the terrace into two. The radiocarbon date of Ota et al. (1991) from the lower strath may have been derived from a reworked shell. On the east bank, the profile of E1 between T4 and T6 is gently sloping with only a small riser at the front edge of T4. We do not map a terrace in here because the morphological expression is indistinct; however, the wide horizontal spacing between T4 and T6 suggests that time may have elapsed between the formation of these terraces. We therefore suggest that T5 is also present on the east bank where it was either weakly developed or has been poorly preserved as a result of aeolian deposition or riser scarp erosion. We retain the age of 1798–1407 cal. yr BP collected by Ota et al. (1991) for this terrace.

T6: As discussed above, we have reasonable evidence from surface morphology for an additional terrace on the west bank that we call T6 (Fig. 5C). On the east bank, our T6 is equivalent to that of Ota et al. (1991) (Fig. 5B). Two radiocarbon samples obtained by Ota et al. (1991) from the east bank, close to the river mouth, date the terrace at 985–854 and 978–828 cal. yr BP.

T7: T7 occurs as a thin strip on the east bank. Our mapping of this terrace agrees with that of Ota et al. (1991) (Fig. 5B,C). The age of this terrace was previously estimated by correlation to a terrace 15 km north along the coast, which has the Loisells Pumice on it. The Loisells Pumice is no longer thought to be everywhere <600 yr BP (Shane et al. 1998), so the age assigned to T7 needs to be reconsidered. We obtained a shell sample from the mudstone platform and it was radiocarbon dated at 1802–1582 cal. yr BP (Fig. 3, Table 1). Given the ages of 985–854 and 978–828 cal. yr BP for T6, we suspect that our shell sample was reworked. It is possible that T7 is also present on the west bank, however dune sands probably bury it (Fig. 2).

Tectonic uplift rates

We agree with Ota et al. (1991) that each terrace was formed by a sudden uplift event that caused the abandonment of the wave-cut surface by the sea (see Ota et al. 1991 for discussion). The New Zealand Holocene eustatic SL curve shows that, since the c. 7 ka culmination, SL has remained near its modern position with only minor fluctuations of the order of <0.5 m (Gibb 1986). We can therefore assume that the present elevation of each terrace above modern mean SL is due almost entirely to tectonic uplift. The likeness of the terrace coverbed sands and constituent shell species to the modern beach intertidal sand and shell accumulations supports the inference that the terraces were formed by coastal processes similar to those operating on the modern beach. We also agree with Ota et al. (1991) that radiocarbon ages of shells from the wave-cut strath are likely to be (at least) slightly older than

Table 2 Age-elevation relationships between the Pakarae River marine terraces including average uplift rates.

Terrace	Elevation of shoreline angle (±0.5 m)	Height difference between terraces (±1 m)	Estimated age (cal. ka BP)	Uncertainty[*]	Time since previous events (ka)	Uncertainty[§]	Uplift rate (wave-cut strath elevation /estimated age: m/ka)	Uncertainty[†]
T1	24		7[a]	±0.5			3.4	±0.2
T2	13.8	10.2[‡]	4.3[b]	±0.2	na[g]	±0.4	3.2	±0.2
T3	11.5	2.3	3.5[c]	±0.1	0.8	±0.3	3.3	±0.2
T4	7.5	4	2.9[d]	±0.2	0.6	±0.2	2.6	±0.2
T5	5.0	2.5	1.6[e]	±0.2	1.3	±0.3	3.13	±0.5
T6	3.0	2	0.9[f]	±0.1	0.7	±0.2	3.3	±0.6
T7	0.5	2.5	–		–		–	
Average		2.7[†] ± 1.1[¶]			0.85[†]	±0.45[¶]	3.2	±0.8[¶]

[*]This uncertainty assumes a normal distribution of ages around the mean, however this is not true for the calibrated ages, but we assume this for simplification.
[†]Calculations do not include difference between T1 and T2.
[‡]Height may reflect erosion of missing terraces between T1 and T2.
[¶]Uncertainty = $\sqrt{[(\text{error}^2) + (\text{error}^2) + \ldots]}$.
[§]Uncertainty = $\sqrt{[(\%\ \text{elevation error})^2 + (\%\ \text{age error})^2]}$.
[a]Aged based on the timing of eustatic SL stabilisation after Gibb (1986); estimated uncertainty of ±500 yr.
[b]Radiocarbon dates from T2, this study and Ota et al. (1991): (4391+4138+4602+4130)/4; uncertainty is the larger half difference between the 2 σ calibrated age of the two samples.
[c]Mid point 3610–3403 cal. yr BP, this study; uncertainty is half the difference between the 2 σ calibrated ages.
[d]Mid point 3047–2738 cal. yr BP, Ota et al. (1991); uncertainty is half the difference between the 2 σ calibrated ages.
[e]Mid point 1798–1407 cal. yr BP, Ota et al. (1991); uncertainty is half the difference between the 2 σ calibrated ages.
[f]Radiocarbon ages from T6, Ota et al. (1991): (985+854+978+828)/4; uncertainty is the larger half difference between the 2 σ calibrated age of the two samples.
[g]Not applicable as there have probably been terraces eroded between T1 and T2.

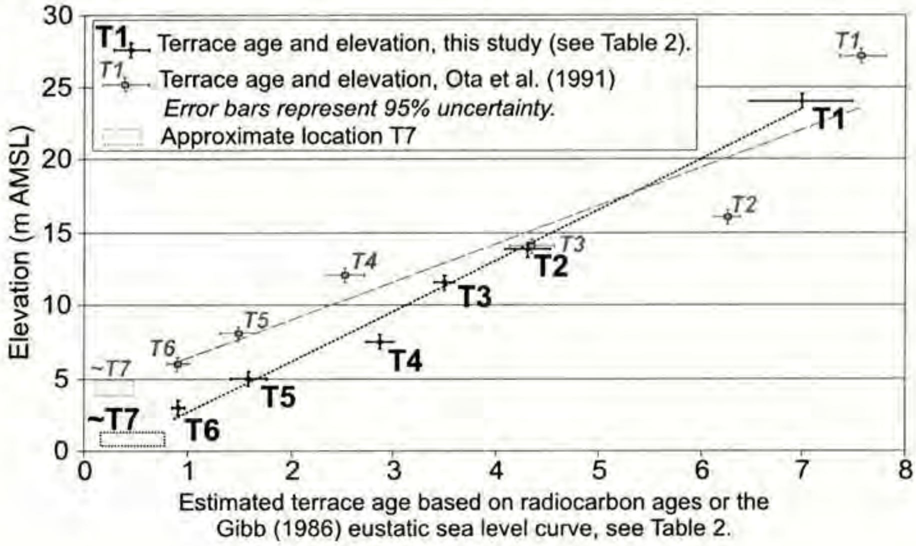

Fig. 6 Estimated terrace age (see Table 2) versus elevation. The ages of Ota et al. (1991) were calibrated (Hughen et al. 2004); the value shown here is the mid-point of the 2 σ calibrated age.

the timing of uplift and their abandonment—assuming that uplift caused the death of the organism. The well-preserved nature of the dated samples suggest there has been very little, if any, reworking the samples (Fig. 3). We use these ages to approximate a maximum limit for the time since uplift.

Our revised terrace ages are summarised in Table 2. On the modern beach the mudstone platform is being cut at approximately the mid-tide level, therefore we assume the uplifted wave-cut strath, measured at the shoreline angle, approximately represents mean SL prior to terrace uplift. The elevation difference between the wave-cut strath and modern mean SL equals the tectonic uplift. The mean uplift rates appear to have been remarkably uniform since c. 7 ka. We calculate an average rate of 3.2 ± 0.8 mm/yr (Fig. 6, Table 2). From T2 to T7 each terrace probably represents one uplift event; the average time interval between events is 850 ± 450 yr and the average magnitude is 2.7 ± 1.1 m per event. These are maximum values; it is possible that terraces produced by smaller events have not been preserved. Discounting the elevation and time difference between T1 and T2, because we believe terraces have been eroded from this part of the terrace sequence, the terrace-forming uplift events at Pakarae have been more regular in terms of magnitude than previously thought (Fig. 6).

One major difference between our terrace distribution interpretation and that of Ota et al. (1991) is the age of our T2. Ota et al. (1991) assigned an age of 6410–6138 cal. yr BP to this terrace, whereas we revise this to c. 4300 cal. yr BP. Our age revision means there is more time between the formation of T1 and T2. The age assignment of Ota et al. (1991) has an age difference of 1670–830 yr between T1 and T2; this study has 3210–2170 yr. A greater age difference between T1 and T2 reconciles better with the very high riser height (10.2 m) between these two terraces. Between T1 and T2 we believe more than one uplift event occurred to account for the high terrace riser. It is unrealistic that a 10.2 m riser was created by a single event when the average riser height of all the younger terraces is c. 2.7 m. Terraces may have formed in the period between T1 and T2 (c. 7000–4300 cal. yr BP) but subsequently eroded.

Pakarae terrace uplift and the role of the Pakarae Fault

We seek to investigate the tectonic structures that have driven the coastal uplift at Pakarae. We can use the geomorphology and ages of the terraces and compare them with block models of how terraces would form under different faulting scenarios. The presence of a scarp of the Pakarae Fault across the <7 ka Pakarae terrace sequence is indisputable evidence that this fault has moved during the Holocene. However, the north–south strike of the fault and the presence of terraces on either side of the fault indicate it is not the sole cause of uplift of the marine terraces. Instead, we infer that the main cause of coastal uplift on both sides of the Pakarae Fault was slip on a westward-dipping offshore reverse fault (Fig. 7A,B). Other than the Pakarae Fault, the onshore region contains no other known active faults except for the Waihau Bay Fault, which is a normal fault located c. 15 km north of Pakarae. Fault scaling relationships imply that with the short surface trace of the Waihau Bay Fault, and its distance from Pakarae, it is unlikely this fault caused uplift at Pakarae.

Slip on the subduction interface is not a likely cause of uplift because preliminary dislocation modelling indicates an unrealistically large amount of slip on the subduction thrust is required to produce uplift of c. 2.7 m at Pakarae (Litchfield & Wilson 2005). Sixty kilometres SSW of Pakarae, the offshore Lachlan reverse fault, dipping 15–20° to the NW, has caused coseismic uplift of Holocene marine terraces c. 5 km westwards on the Mahia Peninsula (Berryman 1993; Barnes et al. 2002). Although no structure analogous to the Lachlan Fault has so far been seismically imaged offshore of Pakarae, we suggest a similar reverse fault may have caused coastal uplift at Pakarae (Fig. 7B). A reverse fault has been mapped offshore of Pakarae by Lewis et al. (1997) and Mazengarb & Speden (2000); however, this mapping was based on an estimated location by Ota et al. (1991). The fault location was estimated by Ota et al. (1991) based upon the distribution of Holocene marine terraces at the Pakarae River mouth and 15 km northeastward along the coastline.

Ota et al. (1991) also suggested that while the main fault driving the coastal uplift at Pakarae was a reverse fault located offshore, the Pakarae Fault also moved simultaneously

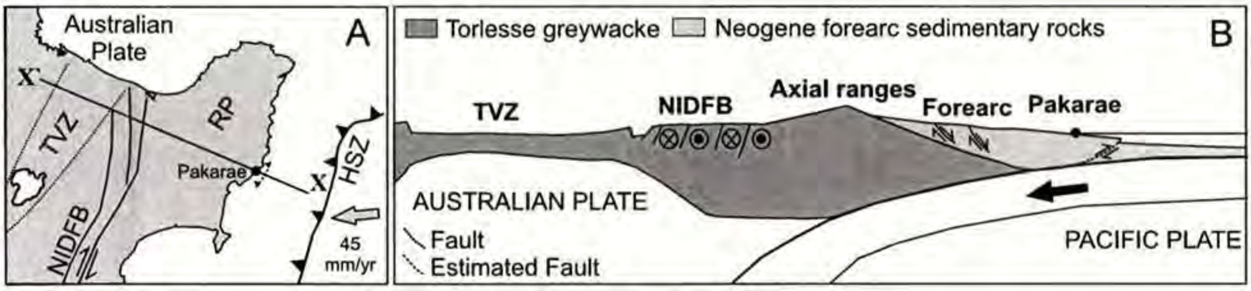

Fig. 7 A, Major tectonic elements of the Raukumara Peninsula sector of the Hikurangi margin. **B**, Schematic cross-section of the Raukumara Peninsula sector of the Hikurangi margin (X–X') showing major upper plate structures and estimated location of a reverse fault offshore of the Pakarae River mouth. RP, Raukumara Peninsula; TVZ, Taupo Volcanic Zone; NIDFB, North Island Dextral Fault Belt; HSZ, Hikurangi Subduction Zone.

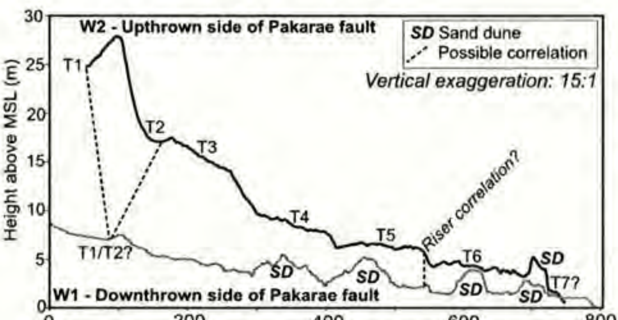

Fig. 8 Comparison of the topographic profiles on the downthrown (W1) and upthrown (W2) sides of the Pakarae Fault with possible correlation points.

with the uplift of the terraces. Correlation of terraces directly across the Pakarae Fault and comparison of riser heights led Ota et al. (1991) to suggest that the Pakarae Fault moved during some terrace uplift events, but that slip on this fault was not the primary cause of the regional coastal uplift. On the downthrown side of the Pakarae Fault, our profile (W1, Fig. 2) does not show the "staircase topography" characteristic of the upthrown side of the fault; rather, it is characterised by gentle slopes and sharp sand dune ridges (Fig. 2). Based on these data we cannot reliably correlate any terraces across the fault (Fig. 8), and suggest there are presently insufficient data to establish a relationship between Pakarae Fault movement and terrace formation. The terraces display a westward tilt towards the Pakarae Fault of 0.19° (Fig. 4), which argues against significant involvement of the Pakarae Fault in terrace uplift, because terraces in the footwall would be expected to have a tilt away from the fault (an eastwards tilt). The regional nature of the coastal uplift signal is corroborated by the similarity in the age of the marine terraces at Puatai Beach and Waihau Bay, 9 and 15 km north of Pakarae (Ota et al. 1991). Together, these datasets imply a domal uplift pattern with a wavelength of uplift along the coast of >15 km, as is consistent with slip on a major offshore fault striking parallel to the coast and dipping to the WNW (Ota et al. 1991). A revision of the Puatai Beach and Waihau Bay Holocene marine terraces and an evaluation of landward tilting on the Pakarae River fluvio-tectonic terraces are currently being prepared with the aim of refining the geometry of a probable causative offshore fault (Litchfield et al. "Coseismic fluvial terraces: an eample from the lower Pakarae River valley, Hikurangi margin, New Zealand" in prep.).

We use a simple schematic block model with an offshore reverse fault striking parallel with the coastline and an onshore normal fault striking perpendicular to the coastline to assess the likely structures driving coastal uplift (Fig. 9). Flexural isostasy dictates that the majority of absolute movement during slip on normal faults occurs through subsidence of the hanging wall (e.g., Jackson et al. 1988). Under various combinations of fault movement our model shows that the Pakarae geomorphology is most compatible with an offshore fault as the primary driver of coastal uplift (Fig. 9), in agreement with the conclusions of Ota et al. (1991).

Slip on a northwest-dipping offshore reverse fault would uplift both sides of the Pakarae Fault (Fig. 9A/1). Any synchronous or subsequent slip on the Pakarae Fault might be anticipated to cause subsidence of the downthrown block relative to MSL but not necessarily any significant vertical movement of the upthrown block relative to MSL (Fig. 9A/2). Vertical slip on the Pakarae Fault, in particular subsidence of its downthrown block, must have been less than the regional uplift related to slip on the offshore reverse fault, or else the western side of the fault would have been drowned due to net subsidence there, or be a flat coastal plain if coastal sedimentation rates were high enough to infill the embayment created by such net subsidence (Fig. 9B). To produce a terrace flight geomorphology similar to that of Pakarae with a downthrown block raised above MSL, these models show that the coastal uplift rate related to slip on the offshore fault must have been greater than the dip-slip rate of the Pakarae Fault (Fig. 9). The landward tilt of the terraces is compatible with back-tilt on an offshore coast-parallel reverse fault (Fig. 4).

The presence of an active reverse fault offshore of the Pakarae River mouth has important geodynamic implications for this sector of the Hikurangi margin. Presently only active normal faults have been mapped on the onshore Raukumara Peninsula (Mazengarb 1984, 1998; Mazengarb & Speden 2000), and geodetic studies show the region is currently undergoing extension and eastward rotation (Walcott 1987; Darby & Meertens 1995; Arnadottir et al. 1999; Wallace et al. 2004). The proposed offshore reverse fault is the first active contractional structure identified in a traverse from the

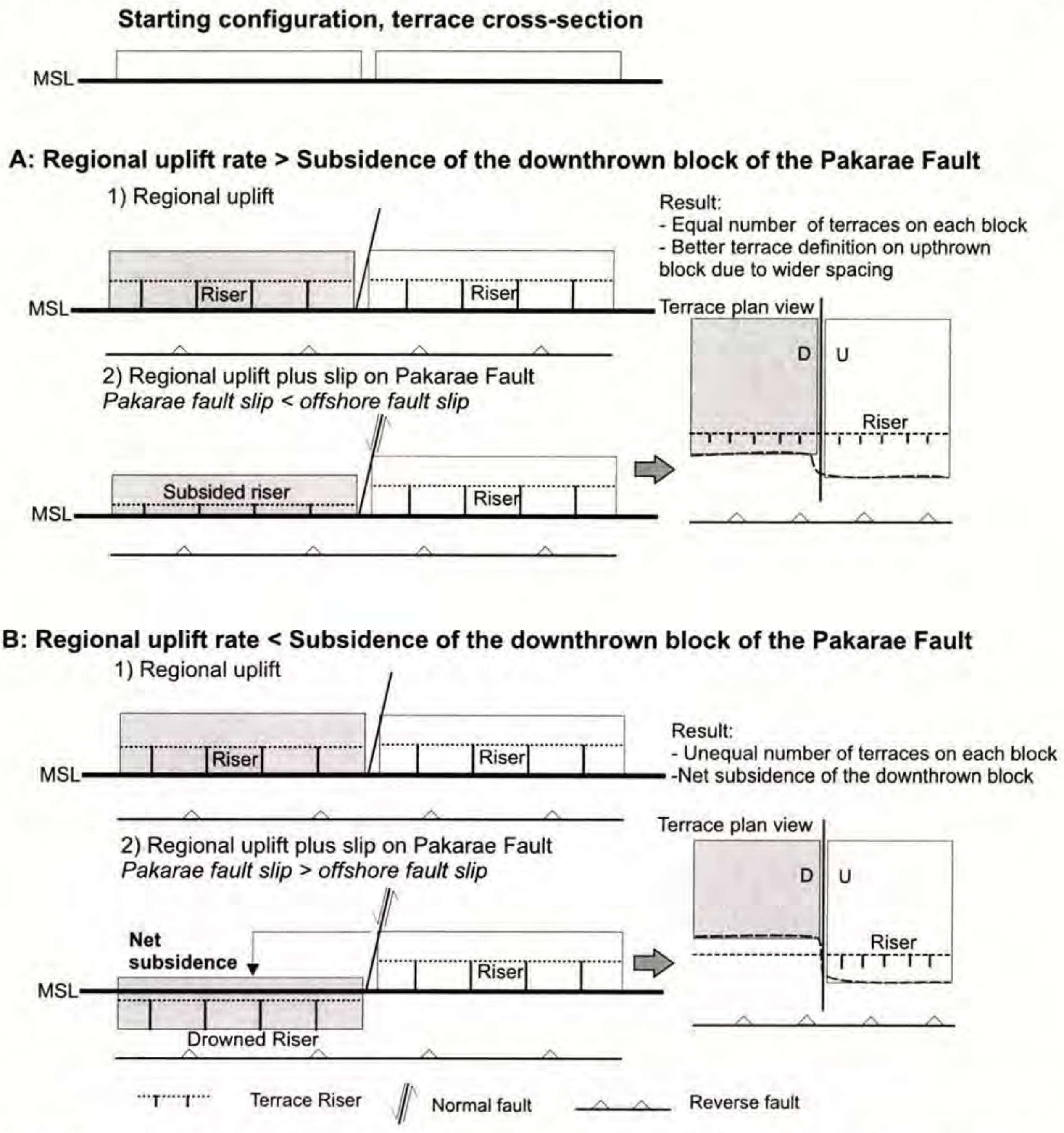

Fig. 9 Block models of an offshore reverse fault parallel with the marine terraces causing regional uplift, and a normal fault onshore perpendicular with the marine terraces. Two combinations of slip are shown, either regional uplift caused by the offshore fault is greater than dip-slip on the normal fault (A) or less than dip-slip on the normal fault (B). MSL = mean sea level.

backarc region to the Hikurangi Subduction Zone (Fig. 7B). Incorporation of offshore reverse faults in future studies of the Raukumara Peninsula is important; for example, examining whether such faults are listric to the plate interface, whether they interact with the interseismically locked portion of the interface, considering if reverse faults may accommodate a portion of the normal plate convergence motion along this segment of the margin, and incorporating faults on the continental shelf into tsunami hazard models of the region.

CONCLUSIONS

Our revision of the marine terrace distribution and chronology at Pakarae has shown that terrace formation and preservation either side of the Pakarae River is more uniform than previously described. Similar to Ota et al. (1991), we map seven terraces in total from T1 (representing the maximum Holocene transgression, and present only on the west bank) to T7 (the youngest terrace, preserved only on the east bank).

Terraces T2 through T6 are present on both sides of the river, although T3 is indistinct on the west bank and T5 is indistinct on the east bank. New age data from the east bank indicates that T2 is c. 4300 cal. yr BP, c. 2000 yr younger than the age of 6314–6195 cal. yr BP assigned by Ota et al. (1991). Terrace uplift has been intermittent. Average time intervals between uplift events range from 1280 to 630 yr and incremental uplift ranges from 2 to 4 m. Average Holocene uplift rates at Pakarae are relatively uniform over the past 7000 yr with a long term uplift rate of 3.2 ± 0.8 mm/yr.

Our study of the terrace geomorphology illustrates the importance of using the wave-cut strath elevation for terrace correlation rather than relying upon surface morphology, which is subject to a range of post-formation changes, especially in the development of coverbeds. It also demonstrates how multiple ages from the same terrace are preferable because shells from the same terrace used for radiocarbon dating can give variable results and have probably, in part, been reworked from older terraces. Future work is needed at this site to refine the terrace chronology, particularly of T7, which is not yet satisfactorily dated. Knowing the time of the most recent earthquake is important because the elapsed time since the last coastal uplift event may be critical to assessing the current seismic hazard at this location. To evaluate the tectonic structure chiefly responsible for terrace formation we need to reliably correlate the terraces across the Pakarae Fault and identify an offshore structure using marine geophysics. Block models indicate an offshore fault drives most or all of the coastal uplift, with synchronous or alternating smaller events on the Pakarae Fault causing relative subsidence of the western block of this normal fault.

ACKNOWLEDGMENTS

This research was funded by an EQC Student Grant (Project 6UNI/501). KJW is supported by the GNS-funded Sarah Beanland Memorial Scholarship. Rodger Sparks and Dawn Chambers of the Rafter Radiocarbon Laboratory are thanked for their contribution to the radiocarbon dating. Reviews by Yoko Ota, Harvey Kelsey, Philip Barnes, and an anonymous reviewer substantially improved this manuscript.

REFERENCES

Arnadottir T, Thornley S, Pollitz F, Darby DJ 1999. Spatial and temporal strain rate variations at the northern Hikurangi margin, New Zealand. Journal of Geophysical Research 104(B3): 4931–4944.

Barnes PM, Nicol A, Harrison T 2002. Late Cenozoic evolution and earthquake potential of an active listric thrust complex above the Hikurangi subduction zone, New Zealand. Geological Society of America Bulletin 114(11): 1379–1405.

Berryman KR 1993. Age, height, and deformation of Holocene terraces at Mahia Peninsula, Hikurangi subduction margin, New Zealand. 1. Tectonics 12(6): 1347–1364.

Berryman KR, Ota Y, Hull AG 1989. Holocene paleoseismicity in the fold and thrust belt of the Hikurangi subduction zone, eastern North Island, New Zealand. Tectonophysics 163: 185–195.

Berryman KR, Ota Y, Hull AG 1992. Holocene coastal evolution under the influence of episodoc tectonic uplift: examples from New Zealand and Japan. Quaternary International 15/16: 31–45.

Collot J-Y, Delteil J, Lewis K, Davy B, Lamarche G, Andru J-C, Barnes P, Chanier F, Chaumillon E, Lallemand S and others 1996. From oblique subduction to intra-continental transpression: structures of the southern Kermadec-Hikurangi margin from multibeam bathymetry, side-scan sonar and seismic reflection. Marine Geophysical Researches 18(2–4): 357–381.

Darby DJ, Meertens CM 1995. Terrestrial and GPS measurements across the Taupo backarc and Hikurangi forearc in New Zealand. Journal of Geophysical Research 100(B5): 8221–8232.

De Mets C, Gordon RG, Argus DF, Stein S 1994. Effect of recent revisions to the geomagnetic reversal timescale on estimates of current plate motions. Geophysical Research Letters 21: 2191–2194.

Froggatt PC, Lowe DJ 1990. A review of late Quaternary silicic and some other tephra formations from New Zealand: their stratigraphy, nomenclature, distribution, volume and age. New Zealand Journal of Geology and Geophysics 33: 89–109.

Gibb JG 1986. A New Zealand regional Holocene eustatic sea-level curve and its application to determination of vertical tectonic movements. A contribution to IGCP-Project 200. In: Reilly WI, Harford BE ed. Recent crustal movements of the Pacific region. Royal Society of New Zealand Bulletin 24: 377–395.

Hughen KA, Baillie MGL, Bard E, Beck JW, Bertrand CJH, Blackwell PG, Buck CE, Burr GS, Cutler KB, Damon PE, Edwards RL and others 2004. Marine04 Marine Radiocarbon Age Calibration, 0–26 cal kyr BP. Radiocarbon 46(3): 1059–1086.

Jackson JA, White NJ, Garfunkel Z, Anderson H 1988. Relations between normal-fault geometry, tilting and vertical motions in extensional terrains: an example from the southern Gulf of Suez. Journal of Structural Geology 10(2): 155–170.

Kingma JT 1964. Sheet 9—Gisborne. Geological map of New Zealand 1:250 000. Wellington, New Zealand, Department of Scientific and Industrial Research.

Lewis KB, Collot J-Y, Davy B, Delteil J, Lallemand S, Uruski C 1997. North Hikurangi GeodyNZ swath maps: depths, texture and geological interpretation 1:500 000. National Institute for Water and Atmospheric Research Miscellaneous Series Chart 72. Wellington.

Litchfield N, Wilson K 2005. Holocene tectonic fluvial terraces at Pakarae River mouth, Gisborne region. Programme and Abstracts, Geological Society of New Zealand 50th Annual Conference, Kaikoura New Zealand. Geological Society of New Zealand Miscellaneous Publication 119A: 45–46.

McFadgen BG 1985. Late Holocene stratigraphy of coastal deposits between Auckland and Dunedin, New Zealand. Journal of the Royal Society of New Zealand 15: 27–65.

Marsden ID 2004. Effects of reduced salinity and seston availability on growth of the New Zealand little-neck clam *Austrovenus stutchburyi*. Marine Ecology Progress Series 266: 157–171.

Marsden ID, Pilkington R 1995. Spatial and temporal variations in the condition of *Austrovenus stutchburyi* Finlay, 1927 (Bivalvia: Veneridae) from the Avon-Heathcote estuary, Christchurch. New Zealand Natural Sciences 22: 57–67.

Mazengarb C 1984. The Fernside Fault: an active normal fault, Raukumara Peninsula, New Zealand. New Zealand Geological Survey Record 3: 98–103.

Mazengarb C 1998. Late Neogene structural development of eastern Raukumara Peninsula: implications for oil exploration. 1998 New Zealand Petroleum Conference Proceedings: 201–205.

Mazengarb C, Speden IG comp. 2000. Geology of the Raukumara area. Institute of Geological & Nuclear Sciences 1:250 000 Geological Map 6. Lower Hutt, New Zealand, Institute of Geological & Nuclear Sciences Limited.

Morton J 2004. Seashore ecology of New Zealand and the Pacific. In: Hayward BW ed. Auckland, Bateman.

Morton J, Miller M 1968. The New Zealand sea shore. London, Collins.

Ota Y, Yamaguchi M 2004. Holocene coastal uplift in the western Pacific Rim in the context of late Quaternary uplift. Quaternary International 120: 105–117.

Ota Y, Berryman KR, Hull AG, Miyauchi T, Iso N 1988. Age and height distribution of Holocene transgressive deposits in eastern North Island, New Zealand. Palaeogeography, Palaeoclimatology, Palaeoecology 68: 135–151.

Ota Y, Hull AG, Berryman KR 1991. Coseismic uplift of Holocene marine terraces in the Pakarae River area, eastern North Island, New Zealand. Quaternary Research 35: 331–346.

Ota Y, Hull AG, Iso N, Ikeda Y, Moriya I, Yoshikawa T 1992. Holocene marine terraces on the northeast coast of North Island, New Zealand, and their tectonic significance. New Zealand Journal of Geology and Geophysics 35: 273–288.

Shane P, Froggatt PC, Smith I, Gregory M 1998. Multiple sources for sea-rafted Loisels Pumice, New Zealand. Quaternary Research 49: 271–279.

Stuiver M, Polach HA 1977. Discussion; reporting of C-14 data. Radiocarbon 19(3): 355–363.

Thornley S 1996. Neogene tectonics of Raukumara Peninsula, northern Hikurangi margin, New Zealand. Unpublished PhD thesis, Victoria University of Wellington, New Zealand.

Vucetich CG, Pullar WA 1964. Stratigraphy of Holocene ash in the Rotorua and Gisborne districts. Part 2. New Zealand Geological Survey Bulletin 73: 43–63.

Walcott RI 1987. Geodetic strain and the deformation history of the North Island, of New Zealand during the late Cainozoic. Philosophical Transactions of the Royal Society of London A321: 163–181.

Wallace LM, Beavan J, McCaffrey R, Darby D 2004. Subduction zone coupling and tectonic block rotations in the North Island, New Zealand. Journal of Geophysical Research 109(B12406): doi:10.1029/2004JB003241.

Wilson KJ, Berryman KB, Cochran UA, Little TA, in press. A Holocene incised valley infill sequence developed on a tectonically active coast: Pakarae River, New Zealand. Sedimentary Geology.

Yoshikawa T 1988. Pattern and rate of tectonic movement and late Quaternary geomorphic development in the Raukumara Peninsula, northeastern North Island, New Zealand. Bulletin of the Department of Geography University of Tokyo 20: 1–28.

New Zealand Journal of Geology & Geophysics, 2007, Vol. 50: 181–191 181
0028–8306/07/5003–0181 © The Royal Society of New Zealand 2007

Distribution, age, and uplift patterns of Pleistocene marine terraces of the northern Raukumara Peninsula, North Island, New Zealand

KATE WILSON[1*]
NICOLA LITCHFIELD[2]
KELVIN BERRYMAN[2]
TIM LITTLE[1]
[1]School of Earth Sciences
Victoria University of Wellington
PO Box 600
Wellington 6140, New Zealand
[2]GNS Science
PO Box 30368
Lower Hutt 5040, New Zealand
*Present address: GNS Science, PO Box 30368, Lower Hutt 5040, New Zealand.

Abstract The distribution and age of Pleistocene marine terraces fringing the northern Raukumara Peninsula, North Island, New Zealand, is revised. Two terraces, the higher Otamaroa Terrace and the lower Te Papa Terrace, are present from the eastern Bay of Plenty to near East Cape. Six optically stimulated luminescence (OSL) ages obtained from the terrace deposits and coverbeds represent the first radiometric ages from these terraces. Loess from the Te Papa Terrace has an age of 62.6 ± 6 ka and the underlying sand has an age of 58.3 ± 4.1 ka. Four OSL ages obtained from sand resting on the bedrock strath of the higher Otamaroa Terrace range from 64.5 ± 4.7 to 79.2 ± 5.5 ka. These OSL ages suggest that the Te Papa Terrace was formed during early Oxygen Isotope Stage (OIS) 3 and the Otamaroa Terrace was formed during OIS 5a. However, global geomorphological and regional loess unit correlations would imply the extensive Otamaroa Terrace correlates with OIS 5e and the loess on the Te Papa Terrace correlates to the Porewan loess of OIS 4, indicating the Te Papa Terrace formed during OIS 5a or earlier. Regardless of terrace age, the morphology of the terraces shows the coastal uplift mechanism is not related to upper plate faults, but is probably driven by deep-seated subduction zone processes.

Keywords Raukumara Peninsula; Quaternary; marine terraces; tectonic uplift rates

INTRODUCTION

This study reviews the distribution and chronology of a set of Pleistocene marine terraces that fringe the western and northeastern coasts of the Raukumara Peninsula (Fig. 1A). The geometry and rate of uplift of these terraces contributes to constraining uplift process boundaries operating across the Raukumara Peninsula and adjacent to the Hikurangi subduction margin. We present the first numeric ages obtained from these terraces and use global positioning system (GPS) elevation measurements along with coverbed stratigraphic studies to produce more accurate maps of the terrace surfaces and their uplift patterns. The terraces have previously been studied in some detail, particularly by Yoshikawa et al. (1980), Iso et al. (1982), Yoshikawa (1988), and Manning (1995). Therefore, we do not re-describe the details of the covered stratigraphy, origin, or distribution of these terraces. Rather, we focus on updating these studies by using modern dating techniques in an effort to better resolve the age of the terraces and placing the deformation patterns in a regional geodynamic context.

The most extensive terrace, named the Otamaroa Terrace (Yoshikawa et al. 1980), has been estimated previously to have formed during Oxygen Isotope Stage (OIS) 5e (Chapman-Smith & Grant-Mackie 1971; Yoshikawa et al. 1980). The lower Te Papa Terrace has been estimated to have formed during OIS 5a (Chapman-Smith & Grant-Mackie 1971; Yoshikawa et al. 1980). The highest terrace, named the Matakaoa Terrace, has a very limited distribution (Yoshikawa et al. 1980). It is thought to represent OIS 7 and has been mapped only at Matakaoa Point with fragmentary occurrence south of Whitianga Bay. Deposits on the terraces have not previously been directly dated; age control has been achieved only through correlation with global eustatic sea-level (SL) records and tephrochronology. Tephrochronology is of limited use in this region because the oldest widespread tephra is the c. 50 ka Rotoehu Tephra, which is present on all the Pleistocene marine terraces.

Raukumara Peninsula is situated inboard of the Hikurangi subduction zone (Fig. 1A,D). The mapped Pleistocene marine terraces studied here extend from a distance of c. 150 km normal to the Hikurangi trough, to within c. 90 km normal to the Hikurangi trough, and they are distributed either side of the northeastern projection of the crest of the Raukumara Range, a major axial range running approximately parallel to the Hikurangi margin (Fig. 1D). The marine terraces are therefore in a unique location to yield information about uplift rates and processes over a wide distance perpendicular to a subduction zone and around the perimeter of a major axial mountain range. Yoshikawa et al. (1980) projected the heights of the terraces to a plane normal to the trend of the East Coast, and they showed that the terraces have been uplifted and tilted to the northwest. These authors inferred that terrace uplift was associated with major earthquakes in the inner Kermadec Trench (Yoshikawa et al. 1980). We will use GPS elevations to obtain a more accurate image of terrace geometry and assess the controlling structure in light of recent active fault data.

G06027; Online publication date 17 July 2007
Received 22 August 2006; accepted 4 May 2007

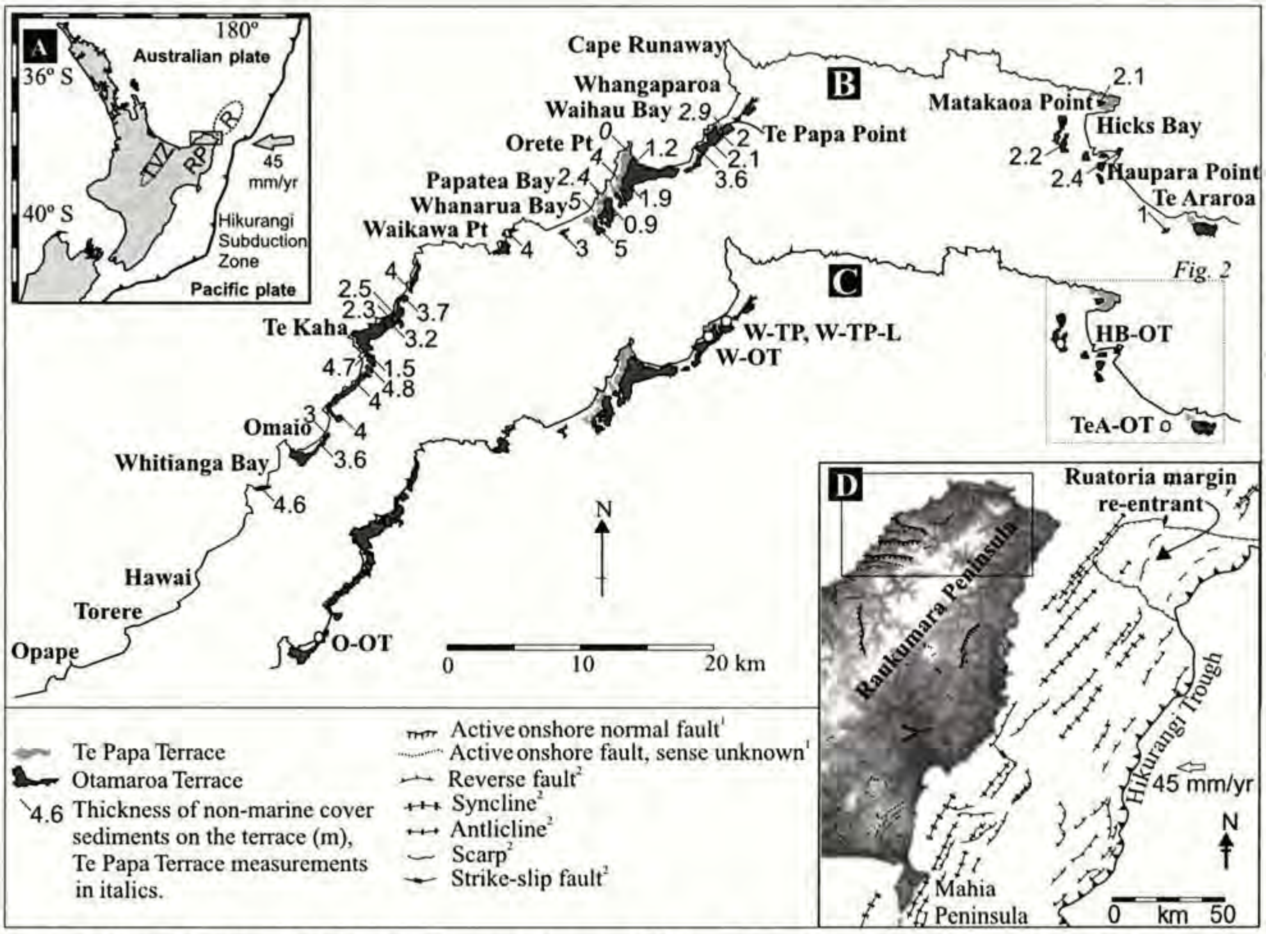

Fig. 1 A, North Island, New Zealand, with major tectonic features. TVZ: Taupo Volcanic Zone, RP: Raukumara Peninsula, R: Raukumara Plain. Relative plate motions after De Mets et al. (1994); Hikurangi subduction deformation front after Collot et al. (1996). **B**, Western and northern coastline of the Raukumara Peninsula with the distribution of the Otamaroa and Te Papa Terraces, location names and the sites where non-marine terrace coverbed thicknesses were measured. **C**, OSL sample locations. **D**, Topography and tectonic features of the Raukumara Peninsula. [1]Onshore active faults from the GNS Science Active Faults Database (http://data.gns.cri.nz/af/). [2]Offshore structures from Lewis et al. (1997).

METHODS

Terrace stratigraphy and distribution

Terrace coverbed descriptions were obtained from natural exposures at 26 locations (Fig. 1B); stratigraphic descriptions are available from the GNS Online Data Repository (http://data.gns.cri.nz/paperdata/index.jsp). We follow the marine terrace terminology of Pillans (1990) and define all sediments on the terrace strath as coverbeds, subdivided into marine and non-marine, or terrestrial. We measured the thickness of the topmost non-marine coverbeds sediments at six additional locations where we did not record an accompanying stratigraphic description. We used aerial photographs together with our stratigraphic studies to map the marine terraces.

Terrace elevations

Terrace surface elevations were measured using a real-time kinematic (RTK) GPS. Control points, including benchmarks, trig stations, and local sea level, were used to calibrate the vertical elevations measured by the GPS. Elevation uncertainties varied between regions depending on the number and uncertainty of the control points measured (the uncertainties for each region were as follows: Hicks Bay area: ±0.07 m, Waihau Bay area: ±0.55 m, Te Kaha area: ±0.77 m, Hawai area: ±0.11 m).

At most locations, an elevation point was measured in approximately the middle of the terrace surface. Where possible we took points from the rear, middle, and front of the terrace (e.g., at Te Kaha and Waihau Bay where the terrace surface was >1 km wide). It is best practice to measure a marine terrace elevation at the strandline, the most landward part of the terrace surface (Pillans 1990); however, the terraces were often too narrow for multiple points to be surveyed, and colluvial fans covered strandlines at many places. Sixty elevation points were collected from the Otamaroa Terrace, the highest and most extensive surface; 15 were collected from the lower Te Papa Terrace. At three locations in Te Araroa, we could not access the terrace surface with the GPS. We estimate the elevations of these terraces from topographic maps with a contour interval of 20 m. We estimate that the uncertainty of these elevations is ±10 m.

Age control

Optically stimulated luminescence (OSL) dating was performed on bulk samples of quartz and feldspar silt-sized grains from the terrace sand and loess coverbeds to estimate the age of the terraces. Six OSL samples were collected (Fig. 2, Table 1): four of these were from the Otamaroa Terrace (samples denoted by "OT") and two from the Te Papa

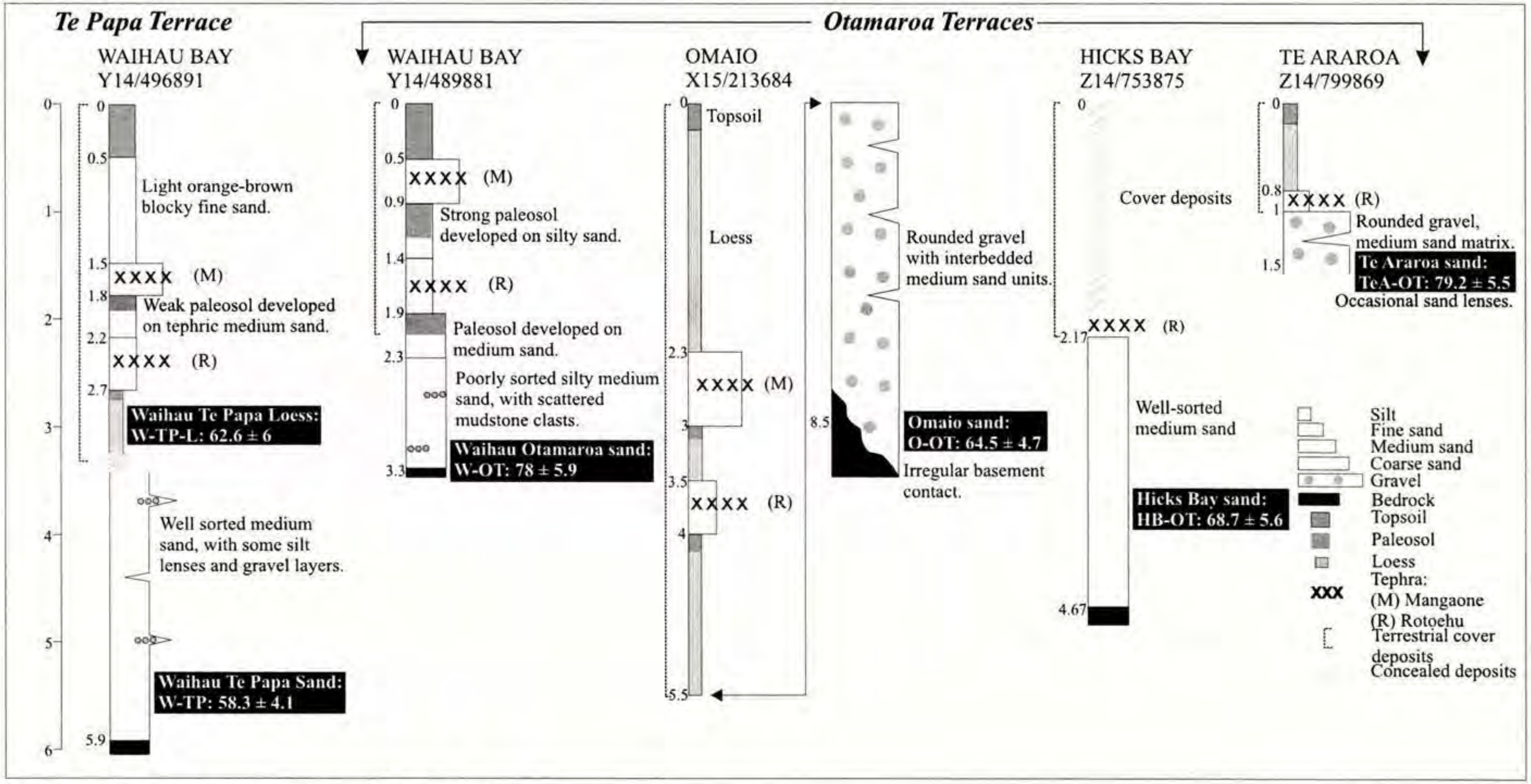

Fig. 2 Stratigraphic columns of terrace coverbeds at the OSL sampling locations.

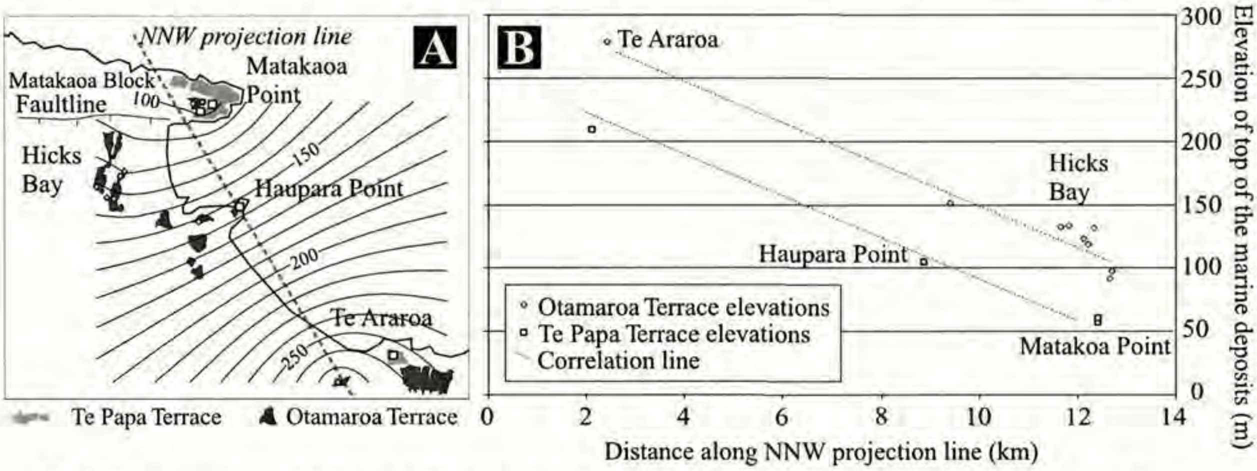

Fig. 3 A, Pleistocene terrace distribution at Matakaoa Point, Hicks Bay, and Te Araroa and locations where the terrace elevation was measured. All points were measured with an RTK GPS except the two locations at Te Araroa, which were estimated from a 1:25 000 topographic map. Contour lines show 10 m intervals on the highest terrace. The normal fault trace along the southern side of the Matakaoa Peninsula is shown. **B**, Elevation of the Otamaroa and Te Papa Terraces projected to a NNE trend line. This graph shows how the two terraces at Matakaoa Point correlate with the Otamaroa and Te Papa Terraces. There is no downthrow to the south of the terraces across the normal fault bounding the east–west-trending Matakaoa block.

Table 1 OSL sampling locations, modern elevations and stratigraphic context of the samples.

Sample name[1]	Location	Grid reference[2]	Elevation (m)	Stratigraphic context	OSL ages (ka)
W-TP	Waihau Bay	Y14/496891	22.8	Sand 0.5 m above bedrock strath.	58.3 ± 4.1
W-TP-L	Waihau Bay	Y14/496891	25.0	Loess overlying the sand of sample W-TP, underlying Rotoehu Tephra.	62.6 ± 6.0
O-OT	Omaio Bay	X15/213684	12.0	Sand lens within gravel, near undulating bedrock strath.	64.5 ± 4.7
W-OT	Waihau Bay	Y14/489881	62.4	Sand overlying bedrock strath.	78.0 ± 5.9
HB-OT	Hicks Bay	Z14/753877	131.2	Sand overlying bedrock strath.	68.7 ± 5.6
TeA-OT	Te Araroa	Z14/834816	279.0	Sand lens within gravel overlying bedrock strath.	79.2 ± 5.5

[1]TP, Te Papa Terrace; OT. Otamaroa Terrace; L, loess sample.
[2]New Zealand Map Grid co-ordinates.

Terrace (samples denoted by "TP"). All the Otamaroa Terrace samples and one sample from the Te Papa Terrace were selected from sediment interpreted to be beach deposits: coarse sands, or sand within gravel. Sampling was undertaken immediately above the bedrock strath so as to date the timing of strath cutting and avoid younger coverbeds (Fig. 2). One loess OSL sample was collected at Waihau Bay from the Te Papa Terrace (W-TP-L). This was collected from a loess layer overlying the sand from which the W-TP sand sample was obtained. The OSL dating was carried out at the Luminescence Dating Laboratory, Victoria University of Wellington. The technical details of the luminescence dating for these samples are described in Rieser (2005, 2006). These technical reports are available from the author by request.

RESULTS

Terrace distribution

On the western side of the Raukumara Peninsula coastline between Whangaparoa and Whitianga Bay, our terrace distribution maps are similar to those of Yoshikawa et al. (1980) and Manning (1995) (Fig. 1B). From Whangaparoa to Papatea Bay, there are two clear terraces—the Otamaroa (highest) and the Te Papa (lowest). From Papatea Bay to Omaio Bay, only the Otamaroa Terrace is present (Fig. 1B).

We do not include any terrace elevations southwest of Whitianga Bay in our analysis of the Pleistocene marine terraces owing to uncertainty about their origins and correlations, although Yoshikawa et al. (1980) and Manning (1995) mapped the Otamaroa Terrace southward to Opape. South of Whitianga Bay, the elevation of the terrace decreases to <20 m, and we found the marine and fluvial terraces became increasingly difficult to distinguish on the basis of geomorphology; the terrace stratigraphy also becomes increasingly ambiguous. Due to the lower uplift rates, there has probably been reworking of terrace sediments by fluvial processes and possibly re-occupation of the terrace. We also did not map terraces on the northern Raukumara Peninsula coastline between Cape Runaway and Matakaoa Point, though Yoshikawa et al. (1980) did map them there. We judged from our field visits that, although there is a marine terrace along most of the coastline, it has a steep surface gradient due to colluvial fan deposition. The terrace strath was difficult to locate, so we did not collect elevation measurements. On the eastern

Table 2 OSL results: radionuclide and water contents, measured a-value and equivalent dose, dose rate, and luminescence age (in bold).

Sample	Lab no.	a-value	dD_c/dt (Gy/ka)[1]	D_e (Gy)	dD/dt (Gy/ka)	Water content δ[2]	U (µg/g) from ^{234}Th	U (µg/g)[3] from ^{226}Ra, ^{214}Pb, ^{214}Bi	U (µg/g) from ^{210}Pb	Th (µg/g)[2] from ^{208}Tl, ^{212}Pb, ^{228}Ac	K (%)	OSL age (ka)
W-TP	WLL4 27	0.055 ± 0.008	01398 ± 0.0070	1015 ± 5.0	1.74 ± 0.09	1.138	0.91 ± 0.15	0.89 ± 0.09	1.08 ± 0.16	3.33 ± 0.06	1.07 ± 0.02	**58.3 ± 4.1**
WTP-L	WLL5 07	0.054 ± 0.003	0.1434 ± 0.0072	112.6 ± 4.8	1.80 ± 0.15	1.334	2.15 ± 0.14	1.90 ± 0.09	1.41 ± 0.11	5.69 ± 0.07	0.90 ± 0.02	**62.6 ± 6.0**
O-OT	WLL5 05	0.074 ± 0.007	0.1594 ± 0.0080	245.9 ± 13.2	3.81 ± 0.19	1.135	2.12 ± 0.20	1.77 ± 0.13	1.61 ± 0.18	7.60 ± 0.10	2.36 ± 0.05	**64.5 ± 4.7**
W-OT	WLL4 28	0.043 ± 0.005	0.1594 ± 0.0080	173.4 ± 7.2	2.20 ± 0.14	1.186	1.34 ± 0.18	1.41 ± 0.10	1.40 ± 0.19	3.88 ± 0.06	1.47 ± 0.03	**78.9 ± 5.9**
HBOT	WWL4 29	0.029 ± 0.004	0.1706 ± 0.0085	135.4 ± 6.0	1.97 ± 0.13	1.210	1.75 ± 0.20	1.35 ± 0.11	1.34 ± 0.20	4.51 ± 0.07	1.28 ± 0.03	**68.7 ± 5.6**
TeAOT	WLL5 06	0.074 ± 0.013	0.1706 ± 0.0085	181.3 ± 8.0	2.29 ± 0.12	1.136	1.75 ± 0.15	1.36 ± 0.10	1.24 ± 0.13	5.27 ± 0.07	1.14 ± 0.03	**79.2 ± 5.5**

[1]Contribution of cosmic radiation to the total dose rate, calculated as proposed by Prescott & Hutton (1994), *Radiation Measurements*, Vol. 23.
[2]Ratio wet sample to dry sample weight. Errors assumed 50% of (δ – 1).
[3]U and Th-content is calculated from the error weighted mean of the isotope equivalent contents.

side of the peninsula, at Hicks Bay and Te Araroa, our terrace distribution agrees with Yoshikawa et al. (1980). However, our terrace correlations differ slightly. The highest terrace on Matakaoa Point was defined by Yoshikawa et al. (1980) as the Matakaoa Terrace, and the lower terrace, the Otamaroa. Based on our new elevation data, we correlate the highest terrace on Matakaoa Point with the Otamaroa Terrace, and the lower Matakaoa Point terrace with the Te Papa Terrace (Fig. 3).

Terrace stratigraphy

Terrace cover deposits varied in thickness throughout the region, from 1.5 to >9 m (Fig. 1B). In the field we estimated the boundary between marine and non-marine deposits using sedimentology. Silt, loess, paleosols, colluvium, poorly sorted gravels, and the interbedded tephras were judged to be non-marine deposits. Well-sorted sands and gravels directly on the terrace strath were judged to be beach deposits.

The identification of beach sands was important for OSL sampling because we aimed to collect sand deposited synchronously with marine terrace incision. The sands sampled for OSL dating did not display any direct evidence of a beach depositional environment (e.g., shells within the sands have probably been leached out). However, the well-sorted nature of the sand and rounded gravels support wave sorting during deposition. Alternative mechanisms for sand and gravel emplacement are colluvial, aeolian, or fluvial deposition. Colluvial sediments were identified by the characteristics of silt matrix-supported angular gravel clasts and irregular bedding. We were careful not to select OSL samples from colluvial sediments. At Waihau Bay, Omaio, and Te Araroa, the sand sampled for OSL dating occurred in close association with gravel; therefore, an aeolian depositional mechanism is unlikely. At Hicks Bay, the sampled sand was well-sorted and did not occur in proximity with gravel (Fig. 2); it is possible this was dune sand. Fluvial deposition of gravels and sands was discounted at most locations where we measured and described the coverbed stratigraphy because there were no nearby fluvial sources. This leaves beach processes as the most likely depositional mechanism of well-sorted sands and gravels, and the modern beach also contains similar deposits. Only the OSL sampling sites at Omaio Bay and Te Araroa were proximal to rivers that may have occupied the terrace strath in the past. Therefore, at these two locations, it is possible that fluvial processes deposited the sampled sands post-terrace incision, rather than beach processes depositing the sand and gravel synchronous with terrace incision.

Loess was identified by sedimentary characteristics such as a massive, homogeneous nature, uniform silt grain size, and blocky texture when dry. Loess units in the study region typically displayed paleosols developed at the top of them, indicative of weathering during warm climatic conditions following loess deposition (Palmer & Pillans 1996).

Two tephras were commonly seen within the non-marine terrace coverbed sequence. These were a coarse-grained, dark orange tephra, and a fine–medium grained, pale creamy tephra. These are identified, respectively, as the Mangaone (c. 28 ka, Froggatt & Lowe 1990) and Rotoehu Tephras (c. 50 ka). Rotoehu Tephra age estimates range from 45 to 65 ka: Berryman (1992) estimates 52 ± 7 ka based on marine terrace correlation; Wilson et al. (1992) estimate 64 ± 4 ka based on radiometric dating of bracketing lavas; and Lian & Shane (2000) estimate 44 ± 3 ka based on OSL dating of bracketing loess. Tephra identification was made with reference to

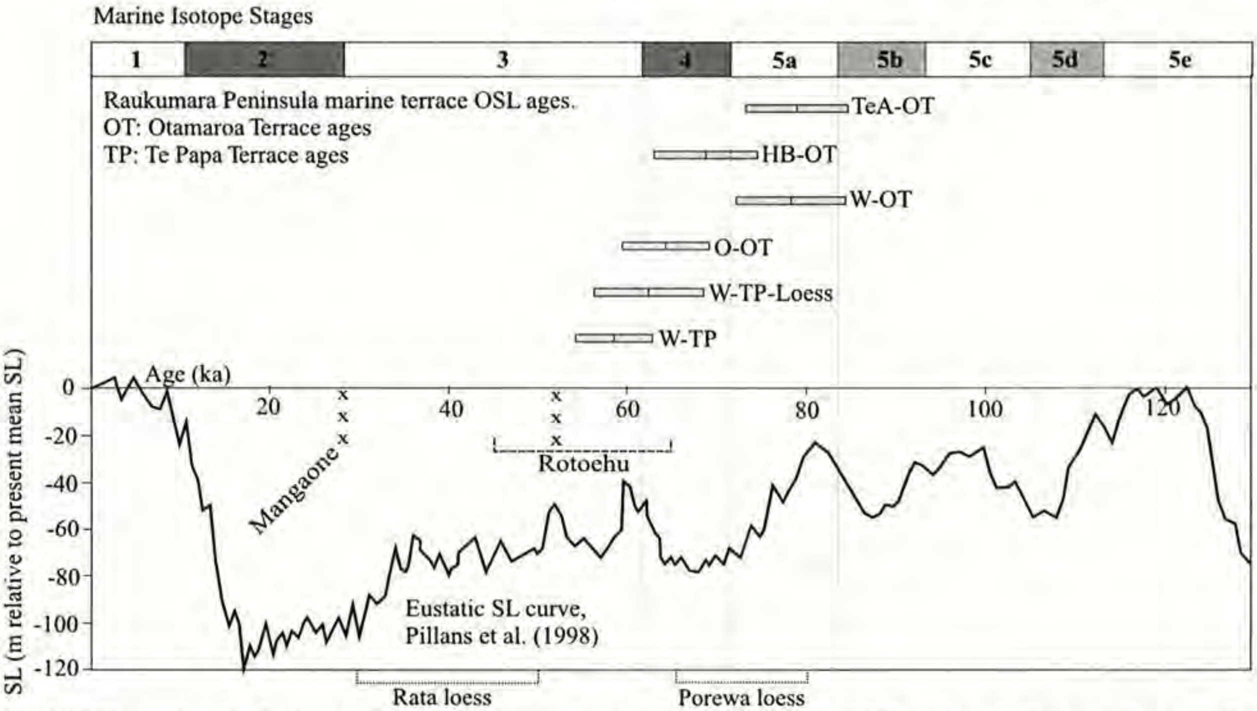

Fig. 4 OSL ages from the Raukumara Peninsula Pleistocene terraces. Samples with suffix "OT" are from the Otamaroa Terrace; suffix "TP" denotes from the Te Papa Terrace. Also shown are the oxygen isotope stage boundaries and the eustatic sea-level curve of Pillans et al. (1998).

the descriptions presented in Iso et al. (1982) and Manning (1995, 1996).

OSL results

The OSL results are shown in Table 2; all ages are presented with a standard error, though the actual error could be significantly larger. The four sand samples from the Otamaroa Terrace yielded ages of 64.5 ± 4.7, 68.7 ± 5.6, 78 ± 5.9, and 79.2 ± 5.5 ka. Sample O-OT, from the Otamaroa Terrace at Omaio, yielded an age of 64.5 ± 4.7 ka, though the sample was noted to be near saturation. Thus, there is a possibility that this sample is slightly older, as the dose-response curve fitting procedures are not very robust for almost saturated samples (Rieser 2005, 2006). The sand sample immediately above the bedrock strath of the Te Papa Terrace (W-TP) yielded an age of 58.3 ± 4.1 ka. The overlying loess (W-TP-L) yielded an age of 62.6 ± 6 ka. Apart from sample O-OT, the dose-response curve fitting for all samples was satisfactory, indicating the samples were not near saturation. There was no evidence of anomalous fading or disequilibrium in the U-series chains, and no other sample anomalies arose during the standard procedures of luminescence measurements (Rieser 2005, 2006).

DISCUSSION

Ages of the Raukumara Peninsula Pleistocene marine terraces

The study of Pleistocene marine terraces globally has shown some general relationships exist between climate, SL, terrace formation, and terrace cover deposits. Marine terrace straths are cut during relative SL highstands, therefore they represent warm climatic periods such as interglacials or interstadials. Beach deposits upon the terrace strath are assumed to be approximately equivalent in age with incision of the terrace strath, or at least represent a minimum age for the terrace. OSL dating, which measures time elapsed since the sediments were last exposed to sunlight, is a useful method to date the beach deposits directly and therefore determine the minimum terrace age.

The sand sample from the Te Papa Terrace at Waihau Bay yielded an OSL age of 58.3 ± 4.1 ka. This result suggests a depositional age of early OIS 3 (Fig. 4). The overlying loess sample collected at the same location yielded an age of 62.6 ± 6 ka. This loess age is slightly older than the underlying sand age; however, the samples are within the 1-sigma uncertainty range of one another (Fig. 4).

Ages obtained from the Otamaroa Terrace cluster around the OIS 5a eustatic SL highstand at 80 ka (Fig. 4). Samples from Te Araroa and Waihau Bay coincide with this age at 79.2 ± 5.5 and 78 ± 5.9 ka, respectively. The sample from Hicks Bay is younger—the depositional age of 68.7 ± 5.6 ka falls within OIS 4, a glacial period. However, within the uncertainty of the OSL age, this sample spans the end of OIS 5a and most of OIS 4 (Fig. 4). The sample from the Otamaroa Terrace at Omaio also falls mainly within OIS 4 at 64.5 ± 4.7 ka but this sample probably has an underestimated age due to saturation (Rieser 2006).

These six OSL ages suggest the Te Papa and Otamaroa Terraces formed during OIS 3 and 5a, respectively. These estimates are different from the earlier study by Yoshikawa et al. (1980), who suggested ages of OIS 5a and 5e. The revised age estimates imply terrace uplift rates higher than previously calculated (Table 3, Fig. 5). For example, an OIS

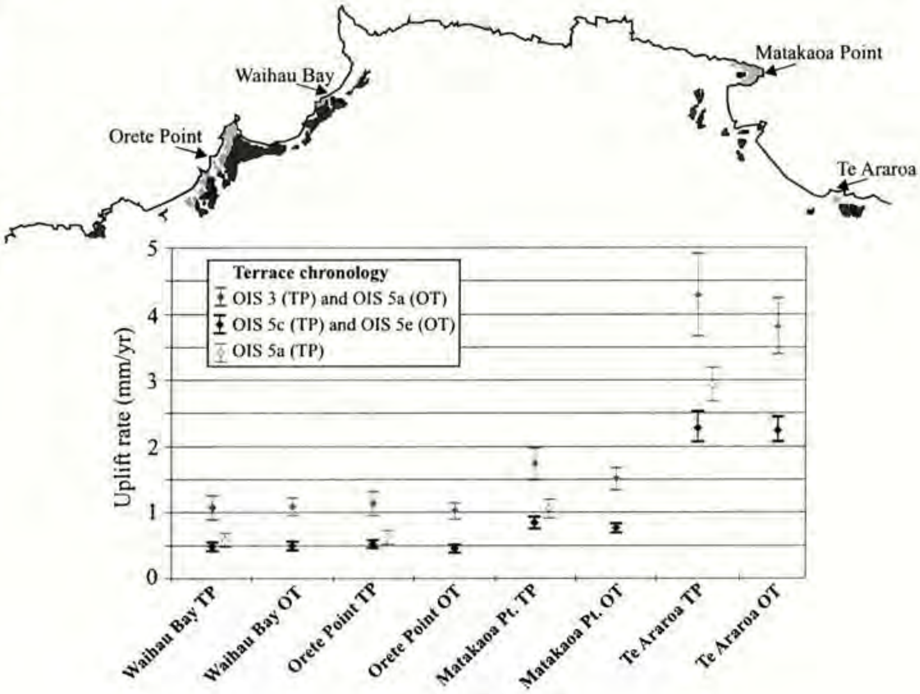

Fig. 5 Comparison of uplift rates at four locations, where the two terraces are adjacent to each other (locations shown on map at the top) using different terrace ages of OIS 3, 5a, 5c and 5e. Uplift rates are calculated using eustatic sea-level estimations of Pillans et al. (1998). Terrace elevation refers to the height of the top of the marine deposits on the terraces relative to modern mean sea level. See Table 3 for discussion of how the uplift rates were calculated.

Table 3 Terrace uplift rates (in bold) for the Te Papa and Otamaroa Terraces at four locations around the Raukumara Peninsula, calculated using the possible terrace ages discussed in the text.

			Estimated terrace age					
			OIS 3/5a		OIS 5c/5e		OIS 5a	
Terrace location	Elevation (m)	Uncertainty (±m)	Uplift rate (mm/yr)*	(Min.–max.)†	Uplift rate (mm/yr)	(Min.–max.)	Uplift rate (mm/yr)	(Min.–max.)
Waihau Bay TP	22.8	0.5	**1.06**	(0.90–1.26)	**0.48**	(0.41–0.56)	**0.59**	(0.49–0.70)
Waihau Bay OT	62.4	0.5	**1.08**	(0.95–1.23)	**0.50**	(0.44–0.57)		
Orete Point TP	26.1	0.5	**1.12**	(0.95–1.32)	**0.52**	(0.45–0.59)	**0.63**	(0.53–0.73)
Orete Point OT	57.0	0.5	**1.01**	(0.89–1.15)	**0.46**	(0.40–0.52)		
Matakoa Point TP	61.0	0.5	**1.71**	(1.49–1.97)	**0.85**	(0.76–0.95)	**1.06**	(0.94–1.21)
Matakoa Point OT	96.0	0.5	**1.50**	(1.35–1.67)	**0.77**	(0.70–0.85)		
Te Araroa TP	210.0	10.0	**4.24**	(3.67–4.91)	**2.27**	(2.03–2.53)	**2.93**	(2.58–3.32)
Te Araroa OT	279.0	10.0	**3.79**	(3.39–4.24)	**2.23**	(2.03–2.45)		

*Uplift rate = (terrace elevation – past eustatic SL[1])/age[1].
†Minimum uplift rate: mimimum uplift [(elevation – uncertainty) – (SL + uncertainty) / maximum age (age + uncertainty). Maximum uplift rate: maximum uplift [(elevation + uncertainty) – (SL – uncertainty) / mimimum age (age – uncertainty).
[1]Past eustatic sea levels estimated from Pillans et al. (1998): (stage, age, sea level); (OIS 3, 59 ± 5 ka, –40 ± 5 m); (OIS 5a, 80 ± 5 ka, –24 ± 5 m); (OIS 5c, 105 ± 5 ka, –28 ± 5 m); (OIS 5e, 125 ± 5 ka, 0 ± 5 m).

5a age for the Otamaroa Terrace at Te Araroa yields an uplift rate of 3.5–4.1 mm/yr (assuming eustatic SL during OIS 5a was –24 ± 5 m; Pillans et al. 1998), whereas an OIS 5e age yields uplift rates of 2.1–2.4 mm/yr (Table 3, Fig. 5).

Three issues arise from a OIS 3 and 5a terrace age revision for the Te Papa and Otamaroa Terraces. Firstly, marine terraces older than OIS 5a are not preserved along the northern Raukumara Peninsula. The eustatic SL highstands of OIS 5c and 5e were higher than the highstands of the OIS 3 and 5a. Therefore, given a consistent or, even slower, uplift rate dating back to c. 125 ka, the OIS 5e and 5c terraces should have formed and be present higher in the landscape, especially in areas of slower uplift rates. Secondly, two of the Otamaroa Terrace OSL samples (HB-OT and O-OT, Fig. 4) imply sand deposition on the marine terrace while eustatic SL was falling. On an uplifting coastline such as the Raukumara Peninsula, marine terrace incision is predicted to start when the rates of eustatic SL rise equal to or exceed the rate of land uplift (cf. Pillans 1990) (Fig. 4). Terrace incision will cease when eustatic SL rates decrease below the land uplift rate. The OSL ages of HB-OT (68.7 ± 5.6 ka) and O-OT (64.5 ± 4.7 ka) imply sand deposition after the peak of OIS 5a, when eustatic SL was falling and terrace incision was unlikely to have been occurring (Fig. 4). Thirdly, the loess mantling the Te Papa Terrace at Waihau Bay must have been deposited during early OIS 3, after incision of the terrace with a sufficient

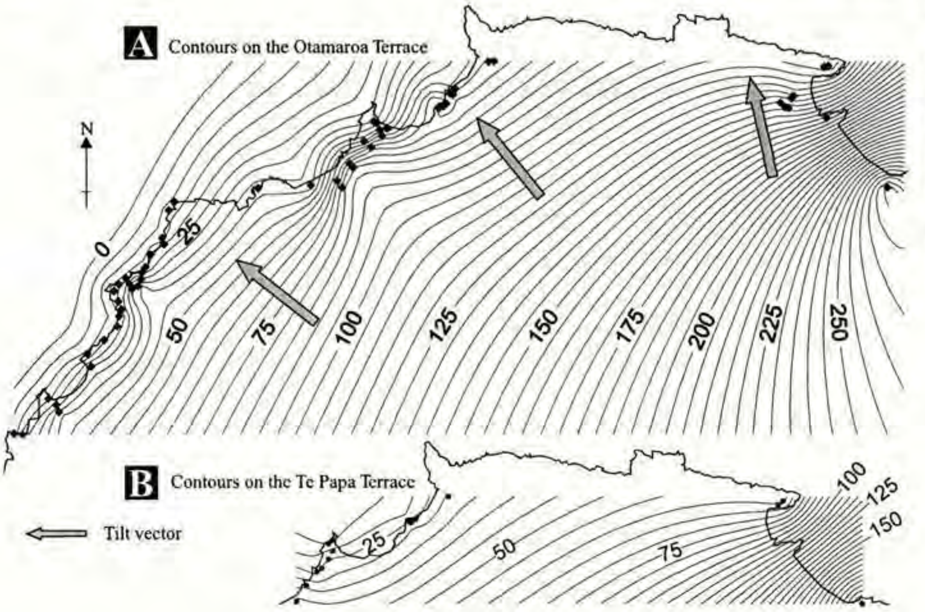

Fig. 6 A, Contours of the Otamaroa Terrace surface, heights are based on the elevation of the top of the marine sediments on the terrace. Contour interval is 5 m. B, Contours on the Te Papa Terrace, 5 m intervals, based on the elevation of the top of the marine deposits on the terrace. Contour maps were created from a gridded version of the data using the Golden Software Surfer surface mapping system.

time lapse for paleosol formation before deposition of the Rotoehu Tephra (Fig. 4). There are no known loess units in New Zealand that correlate to this age.

These three issues suggest a more critical appraisal of the OSL ages is warranted. The OSL age of 62.6 ± 6 ka for the Waihau Bay loess falls within OIS 4, suggesting a correlation to the widespread Porewa loess (Milne & Smalley 1979; Kennedy 1988, 1994; Litchfield & Rieser 2005). This is consistent with the presence of the Rotoehu tephra overlying this loess, with a paleosol developed in between. This stratigraphic correlation would imply the Te Papa Terrace was formed during or before OIS 5a, not during OIS 3 as implied by the sand OSL age from beneath the loess. Furthermore, the well-documented extent of the OIS 5e terrace globally (e.g., Bloom et al. 1974; Hsu 1992; Kelsey & Bockheim 1994; Pillans 1994; Murray-Wallace 2002; De Diego-Forbis et al. 2004; Marquardt et al. 2004) would suggest the Otamaroa Terrace was more likely to have formed during OIS 5e. Comparisons of uplift rates using different terrace ages show that for OIS 3/5a and OIS 5c/5e terrace ages the uplift rates remain steady during the late Pleistocene (Fig. 5). However, if an OIS 5a/5e terrace age combination is used, then uplift rates must have increased by 30% between OIS 5e and OIS 5a (from 2.23 mm/yr to 2.93 mm/yr; Table 3, Fig. 5). No known tectonic perturbations occurred during the time period from OIS 5e to 5a (125–80 ka) that may have caused accelerated uplift, therefore, if an age of OIS 5e is adopted for the Otamaroa Terrace, the Te Papa Terrace is most likely to have an age of OIS 5c.

A terrace chronology of >OIS 5a and OIS 5e for the Te Papa and Otamaroa Terraces, respectively, is consistent with regional loess chronology and geomorphological characteristics of Pleistocene marine terraces, but conflicting with all the OSL ages, except for the Waihau Bay loess. Although detailed description and analysis of the OSL technique is beyond the scope of this paper, we briefly examine some of the uncertainties in this relatively new technique that may be contributing to younger ages.

The possibility that the sand samples were not fully reset during deposition is discounted because this would result in older, rather than younger ages. Anomalous fading is also discounted because there was no sign shown by the routine 6 month testing for each of these samples. The only reported problem with fitting of the dose-response curves was for sample O-OT, which showed near-saturation signals. Thus, the age for this sample may be considered a minimum.

There are other possible reasons that the sample ages may be underestimated. (1) The sampled sands may have been deposited a significant amount of time after terrace formation. Terrestrial processes of erosion and resedimentation of cover sediments on the terrace strath would result in sediment ages younger than the terrace formation age. However, it is unlikely that the five sand samples we collected, from two terraces and at four widely spaced locations, would have all been affected by the same erosion and redeposition process. (2) The silt fractions from the beach sand samples were used for the OSL dating, and it is conceivable that this silt has filtered down the sediment profile from the younger deposits above, hence yielding a younger age. (3) It is also possible that the silt in this region does not contain sufficient amounts of K-feldspar for OSL dating. (4) There may be an as-yet-unidentified technical problem with the OSL dating process for silt samples extracted from sandy sediments. All of these reasons suggest that further testing of the OSL technique for dating beach sands using the silt fraction should be undertaken.

Deformation of the marine terraces in the context of Hikurangi subduction margin tectonics

The continuity of the Pleistocene marine terraces around the Raukumara Peninsula coastline means we are confident that the mapped Te Papa and Otamaroa Terrace surfaces are representative of the same time period at all locations. This means that, regardless of the terrace age, the terrace surface was originally horizontal with respect to SL and its deformation since is a reflection of the spatial patterns of tectonic processes. The morphology of the Otamaroa Terrace displays a distinctive northwestward tilt (Fig. 6A). The contour map shows some compression of the contours at Te Kaha and Orete Point because the Otamaroa Terrace is wide at these locations

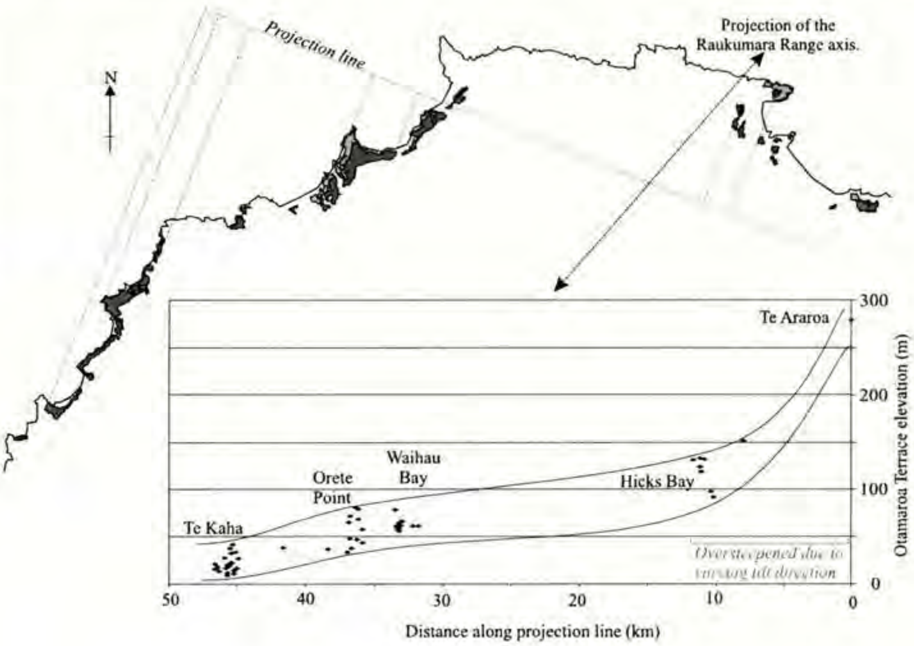

Fig. 7 Otamaroa Terrace elevations with distance from Te Araroa projected to a westnorthwest trend (approximately normal to the trend to the Hikurangi Subduction Zone. The dominant tilt direction in the Matakaoa Point to Te Araroa region is to the northnorthwest, therefore the projected tilt for this region shown in the graph is artificially oversteepened. Refer to Fig. 3B for a more accurate representation of tilt in this area.

and we were able to measure terrace elevations from the front, middle, and rear of the terraces, and the contours reflect the seaward slope of the terrace. The Te Papa Terrace, with more limited spatial extent, also shows the same morphology and northwestward tilt (Fig. 6B). The tilt on the Te Papa Terrace is not as steep compared with the Otamaroa Terrace. The similarity in geometry and progressive tilting through time indicates the same mechanism operated to uplift both terraces. The tilt vector of the terraces is approximately normal to the strike of the Raukumara Peninsula and the Hikurangi Trench (Fig. 7). This suggests that uplift of the terraces is related to Hikurangi Subduction Zone processes. However, the lack of mapped active faults implies it is not an upper plate fault accommodating the uplift. Rather, there are probably deeper lower-crust to upper-mantle processes controlling the uplift pattern (e.g., Reyners & McGinty 1999; Litchfield et al. 2007). Also, the location of greatest terrace uplift at Te Araroa is offset by a distance of c. 13 km from the projected northwestward trend of the axis of the Raukumara Range. This may imply that the crest of the Raukumara Range does not represent the zone of greatest uplift of the Raukumara Peninsula or that the zone of uplift has shifted westward during the late Pleistocene.

The terrace tilt is very steep and has a more northerly orientation on the eastern side of the peninsula from Matakaoa Point to Te Araroa (Fig. 3, 7). However, the terrace elevations in Fig. 7 have been projected to a WNW projection line, which is approximately parallel with the tilt on most of the terraces, except those in the Hicks Bay to Te Araroa region that tilt to the NNW. Therefore, the terrace tilt in Fig. 7 is artificially oversteepened. If the projection line for this region were in a more northerly direction, the terrace tilt would be slightly less (cf. Fig. 3). There are no known onshore or near-offshore active faults that can account for this geometry (Fig. 1D) (Collot et al. 1996; Lewis et al. 1997; Mazengarb & Speden 2000). The more northerly tilt direction of the terraces in this region may be related to the offshore transition into the Raukumara Plain, a long-lived deep forearc basin immediately north of Matakaoa Point (Fig. 1A) (Gillies & Davey 1986; Davey et al. 1997).

CONCLUSIONS

This study presents the first radiometric dating of the Raukumara Peninsula Pleistocene marine terraces. Five OSL ages from sand deposits on the terrace straths suggest that the Otamaroa Terrace was formed during OIS 5a and the Te Papa Terrace was formed during OIS 3. However, the OSL age of loess on the Te Papa Terrace suggests the loess unit may correlate with the OIS 4 Porewa loess, therefore requiring the Te Papa Terrace to have formed before OIS 4 and conflicting with the sand OSL age from the same location. Furthermore, if the Otamaroa Terrace was formed during OIS 5a, then this means the OIS 5e terrace is not present on the Raukumara Peninsula. This is unusual as the OIS 5e marine terrace is globally common and often the only Pleistocene marine terrace present on stable and uplifting coastlines. These results, therefore, do not satisfactorily resolve the age of the Raukumara Peninsula Pleistocene terraces but they do raise important questions regarding either the use of loess stratigraphy and geomorphic correlations to date marine terraces or the application of OSL dating to beach sands. The geometry of the Raukumara Peninsula terraces shows a strong northwest tilt which cannot be attributed to any known active faults in the region. We suggest that upper mantle and lower crust processes related to the Hikurangi Subduction Zone control the geometry and uplift of the terraces.

ACKNOWLEDGMENTS

This research was funded by an EQC Student Grant (Project 6UNI/501). KJW was supported by the GNS Science Sarah Beanland Memorial Scholarship. Uwe Rieser of the Victoria University of Wellington Luminescence Dating Laboratory is thanked for his contribution to the luminescence dating. The manuscript was improved thanks to reviews by Alan Palmer and Colin Murray-Wallace.

REFERENCES

Berryman K 1992. A stratigraphic age of Rotoehu ash and late Pleistocene climate interpretation based on marine terrace chronology, Mahia Peninsula, North Island, New Zealand. New Zealand Journal of Geology and Geophysics 35(1): 1–7.

Bloom AL, Broecker WS, Chappell J, Matthews RK, Mesolella KJ 1974. Quaternary sea level fluctuations on a tectonic coast: new $^{230}Th/^{234}U$ dates from the Huon Peninsula, New Guinea. Quaternary Research 4: 185–205.

Chapman-Smith M, Grant-Mackie JA 1971. Geology of the Whangaparoa area, eastern Bay of Plenty. New Zealand Journal of Geology and Geophysics 14: 3–38.

Collot J-Y, Delteil J, Lewis K, Davy B, Lamarche G, Andru J-C, Barnes P, Chanier F, Chaumillon E, Lallemand S and others 1996. From oblique subduction to intra-continental transpression: structures of the southern Kermadec-Hikurangi margin from multibeam bathymetry, side-scan sonar and seismic reflection. Marine Geophysical Researches 18(2–4): 357–381.

Davey FJ, Henrys S, Lodolo E 1997. A seismic crustal section across East Cape convergent margin, New Zealand. Tectonophysics 269: 199–215.

De Diego-Forbis T, Douglas R, Gorsline D, Nava-Sanchez E, Mack L, Banner J 2004. Late Pleistocene (last interglacial) terrace deposits, Bahia Coyote, Baja California Sur, Mexico. Quaternary International 120: 29–40.

De Mets C, Gordon RG, Argus DF, Stein S 1994. Effect of recent revisions to the geomagnetic reversal timescale on estimates of current plate motions. Geophysical Research Letters 21: 2191–2194.

Froggatt PC, Lowe DJ 1990. A review of late Quaternary silicic and some other tephra formations from New Zealand: their stratigraphy, nomenclature, distribution, volume and age. New Zealand Journal of Geology and Geophysics 33: 89–109.

Gillies PN, Davey FJ 1986. Seismic reflection and refraction studies of the Raukumara forearc basin, New Zealand. New Zealand Journal of Geology and Geophysics 29: 391–403.

Hsu JT 1992. Quaternary uplift of the Peruvian coast related to the subduction of the Nazca Ridge: 13.5 to 15.6 degrees latitude. Quaternary International 15/16: 87–97.

Iso N, Okada A, Ota Y, Yoshikawa T 1982. Fission-track ages of late Pleistocene tephras on the Bay of Plenty coast, North Island, New Zealand. New Zealand Journal of Geology and Geophysics 25: 295–303.

Kelsey HM, Bockheim JG 1994. Coastal landscape evolution as a function of eustasy and surface uplift rate, Cascadia margin, southern Oregon. Geological Society of America Bulletin 106: 840–854.

Kennedy N 1988. Late Quaternary loess associated with the Mamaku Plateau, North Island, New Zealand. In: Eden DN, Furkert RJ ed. Loess: its distribution, geology and soils. Rotterdam, A A Balkema. Pp. 71–80.

Kennedy N 1994. New Zealand tephro-chronology as a tool in geomorphic history of the c. 140 ka Mamaku Ignimbrite Plateau and in relating oxygen isotope stages. Geomorphology 9: 97–115.

Lewis KB, Collot J-Y, Davy B, Delteil J, Lallemand S, Uruski C 1997. North Hikurangi GeodyNZ swath maps: depths, texture and geological interpretation 1:500 000. National Institute for Water and Atmospheric Research Miscellaneous Series Chart 72. Wellington.

Lian OB, Shane P 2000. Optical dating of paleosols bracketing the widespread Rotoehu Tephra, North Island, New Zealand. Quaternary Science Reviews 19(16): 1649–1662.

Litchfield N, Rieser U 2005. Optically stimulated luminescence age constraints for fluvial aggradation terraces and loess in the eastern North Island, New Zealand. New Zealand Journal of Geology and Geophysics 48: 581–589.

Litchfield NJ, Ellis S, Berryman K, Nicol A 2007. Subduction related uplift in the Hikurangi margin, New Zealand. Journal of Geophysical Research (Earth Surface). vol. 112, FO2021, doi: 10.1029/2006JF000535, 2007.

Manning DA 1995. Late Pleistocene tephrostratigraphy of the eastern Bay of Plenty region, New Zealand. Unpublished PhD thesis, Victoria University of Wellington, Wellington, New Zealand.

Manning DA 1996. Middle–late Pleistocene tephrostratigraphy of the eastern Bay of Plenty, New Zealand. Quaternary International 34–36: 3–12.

Marquardt C, Lavenu A, Ortleib L, Godoy E, Comte D 2004. Coastal neotectonics in Southern Contral Andes: uplift and deformation of marine terraces in Northern Chile (27 degrees south). Tectonophysics 394: 193–219.

Mazengarb C, Speden IG 2000. Geology of the Raukumara area. Institute of Geological & Nuclear Sciences 1:250 000 Geological Map 6. Lower Hutt, New Zealand. Institute of Geological & Nuclear Sciences Limited.

Milne JDG, Smalley IJ 1979. Loess deposits in the southern part of the North Island of New Zealand: an outline stratigraphy. Acta Geologica Academiae Sientiarum Hungaricae Tomus 22: 197–204.

Murray-Wallace CV 2002. Pleistocene coastal stratigraphy, sea-level highstands and neotectonism of the southern Australian passive continental margin—a review. Journal of Quaternary Science 17(5–6): 469–489.

Palmer A, Pillans B 1996. Record of climatic fluctuations from ca. 500 ka loess deposits and paleosols near Wanganui, New Zealand. Quaternary International 34–36: 155–162.

Pillans B 1990. Pleistocene marine terraces in New Zealand: a review. New Zealand Journal of Geology and Geophysics 33: 219–231.

Pillans B 1994. Direct marine-terrestrial correlations, Wanganui Basin, New Zealand: the last 1 million years. Quaternary Science Reviews 13: 189–200.

Pillans B, Chappell J, Naish T 1998. A review of the Milankovich climate beat: template for Plio-Pleistocene sea-level changes and sequence stratigraphy. Sedimentary Geology 122: 5–21.

Reyners M, McGinty P 1999. Shallow subduction tectonics in the Raukumara Peninsula, New Zealand, as illuminated by earthquake focal mechanisms. Journal of Geophysical Research 104(B2): 3025–3034.

Rieser U 2005. Determination of sediment deposition ages by luminescence dating. Victoria University of Wellington Technical Report 05/11.

Rieser U 2006. Determination of sediment deposition ages by luminescence dating. Victoria University of Wellington Technical Report 06/11.

Wilson CJN, Houghton BF, Lanphere MA, Weaver SD 1992. A new radiometric age estimate for the Rotoehu Ash from Mayor Island volcano, New Zealand. New Zealand Journal of Geology and Geophysics 35: 371–374.

Yoshikawa T 1988. Pattern and rate of tectonic movement and Late Quaternary geomorphic development in the Raukumara Peninsula, northeastern North Island, New Zealand. Bulletin of the Department of Geography University of Tokyo 20: 1–28.

Yoshikawa T, Ota Y, Yonekura N, Okada A, Iso N 1980. Marine terraces and their tectonic deformation on the northeast coast of the North Island, New Zealand. Geographical Review of Japan 53(4): 238–262.

ABSTRACT

The coastal geomorphology of the Raukumara Peninsula, North Island, New Zealand, is investigated with the aim of understanding the geodynamics of this segment of the Hikurangi subduction zone. There are few active faults on the Raukumara Peninsula and there have been no historical subduction earthquakes on this part of the margin. Geodetic and geologic evidence suggests the onshore forearc is extending and sliding trenchward. However, Holocene and Pleistocene terraces that have some of the highest uplift rates and elevation in New Zealand occur in this region. Sediment underplating has previously been suggested as a cause of coastal forearc uplift, yet the inferred gradualness of this process does not reconcile with the inferred episodic nature of uplift suggested by stepped Holocene marine terraces along the Raukumara Peninsula. This study focuses on resolving these apparent inconsistencies in the current knowledge of the Raukumara sector of the Hikurangi margin by using the mechanisms of coastal uplift to improve our general understanding of forearc deformation processes.

The mid to late Holocene marine terrace chronology and distribution at the Pakarae River mouth locality on the central Raukumara Peninsula eastern coastline is revised. The coverbed sediments and morphology of the terrace surfaces and straths there are consistent with abandonment of each terrace during a coseismic coastal uplift event. The terraces are offset across the Pakarae Fault, a normal fault, but tilt vectors of the terraces suggest the dominant structure driving uplift is instead an offshore reverse fault in the upper plate of the subduction zone. The highest Holocene marine terrace at the Pakarae River mouth is underlain by a transgressive fluvio-estuarine sequence that documents infilling of the Pakarae River paleo–valley from ~ 10,000 – 7,000 cal. yrs B.P. prior to eustatic sea level stabilisation. This sequence is an example of a valley infill sequence modified by tectonic uplift. By comparing it with facies models developed from stable coastlines a new facies architecture model is developed for incised valley infilling during conditions of synchronous eustatic sea level rise and tectonic uplift.

The sedimentology and biostratigraphy of the Pakarae River incised valley infill sequence is also used to reconstruct the paleoenvironmental evolution of the paleo-valley during the early Holocene. Two estuarine units display sudden vertical transitions to floodplain sediments implying significant marine regressions. During the depositional period, however, eustatic sea level was rapidly rising. The marine regressions, and associated estuary abandonment, are therefore attributed to coseismic coastal uplift events, occurring at ~9,000 and ~8,500 cal. yrs B.P. A third uplift between 8,500 and ~7,350 cal. yrs B.P. is inferred from a significant difference between the amount of sediment preserved and the predicted sediment thickness according to the eustatic SL curve. This study demonstrates the utility of the stratigraphic analysis of incised valley infill sequences for neotectonic investigations on active coasts. In practice the application of incised valley infill analysis allows extension of coastal paleoseismic histories back prior to the time of eustatic sea level rise culmination. The combination of the Pakarae River mouth marine terrace and sedimentary infill sequence data yields the longest record of coastal paleo-earthquakes yet constructed globally.

Along the northeastern coastline of the Raukumara Peninsula a variety of Holocene coastal features have been studied to determine the uplift mechanism of this region. Topographic and coverbed stratigraphic data from previously interpreted coseismic marine terraces at the Horoera and Waipapa localities, east of Te Araroa, indicate that, despite their stepped surface morphology, they are not of marine origin and thus cannot be attributed to coseismic coastal uplift events. Paleoenvironmental analysis of drill cores of early Holocene sediments underlying the Hicks Bay flats shows a typical incised valley infill sequence with gradual transitions from fluvial to estuarine and back to fluvial. However, there are significant differences between the thickness of preserved intertidal infill sediments and the amount of space created by eustatic sea level rise. Therefore, uplift did occur during early Holocene evolution of the Hicks Bay paleo-estuary, but at this location there is no evidence of any sudden or coseismic land elevation changes. The beach ridge sequence of Te Araroa slopes gradually toward the present day coast with no evidence of coseismic steps. It is inferred the evolution of the beach ridges was controlled by a variable sediment supply rate in the context of a background tectonic uplift rate that was geologically continuous rather than punctuated. Although no individual dataset from the Holocene coastal features of the northeastern Raukumara Peninsula can uniquely resolve the mechanism of uplift, a careful evaluation and integration of all available evidence indicates uplift of this region has been driven by a gradual and aseismic mechanism. Pleistocene marine terraces fringing the northern coastline of the Raukumara Peninsula, and overlapping with the northeastern Raukumara Peninsula study area, display a northwest tilt. The tilt vector steepens and rotates gradually northward on the eastern side of the Peninsula. As there are no upper plate active faults that can account for this geometry, it is concluded that the buoyancy of underplated sediment beneath the forearc drives aseismic uplift of this region.

The Holocene coastal uplift mechanism data from the Pakarae River mouth and the northeastern Raukumara Peninsula are integrated with other coastal geomorphic data from the Raukumara Peninsula in this thesis. Distinct spatial variations in the coastal uplift rates and mechanisms are seen. The main parameter controlling the distribution of aseismic and coseismic deformation processes is inferred to be the distance of the forearc from the Hikurangi Trough, and depth to the underlying plate interface. Three margin-parallel zones of forearc uplift mechanisms are identified: (1) a zone of coseismic uplift on upper plate contractional faults located within 20 – 80 km of the trench; (2) a passive inner forearc zone at a margin-normal distance of ~80-120 km from the trench, in which vertical tectonic movement is controlled by distal upper plate structures and or slip on the plate interface; and (3) a zone of aseismic uplift driven by sediment underplating located at a margin-normal distance of ~120 – 180 km of the trench, also encompassing the Raukumara Ranges. Each of the zones has specific seismic hazard implications. Reverse faults within the coseismic uplift zone pose a significant seismic and tsunami hazard to Raukumara Peninsula coastal communities, while seismic hazard in the zone of aseismic uplift is probably less than previously thought. The passive forearc zone probably experiences uplift or subsidence during plate interface rupturing earthquake and therefore it may be the only one of the three zones that has the potential to record past subduction earthquakes. This study demonstrates the value of coastal geomorphology and stratigraphic studies in subduction zone neotectonic and paleoseismology studies. Variances in coastal uplift mechanisms across the Raukumara Peninsula are related to spatial position within the Hikurangi subduction margin and this has implications for our understanding of forearc deformation processes along the length of the margin.

MECHANISMS OF LATE QUATERNARY COASTAL UPLIFT ALONG THE RAUKUMARA PENINSULA SEGMENT OF THE HIKURANGI MARGIN, NORTH ISLAND, NEW ZEALAND.

Report prepared for the Earthquake Commission

Project Number 6UNI/501

June, 2007.

TABLE OF CONTENTS

CHAPTER FIVE

Holocene coastal evolution and uplift mechanisms of the northeastern Raukumara Peninsula, North Island, New Zealand. 97

CHAPTER SIX

Distribution, age and uplift patterns of Pleistocene marine terraces of the northern Raukumara Peninsula, North Island, New Zealand. 141

CHAPTER 7

Relationships between late Quaternary coastal geomorphology and subduction zone geodynamics of the Raukumara Sector of the Hikurangi margin. 159

CHAPTER 8

Conclusions 205

LIST OF FIGURES

CHAPTER 1

CHAPTER 2

CHAPTER 3

CHAPTER 4

CHAPTER 5

CHAPTER 6

CHAPTER 7

List of Tables

Chapter 2

Chapter 3

Chapter 4

Chapter 5

Chapter 6

CHAPTER ONE

INTRODUCTION: THE HIKURANGI MARGIN, SEISMIC HAZARD AND COASTAL GEOMORPHOLOGY

1.1. Introduction

Plate convergence at the Hikurangi subduction margin directly controls the geomorphology, structure and seismicity of the East Coast of the North Island, New Zealand. Because no large subduction earthquakes have taken place historically, the plate interface represents potentially the most significant, yet least well-constrained seismic hazard in New Zealand. Until recently, there has been a comparative under-appreciation of how the geomorphology of the margin can yield information on the geodynamics of the subduction zone. This report contributes to our understanding of the Hikurangi subduction zone specifically by using coastal geomorphology and stratigraphy to document rates, styles and mechanisms of forearc uplift mechanisms, and we aim to relate this to plate boundary processes and seismic hazard.

The focus of this report, based on the PhD thesis of Kate Wilson, is the Raukumara Peninsula sector of the Hikurangi margin (Fig. 1). This northeastern coastline has some of the most spectacular uplifted Holocene and Pleistocene marine terraces of anywhere in New Zealand (Figs. 2 –5, Yoshikawa et al., 1980; Ota et al., 1988; Ota et al., 1992; Berryman, 1993a, b). A key observation that was initially identified was that these marine terraces are geomorphically similar to other marine terraces of the Wairarapa and Wellington regions, at the southwestern end of the Hikurangi margin (Fig. 1), but despite the this apparent similarity, geophysical studies of seismicity and geodesy, and structural geology, indicate there are significant changes in how plate convergence is accommodated along the strike of the margin between these two regions (Collot et al., 1996; Beanland and Haines, 1998; Reyners, 1998; Wallace et al., 2004). Thus, a paradox of similar coastal geomorphology under different tectonic regimes appears to exist along the Hikurangi margin. Therefore, one of the main questions addressed in this thesis is what is the mechanism of coastal uplift of the Raukumara Peninsula and is it different from that farther to the south?

On the southern margin, the prevalence of active contractional faults and historical records of coseismic coastal uplift results in a widely held acceptance that terraces here are uplifted in discrete events and this deformation is accommodated by upper plate reverse faults. On the Raukumara Peninsula, the virtual absence of recognised active faulting and proposed trenchward gravitational collapse and expansion of the forearc (Thornley, 1996; Arnadottir et al., 1999) beg the question of what structures control the uplift of these terraces? Are they uplifted by aseismic or coseismic mechanisms? Is the deformation accommodated by the plate interface, upper plate faults or, as yet, unidentified structures?

A variety of tools are used in this project to understand the coastal geomorphic evolution and its relationship to neotectonism. At several sites previously-used methods such as surveying, radiocarbon dating and stratigraphic studies are applied. At two locations biostratigraphy and facies architecture of incised valley infill sedimentary sequences are used to document paleoenvironmental evolution of valleys under conditions of rising eustatic sea level and tectonic uplift. Biostratigraphic studies of marginal marine sediments have been used extensively in New Zealand (for example, Hayward et al., 2004; Hayward et al., 2006; Cochran et al., 2006) and globally (for example, Atwater, 1987; Darienzo et al., 1994; Hemphill-Haley, 1995; Nelson et al., 1996; Clague, 1997) to infer coastal paleoseismic events. At some subduction margins, such as Cascadia, tidal wetland biostratigraphy provides the key evidence for past great earthquakes (Atwater, 1987; Hemphill-Haley, 1995). Thus, the value of marginal marine biostratigraphy has been proven. However, a common theme of these previous studies has been their use, firstly, in regions dominated by coseismic subsidence events and, secondly, during Late Holocene time periods when sea level has been approximately stable. In this study the biostratigraphic technique is used at locations on the Raukumara Peninsula that are undergoing tectonic uplift and applied to the early Holocene period when eustatic sea level was rapidly rising. Therefore while the primary aim of this thesis is to understand relationships between coastal geomorphology and subduction zone geodynamics, we also aim to develop a new methodology that uses the stratigraphy of incised valleys as a tool to constrain the rate and tempo of coastal uplift, and to reconstruct the paleoseismic history at such sites.

In Chapter Two we present a timely revision of the marine terrace distribution and chronology at the Pakarae River mouth, one of the most well-documented coastal uplift locations of the Raukumara Peninsula (Figs. 1, 2). Here seven mid-late Holocene marine terraces were identified by Ota et al. (1991) and uplifted early Holocene estuarine sediments were described by Berryman et al. (1992). This location provided an opportunity to test whether rapid uplift at this site is driven by coseismic uplift on faults or whether other, more gradual processes operate here. Utilising modern methods of surveying and AMS radiocarbon dating, we constrain the timing and magnitude of coastal uplift at this location to a higher degree of precision than previously, and assess the tilt vectors on the terraces to estimate the probable location of the fault accommodating uplift.

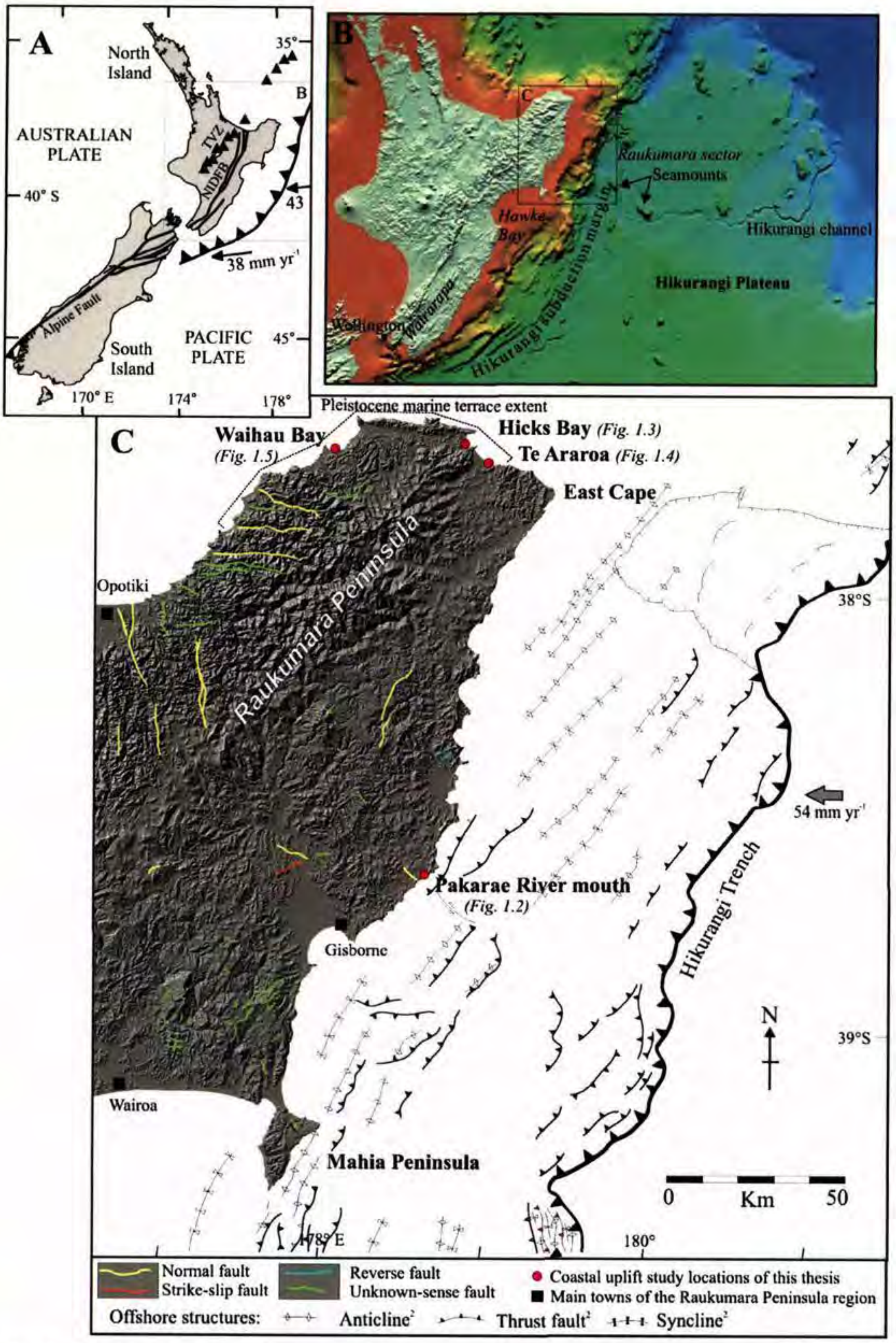

Fig. 1. (A) Major tectonic elements of New Zealand. The major fault lines (black lines) and the volcanic arc (black triangles) are shown (NIDFB: North Island dextral fault belt, TVZ: Taupo Volcanic Zone).Plate motions rates after De Mets et al. (1994). **(B)** Geographic regions, bathymetry and offshore geologic features of the Hikurangi subduction margin (map source: CANZ Group, 1996). **(C)** Shaded relief image of the Raukumara sector of the Hikurangi subduction zone. Active faults are shown (onshore faults source: New Zealand Active Faults Database, http://data.gns.cri.nz/af/, offshore faults source: Lewis, 1997) as are the coastal geomorphology study locations of this thesis and the main settlements of the region. Plate motion rate of Pacific-Kermadec convergence after Collot et al. (2001).

The main focus of the Pakarae River mouth study is on the early Holocene uplifted incised valley infill sequence, now exposed along the Pakarae River banks (Fig. 2). This sequence was first identified by Berryman et al. (1992) when the sediments were dated and shown to have been deposited within the Pakarae River paleo-valley when sea level was still rising due to post-glacial melt. In Chapter Three the sequence is revisited and we present a detailed examination of the sedimentology, biostratigraphy and chronology of the sediments at multiple riverbank exposures. Biostratigraphy yields excellent paleoenvironmental control and several alternations between estuarine and fluvial environments can be seen. However, to understand the tectonic significance of how the paleoenvironmental facies are distributed in this paleo-valley exposure the sequence must be placed in a context that enables comparisons with equivalent deposits on stable coastlines. Several facies models have been developed for incised valley infill sequences on stable coasts due to their applicability in recording past eustatic sea level and climate changes. In Chapter Three a facies model is presented for incised valley infill sequences on tectonically active coastlines, based upon the Pakarae River mouth stratigraphic sequence.

With a context established for incised valley infill sequences on active coasts, in Chapter Four we identify which paleoenvironmental facies transitions at the Pakarae River mouth are part of a predictable valley infilling sequence under rising eustatic sea level and which transitions are anomalous, hence more likely to be related to tectonic events. Models of palaeographic evolution of the Pakarae River paleo-valley have been developed and the timing and magnitude of uplift events that occurred during infilling of the valley have been assessed. This chapter demonstrates that incised valley infill sequences can be used as a new approach or tool in paleoseismic investigations of coastal locations, and biostratigraphy of these sequences can constrain the rate at which tectonic processes took place.

The other coastal region of the Raukumara Peninsula studied is the northeastern portion (Fig. 1); here there is a rich record of both Holocene and Pleistocene uplifted marine deposits (Figs. 3, 4). In Chapter Five two marine terrace sequences near East Cape that were previously thought by Ota et al. (1992) to have been coseismically uplifted are re-evaluated. Coverbed stratigraphy and topographic surveying are used to determine the origin of the terraces. The remarkable uplifted beach ridge sequence at Te Araroa is also revisited. Here additional age control and ridge topography are used to re-assess the mechanism of beach ridge uplift (Fig. 4). A study of the transgressive marine sediments infilling the Hicks Bay paleo-valley is also presented in Chapter Five (Fig. 5). This study uses a similar methodology to the Pakarae River mouth study, except at Hicks Bay drill cores of the transgressive sediments rather than outcrop are the primary data source. Biostratigraphy is used to constrain the sediment depositional environments, and paleogeographic models of the infilling valley are developed. Again, the utility of transgressive marine sediments in coastal neotectonic studies is demonstrated.

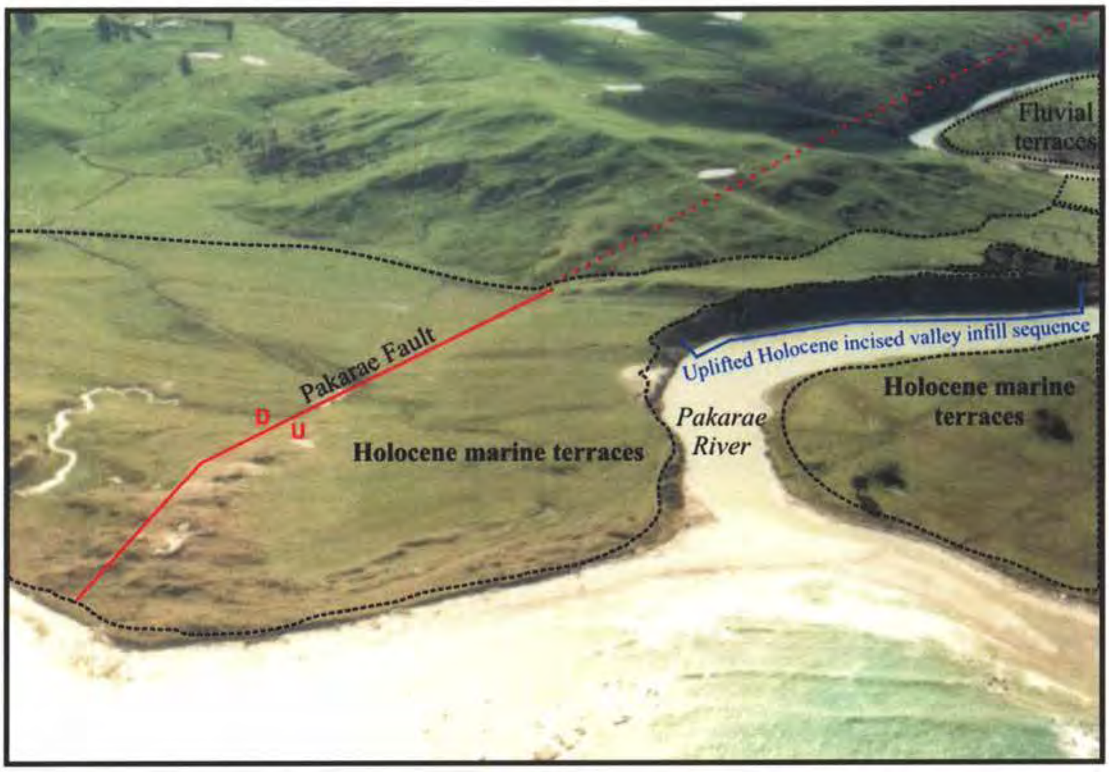

Fig. 2. The Pakarae River mouth site on the Raukumara Peninsula with significant coastal geomorphic features. View looking to the northwest, photo by Lloyd Homer.

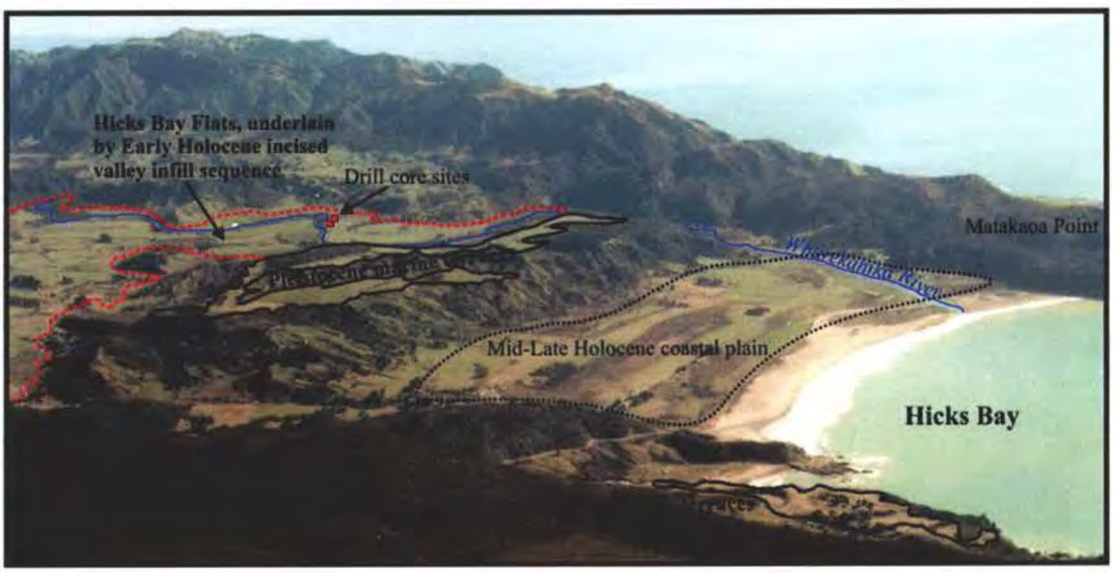

Fig. 3. The Hicks Bay locality on the northeastern Raukumara Peninsula with significant coastal geomorphic features. View looking toward the north-northwest, photo by Lloyd Homer.

At Te Araroa, the Pleistocene marine terraces of the northern Raukumara Peninsula reach their maximum elevation of ~ 300 m (Fig. 4). Although previously studied by Yoshikawa et al. (1980), age constraints on these terraces are poor. In Chapter Six the dating results obtained from the terraces and discussion of terrace geometry in relation to active faults and forearc structures are presented. The continuity of these Pleistocene terraces, along approximately 90 km of coastline (Fig. 1, 5), provides an opportunity to extend the spatial and temporal scale of the coastal geomorphic study.

The Holocene coastal geomorphology at the Pakarae River mouth and around the northeastern part of the Peninsula has been studied in detail and yields evidence of coseismic Holocene uplift mechanism at the Pakarae locality and aseismic, apparently continuous uplift at the northeast tip of the Peninsula. In Chapter Seven data from the previous papers are integrated with other regional coastal geomorphic studies. Reconnaissance level studies of many other coastal locations on the Raukumara Peninsula have been presented by Ota et al. (1988), and Ota et al. (1992). Uplift rates presented in those studies are valuable data, although the interpretation of coseismic uplift mechanisms in those areas is not proven. The only other coastal reach where detailed coastal uplift mechanism studies have been undertaken is from Mahia Peninsula to Wairoa (Fig. 1). Studies of vertical deformation along this, southernmost portion of the Raukumara Peninsula have been presented by Berryman (1993a, b) and Cochran et al. (2006). This information is integrated with the new data of this study to provide insights into the mechanics of deformation of the Hikurangi subduction margin from three locations evenly spaced ~ 80 – 100 km apart along the strike of the Raukumara sector.

The final discussion, presented in Chapter Seven, assesses how the spatial pattern of coastal deformation across the Raukumara Peninsula can be related to the Hikurangi subduction zone. Major questions, such as: do uplift mechanisms vary along the Raukumara sector, what parameters control the distribution of uplift mechanisms, and importantly, how does this study of coastal uplift mechanisms relate to other sources of information about Raukumara Peninsula deformation, are addressed. Other sources of information include seismicity (earthquake focal mechanisms and seismic velocity modelling), GPS-measured deformation, structural geology, and Late Quaternary fluvial terrace uplift studies. The contribution of coastal geomorphology to constraining seismic sources and seismic hazard in the Raukumara sector of the subduction margin is also discussed.

Fig. 4. The Te Araroa locality on the northeastern Raukumara Peninsula with significant coastal geomorphic features. View looking towards the southeast, photo by Lloyd Homer.

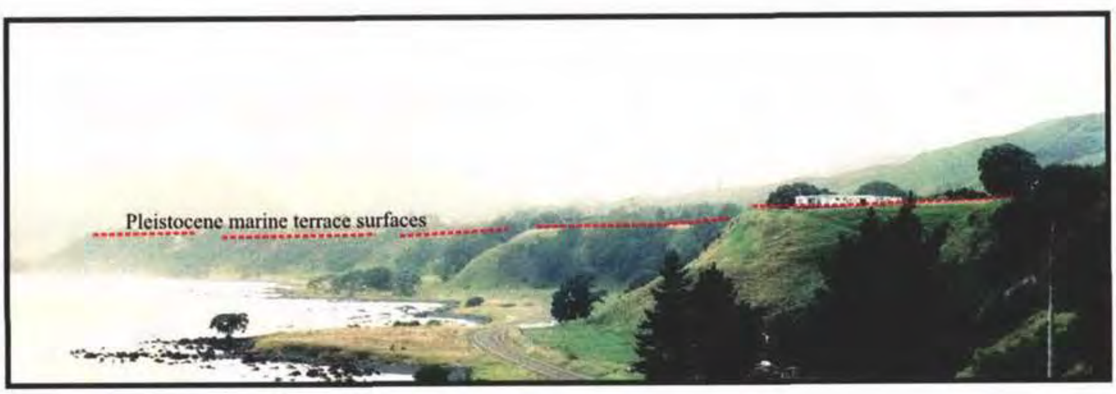

Fig. 5. The Waihau Bay coastline, located at the northwestern edge of the Raukumara Peninsula with uplifted Pleistocene marine terrace surfaces. View looking towards the north.

1.2. Report format

This report has been adapted from Kate Wilson's PhD thesis. The research is presented in six main chapters with brief introductory and concluding chapters. Chapters two to six have been published, or are presently in press, in international earth science journals. Chapter seven is currently in preparation for journal submission. We have tried to minimise repetition between chapters but some is unavoidable to the ensure completeness of each paper, particularly in sections that describe regional settings and previous work. Appendices are included at the end of the relevant chapter, as are references.

1.3. References

Arnadottir, T., S. Thornley, F. Pollitz, F. and D. J. Darby (1999). "Spatial and temporal strain rate variations at the northern Hikurangi margin, New Zealand." Journal of Geophysical Research **104**(B3): 4931-4944.

Atwater, B. F. (1987). "Evidence for great Holocene earthquakes along the outer coast of Washington State." Science **236**: 942-944.

Beanland, S. and J. Haines (1998). "The kinematics of active deformation in the North Island, New Zealand, determined from geologic strain rates." New Zealand Journal of Geology and Geophysics **41**: 311-323.

Berryman, K. R. (1993a). "Age, height, and deformation of Holocene terraces at Mahia Peninsula, Hikurangi subduction margin, New Zealand. 1." Tectonics **12**(6): 1347-1364.

Berryman, K. R. (1993b). "Distribution, age, and deformation of Late Pleistocene marine terraces at Mahia peninsula, Hikurangi subduction margin, New Zealand." Tectonics **12**(6): 1365-1379.

Berryman, K. R., Y. Ota and A. G. Hull (1992). "Holocene evolution of an estuary on a tectonically rising coast: the Pakarae River locality, eastern North Island, New Zealand." Sedimentary Geology **80**: 151-162.

CANZ Group. (1996). "Undersea New Zealand" New Zealand region physiography, 1:4,000,000. NIWA Chart Series 74.

Clague, J. J. (1997). "Evidence for large earthquakes at the Cascadia subduction zone." Reviews of Geophysics **35**(4): 439-460.

Cochran, U., K. Berryman, D. Mildenhall, B. Hayward, K. Southall, C. Hollis, P. Barker, L. Wallace, B. Alloway and K. Wilson (2006). "Paleoecological insights into subduction zone earthquake occurrence, eastern North Island, New Zealand." Geological Society of America Bulletin, **118**(9/10): 1051-1074.

Collot, J.-Y., J. Delteil, K. Lewis, B. Davy, G. Lamarche, J.-C. Andru, P. Barnes, F. Chanier, E. Chaumillon, S. Lallemand, B. M. De Lepinay, A. Orpin, B. Pelletier, M. Sosson, Toussaint and C. Uruski (1996). "From oblique subduction to intra-continental transpression: structures of the southern Kermadec-Hikurangi margin from multibeam bathymetry, side-scan sonar and seismic reflection." Marine Geophysical Researches **18**(2-4): 357-381.

Collot, J.-Y., K. Lewis, G. Lamarche and S. Lallemand (2001). "The giant Ruatoria debris avalanche on the northern Hikurangi margin, New Zealand; results of oblique seamount subduction." Journal of Geophysical Research **106B**(9): 19271-19297.

Darienzo, M. E., C. D. Peterson and C. Clough (1994). "Stratigraphic evidence for great subduction-zone earthquakes at four estuaries in Northern Oregon, U. S. A." Journal of Coastal Research **10**: 820-876.

De Mets, C., R. G. Gordon, D. F. Argus and S. Stein (1994). "Effect of recent revisions to the geomagnetic reversal timescale on estimates of current plate motions." Geophysical Research Letters **21**: 2191-2194.

Hayward, B. W., U. Cochran, K. Southall, E. Wiggins, H. R. Grenfell, A. Sabaa, P. R. Shane and R. Gehrels (2004). "Micropalaeontological evidence for the Holocene earthquake history of the eastern Bay of Plenty, New Zealand, and a new index for determining the land elevation record." Quaternary Science Reviews **23**: 1651-1667.

Hayward, B. W., H. R. Grenfell, A. Sabaa, R. Carter, U. Cochran, J. H. Lipps, P. Shane and M. S. Morley (2006). "Micropaleontological evidence of large earthquakes in the past 7200 years in southern Hawke's Bay, New Zealand." Quaternary Science Reviews **25**(11-12): 1186-1207.

Hemphill-Haley, E. (1995). "Diatom evidence for earthquake-induced subsidence and tsunami 300 yr ago in southern coastal Washington." Geological Society of America Bulletin **107**: 367-378.

Lewis, K. B., J.-Y. Collot, B. Davy, J. Delteil, S. Lallemand and C. Uruski (1997). "North Hikurangi GeodyNZ swath maps: depths, texture and geological interpretation 1: 500 000." National Institute for Water and Atmospheric Research miscellaneous series chart 72. Wellington.

Nelson, A. R., I. Shennan and A. J. Long (1996). " Identifying coseismic subsidence in tidal-wetland stratigraphic sequences at the Cascadia subduction zone of western North America." Journal of Geophysical Research **101**: 6115-6135.

Ota, Y., K. R. Berryman, A. G. Hull, T. Miyauchi and N. Iso (1988). "Age and height distribution of Holocene transgressive deposits in eastern North Island, New Zealand." Palaeogeography, Palaeoclimatology, Palaeoecology **68**: 135-151.

Ota, Y., A. G. Hull and K. R. Berryman (1991). "Coseismic uplift of Holocene marine terraces in the Pakarae River area, eastern North Island, New Zealand." Quaternary Research **35**: 331-346.

Ota, Y., A. G. Hull, N. Iso, Y. Ikeda, I. Moriya and T. Yoshikawa (1992). "Holocene marine terraces on the northeast coast of North Island, New Zealand, and their tectonic significance." New Zealand Journal of Geology and Geophysics **35**: 273-288.

Reyners, M. (1998). "Plate coupling and the hazard of large subduction thrust earthquakes at the Hikurangi subduction zone, New Zealand." New Zealand Journal of Geology and Geophysics **41:** 343-354.

Thornley, S. (1996). "Neogene tectonics of Raukumara Peninsula, Northern Hikurangi margin, New Zealand." Victoria University of Wellington **Unpublished PhD thesis**.

Wallace, L. M., J. Beavan, R. McCaffrey and D. Darby (2004). "Subduction zone coupling and tectonic block rotations in the North Island, New Zealand." Journal of Geophysical Research **109**(B12406): doi:10.1029/2004JB003241.

Wilson, K.J., K.R. Berryman, N.J. Litchfield, and T.A. Little (2006). A revision of Mid to Late Holocene marine terrace distribution and chronology at New Zealand's most tectonically active coastal location, Pakarae River, North Island, New Zealand. New Zealand Journal of Geology and Geophysics, **49**(4): 477-489.

Yoshikawa, T., Y. Ota, N. Yonekura, A. Okada and N. Iso (1980). "Marine terraces and their tectonic deformation on the northeast coast of the North Island, New Zealand." Geographical Review of Japan **53**(4): 238-262.

CHAPTER TWO

A REVISION OF MID TO LATE HOLOCENE MARINE TERRACE DISTRIBUTION AND CHRONOLOGY AT NEW ZEALAND'S MOST TECTONICALLY ACTIVE COASTAL LOCATION, PAKARAE RIVER MOUTH, NORTH ISLAND, NEW ZEALAND.

Published: Wilson, K., Berryman, K., Litchfield, N., Little, T. 2006. New Zealand Journal of Geology and Geophysics, Vol. 49, 477-489.

Abstract

A suite of seven marine terraces at the Pakarae River mouth, New Zealand provide evidence for the highest Holocene coastal uplift rates adjacent to the Hikurangi Subduction Zone. New elevation, coverbed stratigraphy, and age data allow for a timely revision of the distribution, nomenclature, and chronology of these terraces. Terrace correlation primarily is based of the elevation of the wave-cut strath. Terrace preservation either side of the river is more equal than previously proposed. The age of abandonment of each terrace is c. 7 ka (T1), 4.3 ka (T2), 3.5 ka (T3), 2.89 ka (T4), 1.6 ka (T5), 0.91 ka (T6), <0.91 ka (T7). The average Holocene tectonic uplift rate at Pakarae is 3.2 ± 0.8 mm/yr. The abandonment of each terrace, from T2 to T7, probably took place after a discrete uplift event. The average time interval between these events is 850 ± 450 yr and the average uplift magnitude is 2.7 ± 1.1 m per event. We infer that uplift has been accommodated by slip on an offshore reverse fault. Normal slip on the Pakarae Fault, at right angles to the margin, occurs at a comparatively slower rate and has probably made little contribution to coastal uplift.

2.1 Introduction

The Pakarae River mouth locality (henceforth called Pakarae) has the greatest number of Holocene marine terraces of any location adjacent to the Hikurangi subduction zone (Berryman et al. 1989; Ota et al. 1991, 1992). Seven terraces elevated above modern mean sea level (MSL) provide evidence of past sudden coastal uplift since sea level (SL) stabilised in the mid Holocene. The well-preserved record of coastal uplift distinguishes the Pakarae location as one of the most tectonically active coastal areas of the Pacific Rim (Berryman et al. 1992; Ota & Yamaguchi, 2004). Accurate knowledge of the timing, frequency, and magnitude of coastal uplift for each event at Pakarae provides a long record of tectonism in the subduction margin. The proximity of the study location to a subduction thrust (that has no historic record of slip during large or great earthquakes), and a normal fault offsetting the terraces locally at Pakarae begs the question of what fault, or faults, are driving the rapid coastal uplift rates along this part of the Hikurangi margin.

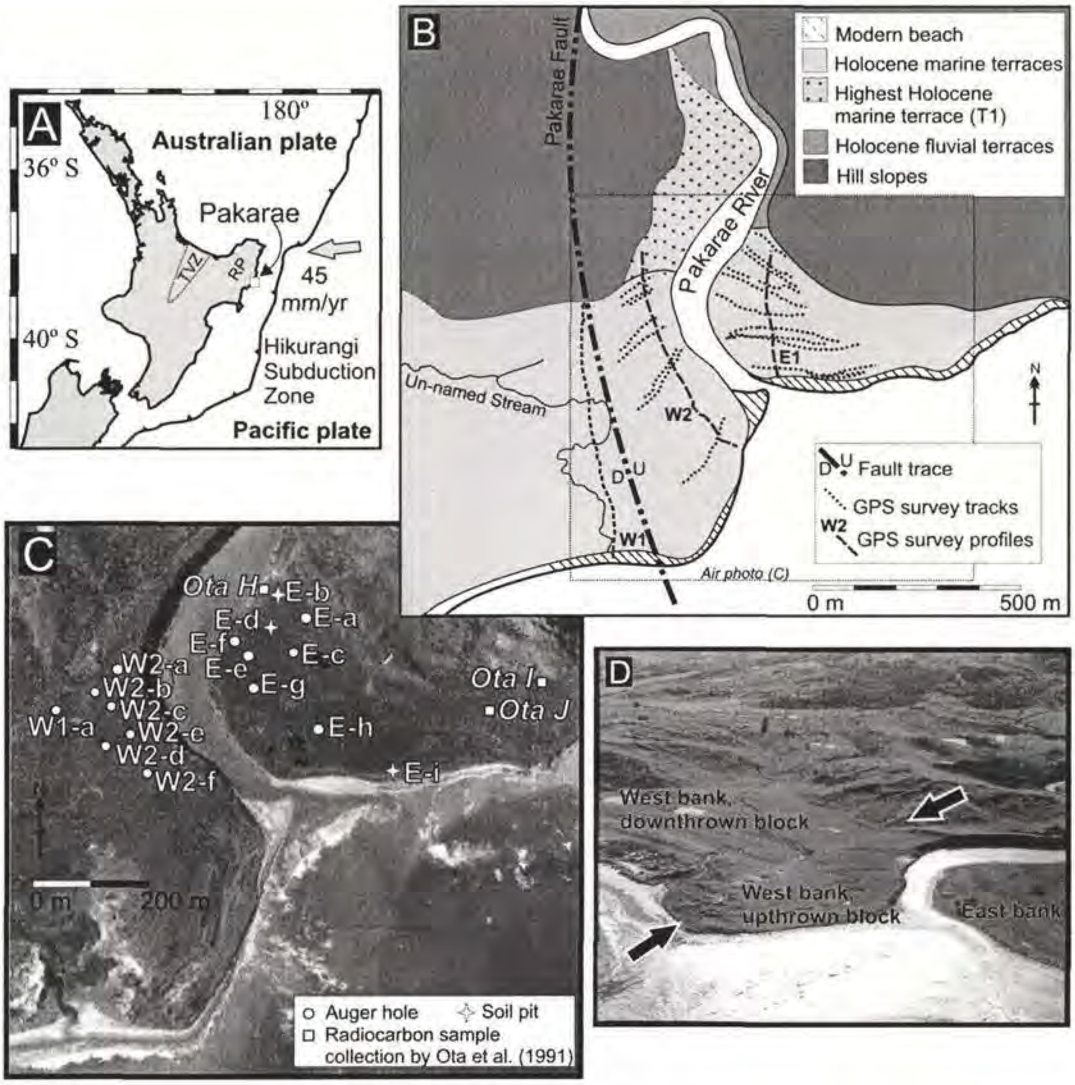

Fig. 1 The Pakarae River mouth locality. **A,** Location map and the Hikurangi Subduction Zone, North Island New Zealand. RP: Raukumara Peninsula, TVZ: Taupo Volcanic Zone. Arrow shows the relative plate motion vector from De Mets et al. (1994). **B,** Major geomorphic features of the Pakarae River mouth and GPS survey lines referred to in text. W1, W2 and E1 refer to elevation profiles shown in Fig. 2. **C,** Locations of cover sediment profiles shown in Fig. 2. Points "Ota ..." are radiocarbon date collection locations of Ota et al. (1991) referred to in text. **D,** Oblique aerial photo of the Pakarae River mouth showing the geomorphology of the Pakarae Fault (arrowed).

Moderate to high late Quaternary coastal uplift rates (0.5 – 3 mm/yr) have been recorded by marine terraces at many locations along the Raukumara Peninsula (Fig. 1A-D); the Pakarae region has the highest Holocene uplift rates recorded along this segment of the Hikurangi margin (Ota, 1987; Ota et al. 1988, 1992; Yoshikawa, 1988; Berryman et al. 1989; Berryman, 1993). Offshore of Pakarae, directly to the east, is the Hikurangi Subduction Zone (Fig. 1A); the continental shelf has been deformed by strike slip, contractional, and extensional faulting, and several margin indentations may indicate previous seamount collisions (Collot et al. 1996). In the vicinity of Pakarae, Oligocene and Miocene marine siltstones and mudstones are juxtaposed across the Pakarae Fault, a north-striking structure on the western side of the Pakarae River (Kingma, 1964; Mazengarb & Speden, 2000). Several short segments of active normal faults have been mapped in the Pakarae region – including the Pakarae Fault (Fig. 1D) and the Waihau Bay Fault, located 10 km north of Pakarae (Mazengarb, 1984, 1998; Mazengarb & Speden, 2000). Walcott (1987) and Thornley (1996) inferred that the Raukumara Peninsula is undergoing margin-normal extension due to uplift driven by sediment underplating. The character of active faulting at Pakarae is therefore of relevance to understanding the geodynamic relationships between onshore normal faults, offshore upper plate compressional structures and the subduction interface.

The Pakarae Holocene marine terraces were previously mapped, correlated, and dated by Ota et al. (1991). Seven terraces, named T1-T7, from oldest to youngest, were recognised at Pakarae. T1 corresponds to the maximum mid-Holocene marine transgression at c. 7 ka (Gibb, 1986). The terraces were correlated across the Pakarae River based on their age and height. Only terraces T4 and T5 were mapped on both sides of the river. Landward tilting of the terraces was indicated by terrace height projections normal to the coast (Ota et al. 1991). The timing of uplift of each terrace was estimated from tephra coverbed distribution and radiocarbon ages of shells that were collected from close to the wave-cut strath. Shells from T1-T6 were collected for radiocarbon dating either from natural river bank exposures of the marine terrace coverbeds on the west bank, or from soil pits excavated on the eastern bank. T7 was dated by correlation to the lowest terrace at Waihau Bay, 15 km north of Pakarae, which is overlain by sea-rafted Loisells Pumice. Originally thought to be uniformly <700 yr BP (McFadgen, 1985), this pumice is now acknowledged to be diachronous in its age at different sites around the New Zealand coastline (Shane et al., 1998).

As part of a broader study at Pakarae we have collected new information on terrace elevation, coverbed stratigraphy, including tephra, and ages of fossils in the terrace deposits. These new data provide the basis for revising the correlation of the terraces across the Pakarae River and for reconsidering the timing and rates of Holocene coastal uplift events. In this study we use 3 GPS elevation profiles across the terraces, 16 terrace cover sediment profiles and 3 new radiocarbon ages to revise the original terrace distribution and chronology detailed by Ota et al. (1991). The geomorphology and age of the raised terraces allow inferences to be made regarding the types of faults are most likely to have played a key role in the uplift of this coast.

2.2 Methods

In this study we use the following terminology: **marine terraces** refer to relict coastal erosion surfaces overlain by marine and non-marine cover sediments; risers separate the terraces. **Wave-cut strath** refers to the surface cut by coastal erosion processes when the surface was approximately at MSL; the **shoreline angle** is the angle formed at the landward edge of a terrace where strath intersects the riser to the higher terrace, the **terrace surface** refers to the modern surface of the terrace, which includes a certain thickness of cover sediments deposited since the sea abandoned the terrace.

A microtopographic survey of the terrace surfaces was carried out using a Real Time Kinematic (RTK) GPS. The elevations have an uncertainty of ±0.16 m at a 95% confidence interval. The perimeter of each terrace on the east bank and on the upthrown side of the fault on the west bank was surveyed. Linear profiles across all terraces were also made: W1 on the west bank on the downthrown side of the fault, and W2 on the west bank, upthrown side of the fault, and E1 on the east bank (Fig. 1B). The stratigraphy of the terrace sediment cover was determined at 16 locations using a hand auger or soil pits (Fig. 1C). Coverbed sediments were described by a visual assessment of their colour and grain size (Fig. 2).

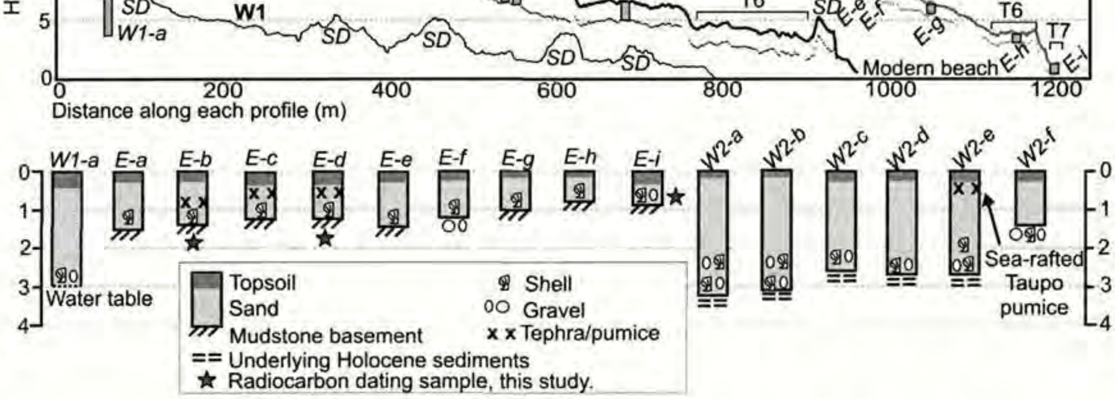

Fig. 2 (Top) GPS height profiles across the Pakarae Holocene marine terraces, location of profiles shown on Fig. 1. Profiles W2 and E1 have the terrace straths plotted based on the amount of cover material on each terrace, location of the soil pits and auger holes shown. Profile E2 not shown as it is similar to E1. See text for discussion of the GPS elevation uncertainties. **(Below)** Simplified coverbed stratigraphy on the Holocene marine terraces from soil pits and augering.

Our height correlations between the terraces are based on the elevation of the wave-cut straths, which we obtained by subtracting the depth of cover sediment from the terrace surface elevation, as determined from the GPS. On approximately half of the terraces we had two measurements of the cover sediment thickness over the wave-cut strath and there was always <0.15 m difference between the two measurements (the average difference was 0.1 m, Fig. 2). Given that 0.1 m is less than the elevation measurement uncertainty on each terrace it was not deemed essential to take more than one measurement of cover sediment thickness per terrace. However, we assign a 95% uncertainty of ± 0.5 m to the elevations of the wave-cut straths to take account of irregularities created by variable erosion of the platforms. To calculate the elevation of the wave-cut strath of the lowest terrace on the west bank we used the cover sediment thickness from the terrace above it as an approximate measure of the cover sediment thickness (Fig. 2); this assumption may result in a slight underestimation of the wave-cut strath elevation as there is a trend of decreasing cover sediment thickness with decreasing age. Therefore the lowest terrace probably has slightly less cover sediment than the one above it. Only one auger hole was taken on the downthrown side of the fault, this sampled the highest terrace. The auger hole reached the water table at 3 m and further sediment recovery was not possible. With the surface elevation of the terraces having an uncertainty of ±0.16 m and the cover sediment thickness variation <0.15 m, we believe ±0.5 m is a conservative estimate of the uncertainty at a 95% confidence interval for the elevation of each of the wave cut straths at the Pakarae River mouth.

Shell material was collected for radiocarbon dating from all auger holes and soil pits (Fig. 2, 3). We always collected shells from as close as possible to the wave-cut strath. These shells occur within coarse sand and mudstone-clast gravels that represent the paleo-beach deposits at the time when the terrace was being cut. Whole shells were collected if present, otherwise well-preserved shell fragments were collected; the shell species have been identified where possible (Fig. 3). Accelerator mass spectrometer (AMS) radiocarbon ages of shells were determined at the Rafter Radiocarbon Laboratory, Institute of Geological and Nuclear Sciences Ltd. We chose to date only terraces which had the highest age uncertainty as most of the terraces have been previously dated by Ota et al. (1991). The radiocarbon ages of Ota et al. (1991) have been calibrated for use in this study using the marine calibrations of Hughen et al. (2004). All radiocarbon ages will be presented as the 2-sigma age estimate in calibrated years before present (cal. yr BP). Tephra was identified by its physical characteristics, age relationships and comparison with tephra isopach maps of Vucetich & Pullar (1964).

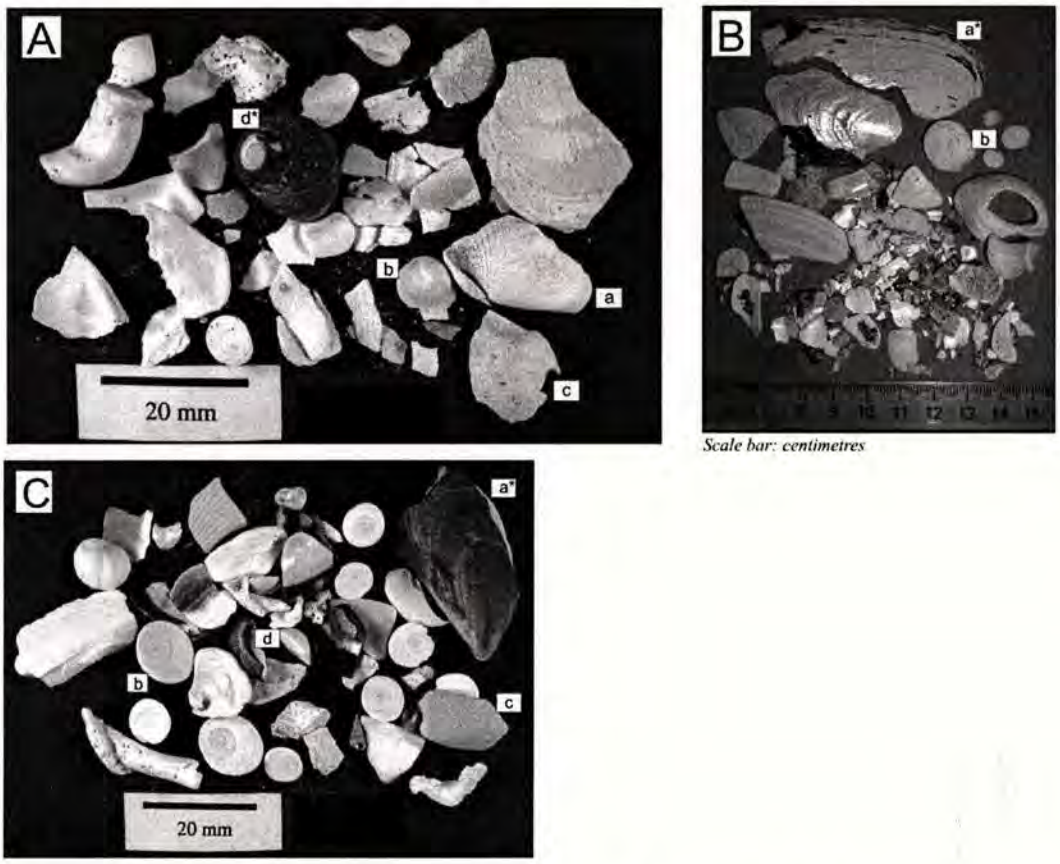

Fig. 3 Shell species and radiocarbon samples from the Pakarae marine terraces. * radiocarbon AMS sample. **A,** T2 North bank (a) Fragment of *Pholadidea* spp, (b) fragments of Cat's Eye (Ataota), *Turbo smaragdus*, (c) fragments of Cockle, *Austrovenus stutchburyi*, (d) Spotted top shell (Maihi), *Melagraphia aethiops* and unidentified shell fragments. **B,** T3 North bank (a) Blue mussel (Toretore), *Mytilus edulis galloprovincialis*, (b) fragments of Cat's Eye (Ataota), *Turbo smaragdus*, (c) fragments of Cockle, *Austrovenus stutchburyi*, (d) Spotted top shell (Maihi), *Melagraphia aethiops* and unidentified shell fragments. **C,** T6 North bank (a) Scimitar shell (Peraro) *Zenatia acinaces*, (b) fragments of Cat's Eye (Ataota), *Turbo smaragdus* and unidentified shell fragments.

2.3 Results

2.3.1 Marine terrace characterisation

RTK GPS profiles oriented approximately normal to the terraces show distinctive staircase topography with flat to gently sloping surfaces separated by steep risers (Fig. 2). The terrace surfaces are up to 120 m wide and display morphology similar to the modern beach mudstone platform, which is exposed from the beach out to c. 150 m offshore within the intertidal surf zone. From terrace profiles W2 and E1 we can identify six terraces on the west bank and six terraces on the east bank of the Pakarae

River. On the downthrown side of the Pakarae Fault (profile W1), separate terraces were not differentiated because they are covered by sand dunes (Fig. 2). Therefore, discussions of the west bank terraces refer to the upthrown side of the fault only.

Cover sediment thickness is greatest on the west bank, while on both sides of the river there is a general decrease in cover sediment thickness with decreasing terrace elevation, possibly reflecting a greater accumulation of aeolian sand over time (Fig. 2). Cover sediment stratigraphy generally fines upwards. The basal deposits sit directly on the wave-cut strath and are everywhere coarse sand with shells (whole shells, and shells hash) and mudstone-clast gravel (Fig. 2). On the east bank all wave cut straths are incised in mudstone. On the west bank all wave cut straths, except underlying the most recent two terraces, are incised into hard, mottled fluvial silts (Fig. 2). These silts were deposited by the Pakarae River during the early Holocene when the coastline was further to the east. Shell species in the beach deposits (Fig. 3) are mostly from rocky shore habitats and all are from intertidal environments (Morton & Miller, 1968; Marsden & Pilkington, 1995; Marsden, 2004; Morton, 2004). The beach deposits are overlain by well-sorted, massive medium sand barren of shells. The change from coarse shelly sand to medium unfossiliferous sand represents a transition between shoreface beach sands and aeolian sands. Dark brown topsoil has developed on the aeolian sand on all terraces.

The depths of cover sediment that we measured on the east bank are similar to those of Ota et al. (1991). Both studies included the use of soil pits to measure sediment thickness above the wave-cut strath. On the west bank our measurements of cover sediment thickness are significantly less than those of Ota et al. (1991) (*cf.* second highest terrace: our study - 3.2 m, Ota et al. 1991 - 5 m). The difference is because we obtained sediment thickness in the middle of the terrace surface, whereas Ota et al. (1991) used outcrops along the riverbank. Our recent observations along the riverbank reveal that much of it has slumped and therefore these outcrops overestimate the thickness of sediment and underestimate the elevation of the wave-cut strath.

2.3.2 Terrace ages

Three new shell radiocarbon ages from the east bank were obtained: from the highest (14 m), second highest (11.5 m) and the lowest (1 m) terraces (Fig. 2, Table 1). The two highest terraces on the east bank have a mantle of Waimihia Tephra (3430 - 3470 cal. yr BP, Froggatt & Lowe, 1990). The Waimihia tephra is identified by its age relationship to the highest terrace (i.e., must be $< c.\ 7 \pm 0.5$ ka BP, the time of eustatic SL stabilisation; Gibb, 1986) and its coarse lapilli texture. The middle terrace of the west bank has a layer of sea-rafted pumice clasts within the sand (section W2-c). We identify this as the Taupo Pumice based on its age relationships to the terraces and other known occurrences of this pumice along the east coast of the North Island. These rounded pumice clasts are up to 5 cm in diameter; they are probably a storm-deposit and indicate that the terrace is older than the age of the Taupo eruption at 1720 – 1600 cal. yr BP (Froggatt & Lowe, 1990).

Table 1: Radiocarbon age data collected during this study from the Pakarae marine terraces.

Sample height (m)	Sample name	Sample Material	Dating Technique	^{13}C (‰)	Radiocarbon Age* (radiocarbon years B.P.)	Calibrated Age** 2 sigma (cal. years B.P.)	Lab number***
14	East highest terrace	Shell, *Melagraphia aethiops*	AMS	1.33	4148 ± 30	4391 - 4138	NZA 22657
11.5	East 2nd highest terrace	Shell, *Mytilus edulis galloprovincialis*	AMS	0.52	3582 ± 30	3610 - 3403	NZA 22659
1	East lowest terrace	Shell, *Zenatia acinaces*	AMS	-8.48	2078 ± 30	1802 - 1582	NZA 22658

* Conventional radiocarbon age before present (1950 AD) after Stuiver and Polach, 1977.

** Marine calibration in calendar years after Hughen et al., 2004. 1 sigma range (68% probability) and 2 sigma range (95% probability) reported.

*** NZA: Institute of Geological and Nuclear Sciences Rafter Radiocarbon Laboratory.

2.4 Discussion

2.4.1 Terrace correlation and chronology

Revised terrace correlations across the Pakarae River are primarily based on new data on the elevation of the shoreline angles and wave-cut straths, and we also use two of the three additional radiocarbon ages (Table 1). We consider that the elevation of the shoreline angle is the most reliable feature for correlating the terraces because the elevation of this would have been the same on both sides of the river.

One potential problem with correlating shoreline angle elevations across the river is the possible influence of tilting due to movement on the Pakarae or other faults. Projections of the terrace surface elevations to an east-west plane striking approximately normal to the Pakarae Fault show a small gradient (0.19°, 3.4 m/km) of terrace tilt towards the west (Fig. 4A), a gradient not significant enough to affect terrace correlations across the c. 100 m wide Pakarae River. Ota et al. (1991) also documented westward tilt normal to the Pakarae Fault. However, they interpreted this as evidence of landward tilt. We confirm landward tilt by projecting the terrace surface elevations to a plane striking normal to the Pakarae River and approximately normal to the Hikurangi subduction margin (Fig. 4). The projected elevations show a 0.23° landward tilt (a gradient of 4.1 m/km, Fig. 4).

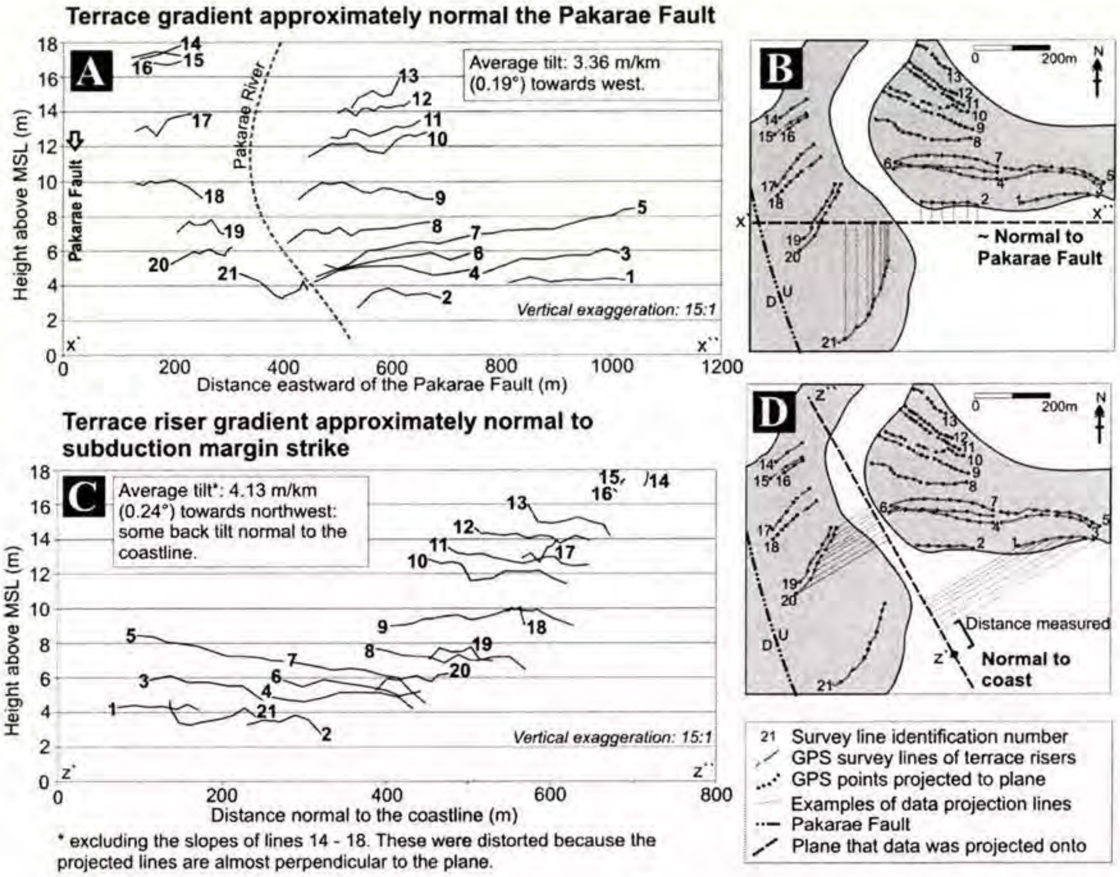

Fig. 4 Height profiles along the Pakarae terrace risers. Riser heights are projected to a plane approximately normal to the Pakarae Fault (A, B) and to a plane approximately normal to the Hikurangi subduction margin (C, D). The profiles test whether the terraces are back tilted relative to the Pakarae Fault or the subduction margin.

Our terrace correlations indicate the presence of seven distinct terraces (Fig. 5). This is the same number as determined by Ota et al. (1991); however, our terrace distribution and correlation is significantly different (*cf.* Fig. 5B, 5C). In several cases there are conflicting radiocarbon ages from, what are interpreted to be, the same terrace. We resolve this by recognising that tephra occurrence provides an age constraint that can help distinguish which radiocarbon ages are more likely to be correct. We then consider from where the radiocarbon samples were collected. Some samples collected by Ota et al. (1991) are from areas where the terraces are indistinct and difficult to map and correlate. Lastly, we give preference to younger radiocarbon ages. We cannot see a mechanism for transporting young shell into the basal beach deposits of higher terraces yet there are several mechanisms by which older shells could be recycled onto lower terraces. The following details the nomenclature, correlation and distribution of each terrace from oldest (T1) to youngest (T7):

***T1*:** The T1 surface is present only on the west bank (Fig. 5B, 5C). Our interpretation as agrees with Ota et al. (1991), that this is the maximum Holocene SL transgression surface of c. 7 ± 500 cal yrs BP (we estimate a 95% uncertainty of 500 yrs for the timing of eustatic SL stabilisation based on Gibb, 1986). The oldest marine sediments underlying this surface have been dated at 7430-7280 cal. yr BP by Wilson et al. (submitted). Therefore constraining the timing of uplift to younger than 7430-7280 cal. yr BP.

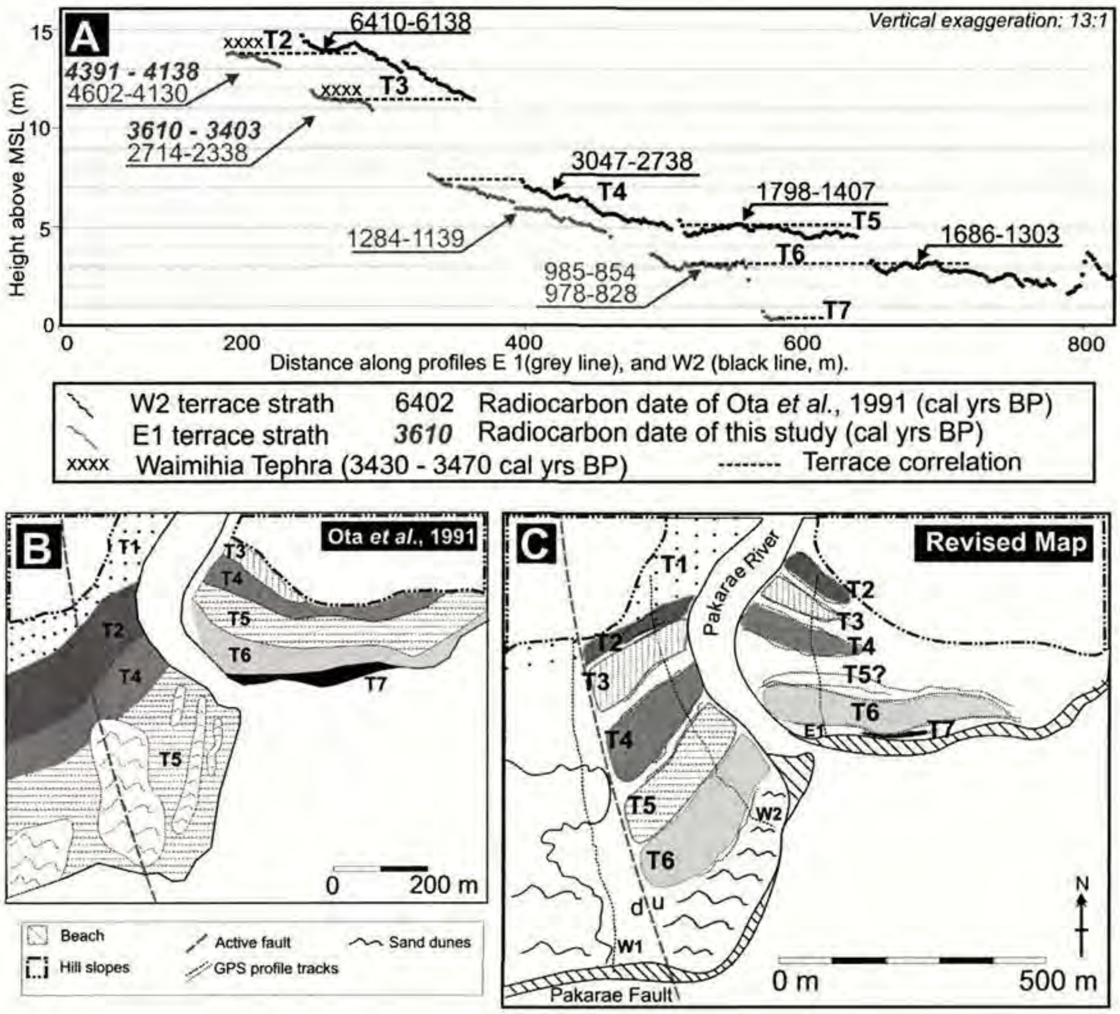

Fig. 5 A, Profiles showing wave-cut surface elevation with radiocarbon dates and surface correlation between the east and west banks of the Pakarae River. **B,** Marine terrace distribution at Pakarae, original map by Ota et al. (1991). **C,** Revised terrace distribution of this study.

T2: T2 is the second highest terrace on the west bank and the highest terrace on the east bank (Fig. 5C). It was previously mapped as T3 on the east bank by Ota et al. (1991) because it had a younger radiocarbon age than the terrace of similar elevation on the west bank terrace (6410 – 6138 cal yr BP on the west bank versus. 4602 – 4130 cal yr BP on the east bank; Ota et al., 1991). Our radiocarbon age of this terrace of 4391 – 4138 cal. yr BP on the west bank supports a younger terrace age of c. 4300 cal yr BP, which is also consistent with the presence of the Waimihia Tephra in the terrace cover sediments. We therefore revise the terrace correlation in spite of the age difference inferred by Ota et al. (1991) because the shoreline angles are almost identical in elevation (c. 14 m AMSL) on both sides of the river. We interpret the older (c. 6.3 ka) radiocarbon age obtained by Ota et al. (1991) from the west bank as a reworked shell.

T3: The T3 terrace is the second highest terrace on the east bank but is less distinct on the west bank (Fig. 2). On the west bank, T3 has a significant surface gradient; however, this gradient is considerably less than that of the other risers and we infer it to be a modified terrace surface. In the field the T3 terrace on the west bank is sufficiently clear that its perimeter could be mapped. The seaward edge of the slope of the wave-cut strath on the west bank is the same elevation as the wave-cut strath of T3 on the east bank. The steeper terrace slope observed on the west bank T3 may result from either poor wave-cut strath planation or more likely due to aeolian sand accumulation towards the rear of the terrace, which would also explain why there is no riser separating T2 and T3 on the west bank. On the east bank T3 is mantled by the Waimihia Tephra (3430 - 3470 cal yrs BP) and we obtained a radiocarbon age of 3610 – 3403 cal yrs BP from beneath the tephra; an age of 2714 – 2338 cal yr BP was obtained by Ota et al. (1991). We prefer our radiocarbon age as an estimate of the age of the second highest terrace because it is compatible with the presence of the overlying 3430 - 3470 cal yrs BP Waimihia Tephra. Furthermore, the location of Ota et al.'s sample yielding the 2714 – 2338 cal yr BP age is farther away from the river mouth at a location where terrace risers become less distinctive. For this reason, we could not map the terrace distribution in the eastern area (Fig. 5C), and it is possible the young age of Ota et al. (1991) is not from a terrace correlative to the second highest terrace as defined by us close to the river. Ota et al. (1991) previously mapped T3 only on the east bank where it was their highest terrace (Fig. 5B). We revise this in light of our new age estimates of the terrace and our data on the wave-cut strath elevations (Fig. 5C).

T4: the T4 terrace is the middle terrace on both banks. Our mapping agrees with Ota et al. (1991) on the west bank but not on the east bank where they called it T5 (Fig. 5B, 5C). We found scattered sea-rafted Taupo Pumice clasts on this terrace on the west bank, as did Ota et al. (1991). They also found the same clasts on what we are calling T4 on the east bank, but despite this they mapped it as T5 on the east side. The mapping of these as different terraces by Ota et al. (1991) is plausible given that the sea-rafted pumice can be of diachronous age and deposited by storm waves some distance from the shoreface, but the simplest interpretation in our view is that these terraces are the same age. The terrace surface of T4 is relatively wide and gently sloping with the shoreline angles at 7.5 m AMSL and mid points of the wave-cut strath at c. 6 m AMSL on both banks. Another distinctive feature common to the T4 terrace on both sides of the river is that the riser on the landward side of the terrace is particularly high; 4 m compared to typical 2 – 2.5 m riser heights for other terraces (Fig. 2). Ota et al. (1991) obtained a radiocarbon date of 3047 – 2738 cal yr BP from this terrace on the west bank and 1284 - 1139 cal yr BP on the east bank. The presence of Taupo Pumice (erupted 1720 – 1600 cal. yr BP, Froggatt & Lowe, 1990) as a storm beach deposit constrains the terrace age to the older date because pumice would not occur as part of the basal beach deposit if the younger age were correct. The east bank radiocarbon sample was collected from a location far to the east of the river mouth (point "Ota-J", Fig. 1C), where the terraces are indistinct and therefore this sample may date a terrace younger than T3. For these reasons we prefer to use the older radiocarbon age of 3047 – 2738 cal yr BP as the age of this terrace.

***T5*:** The T5 terrace is distinctive on the west bank but poorly developed or preserved on the east bank (Fig. 2, 5). On the west bank, T5 is wide and gently sloping with sharp 1 – 2 m risers above and below. Ota et al. (1991) also mapped this surface as T5 (Fig. 5B); however, their T5 is wider than our definition of T5 (Fig. 5C). The narrowing of T5 between interpretations is because we have subdivided Ota et al.'s T5 into T5 and T6 terraces. Both our profiles and that of Ota et al. (1991) show a step in the surface topography of c. 1.5 m at our T5/T6 riser; however, Ota et al. (1991) did not split the terrace here apparently because the lower section yielded a similar radiocarbon date to the upper one (1783 – 1418 cal yr BP upper strath, 1680 – 1307 cal yr BP lower strath). We do not have any auger holes from the lower surface to verify that there is a step down in the wave-cut strath elevation but the surface topography is clearly stepped and therefore we have divided the terrace into two. The radiocarbon date of Ota et al. (1991) from the lower strath may have been derived from a reworked shell. On the east bank the profile of E1 between T4 and T6 is gently sloping with only a small riser at the front edge of T4. We do not map a terrace in here because the morphological expression is indistinct; however, the wide horizontal spacing between T4 and T6 suggests that time may have elapsed between the formation of these terraces. We therefore suggest that T5 is also present on the east bank where it was either weakly developed or has been poorly preserved as a result of aeolian deposition or riser scarp erosion. We retain the age of 1798– 1407 cal yr BP collected by Ota et al. (1991) for this terrace.

***T6*:** As discussed above we have reasonable evidence from surface morphology for an additional terrace on the west bank that we call T6 (Fig. 5C). On the east bank our T6 is equivalent to that of Ota et al. (1991) (Fig. 5B). Two radiocarbon samples obtained by Ota et al. (1991) from the east bank, close to the river mouth, date the terrace at 985 – 854 and 978 – 828 cal yr BP

***T7*:** T7 occurs as a thin strip on the east bank. Our mapping of this terrace agrees with that of Ota et al. (1991) (Fig. 5B, 5C). The age of this terrace was previously estimated by correlation to a terrace 15 km north along the coast, which has the Loisells Pumice on it. The Loisells Pumice is no longer thought to be everywhere <600 yr BP (Shane et al., 1998) so the age assigned to T7 needs to be reconsidered. We obtained a shell sample from the mudstone platform and it was radiocarbon dated at 1802 – 1582 cal. yr BP (Fig. 3, Table 1). Given the ages of 985 – 854 and 978 – 828 cal yr BP for T6, we suspect that our shell sample was reworked. It is possible that T7 is also present on the west bank, however dune sands probably bury it (Fig. 2).

2.4.2 Tectonic uplift rates

We agree with Ota et al. (1991) that each terrace was formed by a sudden uplift event that caused the abandonment of the wave-cut surface by the sea (see Ota et al., 1991, for discussion). The New Zealand Holocene eustatic SL curve shows that, since the c. 7 ka culmination, SL has remained near its modern position with only minor fluctuations of the order of <0.5 m (Gibb, 1986). We can therefore assume that the present elevation of each terrace above modern mean SL is due almost entirely to tectonic uplift. The likeness of the terrace coverbed sands and constituent shell species to the modern beach intertidal sand and shell accumulations supports the inference that the terraces were formed by coastal processes similar to those operating on the modern beach. We also agree with Ota et al. (1991) that radiocarbon ages of shells from the wave cut strath are likely to be (at least) slightly older than the timing of uplift and their abandonment - assuming that uplift caused the death of the organism. The well-preserved nature of the dated sampled suggest there has been very little, if any reworking the samples (Fig. 3). We use these ages to approximate a maximum limit for the time since uplift.

Our revised terrace ages are summarised in Table 2. On the modern beach the mudstone platform is being cut at approximately the mid-tide level, therefore we assume the uplifted wave-cut strath, measured at the shoreline angle, approximately represents mean SL prior to terrace uplift. The elevation difference between the wave cut strath and modern mean SL equals the tectonic uplift. The mean uplift rates appear to have been remarkably uniform since c. 7ka. We calculate an average rate of 3.2 ± 0.8 mm/yr (Fig. 6, Table 2). From T2 to T7 each terrace probably represents one uplift event; the average time interval between events is 850 ± 450 yr and the average magnitude is 2.7 ± 1.1 m per event. These are maximum values; it is possible that terraces produced by smaller events have not been preserved. Discounting the elevation and time difference between T1 and T2, because we believe terraces have been eroded from this part of the terrace sequence, the terrace-forming uplift events at

Pakarae have been more regular in terms of magnitude than previously thought (Fig. 6).

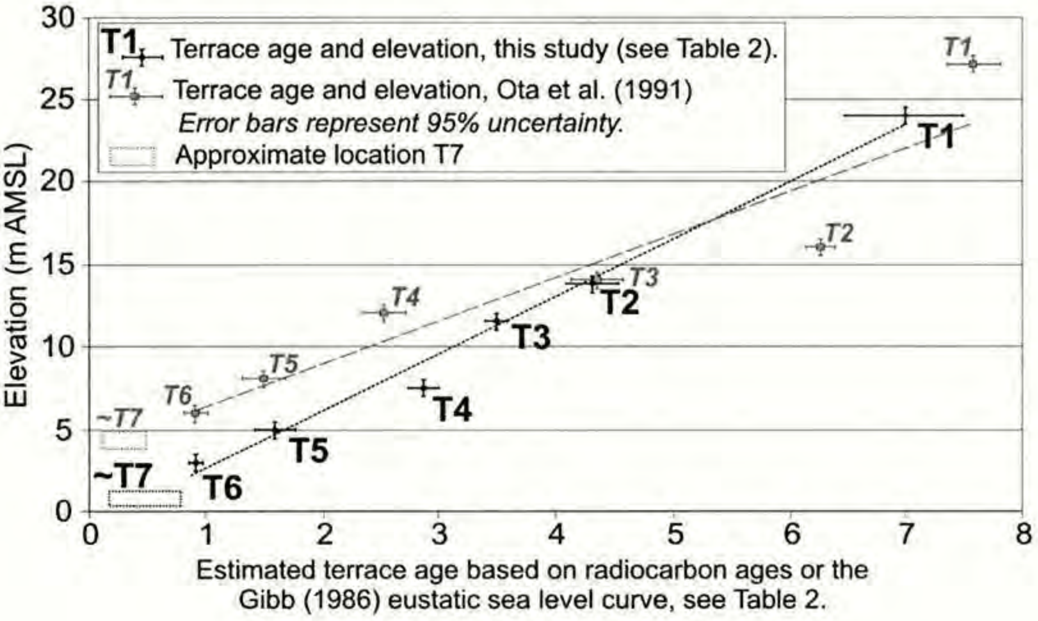

Fig. 6 Estimated terrace age (see Table 2) versus elevation. Elevation and ages from this study in black (see Table 2), from Ota et al. (1991) in grey. The ages of Ota et al. (1991) were calibrated (Hughen et al., 2004), the value shown here is the mid-point of the 2-sigma calibrated age.

One major difference between our terrace distribution interpretation and that of Ota et al. (1991) is the age of our T2. Ota et al. (1991) assigned an age of 6410 BP to 6138 cal yr BP to this terrace, whereas we revise this to c. 4300 cal yr BP. Our age revision means there is more time between the formation of T1 and T2 in our revision. The age assignment of Ota et al. (1991) has an age difference of 1670 - 830 yr between T1 and T2; this study has 3210 - 2170 yr. A greater age difference between T1 and T2 reconciles better with the very high riser height (10.2 m) between these two terraces. Between T1 and T2 we believe more than one uplift event occurred to account for the high terrace riser. It is unrealistic that a 10.2 m riser was created by a single event when the average riser height of all the younger terraces is c. 2.7 m. Terraces may have formed in the period between T1 and T2 (c. 7000 - 4300 cal yr BP) but subsequently eroded.

Table 2: Age-elevation relationships between the Pakarae River marine terraces including average uplift rates.

Terrace	Elevation of shoreline angle (± 0.5 m)	Height difference between terraces (± 1 m)	Estimated age (cal ka BP)	Uncertainty*	Time since previous events (ka)	Uncertainty	Uplift rate (wave-cut strath elevation / estimated age: m/ka)	Uncertainty**
T1	24		7[a]	± 0.5			3.4	± 0.2
T2	13.8	10.2[+]	4.3[b]	± 0.2	N.A[g]	± 0.4	3.2	± 0.2
T3	11.5	2.3	3.5[c]	± 0.1	0.8	± 0.3	3.3	± 0.2
T4	7.5	4	2.9[d]	± 0.2	0.6	± 0.2	2.6	± 0.2
T5	5.0	2.5	1.6[e]	± 0.2	1.3	± 0.3	3.13	± 0.5
T6	3.0	2	0.9[f]	± 0.1	0.7	± 0.2	3.3	± 0.6
T7	0.5	2.5	-		-		-	
Average		2.7** ± 1.1[++]			0.85**	± 0.45[++]	3.2	± 0.8[++]

\+ Height may reflect erosion of missing terraces between T1 and T2.

++ Uncertainty = $\sqrt{[(\text{error}^2) + (\text{error}^2) + \ldots]}$.

* This uncertainty assumes a normal distribution of ages around the mean, however this is not true for the calibrated ages, but we assume this for simplification.

** Calculations do not include difference between T1 and T2.

*** Uncertainty = $\sqrt{[(\%\ \text{elevation error})^2 + (\%\ \text{age error})^2]}$.

a Aged based on the timing of eustatic SL stabilisation after Gibb, 1986, estimated uncertainty of ± 500 yrs.

b Radiocarbon dates from T2, this study and Ota et al, 1991: (4391+4138+4602+4130)/4, uncertainty is the larger half difference between the 2 sigma calibrated age of the two samples.

c Mid point 3610-3403 cal yr BP, this study, uncertainty is half the difference between the 2 sigma calibrated ages.

d Mid point 3047-2738 cal yr BP, Ota et al, 1991, uncertainty is half the difference between the 2 sigma calibrated ages.

e Mid point 1798-1407 cal yr BP, Ota et al, 1991, uncertainty is half the difference between the 2 sigma calibrated ages.

f Radiocarbon ages from T6, Ota et al, 1991: (985+854+978+828)/4, uncertainty is the larger half difference between the 2 sigma calibrated age of the two samples.

g Not applicable as there are have probably been terraces eroded from between T1 and T2.

2.4.3 Pakarae terrace uplift and the role of the Pakarae Fault

We seek to investigate the tectonic structures that have driven the coastal uplift at Pakarae. We can use the geomorphology and ages of the terraces and compare them with block models of how terraces would form under different faulting scenarios. The presence of a scarp of the Pakarae Fault across the <7 ka Pakarae terrace sequence is indisputable evidence that this fault has moved during the Holocene. However, the N-

S strike of the fault and the presence of terraces on either side of the fault indicate it is not the sole cause of uplift of the marine terraces. Instead, we infer that the main cause of coastal uplift on both sides of the Pakarae Fault was slip on a westward-dipping offshore reverse fault (Fig. 7A, B). Other than the Pakarae Fault, the onshore region contains no other known active faults except for the Waihau Bay Fault, which is a normal fault located c. 15 km north of Pakarae. Fault scaling relationships imply that with the short surface trace of the Waihau Bay Fault and its distance from Pakarae, it is unlikely this fault caused uplift at Pakarae.

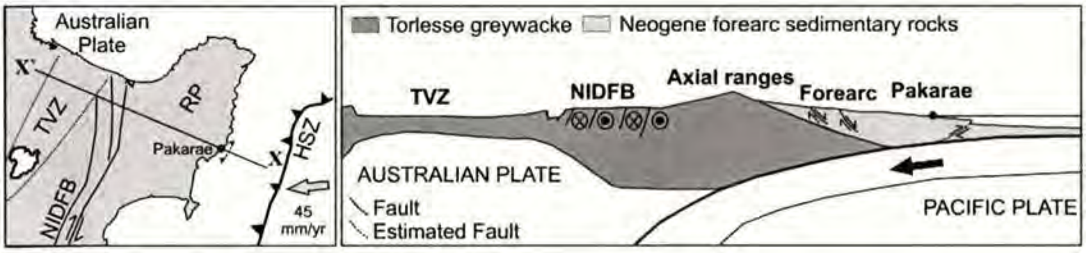

Fig. 7 A, Major tectonic elements of the Raukumara Peninsula sector of the Hikurangi Margin. **B,** Schematic cross-section of the Raukumara Peninsula sector of the Hikurangi Margin (X-X') showing major upper plate structures and estimated location of a reverse fault offshore of the Pakarae River mouth. RP: Raukmara Peninsula, TVZ: Taupo Volcanic Zone, NIDFB: North Island Dextral Fault Belt, HSZ: Hikurangi Subduction Zone.

Slip on the subduction interface is not a likely cause of uplift because preliminary dislocation modelling indicates an unrealistically large amount of slip on the subduction thrust is required to produce uplift of c. 2.7 m at Pakarae (Litchfield & Wilson, 2005). Sixty kilometres SSW of Pakarae, the offshore Lachlan reverse fault, dipping 15-20° to the NW, has caused coseismic uplift of Holocene marine terraces c. 5 km westwards on the Mahia Peninsula (Berryman, 1993; Barnes et al. 2002). Although no structure analogous to the Lachlan Fault has so far been seismically imaged offshore of Pakarae, we suggest a similar reverse fault may have caused coastal uplift at Pakarae (Fig. 7B). A reverse fault has been mapped offshore of Pakarae by Lewis et al. (1997) and Mazengarb & Speden (2000) however this mapping was based on an estimated location by Ota et al. (1991). The fault location was estimated by Ota et al. (1991) based upon the distribution of Holocene marine terraces at the Pakarae River mouth and 15 km northeastward along the coastline.

Ota et al. (1991) also suggested that while the main fault driving the coastal uplift at Pakarae was a reverse fault located offshore, the Pakarae Fault also moved simultaneously with the uplift of the terraces. Correlation of terraces directly across the Pakarae Fault and comparison of riser heights led Ota et al. (1991) to suggest that the Pakarae Fault moved during some terrace uplift events, but that slip on this fault was not the primary cause of the regional coastal uplift. On the downthrown side of the Pakarae fault, our profile (W1, Fig. 2) does not show the "staircase topography" characteristic of the upthrown side of the fault; rather, it is characterised by gentle slopes and sharp sand dunes ridges (Fig. 2). Based on these data we cannot reliably correlate any terraces across the fault (Fig. 8) and suggest there is presently insufficient data to establish a relationship between Pakarae Fault movement and terrace formation. The terraces display a westward tilt, towards the Pakarae Fault, of 0.19° (Fig. 4), which argues against significant involvement of the Pakarae Fault in terrace uplift because terraces in the footwall would be expected to have a tilt away from the fault (an eastwards tilt). The regional nature of the coastal uplift signal is corroborated by the similarity in the age of the marine terraces at Puatai Beach and Waihau Bay, 9 and 15 km north of Pakarae (Ota et al. 1991). Together these datasets imply a domal uplift pattern with a wavelength of uplift along the coast of >15 km, as is consistent with slip on a major offshore fault striking parallel to the coast and dipping to the WNW (Ota *et al.*, 1991). A revision of the Puatai Beach and Waihau Bay Holocene marine terraces and an evaluation of landward tilting on the Pakarae River fluvio-tectonic terraces are currently being prepared with the aim of refining the geometry of a probable causative offshore fault (Litchfield et al. in preparation).

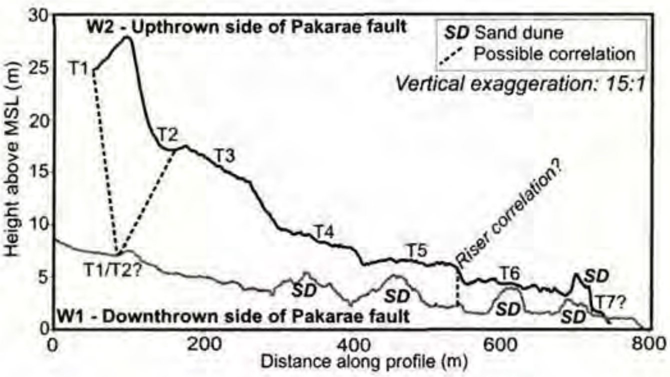

Fig. 8 Comparison of the topographic profiles on the downthrown (W1) and upthrown (W2) sides of the Pakarae Fault with possible correlation points.

We use a simple schematic block model with an offshore reverse fault striking parallel with the coastline and an onshore normal fault striking perpendicular to the coastline to assess the likely structures driving coastal uplift (Fig. 9). Flexural isostasy dictates that the majority of absolute movement during slip on normal faults occurs through subsidence of the hanging wall (e.g., Jackson et al. 1988). Under various combinations of fault movement our model shows that the Pakarae geomorphology is most compatible with an offshore fault as the primary driver of coastal uplift (Fig. 9), in agreement with the conclusions of Ota et al. (1991).

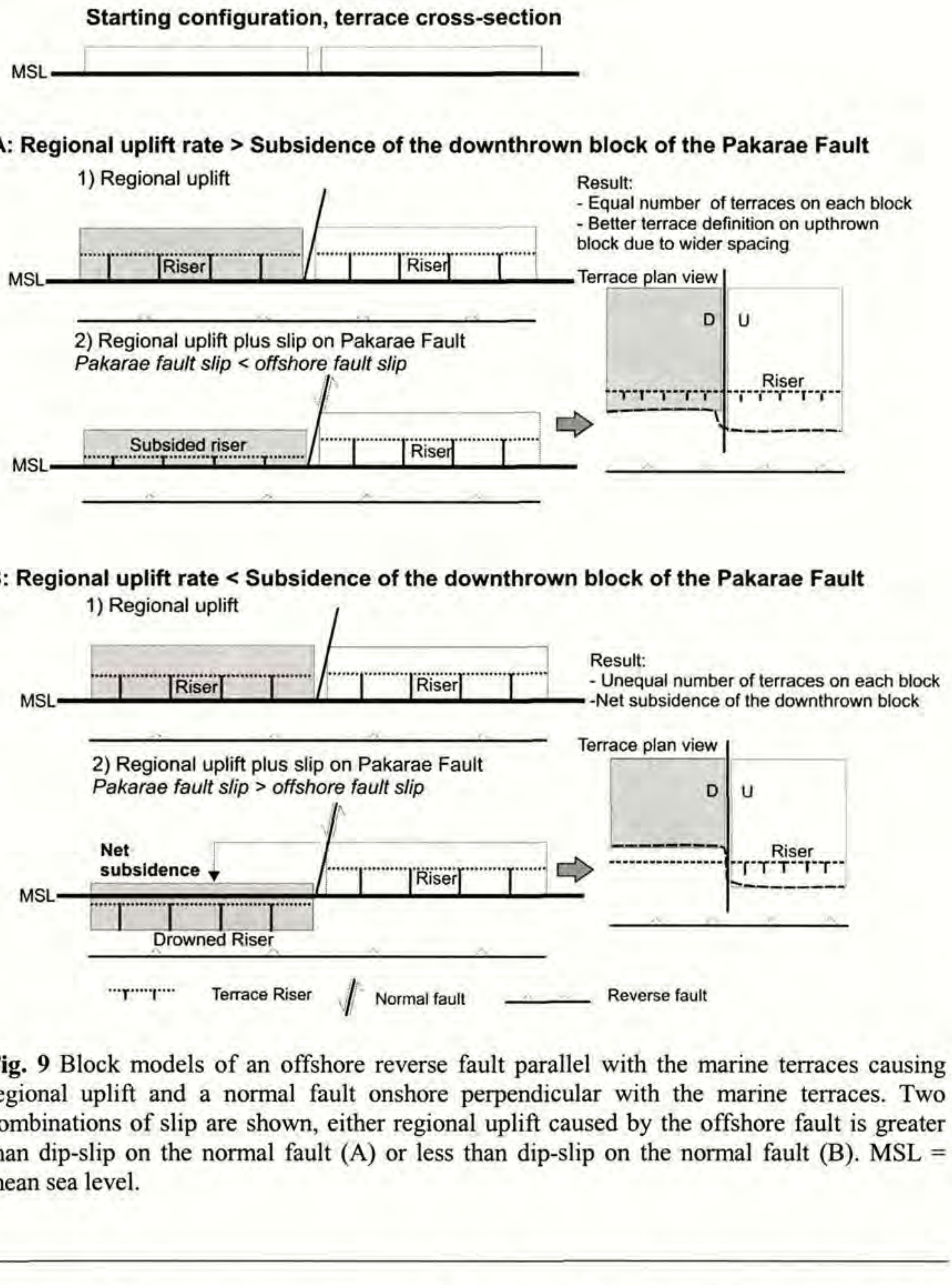

Fig. 9 Block models of an offshore reverse fault parallel with the marine terraces causing regional uplift and a normal fault onshore perpendicular with the marine terraces. Two combinations of slip are shown, either regional uplift caused by the offshore fault is greater than dip-slip on the normal fault (A) or less than dip-slip on the normal fault (B). MSL = mean sea level.

Slip on a northwest-dipping offshore reverse fault would uplift both sides of the Pakarae Fault (Fig. 9A/1). Any synchronous or subsequent slip on the Pakarae Fault might be anticipated to cause subsidence of the downthrown block relative to MSL but not necessarily any significant vertical movement of the upthrown block relative to MSL (Fig. 9A/2). Vertical slip on the Pakarae Fault, in particular subsidence of its downthrown block, must have been less than the regional uplift related to slip on the offshore reverse fault or else the western side of the fault would have been drowned due to net subsidence there, or be a flat coastal plain if coastal sedimentation rates were high enough to infill the embayment created by such net subsidence (Fig. 9B). To produce a terrace flight geomorphology similar to that of Pakarae with a downthrown block raised above MSL, these models show that the coastal uplift rate related to slip on the offshore fault must have been greater than the dip-slip rate of the Pakarae Fault (Fig. 9). The landward tilt of the terraces is compatible with back-tilt on an offshore coast-parallel reverse fault (Fig. 4).

The presence of an active reverse fault offshore of the Pakarae River mouth has important geodynamic implications for this sector of the Hikurangi margin. Presently only active normal faults have been mapped on the onshore Raukumara Peninsula (Mazengarb, 1984, 1998; Mazengarb & Speden, 2000) and geodetic studies show the region is currently undergoing extension and eastward rotation (Walcott 1987; Darby & Meertens 1995; Arnadottir et al. 1999; Wallace et al. 2004). The proposed offshore reverse fault is the first active contractional structure identified in a traverse from the backarc region to the Hikurangi Subduction Zone (Fig. 7B). Incorporation of offshore reverse faults in future studies of the Raukumara Peninsula is important, for example, examining whether such faults are listric to the plate interface, whether they interact with the interseismically locked portion of the interface, considering if reverse faults may accommodate a portion of the normal plate convergence motion along this segment of the margin, and incorporating faults on the continental shelf into tsunami hazard models of the region.

2.5 Conclusions

Our revision of the marine terrace distribution and chronology at Pakarae has shown that terrace formation and preservation either side of the Pakarae River is more uniform than previously described. Similar to Ota et al. (1991), we map seven terraces in total from T1 (representing the maximum Holocene transgression, and present only on the west bank) to T7 (the youngest terrace, preserved only on the east bank). Terraces T2 through T6 are present on both sides of the river although T3 is indistinct on the west bank and T5 is indistinct on the east bank. New age data from the east bank indicates that T2 is c. 4300 cal yr BP, approximately 2000 yr younger than the age of 6314 – 6195 cal yr BP assigned by Ota et al. (1991). Terrace uplift has been intermittent. Average time intervals between uplift events range from 1280 to 630 yr and incremental uplift ranges from 2 – 4 m. Average Holocene uplift rates at Pakarae are relatively uniform over the past 7 ka with a long term uplift rate of 3.2 ± 0.8 mm/yr.

Our study of the terrace geomorphology illustrates the importance of using the wave-cut strath elevation for terrace correlation rather than relying upon surface morphology, which is subject to a range of post-formation changes, especially in the development of coverbeds. It also demonstrates how multiple ages from the same terrace are preferable because shells from the same terrace used for radiocarbon dating can give variable results and have probably, in part, been reworked from older terraces. Future work is needed at this site to refine the terrace chronology, particularly of T7, which is not yet satisfactorily dated. Knowing the time of the most recent earthquake is important because the elapsed time since the last coastal uplift event may be critical to assessing the current seismic hazard at this location. To evaluate the tectonic structure chiefly responsible for terrace formation we need to reliably correlate the terraces across the Pakarae Fault and identify an offshore structure using marine geophysics. Block models indicate an offshore fault drives most or all of the coastal uplift with synchronous or alternating smaller events on the Pakarae Fault causing relative subsidence of the western block of this normal fault.

Acknowledgements

This research was funded by an EQC Student Grant (Project 6UNI/501). KJW is supported by the GNS-funded Sarah Beanland Memorial Scholarship. Rodger Sparks and Dawn Chambers of the Rafter Radiocarbon Laboratory are thanked for their contribution to the radiocarbon dating. Reviews by Yoko Ota, Harvey Kelsey, Philip Barnes and an anonymous reviewer substantially improved this manuscript.

References

Arnadottir T, Thornley S, Pollitz F, F., Darby DJ 1999. Spatial and temporal strain rate variations at the northern Hikurangi margin, New Zealand. Journal of Geophysical Research 104(B3): 4931-4944.

Barnes PM, Nicol A, Harrison T 2002. Late Cenozoic evolution and earthquake potential of an active listric thrust complex above the Hikurangi subduction zone, New Zealand. Geological Society of America Bulletin 114(11): 1379-1405.

Berryman KR 1993. Age, height, and deformation of Holocene terraces at Mahia Peninsula, Hikurangi subduction margin, New Zealand. 1. Tectonics 12(6): 1347-1364.

Berryman KR, Ota Y, Hull AG 1989. Holocene paleoseismicity in the fold and thrust belt of the Hikurangi subduction zone, eastern North Island, New Zealand. Tectonophysics 163: 185-195.

Berryman KR, Ota Y, Hull AG 1992. Holocene coastal evolution under the influence of episodoc tectonic uplift: examples from New Zealand and Japan. Quaternary International 15/16: 31-45.

Collot J-Y, Delteil J, Lewis K, Davy B, Lamarche G, Andru J-C, Barnes P, Chanier F, Chaumillon E, Lallemand S and others 1996. From oblique subduction to intra-continental transpression: structures of the southern Kermadec-Hikurangi margin from multibeam bathymetry, side-scan sonar and seismic reflection. Marine Geophysical Researches 18(2-4): 357-381.

Darby DJ, Meertens CM 1995. Terrestrial and GPS measurements across the taupo backarc and Hikurangi forearc in New Zealand. Journal of Geophysical Research 100(B5): 8221-8232.

De Mets C, Gordon RG, Argus DF, Stein S 1994. Effect of recent revisions to the geomagnetic reversal timescale on estimates of current plate motions. Geophysical Research Letters 21: 2191-2194.

Froggatt PC, Lowe DJ 1990. A review of late Quaternary silicic and some other tephra formations from New Zealand: their stratigraphy, nomenclature, distribution, volume and age. New Zealand Journal of Geology and Geophysics 33: 89-109.

Gibb JG 1986. A New Zealand regional Holocene eustatic sea-level curve and its application to determination of vertical tectonic movements, A contribution to IGCP-Project 200. Recent Crustal Movements of the pacific Region., Bulletin of the Royal Society of New Zealand. Pp. 377-395.

Hughen KA, Baillie MGL, Bard E, Beck, J. W. , Bertrand CJH, Blackwell PG, Buck CE, Burr GS, Cutler KB, Damon PE, Edwards RL and others 2004. Marine04 Marine Radiocarbon Age Calibration, 0–26 Cal Kyr BP. Radiocarbon 46(3): 1059-1086.

Jackson JA, White NJ, Garfunkel Z, Anderson H 1988. Relations between normal-fault geometry, tilting and vertical motions in extensional terrains: an example from the southern Gulf of Suez. Journal of Structural Geology 10(2): 155-170.

Kingma JT 1964. Sheet 9, Gisborne (1st Ed.) Geological Map of New Zealand 1 : 250 000 DSIR. Department of Scientific and Industrial Research, Wellington.

Lewis KB, Collot J-Y, Davy B, Delteil J, Lallemand S, Uruski C 1997. North Hikurangi GeodyNZ swath maps: depths, texture and geological interpretation 1: 500 000. National Institute for Water and Atmospheric Research miscellaneous series chart 72. Wellington.

Litchfield N, Wilson K 2005. Holocene tectonic fluvial terraces at Pakarae River mouth, Gisborne region. Programme and Abstracts, Geological Society of New Zealand 50th Annual Conference, Kaikoura New Zealand. Geological Society of New Zealand Misc. Publ. 119A, 45-46.

Litchfield N, Wilson K, Berryman K, Wallace L in preparation. Coseismic fluvial terraces: an example from the lower Pakarae River valley, Hikurangi Margin, New Zealand.

Marsden ID 2004. Effects of reduced salinity and seston availability on growth of the New Zealand little-neck clam *Austrovenus stutchburyi*. Marine Ecology Progress Series 266(157-171).

Marsden ID, Pilkington R 1995. Spatial and temporal variations in the condition of *Austrovenus stutchburyi* Finlay, 1927 (Bivalvia: Veneridae) from the Avon-Heathcote estuary, Christchurch. New Zealand Natural Sciences 22: 57-67.

Mazengarb C 1984. The Fernside Fault: an active normal fault, Raukumara Peninsula, New Zealand. New Zealand Geological Survey Record 3: 98-103.

Mazengarb C 1998. Late Neogene structural development of eastern Raukumara Peninsula: Implications for oil exploration. 1998 New Zealand Petroleum Conference Proceedings: 201 - 205.

Mazengarb C, Speden, IG (Compilers) 2000. Geology of the Raukumara area. Institute of Geological & Nuclear Sciences 1:250,000 Geological Map 6. Institute of Geological and Nuclear Sciences Limited, Lower Hutt, New Zealand.

McFadgen BG 1985. Late Holocene stratigraphy of coastal deposits between Auckland and Dunedin, New Zealand. Journal of the Royal Society of New Zealand 15: 27-65.

Morton J 2004. Seashore ecology of New Zealand and the Pacific, Hayward, B. W. (scientific editor), Bateman, Auckland.

Morton J, Miller M 1968. The New Zealand sea shore. Collins, London.

Ota, Y (Editor) 1987. Holocene coastal tectonics of eastern North Island, New Zealand. *In* "A preliminary report on late Quaternary seismo-tectonic movement in the Circum Pacific area, 1st survey (1985/86)."

Ota Y, Berryman KR, Hull AG, Miyauchi T, Iso N 1988. Age and height distribution of Holocene transgressive deposits in eastern North Island, New Zealand. Palaeogeography, Palaeoclimatology, Palaeoecology 68: 135-151.

Ota Y, Hull AG, Berryman KR 1991. Coseismic uplift of Holocene marine terraces in the Pakarae River area, eastern North Island, New Zealand. Quaternary Research 35: 331-346.

Ota Y, Yamaguchi M 2004. Holocene coastal uplift in the western Pacific Rim in the context of Late Quaternary uplift. Quaternary International 120: 105-117.

Ota Y, Hull AG, Iso N, Ikeda Y, Moriya I, Yoshikawa T 1992. Holocene marine terraces on the northeast coast of North Island, New Zealand, and their tectonic significance. New Zealand Journal of Geology and Geophysics 35: 273-288.

Shane P, Froggatt PC, Smith I, Gregory M 1998. Multiple sources for sea-rafted Loisels Pumice, New Zealand. Quaternary Research 49: 271-279.

Stuiver M, Polach HA 1977. Discussion; reporting of C-14 data. Radiocarbon 19(3): 355-363.

Thornley S 1996. Neogene tectonics of Raukumara Peninsula, Northern Hikurangi margin, New Zealand. Victoria University of Wellington Unpublished PhD thesis.

Vucetich CG, Pullar WA 1964. Stratigraphy of Holocene ash in the Rotorua and Gisborne districts. Part 2. New Zealand geological Survey Bulletin 73: 43-63.

Walcott RI 1987. Geodetic strain and the deformation history of the North Island, of New Zealand during the late Cainozoic. Philosophical Transactions of the Royal Society of London A 321: 163-181.

Wallace LM, Beavan J, McCaffrey R, Darby D 2004. Subduction zone coupling and tectonic block rotations in the North Island, New Zealand. Journal of Geophysical Research 109(B12406): doi:10.1029/2004JB003241.

Wilson KJ, Berryman KB, Cochran UA, Little TA, submitted. A Holocene incised valley infill sequence developed on a tectonically active coast: Pakarae River, New Zealand. Sedimentary Geology.

Yoshikawa T 1988. Pattern and rate of tectonic movement and Late Quaternary geomorphic development in the Raukumara Peninsula, northeastern North Island, New Zealand. Bulletin of the Department of Geography University of Tokyo 20: 1-28.

CHAPTER THREE

A HOLOCENE INCISED VALLEY INFILL SEQUENCE DEVELOPED ON A TECTONICALLY ACTIVE COAST: PAKARAE RIVER, NEW ZEALAND.

Published: Wilson, K., Berryman K., Cochran, U., Little, T. 2007. Sedimentary Geology. Vol. 197, 333-354.

Abstract

A sequence of fluvio-estuarine sediments exposed beneath the highest Holocene marine terrace at Pakarae, North Island, New Zealand, records the early-mid Holocene infilling of the Pakarae valley. This sequence was developed on an active, coseismically uplifting coastline and provides a valuable comparison to widely used facies models for estuaries, which were developed exclusively from stable coastal settings. We describe eight sedimentary sections, distributed along a 220 m stretch of riverbank and present twelve new radiocarbon ages. Sedimentology and benthic foraminifera are used to divide the sequence into eight bio-lithofacies. These units are grouped into four paleoenvironmental facies associations: barrier, estuarine, estuary-head delta and floodplain. We compare the distribution of the Pakarae paleoenvironmental facies associations to those in models of incised-valley infill sequence models and case studies of infilled valleys. These data allow us to present new contributions to the development of a facies model for the sedimentary infilling of an incised valley system that was experiencing coseismic uplift synchronous with deposition. We suggest the distinctive characteristics of such a model would include (1) part, or all, of the transgressive and lowstand sequences may now lie above modern sea level, (2) the transgressive sedimentary sequence is typically condensed relative to the coeval amount of eustatic sea level (SL) rise that occurred during that period, and (3) evidence of relative SL falls, such as transitions from estuarine to fluvial environments, despite conditions of rapid and continuous eustatic SL rise.

3.1. Introduction

A common feature to studies of sedimentary sequences that have accumulated as fill deposits in formerly incised valleys is their location on stable coastlines. Here we study a sedimentary sequence at Pakarae, North Island, New Zealand, to develop a facies architecture model for incised valley infill sequences that is applicable to active coseismically uplifting coastlines. Several conceptual models have been developed to explain the distribution of facies within drowned valleys (Roy, 1984; Dalrymple et al., 1992; Allen and Posamentier, 1994; Heap et al., 2004). These models have been useful for assessing the petroleum potential of ancient transgressive estuarine sediments and the significance of these as sequence boundaries in oil exploration, and, more recently, to reconstruct Holocene post-glacial sea level (SL) changes, as is important for climate change studies. These models are now widely accepted and cited. However, taking into account that a large proportion of the world's coastlines are in regions of active tectonics, it is timely to consider how incised valley infill sequences differ according to tectonic setting. Results from this study show that past tectonic movements significantly influence sequences of incised valleys; recognition of this can improve interpretations of infill sequences for the purposes of petroleum research and the reconstruction of Holocene SL change.

At the Pakarae River mouth a raised sequence of marine terraces attest to late Holocene coseismic uplift events with a recurrence interval of ca. 850 yrs (Fig. 1, Ota et al., 1991). The highest terrace, which corresponds with the maximum Holocene flooding surface, is underlain by a sequence of estuarine, fluvial and marine sediments that were deposited under conditions of rising sea level (SL). These are now exposed above sea level due to continuing tectonic uplift (Berryman et al., 1992). These sediments provide an opportunity to study the stratigraphic development of incised valleys under conditions of rising eustatic SL and coseismic uplift. Our approach uses sedimentology, macropaleontology and micropaleontology (benthic foraminifera) to reconstruct the paleoenvironments that accompanied infilling of the Pakarae incised valley, on the East Coast of the North Island, New Zealand. In comparison with previous work on the incised valley infill sequences our study is unique as we are able to observe outcrop exposure of the Holocene sequences rather than making reconstructions based on cores and, or, seismic images.

3.1.1 Models of Incised-Valley infilling

Three widely recognised models of incised-valley infill have been developed by Roy, (1984), Dalrymple et al. (1992) and Allen and Posamentier (1993, 1994). As mentioned above, these were all developed for stable coastlines. Here we summarise these models and compare their settings to that of Pakarae valley.

The three incised-valley infill models are similar to one another in their recognition of three to four main sedimentary environments. All models recognise a fluvial/floodplain environment, a central estuary basin and a barrier environment. Dalrymple et al. (1992) also includes a fluvial delta environment at the head of the estuary and Allen and Posamentier (1993, 1994) include a shoreface environment. The models of valley infilling predict that these environments will translate landward under rising SL. Once the SL highstand (maximum flooding surface) is attained the estuary is subsequently infilled by fluvial sediments that prograde seaward.

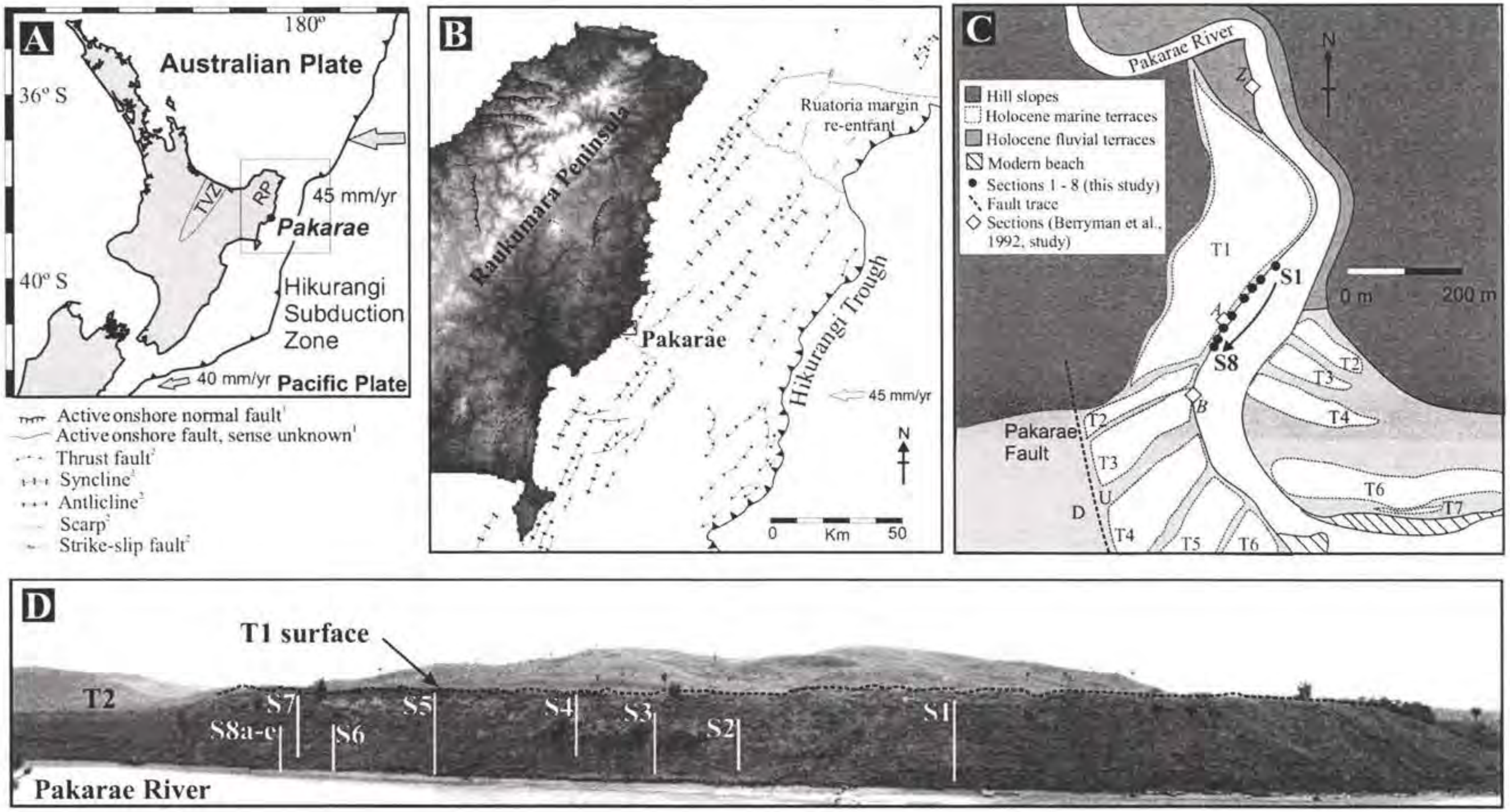

Figure 1. (A) North Island, New Zealand with major tectonic features. TVZ: Taupo volcanic zone, RP: Raukumara Peninsula. Continental-oceanic convergence at the latitude of the Raukumara Peninsula is oblique; the Pacific Plate has a velocity of 45 mm/yr relative to the Australian Plate (Beavan and Haines, 2001; De Mets et al., 1994). Hikurangi subduction deformation front after Collot et al. (1996). **(B)** Topography and tectonic features of the Raukumara Peninsula. [1]Onshore active faults from the GNS Science Active Faults Database (http://data.gns.cri.nz/af/). [2] Offshore structures from Lewis et al. (1997). **(C)** Pakarae River mouth with major geomorphic elements, marine terraces (after Wilson et al., submitted) and stratigraphic section locations (S1-S8). **(D)** The Pakarae riverbank, transgressive sedimentary sequence exposures beneath TI (highest Holocene marine transgression surface) with Sections 1 - 8e. The riverbank is 25 m high.

Based on the Roy (1984) classification the Pakarae valley is comparable to the drowned river valley estuary. According to the Dalrymple et al. (1992) model the Pakarae River valley would be classified as a wave-dominated estuary (as opposed to tide-dominated).. The case studies of individual Holocene estuarine infill sequences, upon which the models are based, have commonly been of large estuaries at the mouths of major rivers that have extensive catchment areas [for example, Hawkesbury River estuary: 109 km length (Roy, 1980); Miramichi River estuary: > 40 km length (Dalrymple et al., 1992); Gironde estuary, 100 km length (Allen and Posamentier, 1993)]. In contrast, the paleo-Pakarae estuary was < 0.5 km wide at the location of the studied sections (Fig. 1), and based on the distribution of estuarine sediments along the riverbank, we estimate the estuary would have been < 1 km in length. For this reason we must consider whether the facies models of Roy (1984), Dalrymple et al. (1992) and Allen and Posamentier (1993), based on studies of larger estuaries, are still applicable when scaled down to this extent. We begin by assuming that scaling is at least approximately valid as we can find no evidence presented in the literature to the contrary. Small estuaries are potentially more suitable for comparison to simplified facies models because multiple tributaries, as found in large estuaries, do not exist.

3.1.2 Tectonic setting of the Pakarae valley

Moderate to high late Quaternary coastal uplift rates have been recorded at many locations along the East Coast of the North Island, an active continental margin inboard of the Hikurangi subduction zone (Fig. 1). The Pakarae locality has the highest Holocene uplift rate identified along this segment of the Australia-Pacific plate boundary at 3.2 ± 0.8 mm/yr (Ota et al., 1988; Yoshikawa, 1988; Berryman et al., 1989; Ota et al., 1991; Ota et al., 1992; Wilson et al., submitted;). The high uplift rate, and evidence for a coseismic uplift process on this coast make Pakarae an ideal location for studying incised valley architecture on a tectonically active coast.

Uplifted forearc basin clastic sediments of Miocene to Pliocene age dominate the eastern region of the Raukumara Peninsula, East Coast, North Island (Fig. 1, Mazengarb and Speden, 2000). In the vicinity of Pakarae, Oligocene and Miocene marine siltstones and mudstones are juxtaposed across the Pakarae Fault, a normal fault, uplifted to the east and striking almost perpendicular to the trend of the subduction zone (Kingma, 1964; Mazengarb and Speden, 2000). This fault offsets the Holocene marine terraces but is not believed to be causing any significant coastal uplift. Rather, an unmapped offshore reverse fault is thought to be responsible for most of the coastal uplift (Ota et al., 1991; Wilson et al., submitted). The Pakarae River has a catchment area of ca. 230 km^2. The modern river mouth has a small sand bar across the mouth, the prevailing longshore current is northerly and the spring tidal range is 1.7 m.

The Pakarae marine terraces were first mapped, correlated, and dated by Ota et al. (1991). They recognised seven terraces, naming them T1-T7 from oldest and highest to youngest and lowest. T1 was recognised as corresponding with the maximum Holocene marine transgression. Wilson et al. (submitted) have revised the distribution of these terraces and their age. These data indicate that uplift over the past 7000 yrs has been achieved by sudden uplift events during which 2 – 2.5 m of coastal uplift has taken place every 850 ± 450 years.

Radiocarbon ages from the fluvio-estuarine sedimentary sequence underlying T1 were presented by Ota et al. (1988). These authors summarised the stratigraphy, but they did not make interpretations concerning the identification and timing of individual uplift events. The sequence was later studied in more detail by Berryman et al. (1992). They used stratigraphy, radiocarbon ages and tephrochronology from three riverbank sections to produce paleogeomorphological maps showing the evolution of the river valley from ca. 9000 to 1000 yrs B.P. A relative sea level curve for the period from 11000 yrs B.P. to present was constructed for this site. Importantly these data showed that during the period 11000 – 7000 calibrated years before present (cal. yrs B.P.), when eustatic SL in the New Zealand region was consistently rising, there were fluctuations in relative SL at Pakarae, including an apparent 4 m fall in relative SL between 10500 – 9500 cal. yrs B.P. This short-term fall was attributed to tectonic and eustatic causes, the eustatic component being based upon correlations to other East Coast locations where trees in growth position aged ca. 10000 cal. yrs B.P. are buried by marine sediments thus indicating a possible hiatus in SL rise at this time (Berryman et al., 1992). A comparison between the amount of eustatic SL rise inferred to have taken place in New Zealand (ca. 34 ± 2 m, Gibb, 1986) from 11000 – 7000 cal. yrs B.P. versus the amount of sediment deposited during that same period in the Pakarae valley (12 m) suggested that as much as 22 ± 2 m of tectonic uplift may have taken place at Pakarae during this period.

Of the three sections (Location A, B and Z) targeted by Berryman et al. (1992), only Location A is in common with the sections that we will examine here (Fig. 1). Their Location Z was revisited by us but will not be used in this study, as there was a lack of recognised marine or estuarine deposits. The approximate site of their Location B was also revisited and again new sites were considered preferable because of uncertainty as to whether the riverbank section was in place or slumped. We believe that most of the section of their Location A has been encompassed by our new sections. However, we cannot exactly correlate our new data with the measured section of Berryman et al. (1992), at Location A, because that section was a composite of several nearby sections.

3.2. Methodology

To construct a facies architecture model from the Pakarae sedimentary sequence we require information on the age and depositional environments of the sediments. To do this we use the radiocarbon dating, tephrochronology, sedimentology, benthic foraminifera and shell assemblages.

3.2.1 Chronology

Radiocarbon ages were collected at significant sedimentary unit contacts to estimate the timing of paleoenvironmental change at Pakarae and to compare these changes with eustatic SL movements. Three conventional radiocarbon ages were obtained on wood (2 small wood branches, one concentration of wood chips). Nine accelerated mass spectrometry (AMS) radiocarbon ages were obtained on marine shells, principally *Austrovenus stutchburyi* or *Paphies australis*. Well-preserved shells were preferentially selected for dating (particularly bivalves with articulated valves) in order to have samples that have undergone as little reworking or transportation as possible. All radiocarbon ages are presented at the 2-sigma age range (95 % probability) and in units of calibrated radiocarbon years before present (cal. yrs B.P.), unless otherwise stated.

A tephra unit correlated within four sections (Sections 5 – 7, and 8d) provided further age control. This tephra was identified on the basis of its glass chemistry and heavy mineralogy and in the context of its bounding radiocarbon ages. Glass shards of 63-250μm size were mounted in epoxy blocks, these were polished and carbon coated. Ten glass shards from the tephra were analysed with a JEOL-733 microprobe using a 10-μm-diameter beam of 8 nA at 15 kV accelerating voltage in the Analytical Facility of Victoria University of Wellington. Heavy mineral identification was done on selected grains using the electron microprobe.

3.2.2 Stratigraphy and sedimentology

Sections were chosen for study along the Pakarae riverbank on the basis of the quality and extent of their exposure and to maximise coverage along the strike of the river. A total of 90 m of vertical section was measured over eight sections (1 – 8). Section 1 is the furthest upstream, with ascending numbers corresponding to sections that are located progressively further downstream. Section 8 is subdivided into 5 small sections (8a – 8e, Fig. 2B). Horizontal bedding was used as the main criterion that a section was in place. At the base of Section 5 we used an auger to retrieve sediments from 1 m deeper than the naturally exposed base of the section. We generally had near-continuous exposure vertically down the riverbank though in some cases (Section 1, 3 and 5) we shifted horizontally along the bedding. The amount of horizontal offset was recorded in each case and it was everywhere < 10 m.

Each section was photographed, measured, described and sampled. Estimates of sediment sorting were made by visual comparison to the charts of Anstey and Chase (1974). Estimates of clast angularity were made by visual comparison with the charts of Powers (1953). Samples of approximately 80 cm^3 were taken from almost every sedimentary unit that we described, larger samples were collected from gravely units. Grain size was estimated in the field and the fraction > 63 microns was measured for samples that underwent micropaleontological processing. Where the beds were greater than 2 cm thick samples were taken 4 - 10 vertical cm apart, if the sediment was particularly homogenous samples were taken at up to 50 cm apart vertically.

The vertical distance of every sedimentary unit contact was measured relative to a reference datum fixed to the top of the exposed section. All heights were later calibrated to elevations in metres above mean sea level (m AMSL) by their relationship to one or more of the 58 elevation control points we had spanning all the sections. On sloping sections all measurements were converted to elevations by taking two points where the elevation was measured (by level or RTK-GPS) and proportionally adjusting the elevation of every depth measurement in between. Elevation uncertainties at the 95% confidence interval range from ± 0.22 – 0.31 m.

3.2.3 Micropaleontological processing

Selected sediment samples were processed for microfossil content to assist with paleoenvironmental interpretation. Microfossils have been demonstrated to be useful in differentiating coastal waterbody types (for example: Darienzo et al., 1994; Hemphill-Haley, 1995; Shennan et al., 1999; Hayward et al., 1999b; Patterson et al., 2000; Hayward et al., 2004). The preservation of diatom and pollen microfossils within the Pakarae sediments was very poor and the results did not contribute to paleoenvironmental interpretation. Benthic foraminifera are common in the Pakarae sediments and these were used in interpretation of the sediment depositional environment.

In total 199 samples were processed for the foraminiferal study, an average of one sample per 0.45 m of section. However, sampling was concentrated around significant stratigraphic contacts and in parts with high unit variability. Samples were processed using the standard techniques of Hayward et al. (1999a). Where possible 100 - 200 benthic foraminifera were picked, 100 tests being considered adequate for environmental assessment using brackish foraminifera (Hayward et al., 1996; Hayward et al., 1999b; Hayward et al., 2004). In some cases when well-preserved benthic foraminifera were very rare we used a floating technique to concentrate the foraminifera. In total 29 samples were floated. Approximately 5 grams of the > 0.063 mm sediment fraction was stirred into sodium polytungstate with a specific gravity of 1.6; the fraction that floated contained the concentrated foraminifera. Identification of the well-preserved foraminifera was made with reference to Hayward et al. (1999a)

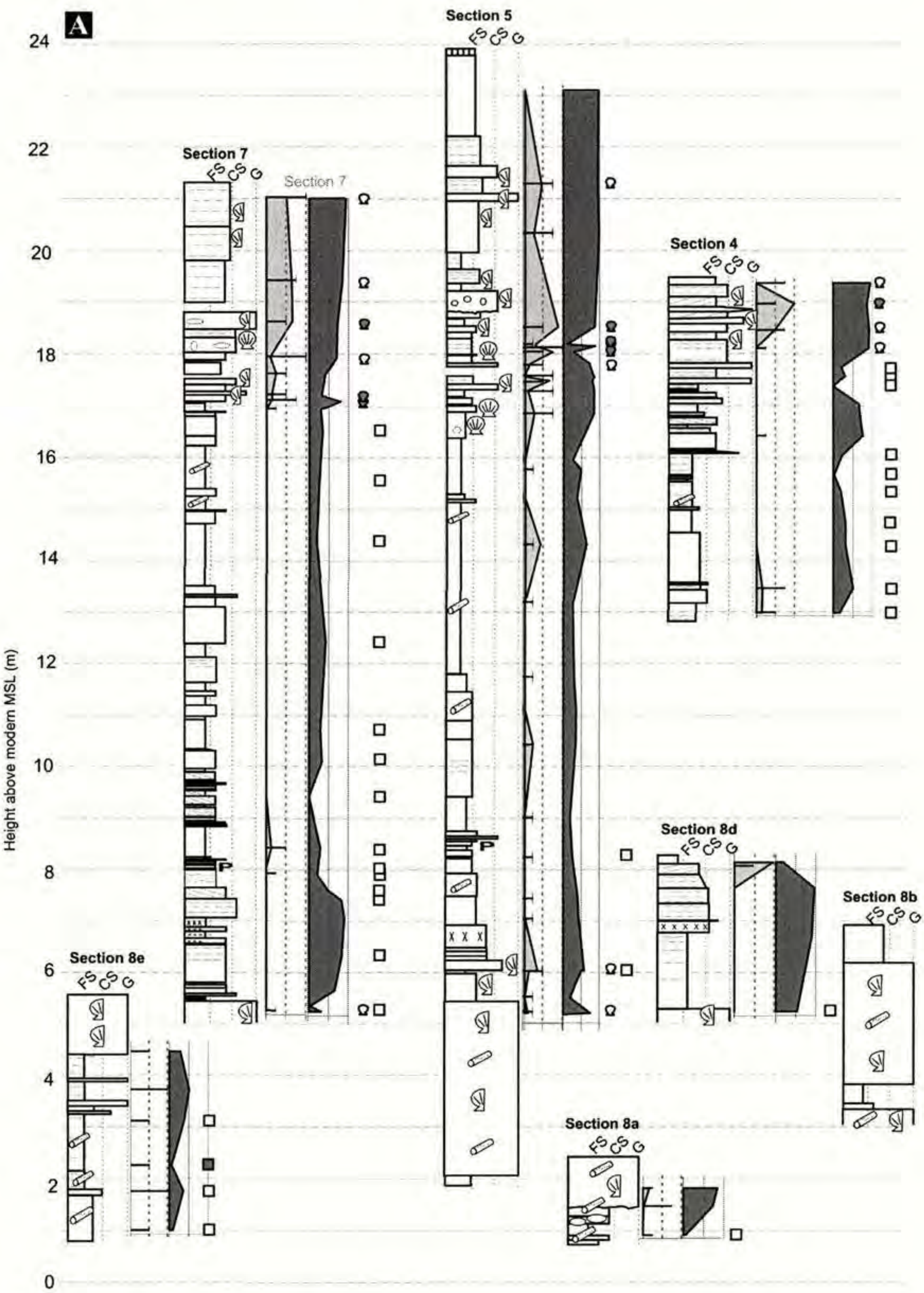

Figure 2. (A) Sedimentology of the Pakarae River incised valley infill sequence. Sedimentary units, grain size, bedding structures and presence of shells and wood are shown. The graphs alongside show the abundance of benthic foraminifera (columns), the percentage of intertidal foraminifera (light grey-shaded line graph), and the percentage of sediment >63 microns in each sample collected for foraminifera analysis (dark grey-shaded line graph). **(B)** Location of sections along the Pakarae riverbank, note the vertical exaggeration. Shaded boxes encompass sections belonging to the same section number.

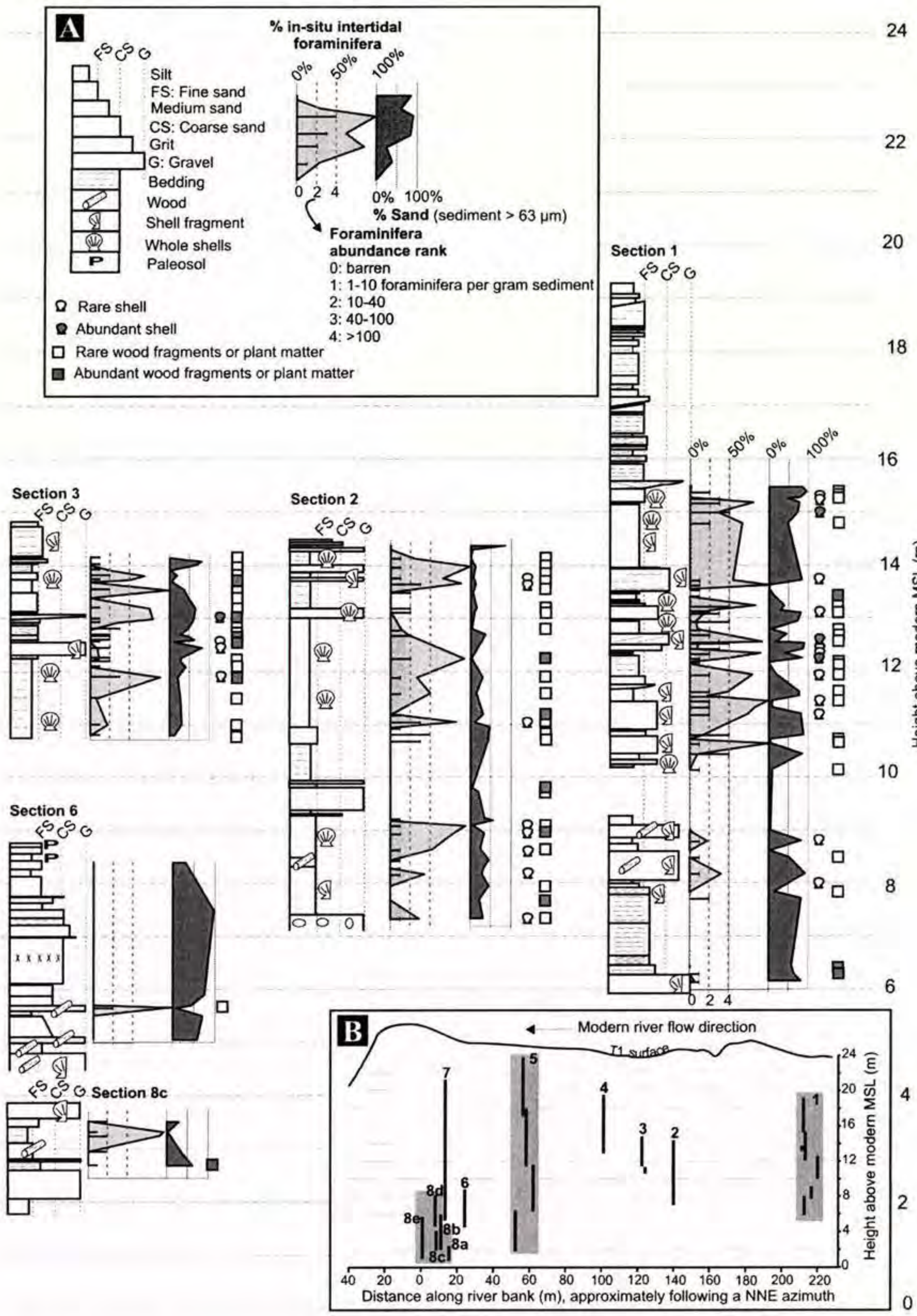

Figure 2 continued.

and Hayward et al. (1997). For each sample the relative amounts of macro shell fragments and wood or plant matter were estimated and noted as either absent, scattered or abundant. The abundance of planktic foraminifera was noted for each sample, but we did not identify or count them as they yield no information about the paleo-elevation of the sediment.

3.3. Results

3.3.1 Chronology

Ages of the infill sediment range from ca. 10230 cal. yrs B.P. at 1.1 m AMSL to ca. 7400 cal. yrs B.P. at 18.3 – 18.7 m AMSL (Table 1). The ages young upwards with the exception of two samples that occur out of chronological order at the > 2 sigma level. In Section 5 the sample at 14.5 m AMSL is a large piece of wood that is not in growth position (Fig. 2). Because this is detrital material it must be older than the sediment that it is preserved within hence the reversed chronology is not a significant concern. A shell sample from Section 4 at 18.9 m AMSL yielded an age of 8350-8170 cal. yrs B.P. and is older than the next sample below it (Section 5 at 18.3 m AMSL). This lower sample has an age of 7530-7280 cal. yrs B.P. It is likely that the higher sample may have been re-deposited.

Table 1: Radiocarbon ages obtained from the Pakarae incised valley infill sequence.

Section	**Sample height (m)**	**Lab number**[1]	**Sample Material**[2]	**Dating Technique**	**^{13}C (‰)**	**Radiocarbon Age**[3] **(radiocarbon years BP)**	**Calibrated Age**[4] **2 sigma (cal. years BP)**
1	**15.2 +/- 0.22**	NZA 21854	A	AMS	-1.27	8056 ± 30	**8590-8410**
1	**10.05 +/- 0.22**	NZA 22529	A	AMS	1.05	8458 ± 35	**9210-8980**
1	**6.3 +/- 0.22**	WK 16864	Wood	Standard	-28.2	8420 ± 59	**9530-9240**
1	**6 +/- 0.22**	NZA 21961	A	AMS	-0.91	8868 ± 30	**9600-9450**
2	**14.15 +/- 0.22**	NZA 22528	A	AMS	1.42	8082 ± 35	**8640-8420**
2	**7.5 +/- 0.22**	NZA 21852	A, B	AMS	-3.71	8338 ± 30	**9010-8770**
4	**18.9 +/- 0.22**	NZA 22526	A, B	AMS	0.98	7791 ± 35	**8350-8170**
5	**18.3 - 18.7 +/- 0.22**	NZA 21851	A, B. C	AMS	-0.49	6847 ± 30	**7430-7280**
5	**14.5 +/- 0.22**	Wk 16454	Wood	Standard	-27.2	8219 ± 52	**9290-9000**
7	**17.15 +/- 0.22**	NZA 22527	A	AMS	0.39	7981 ± 35	**8540-8360**
8a	**1.1 +/- 0.31**	Wk 16453	Wood	Standard	-28	9158 ± 52	**10420-10180**
8b	**4.4 +/- 0.31**	NZA 21853	A	AMS	-2.9	9266 ± 30	**10200-9990**

[1] Wk: The University of Waikato Radiocarbon Dating Laboratory; NZA: Institute of Geological and Nuclear Sciences Rafter Radiocarbon Laboratory.
[2] Shell: A: *Austrovenus stutchburyi*, B: *Paphies australis*, C: *Melagraphia aethiops*.
[3] Conventional radiocarbon age before present (1950 AD) after Stuiver and Polach, 1977.
[4] Calibrated age in calendar years. Wood ages calibrated using Southern Hemisphere atmospheric data of McCormac et al. (2004) marine ages calibrated using data from Hughen et al (2004). Radiocarbon ages calibrated using OxCal v3.10.

The tephra layer that occurs at ca. 7 m AMSL in Sections, 5, 6, 7, and 8d has a major element glass chemistry characteristic of the Okataina volcanic centre and it contains the diagnostic heavy mineral cummingtonite (referenced to datasets in Lowe, 1988, Stokes and Lowe, 1988, and Froggatt and Rogers, 1990, Table 2). Cummingtonite is a heavy mineral present in only three Okataina volcanic centre tephras: the Rotoehu (ca. 50000 cal. yrs B.P.), the Rotoma (9464-9531 cal. yrs B.P.) and the Whakatane (5465 – 5590 cal. yrs B.P. (Froggatt and Lowe, 1990). The bounding radiocarbon ages indicate this is the Rotoma tephra. Berryman et al. (1992) also identified this tephra as Rotoma, although their assignment was based only on bracketing radiocarbon ages. Our geochemical analyses confirm that tephra preserved in the riverbank sections is the Rotoma. Tephra isopach maps of Vucetich and Pullar (1964), suggest the Rotoma ash should be <7.5 cm thick in the Pakarae region and this is compatible with our observations of the outcrop where the tephra appears to be largely reworked with only the thin fining-upwards layers at the base being a primary airfall deposit.

Table 2: Major element glass chemistry and heavy mineral chemistry of the tephra within Sections 5 – 8 at 7 m AMSL. The glass geochemistry is characteristic of an Okataina Volcanic Centre source (referenced to datasets in Stokes and Lowe, 1988, and Lowe, 1988). Cummingtonite was also detected in the tephra using the electron microprobe, four grains were analysed and the results closely match the cummingtonite analyses of Froggatt and Rogers (1990).

Element	**Glass (n=10)**		**Cummingtonite (n=4)**	
	Average %	1 σ	Average %	1 σ
SiO2	78.37	0.30	52.63	1.41
Al2O3	12.44	0.17	0.29	0.08
TiO2	0.13	0.05	1.32	0.64
FeO	0.96	0.06	21.30	2.79
MnO	0.08	0.03	1.21	0.62
MgO	0.12	0.02	21.62	2.17
CaO	0.81	0.09	1.49	0.38
Na2O	3.63	0.16	0.12	0.20
K2O	3.30	0.10	0.03	0.02
Cl	0.17	0.04	-	-

3.3.2 Foraminifera

Of the 199 samples analysed, 56 were barren of foraminifera (either benthic and planktic) and only 36 samples had sufficient foraminifera for > 100 benthic specimens to be counted (Fig. 2). Two populations of foraminifers were recognised: one poorly-preserved and one well-preserved. The presence or absence of foraminifera and relative proportions of poorly- to well-preserved foraminifera formed the basis for four foraminiferal assemblages to be distinguished. The assemblages are (1) barren, (2) reworked, (3) marginal-estuarine and (4) intertidal (Fig. 3). The spatial distribution and composition of each assemblage are described in Fig. 3.

The poorly-preserved tests are typically fragmented and encrusted, some are infilled with sediment or a chemical precipitate such as pyrite. Most specimens were unidentifiable but those that could be identified included *Bolivina* spp, *Bulimina* spp, *Fissurina* spp, *Globocassidulina* spp, *Laevidentalina* spp, *Notorotalia* spp, *Trifarina* spp, and *Uvigerina* spp. Many of these species are typical of fully marine conditions in outer harbours and on the mid to inner shelf, some are known to have been extinct before the Holocene (Hayward et al., 1999a). We conclude the poorly preserved specimens were probably reworked from the Miocene-Pleistocene sedimentary bedrock of the Pakarae River catchment (Mazengarb and Speden, 2000). For this reason we group them in an "Other" category of foraminifera in the census and in foraminifera assemblage descriptions (Fig. 3).

The well-preserved benthic foraminifera are characterised by whole, clear and clean tests, and provide a stark contrast to the reworked specimens (Fig. 3). *Ammonia parkinsonia f. aoetana* is the dominant well-preserved species. Well-preserved *Elphidium excavatum f. excavatum* were rare and only identified in nine samples. *A. aoteana* and *E. excavatum* are common species in brackish to very slightly brackish environments. *A. aoteana* is often a dominant species in the intertidal and subtidal zones of lower estuaries and mid to inner areas of enclosed harbours (Hayward et al., 1999a). The well-preserved nature of these specimens indicates that they are *in situ* fossils.

The difference between the marginal-estuarine and intertidal assemblages is based on the number of well-preserved ($\approx$*in situ*) foraminifera picked from each sample. We do not use the percentage of *in situ* tests as this can cause an artificial bias in those samples with extremely low abundances. Approximately equal sample sizes were scanned for foraminifera therefore the numbers of foraminifera picked are comparable measures. The foraminiferal assemblages tend to be clustered together at varying elevations within the sections (Fig. 3). Intertidal assemblages are notably clustered between ca.16 and 10 m AMSL in the upstream Sections 1, 2, and 3, and between 17 and 20 m AMSL in the downstream Sections 7 and 5 (Fig. 3).

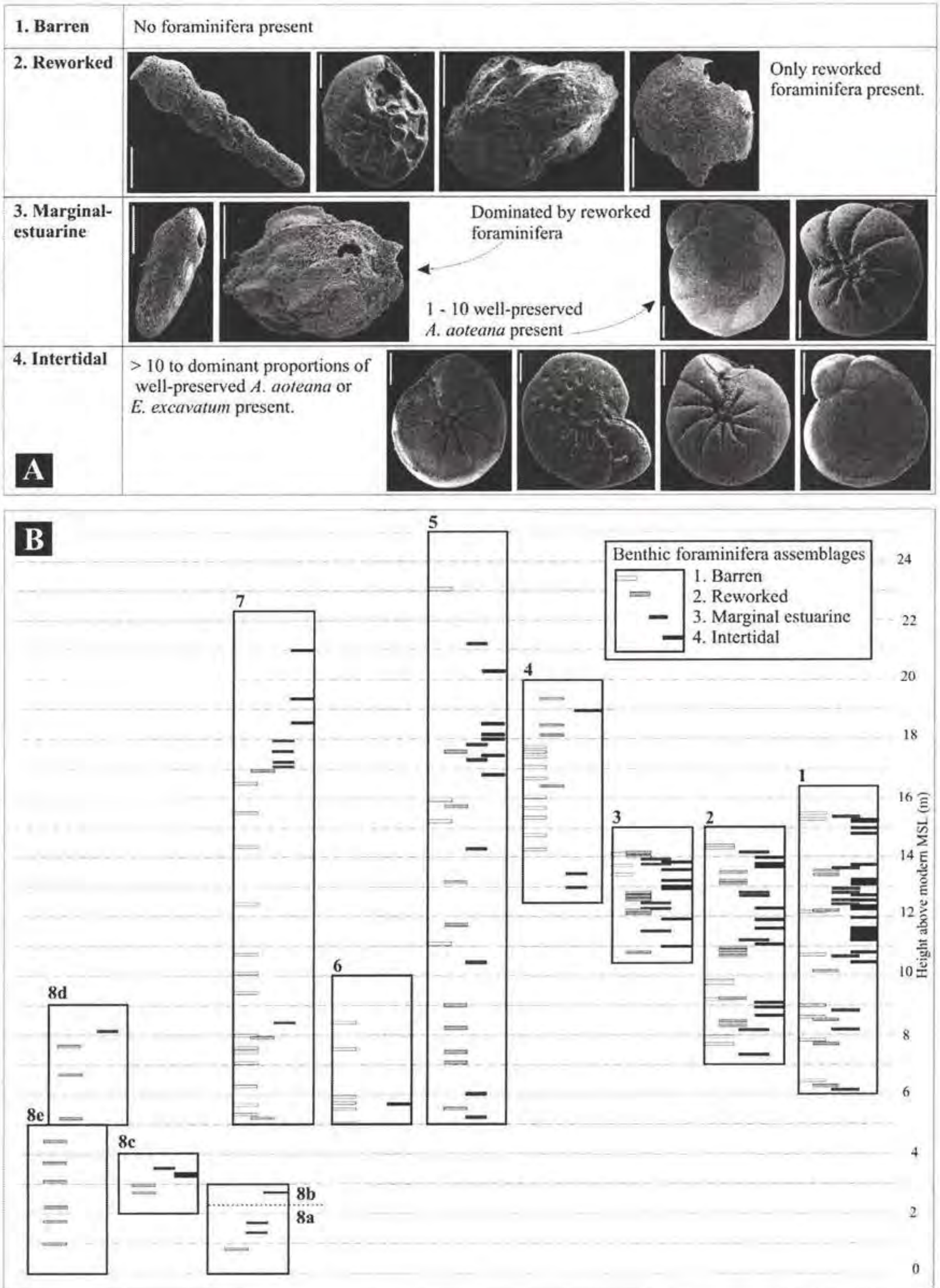

Figure 3. (A) Benthic foraminifera assemblages, with representative images of the specimens within each group. The white bars in each image represent 100 microns. **(B)** Distribution of the foraminifera assemblages in the Pakarae sections.

3.3.3 Bio-lithofacies

Ten bio-lithofacies (Facies 1 – 10) are recognised within the studied sedimentary sequences. We define a bio-lithofacies as a sedimentary unit with a characteristic lithology and biological assemblage. The sedimentary and faunal characteristics of each facies, and their distribution, are described in Table 3. Here we interpret the depositional environment of each facies.

Facies 1: Non-fossiliferous silt and sand units 0.2 – 8 m thick.

As it is the most widespread unit, the depositional environment of this facies is of critical importance to this study. We infer that the most likely depositional environment is fluvial. Evidence for this includes the complete absence of marine fauna, the silty nature of the sediments, channelling, and its content of scattered detrital wood.

Marine fauna could be absent from this unit for reasons other than the sediment having been deposited in a non-marine environment. For example (i) there could be poor marine fossil preservation because the calcareous shells and foraminifera tests may have been leached out by acidic ground water; (ii) the marine environment may not have suited the specific living preferences of the marine fauna; or (iii) sediment deposition rates could have been so high that the marine fauna are either highly "diluted" or could not survive under such rapid sedimentation. With the available data we suggest that the non-fossiliferous facies was deposited in a fluvial environment.

Facies 2: Thick shelly gravel units 0.5-3.5 m thick.

We interpret this facies to have been deposited in a fluvial delta environment at the head of a paleo-estuary, henceforth called the estuary-head delta. The very poor sorting and clast angularity suggests short transport distances for the clasts. The marginal-estuarine foraminifera assemblages and juvenile intertidal *A. stutchburyi* shells indicate the sediment must have been deposited within reach of tidal flow. Radiocarbon ages from below and within the facies at the downstream end of the sections suggest rapid deposition of the gravel (*cf.* wood age of 10200 – 9990 cal. yrs B.P. at 1.1 m AMSL in Section 8a and shell age of 10200-9990 cal. yrs B.P. at 4.4 m AMSL in Section 8b, Fig. 4). The facies displays variable thicknesses along the riverbank; this may be because its distribution was controlled by proximity to the bedrock high (beneath Sections 1 and 2) which was the source of the gravels (Fig. 4).

Table 3: Distribution and sedimentary characteristics of the bio-lithofacies of the Pakarae infill sequence.

Bio-lithofacies	Distribution	Characteristics	Interpretation of depositional environment
Unfossiliferous gravel	S2, ~10 m; S6, 8c, 8e, 2 – 6 m.	Beds < 0.6 m thick; clast-supported gravel; angular – subrounded mudstone clasts 2 – 40 mm diameter. Matrix of silty medium sand to coarse sand. Always have sharp bounding contacts.	Fluvial channel lags.
Thin shelly gravel	S5, ~22 m; S4, 5, 7, 12 – 13 m; S1, 8 – 9 m.	Beds < 0.5 m thick; rounded – subangular mudstone clasts, 2 – 150 mm diameter. Clast and matrix supported (matrix of coarse sand). Abundant fragments of *A. stutchburyi* and *P. australis*. Fragmentation degree varies from shell grit to whole bivalve halves. Basal contacts sharp and wavy.	Estuarine tidal channel lags.
Thick shelly gravel	S1, 2, 5 – 7, 8a – 8e, 7 – 1 m.	Beds 0.5 – 3.5 m thick. Very poor sorting, clasts vary 2 – 150 mm diameter. Dominantly subangular clasts, occasional rounded and angular clasts. Clast-supported with a silt matrix. Occasional small twigs and detrital wood. Rare juvenile *A. stutchburyi* shells and micromolluscs. Sharp bounding contacts. Three matrix samples contained marginal-estuarine foram assemblages; one sample contained a reworked assemblage.	Estuary-head delta.
Shelly well-sorted sands	S4, 5, 7, > 20 m.	Beds up to 2 m thick. Well-sorted medium to coarse sand. Occasional centimetre scale lenticular cross-bedding and mm-scale laminiations. Occasional shells, some identified as *A. stutchburyi*. Six samples analysed for formainifera: one barren, one reworked, one marginal-estuarine and three intertidal assemblages.	Barrier.
Unfossiliferous well-sorted sands	S6, 7, 8d, 7 – 8 m.	Well-sorted medium to coarse sand with mm-scale laminiations. All bounding contacts sharp. Six foram samples: a mixture of reworked and barren assemblages.	Reworked tephra and fluvial sands.
Silt and sand with adundant marine fauna	S1, 10 – 15 m; S2 and S3, 11 – 14 m; S4, ~ 19 m, S5, 16 – 19 m; S 6, 8b, 8c, 2 – 6 m.	Silt and silty fine sand, beds are usually massive, some display faint mm to centimetre scale laminae; rare units with centimetre-scale lenticular cross-beds and millimetre-scale flaser bedding. Most bounding contacts are sharp and there are frequent scoured angular unconformities indicating channelling. Abundant whole and in-situ *P. australis* and *A. stutchburyi* shells. Foraminifera assemblages dominantly intertidal.	Estuary central basin.
Silt and sand with rare marine fauna	S1, rare 10 – 15.5 m; S2, rare 7 – 14.5 m; S3, rare 11.5 - 14 m; S4, 13 – 13.5 m; S5, rare 6 – 18 m; S7, 17 – 18.5 m; S7, 8b, 8d, rare 2.5 – 8 m.	Silt or silty fine to medium sand, occasional detrital wood chips less than 20 mm in length. Beds are usually massive, rare units with millimetre to centimetre-scale horizontal and wavy laminations. Foraminifer assemblages dominantly marginal-estuarine.	Estuarine margins.
Unfossiliferous silt and sand	S1, > 15 m, 6 – 8 m, 12 – 14 m; S2, 9 – 11 m, 7 – 8 m, 12 – 14 m; S3, > 14 m, 11 – 14 m; S4, 13.5 – 18.5 m; S5, 5.5 – 16 m, < 2 m; S6, 4 – 9 m; S7, 8.5 – 17 m; S7, 6.5 – 5.5 m; S8a – 8d, varying elevations; 8e, 0.9 – 3.4 m.	Silt and silty fine to medium sand; detrital wood common with branches up to 200 mm diameter. Units commonly massive; occasional millimetre to centimetre-scale horizontal bedding. Gradational bounding contacts. Occasional coarser-grained units (medium sand to coarse sand) with unconformable wavy basal contacts. Marine indicators absent. Foraminifera assemblages are either barren or reworked.	Fluvial.
Tephra	S5 – 7, 8d, 6 – 7 m.	Beds 0.85 - 0.24 m thick. Very sharp bounding contacts. ~150 mm of medium-coarse millimetre-scale shower-bedded grains at the base all units, upper parts very fine grained with massive beds of clay-sized glass particles.	Primary airfall tephra at base, reworked tephra at top.
Paleosols	S5 – 7, occasional between 8 – 9 m.	Silt units characterised by a dark brown tint in the sediment due to a high organic content and by a crumbly texture and greasy feel due to high clay content.	Period of non-deposition.

Facies 3: Non-fossiliferous gravel beds 0.2-0.6 m thick.

The non-fossiliferous gravel facies is most likely a fluvial channel deposit because of the thin nature of the beds and high-energy currents implied by the presence of large clasts. A non-marine environment is indicated by the absence of shells in the gravel. The range of clast sizes and the angularity of clasts suggest that the gravel has not been transported far, particularly since the clasts consist chiefly of mudstone, a soft lithology that would be quickly rounded during transport. The mudstone clasts are of identical lithology to that of the local outcrops of Neogene bedrock, thus supporting a nearby source. The poor sorting and angularity of clasts might suggest a colluvial depositional environment, but bedding indicates fluvial deposition of this proximally derived gravel.

Facies 4: Silt and sand units with abundant marine fauna, 0.1 – 1.5 m thick.

We interpret the depositional environment of this facies to be the central basin of an estuary. The primary evidence of this are abundant whole and *in situ P. australis* and *A. stutchburyi* shells and the intertidal foraminifera assemblages (Table 3). Observed and measured grain size variation between sand and silt and evidence of channelling is consistent with an estuarine environment subject to varying current energies and meandering tidal channels (Fig. 2).

Facies 5: Silt and sand units with rare marine fauna 0.1 – 1.5 m thick.

The distinguishing feature of this bio-lithofacies is the occurrence of marginal-estuarine foraminifera assemblages (Fig. 3). The benthic foraminifer *A. aoteana* indicate this unit probably deposited close to an estuary, perhaps between mean high water and extreme high water spring level. However, the abundances are so low it is conceivable that either the depositional site was only inundated during extreme high tides or storm surges, or that the intertidal forams could have been wind-blown up river.

Facies 6: Thin shelly gravel units <0.5 m thick.

The thin shelly gravel layers are interpreted as estuary tidal channel lags. The scoured bases, abundant fragmented shells and large clast sizes indicate a high-energy depositional environment. The shell species consist of *Austrovenus stutchburyi* and *Paphies australis,* both of which inhabit sheltered, marine to brackish-marine, intertidal environments (Morton and Miller, 1968; Hayward et al., 1999a; Hayward et al., 1999b). The foraminifera assemblages are dominantly estuarine to marginal-estuarine therefore both the macro- and mircofauna indicate a brackish-marine, intertidal paleoenvironment.

Facies 7: Tephra

The lenticular shape of the tephra (correlations between the units suggests a horizontal top and curved concave-up base, Fig. 4), and the considerable thickness of very fine reworked tephra suggest that the depositional environment may have been an abandoned oxbow or backwater swamp of the Pakarae River. Such a low-energy paleoenvironment would have been required to preserve the tephra, and allow the clay-sized glass particles to settle out of suspension. The lack of marine indicators in the surrounding tephra lense argues against deposition within an estuary.

Facies 8: Non-fossiliferous well-sorted sand units 0.4 – 1 m thick.

This sand was probably deposited in a fluvial environment as it contains no shells or foraminifera. Most of the grains consist of volcanic glass, suggesting reworking of the underlying Rotoma tephra, with subordinate amounts of quartz grains.

Facies 9: Paleosol

The paleosol units occur within silt, where they are characterised by a dark brown tint signifying a higher organic content and they have a crumbly texture with a greasy feel due to high clay content. Paleosols record a prolonged period during which the sediment surface was above water and not undergoing continuous sedimentation thereby allowing soil to develop.

Facies 10: Shelly well-sorted sand units up to 2.5 m thick.

We interpret the shelly well-sorted sand to have been deposited near the mouth of an estuary inside a wave-dominated barrier, probably representing the flood tidal delta. The clean, well-sorted nature of the facies is characteristic of sediments sorted by waves and tidal currents (Allen and Posamentier, 1993; Roy et al., 1994). The occasional *A. stutchburyi* shells and dominantly intertidal foraminifera assemblages are consistent with an intertidal environment.

3.3.4 Paleoenvironmental facies associations and correlations between sections.

With the exception of the paleosols and tephra facies, which can be correlated reliably between sections, the rest of the bio-lithofacies have highly variable distribution and correlation of individual units is not feasible. This is why we simplify the stratigraphy further by adopting four basic paleoenvironmental facies associations to enable correlation between the sections (Fig. 4). We define a paleoenvironmental facies association as a package of bio-lithofacies from a similar depositional paleoenvironment. Four paleoenvironmental facies associations are recognised within the Pakarae sequence: barrier, estuarine, estuary-head delta and floodplain. The composition of each of these is described below:

- The floodplain paleoenvironmental facies association is comprised of Facies 1, non-fossiliferous silts and sand, Facies 3, non-fossiliferous gravel bio-lithofacies and Facies 8, non-fossiliferous well-sorted sands.
- The estuarine paleoenvironmental facies association is composed mainly of Facies 4, silt and sand with abundant marine fauna and Facies 6, thin shelly gravels. Both the floodplain and estuarine paleoenvironmental facies associations include occasional units of Facies 5 (silts and sand with rare marine fauna). Because Facies 5 is interpreted as a marginal-estuarine deposit we package it within the paleoenvironmental facies association of the surrounding bio-lithofacies.
- The estuary-head delta paleoenvironmental facies association consists of Facies 2, thick shelly gravel bio-lithofacies. With increasing distance from the bedrock high these coarse gravel sediments become interfingered with units of Facies 1, non-fossiliferous silts, and Facies 4, silts with abundant marine fauna.
- The barrier paleoenvironmental facies association is dominated by Facies 10, shelly well-sorted sands and also includes some units of Facies 6, thin shelly gravels.

3.4. Discussion

To characterise the facies architecture of an incised valley on a tectonically active coast we compare the paleoenvironmental facies association distribution profile we have developed from Pakarae (Fig. 4) to facies models for stable coasts (Fig. 5A, B, D Roy, 1984, Allen and Posamentier, 1993; Dalrymple et al., 1992) and case studies of infilled Holocene estuaries on stable coasts (for example, Fletcher III et al., 1990; Chappell, 1993; Woodroffe et al., 1993; Nichol et al., 1996; Woodroffe, 1996; Lessa et al., 1998; Long et al., 1998; Dabrio et al., 2000; Sloss et al., 2005, 2006). We then modify these models to better reflect the expected architecture of valley infill on tectonically active coasts.

Figure 4. Bio-lithofacies and paleoenvironmental facies associations of the Pakarae River sections, correlations between the sections based on stratigraphy and paleoenvironmental interpretations. Tidal ravinement surface and transgressive surface after the terminology of Allen and Posamentier (1993).

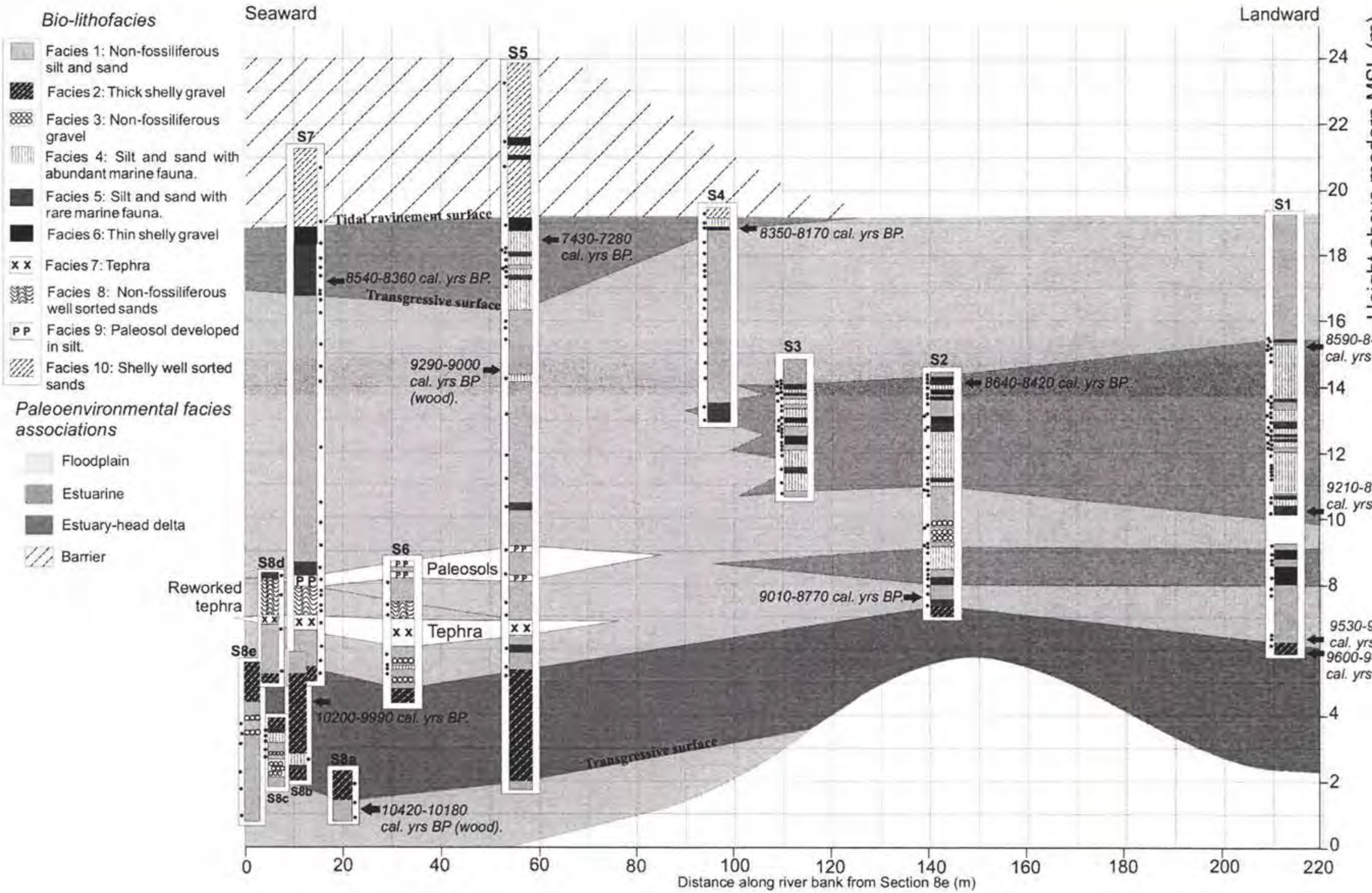
Bio-lithofacies
Facies 1: Non-fossiliferous silt and sand
Facies 2: Thick shelly gravel
Facies 3: Non-fossiliferous gravel
Facies 4: Silt and sand with abundant marine fauna.
Facies 5: Silt and sand with rare marine fauna.
Facies 6: Thin shelly gravel
Facies 7: Tephra
Facies 8: Non-fossiliferous well sorted sands
Facies 9: Paleosol developed in silt.
Facies 10: Shelly well sorted sands
Paleoenvironmental facies associations
Floodplain
Estuarine
Estuary-head delta
Barrier
Seaward
Landward
S1
S2
S3
S4
S5
S6
S7
S8a
S8b
S8c
S8d
S8e
Tidal ravinement surface
Transgressive surface
Transgressive surface
7430-7280 cal. yrs BP.
8350-8170 cal. yrs BP.
8540-8360 cal. yrs BP.
9290-9000 cal. yrs BP (wood).
8590-8410 cal. yrs BP.
8640-8420 cal. yrs BP.
9210-8980 cal. yrs BP.
9010-8770 cal. yrs BP.
9530-9240 cal. yrs BP.
9600-9450 cal. yrs BP.
10200-9990 cal. yrs BP.
10420-10180 cal. yrs BP (wood).
Paleosols
Reworked tephra
Tephra
Height above modern MSL (m)
Distance along river bank from Section 8e (m)

3.4.1 Comparisons of Pakarae stratigraphy to stable coast models of incised valley infilling

The paleoenvironmental facies associations we identify have been developed on their own merits, but many do have similarities with the facies divisions of Dalrymple et al. (1992), Roy (1984) and Allen and Posamentier (1993, Fig. 5A, B, D). Our barrier paleoenvironmental facies association is comparable to the barrier-shoreface facies of Dalrymple et al. (1992), the estuary mouth facies of Allen and Posamentier (1993), and the tidal delta sand of Roy (1984). The estuarine paleoenvironmental facies association of this study is similar to the central basin facies of Dalrymple et al. (1992), the tidal estuarine sand and mud facies of Allen and Posamentier (1993), and the estuarine mud facies of Roy (1984). The Pakarae estuarine facies, consisting of silts, sands and occasional thin shelly gravels, is generally coarser and more variable than the equivalent facies described by Roy (1984), Dalrymple et al. (1992), and Allen and Posamentier (1993), which are dominantly or entirely muds or silts. Nevertheless our Pakarae data benefits from micro- and macrofossil data to confirm the estuarine paleoenvironment. The coarser sediment and greater variability of this facies at Pakarae is probably due to the relatively restricted space in the Pakarae incised valley, which may have inhibited the development of a deep central basin where fine sediments could uniformly accumulate. The estuary-head delta paleoenvironmental facies association of Pakarae is similar to the bay-head delta facies of Dalrymple et al. (1992). Bay-head and estuary-head are interchangeable terms and refer to the same physiographic location within an estuary; we henceforth use the term "estuary-head". Our floodplain paleoenvironmental facies association corresponds to the alluvial package of Dalrymple et al. (1992), the fluvial or floodplain packages of Allen and Posamentier (1993) and Roy (1984). The recognition of fluvial sediments in these studies is based on an absence of evidence of marine or tidal processes in the sediment deposition, similar to the criteria we have used at Pakarae.

The stratigraphic framework of Pakarae is simplified by the use of paleoenvironmental facies associations (Fig. 4). This allows correlation of groups of bio-lithofacies from similar depositional environments. The spatial and chronological relationships between the paleoenvironmental facies associations forms the basis of our comparisons with stable coast facies models of incised-valley infill. This is also a significant improvement upon the previous data collected from Pakarae by Berryman et al. (1992) which used three widely spaced sections between which unit correlation was not possible and did not utilise paleoenvironmental data from microfossils.

There are two elements of similarity between Pakarae facies distribution and the facies models of Dalrymple et al. (1992), Roy (1984) and Allen and Posamentier (1994, Fig. 5A, B, D): (1) the occurrence of floodplain sediments at the base of the sequence and the immediately overlying estuary-head delta facies; (2) the occurrence of barrier sands at the top of the sequence. The major difference between Pakarae valley sequence and existing stable-coast models is within the middle part of the infill sequence where estuarine and fluvial facies alternate at Pakarae instead of displaying a deepening central estuary basin facies as predicted in the models. We discuss the similarities first, and then the important differences.

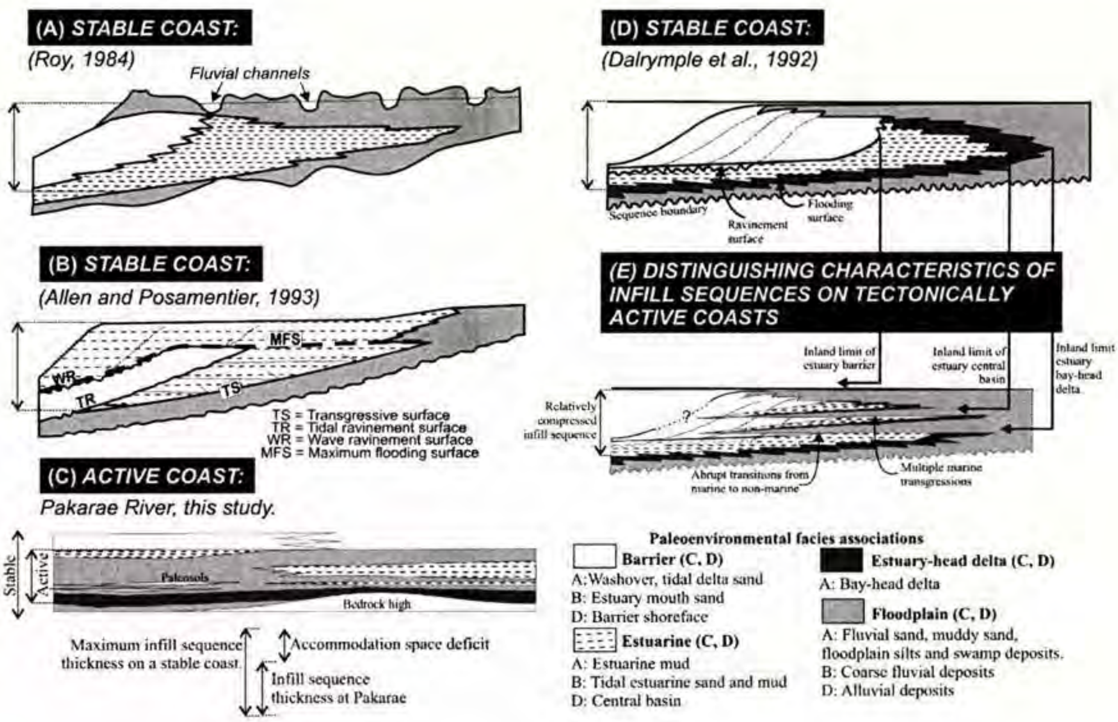

Figure 5. Comparisons between incised-valley facies models of stable coasts **(A, B, D)**, and an active coast **(C)**, and a model for the distinguishing characteristics of an infill sequence on a tectonically active coast **(E)**. All thicknesses (denoted by the vertical arrows) are relative. **(A)** Stable coast facies model Roy (1984), central estuarine basin mud facies in the middle, thinning landward, underlain and overlain by fluvial sediments. **(B)** Stable coast facies model Allen and Posamentier (1993), thick estuarine facies in middle thinning landward. **(C)** Uplifting active coast, Pakarae River (this study), includes three estuarine paleoenvironmental facies associations, two of which pinch out seaward within a floodplain paleoenvironmental facies association. **(D)** Stable coast facies model Dalrymple et al. (1992), thick central estuarine basin facies in middle thinning landward, underlain and overlain by fluvial sediments. **(E)** Modification of a stable coast infill model to better reflect the distinguishing characteristics produced by a tectonically active coast.

It is significant that both the basal floodplain and capping barrier package are present at Pakarae because it suggests that the whole sequence of the Holocene valley infill is represented in the outcrop exposures. We infer there is no additional valley infill below the extent of the exposures we have documented at Pakarae. A juvenile *A.*

stutchburyi shell from the lowest estuary-head package is dated at 10200-9990 cal. yrs B.P. (Table 1). At this time eustatic SL was ca. 23 m below modern MSL (Gibb. 1986). The present elevation of this shell sample at 4.4 ± 0.31 m indicates an uplift rate of 2.7 ± 0.5 mm/yr since its deposition. This is within the uncertainty range of the late Holocene uplift rate calculated at Pakarae from the elevation of marine terraces (3.2 ± 0.8 mm/yr, Wilson et al., submitted). We infer the incised valley floor that was inundated at ca. 10000 cal. yrs B.P. probably now resides close to modern MSL, assuming that the average uplift rate has been constant for the past 10000 yrs. This supports our inference that there is no valley infill below the Pakarae riverbank exposures.

The presence of a laterally continuous layer of the estuary-head delta paleoenvironmental facies (extending the full 220 m length of the sections) deposited on top of the basal fluvial deposits at Pakarae is consistent with the Dalrymple et al. (1992) facies model (Fig. 5D). The base of the estuary head paleoenvironmental facies association is termed the "flooding surface" by Dalrymple et al. (1992), and the "transgressive surface" by Allen and Posamentier (1994). The gravel-rich, carbonate poor nature of the estuary-head delta paleoenvironmental facies does contrast with the transgressive sand sheet described by Sloss et al. (2005, 2006) in their infilling models of two Australian estuaries, Burrill Lake and Lake Illawarra. They noted a basin-wide, carbonate-rich sand sheet as the initial transgressive marine unit in two incised valleys. Lacking in lithic components, they suggested the sand was sourced from the continental shelf rather than the catchment (Sloss et al., 2005) and this may explain why a similar unit is not seen in the Pakarae River incised valley. The more youthful landscape of the eastern North Island has higher erosion rates relative to southeastern Australia therefore the Pakarae River incised valley receives a higher catchment sediment input, most likely masking any contribution of continental shelf sand to the transgressive marine unit. At Pakarae the gravel-rich estuary-head delta paleoenvironmental facies marks the start of the post-glacial marine transgression along this part of the incised valley. Radiocarbon ages from juvenile *A. stutchburyi* shells within this facies indicate that the estuary head shifted landward ca. 200 m between 10200-9990 cal. yrs B.P. and 9600-9450 cal. yrs B.P. (Fig. 4, Table 1).

The distribution of paleoenvironmental facies associations in the middle section at Pakarae, between the estuary-head delta package and the barrier sands, does not reconcile with the common stable-coast facies models (Dalrymple et al., 1992; Roy, 1984; Allen and Posamentier, 1994). In this part of the section sediments of the central estuary basin would be expected (Fig. 5A, B, D). In contrast, the sediments at Pakarae between the basal estuary-head delta and capping paleoenvironmental facies associations show a complex alternation and interfingering of floodplain and estuarine paleoenvironmental facies associations (Figs. 4 and 5C). We consider this to be an important characteristic of the facies architecture of incised valley infill sequences on coseismically uplifting coastlines.

There are three units of estuarine paleoenvironmental facies association sediments in the middle stratigraphic section of the Pakarae incised valley infill sequence. The highest and youngest estuarine paleoenvironmental facies association is at the seaward end of the sections. It overlies a floodplain facies, pinches out landward into floodplain sediments and grades upwards into estuary barrier sands. This paleoenvironmental facies association distribution can be likened to a typical transgressive estuarine sequence (Fig. 4). The upper estuarine unit is thickest at the seaward end and its base is erosional above silts of the floodplain paleoenvironmental facies association (Fig. 2). The basal unconformity represents a transgressive surface, after Allen and Posamentier (1994) (Fig. 5B). The estuarine silts and sands contain *in-situ* intertidal foraminifera and the shells of *A. stutchburyi* and *P. australis*, common intertidal brackish-marine species. The estuarine unit coarsens upward into cross-bedded barrier sands. The thin gravel beds at ca. 19 m AMSL in Sections 5 and 7 probably represent tidal channels at the estuary barrier (Fig. 2), corresponding to a tidal ravinement surface (Fig. 4, Fig. 5B, Allen and Posamentier, 1994).

The lower and middle estuarine paleoenvironmental facies associations are located at the landward end of the sections (Fig. 4). Both units appear to either pinch out or gradationally merge seaward into a fluvial facies which lies at the same elevation in the seaward sections, though the contact between the estuarine and floodplain paleoenvironmental facies associations is concealed (Fig. 4). Floodplain sediments overlie both estuarine units. These lower two units of the estuarine paleoenvironmental facies association do not reconcile with existing models of incised valley infilling because in this section the marine environment should, if anything, become deeper due to rising eustatic SL. We have not conclusively resolved why this is so but can propose four possible scenarios:

(1) The non-marine sediments were deposited prior to estuary establishment: For example there may have been alluvial aggradation or colluvial fan deposition at the locations of Sections 5 and 7 before the estuarine sediments of Sections 1 – 4 were deposited.
(2) Birds-foot estuary-head delta morphology: A splayed fluvial delta front, in which there was switching between distributaries (e.g. a prodelta environment). Localised lobes of rapid sediment deposition that inhibited marine fauna colonisation, may account for the close juxtaposition of non-marine and marine-influenced sediments.
(3) The paleo-estuary was not oriented in the same direction as the modern river mouth: The former river mouth may have been in a different location therefore the paleo-seaward direction could have been different from the modern seaward.
(4) The estuarine paleoenvironmental facies associations were once continuous in the seaward direction, but have been removed by fluvial cut

and fill subsequent to tectonic uplift, coastal emergence, and consequent river baselevel fall.

None of these scenarios are completely satisfactory to explain the juxtaposition of seaward non-marine sediments at equivalent elevations to landward estuarine sediments. Colluvial fan deposition (scenario 1) is inconsistent with the silty laminations and cross-bedding displayed by the seaward floodplain unit. A floodplain aggradation mechanism implies ca. 7 m of floodplain sediment was deposited within ca. 400 yrs at a location very close to the coastline (*cf.* elevation of the ca. 9500 cal. yrs B.P. Rotoma tephra at 7 m and wood aged ca. 9100 cal. yrs B.P. at 14 m in Section 5), whilst leaving an area of lower elevation landward into which the middle estuarine paleoenvironmental facies association was deposited after ca. 9100 cal. yrs B.P. (indicated by shell age of 9210-8980 cal. yrs B.P. at 10 m elevation in Section 1). One might expect a river to grade to a consistent base level, and not form the significant topography implied by this scenario.

A splayed delta-front is possible (scenario 2) but it implies the sediments barren of marine fauna (now identified by us as floodplain sediments) were deposited rapidly in an estuary, seaward of locations inhabited by a rich estuarine fauna, without entraining any marine fauna. Furthermore the restricted space in the Pakarae valley means the development of a splayed delta is unlikely. For the same reason, an alternative river mouth orientation (scenario 3) is improbable. Marine terraces on the east side of the river are underlain by mudstone bedrock. Therefore the paleo-river mouth cannot have flowed east, this only leaves a narrow valley width open to the west.

Scenario 4, post-uplift fluvial cut-and-fill, is the preferred scenario because it is known from the late Holocene marine terraces that tectonic uplift at the Pakarae River mouth occurs at intervals of ca. 850 yrs (Ota et al., 1991; Wilson et al., submitted); therefore it most likely also occurred during deposition of the infill sequence. River incision following a sudden base level fall, caused by coastal uplift during an earthquake, is likely. The paleosol layer near the base of the fluvial package at 9 m, approximately the same elevation as the lowest estuarine unit, is interpreted as an unconformity because it indicates a hiatus in sedimentation. An issue with this scenario is that the floodplain paleoenvironmental facies association seaward of the middle estuarine unit is relatively uniform and there are no indications of an unconformity that may be equivalent an incision event following abandonment of the middle landward estuarine unit. The 2.5 m thickness of the floodplain sequence between the middle and upper estuarine units is significant and possibly represents rapid deposition of a large fluvial sediment pulse. The sediment pulse was probably due to catchment destabilisation triggered by an earthquake, probably the same event that caused abandonment of the middle estuarine unit.

The Pakarae stratigraphy is compared with case studies of incised valley infills as an additional check on whether our interpretation of fluvial package in the middle section of the Pakarae stratigraphy is anomalous (for example: Fletcher III et al., 1990; Chappell, 1993; Woodroffe et al., 1993; Nichol et al., 1996; Woodroffe, 1996; Heap and Nichol, 1997; Lessa et al., 1998; Long et al., 1998; Dabrio et al., 2000; Heap et al., 2004; Sloss et al., 2005). While there are some details of the stratigraphy that differ between these case studies and the facies models this is probably due to varying sediment supply rates, estuary sizes and tidal ranges. Overall, there is a broad consistency between the examples and the stable coast models. The main signature is of a transgressive sequence of non-marine sediments, followed by estuarine sediments that become progressively increasingly marine-influenced, and then a reversion back to non-marine sediments.

The study of Dabrio et al. (2000) is particularly comparable to our Pakarae study as similar biostratigraphic tools were used at two river valleys in the south of Spain. Within the Guadalete River trangressive sequence the fauna (benthic foraminifera and shells) show a transition from low-diversity, restricted water assemblage to an increasingly diverse, open-water fauna as SL reached maximum flooding. The highstand sediments are represented by a transition back to low-diversity restricted water fauna as a result estuary infilling (Dabrio et al., 2000). A comparable biostratigraphic sequence is not evident at Pakarae. The middle and lower estuarine units of Sections 1-3 show no apparent increase in marine influence or species diversity. The upper estuarine unit of Sections 4, 5 and 7, show some evidence of increasing marine influence: the foraminifera assemblages change from rare intertidal to abundant intertidal species between 16 – 20 m AMSL (Fig. 3), however there is no change in species diversity.

An alternating fluvial-estuarine-fluvial succession was suggested by Dalrymple et al. (1992) to occur if sea level fell before a valley was full. Subsequent sea level rise was predicted to deposit a second valley fill sequence over the incised remnants of the former fill sequence, resulting in a stacked pattern (for example, the three stacked Pleistocene channel fill sequences underlying Chesapeake Bay, Colman and Mixon, 1988). It is not surprising that there are similarities between the Pakarae sequence and that such as Chesapeake Bay as both are related to intermittent marine regressions within an overall trend of rising SL. However, the documentation of alternating fluvial-estuarine facies at Pakarae is the first of its kind to be recognised. Firstly, the Pakarae sedimentary successions are of Holocene age, and secondly, the marine regressions are tectonically-induced rather than eustatic SL change. The extent to which the detailed nature of the estuarine-fluvial transition preserved at Pakarae is analogous to a eustatic SL-related transition is unknown given that the marine regressions at Pakarae were sudden whereas eustatic SL change occurs gradually.

The coseismic marine regressions that appear to have occurred during infilling of the Pakarae incised valley probably had a similar geomorphic effect to sudden infilling of the incised valley. This raises the question of whether a delta ever developed at the mouth of the Pakarae River following uplift events, an evolutionary pathway suggested by Boyd et al. (1992) and Heap et al. (2004) to occur once estuaries infill either under falling or stable eustatic SL conditions. Any early Holocene deltaic deposits of the Pakarae River would have been deposited seaward of the present riverbank outcrops, therefore they would have since been removed by erosion. It is possible that immediately following uplift events the sediment delivery at the Pakarae river mouth was high enough to overwhelm the rates of eustatic SL rise and create a delta. However, the alternating fluvial-estuarine sequence preserved along the riverbank indicates that the rate of eustatic SL rise was eventually sufficient to develop an estuary in the incised valley, which was maintained until the next uplift event.

A recent study by Sakai et al. (2006) addressed a similar question to this study: to interpret the tectonic controls on incised valley infilling on an uplifting coastline in Japan. Evidence for three uplift events of the Isumi River lowlands was found. An early Holocene event at ca. 9000 cal. yrs B.P., during the period of eustatic SL rise, was identified by an age gap in landward cores and a correlative period of very rapid sediment progradation within a marine silt sequence in the seaward cores. The rapid sedimentation and associated progradation was interpreted to be the result of increased erosion, probably related to an earthquake (Sakai et al., 2006). Other events younger than the culmination of eustatic SL rise, at 6,400 and 3,500 cal. yrs B.P., were identified by uplifted terraces and were associated with barrier establishment and enclosure of a lagoon. Our resolution of rapid deposition events is constrained by less age control than the Sakai et al. (2006) study, but it is possible that the middle, seaward floodplain paleoenvironmental facies association at Pakarae is an example of the rapid sedimentation and fluvial progradation event demonstrated at the Isumi River.

Comparison between Pakarae and the Isumi River sequence illustrates that the preserved sedimentary signature of an uplift event within a transgressive estuarine sequence depends on the location of the preserved sequence within the incised valley. For example, the preserved Pakarae sequences were probably near the landward edge of the estuary and seaward of this point there were probably pulses of rapidly accumulating sediment corresponding to each coseismic event and associated catchment destabilisation. The more landward parts of estuaries probably record hiatuses or unconformities, while seaward portions may respond with sediment progradation.

3.4.2 Development of a facies architecture model for an incised valley infill sequence on a coastline undergoing coseismic uplift.

Both the Pakarae and Isumi River examples demonstrate that there are significant differences between the incised valley infill sequences of stable and active coasts. Therefore we can begin to develop a modified facies model of the sedimentary infilling of an incised valley system that was experiencing coseismic uplift synchronous with deposition (Fig. 5E). The characteristics of this can be used to recognise similar tectonic settings in the ancient sedimentary record.

On a coastline undergoing uplift synchronously with eustatic SL rise, we predict the transgressive estuarine sequence will be compressed and will not extend as far inland relative to that on a stable coastline (Fig. 5E). If uplift occurred suddenly (i.e. by earthquakes) one might expect abrupt lateral shifts in the paleoenvironment thus sharp facies boundaries. For example, the estuarine central basin sediments might slowly transgress landward during eustatic SL rise, suddenly retreat seaward synchronous with an uplift event, and then subsequently resume gradual landward movement under the continuing eustatic SL rise. This would produce a saw-tooth pattern of interfingering fluvial and estuarine facies at the landward margin (Fig. 5E). If coastal uplift occurred continuously and aseimically this would result in a compressed estuarine sequence with gradational facies transitions. No SL regressions would be recorded if the uplift was always less than the rate of eustatic SL rise rate.

We can demonstrate that the Pakarae valley infill sequence is compressed by comparing the preserved thickness of infill to the eustatic New Zealand SL curve (Gibb, 1986). To do this we have to assume that sedimentation rates in the paleo-valley approximately kept pace with eustatic SL rise. This is indicated by the presence of intertidal foraminifera and bivalves throughout the estuarine paleoenvironmental facies associations. There is 14.1 ± 0.38 m between the oldest and youngest shell radiocarbon samples. An age of 10200-9990 cal. yrs B.P. was obtained from a shell at 4.4 m AMSL, and an age of 7430-7280 cal. yrs B.P. was obtained from 18.5 m AMSL (Fig. 4, Table 1). According to the Gibb (1986) eustatic SL curve there was 21 ± 2 m of eustatic SL rise between these two ages. An uncertainty of ± 2 m to this value to reflect the uncertainty of the eustatic SL curve. SL rise creates accommodation space for sedimentation within incised valleys. If sedimentation within the Pakarae incised valley kept pace with the creation of accommodation space by SL rise then 21 ± 2 m of sediment is expected to have been deposited between these two dated shells. The differential between the preserved sediment thickness (14.1 ± 0.38 m) and the accommodation space created during this period (21 ± 2 m) is 6.9 ± 2.04 m (uncertainty calculated as the square root of the sum of the variances, Fig. 4, Table 1). We call this residual the accommodation space deficit (Fig. 5). The substantial deficit between the highest and lowest dated shells is an indicator that the transgressive sequence at Pakarae is compressed relative to that which would be expected on a stable coast. The accommodation space deficit value of 6.9 ± 2.04 m is a significant refinement on the Berryman et al. (1992) study that estimated an accommodation space deficit of ca. 22 m for the Pakarae sequence. Our new estimate benefits from better paleoenvironmental and age control.

We cannot compare the inland extent of the marine sediments at Pakarae to other incised valleys because the geomorphology of Pakarae is unique. The initial depth and slope of the paleo-fluvial valley and rates of fluvial sediment delivery to the coast determine how far inland the maximum Holocene SL transgression reached and these vary with each valley.

Another distinguishing feature we identify for incised valley infills on coseismically uplifting coasts is a distinctive saw-tooth pattern stratigraphy (Fig. 5E). This is created by multiple cycles of sudden SL regressions (earthquakes) followed by gradual SL transgressions (eustatic SL rise). This is in contrast to an aseismic, gradual uplift mechanism, which might instead produce a compressed infill sequence with no reversals in the SL trend. While the paleoenvironmental package distribution of Pakarae has not produced an obvious saw tooth pattern (Fig. 5C), the alternations of fluvial and estuarine paleoenvironmental facies indicates that more than one SL transgression occurred during the valley infilling. The three separate estuarine units indicate at least three periods of marine transgression into the Pakarae paleo-valley. The Pakarae stratigraphy actually indicates that a saw-tooth pattern stratigraphy is perhaps oversimplified and more complex sedimentation patterns are likely because of local circumstance, particularly with rapid fluvial sediment delivery due to catchment destabilisation following earthquakes. The feature of landward estuarine package juxtaposed at the same elevation with an fluvial paleoenvironmental facies in the seaward direction is evidence of this. Evidence of SL reversals in the form of transitions from marine to fluvial environments despite continuous eustatic SL rise, is a remarkable stratigraphic feature at Pakarae and we believe it is an important characteristic of incised valley infills on coseismic tectonically active coasts.

It is possible that fluvial sedimentation pulses rather than uplift could produce saw-tooth stratigraphic patterns and vertical transitions from estuarine to fluvial packages. Both would cause seaward movement of the shoreline and preserve stratigraphic signature of a marine regression stratigraphic signature. However, with SL rising at such fast rates during the early Holocene we believe that it is unlikely that fluvial sedimentation could have been rapid enough to cause seaward movement of the coastline, and this mechanism does not explain the accommodations space deficits recorded at Pakarae. Furthermore, the mostly likely cause of a sediment pulse is destabilisation of the catchment triggered by an earthquake. Offshore sediment cores have shown no evidence of sedimentation pulses during the early Holocene which could be related to earthquakes (Foster and Carter, 1997; Carter et al., 2002; Orpin, 2004), and sediment pulses are unlikely to be climate-related as this is a period of expanding vegetation and slope stabilisation (McGlone et al., 1994).

This discussion shows that some features of the Pakarae sedimentary can be related to the occurrence of coseismic uplift during infilling of the incised valley. We suggest these may be characteristics that can be integrated into a facies model of incised valley infill on active margins. However, the general applicability of these features is yet to be tested. The Pakarae River is an ideal location for this type of study due to the abundant outcrop data, small size and a well-documented history of coseismic uplift events. Conversely, we do not know how the small size of the Pakarae incised valley and the high sediment input rates of the region affect the facies development, hence its value as a representative sequence is not known. Future work on uplifted incised valley infill sequences in other tectonically active regions will help to resolve this and to further refine a facies model for infill sequences on active coasts.

3.5. Conclusions

The stratigraphy preserved beneath the highest late Holocene marine terrace represents infilling of the Pakarae incised valley during early Holocene post-glacial SL rise. This example of infilling of an incised valley on a tectonically active coast provides a timely comparison with established facies models of incised valley infills, which have been developed exclusively for stable coasts (Roy, 1984; Dalrymple et al., 1992; Allen and Posamentier, 1994). At Pakarae the basal fluvial package, the immediately overlying estuary-head delta package, and the capping barrier package correlate well with models of incised valley infill and indicate that the complete sequence of incised valley infill is present within the Pakarae outcrops. The middle section of the Pakarae stratigraphy displays complex alternations of estuarine and fluvial environments and thus differs from facies architecture models of stable coasts, which display only central estuarine basin sediments in this section. These differences are probably related incision of the fluvial system in response to a fall in base level coupled with rapid delivery of large volumes of earthquake-generated sediment in the catchment following uplift.

Pakarae demonstrates that on coseismic uplifting coastlines distinctive incised valley infill facies architecture is developed and it is timely for a new facies model for such a setting to be developed. The distinguishing characteristics may include: (1) part, or all, of the transgressive and lowstand sequences can be above modern SL, (2) during the period of eustatic SL rise up to the culmination age (c. 7000 cal. yrs B.P. in New Zealand) the infill sedimentary sequence is thinner than the amount of eustatic SL rise that occurred during that period, (3) evidence of relative SL falls (tectonic uplift), such as transitions from estuarine to fluvial environments, during periods of time when SL was constantly rising, and (4) periods of rapid fluvial sedimentation that may represent catchment destabilisation following earthquakes.

Acknowledgements

This research was funded by an Earthquake Commission Student Grant (Project 6UNI/501). Kate Wilson was supported by the GNS Science Sarah Beanland Memorial Scholarship. Dr Rodger Sparks and Dawn Chambers of the Rafter Radiocarbon Laboratory are thanked for their contribution to the radiocarbon dating. Dr Bruce Hayward and Ashwaq Sabba are gratefully thanked for assistance and advice with foraminifera identification. Hannu Seebeck, Matt Hill and Vicente Perez provided fieldwork assistance. Dr Craig Sloss, Dr Andrew Heap and one anonymous reviewer are thanked for their reviews, which significantly improved this manuscript.

References

Allen, G.P., Posamentier, H.W., 1993. Sequence stratigraphy and facies model of an incised valley fill: the Gironde estuary, France. Journal of Sedimentary Petrology, 63(3): 378-391.

Allen, G.P., Posamentier, H.W., 1994. Transgressive facies and sequence architecture in mixed tide- and wave-dominated incised valleys: example from the Gironde estuary, France. In: Dalrymple, R. W., Boyd, R., Zaitlin, B. A. (Eds.), Incised-valley systems: origin and sedimentary sequences, SEPM Special Publication 51, Tulsa, Oklahoma., pp. 225-241.

Anstey, R.L., Chase, T.L., 1974. Environments through time. Burgess Publishing Ltd., Minneapolis, 136 p.

Beavan, J., Haines, J., 2001. Contemporary horizontal velocity and strain rate fields of the Pacific-Australian plate boundary zone through New Zealand. Journal of Geophysical Research, 106(B1): 741-770.

Berryman, K.R., Ota, Y., Hull, A.G., 1989. Holocene paleoseismicity in the fold and thrust belt of the Hikurangi subduction zone, eastern North Island, New Zealand. Tectonophysics, 163: 185-195.

Berryman, K.R., Ota, Y., Hull, A.G., 1992. Holocene evolution of an estuary on a tectonically rising coast: the Pakarae River locality, eastern North Island, New Zealand. Sedimentary Geology, 80: 151-162.

Boyd, R., Dalrymple, R.W., Zaitlin, B.A., 1992. Classification of clastic depositional environments. Sedimentary Geology, 80: 139-150.

Carter, L., Manighetti, B., Elliot, M., Trustrum, N., Gomez, B., 2002. Source, sea level and circulation effects on the sediment flux to the deep ocean over the past 15 ka off eastern New Zealand. Global and Planetary Change, 33: 339-355.

Chappell, J., 1993. Contrasting sedimentary geologies of lower Daly River, northern Australia, and lower Sepik-Ramu, Papua New Guinea. Sedimentary Geology, 83: 339-358.

Collot, J.-Y., J. Delteil, K. Lewis, B. Davy, G. Lamarche, J.-C. Andru, P. Barnes, F. Chanier, E. Chaumillon, S. Lallemand, B.M. De Lepinay, A. Orpin, B. Pelletier, M. Sosson, Toussaint, C. Uruski., 1996. From oblique subduction to intra-continental transpression: structures of the southern Kermadec-Hikurangi margin from multibeam bathymetry, side-scan sonar and seismic reflection. Marine Geophysical Researches, 18(2-4): 357-381.

Colman, S.M., Mixon, R.B., 1988. The record of major Quaternary sea-level changes in a large coastal plain estuary, Chesapeake Bay, eastern United States. Palaeogeography, Palaeoclimatology, Palaeoecology, 68: 99-116.

Dabrio, C. J., Zazo, C., Goy, J. L., Sierro, F. J., Borja, F., Lario, J., Gonzalez, J. A., Flores, J. A., 2000. Depositional history of estuarine infill during the last postglacial transgression (Gulf of Cadiz, Southern Spain). Marine Geology, 162: 381-404.

Dalrymple, R.W., Zaitlin, B.A., Boyd, R., 1992. Estuarine facies models: conceptual basis and stratigraphic implications. Journal of Sedimentary Petrology, 62(6): 1130-1146.

Darienzo, M.E., Peterson, C.D., Clough, C., 1994. Stratigraphic evidence for great subduction-zone earthquakes at four estuaries in Northern Oregon, U. S. A. Journal of Coastal Research, 10: 820-876.

De Mets, C., Gordon, R.G., Argus, D.F., Stein, S., 1994. Effect of recent revisions to the geomagnetic reversal timescale on estimates of current plate motions. Geophysical Research Letters, 21: 2191-2194.

Fletcher III, C.H., Knebel, H.J., Kraft, J.C., 1990. Holocene evolution of an estuarine coast and tidal wetlands. Geological Society of America Bulletin, 102: 283-297.

Foster, G., Carter, L., 1997. Mud sedimentation on the continental shelf at an accretionary margin - Poverty Bay, New Zealand. New Zealand Journal of Geology and Geophysics, 40: 157-173.

Froggatt, P.C., Lowe, D.J., 1990. A review of late Quaternary silicic and some other tephra formations from New Zealand: their stratigraphy, nomenclature, distribution, volume and age. New Zealand Journal of Geology and Geophysics, 33: 89-109.

Froggatt, P.C., Rogers, G.M., 1990. Tephrostratigraphy of high-altitude peat bogs along the axial ranges, North Island, New Zealand. New Zealand Journal of Geology and Geophysics, 33: 111-124.

Gibb, J.G., 1986. A New Zealand regional Holocene eustatic sea-level curve and its application to determination of vertical tectonic movements. In: Reilly, W. I., Harford, B. E. (Eds.) Recent Crustal Movements of the Pacific Region. The Royal Society of New Zealand Bulletin 24, Wellington, pp. 377-395.

Hayward, B.W., Grenfell, H.R., Cairns, G., Smith, A., 1996. Environmental controls on benthic foraminiferal and thecamoebian associations in a New Zealand tidal inlet. Journal of Foraminiferal Research, 26: 150-171.

Hayward, B.W., Grenfell, H.R., Reid, C. and Hayward, K., 1999a. Recent New Zealand shallow-water benthic foraminifera: taxonomy, ecologic dstribution, biogeography, and use in paleoenvironmental assessment. Institute of Geological and Nuclear Sciences Monograph 21, Lower Hutt, New Zealand, 264 p.

Hayward, B.W., Grenfell, H.R. and Scott, D.B., 1999b. Tidal range of marsh foraminifera for determining former sea-level heights in New Zealand. New Zealand Journal of Geology and Geophysics, 42: 395-413.

Hayward, B.W., Hollis, C.J. and Grenfell, H.R., 1997. Recent Elphidiidae (Foraminiferida) of the South-west Pacific and fossil Elphidiidae of New Zealand. Institute of Geological and Nuclear Sciences Monograph 16, Lower Hutt, New Zealand, 170 p.

Hayward, B.W., Scott, G.H., Grenfell, H.R., Carter, R., Lipps, J.H., 2004. Techniques for estimation of tidal elevation and confinement (~ salinity) histories of sheltered harbours and estuaries using benthic foraminifera: examples from New Zealand. The Holocene, 14(2): 218-232.

Heap, A.D., Nichol, S.L., 1997. The influence of limited accommodation space on the stratigraphy of an incised-valley succession: Weiti River estuary, New Zealand. Marine Geology, 144(1-3): 229-252.

Heap, A.D., Bryce, S., Ryan, D.A., 2004. Facies evolution of Holocene estuaries and deptas: a large-sample statistical study from Australia. Sedimentary Geology, 168: 1-17.

Hemphill-Haley, E., 1995. Diatom evidence for earthquake-induced subsidence and tsunami 300 yr ago in southern coastal Washington. Geological Society of America Bulletin, 107: 367-378.

Hughen, K.A., Baillie, M G. L., Bard, E., Bayliss, A., Beck, JW., Bertrand, C., Blackwell, P. G., Buck, C. E., Burr, G., Cutler, K. B., Damon, P. E., Edwards, R. L., Fairbanks, R. G., Friedrich, M., Guilderson, T. P., Kromer, B., McCormac, F. G., Manning, S., Bronk Ramsey, C., Reimer, P. J., Reimer, R. W., Remmele, S., Southon, J. R., Stuiver, M., Talamo, S., Taylor, F. W., van der Plicht, J., Weyhenmeyer, C. E., 2004. Marine04 Marine Radiocarbon Age Calibration, 0–26 Cal Kyr BP. Radiocarbon, 46(3): 1059-1086.

Kingma, J.T., 1964. Sheet 9, Gisborne (1st Ed.) Geological Map of New Zealand 1 : 250 000. Department of Scientific and Industrial Research, Wellington.

Lessa, G.C., Meyers, S.R., Marone, E., 1998. Holocene stratigraphy in the Paranagua Bay estuary, southern Brazil. Journal of Sedimentary Research, 68(6): 1060-1076.

Lewis, K.B., Collot, J. –Y., Davy, B., Delteil, J., Lallemand, S., Uruski, C., 1997. North Hikurangi GeodyNZ swath maps: depths, texture and geological interpretation 1: 500 000. National Institute of Water and Atmospheric Research Miscellaneous Series Chart 72. Wellington, New Zealand.

Long, A. J., Innes, J. B., Kirby, J. R., Lloyd, J. M., Rutherford, M. M., Shennan, I., Tooley, M. J., 1998. Holocene sea-level change and coastal evolution in the Humber estuary, eastern England: an assessment of rapid coastal change. The Holocene, 8(2): 229-247.

Lowe, D.J., 1988. Late Quaternary volcanism in New Zealand: towards an integrated record using distal airfall tephras in lakes and bogs. Journal of Quaternary Science, 3(2): 111-120.

Mazengarb, C., Speden, I.G. (compilers), 2000. Geology of the Raukumara area. Institute of Geological & Nuclear Sciences 1:250,000 Geological Map 6. Institute of Geological and Nuclear Sciences Limited, Lower Hutt, New Zealand.

McCormac, F. G., Hogg, A. G., Blackwell, P. G., Buck, C. E., Higham, T. F. G., Reimer, P. J., 2004. SHCal04 Southern Hemisphere Calibration, 0 - 26 ka cal BP. Radiocarbon 46, 1087-1092.

McGlone, M.S., Anderson, A.J., Holdaway, R.N., 1994. An ecological approach to the Polynesian settlement of New Zealand. In: D.G. Sutton (Ed.), The Origins of the First New Zealanders. Auckland University Press, Auckland, pp. 136– 163.

Morton, J., Miller, M., 1968. The New Zealand sea shore, Collins, London. 638 p.

Nichol, S.L., Boyd, R., Penland, S., 1996. Sequence stratigraphy of a coastal-plain incised valley estuary: Lake Calcasieu, Louisiana. Journal of Sedimentary Research, 66(4): 847-857.

Orpin, A., 2004. Holocene sediment deposition on the Poverty-slope margin by the muddy Waipaoa River, East Coast New Zealand. Marine Geology, 209: 69-90.

Ota, Y., Berryman, K.R., Hull, A.G., Miyauchi, T., Iso, N., 1988. Age and height distribution of Holocene transgressive deposits in eastern North Island, New Zealand. Palaeogeography, Palaeoclimatology, Palaeoecology, 68: 135-151.

Ota, Y., Hull, A.G., Berryman, K.R., 1991. Coseismic uplift of Holocene marine terraces in the Pakarae River area, eastern North Island, New Zealand. Quaternary Research, 35: 331-346.

Ota, Y., Hull, A. G., Iso, N., Ikeda, Y., Moriya, I., Yoshikawa, T., 1992. Holocene marine terraces on the northeast coast of North Island, New Zealand, and their tectonic significance. New Zealand Journal of Geology and Geophysics, 35: 273-288.

Patterson, R.T., Hutchinson, I., Guilbault, J.-P., Clague, J.J., 2000. A comparison of the vertical zonation of diatom, foraminifera, and macrophhyte assemblages in a coastal marsh: implications for greater paleo-sea level resolution. Micropaleontology, 46(3): 229-244.

Powers, M.C., 1953. A new roundness scale for sedimentary particles. Journal of Sedimentary Petrology, 23: 117-119.

Roy, P. S., Thom, B. G., Wright, L. D. 1980. Holocene sequences on an embayed high-energy coast: an evolutionary model. Sedimentary Geology, 26: 1-19.

Roy, P.S., 1984. New South Wales Estuaries: their origin and evolution. In: Thom, B. G. (Ed.), Coastal Geomorphology in Australia. Academic Press, Sydney, Australia, pp. 99-121.

Roy, P.S., Cowell, P.J., Ferland, M.A., Thom, B.G., 1994. Wave-dominated coasts. In: Carter, R. W. G., Woodroffe, C. D. (Eds.), Coastal evolution: Late Quaternary shoreline morphodynamics. Cambridge University Press, Cambridge, pp. 121-186.

Sakai, T., Fujiwara, O., Kamataki, T., 2006. Incised-valley-fill succession affected by rapid tectonic uplifts: An example from the uppermost Pleistocene to Holocene of the Isumi River lowland, central Boso Peninsula, Japan. Sedimentary Geology, 185: 21-39.

Shennan, I., Scott, D.B., Rutherford, M., Zong, Y., 1999. Microfossil analysis of sediments representing the 1964 earthquake, exposed at Girdwood Flats, Alaska, USA. Quaternary International, 60: 55-73.

Sloss, C.R., Jones, B.G., Murray-Wallace, C.V., McClennen, C.E., 2005. Holocene sea level fluctuations and the sedimentary evolution of a barrier estuary: Lake Illawarra, New South Wales, Australia. Journal of Coastal Research, 21(5): 943-959.

Sloss, C. R., Jones, B. G., McClennen, C. E., de Carli, J., Price, D. M., 2006. The geomorphological evolution of a wave-dominated barrier estuary: Burrill Lake, New South Wales, Australia. Sedimentary Geology 187(3-4): 229-249.

Stokes, S., Lowe, D.J., 1988. Discriminant function analysis of late Quaternary tephras from five volcanoes in New Zealand using glass shard major element chemistry. Quaternary Research, 30: 270-283.

Stuiver, M. and Polach, H.A., 1977. Discussion: reporting of C-14 data. Radiocarbon, 19(3): 355-363.

Vucetich, C.G., Pullar, W.A., 1964. Stratigraphy of Holocene ash in the Rotorua and Gisborne districts. Part 2. New Zealand geological Survey Bulletin, 73: 43-63.

Wilson, K.J., Berryman, K.R., Litchfield, N.J. and Little, T.A., submitted, New Zealand Journal of Geology and Geophysics. A revision of Mid to Late Holocene marine terrace distribution and chronology at New Zealand's most tectonically active coastal location, Pakarae River, North Island, New Zealand.

Woodroffe, C.D., 1996. Late Quaternary infill of macrotidal estuaries in northern Australia. In: Nordstrum, K. F., Roman, C. T (Eds.) Estuarine Shores: Evolution, Environments and Human Alterations. John Wiley & Sons Ltd., Chichester, pp. 89-114.

Woodroffe, C.D., Mulrennan, M.E., Chappell, J., 1993. Estuarine infill and coastal progradation, southern van Diemen Gulf, northern Australia. Sedimentary Geology, 83: 257-275.

Yoshikawa, T., 1988. Pattern and rate of tectonic movement and Late Quaternary geomorphic development in the Raukumara Peninsula, northeastern North Island, New Zealand. Bulletin of the Department of Geography University of Tokyo, 20: 1-28.

CHAPTER FOUR

EARLY HOLOCENE PALEOSEISMIC HISTORY AT THE PAKARAE LOCALITY, EASTERN NORTH ISLAND, NEW ZEALAND, INFERRED FROM TRANSGRESSIVE MARINE SEQUENCE ARCHITECTURE.

Wilson, K., Berryman, K., Cochran, U., Little, T. In press. Tectonics.

Abstract

Early Holocene transgressive marine deposits infilling the Pakarae River paleo-valley are used to extend the paleoseismic history of the Pakarae River locality, East Coast, North Island, New Zealand, back in time prior to eustatic sea level stabilization at ~ 7 ka cal. B.P. Paleoenvironmental evolution of the Pakarae River paleo-valley from 7 – 10 ka cal. B.P is reconstructed using sedimentology and biostratigraphy. Two estuarine units display sudden vertical transitions to floodplain sediments implying significant marine regressions and estuary abandonment. These regressions are attributed to coseismic coastal uplift events at ~9,000 and ~8,500 cal. yrs B.P. A third uplift between 8,500 and ~7,350 cal. yrs B.P. is inferred from a significant difference between the amount of sediment preserved and the predicted sediment thickness according to the eustatic sea level curve. This study demonstrates the utility of the analysis of transgressive deposits and their paleoenvironmental characteristics for neotectonic investigations on active coasts.

4.1. Introduction

With rising awareness of the devastating effects of subduction zone earthquakes, long-term records of plate interface and upper plate paleoseismicity are becoming increasingly important. Coastal environments are commonly the only places that preserve a record of such events; for example, coseismic subsidence is often documented by drowning of tidal marsh sequences, and uplift recorded by abandonment of marine terraces on parts of the coastline favourable for their preservation (e.g. Atwater, 1987; Clague, 1997; Darienzo, et al., 1994; Marshall and Anderson, 1995; Merritts, 1996; Zachariasen, et al., 1999). The duration of these records is commonly limited by the time elapsed since stabilization of post-glacial eustatic sea level (SL). This is because modern SL can be used as a datum against which to measure non-eustatic (i.e. tectonic) effects. Here we extend the paleoseismic history at the Pakarae River mouth (henceforth called the Pakarae locality), New Zealand's most tectonically active coastal location, back beyond the time of eustatic SL stabilization at ~ 7 ka (Gibb, 1986) by unravelling an event history in the transgressive fluvio-marine sequence.

Tectonic uplift since ~ 7 ka, taking place at an average rate of 3.2 ± 0.8 mm/yr, is recorded at the Pakarae River mouth, North Island, New Zealand, by a flight of seven Holocene marine terraces (Ota et al., 1991; Wilson et al., 2006). Prior to 7 ka the incised valley of the Pakarae River was infilled by a transgressive sedimentary sequence under conditions of rapidly rising eustatic SL (Berryman et al., 1992). Wilson et al. (in press-a) have demonstrated that tectonic uplift occurred during deposition of the sequence, and was a major control on the facies distribution. Here we further investigate the paleogeographic evolution and tectonic history of the Pakarae paleo-estuary by applying two methods to identify the timing of tectonic uplift that has affected the transgressive estuarine sequence. One method is to compare the thickness of the estuarine section with that on a stable coast. On stable coasts the thickness of sediment should approximately equal the amount of eustatic SL rise. If tectonic uplift occurs during transgression the total thickness of sediment will be less than the amount of eustatic SL rise. The deficit will approximately equal the tectonic uplift component, though this does rely on several assumptions such as sedimentation rates keeping pace with eustatic SL rise and estuary infilling being controlled by eustatic SL rise rather than fluvial aggradation. This technique is most effective where it can be demonstrated, particularly using microfauna, that the infilling sediment is consistently from an intertidal environment, which implies sedimentation rates equal the rate of eustatic SL rise and a lack of fluvial aggradation. The second, and most important, method employed is to use the paleoenvironmental facies architecture to detect sudden marine regressions that identify tectonic event horizons. We use the sedimentological and paleoenvironmental data reported by Wilson et al. (in press-a) to constrain a paleogeographic model of the Pakarae locality coastal evolution during the early Holocene and discuss evidence for the timing and magnitude of early Holocene uplift events at the Pakarae locality. Transgressive marine sequence analysis is an emerging field of coastal paleoseismology that enables us to extending the paleoseismic history of this significant location adjacent to the Hikurangi subduction zone.

The Pakarae locality is an important site along this sector of the margin because the Holocene record there can be used to place constraints on the boundaries of various upper plate strain domains, and to clarify where episodic (coseismic) versus aseismic tectonic processes may have operated along the Hikurangi margin. The Pakarae River mouth is situated on the southeastern Raukumara Peninsula, ~ 65 km inboard of the Hikurangi subduction trough on the eastern coast of North Island, New Zealand (Fig. 1). No subduction earthquakes have occurred in historic times along this section of the margin. The presence of a stepped sequence of Holocene coseismic marine terraces at the Pakarae River mouth has been interpreted to record permanent uplift and is most likely a consequence of faulting in the upper plate of this subduction zone (Ota et al., 1991; Wilson et al., 2006). Alternatively, sediment underplating (inferred from seismic velocities which image a weak zone along the plate interface) has been suggested as a cause of long term uplift of Raukumara Peninsula (Eberhart-Phillips and Reyners, 1999; Litchfield et al., in press; Reyners et al., 1999; Walcott, 1987). Normal faulting is persistent in the Raukumara Range but reverse faults are inferred in the coastal area and offshore (Lewis et al., 1997; Mazengarb, 1984; Mazengarb and Speden, 2000).

The Pakarae River mouth marine terraces were first mapped, correlated, and dated by Ota et al. (1991). Seven terraces were recognised and named T1-T7 from oldest to youngest. T1 was recognised by Berryman et al. (1992) as corresponding with the maximum Holocene marine transgression, which in the New Zealand region occurred ~ 7 cal. ka BP (Gibb, 1986). The age of uplift of each terrace was estimated from radiocarbon dates and tephra distribution by Ota et al. (1991). This chronology has been revised by Wilson et al. (2006). Although the Pakarae Fault, a reactivated Tertiary normal fault near the Pakarae River mouth, was argued to have moved during terrace uplift events, it did not rupture with every terrace-forming event. Rather uplift was inferred to have been driven by slip on an active reverse fault located a few kilometres offshore of the Pakarae River mouth (Ota et al., 1991). As part of this original study, Ota et al. (1988) presented radiocarbon dates from the sedimentary sequence underlying T1 and made summaries of the stratigraphy but no further interpretations were made.

The Pakarae River mouth transgressive sequence was interpreted in more detail by Berryman et al. (1992). Stratigraphy, radiocarbon dates and tephrochronology were used to produce paleogeographic maps showing evolution from 9 – 1 ka B. P. and they constructed a relative SL curve for the Pakarae locality from 11 ka B. P. to present day. Berryman et al. (1992) showed there was a deficit in the amount of sediment preserved when compared to the amount of accommodation space created by eustatic SL rise, as estimated from the Gibb (1986) SL curve. They attributed the deficit to tectonic uplift during deposition of the sequence but specific events could not be identified on the basis of their data. Unconformities and weathering horizons within the sequence were mentioned and inferred to be indicative of uplift events. Berryman et al. (1992) inferred a regression in the relative SL curve for the Pakarae locality at ~10.5 – 9.5 cal. yrs B.P. This was attributed to a eustatic SL fall rather than a tectonic uplift event because of (1) correlation to similar-aged trees growing in and overwhelmed by estuarine deposits at several other sites along the East Coast, and (2) correlation with a change in the trend of the Gibb (1986) eustatic SL curve.

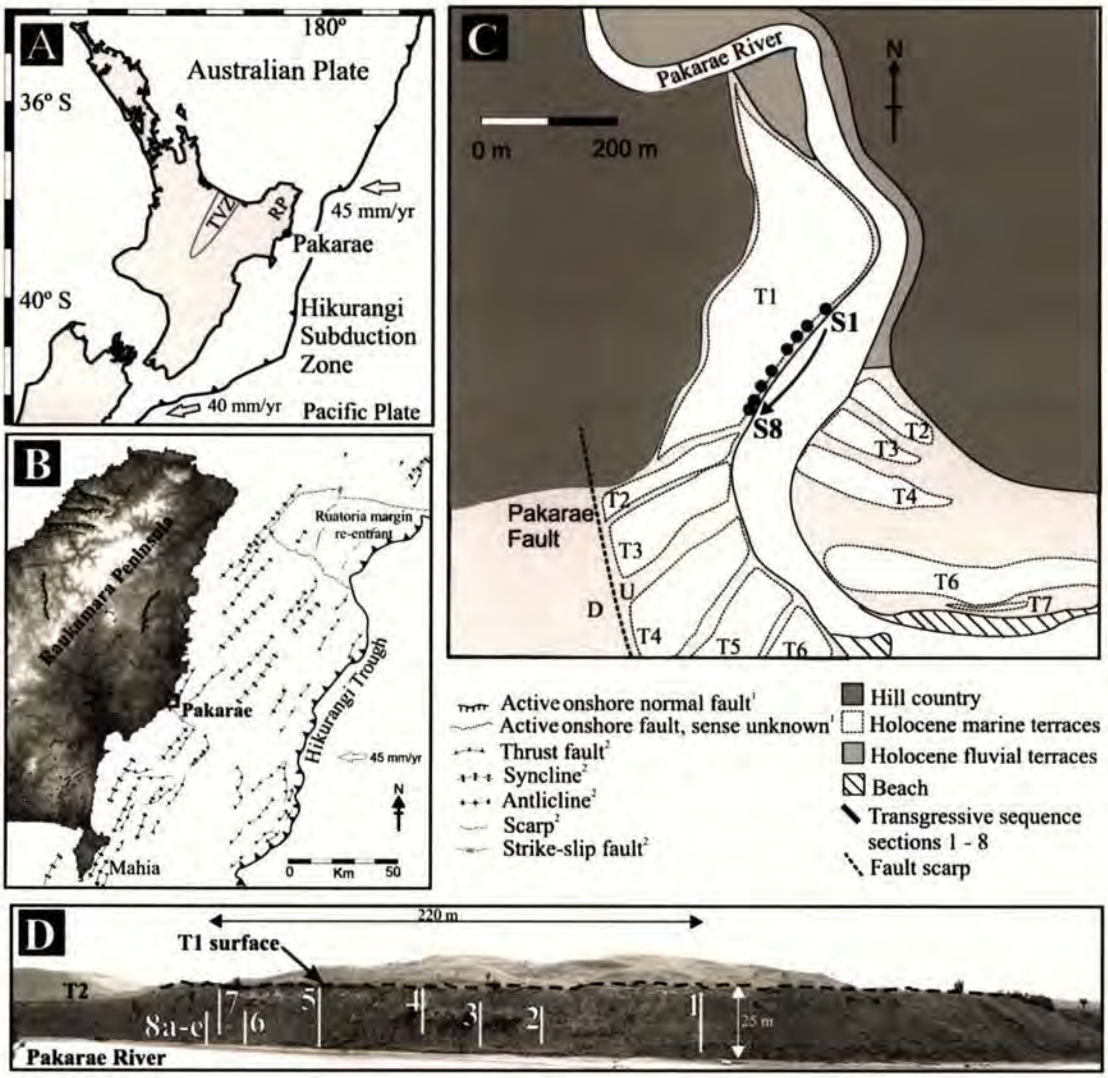

Figure 1. (A) North Island, New Zealand with major tectonic features. TVZ: Taupo volcanic zone, RP: Raukumara Peninsula. Relative plate motions after De Mets et al. (1990, 1994); Hikurangi subduction deformation front after Collot et al. (1996). (B) Topography and tectonic features of the Raukumara Peninsula. [1]Onshore active faults from the GNS Science Active Faults Database (http://data.gns.cri.nz/af/). [2] Offshore structures from Lewis et al. (1997). (C) Pakarae River mouth with major geomorphic elements, marine terraces (after Wilson et al., 2006) and stratigraphic section locations. (D) Pakarae River, transgressive exposures beneath TI (highest Holocene marine transgression surface) with Sections 1 - 8e. Riverbank is ~ 25 m high.

Wilson et al. (in press-a) recently examined the Pakarae River mouth sedimentary sequence; they re-measured one section in common with the Berryman et al. (1992) study and described seven new riverbank sections spanning a 220 m stretch of the riverbank. Twelve new radiocarbon ages were presented. Sedimentology and benthic foraminifera assemblages were used to define four broad paleoenvironmental facies associations (Fig. 2), the distribution of which was used to develop a facies architecture model for sediment infill of an incised valley in an uplifting tectonic setting. In this paper we combine all the available stratigraphic data and facies model results previously presented to (1) develop models of the paleogeographic evolution of the Pakarae River paleo-estuary; and (2) identify and date specific tectonic event horizons.

4.2. Methodology

4.2.1 Reconstruction of the Pakarae locality paleoenvironments

The facies architecture profile developed from the Pakarae riverbank sections (Wilson et al., in press-a) provides the basis for paleogeographic reconstructions (Fig. 2). On the basis of sedimentology and foraminifera data eight bio-lithofacies were identified in the Pakarae riverbank sequence, these were: non-fossiliferous gravels (interpreted as a fluvial channel lag); thin shelly gravels (estuarine tidal channel lags); thick shelly gravels (estuary-head delta); shelly well-sorted sands (barrier environment); non-fossiliferous well-sorted sands (reworked tephra and fluvial sand); silt and sand with abundant marine fauna (central estuary basin); silt and sand with rare marine fauna (estuarine margin); and non-fossiliferous silt and sand (fluvial) (Fig. 2, Wilson et al., in press-a). From these eight bio-lithofacies four paleoenvironmental facies associations are distinguished, namely, floodplain, estuary-head delta, estuarine, and barrier (Fig. 2).

The paleogeographic models of the Pakarae paleo-estuary were constructed sequentially with stepwise addition of each sedimentary unit, starting with the basal floodplain deposit resting on a bedrock surface. For each facies or stratigraphic unit we develop an associated plan-view of the paleogeography of the Pakarae River valley that satisfies the preserved distribution of the facies. Each of our paleogeographic reconstructions of the Pakarae River valley represents our best-fit model, but they are not unique because of the limited exposure available in outcrop. For all paleoenvironmental facies within each time slice we aimed to satisfy the following criteria (in no order of relative importance): (i) the predicted spatial relationships of the Pakarae River mouth paleoenvironments to one another, (ii) the temporal relationships between eustatic SL data and the radiocarbon ages within the Pakarae River mouth sedimentary sequence, (iii) the average timing and magnitude of uplift events at the Pakarae locality as inferred by the post-7 ka marine terraces. These criteria are discussed further below.

Figure 2. Bio-lithofacies and paleoenvironmental facies associations of the Pakarae River incised valley infill sedimentary sequence after Wilson et al. (in press). Locations of section photos in proceeding figures shown.

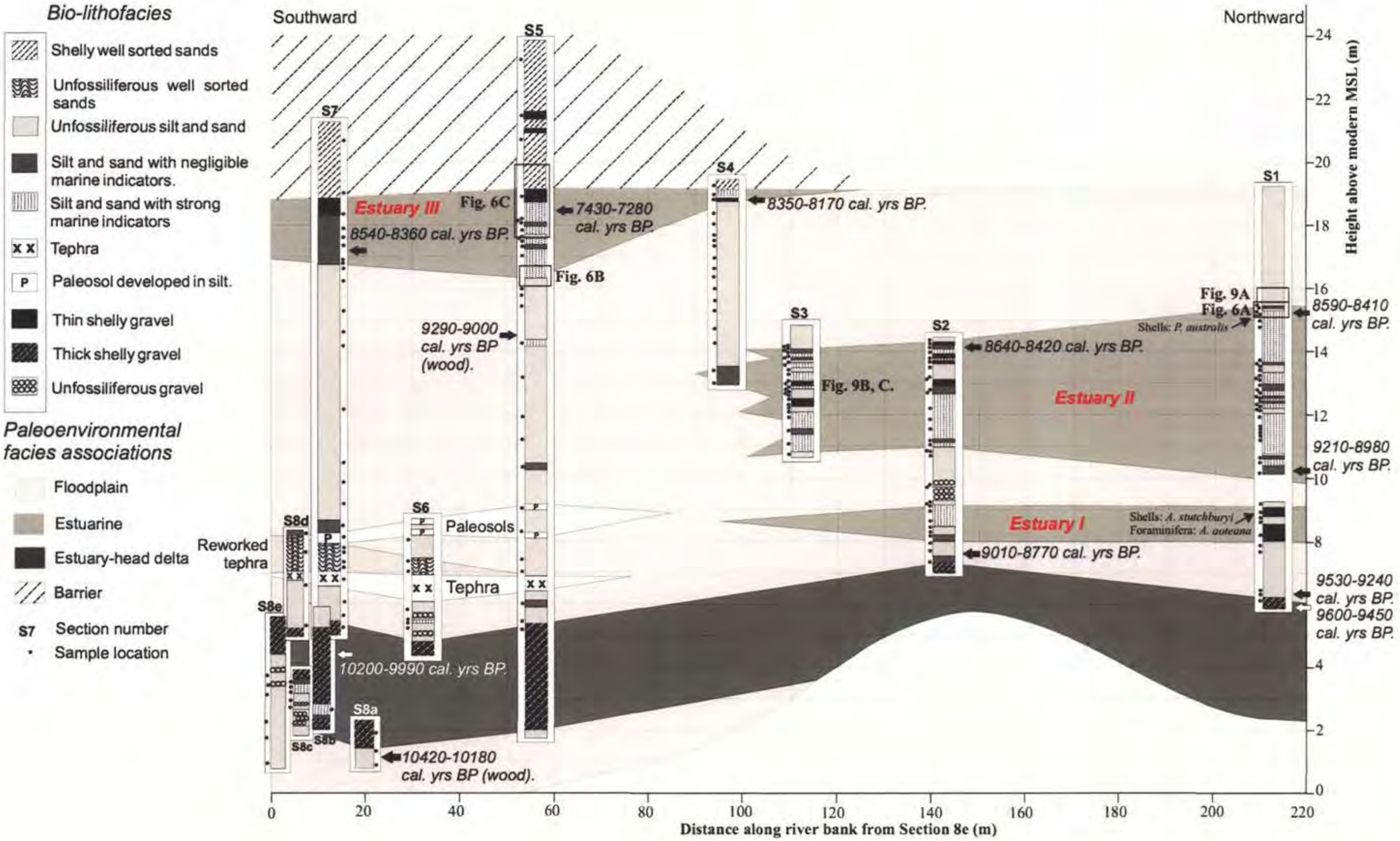

Bio-lithofacies
Shelly well sorted sands
Unfossiliferous well sorted sands
Unfossiliferous silt and sand
Silt and sand with negligible marine indicators.
Silt and sand with strong marine indicators
Tephra
Paleosol developed in silt.
Thin shelly gravel
Thick shelly gravel
Unfossiliferous gravel
Paleoenvironmental facies associations
Floodplain
Estuarine
Estuary-head delta
Barrier
S7 Section number
Sample location
Southward
Northward
S1
S2
S3
S4
S5
S6
S7
S8a
S8b
S8c
S8d
S8e
Estuary III
Estuary II
Estuary I
Fig. 6C
Fig. 6B
Fig. 6A
Fig. 9A
Fig. 9B, C.
7430-7280 cal. yrs BP.
8350-8170 cal. yrs BP.
8540-8360 cal. yrs BP.
9290-9000 cal. yrs BP (wood).
8590-8410 cal. yrs BP.
Shells: P. australis
8640-8420 cal. yrs BP.
9210-8980 cal. yrs BP.
Shells: A. stutchburyi
Foraminifera: A. aoteana
9010-8770 cal. yrs BP.
9530-9240 cal. yrs BP.
9600-9450 cal. yrs BP.
Paleosols
Reworked tephra
Tephra
10200-9990 cal. yrs BP.
10420-10180 cal. yrs BP (wood).
Height above modern MSL (m)
Distance along river bank from Section 8e (m)

- *The predicted spatial relationships of the Pakarae River mouth paleoenvironments:*

Based on depositional models developed for Holocene infilling of incised valleys (Roy, 1984; Dalrymple et al., 1992; Allen and Posamentier, 1993) we expect that each of the four depositional environments identified in Pakarae River mouth sedimentary sequence should have a predictable spatial relationship to one another. In a landward to seaward direction, in plan view, the order of the facies should be: floodplain, estuary-head delta, estuary, and then a estuary mouth barrier. These models are based upon eustatic SL rise being the main parameter controlling the facies relationship, rather than fluvial processes such as river mouth progradation or regression. At the Pakarae River mouth the estuary head-delta facies may not always occur between the floodplain and estuarine facies because its distribution appears to be chiefly controlled by proximity to a local gravel supply (Wilson et al., in press-a). Therefore, in our models we generally show the floodplain facies merging directly into the estuarine facies. No modern estuary exists at the Pakarae River mouth to use as an analogue; hence we use only the outcrop data as a guide to the size and length of the paleo-estuary.

The proximity of the river to base level has important implications for the amount of fluvial aggradation that could have occurred while still maintaining the rivers longitudinal profile. However, beyond outcrop data we cannot constrain the position of river mouth relative to the shoreline or the valley paleo-slope, thus the possible thickness of fluvial aggradation cannot be estimated. While it would be interesting to know how high the river could have aggraded to this is not critical to our interpretation of uplift events. In all cases where fluvial aggradation is a possibility it occurs stratigraphically above an estuarine unit therefore we suggest the shoreline and river base level must have been nearby.

- *SL constraints imposed by the eustatic SL data of Gibb (1986) and the radiocarbon age control within the Pakarae River mouth sedimentary sequence:*

The eustatic SL curve provides an estimate of the amount of sediment that should be deposited between age control points. As eustatic SL rose, accommodation space within the paleo-valley was created. If sedimentation rates within the paleo-estuary approximately kept pace with the rate of accommodation space creation (as supported by the presence of intertidal microfauna throughout the sequence, Wilson et al., in press-a), the sediment thickness between two age control points should approximate the amount of eustatic SL that occurred during that time interval. In our paleoenvironmental reconstructions we compare the present elevations of the radiocarbon dated shells with the eustatic SL at the time of their deposition to assess whether the sediment thickness between the shells is consistent with the estimated amount of eustatic SL rise or if there is a significant difference. For each radiocarbon age we take the midpoint of the 2-sigma calibrated age range and project this across to the midpoint of the SL curve envelope, and use the eustatic SL at this midpoint as the estimate of eustatic SL at that time (Fig. 3). The New Zealand eustatic SL curve was developed by Gibb (1986) using wood and shell radiocarbon ages selected from tectonically stable parts of the New Zealand coastline (Fig. 3). Taking the upper and lower bounds of the eustatic SL curve envelope produces a wide range of eustatic SL elevations; there can be up to 15 m of uncertainty where the curve is very steep (Fig. 3). For consistency we take the mid-point eustatic SL and apply an arbitrary uncertainty of ± 2 m at a 95% confidence interval to all paleo-SL estimates. We try to produce paleoenvironmental reconstructions where the eustatic SL change between each age control point is within 2 m of the change predicted by the eustatic SL curve.

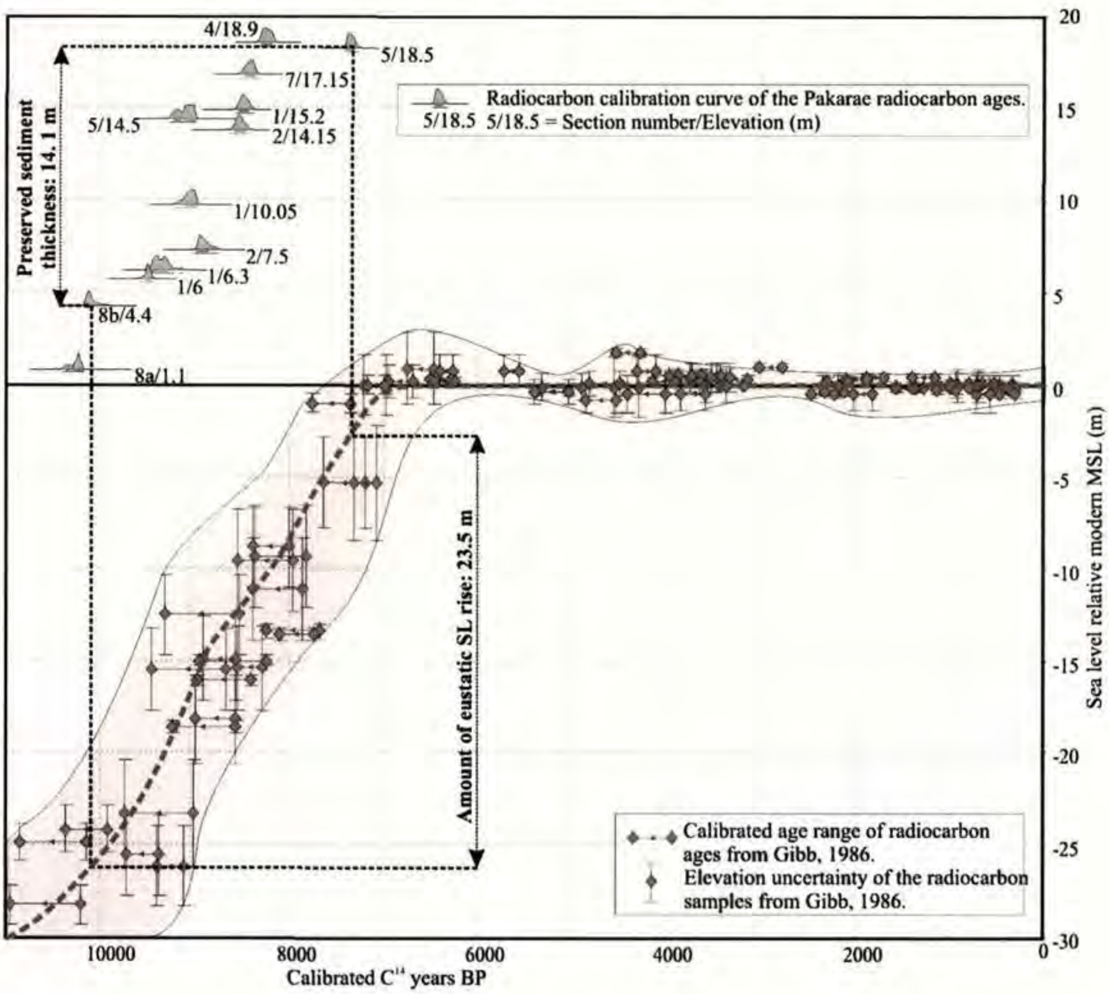

Figure 3. Pakarae transgressive sequence radiocarbon ages plotted at their modern elevation (m AMSL) and the data of Gibb (1986) to envelope the New Zealand eustatic SL curve. Radiocarbon ages calibrated using OxCal v3.10 Bronk Ramsey (2005), marine samples calibrated using the calibration curve of Hughen et al. (2004) and wood samples calibrated using Southern Hemisphere atmospheric data from McCormac et al. (2004). Dashed lines and arrows show a comparison between the thickness of sediment preserved at Pakarae and the amount of eustatic SL rise that occurred from ~10100 cal. yrs B.P. to ~7300 cal. yrs B.P. The deficit between these two measurements approximates the net amount of tectonic uplift that occurred during that time interval.

When considering preserved sediment thicknesses and relationships to eustatic SL changes we do not account for the affects of post-depositional sediment compaction. A study of Holocene intertidal sediments infilling the Forth Valley, Scotland, by Paul and Barras (1998) examined the effects of compaction on silty clays with shelly lenses, similar to the Pakarae River mouth sediments. They found that over a 20 m thickness of sediment a maximum of 2.5 m of correction was required to approximately account for the affects of compaction. This equates with a mid-section correction of ~10% of the bed thickness (Paul and Barras, 1998). Therefore, it is likely that the Pakarae River mouth sediments have compacted slightly but the correction required to account for this is minor in comparison to the magnitudes of eustatic and tectonic relative SL changes that we will be discussing. Furthermore, the gravel layers within the Pakarae River mouth sequence probably undergo little to no post-depositional compaction. The clast-supported nature of the gravels means that water expulsion has little effect on bed thickness.

- *The average< 7 ka timing and magnitude of tectonic events at Pakarae:*

The marine terraces at the Pakarae River mouth record tectonic uplift subsequent to the stabilization of SL at ~ 7 ka. During that time sudden uplift events have occurred at an average interval of 850 ± 450 yrs with an average coastal uplift magnitude of 2.7 ± 1.1 m per event (Ota et al., 1991; Wilson et al., 2006). It is possible that the characteristics of tectonic uplift at the Pakarae locality changed during the Holocene, nevertheless our paleoenvironmental models for the early Holocene attempt to stay within the uncertainties of the post-7 ka single uplift event measurements.

4.2.2 Age control

Age control is derived from radiocarbon ages and the tephrochronology presented in Wilson et al. (in press-a). Nine estuarine shell radiocarbon ages and three detrital wood radiocarbon ages were obtained from throughout the Pakarae valley infill sedimentary sequence (Fig. 3, Table 1). The tephra at ~ 7 m AMSL in Sections 5 – 8 is identified as the Rotoma (9535 – 9465 cal. yrs B.P., Froggatt and Lowe, 1990).

Table 1: Radiocarbon ages obtained from the Pakarae River mouth transgressive sedimentary sequence.

Section	Sample height (m)	Lab number[1]	Sample Material[2]	Dating Technique	^{13}C (‰)	Radiocarbon Age[3] (radiocarbon years BP)	Calibrated Age[4] 2 sigma (cal. years BP)	Sample living depth[5]
1	**15.2 +/- 0.22**	NZA 21854	A	AMS	-1.27	8056 ± 30	**8590-8410**	-0.2
1	**10.05 +/- 0.22**	NZA 22529	A	AMS	1.05	8458 ± 35	**9210-8980**	-0.2
1	**6.3 +/- 0.22**	WK 16864	Wood	Standard	-28.2	8420 ± 59	**9530-9240**	?
1	**6 +/- 0.22**	NZA 21961	A	AMS	-0.91	8868 ± 30	**9600-9450**	-0.2
2	**14.15 +/- 0.22**	NZA 22528	A	AMS	1.42	8082 ± 35	**8640-8420**	-0.2
2	**7.5 +/- 0.22**	NZA 21852	A, B	AMS	-3.71	8338 ± 30	**9010-8770**	-0.2
4	**18.9 +/- 0.22**	NZA 22526	A, B	AMS	0.98	7791 ± 35	**8350-8170**	-0.2
5	**18.3 - 18.7 +/- 0.22**	NZA 21851	A, B. C	AMS	-0.49	6847 ± 30	**7430-7280**	-0.2
5	**14.5 +/- 0.22**	Wk 16454	Wood	Standard	-27.2	8219 ± 52	**9290-9000**	?
7	**17.15 +/- 0.22**	NZA 22527	A	AMS	0.39	7981 ± 35	**8540-8360**	-0.2
8a	**1.1 +/- 0.31**	Wk 16453	Wood	Standard	-28	9158 ± 52	**10420-10180**	?
8b	**4.4 +/- 0.31**	NZA 21853	A	AMS	-2.9	9266 ± 30	**10200-9990**	-0.2

[1] Wk: The University of Waikato Radiocarbon Dating Laboratory; NZA: Institute of Geological and Nuclear Sciences Rafter Radiocarbon Laboratory.
[2] Shell: A: *Austrovenus stutchburyi*, B: *Paphies australis*, C: *Melagraphia aethiops*.
[3] Conventional radiocarbon age before present (1950 AD) after Stuiver and Polach, 1977. Radiocarbon 19: 355-363.
[4] Calibrated age in calendar years. Wood ages calibrated using Southern Hemisphere atmospheric data of McCormac et al (2004), marine ages calibrated using data from Hughen et al (2004). Radiocarbon ages calibrated using OxCal v3.10.
[5] Estimated based on *Austrovenus stutchburyi* living at mean sea level and burrowing to a depth of 0.2m below the sediment surface.

4.3. Results: Paleogeographic evolution of the Pakarae River paleo-estuary

4.3.1 Models of estuary evolution

We identify eight stages of paleogeographic evolution of the Pakarae River paleo-estuary. There is evidence for at least two significant marine regressions that we suggest are tectonically driven coastal uplift events. A third uplift event is inferred from a significant accommodation space deficit.

I. Marine transgression A: ~10.25 – 9.5 ka.

The oldest sedimentary unit is an alluvial unit that represents SL lowstand deposition. The floodplain facies, consisting of massive silt with occasional gravel beds, forms the basal surface upon which transgressive marine deposits subsequently accumulated. Detrital wood within the basal floodplain facies has a radiocarbon age of 10420-10180 cal. yrs B.P. cal. yrs B.P. Estuary-head delta deposits overly the floodplain facies. These deltaic deposits appear as a laterally continuous unit of gravel. The poorly sorted nature and clast angularity implies a short transportation distance of the sediments. We infer that the gravel clasts were sourced from the mudstone bedrock high that outcrops at the base of Section 1 or from hillsides flanking the Pakarae River valley. Prior to gravel deposition, at ~10,300 cal. yrs B.P., New Zealand eustatic SL was ~ -24±2 m and rising at ~7 mm/yr. The estuary-head delta sediments probably represent the first incursion of the marine environment into the incised valley that the Pakarae River had cut during the previous glacial lowstand. Two radiocarbon ages from estuarine shells within the estuary head deltaic gravels indicate the sedimentary unit decreases in age towards the north (Fig. 2). This is consistent with a transgressive marine sequence. Our paleogeographic reconstruction shows a transgressive estuary with gravel deposition around the bedrock high (Fig. 4.1).

II. Marine transgression A continued: ~9.5 – 9 ka.

Overlying the estuary head gravels are floodplain and estuarine sediments. The non-marine sediments may have accumulated around a topographic high created above the basement outcrop at the base of Section 2. The Rotoma tephra was deposited and preferentially accumulated in the downstream sections (S5 – S8). The overthickening and lenticular shape of the tephra probably represents infilling of an abandoned oxbow of the river. This suggests that the river mouth was located farther to the west than it is at present. Estuarine facies were deposited in the sections S1 and S2 up to ~ 9 ka. This unit is called Estuary I (Fig. 4.2).

III. Uplift Event A: ~9 ka.

At an elevation of ~ 9 m AMSL the Estuary I facies is overlain by floodplain sediments and, at equivalent elevations in the southern sections, a series of paleosols are present. Both of these transitions provide evidence of a significant, and sudden marine regression. Eustatic SL was rising during this time period and estuarine facies might therefore be expected to be overlain, in a normal stratigraphic order, by increasingly marine-influenced sediment.

Figure 4. Paleogeographic evolution of the Pakarae River, reconstruction of preserved stratigraphy and relative SL changes from ~10 - 7 ka.

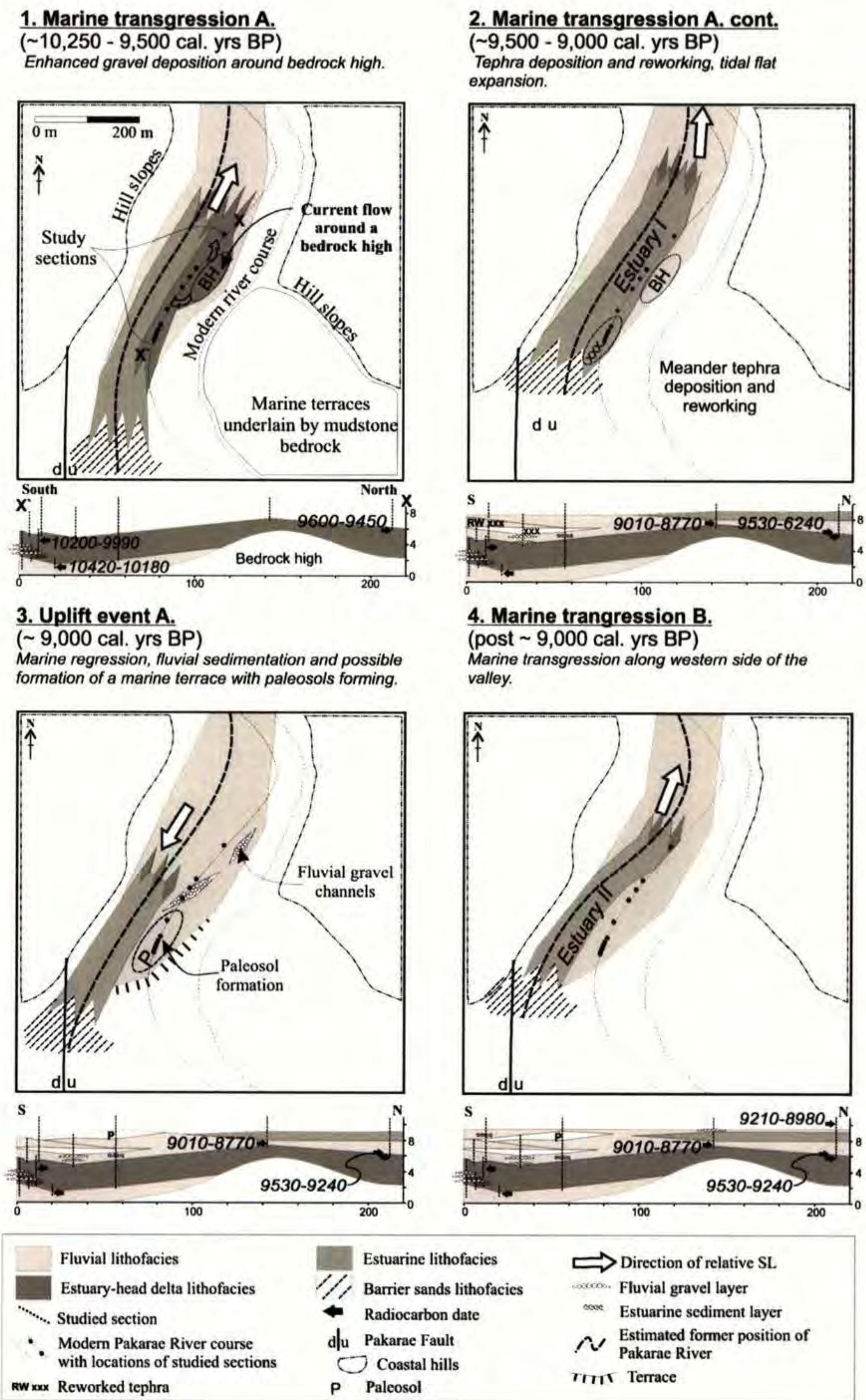

1. Marine transgression A.
(~10,250 - 9,500 cal. yrs BP)
Enhanced gravel deposition around bedrock high.
0 m
200 m
N
Hill slopes
Study sections
Current flow around a bedrock high
BH
Modern river course
Hill slopes
Marine terraces underlain by mudstone bedrock
d u
South
North
X
X
9600-9450
10200-9990
10420-10180
Bedrock high
2. Marine transgression A. cont.
(~9,500 - 9,000 cal. yrs BP)
Tephra deposition and reworking, tidal flat expansion.
N
Estuary I
BH
Meander tephra deposition and reworking
d u
S
N
RW xxx
xxx
9010-8770
9530-6240
3. Uplift event A.
(~ 9,000 cal. yrs BP)
Marine regression, fluvial sedimentation and possible formation of a marine terrace with paleosols forming.
N
Fluvial gravel channels
P
Paleosol formation
d u
S
N
P
9010-8770
9530-9240
4. Marine trangression B.
(post ~ 9,000 cal. yrs BP)
Marine transgression along western side of the valley.
N
Estuary II
d u
S
N
9210-8980
P
9010-8770
9530-9240
0
100
200
0
4
8
Fluvial lithofacies
Estuary-head delta lithofacies
Studied section
Modern Pakarae River course with locations of studied sections
RW xxx Reworked tephra
Estuarine lithofacies
Barrier sands lithofacies
Radiocarbon date
d u Pakarae Fault
Coastal hills
P Paleosol
Direction of relative SL
Fluvial gravel layer
Estuarine sediment layer
Estimated former position of Pakarae River
Terrace

5. Marine trangression B. cont.
(~ 9,000 - 8,500 cal. yrs BP)
Marine transgression - main estuary basin infills synchronous with fluvio-tidal sedimentation in the southeast of the valley.

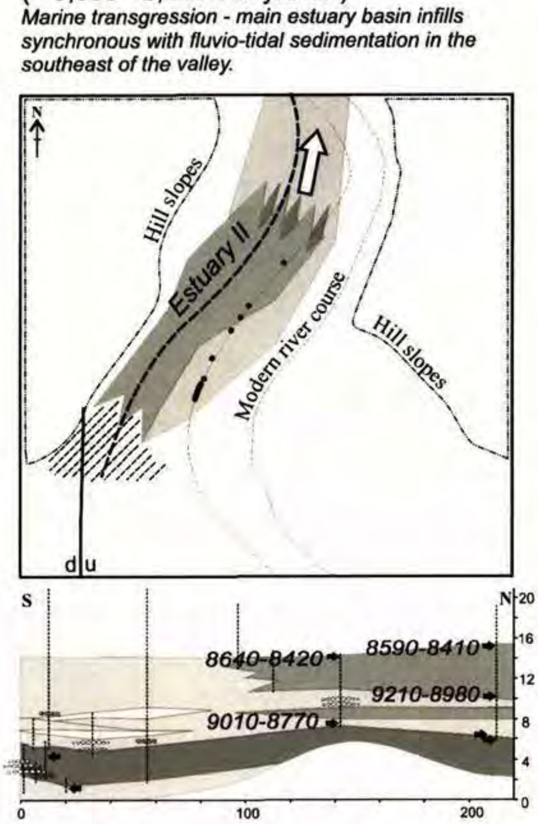

6. Uplift Event B.
(~ 8,500 cal. yrs BP)
Marine regression, fluvial sedimentation pulse.

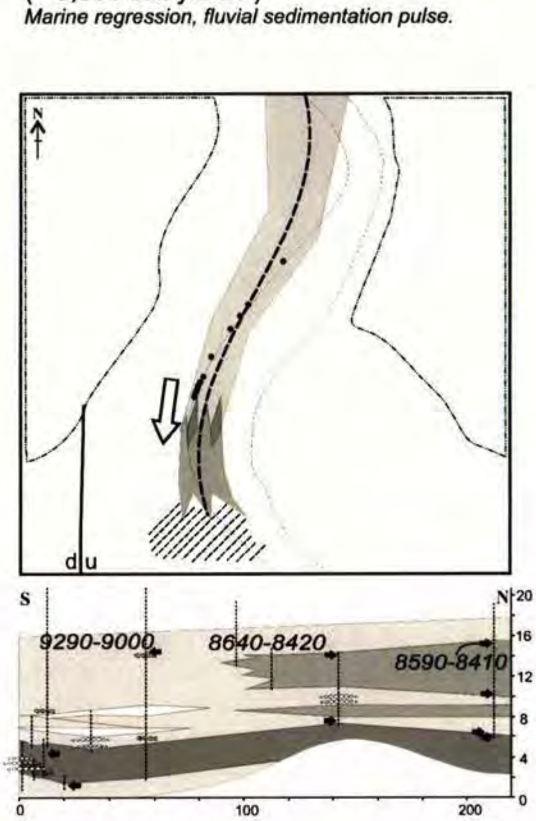

7. Marine trangression C.
(~ 8,500 - 7,400 cal. yrs BP)
Marine transgression - tidal channel cut into fluvial sediments.

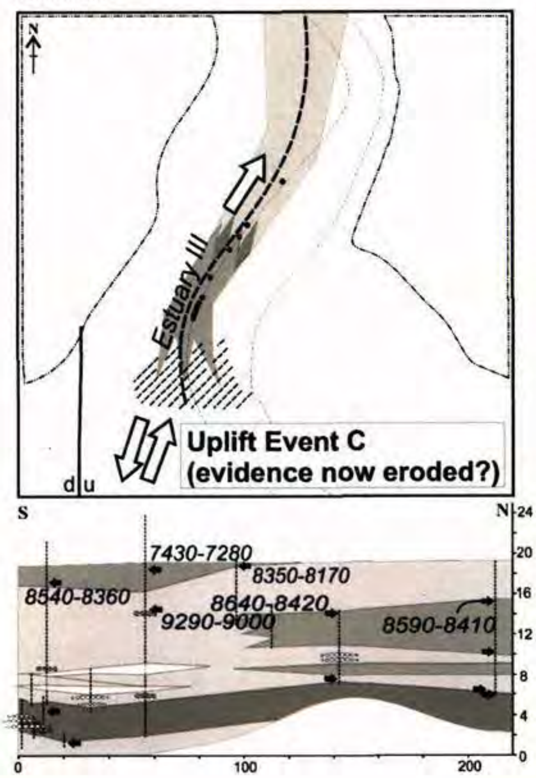

8. Estuary infilling.
(post ~ 7,400 cal. yrs BP)
Beach barrier progrades into estuary from seaward side, fluvial sediments infill from the landward side.

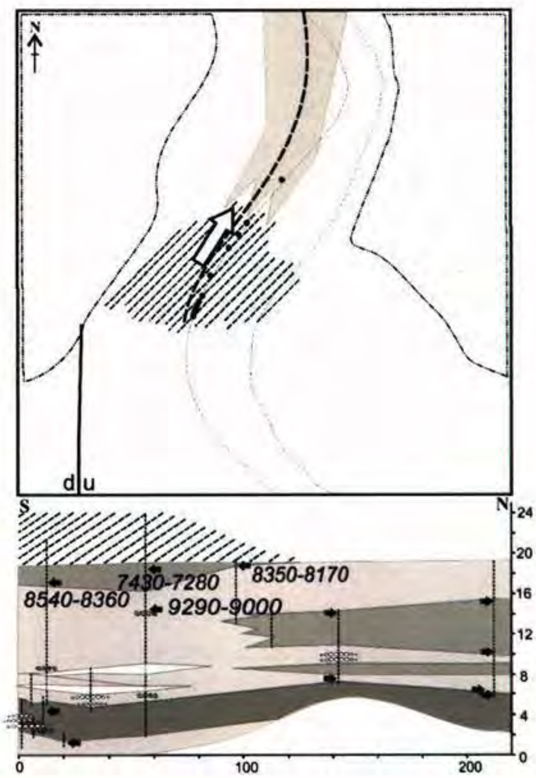

That Estuary I is instead overlain by non-marine floodplain sediments indicates either that there was a fall in SL due to tectonic uplift or that there was rapid fluvial progradation. The paleosols in Sections 5 – 7 occur within floodplain silts. Paleosols represent a period of time when a surface didnot receive sediment, and a soil was allowed to develop. Therefore, rapid fluvial progradation is unlikely to have occurred at this time. It is more likely that the river was subject to a fall in its base level, a change that lowered the elevation at which fluvial sediments were deposited. A fall in river base level is consistent with a marine regression. This could have been caused by eustatic SL fall, a change in fluvial discharge or tectonic uplift. The New Zealand eustatic SL curve of Gibb (1986) is not of sufficient resolution to discount a eustatic SL fall. Carter et al. (1986) used submerged shorelines in the southwest Pacific to infer the ages of several stillstands, or hiatuses, during Holocene SL rise. The ages of the stillstands do not, however, coincide with the estimated ~9 ka environmental change at Pakarae, and a stillstand would not trigger fluvial incision into an already existing estuary. Furthermore, sea level falls can result in fluvial channel readjustments (e.g. changes to sinuosity or bed roughness) rather than incision (Schumm, 1993; Holbrook and Schumm, 1999; Wellner and Bartek, 2003). Assuming the Estuary I was close to the shoreline, a change in river discharge or decreased sediment supply would not have caused a significant (if any) incision due to its proximity to the base level. Furthermore, a change in fluvial discharge is most likely to be climatically controlled, hence of regional extent. However, eastern North Island offshore sediment cores do not display any significant changes in sediment flux at this time (Foster and Carter, 1997; Carter et al., 2002).
Sharp changes from intertidal foraminifera assemblages to foraminifera-barren ones at the Estuary I-floodplain contact suggests that this base level fall was sudden (Wilson et al., in press-a). The paleogeographic reconstruction shows a southward shift in the marine-floodplain interface (Fig. 4.3). The floodplain environment moved over Sections 1 - 2, at Sections 5 – 7 a fluvial terrace formed upon which the paleosols developed. This terrace is analogous to the fluvio-tectonic terraces present at the modern Pakarae river mouth. There is no evidence in outcrop of a scour surface that records the river base level fall. This would provide further evidence of fluvial incision but could probably only be located by drilling. Eustatic SL was rising during this period, therefore the most likely cause of a marine regression is tectonic uplift, we call this Uplift Event A. Uplift must have been of a sufficiently large amount to elevate the more southern sections (Sections 5 – 7) above the depositional height of floodplain sediments (although we cannot quantify this amount) and to raise Estuary I out of intertidal range. Estuary I contains foraminifera assemblages dominated by *A. aoteana* (a species dominant at intertidal-subtidal elevations in brackish environments, Hayward et al., 1999) and fragments of *A. stutchburyi* (a common estuarine shell that lives between MSL – subtidal elevations, Marsden and Pilkington, 1995, Morton, 2004, Fig. 2). The occurrence of these two species together suggests that the sediment of Estuary I was deposited at MSL or slightly deeper. The Pakarae River mouth beach has a spring tidal range of 1.7 m. Therefore the only firm

constraint we can place on the magnitude of Uplift Event A is that it was probably >0.85 m. The amount of uplift can also be roughly estimated from the paleosols. If it takes approximately 200-300 years for a soil to develop on a fluvial terrace, and eustatic SL was rising at ~ 7 mm yr^{-1}, then the terrace must have been uplifted by > 1.4 – 2.1 m to allow sufficient elevation before marine inundation resumed.

IV. Marine transgression B: post-9 ka.

Floodplain sediments were deposited in all sections following the above inferred uplift event. As discussed, the southern sections must have been subaerial for sufficient periods of time to allow paleosols to form. Two to three paleosol units can be distinguished. This shows there may have been intermittent flooding of the surface as the base level of the river increased in elevation with rising eustatic SL before it was completely overwhelmed by fluvial sedimentation. In the northern sequence (in Sections 1 and 2) 1-2 m of fluvial silt and gravel was deposited over the silty clay sediments of Estuary I. When eustatic SL became high enough following Uplift Event A, an estuary called Estuary II was re-established in the northern sections. *A. stutchburyi* shells from the base of Estuary II have a radiocarbon age of 9210-8980 cal. yrs B.P. This age overlaps (at the 2-sigma interval) with a shell age at the base of Estuary I (Fig. 4.4). We suggest that the shells at the base of Estuary II were reworked from deposits at the top of Estuary I. No cross-cutting occurs between Estuaries I and II in the outcrop but these radiocarbon ages suggest it does occur elsewhere in the sequence. At the same time that Estuary II re-established in Sections 1 and 2, non-marine sedimentation continued in the southern sections. This apparent anomaly of having non-marine sedimentation south, or in the possible seaward direction, of a marine environment is discussed further below (Section 3.1, V).

V. Marine transgression B continued: 9 – 8.5 ka.

Estuary II was infilled during Marine Transgression B (Fig. 4.5). The thickness of the intertidal estuarine infill ranges from 3.5 – 5.5 m (decreasing thickness southward, Fig. 2). Radiocarbon ages from the top of Estuary II range between 8640 – 8410 cal. yrs B.P. (Fig. 4.5). We therefore estimate that estuary infilling ceased at ~ 8.5 ka. Infilling of Estuary II took place over ~ 500 years. During the time period of infilling between 9 – 8.5 ka, there was ~ 5 – 8 m of eustatic SL rise. Accounting for uplift in Event A of ~2-3 m, 1 m of fluvial deposition and the 5.5 m of estuarine sediment in Section 1, the thickness of the Estuary II facies is consistent with the amount of eustatic SL rise during this time interval (within the uncertainty of the radiocarbon ages and the eustatic SL curve, Fig. 3).

Floodplain facies were deposited southward of Estuary II. The southward direction is the modern seaward direction. If we assume that the paleo-estuary was always aligned approximately north-south (this is reasonable given the valley is bedrock controlled) then it appears that non-marine sediments accumulated seaward of Estuary II. How this sedimentation pattern could have occurred is not fully resolved. We offer four possible paleogeographic scenarios including: (A) *the paleo-river mouth may have* *been in a different location* therefore producing a different flooding pattern, (B) *Birds-foot fluvial delta.* The southward non-marine sediments were deposited as lobes within an estuarine environment in which localised sedimentation rates were too high for marine fauna to survive or they are too heavily diluted to be detected; (C) *Colluvial fans* were depositing sediment above MSL in the southern sections or (D) *Fluvial cut-and-fill:* originally present estuarine sediments were removed from the southern sections by post-uplift incision to be replaced by younger floodplain sediments (Fig. 5). It is not well determined whether the floodplain facies of the southern sections was emplaced prior to, synchronously with, or after emplacement of Estuary II. A detrital wood fragment radiocarbon age of 9290-9000 cal. yrs B.P. from the floodplain facies of Section 5 is older than estuarine shell ages from equivalent elevations in Sections 1 and 2 (radiocarbon ages of 8640-8420 and 8590-8410 cal. yrs B.P., Fig. 2). This supports model B (birds foot delta) or model C (colluvial fan) as both of these scenarios require emplacement of the southern non-marine sediment prior to estuary establishment in the northern sections. However, because the wood is detrital and could have been reworked, while the shells are *in-situ,* the wood age is a less reliable indicator of sediment depositional age than the shells.

None of these scenarios are entirely consistent with the stratigraphic and age data of the Pakarae River mouth sedimentary sequence. A combination of the above processes may be responsible. The width of the Pakarae River paleo-valley (<200 m) is relatively narrow and leaves little room for multiple, or migrating sediment deposition lobes. An *alternative river mouth orientation* (model A) is unlikely because marine terraces on the east side of the river are underlain by mudstone bedrock. Therefore the paleo-river mouth cannot have been located to the east, this only leaves a narrow valley width open to the west (<140 m). Such a small shift in the river mouth location is not likely to have caused a radically different flooding pattern in the Pakarae valley and the proximity to the paleo-shoreline would have limited the elevation to which fluvial sediments may have been deposited. The *birds-foot delta scenario* unrealistically implies that sediment delivered to the estuary by the river bypassed Sections 1-3, without entraining any of the inhabitant marine fauna and preferentially settled seaward in Sections 5 and 7. To inhibit colonization by marine fauna we have implied that sedimentation rates must have been very rapid. However Section 1 indicates sedimentation rates here were approximately equal to the rate of eustatic SL rise. By inference, rates in Sections 5 and 7 must have been greater than the rate of eustatic SL rise. Therefore sediment would have quickly built up above MSL. *Colluvial fan deposition* is inconsistent with the presence of horizontal sedimentary bedding structures seen throughout the non-marine facies. Post-uplift fluvial cut-and-fill is possible, although there are no detectable unconformities evident of an incision horizon within the non-marine sediments of Sections 5 and 7.

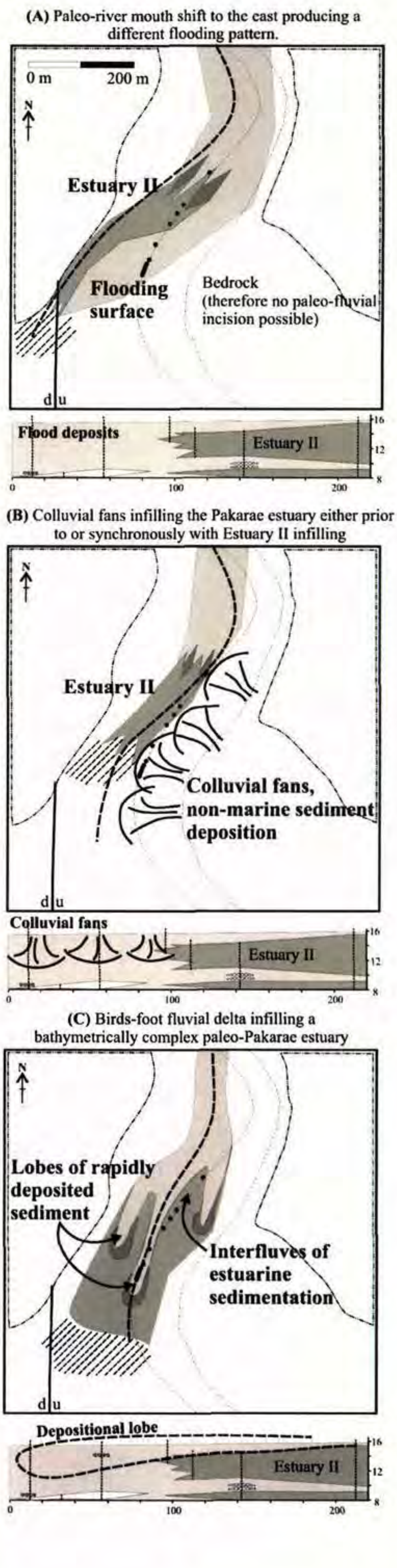

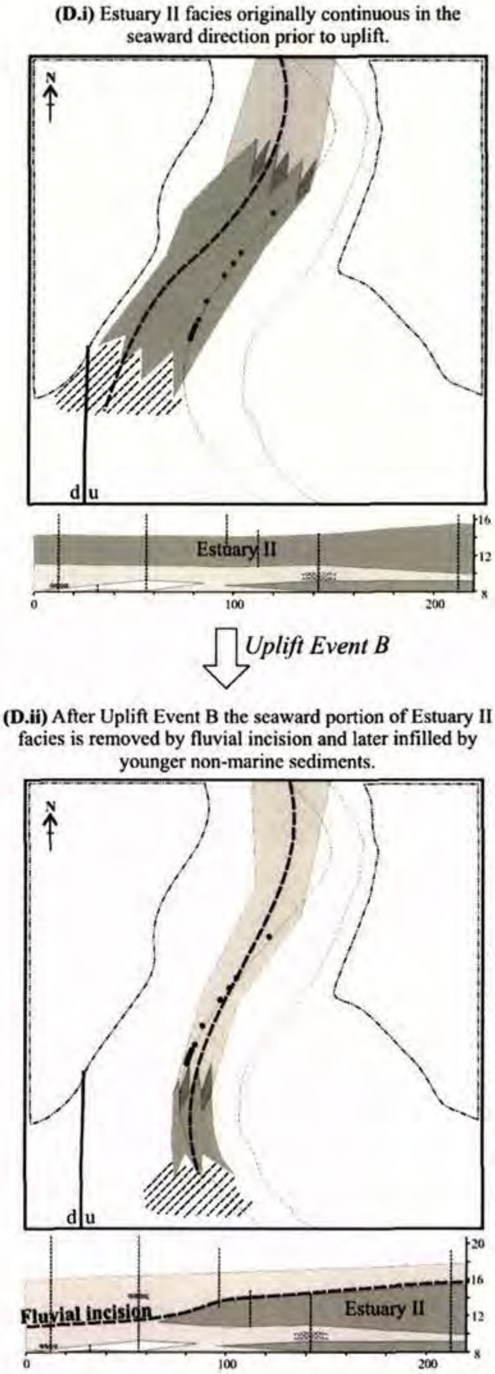

Figure 5. Four scenarios to explain the juxtaposition of seaward barren sediments against landward estuarine sediments with a rich marine fauna in the Pakarae paleo-valley (see Fig. 4.4 for the map legend). (A) Alternative paleo-river mouth orientation. (B) Colluvial fans entering paleo-estuary. (C) Birds-foot fluvial delta infilling the paleo-estuary. (D.i and D.ii) Post-uplift fluvial incision removing seaward Estuary II facies.

VI. Uplift Event B: ~8.5 ka.

Abandonment of Estuary II occurred ~8.5 ka. Like the abandonment of Estuary I, this regressive estuarine-floodplain transition is inconsistent with rising eustatic SL and could represent either a tectonic uplift or fluvial progradation (Fig. 4.6). The radiocarbon ages of the highest shells in Sections 1 and 2 are statistically indistinguishable with ages of 8590-8410 and 8640-8420 cal. yrs B.P., respectively. This synchronicity in paleoenvironmental change at these two locations is consistent with a sudden tectonic uplift event. If fluvial progradation caused estuary abandonment, then the shell ages from the top of the estuarine facies would be expected to get younger seaward. A layer of *P. australis* shells characteristically marks the contact between marine and floodplain sediments in Sections 1-3 (Figs. 2, 6). The abrupt changes in the foraminifera assemblages (from intertidal to barren), and the presence of life assemblages of *P. australis* indicate marine regression from this site was rapid. Life assemblages are those in which there are a range of shells from juvenile to adult. Hull (1987) infers sudden death from the preservation of life assemblages because if the environmental change was gradual then the smaller, and younger, species component of the assemblage would have moved to more suitable environments. Again, eustatic SL was rising during this time period therefore, a tectonic uplift event is the most likely explanation for the marine regression, we call this Uplift Event B (Fig. 4.6).

VII. Marine transgression C: 8.5 – 7.4 ka.

The highest elevation and youngest estuarine facies, correlated between Sections 4, 5 and 7, represents Estuary III. This estuary evolved due to eustatic SL transgression (Fig. 4.7). Three radiocarbon ages have been obtained from this facies (Table 1). Two ages of poorly preserved shells at the base of the facies are 8350-8170 cal. yrs B.P. (Sections 4, 18.9 m) and 8540-8360 cal. yrs B.P. (Section 7, 17.15 m). Well-preserved shells from near the top of the facies have an age of 7430-7280 cal. yrs B.P. (Section 5, 18.3-18.7 m). The large age differences and contrasts in shell preservation imply two shell populations within Estuary III. We suggest that the older, degraded shells are reworked. They may have been transported from the seaward part of Estuary III when it was initially established seaward of its present location or removed from the top of Estuary II if it has been incised by Estuary III elsewhere in the sequence. The base of the estuarine facies is sharp and probably represents a transgressive surface (in the nomenclature of Dalrymple et al., 1992 and Allen and Posamentier, 1993; Fig. 6).

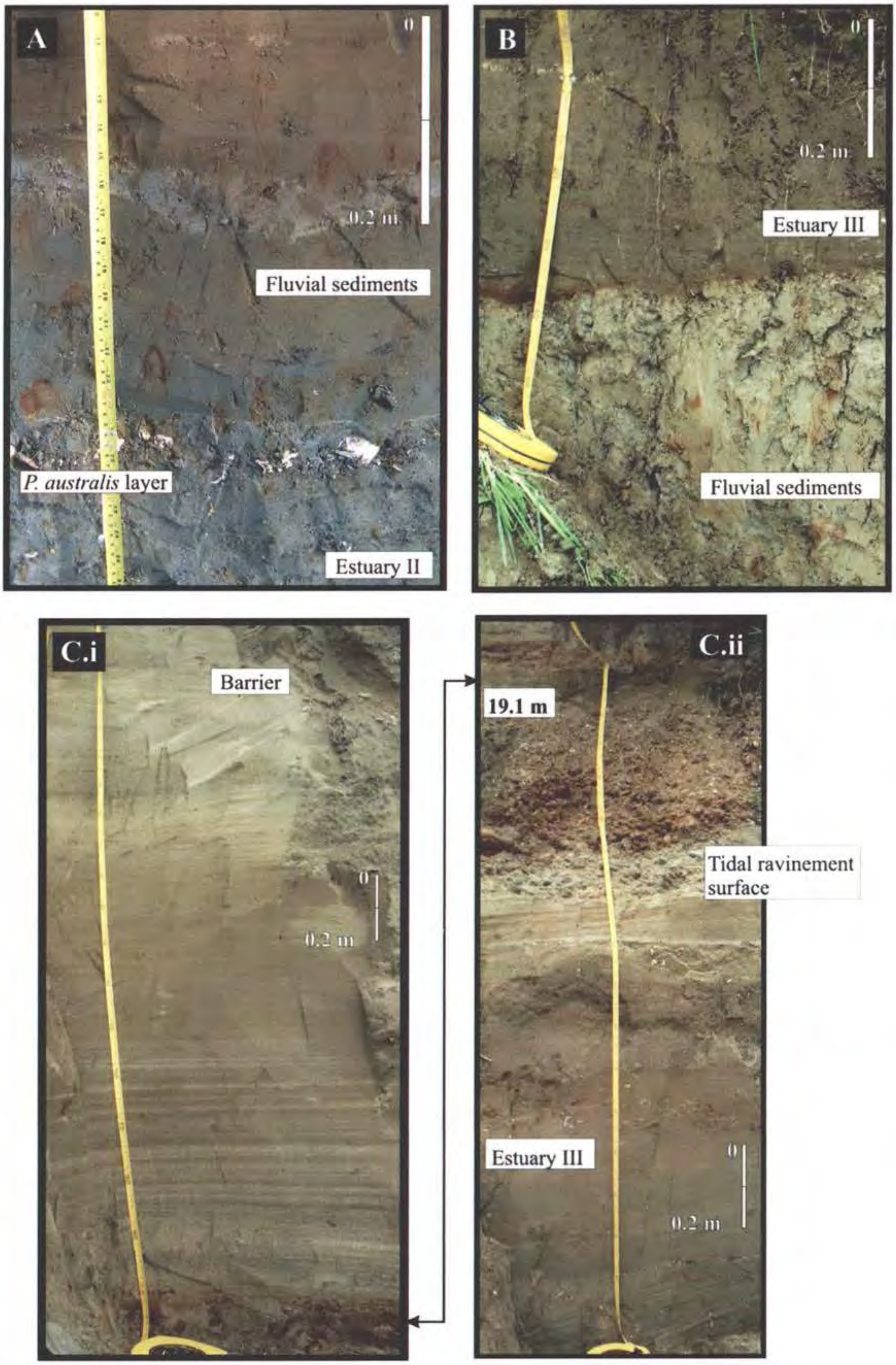

Figure 6. (A) Section 1, facies contact between Estuary II and fluvial sediments at ~15.3 m AMSL. Shells are P. australis. (B) Sections 5, facies contact between fluvial sediments and the base of Estuary III, ~ 16.2 m AMSL. (C) Section 5, facies contact between barrier sands and the top of Estuary III; C.i: ~19 - 20 m AMSL; C.ii: ~19-17.5 m AMSL.

If we assume the shell age of 7430-7280 cal. yrs B.P. is from an in-situ sample and representative of the age of infilling of Estuary III then there was an interval of ~ 1160 yrs between the occupations of Estuary II and Estuary III (calculated from the difference between the mid-points of the bounding radiocarbon ages). During this time interval there was ~ 10±2 m of eustatic SL rise (Fig. 3). The elevation difference between the in-place dated shells in Estuary II and Estuary III is 3.5 m. The calculated accommodation space deficit (the difference between preserved sediment thickness and the amount accommodation space created by eustatic SL rise) is ~ 6.5± 2 m (Fig. 7). One uplift event horizon has been identified during this time period: that at the top of Estuary II, inferred to represent Uplift Event B. It is unlikely, however, that a single event could account for the entire accommodation space deficit of ~6.5 m. For example the M_W 7.4 1931 Napier earthquake produced a maximum of 3.5 m of coastal uplift (Hull, 1990) and by comparison of the faults rupture areas, Berryman (1993) estimated events of M_W 7.5-8 were required to uplift the Mahia Peninsula marine terraces up to 4 m. Average uplift magnitudes at the Pakarae River mouth are 2.7 ± 1.1 m per event (Ota et al., 1991; Wilson et al., 2006). The accommodation space deficit of ~ 6.5 m probably represents at least two uplift events: Uplift Event B as well as an inferred, Uplift Event C. This scenario would be broadly consistent with the uplift event frequency inferred from the marine terrace data. Marine terraces were formed at intervals of 850 ± 450 yrs (Wilson et al., 2006), and the accommodation space deficit of 6.5 m accumulated over ~1160 yrs, therefore two uplift events within this time interval is feasible. Evidence for Uplift Event C was probably recorded in the sedimentary sequence seaward of Section 7. This part of the sequence has been eroded during marine terrace formation.

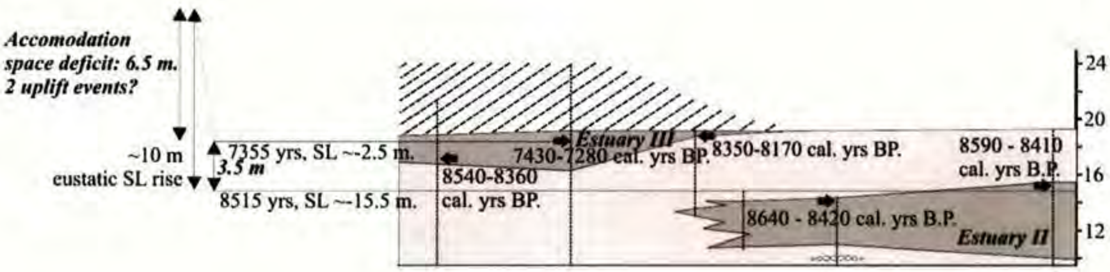

Figure 7. Relationships between preserved sediment thickness and amounts of eustatic SL rise for the time period between the deposition of Estuary II and Estuary III.

VIII. Estuary infilling and marine regression: post 7.4 ka.

The upper contact between Estuary III and the barrier sands is gradational (Fig. 6). This unit represents infilling of the paleo-estuary during the last several hundred years of eustatic SL rise (~7.4 – 7 ka, Fig. 4.8). Some scouring at the base of tidal channel gravels can be seen (Fig. 6), consistent with a tidal ravinement surface (after Dalrymple et al., 1992). The barrier sands grade upward into aeolian sands. After ~ 7 ka marine regression continued due to repeated tectonic uplift events during the subsequent period of stable eustatic SL, as recorded by the mid to late Holocene marine terraces.

4.4. Discussion

4.4.1 Chronology of relative SL change

Our paleogeographic reconstructions have been used to identify three previously unrecognized uplift events in the Holocene: two event horizons are distinguished by abrupt regressions within the Pakarae River sedimentary sequence (Uplift Events A and B) and a third, younger uplift event is inferred from a significant accommodation space deficit between 8.5 – 7.4 ka B.P. (Uplift Event C). The oldest event (Uplift Event A) occurred ~9210-8770 cal. yrs B.P. The magnitude of uplift was >0.85 m and was sufficient enough to cause the river to abandon its bed (creating a fluvial terrace) and grade to a new base level (Section 3.1-III). The timing of the second event, Uplift Event B, is well-constrained by two radiocarbon ages dating the death of shells due to estuary abandonment. This occurred at 8640-8410 cal. yrs B.P. The third event, Uplift Event C, occurred in the time interval between the Uplift Event B and 7430-7280 cal. yrs B.P. No magnitude constraints can be placed on the Uplift Events B and C. However, accommodation space deficits suggest a combined vertical movement of 6.5 ± 2 m. A new relative Holocene SL curve for the Pakarae locality has been constructed using data presented here and marine terrace data of Ota et al. (1991) and Wilson et al. (2006, Fig. 8).

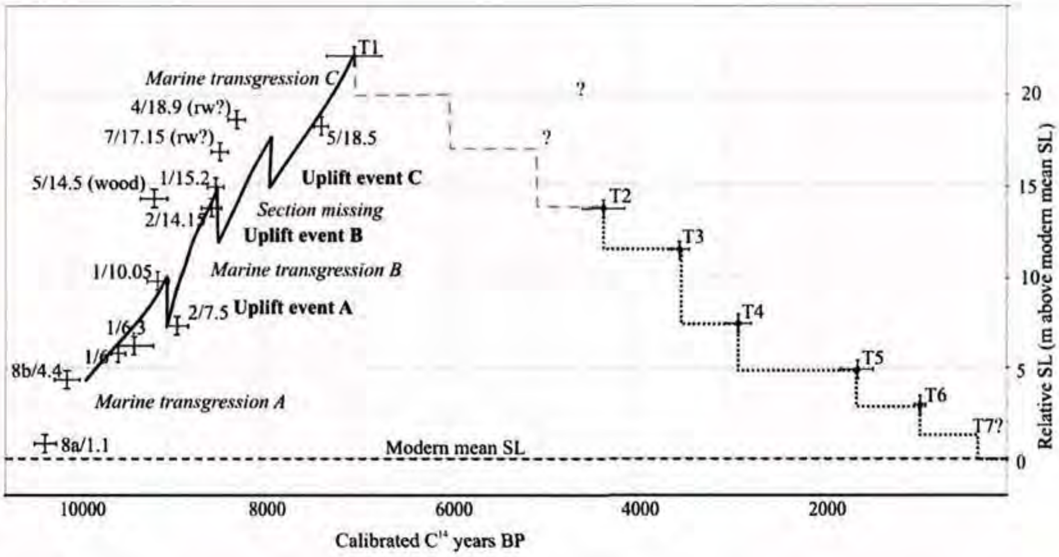

Figure 8. Pakarae locality Holocene relative SL curve. Transgressive sequence data presented in this study and the post- 7 ka marine terrace data presented in Wilson (2006). (rw?): probable reworked sample.

The relative SL curve is a significant revision of the previous curve constructed for the Pakarae locality by Berryman et al. (1992). The Berryman et al. curve showed a similar trend but evidence of pre-7 ka uplift was based only on accommodation space deficits, not on specific facies distributions, and individual events were not delineated. As previously discussed, Berryman et al. (1992) suggested a relative SL fall at ~10500 – 9500 cal. yrs B.P., which they inferred to have been a eustatic regression rather than tectonic one based partly on correlation to the eustatic SL curve. Recent calibration of the Gibb (1986) SL curve does not show the equivalent change in trend at ~10.5 – 9.5 cal. yrs B.P. Our data does not support an uplift event during this time period. However, if one did occur near 10500 cal. yrs B.P. the Pakarae River mouth sedimentary sequence would have been unlikely to preserve a record of it, as the sequence is younger than ~10400 cal. yrs B.P. and the location was probably undergoing terrestrial (floodplain) sedimentation at that time.

4.4.2 Uplift Rates

The radiocarbon ages obtained from the Pakarae River transgressive sequence, in combination with the Gibb (1986) eustatic SL data, can be used to calculate average uplift rates over time periods extending back to ~ 10000 cal. yrs B. P. (Table 2). We obtain an average uplift rate is 3.15 ± 0.8 mm/yr (excluding the wood radiocarbon ages as the depositional elevation of these samples relative to MSL is uncertain). This rate is of the same as that calculated using the younger Pakarae River mouth marine terrace data (Wilson et al., 2006) and indicates steady average uplift rates of the Pakarae locality since ~ 10000 cal. yrs B.P.

4.4.3 Tsunami events

With such a high frequency of coastal uplift (i.e. earthquake) events Pakarae River mouth is an obvious candidate for tsunami inundation. Tsunamigenic sources include an offshore thrust fault, the Pakarae normal fault, the Hikurangi subduction interface, trans-Pacific tsunamis (particularly from South America), submarine landslides, and other offshore faults such as the Lachlan Fault. Tsunami deposits can be recognised as anomalous high-energy influxes into low-energy environments (Cochran, 2002; Goff et al., 2001). There are many high-energy sedimentary layers in the Pakarae River sedimentary sequence that could be indicative of tsunamis. However, in general the sequence is too variable to be able to isolate anomalous deposits and unequivocally attribute them to a tsunami. Our facies analysis has shown that this paleo-estuary was extremely dynamic. It would be difficult to distinguish tsunami-emplaced layers from other high-energy environments or events such as tidal channels, storm deposits, and flood deposits. For example, Fig. 9B and 9C show two shell and gravel layers within laminated estuarine silts. These gravel layers could be tsunami deposits, suggesting a high frequency of events, or they could represent migrating tidal channel lags within the estuary. Mapping the extent of the deposits would be required to differentiate between channel and more extensive flood or tsunami deposits.

Table 2: Calculation of Holocene uplift rates as estimated from radiocarbon ages obtained from the Pakarae River mouth transgressive sedimentary sequence.

Section	Sample height (m)	Calibrated Age** 2 sigma (cal. years BP)	Sea level at time of deposition (m) [1]	Total uplift (m) [2]	Uplift rate (mm/yr) [3]	Minimum uplift rate (mm/yr) [4]	Maximum uplift rate (mm/yr) [5]
1	15.2 +/- 0.22	8590-8410	-12	27	3.2	2.9	3.4
1	10.05 +/- 0.22	9210-8980	-19	28.85	3.2	2.9	3.4
1	6.3 +/- 0.22	9530-9240	-20	26.1	2.8*	2.5	3.0
1	6 +/- 0.22	9600-9450	-22	27.8	2.9	2.7	3.2
2	14.15 +/- 0.22	8640-8420	-12.5	26.45	3.1	2.8	3.4
2	7.5 +/- 0.22	9010-8770	-18	25.3	2.8	2.6	3.1
4	18.9 +/- 0.22	8350-8170	-12.5	31.2	3.8	3.5	4.1
5	18.3 - 18.7 +/- 0.22	7430-7280	-2.5	20.8	2.8	2.5	3.1
5	14.5 +/- 0.22	9290-9000	-19.5	34	3.7*	3.4	4.0
7	17.15 +/- 0.22	8540-8360	-14.5	31.45	3.7	3.4	4.0
8a	1.1 +/- 0.31	10420-10180	-27	28.1	2.7*	2.5	3.0
8b	4.4 +/- 0.31	10200-9990	-26	30.2	3.0	2.8	3.2
				Average	3.15		
				2 SD	0.8		

[1] Sea level estimated using Gibb (1986) New Zealand Holocene sea level curve, the mid-point of the 2σ calibrated radiocarbon age is projected to the SL curve, we estimate an uncertainty of ± 2 m using this method.
[2] Total uplift = modern sample elevation – eustatic SL at time of deposition.
[3] Uplift rate = (total uplift) / (mid-point of the 2σ calibrated radiocarbon age)
[4] Minimum uplift rate = (total uplift - 2 m)/(maximum 2σ calibrated age)
[5] Maximum uplift rate = (total uplift + 2 m)/(minimum 2σ calibrated age)
[6] Wood samples: may have been deposited above MSL therefore these are maximum uplift rates.

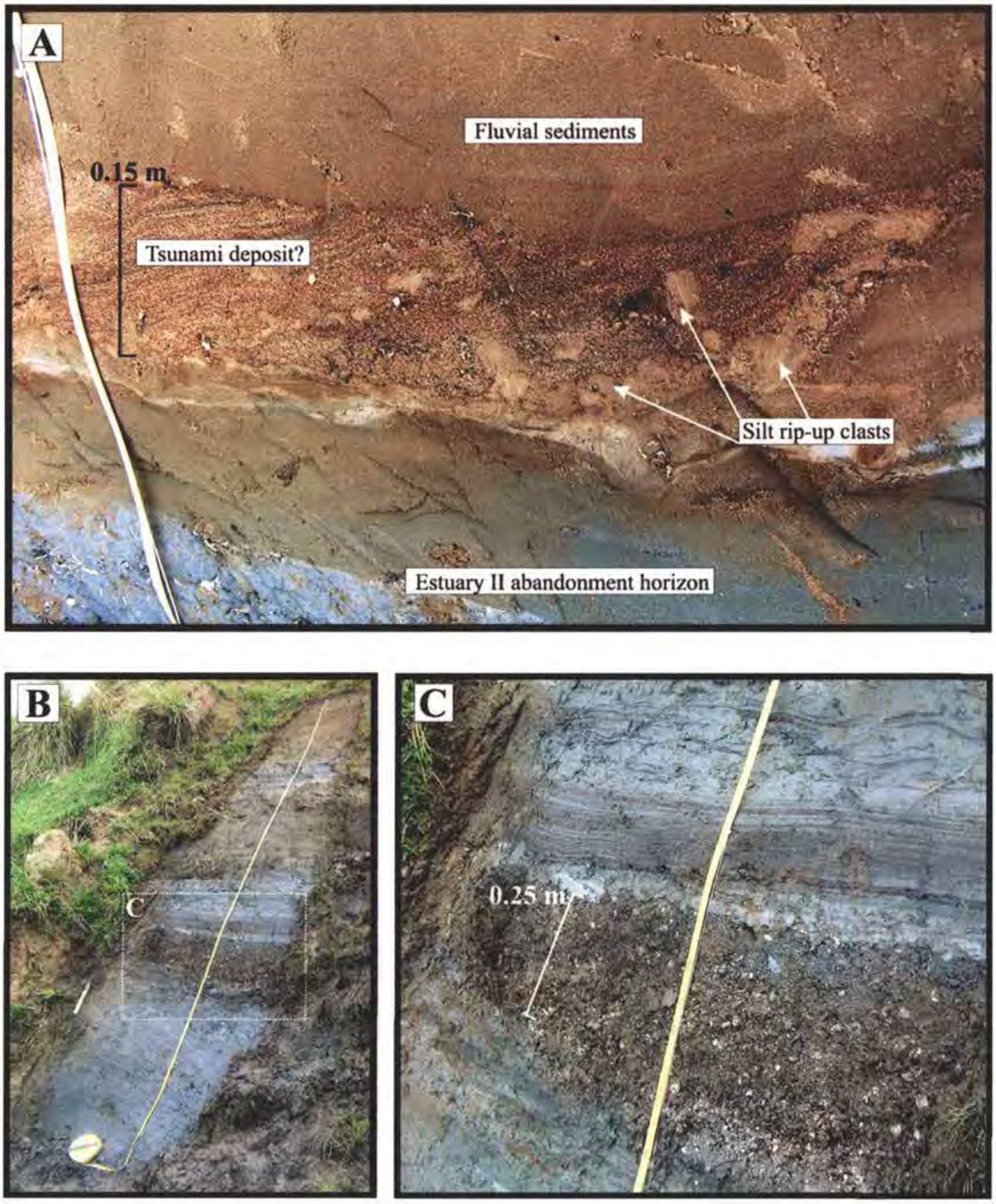

Figure 9. Examples of high-energy sedimentary units within low-energy paleoenvironments. (A) Section 1, ~ 15 - 16 m AMSL. (B) Section 3, ~11 - 15.8 m AMSL. (C) Section 3, 12 - 13 m AMSL.

One unit that we suggest may be a tsunami deposit is a coarse sand layer within Section 1 at ~ 15.5 m AMSL (Fig. 9A). The base of this unit is erosional and it contains entrained silt rip-up clasts; the sand displays unidirectional, high angle bedding. There are scattered shells even though the unit occurs within floodplain sediments. These features are all indicative of a tsunami deposit. However, the unit occurs 0.23 m above the horizon marking the abandonment of Estuary II, a horizon which has been identified as representing Uplift Event B. The unit cannot be correlated to Sections 2 and 3, which also display the uplift event horizon. If the coarse sand influx was a tsunami generated by the uplift event then we are uncertain what the intervening 0.23 m of silt sediment represents. It may be that sediment was deposited immediately following Uplift Event B (though it does not display any chaotic or colluvial-type sediments). Alternatively the tsunami deposit may be unrelated to Uplift Event B, and may have been from a different tsunamigenic source. This layer has a depositional age of < 8600 cal. yrs B.P. A possible tsunami deposit dated at ~ 8000 cal. yrs B.P. has been identified within a paleo-estuary sequence at Hicks Bay, 100 km north of the Pakarae locality (Wilson et al., in press-b). These tsunami deposits may correlate and be indicative of a regional tsunamigenic source such as the Hikurangi subduction interface or a trans-Pacific Ocean tsunami. These examples demonstrate the complexity of distinguishing tsunami deposits within a dynamic estuary such as Pakarae River mouth.

4.4.4 The interpretation of transgressive sequences for paleoseismology

We identify three major reasons why transgressive deposits are useful in coastal paleoseismic studies: (1) the ability to extend earthquake records prior to the time of eustatic SL stabilization, (2) potential for application on coastlines that do not preserve marine terraces, and (3) the ability to distinguish mechanisms of uplift on coastlines without historical occurrences of coseismic uplift. These are discussed further:

1. As previously stated, coastal neotectonic studies are frequently limited by the length of time since eustatic SL stabilization. This study has demonstrated that transgressive fluvio-marine deposits can record evidence of tectonic events prior to eustatic SL stabilization for the Holocene. This technique may therefore be particularly valuable in regions with long recurrence intervals.

2. During post-glacial SL rise estuaries were probably widespread along the New Zealand coastline, as they were globally. These are now largely infilled but the sequences may have untapped potential for coastal neotectonic studies if the locations do not display marine terraces. Many areas of the New Zealand coast are undergoing erosion, therefore where marine terraces are not well-formed or have not been preserved, transgressive sequences can be a tool for determining uplift rates and mechanisms.

3. On some coastlines there may be uncertainty over tectonic uplift mechanisms. Marine terraces are frequently assumed to be coseismic landforms; however terrace morphology can be created by other processes, and on coastlines where there have been no historical occurrences of coseismic uplift this is an important issue. For example, gradual uplift coupled with periods of storminess or varying sediment supply, may create benched coastlines. Usually these scenarios can be tested by collecting a suite of radiocarbon samples from the same marine terrace to test their coherence (Berryman, 1993; Ota et al., 1991), and in rare cases by studying the

ecological assemblages on the terrace straths (Hull, 1987). This study has shown that the style of uplift events (sudden or gradual, i.e. coseismic or aseismic) can be estimated from the marine transgression fill deposits. This technique may provide a more accurate determination of uplift mechanisms than marine terraces. At the Pakarae locality the synchronicity of abandonment of Estuary II, the apparent estuary-wide nature of the paleoenvironmental change and the very sharp facies contacts at the top of Estuaries I and II, are indicators that uplift was widespread and sudden. The preservation of a life assemblage of *P. australis* at the top of Estuary II is a good indicator of sudden environmental changes, as is the sharp transition from intertidal foraminifera assemblages to sediments barren of foraminifera. In locations where there is uncertainty about the uplift mechanism of marine terraces, we suggest transgressive deposits, if accessible, may be useful in resolving this.

4.4.5 Limitations of neotectonic analysis of transgressive deposits

While the use of transgressive deposits in detecting uplift events has been successful at the Pakarae locality, there are also several limitations. Firstly, detailed local knowledge of post-glacial eustatic SL rise is essential, and in areas undergoing glacio-isostatic rebound, tectonic uplift signals may be more difficult to isolate. Secondly, it is not always possible to quantify the amount of uplift that occurs with each event. Quantification is limited by the accuracy of the eustatic SL curve and by the paleoenvironmental bathymetric control. At the Pakarae locality paleoenvironmental control is relatively weak because only in-situ *A. aoteana* foraminifera were preserved. This is a common intertidal species; hence its presence places relatively little control on the position of paleo-mean SL. Foraminifera with greater SL sensitivity can generally be found at estuary margins. Therefore, there is potential to place better constraints of the amounts of uplift if the exposures are in the right location, or if drill cores can reach marginal-estuarine locations. Thirdly, a wide spatial distribution of exposures (or drill cores) is needed to detect each event. Correlation of events across different sections is needed to understand the paleogeography of the valley. Even at the Pakarae River mouth, a relatively small paleo-valley, direct stratigraphic evidence of Uplift Event C is missing and was probably only recorded further seaward. Availability of age control also potentially limits the interpretation of uplift events from transgressive sequences. Only Uplift Event B has been accurately dated within the Pakarae River mouth sequence. There appears to be a high degree of shell reworking and this has limited the age constraints we can place on Uplift Event A. Sediment reworking is probably a common characteristic of uplifting transgressive estuaries; with rapid sediment depocentre changes as a result of alternating eustatic SL rises (causing landward movement) and tectonic uplift events (causing seaward retreat).

4.5. Conclusions

A fluvio-estuarine transgressive sequence has been used to identify tectonic uplift events that occurred during infilling of the Pakarae River incised valley. Stratigraphic evidence suggests there was abandonment of two estuarine units (at ~ 9,000 and 8,600 cal. yrs B.P.) and microfaunal evidence suggests the paleoenvironmental change was sudden. We attribute these characteristics to rupture of an offshore reverse fault producing coseismic coastal uplift. A third uplift event at prior to ~7,350 cal. yrs B.P. is inferred from a significant accommodation space deficit.

This study has extended the paleoseismic history of the Pakarae locality to cover the past 10000 years. This is possibly the longest continuous record of coastal paleoseismology in the world. A long record has been attained through the combined use of marine terrace data, post-dating the culmination of eustatic SL rise, and by the use of transgressive marine facies architecture, which relies upon constantly rising eustatic SL. The use of biostratigraphy to document the sudden nature of paleoenvironmental change adds robustness to inferences based on the marine terraces that uplift on this part of the Hikurangi margin occurs by coseismic processes.

Acknowledgements

This research was funded by an EQC Student Grant (Project 6UNI/501). KJW was supported by the GNS Science Sarah Beanland Memorial Scholarship. Rodger Sparks and Dawn Chambers of the Rafter Radiocarbon Laboratory are thanked for their contribution to the radiocarbon dating. Hannu Seebeck, Matt Hill and Vicente Perez provided fieldwork assistance. This manuscript was improved thanks to reviews by John Holbrook and one anonymous reviewer.

References

Allen, G.P., and H.W. Posamentier, Sequence stratigraphy and facies model of an incised valley fill: the Gironde estuary, France., *Journal of Sedimentary Petrology, 63*, 378-391, 1993.

Atwater, B. F. Evidence for great Holocene earthquakes along the outer coast of Washington State. *Science, 236*, 942-944, 1987.

Berryman, K.R., Age, height, and deformation of Holocene terraces at Mahia Peninsula, Hikurangi subduction margin, New Zealand. *Tectonics, 12*, 1347-1364, 1993.

Berryman, K.R., Y. Ota, and A.G. Hull, Holocene evolution of an estuary on a tectonically rising coast: the Pakarae River locality, eastern North Island, New Zealand., *Sedimentary Geology, 80*, 151-162, 1992.

Carter, L., B. Manighetti, M. Elliot, N. Trustrum and B. Gomez. Source, sea level and circulation effects on the sediment flux to the deep ocean over the past 15 ka off eastern New Zealand. *Global and Planetary Change, 33*, 339-355, 2002.

Carter, R. M., L. Carter and D. P. Johnson. Submergent shorelines in the SW Pacific: evidence for an episodic post-glacial transgression. *Sedimentology 33*: 629-649, 1986.

Clague, J. J. Evidence for large earthquakes at the Cascadia subduction zone. *Reviews of Geophysics, 35*, 439-460, 1997.

Cochran, U., Detection of large Holocene earthquakes in the sedimentary record of Wellington, New Zealand using diatom analysis., Unpublished PhD thesis, Victoria University of Wellington, Wellington, 2002.

Collot, J.-Y., J. Delteil, K. Lewis, B. Davy, G. Lamarche, J.-C. Andru, P. Barnes, F. Chanier, E. Chaumillon, S. Lallemand, B.M. De Lepinay, A. Orpin, B. Pelletier, M. Sosson, Toussaint, and C. Uruski, From oblique subduction to intra-continental transpression: structures of the southern Kermadec-Hikurangi margin from multibeam bathymetry, side-scan sonar and seismic reflection., *Marine Geophysical Researches, 18*, 357-381, 1996.

Dalrymple, R.W., B.A. Zaitlin, and R. Boyd, Estuarine facies models: conceptual basis and stratigraphic implications, *Journal of Sedimentary Petrology, 62*, 1130-1146, 1992.

Darienzo, M. E., C. D. Peterson, and C. Clough, Stratigraphic evidence for great subduction-zone earthquakes at four estuaries in Northern Oregon, U. S. A., *Journal of Coastal Research, 10*, 820-876, 1994.

De Mets, C., R.G. Gordon, D.F. Argus, and S. Stein, Current plate motions, *Geophysics Journal International, 101*, 425-478, 1990.

De Mets, C., R.G. Gordon, D.F. Argus, and S. Stein, Effect of recent revisions to the geomagnetic reversal timescale on estimates of current plate motions., *Geophysical Research Letters, 21*, 2191-2194, 1994.

Eberhart-Phillips, D., and M. Reyners, Plate interface properties in the northeast Hikurangi subduction zone, New Zealand, from converted seismic waves., *Geophysical Research Letters, 26*, 2565-2568, 1999.

Foster, G. and L. Carter, Mud sedimentation on the continental shelf at an accretionary margin - Poverty Bay, New Zealand. *New Zealand Journal of Geology and Geophysics, 40,* 157-173, 1997.

Froggatt, P.C., and D.J. Lowe, A review of late Quaternary silicic and some other tephra formations from New Zealand: their stratigraphy, nomenclature, distribution, volume and age., *New Zealand Journal of Geology and Geophysics, 33*, 89-109, 1990.

Gibb, J.G., A New Zealand regional Holocene eustatic sea-level curve and its application to determination of vertical tectonic movements, A contribution to IGCP-Project 200., in *Recent Crustal Movements of the pacific Region.*, vol. 24, pp. 377-395, Bulletin of the Royal Society of New Zealand., 1986.

Goff, J.R., C. Chague-Goff, and S.L. Nichol, Paleotsunami deposits: a New Zealand perspective., *Sedimentary Geology, 143*, 1-6, 2001.

Hayward, B.W., H.R. Grenfell, C. Reid, and K. Hayward, *Recent New Zealand shallow-water benthic foraminifera: taxonomy, ecologic dstribution, biogeography, and use in paleoenvironmental assessment.*, Institute of Geological and Nuclear Sciences Monograph 21. 264 p. Lower Hutt, New Zealand: Institute of Geological and Nuclear Sciences Limited., 1999.

Holbrook, J. and S. A. Schumm, Geomorphic and sedimentary response of rivers to tectonic deformation: a brief review and critique of a tool for recognizing subtle epeirogenic deformation in modern and ancient settings. *Tectonophysics, 305*: 287-306, 1999.

Hughen, K.A., M.G.L. Baillie, E. Bard, Beck, J. W. , C.J.H. Bertrand, P.G. Blackwell, C.E. Buck, G.S. Burr, K.B. Cutler, P.E. Damon, R.L. Edwards, R.G. Fairbanks, M. Friedrich, T.P. Guilderson, B. Kromer, G. McCormac, S. Manning, B.B. Ramsey, P.J. Reimer, R.W. Reimer, S.S. Remmele, J. R., M. Stuiver, S. Talamo, F.W. Taylor, J. van der Plicht, and C.E. Weyhenmeyer, Marine04 Marine Radiocarbon Age Calibration, 0–26 Cal Kyr BP, *Radiocarbon, 46*, 1059-1086, 2004.

Hull, A.G., A late Holocene marine terrace on the Kidnappers Coast, North Island, New Zealand: some implications for shore platform development processes and uplift mechanisms., *Quaternary Research, 28*, 183-195, 1987.

Hull, A. G. Tectonics of the 1931 Hawke's Bay earthquake, *New Zealand Journal of Geology and Geophysics, 33*, 309-320, 1990.

Lewis, K.B., J.-Y. Collot, B. Davy, J. Delteil, S. Lallemand, and C. Uruski, North Hikurangi GeodyNZ swath maps: depths, texture and geological interpretation 1: 500 000., *National Institute for Water and Atmospheric Research miscellaneous series chart 72. Wellington.*, 1997.

Litchfield, N.J., S. Ellis, K. Berryman, and A. Nicol, Subduction related uplift in the Hikurangi Margin, New Zealand., *JGR, Earth Surface.*, in press.

Marsden, I.D., and R. Pilkington, Spatial and temporal variations in the condition of *Austrovenus stutchburyi* Finlay, 1927 (Bivalvia: Veneridae) from the Avon-Heathcote estuary, Christchurch., *New Zealand Natural Sciences, 22*, 57-67, 1995.

Marshall, J. S., and R. S. Anderson. Quaternary uplift and seismic cycle deformation, Peninsula de Nicoya, Costa Rica, *Geological Society of America Bulletin, 107*, 463-473, 1995.

Mazengarb, C., The Fernside Fault: an active normal fault, Raukumara Peninsula, New Zealand., *New Zealand Geological Survey Record, 3*, 98-103, 1984.

Mazengarb, C., and I.G. Speden (compilers), Geology of the Raukumara area, Institute of Geological & Nuclear Sciences 1:250,000 geological map 6. Institute of Geological and Nuclear Sciences Limited, Lower Hutt, New Zealand., 2000.

McCormac, F.G., A.G. Hogg, P.G. Blackwell, C.E. Buck, T.F.G. Higham, and P.J. Reimer, SHCal04 Southern Hemisphere Calibration, 0 - 26 ka cal BP., *Radiocarbon, 46*, 1087-1092, 2004.

Merritts, D. J., The Mendecino triple junction: Active faults, episodic coastal emergence, and rapid uplift, *Journal of Geophysical Research, 101*, 6051-6070, 1996.

Morton, J., *Seashore ecology of New Zealand and the Pacific*, Hayward, B. W. (scientific editor), Bateman, Auckland, 2004.

Ota, Y., K.R. Berryman, A.G. Hull, T. Miyauchi, and N. Iso, Age and height distribution of Holocene transgressive deposits in eastern North Island, New Zealand., *Palaeogeography, Palaeoclimatology, Palaeoecology, 68*, 135-151, 1988.

Ota, Y., A.G. Hull, and K.R. Berryman, Coseismic uplift of Holocene marine terraces in the Pakarae River area, eastern North Island, New Zealand., *Quaternary Research, 35*, 331-346, 1991.

Paul, M.A., and B.F. Barras, A geotechnical correction for post-depositional sediment compression: examples from the Forth valley, Scotland., *Journal of Quaternary Science, 13*, 171-176, 1998.

Reyners, M., D. Eberhart-Phillips, and G. Stuart, A three-dimensional image of shallow subduction: crustal structure of the Raukumara Peninsula, *Geophysical Journal International, 137*, 873-890, 1999.

Roy, P.S., New South Wales Estuaries: their origin and evolution, in *Coastal Geomorphology in Australia*, pp. 99-121, Academic Press Australia, 1984.

Schumm, S. A., River response to baselevel change: implications for sequence stratigraphy. *Journal of Geology, 101*: 279-294, 1993.

Walcott, R.I., Geodetic strain and the deformation history of the North Island, of New Zealand during the late Cainozoic, *Philosophical Transactions of the Royal Society of London A, 321*, 163-181, 1987.

Wellner, R. W. and L. R. Bartek, The effect of sea level, climate, and shelf physiography on the development of incised-valley complexes: a modern example from the East China Sea. *Journal of Sedimentary Research, 73*: 926-940, 2003.

Wilson, K.J., K. Berryman, U. Cochran, and T. A. Little, A facies architecture model for Holocene incised valley infill on a tectonically active coast: Pakarae River, New Zealand., *Sedimentary Geology*, in press-a.

Wilson, K., K. Berryman, U. Cochran, and T. Little, Holocene coastal evolution and uplift mechanisms of the northeastern Raukumara Peninsula, North Island, New Zealand., *Quaternary Science Reviews*, in press-b.

Wilson, K.J., K.R. Berryman, N.J. Litchfield, and T.A. Little, A revision of Mid to Late Holocene marine terrace distribution and chronology at New Zealand's most tectonically active coastal location, Pakarae River, North Island, New Zealand., *New Zealand Journal of Geology and Geophysics, 49*, 477-489, 2006.

Zachariasen, J., K. Sieh, F. W. Taylor, R. L. Edwards, and W. S. Hantoro, Submergence and uplift associated with the giant 1833 Sumatran subduction zone earthquake: evidence from coral microatolls, *Journal of Geophysical Research, 104*, 895-919, 1999.

CHAPTER FIVE

HOLOCENE COASTAL EVOLUTION AND UPLIFT MECHANISMS OF THE NORTHEASTERN RAUKUMARA PENINSULA, NORTH ISLAND, NEW ZEALAND.

Published: Wilson, K., Berryman, K., Cochran, U., Little, L. 2007. Quaternary Science Reviews, Vol. 26, 1106-1128.

Abstract

The coastal geomorphology of the northeastern Raukumara Peninsula, New Zealand, is examined with the aim of determining the mechanisms of Holocene coastal uplift. Elevation and coverbed stratigraphic data from previously interpreted coseismic marine terraces at Horoera and Waipapa indicate that, despite the surface morphology, there is no evidence that these terraces are of marine or coseismic origin. Early Holocene transgressive marine deposits at Hicks Bay indicate significant differences between the thickness of preserved intertidal infill sediments and the amount of space created by eustatic sea level rise, therefore uplift did occur during early Holocene evolution of the estuary. The paleoecology and stratigraphy of the sequence shows no evidence of sudden land elevation changes. Beach ridge sequences at Te Araroa slope gradually toward the present day coast with no evidence of coseismic steps. The evolution of the beach ridges was probably controlled by sediment supply in the context of a background continuous uplift rate. No individual dataset uniquely resolves the uplift mechanism. However, from the integration of all evidence we conclude that Holocene coastal uplift of this region has been driven by a gradual, aseismic mechanism. An important implication of this is that tectonic uplift mechanisms do vary along the East Coast of the North Island. This contrasts with conclusions of previous studies, which have inferred Holocene coastal uplift along the length of the margin was achieved by coseismic events. This is the first global example of aseismic processes accommodating uplift at rates of > 1 mm yr^{-1} adjacent to a subduction zone and it provides a valuable comparison to subduction zones dominated by great earthquakes.

5.1. Introduction

The interpretation of Holocene coseismic uplift along the East Coast of the North Island, New Zealand, despite changes in upper plate structures and Hikurangi subduction zone dynamics is examined in this study. Early Holocene transgressive marine sediments and mid-late Holocene marine terraces occur extensively along the East Coast adjacent to the Hikurangi subduction zone (Ota, 1987; Ota et al., 1988; Ota et al., 1992). At several localities on the central and southern East Coast detailed studies have produced sound evidence of terrace formation by sudden, episodic uplift processes, that are by inference, coseismic (Berryman, 1993; Hull, 1987; Ota et al., 1991). Other terraces along this margin with similar geomorphology have been presumed to be coseismically uplifted.

This study focuses on the northeastern tip of the Raukumara Peninsula, at the northern end of the onland Hikurangi margin (Fig. 1A, inset). There, suites of 4 – 5 marine terraces were recorded by Ota et al., (1992). These terraces are geomorphically similar to those on the southern margin suggesting their origin by a common uplift mechanism. However, in the Raukumara Peninsula region upper plate compressional structures are absent or poorly expressed and there have been no large historical earthquakes. This contrasts with the central and southern Hikurangi margin where upper plate thrust faults are common both on and offshore and where coseismic coastal uplift has taken place in historic time (for example, the 1931 Napier earthquake and 1855 Wairarapa earthquake).

It is important to determine the mechanism of tectonic uplift along the Raukumara Peninsula particularly due to the poorly known hazard of a great subduction earthquake (Stirling et al., 2002). There have been no subduction earthquakes in historic times but the occurrence of uplifted Holocene coastal features along the Raukumara Peninsula raises the question of whether these are related to great paleo-earthquakes. This sector of the margin is presently estimated to be weakly coupled compared to the southern Hikurangi margin (Reyners, 1998; Wallace et al., 2004. Therefore this location also provides an interesting study of how upper plate deformation varies with interplate coupling strength - variables that can be rarely tested on other global subduction margins.

We revisit the marine terraces at Horoera and Waipapa (Fig. 1A) to evaluate whether or not they were uplifted coseismically. In addition a geomorphic study of the late Holocene beach ridge sequence at Te Araroa (TA, Fig. 1B) and a paleoenvironmental study of the early Holocene uplifted transgressive marine deposits in nearby Hicks Bay (HB, Fig. 1C) were undertaken to further assess rates and processes of Holocene tectonic uplift in the northeastern (NE) Raukumara Peninsula. In this paper we present a summary of the regional geology and previous work related to all study sites: Horoera, Waipapa, HB and TA. We then outline the methodology of this study and summarize the results at each location in turn. The data from each site is integrated and analysed in the context of determining the regional Holocene mechanism of uplift and its relationship to the geodynamics of the Hikurangi margin.

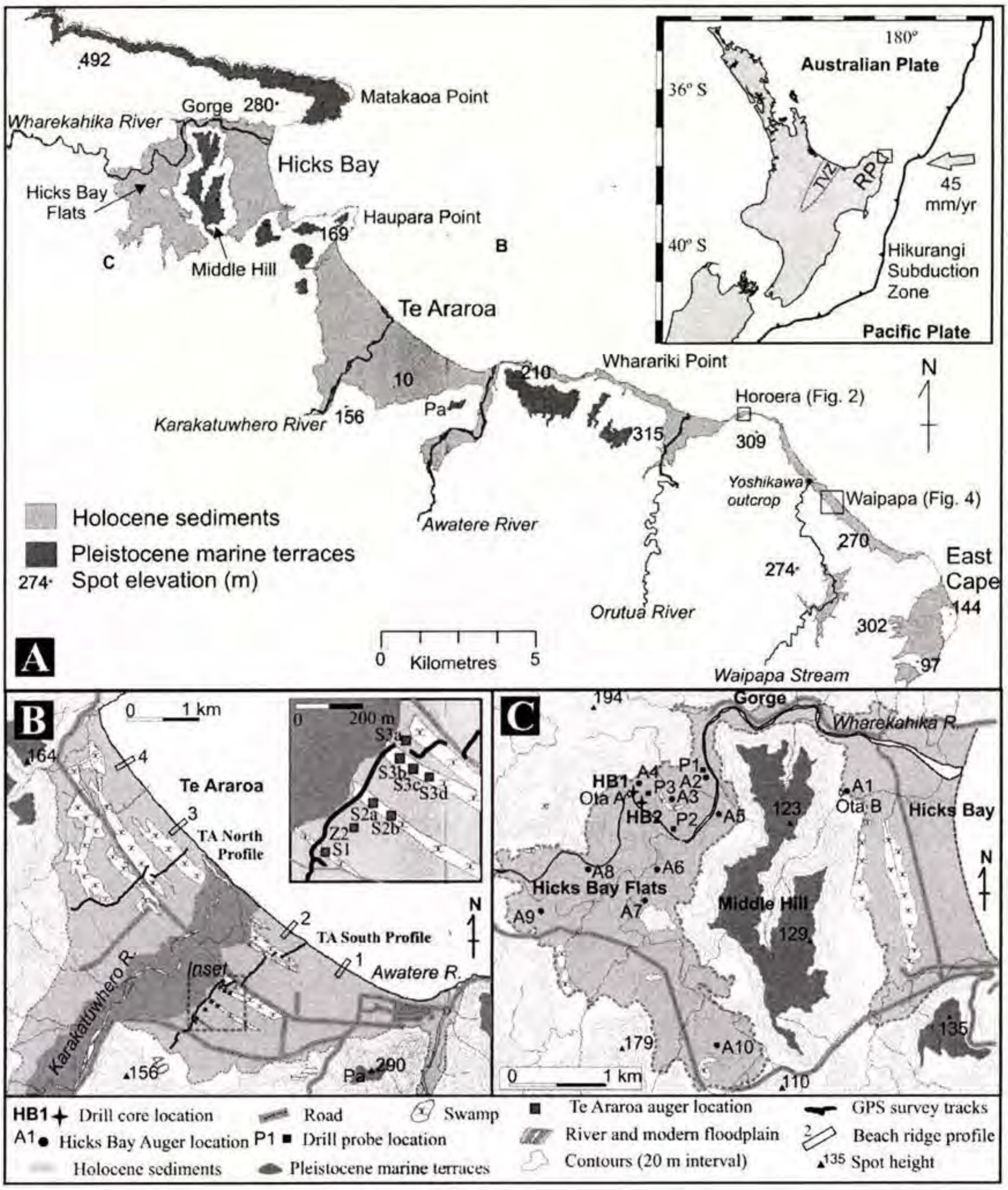

Fig. 1: Location map of the northeastern Raukumara Peninsula region. Inset: Plate tectonic setting of the Raukumara Peninsula (RP: Raukumara Peninsula, TVZ: Taupo Volcanic Zone). (B) Topography of the Te Araroa area with locations auger profiles, GPS survey tracks and locations of modern beach ridge profiles. (C) Topography of the Hicks Bay area with locations of core, probe and auger profiles.

5.2. Tectonic setting

The Raukumara Peninsula is located at the northeastern end of the East Coast of the North Island; HB, TA and East Cape are located at the northeastern tip of the peninsula (Fig. 1A). The Hikurangi Trough lies approximately 60 km offshore to the east of HB-TA. Convergence between the Australian and Pacific Plates occurs at ~45 mm yr^{-1} at an azimuth of 266° (De Mets et al., 1990; 1994). The local geology near HB-TA consists of Pliocene forearc basin muddy sandstones of the Mangaheia Group or Early Cretaceous to Eocene igneous rocks (Matakaoa Volcanics) of the Miocene East Coast Allocthon (Mazengarb and Speden, 2000).

In stark contrast with the central to southern parts of the Hikurangi margin, the Raukumara Peninsula contains few known active onshore faults. Mazengarb and Speden (2000) note that mapped active fault segments are typically short and these faults have a normal sense of slip (Ota et al., 1991, Mazengarb, 1984). Inactive faults on the Raukumara Peninsula generally strike northwest, approximately perpendicular to the emplacement direction of the East Coast Allocthon and are primarily Early Miocene-age thrust faults (Mazengarb and Speden, 2000).

5.3. Previous studies of NE Raukumara Peninsula Quaternary coastal geology

Holocene deposits in the HB-TA regions were first descibed by Henderson and Ongley (1920) and Ongley and MacPherson (1928). Garrick (1979) mapped beach ridges at TA and presented two profiles from the southeastern side of the Karakatuwhero River (Fig. 1B). Three radiocarbon ages of shells collected within 320 m of the modern beach shore, yielded ages of < 1068 cal. yrs B.P., establishing the Holocene age of the beach ridges. Projecting the average progradation rate (derived from the oldest of these radiocarbon ages) back to the highest beach ridge inland, Garrick (1979), calculated an average beach ridge uplift rate of 1.5 mm yr^{-1}. Garrick (1979) divided the beach ridges into four zones separated by intervening swamps that he called Coastal Revisions (CR1 – CR3). Each Revision was proposed to have formed during a period of coastal erosion; although, Garrick (1979) suggested that the oldest zone (CR3) may have formed instead as a result of relatively fast coastal emergence. Ota et al. (1992) subsequently mapped the beach ridges at TA, dividing them into 5 Zones (named I – V). The zones were defined by the continuity of beach ridges. They recognised two, 2 m high, scarps between Zones III-IV and IV-V. The swamps between zones II – V coincide with the Coastal Revisions of Garrick (1979). Ota et al. (1992) did not discuss the formation of the TA beach ridges or mechanisms of their subsequent uplift.

Yoshikawa et al. (1980) included the Holocene terraces of the HB-TA, East Cape and Whangaparoa (on the northwestern side of the Raukumara Peninsula, 25 km west of

HB) into a single landform which they referred to as the Te Araroa terrace. They noted at least 3 to 4 sub-levels of terraces within this larger terrace and presented a profile across marine terraces at Waipapa Stream (Fig. 1A). Maps of marine terraces from HB to East Cape, and 26 radiocarbon ages from Holocene deposits in the region were presented by Ota et al. (1992). These authors recognised three marine terraces at HB based on aerial photograph interpretation, with the lowest and highest terraces continuing inland behind Middle Hill. An exposure along the Wharekahika River called "Location A" (henceforth called Ota A) includes abundant *Austrovenus stutchburyi* shells (a common estuarine species); the highest elevation shell bed yielded a radiocarbon age of 7662-7429 cal. yrs B.P. They identified an overlying tephra as the Whakatane tephra (5590 - 5465 cal. yrs B.P., Froggatt and Lowe, 1990). Ota et al. (1992) mapped marine terraces almost continuously from the Awatere River mouth to East Cape, recognising up to five terraces at the Orutua River mouth and Horoera Point, and three at Waipapa Stream mouth (Fig. 1A). All radiocarbon ages presented by these authors from shells within the terrace cover deposits were < 1240 – 930 cal. yrs B.P. Ota et al. (1992) interpreted all of these late Holocene terraces as having been uplifted suddenly during earthquakes.

5.4. Methods

5.4.1 Elevation measurements

All elevations and topographic profiles measured in this study were obtained using a real-time kinematic GPS. In each of the three study areas several datums, such as geodetic benchmarks and tide levels, were measured to provide calibration to the position of mean sea level (MSL). The uncertainty of each calibration point relative to MSL dictates the accuracy of the elevation measurements; hence the overall uncertainty varies between the regions. At Horoera and Waipapa one benchmark, four high tide points and two mid-tide sea level points were used as calibration points, elevations in this area have a 95% uncertainty of ±0.22 m. At Te Araroa three benchmarks, three estimated high tide markers and two measurements of the tide level at certain times of the day were used and the elevation measurements here have a 95% uncertainty of ± 0.42 m. At Hicks Bay three benchmarks, and one high tide measurement resulted yield an uncertainty of ± 0.3 m.

5.4.2 Geomorphic analysis of the Horoera and Waipapa coastal terraces

At Horoera nine topographic profiles were measured normal to the shoreline and strike of the terraces (Fig. 2, P1-P9), and ten profiles parallel with the shoreline and strike of the terraces were obtained at the front and rear of each terrace (Fig. 2, 1F – 5F and 1R – 5R). At Waipapa three topographic profiles, all normal to the shoreline and to the strike of the terraces, were obtained. Twenty auger holes were hand-drilled on the Horoera terraces, and eight on the Waipapa terraces, to examine the stratigraphy of their cover sediments.

5.4.3 Te Araroa Beach Ridges

Elevation profiles, TA North and TA South, were taken across the coastal plain either side of the Karakatuwhero River at TA (Fig. 1B). Where swamps could not be crossed (particularly on TA North) several short segments of profile have been joined together with the intervening distance left blank. Seven hand augers were drilled on the Te Araroa plain, most of them within swamps (Fig. 1B inset, named S1 – S3a and Z2). The sedimentary characteristics were visually assessed and samples were taken at significant unit boundaries. Three samples were processed for diatom content using the same techniques as will be described for the Hicks Bay study. Two radiocarbon samples of wood were obtained from auger holes S1 and S3d. All radiocarbon ages are presented at the 2-sigma age range (95% probability) and as calibrated radiocarbon years, unless otherwise stated.

The glass geochemistry of three tephra samples from the augers S1 and S2a were analysed. Glass shards of 63-250μm size were mounted in epoxy blocks, these were polished and carbon coated. At least ten glass shards from the tephra were analysed with a JEOL-733 microprobe in the Analytical Facility of Victoria University of Wellington, using a 10-μm-diameter beam of 8 nA at 15 kV accelerating voltage.

5.4.4 Hicks Bay Paleo-estuary

Stratigraphic descriptions of sediments infilling the HB Flats were obtained from natural exposures and auger holes at 10 locations (A1-A10, Fig. 1C). These data along with five cone penetrometer probes allowed us to locate suitable places for collecting drill cores. A hydraulic, truck-mounted drill rig collected sediment cores HB1 and HB2 (Fig. 1C). Hollow-stem augers, with an inside diameter of 85 mm, were used to simultaneously advance the hole and take "undisturbed" core samples. Core samples were taken in a thin-walled stainless steel liner at intervals of approximately 0.5 m. The cores were extruded into PVC liners. All surfaces of the core were scraped to remove the outer ~ 5 mm of sediment to reduce the chance of contamination by sediment smearing inside the core liner. In some sections, particularly near the top, there is some compression of the sediment so that when the core was extruded it had a length < 0.5 m. The method of coring means that the whole sequence was captured, but we leave a blank space on the corelogs where compression occurred. There was no evidence of core disturbance during drilling. Cores were logged in the field with a visual assessment of the sediment type, grainsize, colour and macrofossil content. Sampling was undertaken in the lab with 20 mm slices of sediment removed and the inner portion of the slices processed for microfossils and isotopes. All cores are stored in the coolstore at Victoria University of Wellington.

Five new radiocarbon ages have been obtained from Hicks Bay: four from the drill cores and one from an auger drilled at the riverbank exposure next to the HB1 drill site. All of these except sample HB1/-0.26 m AMSL were fragments of *A. stutchburyi*; HB1/-0.26 m AMSL was a small twig (~30 mm long, 5 mm diameter).

5.4.4.1. Micropaleontology study

- **Foraminifera**: Ninety-one samples were selected from HB1 and HB2 for a foraminifera study. Samples were processed using the standard techniques of Hayward et al. (1999a). Where possible 100 - 200 benthic foraminifera were picked, ~ 100 tests being adequate for environmental assessment using brackish foraminifera (Hayward et al., 1996; Hayward et al., 1999b; Hayward et al., 2004). Only well-preserved foraminifera were identified, identification was made with reference to Hayward et al. (1999a, 1997), and personal communication with B. Hayward and A. Sabaa (Geomarine Research, May 2004). The relative amounts of macro shell fragments and wood or plant matter in each sample were estimated and planktic foraminifera were counted but not identified. In some cases when well-preserved benthic foraminifera were very rare we used a floating technique to concentrate the foraminifera. In total 21 samples were floated. Approximately 5 grams of the >0.063 mm sediment fraction was stirred into sodium polytungstate with a specific gravity of 1.6; the fraction that floated contained the concentrated foraminifera.
- **Palynology**: Nine samples from cores HB1 and HB2 were processed for spores and pollen following the standard technique of Moore and Webb (1978) and Moore et al. (1991). Bill McLea (VUW) identified the pollen species.
- **Diatoms**: Sixteen samples from HB1 and HB2, and five sampled from Ota A, A8 and A10 were analysed for diatom content. Twelve of these samples were fully processed by a standard method as described in Cochran et al. (2006). Diatom species were identified at x1600 magnification with reference to standard floras (eg, Krammer and Lange-Bertalot, 1991-2000; Hartley, 1996; Witkowski et al., 2000). Where possible the species were assessed for their salinity and habitat preferences taken from van Dam et al. (1994) and Round et al. (1990) and the above floras. The remaining nine samples were assessed by placing a wet smear of sediment on the slide and checking for the presence or absence of diatoms.

5.4.4.2 Stable isotopes

Thirty-one samples from HBI between 10.3 m to 6.2 m AMSL were selected for C and N stable isotope study. Sediment samples of ~ 10 g were finely ground and homogenised with a mortar and pestle. Samples were run on a Europa Geo 20-20 mass spectrometer in continuous flow with an ANCA (automatic N and C analyser) elemental analyser at the Rafter Stable Isotope Laboratory. Whole sediment samples were run for total carbon and nitrogen content (%C and %N), and carbon and nitrogen isotopes ($\delta^{13}C$ and $\delta^{15}N$). A split of the whole sample was treated with 1N HCl overnight to demineralise the sediment. The split was run on the ANCA again to get total organic carbon and nitrogen content (%TOC and %TON). Inorganic carbon (% $CaCO_3$) contribution was calculated from % C (total) – % TOC (organic).

5.5. Results

5.5.1 Horoera and Waipapa terrace stratigraphy and geomorphology

All auger profiles on the Horoera terraces revealed a ~ 0.2-0.3 m interval of sandy topsoil overlying orange-grey mottled silt on bedrock. All but four of the augers reached the mudstone bedrock (Fig. 2A). Mudstone pebbles that could not be drilled through were encountered in Augers H1-H2 and H10-H11. Shell fragments were found at the base of H1-H2. Auger holes H18 and H20 contained a <10 mm thick layer of fine-grained white tephra.

The sharpness of definition of the terrace risers deteriorates to the west, away from the Mangakino Stream (Fig. 2C). Five terraces can be identified in profiles P1-P4. From P5 to P9 the only riser that is continuously recognisable is that between terraces 3 and 4 (Fig. 2C). The elevation of the terraces decreases from east to west (Fig. 2D). The average height decrease (measured along the strike of the terrace risers) from east to west over a distance of ~ 100 m is ~0.5 m (Fig. 2D). The mudstone bedrock increases in elevation landward at approximately the same gradient as the terrace surfaces and the cover sediments are nearly constant in thickness. Repeated augers bounding the ~ 2 m riser between terraces 2 and 3 however, shows that there is not an equivalent elevation change on the basement surface as there is at the surface (Fig. 2B). For example in P2 there is a well-defined 2.5 m riser between terraces 2 and 3, yet the elevation of the mudstone bedrock on either side of the surface riser changes by only 0.5 m (Fig. 2B).

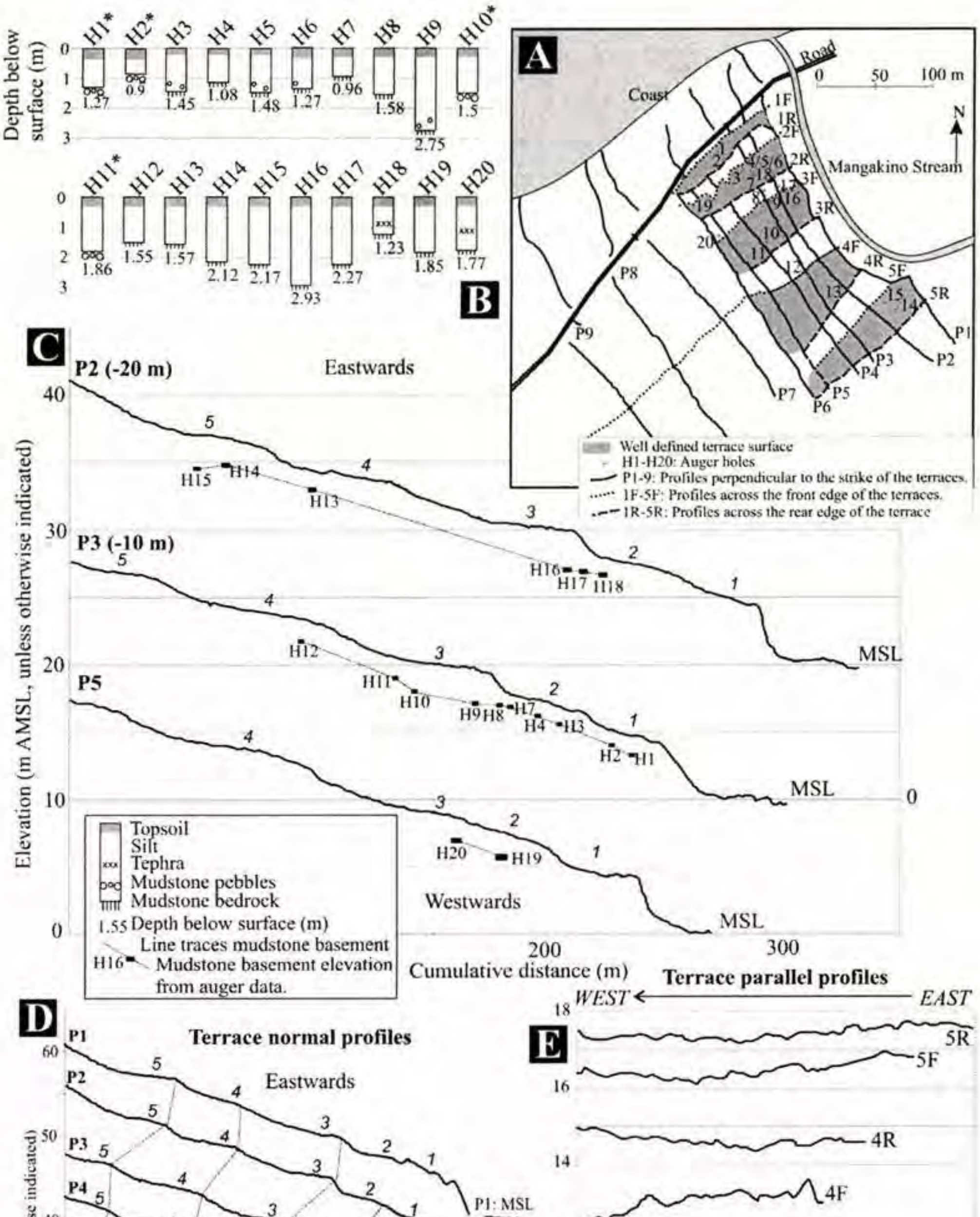

Fig. 2: (A) Location of elevation profiles and auger holes on the Horoera terraces. (B) Stratigraphy of auger profiles H1-H20 on the Horoera terraces, * denotes augers that did not reach the mudstone bedrock. (C) Profiles 1,3 and 5 (crossing perpendicular to the strike of the terraces) with the bedrock elevations projected onto them. Terraces are numbered 1-5. (D) Profiles 1-9 with terraces 1-5 labeled, dotted lines trace the recognisable risers along the strike of the terraces. (E) Elevation profiles along following the strike of the terraces along the front (1F-5F) and rear (1R-5R) of the terraces.

Only one auger at Waipapa reached the underlying mudstone bedrock at a depth below the surface of 4.6 m (W1a, Fig. 3B). All other augers reached the water table and drilling could not go further, therefore the measurements record the minimum thickness of coverbed material on the terraces. All augers, except those on Terrace 2, recovered homogenous fine-medium well-sorted grey sand. Augers W2a and W2b recovered grey-brown silt.

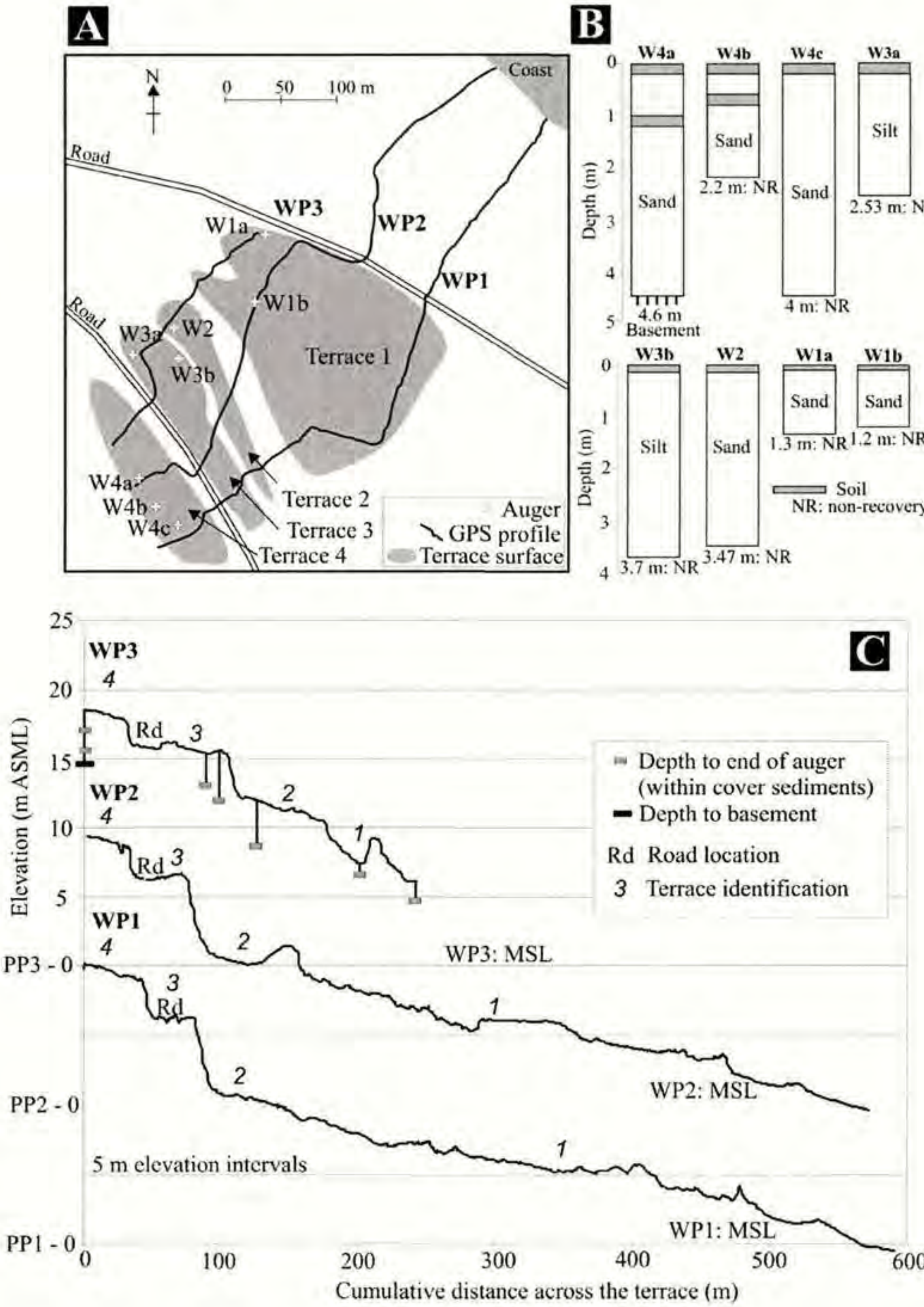

Fig. 3: (A) Location map of the Waipapa terraces, profiles and auger holes, and approximate boundaries of the terraces shown. (B) Auger hole stratigraphy. (C) Elevation profiles, WP1-WP3, with the auger hole depths projected to WP3.

Waipapa terraces 3 and 4 are relatively narrow with very sharp risers and almost horizontal terrace surfaces (although the landward edge of Terrace 3 has been disturbed by the gravel road, Fig. 3A, C). Terrace 4 increases in height along strike towards the south by approximately 1.5 m over 100 m. The riser between terraces 3 and 2 remains very steep along strike increasing in height from 3 m in the north to 6 m in the south (Fig. 3C). Terrace 2 decreases in definition and elevation towards the south. Terrace 1 is very wide with a gentle slope, and the riser between terrace 1 and 2 decreases in definition toward the south. A riser between terrace 1 and the modern beach cannot be distinguished either in the field or on the elevation profiles.

The amount of sand or silt cover on the terraces is generally greater than the height of the adjacent seaward riser. For example, the thickness of sand on Terrace 4 is 4.6 m and the riser height between Terraces 4-3 is 3.5 m. On terrace 3 there is a minimum of 3.7 m of silt, compared with the Terrace 3-2 riser height of 3 m. Terrace 2 has a minimum of 3.5 m of sand cover and an adjacent Terrace 2-1 riser height of up to 3 m (Fig. 3).

5.5.2 Te Araroa Beach Ridge Sequence

The elevation profiles of TA North and TA South are similar to one another in the section extending from the beach to ~400 m inland (Fig. 4 B, C). Both display 6 well-defined beach ridges with an amplitude of ~0.5 m. The average elevation of the ridges over the 400 m increases by 0.8 m in the TA South profile, and 1.2 m in the TA North profile (Fig. 4B, C). The modern storm ridge of TA North is ~0.9 m lower than the equivalent in TA South. We observed a gradual northwards decrease of modern storm ridge elevation along the TA shoreline (Fig. 4D). This is attributed to the dominant sediment source, the Awatere River, being at the south end of the bay.

From ~ 400 m inland to the back of the coastal plain (to the edge of the colluvial fans at ~2000 m inland) the two profiles are dissimilar. On the inland coastal plain to the north of the river there are numerous swampy areas and several sand dunes (Fig. B). The beach ridges on the TA North profile are indistinct at >750 m inland and large steps of 1-2 m in the profile can be seen particularly around the road and sand dune (Fig. 4B). The TA South profile is preferred for geomorphic interpretation because it appears to have fewer swamps, suggesting less possible fluvial modifications to the beach ridges, and it has no sand dunes (Fig. 4C).

The TA South profile shows beach ridges up to 2100 m inland with ridge definition deteriorating inland (Fig. 4C). Four swamps that can be seen on aerial photos can be distinguished on the elevation profiles (S1-S4, Fig. 4C). We identify five zones of beach ridges (Z1-Z5, Fig. 4C), these are the same zones as Ota et al. (1992) identified except that we divide their Zone II into two separate zones (Z1 and Z2), we do not identify anything equivalent to the Ota et al. (1992) Zone I, which they only locate on the northern side of the river.

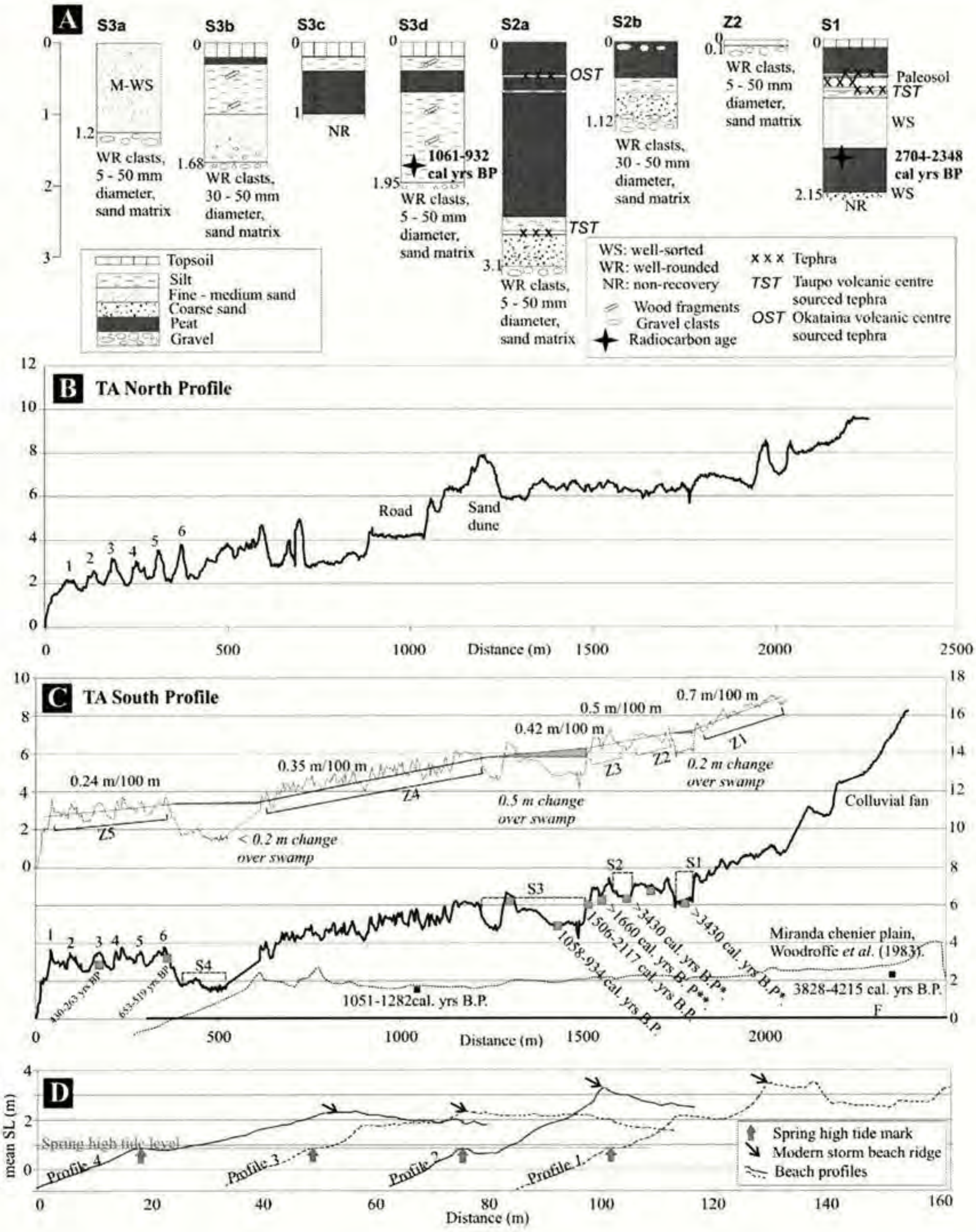

Fig. 4 : Te Araroa Beach Ridges (A) Auger stratigraphy (locations shown on Fig. 12). (B) TA South elevation profile. Top profile shows the names of the beach ridge zones (Z1 - Z5) and the gradient of each zone and the amount of elevation change across the swamps. The middle profile shows the names of each swamp zone (S1 - S4), and radiocarbon ages from this study and Garrick (1979), Ota et al. (1992) and this study. (C) TA North elevation profile. (D) Profiles from the intertidal wave zone to the crest of the modern storm beach ridge at four locations along the Te Araroa beach (Profiles 1 - 4, south to north respectively, see locations Fig. 12). Main sediment source is to the south. * Waimihia tephra, 3375 - 3485 cal. yrs B.P. (Froggatt and Lowe, 1990). ** Sea-rafted Taupo pumice identified by Ota et al., 1992, eruption age of 1720 - 1600 cal. yrs B.P. (Froggatt and Lowe, 1990).

Lines projected through the midpoint of all the beach ridges of each zone of TA South show that the average beach ridge elevation increases landward. The gradients vary from 0.24 m/100 m to 0.7 m/100 m (Fig. 4C). Twenty-seven beach ridges have been identified on the TA South profile; the average elevation difference between the successive ridge crests is 0.17 m.

Table 1. Diatom results from Hicks Bay cores, HB1 and HB2, and the Te Araroa beach plain.

Location/Core	Elevation (m AMSL)	Depth (m)	Processing method	Diatom observations	Paleoenvironmental interpratation
Hicks Bay					
Ota A	6.3		Smear	Rare brackish marine diatoms	Brackish-marine
Ota A	3.5		Smear	Barren	Possibly overbank silts, or diatoms not preserved
HB1	9.96		Smear	Barren	" "
HB1	9.36		Smear	Barren	" "
HB1	8.36		Full	Sparse well-preserved brackish marine diatoms	Brackish-marine
HB1	7.96		Full	" "	Brackish-marine
HB1	7.46		Full	" "	Brackish-marine
HB1	5.78		Full	" "	Brackish-marine
HB1	3.62		Full	" "	Brackish-marine
HB1	-0.16		Full	" "	Brackish-marine
HB1	-0.26		Full	" "	Brackish-marine
HB2	9.2		Smear	Barren	Possibly overbank silts, or diatoms not preserved
HB2	8.82		Smear	Barren	" "
HB2	8.11		Full	Sparse well-preserved brackish marine diatoms	Brackish-marine
HB2	6.02		Full	" "	Brackish-marine
HB2	5.66		Full	" "	Brackish-marine
HB2	4.84		Full	" "	Brackish-marine
HB2	3.76		Full	" "	Brackish-marine
A8		-4.5	Smear	Abundant well-preserved freshwater diatoms	Freshwater, not overbank silts
A8		-5.8	Smear	Moderate concentrations of well-preserved freshwater diatoms	Freshwater, not overbank silts
A10		-1.35	Smear	Fragments of fresh water diatoms	Probably overbank silts
Te Araroa Plain					
S3b		0.98	Smear	Barren	Probably overbank silts
S3d		0.9	Smear	Barren	Probably overbank silts
S2b		0.67	Smear	Abundant freshwater diatoms	Wetland with some ponded open water.

The beach ridges are composed of well-rounded greywacke gravel clasts that are generally 10 – 50 mm in diameter. On the southern coastal plain there is very little sand cover (auger Z2, ~1700m inland has only 0.1 m of cover sand, Fig. 4A). The intervening swamps are infilled with silt and peat (S3b-d, S2a-b, and S1, Fig. 4A). Three silt samples were analysed for diatoms (Table 1). The silt from S2b contained abundant, freshwater diatoms indicative of a freshwater, ponded wetland. The other two samples, from S3b and S3d were barren of diatoms; these are interpreted as overbank silts.

Table 2. Radiocarbon ages obtained from Te Araroa and Hicks Bay.

Sample name*	**Sample Material**	**Lab number[2]**	**Dating Technique**	**^{13}C (‰)**	**Radiocarbon Age[3] (radiocarbon years BP)**	**2-sigma calibrated age[4] (cal. years BP)**
S3d/1.6 - 1.8 m depth	Detrital organic matter within silt	NZA 22393	AMS	-26.85	1142 ± 30	***1058 - 934***
S1/1.59 m depth	Peat	NZA 22394	AMS	-27.49	2485 ± 30	***2701- 2351***
HB1/0.16 m AMSL	*A. stutchburyi*	NZA 21087	AMS	-1.04	8276 ± 35	***8970 - 8679***
HB1/-0.26 m AMSL	Wood	NZA 20754	AMS	-28.66	7678 +/- 30	***8535- 8369***
HB2/1.9 m AMSL	*A. stutchburyi*	NZA 22544	AMS	1.26	7812 ± 35	***8359 - 8185***
HB2/5.2 m AMSL	*A. stutchburyi*	NZA 20910	AMS	-0.48	7360 +/- 35	***7920 - 7731***
Ota A 2.5 m AMSL[1]	*A. stutchburyi*	NZA 17348	AMS	-0.06	7824 +/- 55	***8390 - 8169***
Ota A 7.2 m AMSL[1]	*A. stutchburyi*	NZA 5461	Standard		7046+/-66	***7646 - 7420***
Ota A 8.6 m AMSL[1]	Wood	GaK 10474	Standard		4470 +/- 180	***5576 - 4531***
Ota A 9.8 m AMSL[1]	Peat	GaK 10473	Standard		5590 +/- 140	***6638 - 5994***

* Elevations within HB1 and HB2 have an uncertainty of ± 0.3 m.
[1] Previously published in Ota et al. (1992).
[2] NZA: Rafter Radiocarbon Laboratory, GaK: Gakushuin University.
[3] Conventional radiocarbon age before present (1950 AD) after Stuiver and Polach, (1977).
[4] Marine dates calibrated using Hughen et al., 2004; terrestrial dates calibrated using McCormac et al., 2004.

Age control on the TA beach ridges comes from previously obtained radiocarbon ages and observations of tephra occurrences (Garrick, 1979, and Ota et al., 1992), new radiocarbon ages presented here, and our tephra analyses. Two new radiocarbon samples were collected from the base of auger holes in swamps S1 and S3 (Table 2). Wood fragments within silt at the base of S3d yielded an age of 1058-934 cal. yrs B.P. A wood sample collected by Ota et al. (1992) from the landward side of this swamp had a radiocarbon age of 1506-2117 cal. yrs B.P. Our radiocarbon age from the base of S3 is consistent with the previously collected data and with the absence of tephra in the swamp, it dates the start of infilling of the swamp, therefore dates the minimum age of the beach ridges immediately landward (in Zone 3). Ota et al. (1992) also observed sea-rafted Taupo pumice on beach ridges within Zone 3, implying the beach ridges were formed prior to 1720 – 1600 cal. yrs B.P. (Froggatt and Lowe, 1990).

Peat from the base of S1 yielded a radiocarbon age of 2701-2351 cal. yrs B.P. The tephra lying approximately 1 m above the radiocarbon sample has a Taupo volcanic centre glass geochemical signature (Supplementary Data B). This tephra was ~ 50 mm thick and composed of coarse lapilli. It is most likely to be the Waimihia tephra, 3375-3485 cal. yrs B.P (Froggatt and Lowe, 1990), which is typically the only coarse grained Taupo volcanic centre tephra found in the East Cape region. The alternative is the Taupo tephra (1720 – 1600 cal. yrs B.P., Froggatt and Lowe, 1990) which has an age consistent with the radiocarbon date but it is usually absent or very fine grained in this region. We infer, based on the grain size characteristics, that the tephra in swamp S1 is the Waimihia. Either it has been redeposited or the radiocarbon age represents younger material (either younger tree roots growing down or contamination during sample collection).

Swamp S2 contains a tephra near the base at –2.6 m depth (auger S2a, Fig. 4A). This is a Taupo volcanic zone sourced tephra (Supplementary Data B) with a coarse lapilli texture, inferred to be the Waimihia tephra. This gives the beach ridges in Zone 2 a minimum age of 3375-3485 cal. yrs B.P. A tephra at -0.5 m in Swamp S2, with an Okataina volcanic centre glass geochemistry, is unidentified. Two shells samples were collected by Garrick (1979) from the beach ridges within Zone 5, these yielded ages of 420-263 and 653-519 cal. yrs B.P (Fig. 4C).

Overall the age control on the oldest beach ridges remains relatively poor, though the start of ridge accretion must be > 3375-3485 cal. yrs B.P (the age of the Waimihia tephra which was found in swamp S1). Using the Waimihia tephra as the minimum age of the beach ridges at the front edge of Zones 1 and 2, the maximum uplift rates can be calculated (Table 3). Uplift rates can also be calculated using the radiocarbon ages of Garrick (1979) and Ota et al. (1992) for Zones 3 and 5. We use the modern elevation of the crest of the beach ridge and subtract the elevation of the modern storm beach ridge (4 m) to get a total amount of uplift (Fig. 4D). The calculated uplift rates range between 0.5 – 2 mm/yr (Table 3).

Table 3. Uplift rates from the TA Beach Ridges

Location	Elevation (m)	Age (ka)	Modern analog elevation (m)	Total uplift (m)	Uplift Rate (m/ka)	Uncertainty
Front edge Z1	8.4	>3.43	4	4.4	1.3	Maximum
Front edge Z2	8	>3.43	4	4	1.2	Maximum
Front edge Z3	7.6	1.8115[1]	4	3.6	2.0	(1.7-2.4)[3]
Back edge Z5	4.3	0.586[2]	4	0.3	0.51	(0.46-0.58)[3]

[1]Radiocarbon age of Ota et al., 1992. Midpoint of the 2σ calibrated age B.P.
[2]Radiocarbon age of Garrick, 1979. Midpoint of the 2σ calibrated age B.P.
[3]Maximum uplift rate = calculated using the minimum age of the 2σ calibrated age range; minimum uplift rate: calculated using the maximum age of the 2σ calibrated age range.

5.5.3 Hicks Bay Paleo-Estuary

5.5.3.1 Hicks Bay Flats Stratigraphy

Shells exposed along the banks of the Wharekahika River on the HB Flats attest to an early Holocene estuarine paleoenvironment in this area (Location Ota A, Fig. C, Ota et al., 1992). This transgressive estuarine sequence was targeted for drilling and paleoenvironmental analysis. For purposes of paleo-sea level studies an ideal place to drill is at the margins of the paleo-estuary where many species of tidal-wetland micro-flora and –fauna have restricted salinity or inundation tolerances and are thus sensitive to changes in MSL (Hayward et al., 1999b; Hayward et al., 2004b; Patterson et al., 2000). Stratigraphic sections of the HB Flats were studied to provide a guide on the extent of the paleo-estuary deposits and eliminate areas with gravel layers that would inhibit drilling.

At most locations inland of the Ota A river outcrop, gravels were encountered in augered holes and by the penetrometer resistance probes (A1-A10, Fig. 1C, Supplementary Data A). At least the upper 4 m of sedimentary infill everywhere on the HB Flats is a mixture of silt and gravel. Similarity between these silts and gravels and modern river sediments implies that they are fluvial deposits: probably overbank (silt) and flood (gravel) deposits. A diatom sample from silts in A10 contained fragments of freshwater diatoms. The fragmented nature of the specimens supports a depositional environment of overbank silts (Table 1).

Diatoms from A8 (Fig. 1C) at 5.8 m below the surface indicated the enclosing silts were deposited in freshwater (Table 1). This was a lower elevation than where estuarine sediments were found downstream at Ota A and A4. We inferred that the location of A8 is probably upstream of the head of the paleo-estuary. Therefore, the distribution of gravels and freshwater sediments left only a small area suitable for drilling. HB1 was drilled on the riverbank next to Ota A, and HB2 is located ~100 m downstream. HB1 was drilled at an elevation of 11.76 m above mean SL (AMSL) and reached a depth of 12 m. HB2 was drilled at an elevation of 11.81 m AMSL and penetrated to 10 m below the surface. All locations within the cores are henceforth referred to by their elevations in metres above mean SL (m AMSL).

5.5.3.2 Cores HB1 and HB2

The sedimentary record preserved in drill cores HB1 and HB2 was subjected to a high-resolution paleoenvironmental study utilising foraminifera, macrofauna, palynology, diatoms and stable isotopes. From the base of both cores (at -0.24 m AMSL in HB1 and 1.9 m AMSL in HB2) up to 3.3 and 4.1 m AMSL in HB1 and HB2 respectively, they are dominated by blue-grey silt with occasional *A. stutchburyi* shells and wood fragments. *A. stutchburyi* is a shallow-burrowing bivalve common, and frequently monospecific, at mid- to low-tide elevations in estuaries and sheltered sand flats (Beu, 2006; Marsden, 2004; Marsden and Pilkington, 1995; Morton and Miller, 1968).

At 3.3 – 4.7 m AMSL in HB1 and 4.1 – 4.7 m AMSL in HB2 there is a unit of medium-coarse grey sand bounded by sharp contacts (Fig. 5). This sandy unit contains wood fragments, coarse shell grit and large *A. stutchburyi* fragments. Above the sand unit up to 7.2 m AMSL (HB1) and 5.2 m AMSL (HB2) is blue-grey silt with occasional *A. stutchburyi* shells and wood fragments. From 7.2 m AMSL (HB1) and 5.2 m AMSL (HB2) up to 8.3 m AMSL both cores are composed of massive silt with occasional wood chips. At ~ 8.3 m in both cores there is a 0.2 m thick silty peat and this is overlain by a fine-grained 10 mm thick tephra. From the tephra up to ~11.6 m AMSL (0.5 m below the surface) there is massive orange-brown silt. At ~11.6 m AMSL there is a 50 mm-thick coarse-grained orange tephra; this is immediately overlain by topsoil.

Fifty-one samples from HB1 were studied for foraminifera. The samples were selected between 10.54 to –0.38 m AMSL, with an average sampling density of 1 per 0.21 m in this interval. Seven samples from above 7.96 m AMSL were barren of foraminifera, as was one sample from below –0.22 m AMSL. Forty samples were selected from HB2 from between 8.12 m to 1.94 m AMSL, a sampling density of one per 0.15 m. Eight samples from above 5.68 m AMSL were barren. In both cores there is a transition from samples containing forams (forams present) to samples barren of forams. We call this the foram P-B (present-barren) transition.

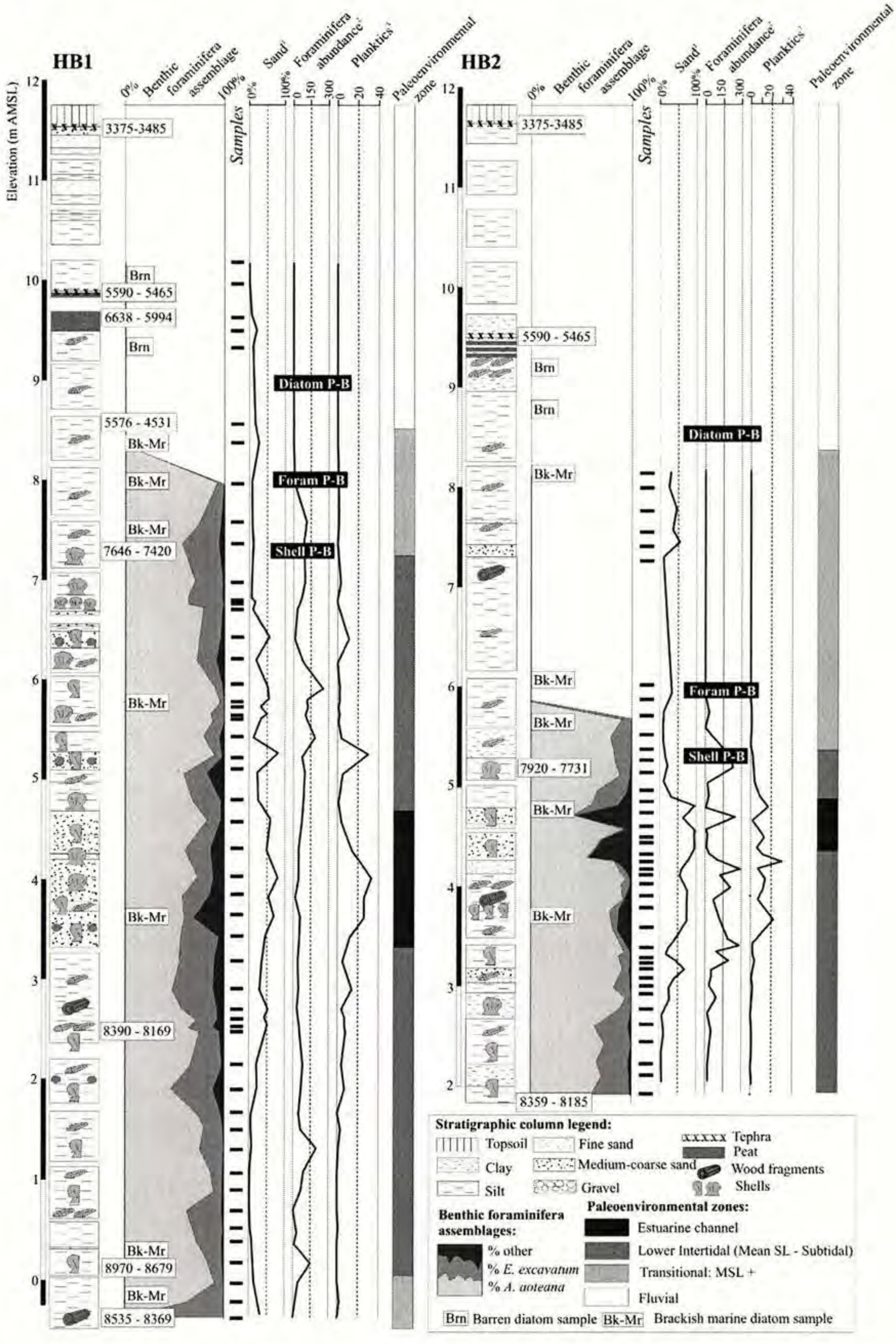

Fig. 5: Cores HB1 and HB2. Stratigraphy, radiocarbon ages, micropaleontology and paleoenvironmental zones. [1] sand = percentage of sediment samples greater than 63 microns, [2] foraminifera abundance = number of benthic foraminifera per gram of sediment, [3] planktics = number of planktics picked per sample.

All samples from HB1 and HB2 containing foraminifera were dominated by *Ammonia parkinsonia f. aoteana* with secondary proportions of *Elphidium excavatum f. excavatum,* and minor amounts of "Other" benthic species (Fig. 5). Common Other species included *Haynesina depressula*, *Elphidium charlottense*, *Notorotalia* species, and *Bulimina* species. *A. aoteana* ranges from 46 – 95% of the assemblage in HB1 and HB2 with an average of 72% in HB1 and 79% in HB2. *E. excavatum* has a range of 1 – 43% and averages 23% in HB1 and 13% in HB2. Others range from 1 – 57%, with an average of 5% in HB1 and 8% in HB2.

A. aoteana is a common species in "brackish to very slightly brackish environments". It is often a dominant species in the intertidal and subtidal zones of the seaward parts of estuaries and mid to inner areas of enclosed harbours (Hayward et al., 1999a). *E. excavatum* is restricted to brackish environments and it usually lives at intertidal depths in the inner-mid zones of estuaries and in enclosed tidal inlets (Hayward et al., 1999a). *H. depressula* is an intertidal, brackish-marine species and *E. charlottense* is a slightly more open-water species. *E. charlottense* occurs most commonly at intertidal-subtidal elevations on sheltered sandy beaches (Hayward et al., 1999a). All the samples analysed for foraminifera assemblages are likely to be from the lower intertidal zone of a sheltered, slightly brackish, estuary.

The change in foraminifera assemblage at the Foram P-B transition is sudden, and there is no gradual decrease in foraminifera abundance approaching this transition (Fig. 5). This transition occurs at a higher elevation than the Shell P-B transition in both cores (0.75 m higher in HB1 and 0.5 m higher in HB2). There is no visual change in core sedimentology at the Shell or Foram P-B transitions. We interpret these transitions to be a gradual environmental change to a less saline or higher elevation setting. It was around this transition that we concentrated sampling for pollen, diatoms, and stable isotopes.

Palynology samples were selected from the HB1 and HB2 cores either side of the foraminifera P-B transition. A sample (HB1/9.86 m AMSL) was taken from a peat unit, and one sample (HB2/1.84 m AMSL) was taken from a unit with abundant *A. stutchburyi* fragments. All samples were dominated by *Cyathea* type pollen with minor amounts of *Podocarpus* type and *Dacrydium cupressinum* pollen (Table 4). These pollen types indicate the regional forest was a lowland podocarp forest, however they yield no information about the environment in the immediate vicinity of the sample location. Pollen from plants such as rushes, sedges, saltwort and mangroves can be indicative of the local environment and have been used elsewhere as corroborative evidence of coastal waterbody and sea level change (Cochran et al., 2006, Goff et al., 2000, Shennan et al., 1994). We conclude that palynology is not suitable for paleoenvironmental interpretation of the HB cores, possibly because the core locations were too far from the estuary margins where saltmarsh plants were growing.

Table 4. Palynological results from Hicks Bay cores, HB1 and HB2.

Core	Elevation (m AMSL)	Monolete spore type	*Cyathea* type	*Dicksonia* type	*Cyperaceae* type	Nothofagus	*Brassica* type	Leptospermum	Poaceae	*Dacrydium cupressinum*	*Podocarpus* type	Ascarina	Phyllocladus	Apiaceae	Olea
HB1	9.96		18				1			4					
HB1	9.86	18	32	3	5	4	1	2	2	22	13	3	2		
HB1	9.36		2												
HB1	8.36		11												
HB1	7.96	5	25							8	2			2	1
HB2	8.82														
HB2	6.02	1	20				1				1				
HB2	5.68	5	6							1					
HB2	1.84	10	25			1				6	4			1	

The highest diatom samples (HB1/9.96, 9.36 and HB2/9.2 and 8.82 m AMSL,) are barren. A barren result from a smear slide means either the diatoms have a very low abundance or they are not present. All other samples from the Hicks Bay cores below HB1/8.36 m AMSL and HB2/8.11 m AMSL contain sparse well-preserved brackish marine diatom assemblages. Abundances were not high enough to warrant full census counts. Above and below the foram P-B transition the diatom assemblages do not change significantly (Table 1). There are several reasons why this is could be so: (1) the foraminifera may not be present in the shallow parts of the cores, above the P-B transition, because of dissolution or extremely low abundances, despite the paleoenvironment remaining the same across the barren-intertidal transition as the diatoms indicate, or (2) there was a small change in salinity across the foram P-B transition that inhibited intertidal foraminifera survival but the environment remained suitable for diatoms.

SEM images of the foraminifera do not provide any strong evidence for poor preservation closer to the foram P-B transition thus suggesting chemical dissolution or mechanical breakage has not been responsible for this transition. This implies the foram P-B transition and the transition from intertidal-shells-present to barren-of-shells is probably a real paleoenvironmental change.

The 31 samples selected for stable isotope study from HB1 span the peat layer (~9.76 m AMSL), the foram P-B transition at 7.96 m AMSL and the start of the *A.*

stutchburyi shells at 7.26 m AMSL (Fig. 6). We selected these samples to test whether C and N isotopic values and ratios showed sensitivity to paleoenvironmental change in the core and if a more detailed study could assist with detecting small paleo-salinity changes. Most of the samples are dominated by silt, though there are some sand samples between 6.8 – 5.8 m AMSL. Variation in sand content does not appear to correlate with any significant isotopic excursion in the sandy regions.

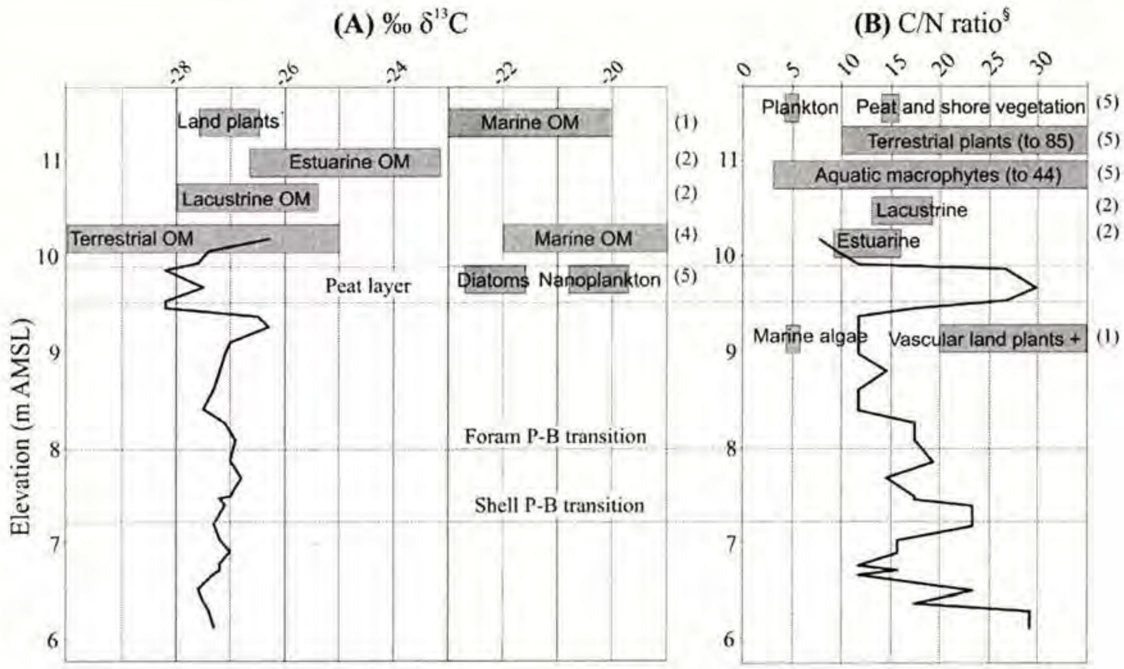

Fig. 6: Stable isotope measurements from the upper 6 m of HB1 with major stratigraphic boundaries marked. (A and B) ‰ $\delta^{13}C$ and C/N ratio of HB1 with superimposed value ranges for terrestrial, estuarine and marine organic matter from several publications. (1) Meyers (1994), (2) Thornton and McManus (1994), (3) Fontugne and Jouanneau (1987), (4) Gearing et al. (1984), (5) Muller and Voss (1999). [1] Land plants with a C4 pathway. § C:N ratio is calculated by an atomic ratio where C:N= $(\%C^{14})/(\%N^{12})$.

Both carbon and nitrogen isotopic values show prominent excursions spanning the peat layer (~-2 m), $\delta^{13}C$ shows an isotopic decrease (Fig. 6A) and C/N increases during this interval (Fig. 6**Fig.** B). The $\delta^{13}C$ plot shows a slight trend toward more negative values below 7.8 m AMSL while the C/N ratio is highly variable below the peat layer but shows an overall increase beneath the foram-P-B transition (Fig. 6).

$\delta^{13}C$ and the C/N ratio have previously been the most useful parameters for distinguishing organic matter provenance (Meyers, 1994; Thornton and McManus, 1994; Muller and Mathesius, 1999). Published observations of freshwater and marine $\delta^{13}C$ values vary slightly, but all agree that marine $\delta^{13}C$ values are higher than freshwater values (Fig. 6A) and higher C/N values are indicative of terrestrial organic matter (Fig. 6B). In both of the HB1 plots of $\delta^{13}C$ and C/N we see the values are not within the range of typical marine organic matter (Fig. 6A, B). We conclude that for the Hicks Bay cores this technique is not a viable tool for distinguishing freshwater and marine paleoenvironments. This is probably because the marine environment at HB was a sheltered intertidal inlet and received a high terrestrial sediment input. We emphasise that this was a test of the technique. Consequently, we have not considered the extent to which the C and N isotopes are affected by factors such as preservation of organic material, transportation, microbial activity, water depth and temperature, water currents, unusual weather events (drought, flood, wind etc). The sharp peaks in all isotopic values at the peat layer indicate that the stable isotopes do reflect significant increases in organic matter. However this is clearly visible in the cores and in this study a quantification of the amount of C (total) is not especially helpful for environmental interpretation and the stable isotopes do not add any higher paleoenvironmental resolution beyond that attained from the microfossils.

5.5.3.3 Age control of Cores HB1 and HB2

Four new radiocarbon dates were collected from the cores, two each from HB1 and HB2 (Table 2). One radiocarbon age was collected from an auger hole at Ota A, and three ages previously collected by Ota et al. (1992) at Ota A have been recalibrated. These four ages from Ota A are directly correlated to their equivalent elevations in HB1 as this core was collected <5 m away from the riverbank exposure. The Waimihia tephra (3485 - 3375 cal. yrs B.P.) is at 11.6 m AMSL in both cores and Whakatane tephra (5590 - 5465 cal. yrs B.P) is at 9.8 m AMSL in HB1 and 9.5 m AMSL in HB2, thus providing additional age control (Fig. 5).

The radiocarbon dates occur in chronological order, younging upwards with increasing elevation, except in two cases (Fig. 5, Table 2). A wood age (5576 – 4531 cal. yrs B.P) collected by Ota et al. (1992) at Ota A/8.6 m is younger than the radiocarbon age from the peat 1.2 m above (6638 – 5994 cal. yrs B.P.) The wood age partly overlaps with and is younger than the Whakatane tephra whereas the peat age is older than the tephra. Due to the overlap with the higher Whakatane tephra, we suggest that the wood age (Ota A/8.6 m) is unreliable and could be a tree root younger than its surrounding sediment. The wood age at HB1/-0.26 m (8535 – 8369 cal. yrs B.P.) is younger than the shell age at 0.42 m above (HB1/0.16 m: 8970 – 8679 cal. yrs B.P.), and it overlaps by 21 years with the 2-σ age of the shell 2.76 m higher at HB1/2.5 m: 8390 – 8169 cal. yrs B.P.). Both shell samples are likely to have been in life position but it is possible that the wood fragment was from a tree root.

The *A. stutchburyi* shell ages are used to date the timing of sediment deposition and for tectonic uplift rate calculations because they are *in-situ* fossils and can be directly related to the paleo-MSL. Observations of the riverbank section adjacent to the HB1 and HB2 core sites (Ota A) from 6.8 m – 7.5 m AMSL are that all the *A. stutchburyi* shells exposed within this section are articulated whole bivalves preserved in growth position. The excellent preservation of the shells in the riverbank, only ~ 5 m from the drill sites allows us to be quite certain that the *A. stutchburyi* fragments retrieved in the cores were formerly whole *in-situ* shells but were broken during drilling or core extrusion, the ability to reconstruct whole shells from the fragments in the further cores supports this. Whilst there have been reported occurrences of transported *A. stutchburyi* found at distances > 20 km from estuaries (Hayward and Stilwell, 1995) these reported shells occurred in association with open beach shell assemblages and only consisted of disarticulated shells. The coupled occurrence of the articulated *A. stutchburyi* fragments with intertidal foraminifera assemblages also suggests the *A. stutchburyi* are *in-situ*. This is further supported by their monospecific occurrence in the cores because *A. stutchburyi* are typically the only species found at intertidal elevations in New Zealand estuaries (Beu, 2006; Healy, 1980). If the *A. stutchburyi* have been reworked then their ages at least represent the maximum age of the enclosing sediment, however for reasons discussed above, we are confident the *A. stutchburyi* are *in-situ* and as such do represent the time of sediment deposition.

5.5.3.4 Hicks Bay Paleoenvironmental Evolution

The sedimentology, foraminifera, macrofauna, and diatom data of the cores is combined to define four paleoenvironmental zones: (1) Estuarine Channel (or Tsunami), (2) Lower Intertidal Estuarine, (3) Fluvial, and (4) Transitional (Fig. 5). The distribution, characteristics and justification for each zone is discussed below.

Estuarine Channel (or Tsunami):

This zone occurs in HB1 at 3.3 – 4.7 m AMSL and at 4.1 – 4.7 m AMSL in HB2 (Fig. 5). The characteristics of this unit are medium-coarse sand, fragmented shells, shell grit, and relatively high proportions of "Other" foraminifera and planktic species. The coarser sand and mechanical breakage of the shells indicates a higher energy depositional environment than the surrounding silts. The high proportion of Other foraminifera, such as the open coast species of *Zealfloris parri* and *Trifarina angulosa* and the high proportion of planktic species, indicates increased hydraulic exchange with the open ocean. We interpret this unit as an estuarine channel because of the evidence of higher energy (tidal currents) and increased open coast hydraulic exchange. This layer also displays several characteristics of a tsunami deposit. For example: it is a distinct sedimentary unit of anomalously coarse sand within silt, the lower contact is sharp and possibly erosional, and it contains deeper water marine foraminifera and is relatively shell-rich (cf. Goff et al., 2001; Goff et al., 2004; Nelson et al., 1996; Shennan et al., 1996). However, we have no data on the spatial extent of the sand layer to test the tsunami theory, for example tsunami deposits typically fine landward (Goff et al., 2001), and the narrow marine inlet of the HB gorge (Fig. C) may restrict the entry of a tsunami into the HB Flats, particularly given eustatic SL was lower than present and the coastline further offshore than present. Future work could focus upon tracing the extent of the sand layer on the HB Flats and correlating the deposit to other coastal locations to resolve this issue. To date no tsunami deposits of ~ 8 ka age have been detected in the region although few studies have been undertaken.

Lower Intertidal:

This zone occurs in HB1 at 0 – 3.3 m and 4.7 – 7.2 m AMSL, and in HB2 at 1.9 – 4.2 m and 4.7 – 5.2 m AMSL (Fig. 5). Sediments of this zone are homogenous blue-grey silts, with scattered *A. stutchburyi* shells (that were probably in-situ prior to drilling disturbance), and occasional small wood fragments. Foraminifera assemblages are dominated by *A. aoteana* and *E. excavatum* and diatom samples are characteristic of brackish marine environments. Our interpretation is of a lower intertidal estuarine paleoenvironment because this is the preferred living environment of the foraminifera and shells. The fine sediment is consistent with deposition in the central part of an estuary where currents generated by both tidal and fluvial energy are at a minimum (Dalrymple et al., 1992).

Fluvial:

The fluvial zone occurs in both cores above 8.5 m AMSL (HB1) and 8.3 m AMSL (HB2) (Fig. 5). Dominated by orange-brown silt, this zone has scattered wood fragments, and both cores contain a 0.1 – 0.3 m thick peat, and two tephra layers. This paleoenvironmental zone is distinguished by a lack of marine indicators: no shells, foraminifera or marine diatoms. The peat layer indicates a fresh water environment existed at least some of the time. The absence of chemical corrosion signals in the foraminifera indicates that groundwater dissolution was not responsible for the absence or calcareous test higher in the cores thus decreased salinity is the most likely reason for their absence. In the cores the silts do not contain any sedimentary structures, however in the adjacent riverbank outcrop some decimetre-thick horizontal layers with gradational contacts can be seen. This is compatible with an overbank fluvial silt depositional environment.

Transitional:

The transitional zone occurs in HB1 between –0.5 – 0 m and 7.2 – 8.5 m AMSL, it is thicker in HB2 where it occurs between 5.2 – 8.3 m AMSL (Fig. 5). Grey-brown silt dominates this zone; there are no shells or foraminifera. However, the diatoms indicate a brackish marine environment. We interpret this as a transitional environment between the intertidal and fluvial environments. Salinity levels probably decreased below the threshold for the foraminifera and shells, but allowed diatoms to persist. Alternatively the diatoms, which are more readily transported, could have been redeposited in this environment.

The early Holocene paleogeography and associated sedimentary infilling of the Hicks Bay Flats can be inferred from the sequence of paleoenvironmental zones and radiocarbon ages in cores HB1 and HB2 and supplemented by outcrop and auger hole data (Fig. 5, Supplementary Data A). We divide the valley evolution into 8 stages (Fig. , 1-8), and this follows a typical incised valley infill sequence of fluvial to estuarine and a return to fluvial conditions following eustatic SL stabilisation (*cf.* Roy 1984; Dalrymple et al. 1992; Allen and Posamentier 1993).

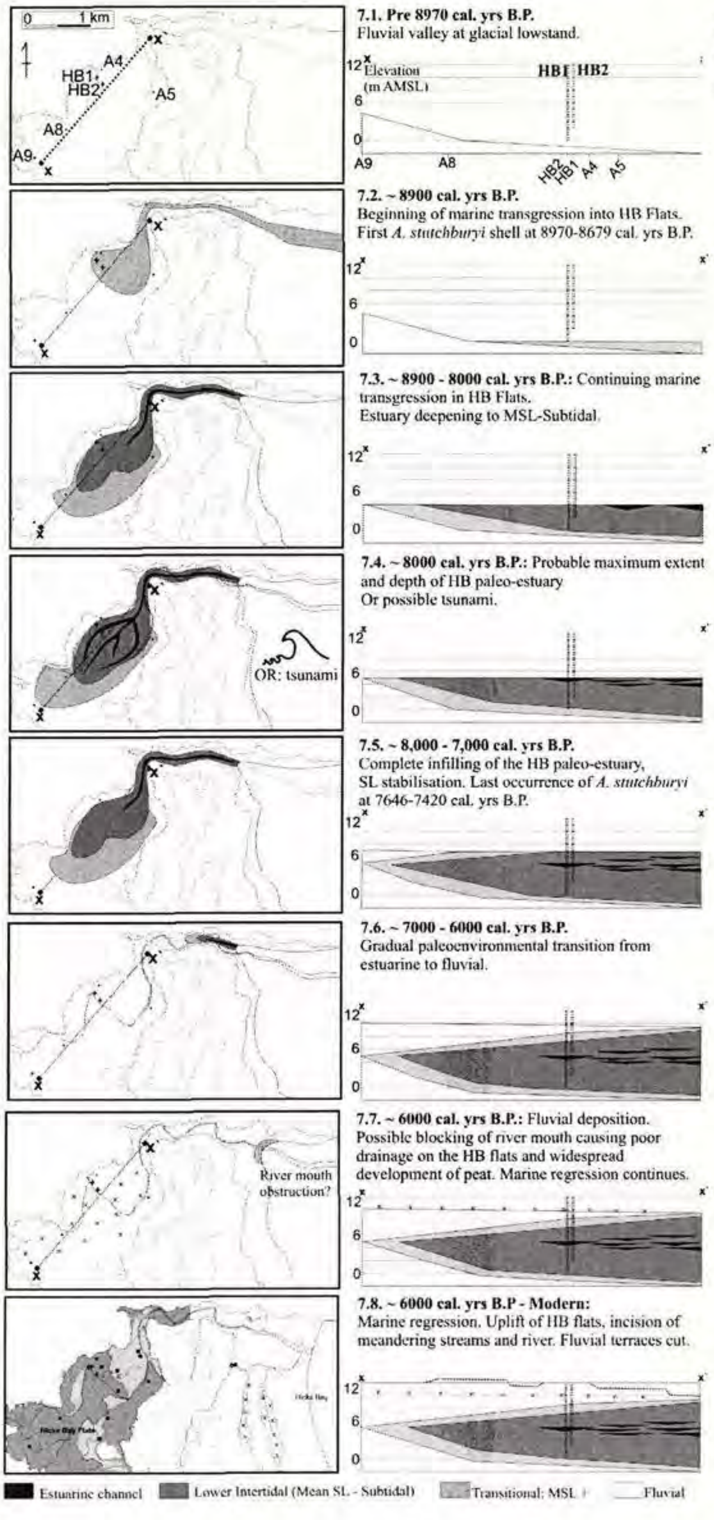

Fig. 7: Paleogeographic evolution of the Hicks Bay Flats in plan and stratigraphic profile view.

Uplift rates, from five shell samples in HB1, HB2 and the riverbank exposure next to HB1, range from 0.9-2.2 mm yr^{-1}, with an average of 1.7 mm yr^{-1} (Table 5). We use only the radiocarbon ages from *A. stutchburyi* shells because we are confident these are in-situ (compared to the wood samples), and for the purposes of calculating accommodation space deficits the *A. stutchburyi* are most likely to have been living at equivalent elevations. *A. stutchburyi* have a living depth range of mid- to low-tide elevations (Beu, 2006; Healy, 1980). In calculating uplift rates we use a living depth of –0.42 ± 0.42 m for the *A. stutchburyi*, which accounts for the shells living at an elevation midway between mid and low tide with a 95% uncertainty spanning the mid-low tide range of 0.85 m (the spring tidal range at HB is 1.7 m, therefore mid-low tide elevations are 0 - -0.85 m AMSL). We suggest that the *A. stutchburyi* are *in-situ*, however if they have been transported they are most likely to have been moved to deeper marine environments, therefore the uplift rates presented here would be minimum rates. The Gibb (1986) eustatic SL curve is used to estimate the position of eustatic SL at the time that the *A. stutchburyi* were living (Fig. 8). Whilst subject to relatively large uncertainties, the Gibb (1986) curve is based upon data collected from tectonically stable regions of New Zealand and is preferable for use in this study in contrast to using a global eustatic SL curve.

Table 5. Tectonic uplift rate calculations from HB. To calculate these uplift rates we estimate the amount of vertical motion, relative to MSL, that each radiocarbon dated sample has been through since its deposition. We use a living depth of -0.42 ±0.42 m AMSL for the living depth of the *A. stutchburyi* (this assumes the shells are in-situ which we judge to be true). The Gibb (1986) New Zealand eustatic SL curve is used estimate the position of eustatic SL at the time of sample deposition with an estimated uncertainty of ± 2 m.

Radiocarbon sample	Present elevation (m AMSL)	Living depth (m)	Age (ka)[1]	Eustatic SL change since deposition (m)[2]	Total uplift since deposition (m)[3]	Uplift rate (mm/yr)[4]	Uplift rate range[5]
Ota A/7.2 m	7.2 ± 0.3	-0.42 ± 0.42	7646 - 7420	2.1 ± 2	8.88 ± 2.07	1.18	0.89-1.48
Ota A/2.5 m	2.5 ± 0.3	-0.42 ± 0.42	8390 - 8169	14.1 ± 2	16.18 ± 2.07	1.95	1.68-2.23
HB1/0.16 m AMSL	0.16 ± 0.3	-0.42 ± 0.42	8970 - 8679	17.5 ± 2	17.24 ± 2.07	1.95	1.69-2.22
HB2/5.2 m AMSL	5.2 ± 0.3	-0.42 ± 0.42	7920 - 7731	6 ± 2	10.78 ± 2.07	1.38	1.1-1.66
HB2/1.9 m AMSL	1.9 ± 0.3	-0.42 ± 0.42	8359 - 8185	14.1 ± 2	15.58 ± 2.07	1.88	1.62-2.16

[1] 2-sigma calibrated radiocarbon age (see Table 2).
[2] Estimated from the Gibb, 1986, eustatic SL curve using the midpoint of the 2-sigma calibrated age and projecting this to the middle of the eustatic SL points (see Fig. 9). We estimate an uncertainty of ± 2 m for estimates of the past eustatic SL using this Holocene SL curve.
[3] Total uplift = (present elevation + eustatic SL change) – living depth. Uncertainty = sum of the squares of the errors of sample elevation, living depth and eustatic SL change estimate.
[4] Uplift rate = total uplift/mid-point of the 2-sigma calibrated radiocarbon age.
[5] Uplift rate range = [(total uplift + 2m)/youngest radiocarbon age] – [(total uplift – 2m)/oldest radiocarbon age)].

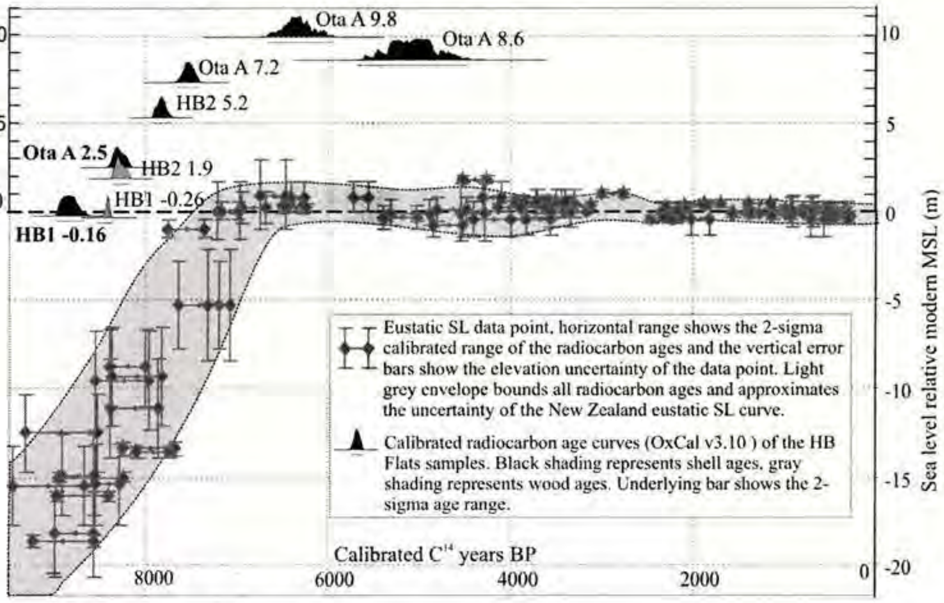

Fig. 8: New Zealand Holocene sea level curve (grey cross-hair data points, after Gibb, 1986) with radiocarbon ages from the HB Flats plotted at their present elevation relative to modern MSL (with an uncertainty of ± 0.3 m). The elevation of the HB Flats radiocarbon ages above the eustatic SL curve represents the total amt of tectonic uplift since sample deposition. Radiocarbon ages plotted using OxCal v3.10 Bronk Ramsey (2005), wood samples calibrated using Southern Hemisphere Atmospheric data from McCormac et al (2004) and shell samples calibrated using Marine data from Hughen et al (2004).

5.6. Discussion: Uplift mechanisms of the northeastern Raukumara Peninsula

5.6.1 Evidence of coseismic uplift

Several lines of evidence have been presented to show the northeastern Raukumara Peninsula has undergone tectonic uplift throughout the Holocene. The critical question we seek to address is how this uplift is achieved? Namely, by sudden, coseismic events, the commonly accepted uplift mechanism for the rest of the Hikurangi margin, or by gradual, aseismic mechanisms?

The most familiar evidence for coseismic coastal uplift along the Hikurangi margin, and globally, are marine terraces whereby the terrace strath is an abandoned surface and the riser approximates the single-event uplift. The terraces at Waipapa and Horoera display a stepped morphology similar to coseismic marine terraces southward along the margin such as at the Pakarae River mouth and Mahia Peninsula (Ota et al., 1991, Berryman, 1993, Wilson et al., 2006) therefore the same uplift mechanism was assumed by Ota et al. (1992). However, the detailed coverbed sedimentology and topographic data we collected is not compatible with the Waipapa and Horoera terraces having a marine origin.

Marine terraces are typically covered in marine deposits such as well-sorted sands, gravels, shells and/or shell hash, comparable to sediments of the modern beach adjacent to the terraces (eg. Hull, 1987; Ota et al., 1991; Berryman, 1993; Wilson et al., 2006). In contrast, no marine deposits were found on any of the Horoera terraces except at the base of Terrace 1. Terraces 2-5 have coverbeds exclusively of silt. The modern beach at Horoera displays a mixture of exposed mudstone platform with abundant rock-boring shells, and coarse shelly sands. We infer that the silt cover on the Horoera terraces is not of marine origin because: (a) it has no modern analogue on the Horoera coastline, (b) it is poorly sorted and fine-grained, not characteristic of wave deposited sediments; and (c) there are no shells within the silt. In contrast the Waipapa terraces are mantled by thick deposits of homogenous medium-fine grained well-sorted sand, these are most likely to be dune sands as the modern beach consists of medium-coarse sand with scattered shells. Auger W4a was the only one to reach the bedrock platform at Waipapa and no coarse sands or shells were encountered on the strath.

The detailed topography of the Waipapa and Horoera terraces also suggests they are not of marine origin. At Horoera the terrace risers appear to be superficial features that do not involve bedrock incision; across the most distinctive terrace riser (that between terraces 3 – 2) there is no accompanying step in the bedrock below it (Fig. 2). The silt coverbeds and observation that the terraces increase in elevation eastward toward the current position of the Mangakino Stream suggests an alluvial fan origin, rather than marine. The stepped surface morphology may have been created by intermittent stream flooding rather than coseismic uplift. Augers H1 and H2, and exposures along the beach at Horoera and in the Mangakino Stream show that Terrace 1 has ~0.5 m of mudstone gravel with rare whole shells on the bedrock strath. It is from this terrace that a shell radiocarbon age of <250 yrs B.P. was obtained by Ota et al. (1992). A marine environment may have covered the bedrock there at some stage, though the bedrock strath was not necessarily wave cut. Moreover, the shells there could be anthropogenic deposits. The Raukumara Peninsula region was settled by Maori 800 – 500 yrs B.P (McGlone et al., 1994). Numerous pas (fortified places) along the coastline attest to Maori occupation of the Horoera area, thus the shells on Terrace 1 could be part of midden deposits.

At Waipapa each terrace has a differing coast-parallel slope inconsistent with wave-cut platform creation (Fig. 3). A degree of along-strike tilt on terraces could be anticipated if uplift of the terraces was controlled by a nearby fault causing differential uplift, or if there was preferential deposition of sediment at one end of a terrace due to alongshore drift or prevailing winds. However, opposing directions of tilt on different terraces is difficult to account for. We suggest the Waipapa terraces are probably depositional landforms created by sand dunes that have been shaped into a terrace-like form by either anthropogenic alterations (the site is close to a Maori pa, these are commonly terraced as part of the fortifications or for cultivation) or fluvial processes.

This re-assessment of the Horoera and Waipapa terraces as non-marine means that they do not provide any evidence of coseismic uplift in this part of the Raukumara Peninsula, as was inferred by Ota et al. (1992). Nonetheless, a wood radiocarbon sample, collected by Yoshikawa et al. (1980) from an riverbank exposure along the Waipapa Stream (labelled "Yoshikawa outcrop", Fig. 1A), indicates this area still has a high coastal uplift rate. The sample had an age of 9900-9400 cal. yrs B.P. and was collected from silt containing marine and estuarine diatoms at 7 m AMSL. This equates with an uplift rate of 2.7 – 3.3 mm/yr (using 22 ± 2 m of eustatic SL rise, Gibb, 1986). The lack of marine terraces indicates that this rapid coastal uplift is either not being accommodated by coseismic movements, or slope and fluvial processes have removed the marine terraces. To further investigate uplift mechanisms of this region this we examine the beach ridge sequence at TA where the wide (>2km) coastal plain suggests there has been no coastal erosion.

It is most likely that the TA beach ridges have accreted since SL stabilisation at ~7 ka therefore the present elevation of the relict beach ridges is the product of tectonic uplift. The decrease in ridge elevation seaward dictates that uplift occurred during accretion of the coastal plain. If the beach ridge sequence was uplifted by discrete coseismic events then, like marine terraces, a step should be present in the sequence. Ota et al. (1992) observed two 2 m scarps at the seaward edge of beach ridge Zones 3 and 4. Their profile was in the same location as our TA South profile. While the equivalent scarps can be seen in the TA South profile, it is important to note that they do not actually equate with a 2 m step in the overall elevation of the beach ridges. Across the width of the swamps adjacent to these scarps (S3 and S4) there is only a slight change in beach ridge elevation (0.5 m across S3 and <0.2 m across S4, Fig. 4C). Three marine terraces on the Hicks Bay coastal plain were mapped by Ota et al. (1992) based on steps identified in aerial photographs. By comparisons to TA we infer the steps recognised by Ota et al. (1992) are those at the landward edge of swamps and like at TA, there is probably no significant net elevation change across the swamps.

With no evidence of coseismic steps in the terrace and beach ridge sequences of the northeastern Raukumara Peninsula we finally question whether the paleo-estuary infill sequence of the HB Flats can be used to elucidate tectonic uplift mechanisms. Estuarine, salt marsh and tidal inlet sediments have been used at subduction zone margins globally to document land elevation changes associated with earthquakes [for example: Atwater (1987); Clague (1997); Darienzo et al. (1994); Hayward et al. (2004a); Nelson et al. (1996); Shennan et al. (1996); Sherrod et al. (2000)] and on passive coasts to document eustatic sea level (SL) changes and glacio-isostatic vertical land movements [for example: Bratton et al. (2003); Dawson et al. (1998); Dawson and Smith (1997); Shennan et al. (1994); Shennan et al. (1995)].

The Hicks Bay paleo-estuary infill sequence has been uplifted either during or since deposition at rates of 0.9 – 2.2 mm yr^{-1} (Table 5, Fig. 8). If this uplift was caused by coseismic mechanisms, we predict the events would be recorded by (1) a sudden paleoenvironmental change reflecting an increase in land elevation. For example, a change from subtidal to MSL elevation or higher, and a freshening of the aquatic environment would be expected. Or (2) an unconformity should occur if the uplifted sediments were exposed subaerially and eroded. During deposition of the early Holocene HB Flats sequence eustatic SL was rising. An uplift event would therefore be recorded as a negative sea level tendency (a marine regression) within a sequence predominantly displaying a positive sea level tendency (a marine transgressive sequence).

Referring back to the record of paleoenvironmental change from the HB cores and examining the sequence in terms of possible uplift events there is only one significant sharp contact: that between lower intertidal sediments and the subtidal estuarine channel (the coarse sand layer at ~ 4 m AMSL in HB1 and HB2, Fig. 5). This sharp sedimentary contact is discounted as being an uplift event because (a) the inferred paleoenvironment goes from lower intertidal to possibly subtidal – a positive sea level tendency consistent with rising eustatic SL; and (b) the sharp contact may represent with scouring at the base of a tidal channel, or tsunami deposition. All other paleoenvironmental zone contacts are gradational.

In the absence of sharp contacts and unconformities in the HB1 and HB2 cores we assess whether there are any marine regressions that may indicate an uplift event. There is only one gradational contact during the time period of rising SL where a negative SL tendency is inferred from the paleoenvironmental data: at ~ 8 – 7 ka where the environment changes from possibly subtidal to lower intertidal (Stage 5, Fig. 7). This transition is sustained therefore it was unlikely to have been an uplift event (which would cause a relatively short-lived sea level regression). The sustained and gradual nature of the paleoenvironmental transition is more likely to be normal infilling of the estuary. That the subtidal-intertidal transition is followed by a gradual change to a fluvial environment coincident with the stabilisation of SL supports an estuary infilling cause for the marine regression.

5.6.2 Alternative uplift mechanisms

The Holocene geomorphic and sedimentary data of the northeastern Raukumara Peninsula coastal region has not yielded evidence of coseismic uplift events, therefore alternative mechanisms of uplift are now considered. Two alternative scenarios are (1) continuous and gradual aseismic uplift and (2) frequent events causing small amounts of uplift that cannot be individually detected by our study methodology.

The TA beach ridge morphology is consistent with a gradual uplift mechanism. The beach ridge sequence displays a seaward slope, implying uplift during beach ridge accretion and progradation. Under a constant uplift process the each new ridge probably forms when the previous ridge reaches a threshold height above MSL. Frequent, small magnitude uplift events as a cause of beach ridge uplift cannot be discounted, but the large number of ridges implies a frequency of events not supported by the historical seismicity catalogue. For example, in zone Z5 and Z4 of the TA South Profile there are 16 beach ridges, a radiocarbon age from the S3 swamp implies all these ridge are less than 1058-934 cal. yrs B.P. This implies a frequency of coastal-uplift causing events of 58 – 66 years yet the historical record, extending back 150 years records only a maximum earthquake size of M_S 6.7 (East Cape, 1914, Dowrick and Smith, 1990) and there is no record of this event causing coastal uplift.

There are several changes in the mean slope of the beach ridge zones; the gradients vary between 0.24 m – 0.7 m per 100m (Fig. 4C). Such changes in slope could be due to (1) uplift rates varying through time, or (2) sediment supply varying through time. Zone 5 has the lowest gradient of 0.24 m/100m and radiocarbon ages suggest this zone is <650 cal. yrs B.P. This age is approximately coincident or slightly post-dates the arrival of Maori in the region (McGlone et al., 1994; Wilmshurst, 1997). Sedimentation pulses have been recorded in several lake cores from the eastern North Island associated with the arrival of Maori and land clearance by fires (Eden and Page, 1998; Wilmshurst, 1997). The rapid development of beach ridge Zone 5 at TA could be in response to enhanced sediment supply due to land burning and clearance by the Maori settlers. This correlation between probable increased sediment supply and lower gradient beach ridge zone suggests that sediment supply is the dominant control on the slope of the beach ridge zones, rather than varying uplift rates.

The estuarine sequence underlying the HB Flats contains no distinct stratigraphic changes that one might attribute to a sudden uplift event. However, we need to consider what the minimum amount of uplift is that would be resolvable with the available data in order to distinguish between continuous and punctuated uplift mechanisms. Most of the sediment in the HB1 and HB2 cores is from a lower intertidal environment. The spring tidal range of HB is 1.7 m and therefore, most of the sediment was deposited between 0 – -0.85 m relative to MSL. Assuming no post-uplift erosion, >0.85 m of uplift would be needed to completely convert this paleoenvironmental zone to an elevation greater than MSL. However, our paleoecological proxies do not resolve a MSL – high tide foraminiferal assemblage. If an uplift event did change the paleoenvironment to above MSL then it would probably be recognisable as a section barren of foraminifera within the lower intertidal sequence. Our sampling resolution of 1 sample per 0.21 m (HB1) or 0.15 m (HB2) is sufficiently dense that we do not think we would have missed such an event. An uplift event of >1.7 m would have elevated the sequence above the high spring tide level. An unconformity, a paleosol or a foraminifera-barren section would probably record subaerial exposure.

This means that uplift of the HB Flats has been accommodated either by constant, gradual uplift, or in intermittent uplift events of <1.7 m, and probably <0.85 m presuming we could recognise a paleoenvironmental change from lower intertidal to MSL-high tide. We can detect if, and approximately how much, uplift occurred during deposition of the sequence by comparing the thickness of sediment preserved with the amount of accommodation space created by eustatic SL rise during the equivalent time period (the accommodation space concept is illustrated in Fig. 9). If no uplift occurred during deposition of the sequence then the thickness of intertidal sediment should approximately equal the amount of space created in the estuary by eustatic SL rise. This assumes that sedimentation within the paleo-estuary approximately kept pace with the rising eustatic sea level. Our paleoenvironmental data shows that within the marine-influenced portion of the cores this is a valid assumption because the foraminifera assemblages consistently represent a lower intertidal environment (with the exception of the thin sedimentary unit representing a tidal channel or tsunami, both of which are still consistent with a lower intertidal elevation).

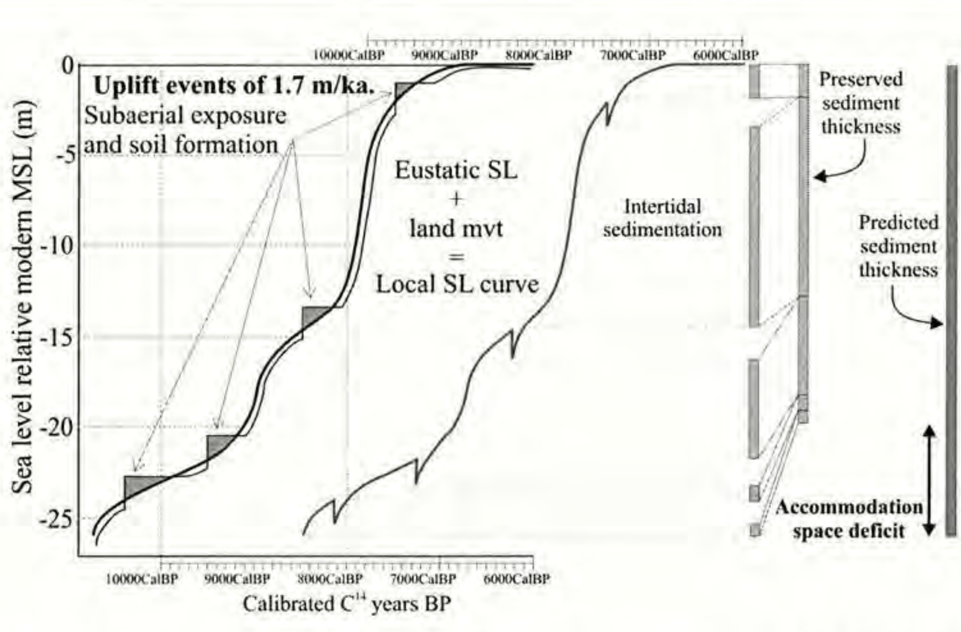

Fig. 9: Cartoon depicting the hypothetical development of a relative SL curve for a site undergoing coseismic uplift during eustatic SL rise. This is based on an uplift rate of 1.7 mm/yr, equating with one uplift event of 1.7 m per ka, it assumes all uplift is accommodated by coseismic movement with no interseismic vertical movement, and that there is no post-uplift erosion of the sequence. This shows how the relative SL curve would have a dominantly positive SL tendency, punctuated by sudden, and short-lived SL falls. If sedimentation kept pace with SL rise then this would result in a lesser thickness of sediment deposited relative to the amount of space created by eustatic SL rise - termed the "accommodation space deficit".

The large uncertainties associated with the eustatic SL curve, and to a lesser degree, with the radiocarbon ages, mean that calculating the exact amount of sediment "missing" within each core is subject to large uncertainties. Post-depositional sediment compaction is not accounted for in the calculations of accommodation space deficits as we consider this to be minor compared with the magnitude of the deficits in question. A study by Paul and Barras (1998) of a sequence of Holocene silty clays with shelly lenses, similar to the Hicks Bay core sediments, found that over a 20 m thickness of sediment a maximum of 2.5 m of correction was required to approximately recalibrate the sediment depths for the affects of compaction. This equates with a mid-section correction of ~10% of the bed thickness (Paul and Barras, 1998).

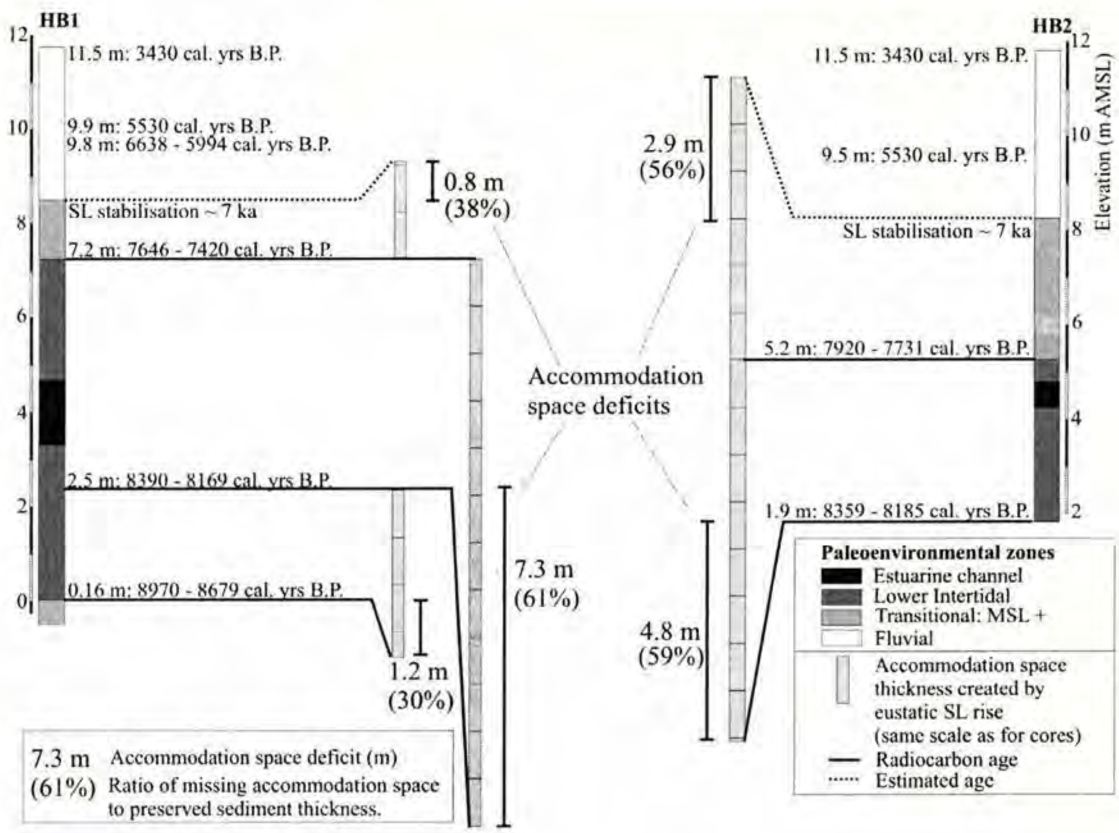

Fig. 10: Thickness of intertidal sediment in HB1 and HB2 compared with the thickness of accommodation space created by rising eustatic SL during the same time period. The elevations within cores HB1 and HB2 have an uncertainty of 0.3 m, estimates of past eustatic SL have an uncertainty of +/- 2 m and are from the Gibb (1986) New Zealand SL curve, shown in Fig. 8.

The available data suggests a consistent accommodation space deficit of ~ 30-60%, over five varying time periods (Fig. 10). The most plausible explanation for this is gradual uplift synchronous with sediment deposition. If uplift had occurred intermittently then periods of time where no uplift occurred would be expected.

Future work using drill cores at more marginal locations on the HB Flats may capture tidal-wetland microfaunal assemblages more sensitive to the rates of sea level changes and provide better resolution to quantify coseismic uplifts less than 0.85 m if they did occur. However, the absence of chaotic or disturbed sedimentary layers within the paleo-estuary sequence suggests there were no environmental perturbations during valley infilling as you might expect earthquake shaking to produce.

To re-assess which of the two uplift mechanisms are most likely for the northeastern Raukumara Peninsula - gradual, aseismic uplift or frequent small events – both the TA beach ridge sequence and the HB paleo-estuary sequence support an aseismic uplift mechanism. Frequent, small events cannot be discounted given the resolution of our data but this is not supported by the relatively undisturbed HB Flats sedimentary sequence or the historical seismicity record of the region.

5.6.3 Global examples of aseismic tectonic uplift and seismic hazard implications.

The recognition of aseismic mechanisms as the most likely driver of tectonic uplift of the northeastern Raukumara Peninsula is significant in a global context as there are very few examples of this worldwide. This location provides us with a valuable contrast to the comparatively well-documented occurrence of coseismic coastal movements associated with great earthquakes at subduction margins with similar rates of plate convergence (e.g. Cascadia and the Nankai Trough). Glacio-isostatic adjustments at high-latitude locations can produce uplift rates at similar magnitudes to, and higher than, the uplift rates recorded in the NE Raukumara Peninsula (for example; Berglund, 2005; Ekman and Makinen, 1996; Forman et al., 2004; James et al., 2000; Larsen et al., 2004; Miettinen, 2004). Aseismic and coseismic uplift mechanisms have contributed to coastal uplift at rates up to 10 mm yr^{-1} at Isla Mocha, Chile (Nelson and Manley, 1992). Both mechanisms of uplift were attributed to rupture and creep on an inferred offshore imbricate thrust fault. Aseismic coastal uplift at ~1 mm/yr has been recorded at eastern Kyushu, Japan, where it has been related to subduction of a buoyant body, the Kyushu-Palau Ridge (Nakada et al., 2002, and references therein). Similar to Kyushu, aseismic uplift of the NE Raukumara Peninsula is probably related to subduction of a buoyant body, namely, the Hikurangi Plateau and associated sediment underplating. The geodynamic significance of this and the relationships between plate coupling and upper plate deformation mechanisms is to be explored further in a following paper (Wilson et al., in preparation).

Identification of aseismic processes accommodating uplift in the NE Raukumara Peninsula region contributes to resolving the seismic hazard of this area. With no large to great subduction zone earthquakes in historical times the Hikurangi subduction zone interface is a significant source of uncertainty in national seismic hazard assessments (Stirling et al., 2002). This study shows there have been no coseismic coastal uplift events, therefore implying no large to great earthquakes have been generated either on the subduction interface or by offshore upper plate faults during the Holocene, along this sector of the Hikurangi margin.

5.7. Conclusions

In summary, our interpretation of the Horoera and Waipapa terraces is that they do not have a marine origin. Therefore they do not provide evidence of coseismic coastal uplift. How then, is the rapid uplift (at rates of 0.5 – 3.3 mm yr^{-1}) achieved? The TA beach ridge sequence does not display any steps indicative of significant coseismic uplift events. Rather, the gradient of the beach ridge zones is approximately constant with small variations probably related to sediment supply fluctuations superimposed on a background uplift rate. The paleoecology of the HB transgressive sequence shows no evidence of coseismic uplift events of a magnitude >0.85 m; all paleoenvironmental transitions appear to be gradational. Accommodation space deficits at varying time intervals indicate that uplift occurred throughout deposition of the HB Flats sedimentary infill sequence.

This combination of different methodologies applied to varying time periods at four different coastal locations leads to our conclusion that a continuous, aseismic process has driven Holocene coastal uplift of the NE Raukumara Peninsula. This is an important outcome for several reasons. Firstly, it is a rare example of aseismic tectonic mechanisms driving coastal uplift in a global context. The second significant implication of these results is that we have shown that Holocene coastal uplift mechanisms do vary along the East Coast of the North Island. This implies that similar coastal geomorphology (for example, raised terraces, wide coastal plains and uplifted estuaries) can be produced by different tectonic processes. Recognition of this brings some reconciliation to the former inconsistency of similar Holocene coastal tectonic processes along the Hikurangi margin, despite the apparent contrasts in upper plate structures.

5.8. Acknowledgements

This research was funded by the Earthquake Commission (Project 6UNI/501). KJW was supported by the GNS Science Sarah Beanland Memorial Scholarship. Peter Barker, assisted by Matt Hill, carried out the drilling. Alvaro Gonzalez and Ruth Wightman provided field assistance. John Begg is thanked for providing the calibrated radiocarbon ages of the Gibb, 1986, eustatic SL data. Bill McLea provided the palynology information, Bruce Hayward and Ashwaq Sabaa are thanked for assisting with foraminifera identification and Karyne Rogers is thanked for her assistance and advice with the stable isotope study. The manuscript was improved by reviews by two anonymous reviewers.

5.9. References

Atwater, B. F., 1987. Evidence for great Holocene earthquakes along the outer coast of Washington State. Science 236, 942-944.

Allen, G. P. and Posamentier, H. W., 1993. Sequence stratigraphy and facies model of an incised valley fill: the Gironde estuary, France. Journal of Sedimentary Petrology 63, 378-391.

Berglund, M., 2005. The Holocene shore displacement of Gastrikland, eastern Sweden: a contribution to the knowledge of Scandinavian glacio-isostatic uplift. Journal of Quaternary Science 20, 519-531.

Berryman, K. R., 1993. Age, height, and deformation of Holocene terraces at Mahia Peninsula, Hikurangi subduction margin, New Zealand. 1. Tectonics 12, 1347-1364.

Beu, A. G., 2006. Marine Mollusca of oxygen isotope stages of the last 2 million years in New Zealand. Part 2. Biostratigraphically useful and new Pliocene to Recent bivalves. Journal of the Royal Society of New Zealand 36, 151-338.

Bratton, J. F., Colman, S. M., Thieler, E. R., and Seal II, R. R., 2003. Birth of the modern Chesapeake Bay estuary between 7.4 and 8.2 ka and implications for global sea level rise. Geo-Marine Letters 22, 188-197.

Clague, J. J., 1997. Evidence for large earthquakes at the Cascadia subduction zone. Reviews of Geophysics 35, 439-460.

Cochran, U., Berryman, K., Mildenhall, D., Hayward, B., Southall, K., Hollis, C., Barker, P., Wallace, L., Alloway, B., and Wilson, K., 2006. Paleoecological insights into subduction zone earthquake occurrence, eastern North Island, New Zealand. Geological Society of America Bulletin 118, 1051-1074.

Dalrymple, R. W., Zaitlin, B. A., and Boyd, R., 1992. Estuarine facies models: conceptual basis and stratigraphic implications. Journal of Sedimentary Petrology 62, 1130-1146.

Darienzo, M. E., Peterson, C. D., and Clough, C., 1994. Stratigraphic evidence for great subduction-zone earthquakes at four estuaries in Northern Oregon, U. S. A. Journal of Coastal Research 10, 820-876.

Dawson, S., Dawson, A. G., and Edwards, K. J., 1998. Rapid Holocene relative sea-level changes in Gruinart, Isle of Islay, Scottish Inner Hebrides. The Holocene 8, 183-195.

Dawson, S., and Smith, D. E., 1997. Holocene relative sea-level changes on the margin of a glacio-isostatically uplifted area: an example from northern Caithness, Scotland. The Holocene 7, 59-77.

De Mets, C., Gordon, R. G., Argus, D. F., and Stein, S., 1990. Current plate motions. Geophysics Journal International 101, 425-478.

De Mets, C., Gordon, R. G., Argus, D. F., and Stein, S., 1994. Effect of recent revisions to the geomagnetic reversal timescale on estimates of current plate motions. Geophysical Research Letters 21, 2191-2194.

Dowrick, D. and Smith, E. G., 1990. Surface was magnitudes of some New Zealand earthquakes 1901-1988. Bulletin of the New Zealand National Society for Earthquake Engineering 23, 198-210.

Eden, D. N., and Page, M. J., 1998. Palaeoclimatic implications of a storm erosion record from late Holocene lake sediments, North Island, New Zealand. Palaeogeography, Palaeoclimatology, Palaeoecology 139, 37-58.

Ekman, M., and Makinen, J., 1996. Recent postgalcial rebound, gravity change and mantle flow in Fennoscandia. Geophysical Journal International 126, 229-234.

Fontugne, M. R., and Jouanneau, J.-M., 1987. Modulation of particulate organic carbon flux to the ocean by a macrotidal estuary: evidence from measurements of carbon isotopes on organic matter from the Gironde system. Estuarine, Coastal and Shelf Science 24, 377-387.

Forman, S. L., Lubinski, D. J., Ingolfsson, O., Zeeberg, J. J., Snyder, J. A., Siegert, M. J., and Matishov, G. G., 2004. A review of postglacial emergence on Svalbard, Franz Josef Land and Novaya Zemlya, northern Eurasia. Quaternary Science Reviews 23, 1391-1434.

Froggatt, P. C., and Lowe, D. J., 1990. A review of late Quaternary silicic and some other tephra formations from New Zealand: their stratigraphy, nomenclature, distribution, volume and age. New Zealand Journal of Geology and Geophysics 33, 89-109.

Garrick, R. A., 1979. Late Holocene uplift at Te Araroa, East Cape, North Island, New Zealand. New Zealand Journal of Geology and Geophysics 22, 131-139.

Gearing, J. N., Gearing, P. J., Rudnick, D. T., Requejo, A. G., and Hutchins, M. J., 1984. Isotopic variability of organic carbon in a phytoplankton-based, temperate estuary. Geochimica et Cosmochimica Acta 48, 1089-1098.

Gibb, J. G. (1986). A New Zealand regional Holocene eustatic sea-level curve and its application to determination of vertical tectonic movements, A contribution to IGCP-Project 200. *In* "Recent Crustal Movements of the pacific Region." pp. 377-395. Bulletin of the Royal Society of New Zealand.

Goff, J. R., Chague-Goff, C., and Nichol, S. L., 2001. Paleotsunami deposits: a New Zealand perspective. Sedimentary Geology 143, 1-6.

Goff, J. R., McFadgen, B. G., and Chague-Goff, C., 2004. Sedimentary differences between the 2002 Easter Storm and the 15th-century Okoropunga tsunami, southeastern North Island, New Zealand. Marine Geology 204, 235-250.

Goff, J. R., Rouse, H. L., Jones, S. L., Hayward, B. W., Cochran, U., McLea, W., Dickinson, W. W., and Morley, M. S., 2000. Evidence for an earthquake and tsunami about 3100-3400 yr ago, and other catastrophic slatwater inundations in a coastal lagoon, New Zealand. Marine Geology 170, 231-249.

Hartley, B. (1996). "An Atlas of British Diatoms." Biopress Ltd, Bristol.

Hayward, B. and Stilwell, J. D., 1995. Floating cockle shells (Austrovenus stutchburyi) - their significance to paleoenvironmental assessments. Tane, 35: 143-148.

Hayward, B. W., Cochran, U., Southall, K., Wiggins, E., Grenfell, H. R., Sabaa, A., Shane, P. R., and Gehrels, R., 2004a. Micropalaeontological evidence for the Holocene earthquake history of the eastern Bay of Plenty, New Zealand, and a new index for determining the land elevation record. Quaternary Science Reviews 23, 1651-1667.

Hayward, B. W., Grenfell, H. R., Reid, C., and Hayward, K. (1999a). "Recent New Zealand shallow-water benthic foraminifera: taxonomy, ecologic dstribution, biogeography, and use in paleoenvironmental assessment." Institute of Geological and Nuclear Sciences Monograph 21. 264 p. Lower Hutt, New Zealand: Institute of Geological and Nuclear Sciences Limited.

Hayward, B. W., Grenfell, H. R., and Scott, D. B., 1999b. Tidal range of marsh foraminifera for determining former sea-level heights in New Zealand. New Zealand Journal of Geology and Geophysics 42, 395-413.

Hayward, B. W., Scott, G. H., Grenfell, H. R., Carter, R., and Lipps, J. H., 2004b. Techniques for estimation of tidal elevation and confinement (~salinity) histories of sheltered harbours and estuaries using benthic foraminifera: examples from New Zealand. The Holocene 14, 218-232.

Healy, W. B. (compiler), 1980. Pauatahanui Inlet - an environmental study. New Zealand Department of Scientific and Industrial Research Information Series 141: 1-198.

Henderson, J., and Ongley, M., 1920. The geology of the Gisborne and Whatatutu Subdivisions, Raukumara Division. New Zealand Geological Survey Bulletin 21.

Hughen, K. A., Baillie, M. G. L., Bard, E., Beck, J. W. , Bertrand, C. J. H., Blackwell, P. G., Buck, C. E., Burr, G. S., Cutler, K. B., Damon, P. E., Edwards, R. L., Fairbanks, R. G., Friedrich, M., Guilderson, T. P., Kromer, B., McCormac, G., Manning, S., Ramsey, B. B., Reimer, P. J., Reimer, R. W., Remmele, S. S., J. R., Stuiver, M., Talamo, S., Taylor, F. W., van der Plicht, J., and Weyhenmeyer, C. E., 2004. Marine04 Marine Radiocarbon Age Calibration, 0–26 Cal Kyr BP. Radiocarbon 46, 1059-1086.

Hull, A. G., 1987. A late Holocene marine terrace on the Kidnappers Coast, North Island, New Zealand: some implications for shore platform development processes and uplift mechanisms. Quaternary Research 28, 183-195.

James, T. S., Clague, J. J., Wang, K., and Hutchinson, I., 2000. Postglacial rebound at the northern Cascadia subduction zone. Quaternary Science Reviews 19, 1527-1541.

Krammer, K., and Lange-Bertalot, H. (1991). "Bacillariophyceae: Achnanthaceae." Gustav Fischer Verlag, Stuttgart.

Krammer, K., and Lange-Bertalot, H. (1999a). "Bacillariophyceae: Bacillariaceae, Epithemiaceae, Surirellaceae." Specktrum Akademischer Verlag, Heidelberg.

Krammer, K., and Lange-Bertalot, H. (1999b). "Bacillariophyceae: Naviculaceae." Specktrum Akademischer Verlag, Heidelberg.

Krammer, K., and Lange-Bertalot, H. (2000a). "Bacillariophyceae: Centrales, Fragilariaceae, Eunotiaceae." Spektrum Akademischer Verlag, Heidelberg.

Krammer, K., and Lange-Bertalot, H. (2000b). "Bacillariophyceae: English and French translation of the keys." Spektrum Akademischer Verlag, Heidelberg.

Larsen, C. F., Motyka, R. J., Freymueller, J. T., Echelmayer, K. A., and Ivins, E. R., 2004. Rapid uplift of southern Alaska caused by recent ice loss. Geophysical Journal International 158, 1118-1133.

Marsden, I. D., 2004. Effects of reduced salinity and seston availability on growth of the New Zealand little-neck clam *Austrovenus stutchburyi*. Marine Ecology Progress Series 266.

Marsden, I. D., and Pilkington, R., 1995. Spatial and temporal variations in the condition of *Austrovenus stutchburyi* Finlay, 1927 (Bivalvia: Veneridae) from the Avon-Heathcote estuary, Christchurch. New Zealand Natural Sciences 22, 57-67.

Mazengarb, C., 1984. The Fernside Fault: an active normal fault, Raukumara Peninsula, New Zealand. New Zealand Geological Survey Record 3, 98-103.

Mazengarb, C., and Speden, I. G. c. (2000). Geology of the Raukumara area. Institute of Geological & Nuclear Sciences 1:250,000 geological map 6. Institute of Geological and Nuclear Sciences Limited, Lower Hutt, New Zealand.

McCormac, F. G., Hogg, A. G., Blackwell, P. G., Buck, C. E., Higham, T. F. G., and Reimer, P. J., 2004. SHCal04 Southern Hemisphere Calibration, 0 - 26 ka cal BP. Radiocarbon 46, 1087-1092.

McGlone, M. S., Anderson, A. J., and Holdaway, R. N. (1994). An ecological approach to the Polynesian settlement of New Zealand. *In* "The Origins of the First New Zealanders." (D. G. Sutton, Ed.), pp. 136– 163. Auckland University Press.

Meyers, P. A., 1994. Preservation of elemental and isotopic source identification of sedimentary organic matter. Chemical Geology 114, 289-302.

Miettinen, A., 2004. Holocene sea-level changes and glacio-isostasy in the Gulf of Finland, Baltic Sea. Quaternary International 120, 91-104.

Moore, P. D., and Webb, J. A. (1978). "An illustrated guide to pollen analysis." Hodder and Stoughton, London.

Moore, P. D., Webb, J. A., and Collinson, M. E. (1991). "Pollen analysis." Blackwell Scientific Publications, Oxford, Boston.

Morton, J., and Miller, M. (1968). "The New Zealand sea shore." Collins, London.

Muller, A., and Mathesius, U., 1999. The paleoenvironments of coastal lagoons in the southern Baltic Sea, I. The application of sedimentary C_{org}/N ratios as source indicators. Palaeogeography, Palaeoclimatology, Palaeoecology 145, 1-16.

Muller, A., and Voss, M., 1999. The paleoenvironments of coastal lagoons in the southern Baltic Sea, II. $d^{13}C$ and $d^{15}N$ ratios of organic matter - sources and sediments. Palaeogeography, Palaeoclimatology, Palaeoecology 145, 17-32.

Nakada, M., Tahara, M., Shimizu, H., Nagaoka, S., Uehira, K., and Suzuki, S., 2002. Late Pleistocene crustal uplift and gravity anomaly in the eastern part of Kyushu, japan, and its geophysical implications. Tectonophysics 351, 263-283.

Nelson, A. R., and Manley, W. F., 1992. Holocene coseismic and aseismic uplift of Isla Mocha, South-Central Chile. Quaternary International 15/16, 61-76.

Nelson, A. R., Shennan, I., and Long, A. J., 1996. Identifying coseismic subsidence in tidal-wetland stratigraphic sequences at the Cascadia subduction zone of western North America. Journal of Geophysical Research 101, 6115-6135.

Ongley, M., and MacPherson, E. O., 1928. The geology of the Waiapu Subdivision, Raukumara Division. New Zealand Geological Survey Bulletin 30.

Ota, Y. (1987). Holocene coastal tectonics of eastern North Island, New Zealand. *In* "A preliminary report on late Quaternary seismo-tectonic movement in the Circum Pacific area, 1st survery (1985/86)."

Ota, Y., Berryman, K. R., Hull, A. G., Miyauchi, T., and Iso, N., 1988. Age and height distribution of Holocene transgressive deposits in eastern North Island, New Zealand. Palaeogeography, Palaeoclimatology, Palaeoecology 68, 135-151.

Ota, Y., Hull, A. G., and Berryman, K. R., 1991. Coseismic uplift of Holocene marine terraces in the Pakarae River area, eastern North Island, New Zealand. Quaternary Research 35, 331-346.

Ota, Y., Hull, A. G., Iso, N., Ikeda, Y., Moriya, I., and Yoshikawa, T., 1992. Holocene marine terraces on the northeast coast of North Island, New Zealand, and their tectonic significance. New Zealand Journal of Geology and Geophysics 35, 273-288.

Patterson, R. T., Hutchinson, I., Guilbault, J.-P., and Clague, J. J., 2000. A comparison of the vertical zonation of diatom, foraminifera, and macrophhyte assemblages in a coastal marsh: implications for greater paleo-sea level resolution. Micropaleontology 46, 229-244.

Paul, M. A. and Barras, B. F. ,1998. A geotechnical correction for post-depositional sediment compression: examples from the Forth valley, Scotland. Journal of Quaternary Science 13, 171-176.

Reyners. M., 1998. Plate coupling and the hazard of large subduction thrust earthquakes at the Hikurangi subduction zone, New Zealand. New Zealand Journal of Geology and Geophysics 41, 343-354.

Round, F. E., Crawford, R. M., and Mann, D. G., 1990. "The Diatoms: Biology and Morphology of the Genera." Cambridge University Press, Cambridge.

Roy, P. S., 1984. New South Wales Estuaries: their origin and evolution. Coastal Geomorphology in Australia, Academic Press Australia: 99-121.

Shennan, I., Innes, J. B., Long, A. J., and Zong, Y., 1994. Late Devensian and Holocene relative sea-level changes at Loch nan Eala, near Arisaig, northwest Scotland. Journal of Quaternary Science 9, 261-283.

Shennan, I., Innes, J. B., Long, A. J., and Zong, Y., 1995. Late Devensian and Holocene relative sea-level changes in Northwestern Scotland: new data to test existing models. Quaternary International 26, 97-123.

Shennan, I., Long, A. J., Rutherford, M. M., Green, F. M., Innes, J. B., Lloyd, J. M., Zong, Y., and Walker, K. J., 1996. Tidal marsh stratigraphy, sea-level change and large earthquakes, I: A 5000 year record in Washington, U.S.A. Quaternary Science Reviews 15, 1023-1059.

Sherrod, B. L., Bucknam, R. C., and Leopold, E. B., 2000. Holocene relative sea level changes along the Seattle Fault at Restoration Point, Washington. Quaternary Research 54, 384-393.

Stirling, M. W., McVerry, G., and Berryman, K. R., 2002. A new seismic hazard model for New Zealand. Bulletin of the Seismological Society of America 92, 1878-1903.

Stuiver, M., and Polach, H. A., 1977. Discussion; reporting of C-14 data. Radiocarbon 19, 355-363.

Thornton, S. F., and McManus, J., 1994. Application of organic carbon and nitrogen stable isotope and C/N ratios as source indicators of organic matter provenance in estuarine systems: evidence from the Tay estuary, Scotland. Estuarine, Coastal and Shelf Science 38, 219-233.

van Dam, H., Mertens, A., and Sinkeldam, J., 1994. A coded checklist and ecological indicator values of freshwater diatoms from the Netherlands. Netherlands Journal of Aquatic Ecology 28, 117-133.

Wallace, L. M., Beavan, J., McCaffrey, R., Darby, D., 2004. Subduction zone coupling and tectonic block rotations in the North Island, New Zealand. Journal of Geophysical Research 109,B12406, doi:10.1029/2004JB003241.

Wilmshurst, J. M., 1997. The impact of human settlement on vegetation and soil stability in Hawke's Bay, New Zealand. New Zealand Journal of Botany 35, 97-111.

Wilson, K.J., Berryman, K.R., Litchfield, N.J. and Little, T.A., 2006. A revision of Mid to Late Holocene marine terrace distribution and chronology at New Zealand's most tectonically active coastal location, Pakarae River, North Island, New Zealand. New Zealand Journal of Geology and Geophysics 49, 477-489.

Wilson, K., Berryman, K., Little, T., Litchfield, N., and Cochran, U., in preparation. Relationship between coastal geomorphology and subduction geodynamics in the Raukumara sector of the Hikurangi subduction zone.

Witkowski, A., Lange-Bertalot, H., and Metzeltin, D., 2000. "Diatom Flora of Marine Coasts I." A. R. G. Gantner Verlag K. G., Ruggell.

Yoshikawa, T., Ota, Y., Yonekura, N., Okada, A., and Iso, N., 1980. Marine terraces and their tectonic deformation on the northeast coast of the North Island, New Zealand. Geographical Review of Japan 53, 238-262.

Wilson et al.

Supplementary material A: Stratigraphic columns from auger holes and sections at Hicks Bay. Locations shown on Fig. 1C.

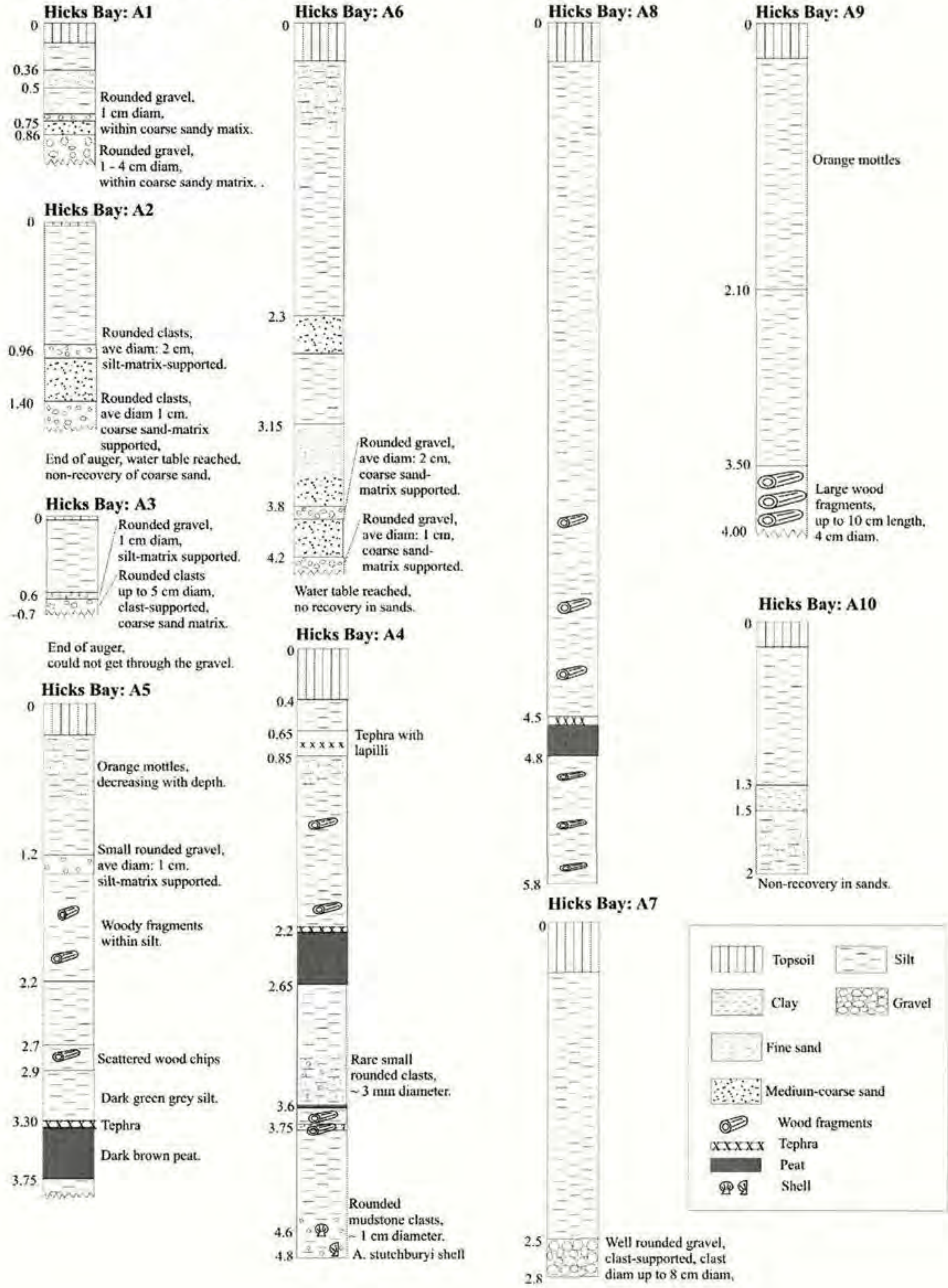

Supplementary Data B: Major element glass geochemistry of tephra from the Te Araroa coastal plain (n = number of glass shards analysed).

	Element										
Sample	**SiO_2**	**Al_2O_3**	**TiO_2**	**FeO**	**MnO**	**MgO**	**CaO**	**Na_2O**	**K2O**	**Cl**	**n**
S1, -0.65 m											
Average	74.8	14.3	0.2	1.7	0.1	0.2	1.9	4.0	2.6	0.1	14
1σ	3.7	2.6	0.1	0.4	0.1	0.1	1.3	0.9	0.6	0.1	
S2a, -2.75 m											
Average	76.0	13.3	0.3	2.0	0.1	0.2	1.5	3.6	2.8	0.2	10
1σ	0.4	0.2	0.0	0.2	0.0	0.0	0.1	0.3	0.1	0.0	
S2a. -0.5 m											
Average	78.1	12.3	0.1	0.9	0.1	0.1	0.6	3.7	3.9	0.2	11
1σ	0.3	0.2	0.0	0.1	0.0	0.0	0.2	0.1	0.3	0.1	

CHAPTER SIX

DISTRIBUTION, AGE AND UPLIFT PATTERNS OF PLEISTOCENE MARINE TERRACES OF THE NORTHERN RAUKUMARA PENINSULA, NORTH ISLAND, NEW ZEALAND.

Published: Wilson, K., Litchfield, N., Berryman, K., Little, T. In press. New Zealand Journal of Geology and Geophysics.

Abstract

The distribution and age of Pleistocene marine terraces fringing the northern Raukumara Peninsula, North Island, New Zealand, is revised. Two terraces, the higher Otamaroa Terrace and the lower Te Papa Terrace, are present from the eastern Bay of Plenty to near East Cape. Six optically stimulated luminescence (OSL) ages obtained from the terrace deposits and coverbeds represent the first radiometric ages from these terraces. Loess from the Te Papa Terrace has an age of 62.6 ± 6 ka and the underlying sand has an age of 58.3 ± 4.1 ka. Four OSL ages obtained from sand resting on the bedrock strath of the higher Otamaroa Terrace range from 64.5 ± 4.7 to 79.2 ± 5.5 ka. These OSL ages suggest that the Te Papa Terrace was formed during early Oxygen Isotope Stage (OIS) 3 and the Otamaroa Terrace was formed during OIS 5a. However, global geomorphological and regional loess unit correlations would imply the extensive Otamaroa Terrace correlates with OIS 5e and the loess on the Te Papa Terrace correlates to the Porewan loess of OIS 4, indicating the Te Papa terrace formed during OIS 5a or earlier. Regardless of terrace age, the morphology of the terraces shows the coastal uplift mechanism is not related to upper plate faults, but is probably driven by deep-seated subduction zone processes.

6.1 Introduction

This study reviews the distribution and chronology of a set of Pleistocene marine terraces that fringe the western and northeastern coasts of the Raukumara Peninsula (Fig. 1A). The geometry and rate of uplift of these terraces contributes to constraining uplift process boundaries operating across the Raukumara Peninsula and adjacent to the Hikurangi subduction margin. We present the first numeric ages obtained from these terraces and use global positioning system (GPS) elevation measurements along with coverbed stratigraphic studies to produce more accurate maps of the terrace surfaces and their uplift patterns. The terraces have previously been studied in some detail before, particularly by Yoshikawa et al. (1980), Iso et al. (1982), Yoshikawa

(1988), and Manning (1995). Therefore, we do not re-describe the details of the covered stratigraphy, origin or distribution of these terraces. Rather we focus on updating these studies by using modern dating techniques in an effort to better resolve the age of the terraces and placing the deformation patterns in a regional geodynamic context.

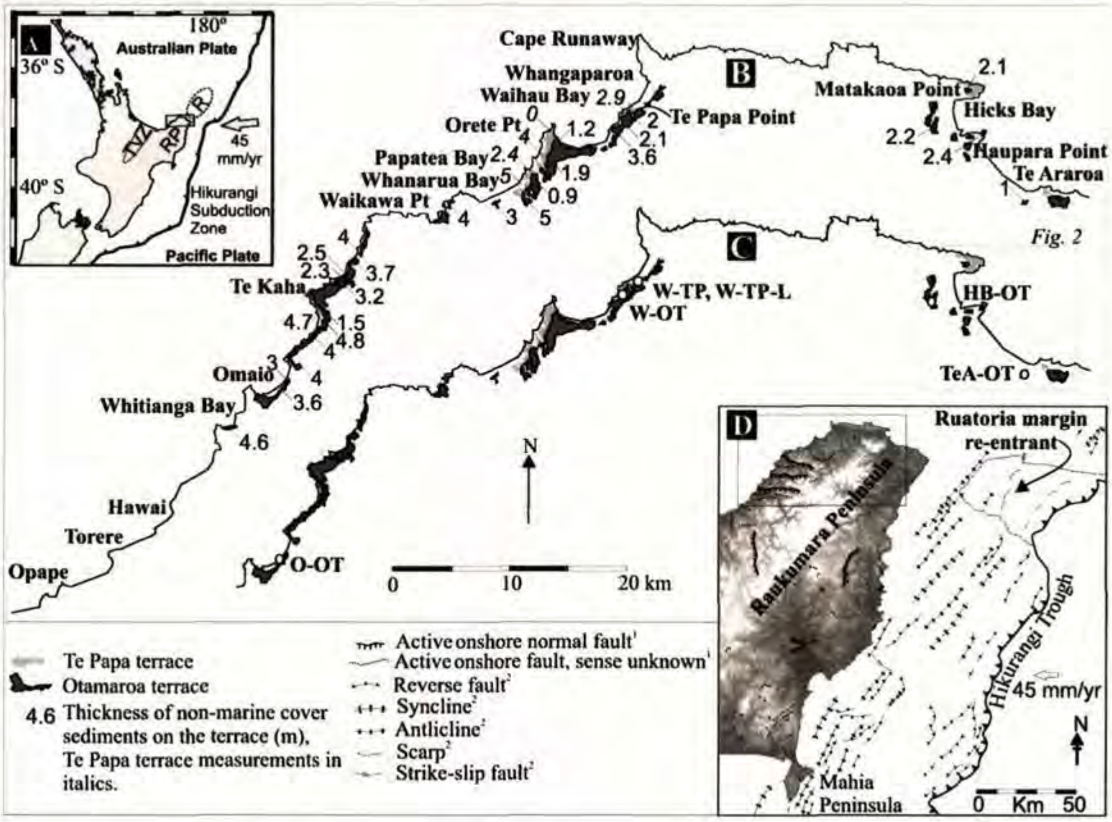

Figure 1. **(A)** North Island, New Zealand with major tectonic features. TVZ: Taupo volcanic zone, RP: Raukumara Peninsula, R: Raukumara Plain. Relative plate motions after De Mets et al., 1994); Hikurangi subduction deformation front after Collot et al. (1996). **(B)** Western and northern coastline of the Raukumara Peninsula with the distribution of the Otamaroa and Te Papa Terraces, location names and the sites where non-marine terrace coverbed thicknesses were measured. **(C)** OSL sample locations. **(D)** Topography and tectonic features of the Raukumara Peninsula. [1] Onshore active faults from the GNS Science Active Faults Database (http://data.gns.cri.nz/af/). [2] Offshore structures from Lewis et al. (1997).

The most extensive terrace, named the Otamaroa Terrace (Yoshikawa et al. 1980), has been estimated previously to have formed in Oxygen Isotope Stage (OIS) 5e (Chapman-Smith & Grant-Mackie 1971; Yoshikawa et al. 1980). The lower Te Papa Terrace has been estimated to have formed during OIS 5a (Chapman-Smith & Grant-Mackie 1971; Yoshikawa et al. 1980). The highest terrace, named the Matakaoa Terrace, has a very limited distribution (Yoshikawa et al. 1980). It is thought to represent OIS 7 and has been mapped only at Matakaoa Point with fragmentary occurrence south of Whitianga Bay. Deposits on the terraces have not previously been directly dated; age control has been achieved only through correlation with global eustatic sea-level (SL) records and tephrochronology. Tephrochronology is of limited use in this region because the oldest widespread tephra is the 50 ka Rotoehu Tephra, which is present on all the Pleistocene marine terraces.

Raukumara Peninsula is situated inboard of the Hikurangi subduction zone (Fig. 1A, D). The mapped Pleistocene marine terraces studied here extend from a distance of c. 150 km normal to the Hikurangi trough, to within c. 90 km normal to the Hikurangi trough and they are distributed either side of the northeastern projection of the crest of the Raukumara Range, a major axial range running approximately parallel to the Hikurangi margin (Fig. 1D). The marine terraces are therefore in a unique location to yield information about uplift rates and processes over a wide distance perpendicular to a subduction zone and around the perimeter of a major axial mountain range. Yoshikawa et al. (1980) projected the heights of the terraces to a plane normal to the trend of the East Coast and they showed that the terraces have been uplifted and tilted to the northwest. These authors inferred that terrace uplift was associated with major earthquakes in the inner Kermadec Trench (Yoshikawa et al. 1980). We will use GPS elevations to obtain a more accurate image of terrace geometry and assess the controlling structure in light of recent active fault data.

6.2 Methods

6.2.1 Terrace stratigraphy and distribution

Terrace coverbed descriptions were obtained from natural exposures at 26 locations (Fig. 1B); stratigraphic descriptions are available from the GNS Online Data Repository (http://data.gns.cri.nz/paperdata/index.jsp). We follow the marine terrace terminology of Pillans (1990) and define all sediments on the terrace strath as coverbeds, subdivided into marine and non-marine, or terrestrial. We measured the thickness of the topmost non-marine coverbeds sediments at six additional locations where we did not record an accompanying stratigraphic description. We used aerial photographs together with our stratigraphic studies to map the marine terraces.

6.2.2 Terrace elevations

Terrace surface elevations were measured using a real-time kinematic (RTK) GPS. Control points, including as benchmarks, trig stations, and local sea level, were used to calibrate the vertical elevations measured by the GPS. Elevation uncertainties varied between regions depending on the number and uncertainty of the control points measured (the uncertainties for each region were as follows: Hicks Bay area: ± 0.07 m, Waihau Bay area: ± 0.55 m, Te Kaha area: ± 0.77 m, Hawai area: ± 0.11 m).

At most locations, an elevation point was measured in approximately the middle of the terrace surface. Where possible we took points from the rear, middle, and front of the terrace (e.g., at Te Kaha and Waihau Bay where the terrace surface was >1 km wide). It is best practice to measure a marine terrace elevation at the strandline, the most landward part of the terrace surface (Pillans, 1990); however, the terraces were often too narrow for multiple points to be surveyed and colluvial fans often covered the strandlines. Sixty elevation points were collected from the Otamaroa Terrace, the highest and most extensive surface; 15 were collected from the lower Te Papa Terrace. At three locations in Te Araroa we could not access the terrace surface with the GPS. We estimate the elevations of these terraces from topographic maps with a contour interval of 20 m. We estimate that the uncertainty of these elevations is ± 10 m.

6.2.3 Age control

Optically stimulated luminescence (OSL) dating was performed on bulk samples of quartz and feldspar silt-sized grains from the terrace sand and loess coverbeds to estimate the age of the terraces. Six OSL samples were collected (Fig. 2, Table 1), four of these were from the Otamaroa Terrace (samples denoted by "OT") and two from the Te Papa Terrace (samples denoted by "TP"). All the Otamaroa Terrace samples and one sample from the Te Papa Terrace were selected from sediment interpreted to be beach deposits: coarse sands, or sand within gravel. Sampling was undertaken immediately above the bedrock strath so to date the timing of strath cutting and avoid younger coverbeds (Fig. 2). One loess OSL sample was collected at Waihau Bay from the Te Papa Terrace (W-TP-L). This was collected from a loess layer overlying the sand from which the W-TP sand sample was obtained. The OSL dating was carried out at the Luminescence Dating Laboratory, Victoria University of Wellington. The technical details of the luminescence dating for these samples are described in Rieser (2005, 2006). These technical reports are available from the author by request.

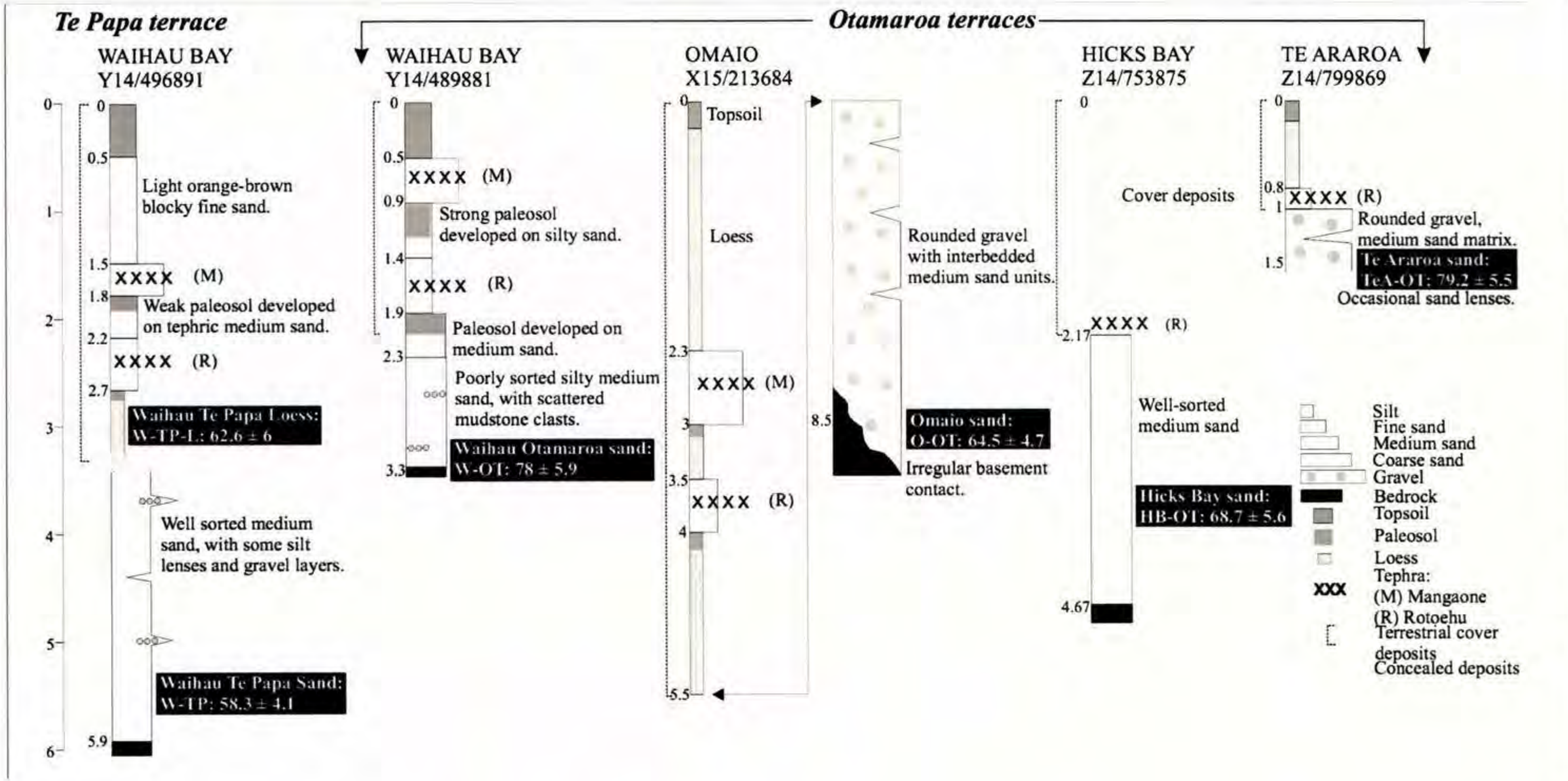

Figure 2. Stratigraphic columns of terrace coverbeds at the OSL sampling locations.

Table 1: OSL sampling locations, modern elevations and stratigraphic context of the samples.

Sample name[1]	Location	Grid reference[2]	Elevation (m)	Stratigraphic context	OSL Ages (ka)
W-TP	Waihau Bay	Y14/496891	22.8	Sand 0.5 m above bedrock strath	58.3 ± 4.1
W-TP-L	Waihau Bay	Y14/496891	25	Loess overlying the sand of sample W-TP, underlying Rotoehu Tephra.	62.6 ± 6
O-OT	Omaio Bay	X15/213684	12	Sand lense within gravel, near undulating bedrock strath.	64.5 ± 4.7
W-OT	Waihau Bay	Y14/489881	62.4	Sand overlying bedrock strath.	78 ± 5.9
HB-OT	Hicks Bay	Z14/753877	131.25	Sand overlying bedrock strath.	68.7 ± 5.6
TeA-OT	Te Araroa	Z14/834816	279	Sand lense within gravel overlying bedrock strath.	79.2 ± 5.5

[1] TP: Te Papa Terrace, OT: Otamaroa Terrace, L: loess sample.
[2] New Zealand Map Grid coordinates

6.3 Results

6.3.1 Terrace distribution

On the western side of the Raukumara Peninsula coastline between Whangaparoa and Whitianga Bay our terrace distribution maps are similar to those of Yoshikawa et al. (1980) and Manning (1995) (Fig. 1B). From Whangaparoa to Papatea Bay there are two clear terraces - the Otamaroa (highest) and the Te Papa (lowest). From Papatea Bay to Omaio Bay only the Otamaroa Terrace is present (Fig. 1).

We do not include any terrace elevations southwest of Whitianga Bay in our analysis of the Pleistocene marine terraces owing to uncertainty about their origins and correlations, although Yoshikawa et al. (1980) and Manning (1995) mapped the Otamaroa Terrace southward to Opape. South of Whitianga Bay, the elevation of the terrace decreases to <20 m and we found the marine and fluvial terraces became increasingly difficult to distinguish on the basis of geomorphology; the terrace stratigraphy also becomes increasingly ambiguous. Due to the lower uplift rates there has probably been reworking of terrace sediments by fluvial processes and possibly re-occupation of the terrace. We also did not map terraces on the northern Raukumara Peninsula coastline between Cape Runaway and Matakaoa Point, though Yoshikawa et al. (1980) did map them there. We judged from our field visits that while there is a marine terrace along most of the coastline, it has a steep surface gradient due to colluvial fan deposition. The terrace strath was difficult to locate so we did not collect elevation measurements. On the eastern side of the Peninsula, at Hicks Bay and Te Araroa, our terrace distribution agrees with Yoshikawa et al. (1980). However, our terrace correlations differ slightly. The highest terrace on Matakaoa Point was defined by Yoshikawa et al. (1980) as the Matakaoa Terrace, and the lower terrace, the Otamaroa. Based on our new elevation data we correlate the highest terrace on Matakaoa Point with the Otamaroa Terrace and the lower Matakaoa Point terrace with the Te Papa Terrace (Fig. 3).

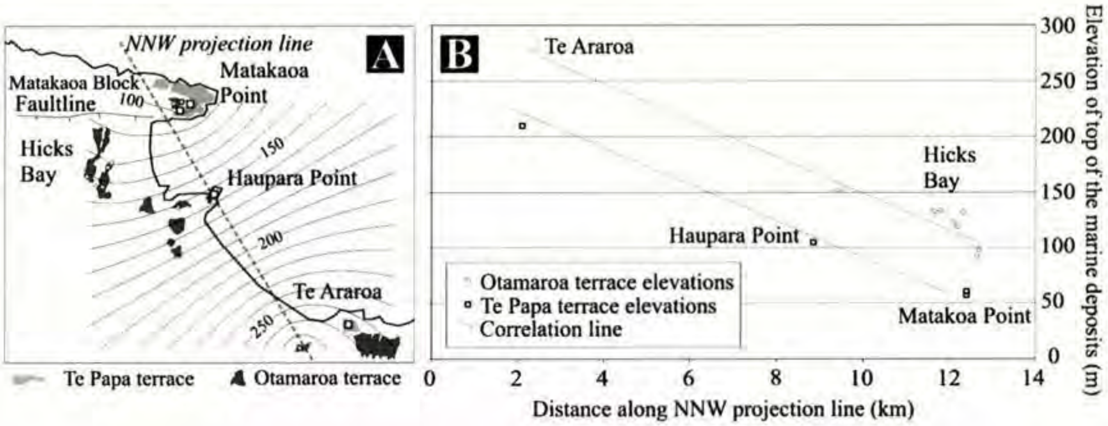

Figure 3. **(A)** Pleistocene terrace distribution at Matakaoa Point, Hicks Bay and Te Araroa and locations where the terrace elevation was measured. All points were measured with an RTK GPS except the two locations at Te Araroa, which were estimated from a 1:25000 topographic map. Contour lines show 10 m intervals on the highest terrace. The normal fault trace along the southern side of the Matakaoa Peninsula is shown. **(B)** Elevation of the Otamaroa and Te Papa Terraces projected to a NNE trend line. This graph shows how the two terraces at Matakaoa Point correlate with the Otamaroa and Te Papa Terraces. There is no downthrow to the south of the terraces across the normal fault bounding the east-west trending Matakaoa block.

6.3.2 Terrace stratigraphy

Terrace cover deposits varied in thickness throughout the region, from 1.5 to >9 m (Fig. 1B). In the field we estimated the boundary between marine and non-marine deposits using sedimentology. Silt, loess, paleosols, colluvium, poorly sorted gravels, and the interbedded tephras were judged to be non-marine deposits. Well-sorted sands and gravels directly on the terrace strath were judged to be beach deposits.

The identification of beach sands was important for OSL sampling because we aimed to collect sand deposited synchronously with marine terrace incision. The sands sampled for OSL dating did not display any direct evidence of a beach depositional environment (e.g., shells within the sands have probably been leached out). However, the well-sorted nature of the sand and rounded gravels support wave sorting during deposition. Alternative mechanisms for sand and gravel emplacement are colluvial, aeolian, or fluvial deposition. Colluvial sediments were identified by the characteristics of silt matrix-supported angular gravel clasts and irregular bedding. We were careful not to select OSL samples from colluvial sediments. At Waihau Bay, Omaio, and Te Araroa the sand sampled for OSL dating occurred in close association with gravel; therefore, an aeolian depositional mechanism is unlikely. At Hicks Bay, the sampled sand was well-sorted and did not occur in proximity with gravel (Fig. 2); it is possible this was dune sand. Fluvial deposition of gravels and sands was discounted at most locations where we measured and described the coverbed stratigraphy because there were no nearby fluvial sources. This leaves beach processes as the most likely depositional mechanism of well-sorted sands and gravels, and the modern beach also contains similar deposits. Only the OSL sampling sites at Omaio Bay and Te Araroa were proximal to rivers that may have occupied the terrace strath in the past. Therefore, at these two locations, it is possible that fluvial processes deposited the sampled sands post- terrace incision, rather than beach processes depositing the sand and gravel synchronous with terrace incision.

Loess was identified by sedimentary characteristics such as a massive, homogeneous nature, uniform silt grain size, and blocky texture when dry. Loess units in the study region typically displayed paleosols developed at the top of them, indicative of weathering during warm climatic conditions following loess deposition (Palmer & Pillans, 1996).

Two tephras were commonly seen within the non-marine terrace coverbed sequence. These were a coarse-grained, dark orange tephra, and a fine to medium grained, pale creamy tephra. These are identified respectively as the Mangaone (c. 28 ka BP, Froggatt and Lowe 1990) and Rotoehu Tephras (c. 50 ka BP). Rotoehu Tephra age estimates range from 45 to 65 ka BP, Berryman (1992) estimates 52 ± 7 ka BP based on marine terrace correlation, Wilson et al. (1992) estimate 64 ± 4 ka BP based on radiometric dating of bracketing lavas, and Lian & Shane (2000) estimate 44 ± 3 ka BP based on OSL dating of bracketing loess. Tephra identification was made with reference to the descriptions presented in Iso et al. (1982) and Manning (1995; 1996).

6.3.3 OSL results

The OSL results are shown in Table 2; all ages are presented with a standard error, though the actual error could be significantly larger. The four sand samples from the Otamaroa Terrace yielded ages of 64.5 ± 4.7, 68.7 ± 5.6, 78 ± 5.9 and 79.2 ± 5.5 ka. Sample O-OT, from the Otamaroa Terrace at Omaio yielded an age of 64.5 ± 4.7 ka, though the sample was noted to be near saturation. Thus, there is a possibility that this sample is slightly older, as the dose-response curve fitting procedures are not very robust for almost saturated samples (Rieser, 2005, 2006). The sand sample immediately above the bedrock strath of the Te Papa Terrace (W-TP) yielded an age of 58.3 ± 4.1 ka. The overlying loess (W-TP-L) yielded an age of 62.6 ± 6 ka. Apart from sample O-OT, the dose-response curve fitting for all samples was satisfactory, indicating the samples were not near saturation. There was no evidence of anomalous fading or disequilibrium in the U-series chains, and no other sample anomalies arose during the standard procedures of luminescence measurements (Rieser 2005; 2006).

Table 2: OSL results: Radionuclide and water contents, measured a-value and equivalent dose, dose rate and luminescence age.

Sample	Lab no.	a-value	dD_c/dt (Gy/ka)[1]	D_e (Gy)	dD/dt (Gy/ka)	Water content δ[2]	U (µg/g) from ^{234}Th	U (µg/g)[3] from ^{226}Ra, ^{214}Pb, ^{214}Bi	U (µg/g) from ^{210}Pb	Th (µg/g)[2] from ^{208}Tl, ^{212}Pb, ^{228}Ac	K (%)	**OSL-age (ka)**
W-TP	WLL427	0.055±0.008	0.1398±0.007	101.5±5	1.74±0.09	1.138	0.91±0.15	0.89±0.09	1.08±0.16	3.33±0.06	1.07±0.02	**58.3±4.1**
W-TP-L	WLL507	0.054±0.003	0.1434±0.0072	112.6±4.8	1.80±0.15	1.334	2.15±0.14	1.90±0.09	1.41±0.11	5.69±0.07	0.90±0.02	**62.6±6.0**
O-OT	WLL505	0.074±0.007	0.1594±0.0080	245.9±13.2	3.81±0.19	1.135	2.12±0.20	1.77±0.13	1.61±0.18	7.60±0.10	2.36±0.05	**64.5±4.7**
W-OT	WLL428	0.043±0.005	0.1594±0.008	173.4±7.2	2.2±0.14	1.186	1.34±0.18	1.41±0.1	1.4±0.19	3.88±0.06	1.47±0.03	**78.9±5.9**
HB-OT	WWL429	0.029±0.004	0.1706±0.0085	135.4±6	1.97±0.13	1.21	1.75±0.2	1.35±0.11	1.34±0.2	4.51±0.07	1.28±0.03	**68.7±5.6**
TeA-OT	WLL506	0.074±0.013	0.1706±0.0085	181.3±8.0	2.29±0.12	1.136	1.75±0.15	1.36±0.10	1.24±0.13	5.27±0.07	1.14±0.03	**79.2±5.5**

[1] Contribution of cosmic radiation to the total doserate, calculated as proposed by Prescott & Hutton (1994), Radiation Measurements, Vol. 23.
[2] Ratio wet sample to dry sample weight. Errors assumed 50% of (δ-1).
[3] U and Th-content is calculated from the error weighted mean of the isotope equivalent contents.

6.4 DISCUSSION

6.4.1 Ages of the Raukumara Peninsula Pleistocene marine terraces

The study of Pleistocene marine terraces globally has shown some general relationships exist between climate, SL, terrace formation, and terrace cover deposits. Marine terrace straths are cut during relative SL highstands, therefore they represent warm climatic periods such as interglacials or interstadials. Beach deposits upon the terrace strath are assumed to be approximately equivalent in age with incision of the terrace strath, or at least represent a minimum age for the terrace. OSL dating, which measures time elapsed since the sediments were last exposed to sunlight, is a useful method to date the beach deposits directly therefore determine the minimum terrace age.

The sand sample from the Te Papa Terrace at Waihau Bay yielded an OSL age of 58.3 ± 4.1 ka. This result suggests a depositional age of early OIS 3 (Fig. 4). The overlying loess sample collected at the same location yielded an age of 62.6 ± 6 ka. This loess age is slightly older than the underlying sand age; however, the samples are within the 1-sigma uncertainty range of one another (Fig. 4).

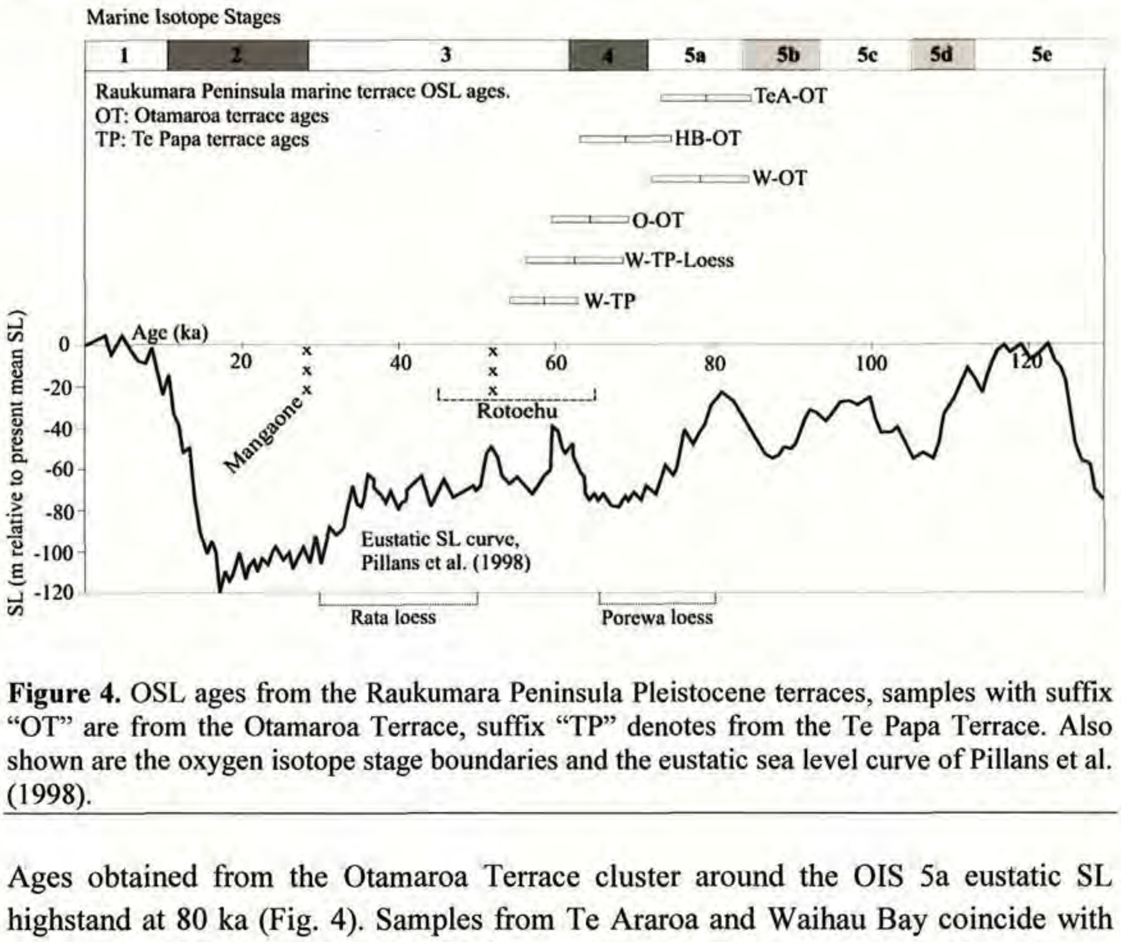

Figure 4. OSL ages from the Raukumara Peninsula Pleistocene terraces, samples with suffix "OT" are from the Otamaroa Terrace, suffix "TP" denotes from the Te Papa Terrace. Also shown are the oxygen isotope stage boundaries and the eustatic sea level curve of Pillans et al. (1998).

Ages obtained from the Otamaroa Terrace cluster around the OIS 5a eustatic SL highstand at 80 ka (Fig. 4). Samples from Te Araroa and Waihau Bay coincide with this age at 79.2 ± 5.5 and 78 ± 5.9 ka respectively. The sample from Hicks Bay is younger, the depositional age of 68.7 ± 5.6 ka falls within OIS 4, a glacial period. However, within the uncertainty of the OSL age, this sample spans the end of OIS 5a and most of OIS 4 (Fig. 4). The sample from the Otamaroa Terrace at Omaio also falls mainly within OIS 4 at 64.5 ± 4.7 ka but this sample probably has an underestimated age due to saturation (Rieser 2006).

These six OSL dates suggest the Te Papa and Otamaroa Terraces formed during OIS 3 and 5a, respectively. These estimates are different from the earlier study by Yoshikawa et al. (1980) who suggested ages of OIS 5a and 5e. The revised age estimates imply terrace uplift rates higher than previously calculated (Table 3, Fig. 5). For example, an OIS 5a age for the Otamaroa Terrace at Te Araroa yields an uplift rate of 3.5-4.1 mm/yr (assuming eustatic SL during OIS 5a was -24 ± 5 m, Pillans et al. 1998), while an OIS 5e age yields uplift rates of 2.1-2.4 mm/yr (Table 3, Fig. 5).

Table 3: Terrace uplift rates for the Te Papa and Otamaroa Terraces at four locations around the Raukumara Peninsula, calculated using the possible terrace ages discussed in the text.

		Estimated terrace age	OIS 3/5a		OIS 5c/5e		OIS 5a	
Terrace location	Elevation (m)	Uncertainty (+/- m)	Uplift rate (mm/yr)*	(Min. – maxi.)**	Uplift rate (mm/yr)	(Min. – maxi.)	Uplift rate (mm/yr)	(Min. – maxi.)
Waihau Bay TP	22.8	0.5	**1.06**	(0.9-1.26)	**0.48**	(0.41-0.56)	**0.59**	(0.49-0.7)
Waihau Bay OT	62.4	0.5	**1.08**	(0.95-1.23)	**0.50**	(0.44-0.57)		
Orete Point TP	26.1	0.5	**1.12**	(0.95-1.32)	**0.52**	(0.45-0.59)	**0.63**	(0.53-0.73)
Orete Point OT	57	0.5	**1.01**	(0.89-1.15)	**0.46**	(0.4-0.52)		
Matakoa Point TP	61	0.5	**1.71**	(1.49-1.97)	**0.85**	(0.76-0.95)	**1.06**	(0.94-1.21)
Matakoa Point OT	96	0.5	**1.50**	(1.35-1.67)	**0.77**	(0.7-0.85)		
Te Araroa TP	210	10	**4.24**	(3.67-4.91)	**2.27**	(2.03-2.53)	**2.93**	(2.58-3.32)
Te Araroa OT	279	10	**3.79**	(3.39-4.24)	**2.23**	(2.03-2.45)		

*Uplift rate = (terrace elevation – past eustatic SL[1])/age[1].
[1] Past eustatic sea levels estimated from Pillans et al. (1998): (stage, age, sea level); (OIS 3, 59 ± 5 ka, -40 ± 5 m); (OIS 5a, 80 ± 5 ka, -24 ± 5 m); (OIS 5c, 105 ± 5 ka, -28 ± 5 m); (OIS 5e, 125 ± 5 ka, 0 ± 5 m).
** Minimum uplift rate: mimimum uplift [(elevation – uncertainty)-(SL+uncertainty) / maximum age (age + uncertainty). Maximum uplift rate: maximum uplift [(elevation + uncertainty)-(SL-uncertainty) / mimimum age (age - uncertainty).

Three issues arise from a OIS 3 and 5a terrace age revision for the Te Papa and Otamaroa Terraces. Firstly, marine terraces older than OIS 5a are not preserved along the northern Raukumara Peninsula. The eustatic SL highstands of OIS 5c and 5e were higher than the highstands of the OIS 3 and 5a. Therefore, given a consistent or, even slower, uplift rate dating back to c.125 ka, the OIS 5e and 5c terraces should have formed and be present higher in the landscape, especially in areas of slower uplift rates. Secondly, two of the Otamaroa Terrace OSL samples (HB-OT and O-OT, Fig. 4) imply sand deposition on the marine terrace while eustatic SL was falling. On an uplifting coastline such as the Raukumara Peninsula, marine terrace incision is predicted to start when the rates of eustatic SL rise equal or exceed that rate of land uplift (*cf.* Pillans 1990, Fig. 4). Terrace incision will cease when eustatic SL rates decrease below the land uplift rate. The OSL ages of HB-OT (68.7 ± 5.6 ka) and O-OT (64.5 ±4.7 ka) imply sand deposition after the peak of OIS 5a, when eustatic SL was falling and terrace incision was unlikely to have been occurring (Fig. 4). Thirdly, the Waihau Bay loess mantling the Te Papa terrace must have been deposited during early OIS 3, after incision of the terrace with a sufficient time lapse for paleosol formation before deposition of the Rotoehu Tephra (Fig. 4). There are no known loess units in New Zealand that correlate to this age.

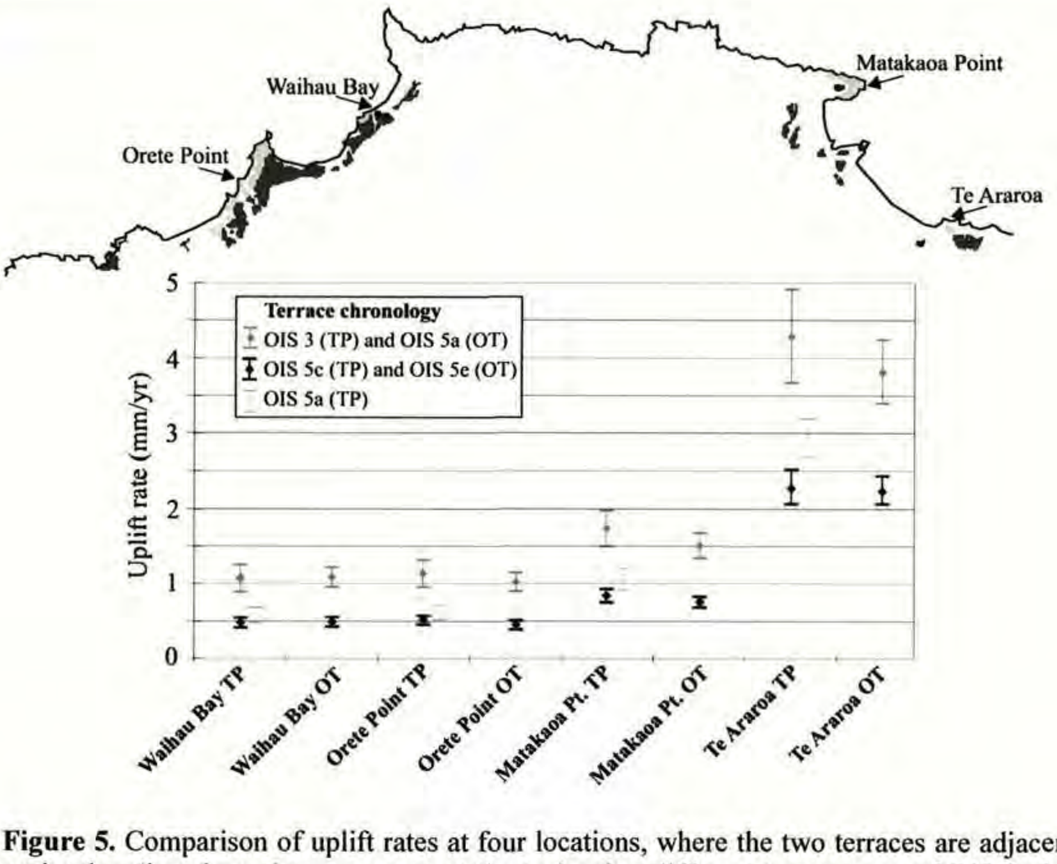

Figure 5. Comparison of uplift rates at four locations, where the two terraces are adjacent to each other (locations shown on map at the top) using different terrace ages of OIS 3, 5a, 5c and 5e. Uplift rates are calculated using eustatic SL estimations of Pillans et al. (1998). Terrace elevation refers to the height of the top of the marine deposits on the terraces relative to modern mean SL. See Table 3 for discussion of how the uplift rates were calculated.

These three issues suggest a more critical appraisal of the OSL ages is warranted. The OSL age of 62.6 ± 6 ka for the Waihau Bay loess falls within OIS 4, suggesting a correlation to the widespread Porewa loess (Milne & Smalley 1979; Kennedy, 1988; 1994; Litchfield & Rieser 2005). This is consistent with the presence of the Rotoehu tephra overlying this loess, with a paleosol developed in between. This stratigraphic correlation would imply the Te Papa terrace was formed during or prior to OIS 5a, not during OIS 3 as implied by the sand OSL age from beneath the loess. Furthermore, the well-documented extent of the OIS 5e terrace globally (e.g., Bloom et al. 1974; Hsu 1992; Kelsey & Bockheim 1994; Pillans 1994; Murray-Wallace 2002; De Diego-Forbis et al. 2004; Marquardt et al. 2004) would suggest the Otamaroa Terrace was more likely to have formed during OIS 5e. Comparisons of uplift rates using different terrace ages shows that for OIS 3/5a and OIS 5c/5e terrace ages the uplift rates remain steady during the late Pleistocene (Fig. 5). However, if an OIS 5a/5e terrace age combination is used then uplift rates must have increased by 30% between OIS 5e and OIS 5a (from 2.23 mm/yr to 2.93 mm/yr, Table 3, Fig. 5). No known tectonic perturbations occurred during the time period from OIS 5e to 5a (125 – 80 ka) that may have caused accelerated uplift, therefore, if an age of OIS 5e is adopted for the Otamaroa Terrace, the Te Papa Terrace is most likely to have an age of OIS 5c.

A terrace chronology of >OIS 5a and OIS 5e for the Te Papa and Otamaroa Terraces, respectively, is consistent with regional loess chronology and geomorphological characteristics of Pleistocene marine terraces, but conflicting with all the OSL ages, except for the Waihau Bay loess. Although detailed description and analysis of the OSL technique is beyond the scope of this paper we briefly examine some of the uncertainties in this relatively new technique that may be contributing to younger ages.

The possibility that the sand samples were not fully reset during deposition is discounted because this would result in older, rather than younger ages. Anomalous fading is also discounted because there was no sign shown by the routine 6 month testing for each of these samples. The only reported problem with fitting of the dose-response curves was for sample O-OT, which showed near-saturation signals. Thus the age for this sample may be considered a minimum.

Other possible reasons that the sample ages may be underestimated include: (1) the sampled sands may have been deposited a significant amount of time after terrace formation. Terrestrial processes of erosion and resedimentation of cover sediments on the terrace strath would result in sediment ages younger than the terrace formation age. However, it is unlikely that the five sand samples we collected, from two terraces and at 4 widely-spaced locations would have all been affected by the same erosion and redeposition process. (2) The silt fractions from the beach sand samples were used for the OSL dating and it is conceivable that this silt has filtered down the sediment profile from the younger deposits above, hence yielding a younger age. (3) It is also possible that the silt in this region does not contain sufficient amounts of K-feldspar for OSL dating. (4) There may be an as yet unidentified technical problem with the OSL dating process for silt samples extracted from sandy sediments. All of these reasons suggest further testing of the OSL technique for dating beach sands using the silt fraction should be undertaken.

6.4.2 Deformation of the marine terraces in the context of Hikurangi subduction margin tectonics

The continuity of the Pleistocene marine terraces around the Raukumara Peninsula coastline means we are confident that the mapped Te Papa and Otamaroa Terrace surfaces are representative of the same time period at all locations. This means that, regardless of the terrace age, the terrace surface was originally horizontal with respect to SL and its deformation since is a reflection of the spatial patterns of tectonic processes. The morphology of the Otamaroa Terrace displays a distinctive northwestward tilt (Fig. 6). The contour map shows some compression of the contours at Te Kaha and Orete Point because the Otamaroa Terrace is wide at these locations and we were able to measure terrace elevations from the front, middle, and rear of the terraces and the contours reflect the seaward slope of the terrace. The Te Papa Terrace, with more limited spatial extent, also shows the same morphology and northwestward tilt (Fig. 6). The tilt on the Te Papa Terrace is not as steep compared with the Otamaroa Terrace. The similarity in geometry and progressive tilting though time indicates the same mechanism operated to uplift both terraces. The tilt vector of the terraces is approximately normal to the strike of the Raukumara Peninsula and the Hikurangi Trench (Fig. 7). This suggests that uplift of the terraces is related to Hikurangi subduction zone processes. However, the lack of mapped active faults implies it is not an upper plate fault accommodating the uplift. Rather there are probably deeper lower-crust to upper-mantle processes controlling the uplift pattern (e.g. Reyners et al. 1999, Litchfield et al. in press). It is also notable that the location of greatest terrace uplift at Te Araroa is offset by a distance of approximately 13 km from the projected northwestward trend of the axis of the Raukumara Ranges. This may imply that the crest of the Raukumara Ranges does not represent the zone of greatest uplift of the Raukumara Peninsula or that the zone of uplift has shifted westward during the late Quaternary.

The terrace tilt is very steep and has a more northerly orientation on the eastern side of the Peninsula from Matakaoa Point to Te Araroa (Fig. 3, 7). It is worth noting however that the terrace elevations in Fig. 7 have been projected to a WNW projection line, which is approximately parallel with the tilt on most of the terraces, except those in the Hicks Bay – Te Araroa region that tilt to the NNW. Therefore, the terrace tilt in Fig. 7 is artificially oversteepened. If the projection line for this region were in a more northerly direction, the terrace tilt would be slightly less (*cf.* Fig. 3). There are no known onshore or near-offshore active faults that can account for this geometry (Fig. 1D) (Collot et al. 1996; Lewis et al. 1997; Mazengarb & Speden 2000). The more northerly tilt direction of the terraces in this region may be related to the offshore transition into the Raukumara Plain, a long-lived deep forearc basin immediately north of the Matakaoa Point (Fig. 1A) (Gillies & Davey 1986; Davey et al. 1997).

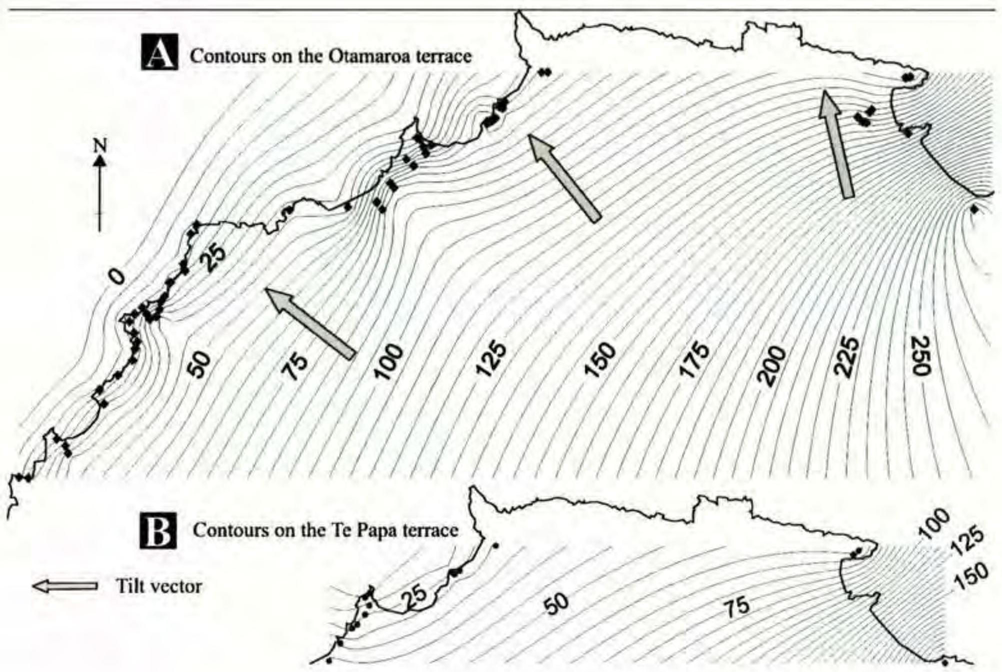

Figure 6. (A) Contours of the Otamaroa Terrace surface, heights are based on the elevation of the top of the marine sediments on the terrace. Contour interval is 5 m. **(B)** Contours on the Te Papa Terrace, 5 m intervals, based on the elevation of the top of the marine deposits on the terrace. Contour maps were created from a grided version of the data using the Golden Software Surfer surface mapping system.

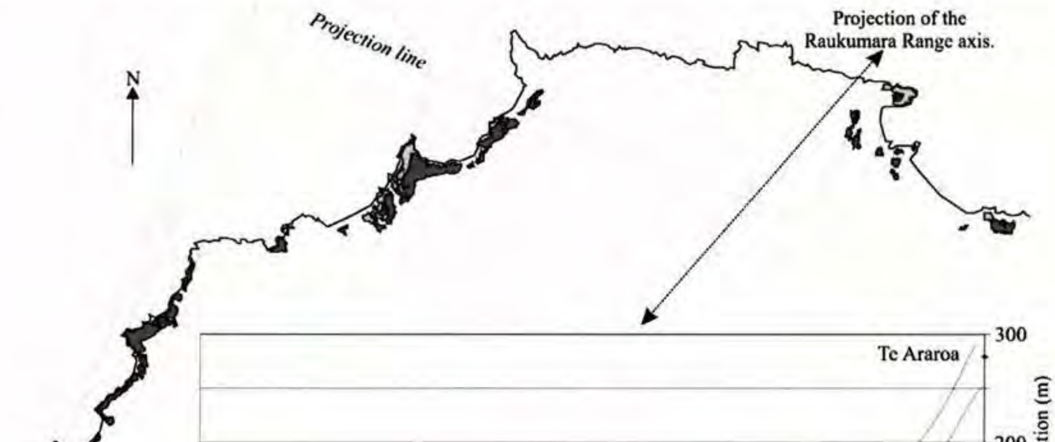

Figure 7. Otamaroa Terrace elevations with distance from Te Araroa projected to a west-northwest trend (approximately normal to the trend to the Hikurangi subduction zone. We note however, that the dominant tilt direction in the Matakaoa Pont to Te Araroa region is to the north-northwest therefore the projected tilt for this region shown in the graph is artificially oversteepened, refer to Fig. 3b for a more accurate representation of tilt in this area.

6.5 Conclusions

This study presents the first radiometric dating of the Raukumara Peninsula Pleistocene terraces. Five OSL ages from sand deposits on the terrace straths suggest that the Otamaroa Terrace was formed during OIS 5a and the Te Papa Terrace was formed during OIS 3. However, the OSL age of loess on the Te Papa Terrace suggests the loess unit may correlate with the OIS 4 Porewan loess, therefore requiring the Te Papa Terrace to have formed prior to OIS 4 and conflicting with the sand OSL age from the same location. Furthermore, if the Otamaroa Terrace was formed during OIS 5a, then this means the OIS 5e terrace is not present on the Raukumara Peninsula. This is unusual as the OIS 5e marine terrace is globally common and often the only Pleistocene marine terrace present on stable and uplifting coastlines. These results, therefore, do not satisfactorily resolve the age of the Raukumara Peninsula Pleistocene terraces but they do raise important questions regarding either the use of loess stratigraphy and geomorphic correlations to date marine terraces or the application of OSL dating to beach sands. The geometry of the Raukumara Peninsula terraces shows a strong northwest tilt which cannot be attributed to any known active faults in the region. We suggest that upper mantle and lower crust processes related to the Hikurangi subduction zone control the geometry and uplift of the terraces.

6.6 Acknowledgements

This research was funded by an EQC Student Grant (Project 6UNI/501). KJW was supported by the GNS Science Sarah Beanland Memorial Scholarship. Uwe Rieser of the Victoria University of Wellington Luminescence Dating Laboratory is thanked for his contribution to the luminescence dating. This manuscript was improved thanks to reviews by Alan Palmer and Colin Murray-Wallace.

6.7 References

Berryman K 1992. A stratigraphic age of Rotoehu ash and late Pleistocene climate interpretation based on marine terrace chronology, Mahia Peninsula, North Island, New Zealand. New Zealand Journal of Geology and Geophysics 35(1): 1-7.

Bloom AL, Broecker WS, Chappell J, Matthews RK, Mesolella KJ 1974. Quaternary sea level fluctuations on a tectonic coast: new 230Th/234U dates from the Huon Peninsula, New Guinea. Quaternary Research 4: 185-205.

Chapman-Smith M, Grant-Mackie JA 1971. Geology of the Whangaparoa area, eastern Bay of Plenty. New Zealand Journal of Geology and Geophysics 14(1): 3-38.

Choi JH, Murray AS, Jain M, Cheong CS, Chang HW 2003. Luminescense dating of well-sorted marine terrace sediments on the southeastern coast of Korea. Quaternary Science Reviews 22: 407-421.

Collot J-Y, Delteil J, Lewis K, Davy B, Lamarche G, Andru J-C, Barnes P, Chanier F, Chaumillon E, Lallemand S and others 1996. From oblique subduction to intra-continental transpression: structures of the southern Kermadec-Hikurangi margin from multibeam bathymetry, side-scan sonar and seismic reflection. Marine Geophysical Researches 18(2-4): 357-381.

Davey FJ, Henrys S, Lodolo E 1997. A seismic crustal section across East Cape convergent margin, New Zealand. Tectonophysics 269: 199-215.

De Mets C, Gordon RG, Argus DF, Stein S 1994. Effect of recent revisions to the geomagnetic reversal timescale on estimates of current plate motions. Geophysical Research Letters 21: 2191-2194.

De Diego-Forbis T, Douglas R, Gorsline D, Nava-Sanchez E, Mack L, Banner J 2004. Late Pleistocene (last interglacial) terrace deposits, Bahia Coyote, Baja California Sur, Mexico. Quaternary International 120: 29-40.

Froggatt PC, Lowe DJ 1990. A review of late Quaternary silicic and some other tephra formations from New Zealand: their stratigraphy, nomenclature, distribution, volume and age. New Zealand Journal of Geology and Geophysics 33: 89-109.

Gillies PN, Davey FJ 1986. Seismic reflection and refraction studies of the Raukumara forearc basin, New Zealand. New Zealand Journal of Geology and Geophysics 29: 391-403.

Hsu JT 1992. Quaternary uplift of the Peruvian coast related to the subduction of the Nazca Ridge: 13.5 to 15.6 degrees latitude. Quaternary International 15/16: 87-97.

Iso N, Okada A, Ota Y, Yoshikawa T 1982. Fission-track ages of late Pleistocene tephras on the Bay of Plenty coast, North Island, New Zealand. New Zealand Journal of Geology and Geophysics 25: 295-303.

Kelsey HM, Bockheim JG 1994. Coastal landscape evolution as a function of eustasy and surface uplift rate, Cascadia margin, southern Oregon. Geological Society of Americe Bulletin 106: 840-854.

Kennedy N 1988. Late Quaternary loess associated with the Mamaku Plateau, North Island, New Zealand. In: Eden DN, Furkert RJ ed. Loess: its distribution, geology and soils. Rotterdam, A A Balkema. Pp. 71-80.

Kennedy N 1994. New Zealand tephro-chronology as a tool in geomorphic history of the c. 140 ka Mamaku Ignimbrite Plateau and in relating oxygen isotope stages. Geomorphology 9: 97-115.

Lewis KB, Collot J-Y, Davy B, Delteil J, Lallemand S, Uruski C 1997. North Hikurangi GeodyNZ swath maps: depths, texture and geological interpretation 1: 500 000. National Institute for Water and Atmospheric Research Miscellaneous Series Chart 72. Wellington.

Lian OB, Shane P 2000. Optical dating of Paleosols bracketing the widespread Rotoehu Tephra, North Island, New Zealand. Quaternary Science Reviews 19(16): 1649-1662.

Litchfield N, Rieser U 2005. Optically stimulated luminescence age constraints for fluvial aggradation terraces and loess in the eastern North Island, New Zealand. New Zealand Journal of Geology and Geophysics 48: 581-589.

Litchfield NJ, Ellis S, Berryman K, Nicol A in press. Subduction related uplift in the Hikurangi Margin, New Zealand. Journal of Geophysical Research (Earth Surface).

Manning DA 1995. Late Pleistocene tephrostratigraphy of the eastern Bay of Plenty region, New Zealand. Unpublished thesis, Unpublished PhD thesis, Victoria University of Wellington.

Manning DA 1996. Middle-late Pleistocene tephrostratigraphy of the eastern Bay of Plenty, New Zealand. Quaternary International 34-36: 3-12.

Marquardt C, Lavenu A, Ortleib L, Godoy E, Comte D 2004. Coastal neotectonics in Southern Contral Andes: uplift and deformation of marine terraces in Northern Chile (27 degrees south). Tectonophysics 394: 193-219.

Mazengarb C, Speden IG 2000 Geology of the Raukumara area, Institute of Geological & Nuclear Sciences 1:250,000 geological map 6. Institute of Geological and Nuclear Sciences Limited, Lower Hutt, New Zealand.

Milne JDG, Smalley IJ 1979. Loess deposits in the southern part of the North Island of New Zealand: an outline stratigraphy. Acta Geologica Academiae Sientiarum Hungaricae, Tomus 22: 197-204.

Murray-Wallace CV 2002. Pleistocene coastal stratigraphy, sea-level highstands and neotectonism of the southern Australian passive continental margin - a review. Journal of Quaternary Science 17(5-6): 469-489.

Palmer A, Pillans B 1996. Record of climatic fluctuations from ca. 500 ka loess deposits and paleosols near Wanganui, New Zealand. Quaternary International 34-36: 155-162.

Pillans B 1990. Pleistocene marine terraces in New Zealand: a review. New Zealand Journal of Geology and Geophysics 33: 219-231.

Pillans B 1994. Direct marine-terrestrial correlations, Wanganui Basin, New Zealand: the last 1 million years. Quaternary Science Reviews 13: 189-200.

Pillans B, Chappell J, Naish T 1998. A review of the Milankovich climate beat: template for Plio-Pleistocene sea-level changes and sequence stratigraphy. Sedimentary Geology 122: 5-21.

Reyners M, McGinty P 1999. Shallow subduction tectonics in the Raukumara Peninsula, New Zealand, as illuminated by earthquake focal mechanisms. Journal of Geophysical Research 104(B2): 3025-3034.

Rieser U 2005. Determination of sediment deposition ages by luminescence dating. Victoria University of Wellington Technical Report 05/11.

Rieser U 2006. Determination of sediment deposition ages by luminescence dating. Victoria University of Wellington Technical Report

Wilson CJN, Houghton BF, Lanphere MA, Weaver SD 1992. A new radiometric age estimate for the Rotoehu Ash from Mayor Island volcano, New Zealand. New Zealand Journal of Geology and Geophysics 35: 371-374.

Yoshikawa T 1988. Pattern and rate of tectonic movement and Late Quaternary geomorphic development in the Raukumara Peninsula, northeastern North Island, New Zealand. Bulletin of the Department of Geography University of Tokyo 20: 1-28.

Yoshikawa T, Ota Y, Yonekura N, Okada A, Iso N 1980. Marine terraces and their tectonic deformation on the northeast coast of the North Island, New Zealand. Geographical Review of Japan 53(4): 238-262.

CHAPTER SEVEN

RELATIONSHIPS BETWEEN LATE QUATERNARY COASTAL GEOMORPHOLOGY AND SUBDUCTION ZONE GEODYNAMICS OF THE RAUKUMARA SECTOR OF THE HIKURANGI MARGIN.

Journal paper in preparation.

Abstract

Subduction zone geodynamics and seismic hazard of the Raukumara sector of the Hikurangi margin forearc, eastern North Island, New Zealand, are poorly understood. Here we assess the coastal neotectonic record of the Raukumara Peninsula, in order to elucidate forearc deformation processes across a margin-normal width of 100 km. We consider how these processes relate to the subduction zone and the implications for the seismic hazard of this sector of the margin. Late Quaternary coastal uplift mechanisms of the Raukumara sector vary between localised zones of coseismic uplift and broader zones of aseismic uplift. Evidence for uplift mechanisms was obtained from detailed studies of Holocene and Pleistocene marine terrace geomorphology and from the stratigraphy of early Holocene transgressive marine sequences at three coastal regions on the Raukumara Peninsula. We propose that the main parameter controlling the spatial distribution of uplift mechanisms is the proximity of the forearc to the Hikurangi Trough and, by inference, the depth to the plate interface below. Three zones of forearc uplift mechanisms are identified: (1) a zone of coseismic uplift on upper plate contractional faults within 20 – 80 km of the trough, (2) a passive inner forearc zone at ~80-120 km from the trough, vertical tectonic movement within this zone is controlled by distal upper plate structures or plate interface paleoseismicity, and (3) a zone of aseismic uplift driven by sediment underplating located ~120 – 180 km of the trough. Changes in the thickness of the upper plate crust and plate coupling along the strike of the Raukumara sector are inferred to be less important in controlling uplift mechanism distribution than changes normal to the margin. The coseismic and aseismic uplift zones have little potential for recording a subduction earthquake history. We identify the passive forearc zone as the most likely region to contain a coastal paleoseismic history of subduction earthquakes because it is less affected by upper plate deformation and displays the general pattern of vertical tectonics predicted to occur during plate interface events. This study demonstrates the utility of studying uplift mechanisms across a broad zone perpendicular to subduction zones. Variances in forearc deformation processes have been documented; these are related to subduction zone geodynamics and are critical in regional-scale seismic hazard assessment.

7.1 Introduction

The Raukumara sector of the Hikurangi margin, East Coast, North Island, New Zealand (Fig. 1A), possesses perhaps some of the least well-understood subduction zone geology of the Hikurangi margin. There are no significant active faults in the onshore forearc (Mazengarb and Speden, 2000), and geophysical studies suggest the forearc is undergoing margin-normal extension (Darby and Meertens, 1995; Arnadottir et al., 1999; Reyners and McGinty, 1999). These observations suggest that the coastline should be subsiding, which is seen at some locations. However, the Raukumara Peninsula also shows some of the highest coastal uplift rates along the Hikurangi margin (Berryman et al., 1989; Ota et al., 1992. Furthermore, the mechanism of these high coastal uplift rates varies spatially between aseismic and coseismic (Berryman, 1993a; Wilson, Ch. 5, Ch. 3). Sediment underplating has been suggested as a cause of forearc uplift (Walcott, 1987; Thornley, 1996), yet the localised zones of coseismic coastal uplift along the Raukumara Peninsula do not reconcile with the broad crustal warping one would expect above ponded sediment in the lower crust. In addition, there have been no large or great earthquakes on the Raukumara Peninsula in historic time and the risk of a plate interface rupture event is poorly constrained (Stirling et al., 2002; Cochran et al., 2006). In the absence of historic events neotectonic interpretation of coastal geomorphology and stratigraphy provides the only record of subduction zone paleoseismology available on active margins, yet the relationship between coastal tectonics of the Raukumara Peninsula and the plate interface is poorly understood for this margin sector.

In this study we review the late Quaternary coastal geomorphology of the Raukumara Peninsula with the aim of understanding some of the geodynamic processes operating on this segment of the Hikurangi margin. We seek to understand what type of structures accommodate coastal uplift on the Raukumara Peninsula, whether these structures have a predictable spatial relationship to the Hikurangi subduction zone, and whether these relationships can be integrated with other geophysical and geologic studies of the Raukumara sector. Essentially, can the coastal neotectonic record be used to shed light on the processes of forearc deformation and what can this tell us about seismic hazard in the region?

Figure 1. (A) Location map of the Raukumara Peninsula, North Island, New Zealand, and the adjacent Hikurangi subduction zone (TVZ: Taupo Volcanic Zone, NIDFB: North Island dextral fault belt). Red lines show the width of the interseismically locked portion of the plate interface, text indicates the strength of plate coupling, after Reyners (1998). Cross-sections X-X` and Y-Y` are adopted from Beanland (1995). *Pacific-Kermadec plate motion after Collot et al. (2001), **Pacific-Australia plate motion after De Mets et al. (1994). **(B)** Localities, coastal tectonics and active onshore faults of the Raukumara Peninsula. Shown is the distribution of Pleistocene marine terraces (grey shade), the number of Holocene marine terraces (boxed numbers) and the elevation of the maximum Holocene marine transgression surface. Only the faults that have had detailed studies undertaken on them are named (PF: Pakarae Fault, FF: Fernside Fault, RF: Repongaere Fault). Data sources are listed in the legend. Dashed grey boxes outline the regions where thorough coastal geomorphic studies have been undertaken, and which are discussed in detail in the text. *Pacific-Kermadec plate motion after Collot et al. (2001). **(C)** Recent seismicity of the Hikurangi margin at depths shallower than 40 km, 1990 -

present day, events > M 3. **(D)** Recent seismicity of the Hikurangi margin at depths shallower greater than 40 km, 1990 - present day, events > M 3. Maps C and D sourced from www.geonet.org.nz.

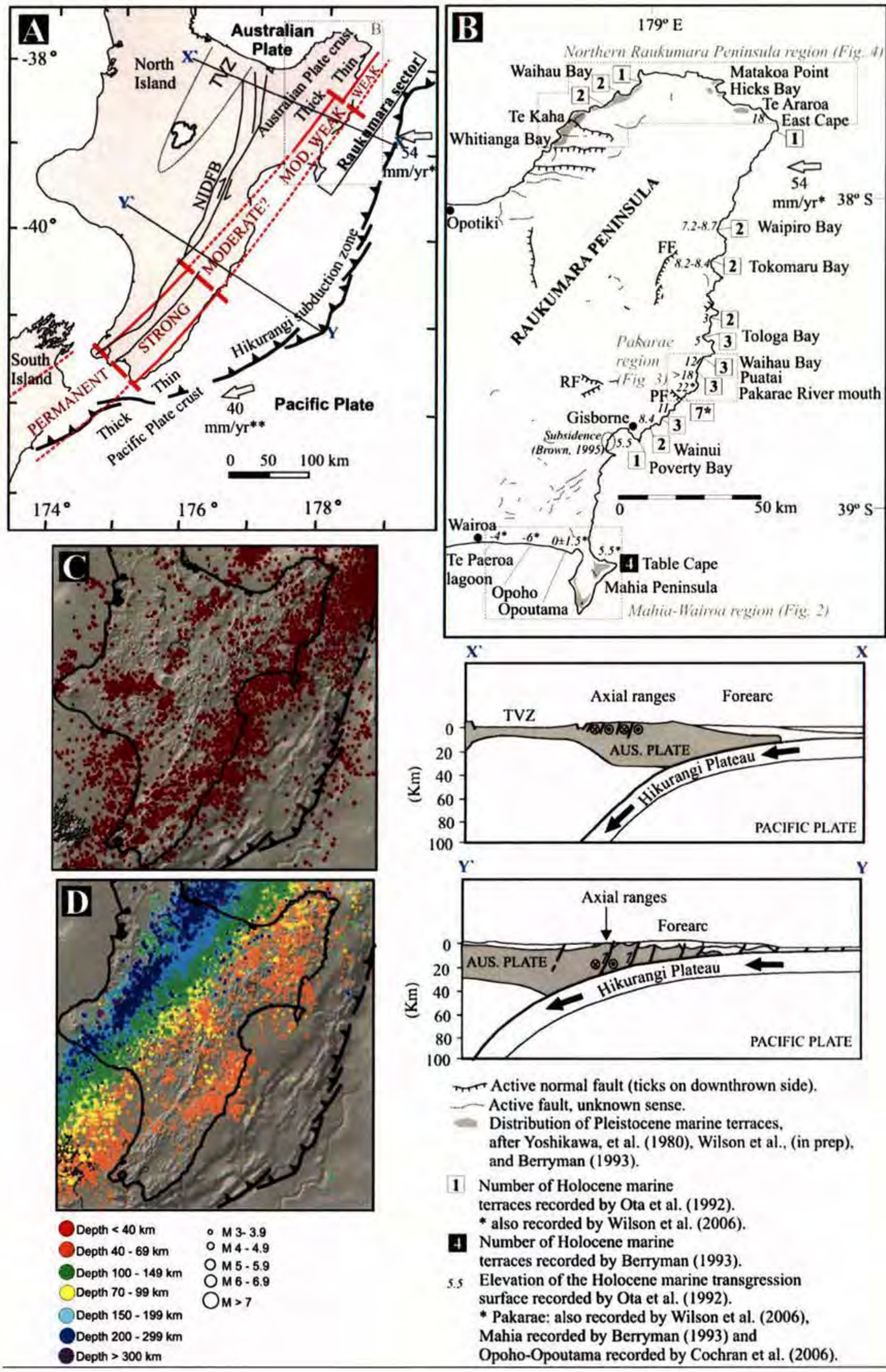

7.2 Previous work

The Hikurangi Trough lies offshore of the East Coast of the North Island and this is the surface manifestation of convergence between the Pacific and Australian Plates (Lewis, 1980; Lewis and Pettinga, 1993, Fig. 1A). The onshore region of the North Island from Cape Palliser in the south to Matakaoa Point in the northeast is known as the Hikurangi margin. Plate convergence rates vary from 54 – 40 mm yr^{-1}, the rate of convergence decreases, and obliquity of convergence increases towards the south (Collot et al., 2001; De Mets et al., 1994). Presently, and for approximately the past 7 Ma, the Hikurangi Plateau, has been subducting along the Hikurangi margin (Reyners et al., 2006). This oceanic crustal Plateau is a Cretaceous large igneous province that is approximately 12 – 15 km thick (Davy and Wood, 1994). A major tectonic feature of the southern and central Hikurangi margin sectors is the North Island dextral fault belt (NIDFB, Fig. 1A). This series of dextral strike slip faults strikes northeast along the eastern side of the axial ranges, at approximately 39° S they strike northward and traverse across the axial ranges to the Bay of Plenty and eastern edge of the TVZ. This major fault system therefore bypasses the Raukumara Peninsula and there is a distinctive absence of active faulting within the onshore forearc of the Raukumara sector.

Interpretations of geodetic data, shallow seismicity and the few active onshore faults in the region suggest the Raukumara Peninsula is currently undergoing margin-normal extension (Darby and Meertens, 1995; Thornley, 1996; Webb and Anderson, 1998; Arnadottir et al., 1999; Reyners and McGinty, 1999). Reyners and McGinty (1999) note that extensional earthquake focal mechanisms occur in the upper 9.5 km of the Raukumara Peninsula crust and compressional thrust faulting occurs below this (Fig. 1C,D). Geodetic measurements by Darby and Meertens (1995), Thornley (1996) and Arnadottir et al. (1999) suggest trenchward extension of the central and eastern Raukumara Peninsula. Few active normal faults have been mapped on the central and eastern Raukumara Peninsula. The three most well-documented faults are the Fernside fault, the Pakarae fault and the Repongaere Fault (Fig. 1B, Mazengarb, 1984; Ota et al., 1991; Wilson, Ch. 2; New Zealand Active Faults Database: http://data.gns.cri.nz/af/index.jsp). These three faults have been active during the Holocene and are short (< 20 km in length) normal faults. Faults such as the Fernside are consistent with the trenchward slumping and extension suggested by Thornley (1996), Arnadottir et al. (1999) and Reyners and McGinty (1999).

Given the absence of active faulting it has long been a question of how the Raukumara Peninsula is uplifting? Sediment underplating was first suggested as a cause of Raukumara Peninsula uplift by Walcott (1987). This theory was largely based on an estimated sediment accretion budget whereby Walcott (1987) compared the amount of sediment estimated to have entered the Hikurangi Trough with the amount of sediment accreted to the forearc. The lack of a modern accretionary wedge adjacent to the Raukumara Peninsula led Walcott (1987) to conclude that sediment entering the subduction zone was ponding beneath the Raukumara Ranges and driving the broad uplift of the Pleistocene marine terraces. Thornley (1996) studied the structural geology, seismicity, geodesy of the Raukumara Peninsula and concluded that the Raukumara Peninsula is undergoing broad antiformal uplift and trenchward extension. Critical wedge models were used to demonstrate that extension is probably due to surficial sliding of Neogene sediments above a detachment layer composed of Paleogene smectite. He inferred the sliding is driven by gravity and maintained by continuous axial range uplift driven by sediment underplating.

Later studies using velocity models, constructed using earthquake arrival time inversions, and seismic attenuation models of the upper plate and subduction interface beneath the Raukumara Peninsula indicated a zone of low velocity and high attenuation directly above the plate interface. This zone is inferred to represent ponded sediment (Eberhart-Phillips and Reyners, 1999; Reyners et al., 1999; Eberhart-Phillips and Chadwick, 2002). The ponded sediment is located deeper than ~ 20 km; it is estimated to be up to 20 km thick and directly underlies the axis of the Raukumara Ranges (Reyners et al., 1999). A channel of subducting sediment ~ 1-2 km thick is inferred on the plate interface along the whole strike of the Raukumara sector (Eberhart-Phillips and Reyners, 1999). Tectonic erosion at the Hikurangi Trough along this portion of the margin provides a sediment source for underplating as the sediment cover on the subducting Plateau is relatively thin at 1 – 1.5 km (Collot et al., 1996). The thickness of the low-velocity zone underlying the Raukumara Peninsula decreases south of a line running approximately between Opotiki and Tologa Bay (Fig. 1A, B), leading Reyners et al. (1999) to infer that the thickness of underplated sediment beneath the Raukumara Peninsula decreases southwestward. They suggest this decrease is related to a change in crustal thickness. Specifically the crust of the northeastern Raukumara Peninsula is ~ 20 km thick and subducted sediment ponds against a relatively strong mantle backstop. In the southwestern Raukumara Peninsula the thickness of the crust increases to ~ 38 km, and the lower crust is relatively weak, allowing sediment subduction to greater depths (Reyners et al., 1999). The body of underplated sediment is not included by Reyners et al. (1999) as part of the Australian plate crust, hence the crustal thickness increases southward despite a substantial thickness (~20 km) of underplated sediment beneath the northern Raukumara Peninsula.

Two recent studies by Upton et al. (2003) and Litchfield et al. (in press) use finite element modelling of a subduction margin to understand the effects that underplated sediment has upon forearc uplift rates. 3D finite-difference modelling by Upton et al. (2003) indicates that an antiformal region of uplift can develop directly above a zone of weaker material in the upper plate. Rates of uplift up to 4 mm yr^{-1} were modelled when a block of weaker material, based on the ponded sediment dimensions of Reyners et al. (1999), was used in the model. The Litchfield et al. (2007) study uses

2D finite element models to test several possible mechanisms of forearc uplift. They demonstrate that sediment underplating could produce uplift of the Raukumara Ranges, although rates of uplift are poorly constrained because the modelling technique dictates that underplated sediment could only be simulated by inducing tectonic erosion at the trough. The study also suggests that subduction of the Hikurangi Plateau may be the cause of widespread low uplift rates (<1 mm yr^{-1}) across the Hikurangi margin and seamount subduction may cause uplift at rates up to 0.7 mm yr^{-1} in localised zones of 20 – 80 km in diameter (Litchfield et al., 2007).

There appears to be less upper plate seismicity on the Raukumara Peninsula relative to the southern Hikurangi margin according to the cumulative number of events greater than or equal to M 4 at depths between 0 – 20 km (Stirling et al., 2002). However, the *b*-value (a parameter that compares the earthquake size distribution of a region to the Gutenberg-Richter relationship) of the Raukumara Peninsula is ~0.9 (Stirling et al., 2002). This value is typically suggests either a reverse faulting province or an incomplete seismic record in which smaller magnitude earthquakes are underestimated in the catalogue. Because the Raukumara Peninsula is a promontory region it is more likely that the distribution of seismic network has resulted in an underestimation of small earthquakes in this region. Therefore the *b*-value indicates that the apparent decrease in upper plate seismicity on the Raukumara Peninsula is therefore probably an artefact of the seismic network distribution rather than a real tectonic signal.

The Raukumara sector plate interface is inferred to be presently weakly coupled relative to the southern sectors of the margin. Plate coupling has been estimated primarily by two methods: firstly by the distribution and nature of earthquake focal mechanisms along the plate interface (Reyners et al., 1998; Reyners and McGinty, 1999) and secondly by modelling GPS velocities (Wallace et al., 2004). These methods provide different ways of estimating plate coupling. The Reyners (1998) study estimates the margin-normal width of the plate interface that is seismically locked (Fig. 1A), whereas the Wallace et al. (2004) study estimates the slip rate deficit between plate convergence and interface movement and uses this to produce a coupling coefficient. Both of these are a measure of the current interseismic coupling state of the interface. Reyners (1998) estimates the width of the locked zone beneath the Raukumara Peninsula to be 20 – 40 km beneath the onshore forearc in the southwest but largely offshore in the northeastern part of the Raukumara Peninsula (Fig. 1A). The Wallace et al. (2004) model shows a relatively uniform coupling coefficient across the Raukumara Peninsula, with only a patch of slightly higher coupling in the Gisborne to Tologa Bay area. Both studies of plate coupling show a gradient in coupling along the strike of the margin, from strongly coupled in the southwest to weakly coupled in the northeast, beneath the Raukumara Peninsula. They suggest there is a correlative decrease in the maximum size of subduction earthquakes that may be generated by plate interface rupture along the margin from southwest to northeast.

The above studies suggest that the Raukumara Peninsula is in a state of margin-normal extension and that the forearc overlies a plate interface that possibly does not generate large to great subduction earthquakes. However moderate to high coastal uplift rates (2-5 mm yr^{-1}) have been recorded at many coastal localities along the peninsula (Ota et al., 1988; 1992). Elsewhere along the margin uplift rates of these magnitudes have been attributed to compressional structures, typically reverse faults listric to the plate interface. This study uses coastal uplift data to make inferences about the geodynamics of the subduction zone, and we will try to address inconsistencies between geophysical and geological methods of studying forearc deformation.

7.3 Raukumara Peninsula coastal geomorphology and uplift mechanisms

The late Quaternary coastal geomorphology of the Raukumara Peninsula has been studied at a reconnaissance level by Ota et al. (1988; 1992) and Brown (1995). These studies documented the occurrence and elevation of the highest Holocene marine transgressive sediments, and the number of Holocene marine terraces (Fig. 1B). Eustatic SL in the New Zealand region stabilised at ~ 7 ka (Gibb, 1986). The surface created when sediments infilled valleys up to the stable SL position is known as the maximum Holocene marine transgression surface (Ota et al., 1988) and it can be used as a marker horizon to estimate the sense and amount of vertical tectonic movement since ~ 7 ka B.P. Ota et al. (1988) measured the maximum Holocene marine transgression surface at elevations between – 4 and 22 m along the Raukumara Peninsula coast (Fig. 1B). Holocene marine terraces represent coastal uplift that has occurred since the time of eustatic SL stabilisation (post-7 ka B.P., Gibb (1986). Between one and seven marine terraces were measured and described by Ota et al. (1988) at 22 locations. However, seven of these locations on the northeastern Raukumara Peninsula have been revised by Wilson (Ch. 5).

The late Quaternary coastal tectonic geomorphology of three regions of the Raukumara Peninsula has been studied in detail: (1) the coastline from Whitianga Bay to East Cape, an area we refer to as the northern Raukumara Peninsula region, (2) the Pakarae region, and (3) Wairoa to Mahia Peninsula region (Fig. 1B). We summarise the results of studies in each of these regions with emphasis on the mechanisms of vertical tectonic movement.

7.3.1 Mahia-Wairoa region

The Holocene coastal geomorphology and stratigraphy of the coastline between Wairoa and Mahia Peninsula has been studied by Ota et al. (1989), Berryman (1993a, b) and Cochran et al. (2006) (Fig. 2). Mid to late Holocene uplift of the Mahia

Peninsula is evidenced by a flight of by 4 to 5 marine terraces (Berryman, 1993a). Sediment cores of mid to late Holocene marginal marine sediments collected at Opoutama show equivocal evidence for vertical movement. Sediment cores at Te Paeroa lagoon and Opoho show the maximum Holocene marine transgression surface presently lying at 4 and 6 m below modern mean SL, this indicates net tectonic subsidence since the time of eustatic SL stabilisation (Cochran et al., 2006).

The Holocene marine terraces at Table Cape and Auroa Point, Mahia Peninsula, display topography, coverbed stratigraphy and radiocarbon age clustering all indicative of uplift by a sudden coseismic mechanism (Berryman, 1993a). Average Holocene uplift rates vary along the coast and range from 2.5 mm yr^{-1} to 0.7 mm yr^{-1}. The structure accommodating uplift is probably the Lachlan Fault, a thrust fault located offshore 5-10 km eastward of Mahia Peninsula (Fig. 2, Barnes et al., 2002). This fault and the associated anticlinal Lachlan Ridge structure are well imaged by hydrocarbon exploration seismic data (Barnes et al., 2002). It is fortuitous that seismic lines can be placed across the southern tip of Mahia Peninsula thus enabling imaging of a cross-section of the Lachlan Ridge structure. The Lachlan Fault dips westward at 55° – 70°, but the gradient decreases with depth to become listric to the subduction interface at ~20 km depth (Barnes et al., 2002). This position is approximately within the middle of that part of the plate interface estimated to be interseismically locked by Reyners (2000, Fig. 1A), but it is not strongly coupled according to the GPS-determined slip deficit (Wallace et al., 2004). A suite of seven Pleistocene marine terraces at Mahia Peninsula attest to coastal uplift dating back to ~ 210 ka (Fig. 2). These terraces display a west-northwest tilt, consistent with uplift on the flank of the Lachlan anticline (Berryman, 1993b).

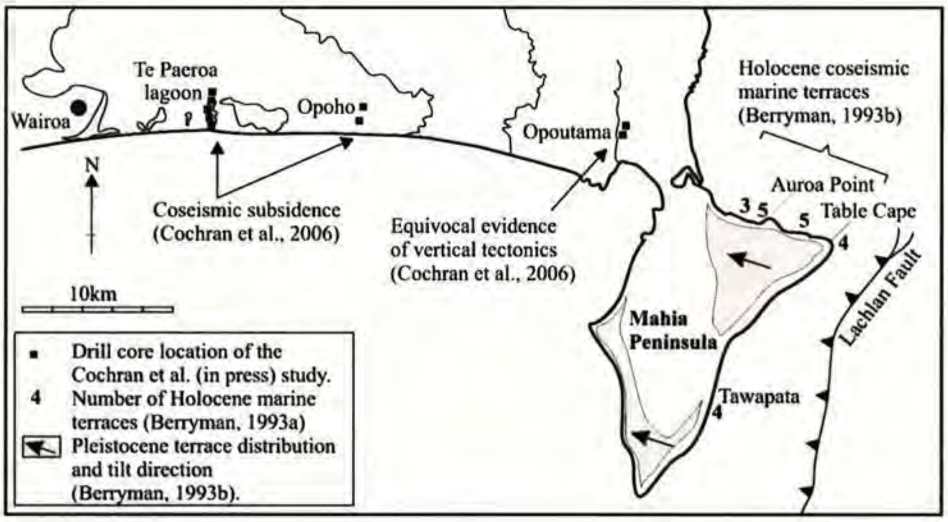

Figure 2. Location map and summary of the coastal neotectonics in the Mahia-Wairoa region. Position of the Lachlan Fault after Barnes et al. (2002). Location of Holocene marine terraces and the distribution of Pleistocene marine terraces are shown.

Two subsidence event horizons have been identified within sediment cores collected from Te Paeroa lagoon and Opoho. The events are identified by rapid paleoenvironmental changes and coincide with probable tsunami deposits; thus a sudden coseismic mechanism is inferred (Cochran et al., 2006). Thus far the subsidence events at Te Paeroa lagoon and Opoho have not been correlated to terrace uplift events at Mahia Peninsula, the age ranges of these two data sets do not coincide. Forward elastic dislocation models indicate the observed pattern of vertical movement recorded at Te Paeroa lagoon, Opoho and Opoutama could be generated by rupture of the subduction interface or the Lachlan fault or by simultaneous rupture of both (Cochran et al., 2006).

7.3.2 Pakarae region

Ota et al. (1991) and Wilson (Ch. 2) have studied the mid to late Holocene marine terraces at the Pakarae River mouth (Fig. 3A, B). The morphology, coverbed stratigraphy and radiocarbon ages of the terraces are consistent with coseismic events causing uplift and abandonment of marine abrasion surfaces. Seven marines terraces record uplift since ~ 7 ka B.P at intervals of 850 ± 450 yrs with an average magnitude of 2.7 ± 1.1 m per event (Fig. 3B, C). The average uplift rate is 3.2 ± 0.8 mm yr^{-1}. A sequence of early Holocene transgressive marine sediments underlying the highest terrace at the Pakarae River mouth has been studied by Berryman et al. (1992) and Wilson (Ch. 3, Ch 4). These studies demonstrated that the infill sequence is thinner than expected given eustatic SL change, implying uplift during deposition. Wilson (Ch. 4) used paleoenvironmental facies architecture to identify three uplift events that occurred during infilling of the Pakarae River paleo-valley in the early Holocene. Significantly, this study used biostratigraphy to demonstrate that changes from estuarine to floodplain paleoenvironments were sudden, verifying that uplift at the Pakarae River mouth occurs by coseismic mechanisms.

At Puatai Beach and Waihau Bay, 9 and 15 km northeast of the Pakarae River mouth respectively, uplift rates of similar magnitudes to the Pakarae River mouth have been estimated from marine terraces (Fig. 3A). This region from Waihau Bay will henceforth be referred to as the Pakarae region (Fig. 3A). Puatai Beach appears to have the highest uplift rates of the three locations and has been suggested to represent the crest of a coast-parallel ellipsoid dome structure. Coseismic uplift of the three locations is thought to be driven by a near-shore reverse fault striking approximately north-notheast (Fig. 3A, Ota et al., 1991; Litchfield and Wilson, 2005; Wilson, Ch. 2). It is likely that this fault lies within 5 km of the coastline. The existence of the fault has not been verified by seismic imaging because available seismic data do not reach this close to the shoreline. Bathymetric data support the existence of active structures offshore of the Pakarae region; Ariel Bank, a north-northeast-striking bathymetric high, approximately 20 km southeast of the Pakarae River mouth is an example (Lewis et al., 1997). A reverse fault directly offshore of the Pakarae region has been mapped by Lewis et al. (1997), though this was based upon the inferences of Ota et al. (1991), rather than seismic or bathymetric data. Recent seismic data collected by the Ministry of Economic Development may help to map the offshore region in greater detail (Ministry of Economic Development Petroleum Report Series PR3136, 2005).

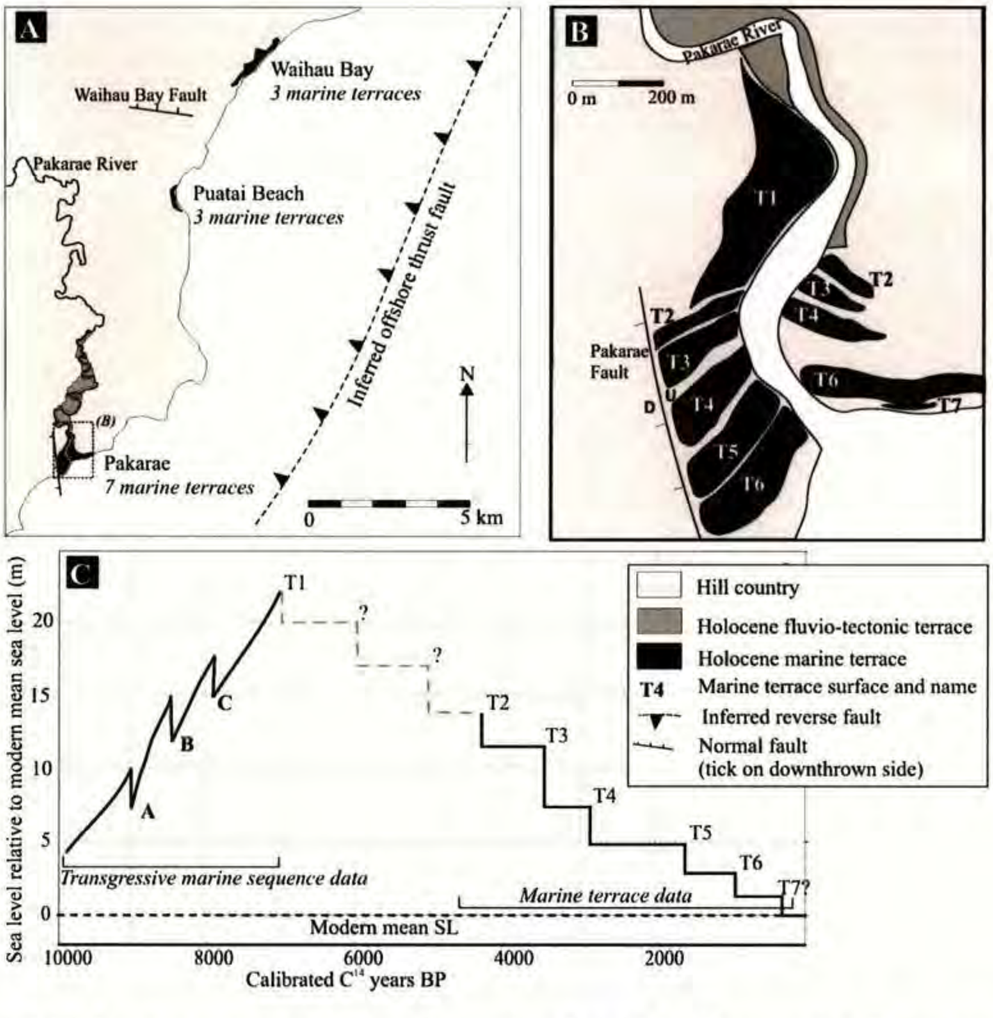

Figure 3 (A) Location map, neotectonics and coastal geology of the Pakarae region. Terrace numbers and inferred offshore fault location after Ota et al. (1991). **(B)** Marine terrace distribution at the Pakarae River mouth, after Wilson, Ch. 2. **(C)** A relative Holocene sea level curve for the Pakarae River mouth locality from Wilson, Ch. 4. Steps within the curve represent sudden relative sea level falls due to coseismic land uplift.

Litchfield and Wilson (2005) studied the surface geometry of late Holocene fluvial terraces along the Pakarae River that grade to the marine terraces. These fluvio-tectonic terraces have a landward tilt and display a fan-like geometry that implies uplift of the terraces was greatest at the coast. The Holocene marine terraces at the Pakarae River mouth also display a landward tilt of 0.24° (Wilson, Ch. 2). Evidence of landward tilt is consistent with uplift along a nearshore reverse fault. Preliminary elastic dislocation modelling using the geometry of the fluvio-tectonic terraces and marine terrace uplift rates indicates that the offshore reverse fault is likely to be very steep and may or may not be listric to the plate interface. No dislocation models could exactly replicate the pattern of uplift created by the Pakarae River mouth-Puatai-Waihau Bay data points. Invoking slip on both the plate interface and the upper plate reverse fault did not help to resolve the model (L. Wallace, *pers.comm.*, Litchfield and Wilson, 2005).

7.3.3 Northern Raukumara Peninsula region

Aspects of the Holocene coastal geomorphology of the northern Raukumara Peninsula, from Hicks Bay to East Cape, have been examined by Garrick (1979), Ota et al. (1992) and Wilson (Ch. 5). Ota et al. (1992) described up to five marine terraces on the coastline east of Te Araroa at Waipapa and Horoera. They inferred from the geomorphology that the terraces were uplifted by coseismic events. Wilson (Ch. 5) undertook detailed topographic surveys and an examination of the cover sediment sequences of the terraces and concluded the terraces did not have a marine origin and therefore yielded no evidence of coseismic uplift events. Wilson (Ch. 5) examined the biostratigraphy and chronology of a transgressive marine sequence infilling the Hicks Bay valley (Fig. 4A). Significant differences between the preserved thickness of intertidal valley infill and the amount of eustatic SL rise during the equivalent time periods indicated the uplift occurred synchronously with deposition of the trangressive sequence. Paleoecological constraints indicate this uplift was probably gradual, though it may have occurred by frequent coseismic events causing <0.85 m of uplift per event. The seaward slope of an uplifted beach ridge sequence at Te Araroa also supports gradual uplift (Fig. 4A). The Wilson (Ch. 5) study concluded that most Holocene uplift in this region was aseismic.

An average Holocene uplift rate of 1.7 ± 0.4 mm yr^{-1} was calculated from the Hicks Bay transgressive marine sequence data. At Te Araroa the Holocene uplift rates are poorly constrained and range between 0.5 and 2 mm yr^{-1}. Yoshikawa et al. (1980) collected a wood sample from a riverbank exposure of silt containing marine and estuarine diatoms at 7 m AMSL along the Waipapa Stream (labelled "Yoshikawa outcrop", Fig. 4A). It yielded a radiocarbon age of 9900-9400 cal. yrs B.P., equating with an uplift rate of $2.7 - 3.3$ mm yr^{-1} (using 22 ± 2 m of eustatic SL rise since its deposition, Gibb, 1986). These few measurements of Holocene uplift indicate that uplift rates in this region increase southeastward towards East Cape.

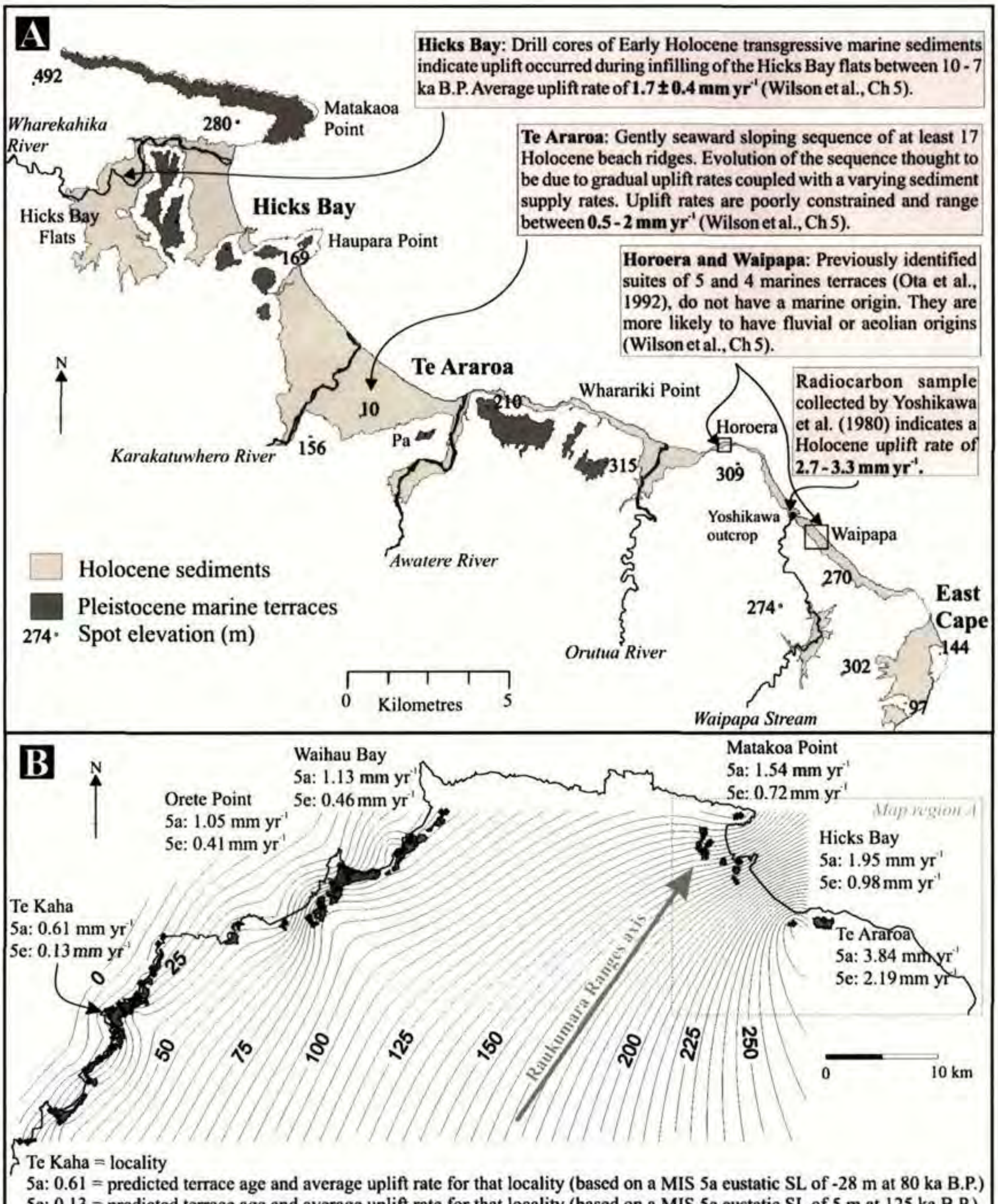

Figure 4 (A) A summary of the Holocene coastal geomorphology of the northern Raukumara Peninsula region from Hicks Bay to East Cape. (B) Distribution of the Otamaroa Pleistocene marine terrace along the northern Raukumara Peninsula coastline. Contour lines represent the smoothed elevation of the surface at the top of marine deposits on the terrace strath (5 m contour interval). As discussed in the text, it is currently uncertain whether this is a Stage 5a (~80 ka) or 5e (~125 ka) terrace; uplift rates for both cases are shown. Map source: Wilson (Ch. 6).

The Pleistocene marine terrace distribution and chronology of the northern Raukumara Peninsula have been studied by Chapman-Smith and Grant-Mackie (1971), Yoshikawa et al. (1980), Yoshikawa (1988) and Wilson (Ch. 6). Two terraces, the higher Otamaroa terrace and the lower Te Papa terrace, almost continuously fringe the northern Raukumara Peninsula coastline from Whitianga Bay to Te Araroa (Fig. 1B, Fig. 4B). The terrace surfaces tilt to the northwest, approximately normal to the trend of the Hikurangi Trough. The tilt vector becomes more northerly towards Te Araroa (Fig. 4B). The age of these terraces is uncertain. Wilson (Ch. 6) presented six OSL ages from terrace cover sediments that suggest the terraces formed during marine isotope stages (MIS) 3 and 5a, in which case the present day elevation differentials between the two terraces imply uplift rates have increased through time. However loess chronology and uplift models, which assume uplift rates have been constant, suggest that the terraces formed during MIS 5c and 5e (Wilson, Ch. 6). The Otamaroa terrace is present in the middle of Hicks Bay, adjacent to the location where drill cores of the Holocene transgressive marine sediments were collected. If the Otamaroa terrace formed during MIS 5a, the average uplift rate for the past ~80 ka is 2 ± 0.2 mm yr^{-1} for the Hicks Bay locality. This is within the uncertainty range of the Holocene uplift rate of 0.9-2.2 mm yr^{-1}, estimated from the uplifted Holocene transgressive marine sediments (Wilson, Ch. 5). If the Otamaroa terrace formed during MIS 5e, the average uplift rate during the past ~125 ka is 1 ± 0.1 mm yr^{-1} for the Hicks Bay locality, which is less than the Holocene uplift rate (Wilson, Ch. 6).

Several east-west trending normal faults have been mapped on the western side of the Raukumara Peninsula (Fig. 1B). However the hanging walls are downthrown in the same direction as the terrace tilt, thus it is difficult to resolve offset given the relatively coarse terrace elevation data (Wilson, Ch. 6). These faults, if active, are not sufficient to drive the uplift and tilting of the Pleistocene terraces as far east as Te Araroa.

We assume here that the aseismic uplift process that is responsible for Holocene uplift at Hicks Bay and Te Araroa (Wilson, Ch. 6) is the same process that has driven uplift of the Pleistocene terraces. Evidence for this includes of (1) possible similarity in Holocene and Pleistocene uplift rates at Hicks Bay; (2) Holocene uplift rates on the eastern side of the Raukumara Peninsula increase toward the southeast, in the same direction as the rise in the Pleistocene terraces; and (3) uplifted Holocene sediments are recorded only in regions where the Pleistocene terraces are higher than ~ 60 m (Fig. 1B, Fig. 4B), implying that the same uplift process controls the distribution of Holocene and Pleistocene terraces.

Crustal doming above a zone of buoyant underplated sediment adjacent to the Hikurangi subduction zone is the most likely driver of aseismic coastal uplift of the northern Raukumara Peninsula region. This mechanism was first suggested by Walcott (1987), though it was largely based on an estimated sediment accretion budget for the Raukumara Peninsula. Here we present several additional lines of evidence that support the theory that sediment underplating is driving uplift of the northern peninsula.

Firstly, the uplifted Pleistocene terraces span a margin-normal width of ~60 km and a margin-parallel length of ~ 60 km (Fig. 4B). Fault scaling relationships imply that if a single fault accommodated uplift of these terraces, the fault would necessarily have a high slip rate (in excess of the maximum terrace uplift rate of 2.2 or 3.8 mm yr^{-1}) and would have to be longer than 60 km in length. There are no known active faults onland near East Cape that could produce the uplift geometry of the Otamaroa Pleistocene terraces (Fig. 1B). A normal fault, downthrown to the southeast, has been mapped near East Cape by Mazengarb and Speden (2000), but there is no evidence it has been active during the Quaternary. In any case, the Pleistocene marine terraces are located in the footwall of this fault and the majority of absolute movement during slip on normal faults occurs through subsidence of the hanging wall (Jackson et al., 1988). There are also no known active faults immediately offshore of the northern Raukumara Peninsula that can explain Pleistocene marine terrace uplift (Fig. 5A, Davey et al., 1997; Lewis et al., 1997; 2004). However, nearshore active faults can be difficult to identify because scarps are eroded by the waves. A recent seismic survey traversing from the head of the Ruatoria margin re-entrant scarp across the northern tip of the Raukumara Peninsula showed no evidence of a reverse fault similar to the Lachlan fault (C. Uruski and D. Barker, *pers. comm.*, Ministry of Economic Development Petroleum Report Series PR3136, 2005). Some anticlinal structures have been mapped offshore of East Cape, but they are more than 30 km offshore and less than 40 km in length (Collot et al., 1996; Lewis et al., 1997; 2004).

Sediment underplating is a viable explanation for northern Raukumara Peninsula uplift because a zone of ponded sediment located above the plate interface has been inferred using velocity and seismic attenuation models models (Eberhart-Phillips and Reyners, 1999; Reyners et al., 1999; Eberhart-Phillips and Chadwick, 2002). Numerical modelling by Upton et al. (2003) and Litchfield et al. (2007) also supports sediment underplating as a mechanism of upper plate uplift along the Hikurangi margin. Surface uplift rates of up to 4 mm yr^{-1} over a zone of weaker material, input to a 3D finite-difference model to simulate ponded sediment, were estimated by Upton et al. (2003). These rates are similar or slightly higher than the Pleistocene terrace uplift rates at Te Araroa (Wilson, Ch. 6). 2D finite element modelling of the northern Hikurangi margin by Litchfield et al. (2007) concluded sediment underplating, caused by tectonic erosion, is the most likely mechanism of axial range uplift in the northern Hikurangi margin. Their model of sediment underplating showed a broad zone of uplift extending a margin-normal distance of ~180 km from the trough.

7.4 A model of Raukumara Peninsula uplift: subduction margin-parallel uplift mechanism zones.

Evidence presented thus far shows that coastal uplift mechanisms of the Raukumara Peninsula are spatially variable. We suggest the most important parameter controlling forearc uplift is the distance from the subduction zone, and by inference, the increasing depth to the underlying plate interface. We propose three margin-parallel tectonic zones operating across the Raukumara sector of the Hikurangi margin (Fig. 5B).

The most outboard zone lies within a margin- normal distance of ~ 20 – 80 km of the Hikurangi Trough, this is the coseismic uplift zone. A central zone, termed the passive inner forearc, lies between a margin normal distance of ~ 80 – 120 km from the trough. The most inboard zone, called the aseismic uplift zone, lies at a distance of greater than ~ 120 km, and extends to ~ 180 km though its westward limit is poorly constrained. The region within 10 – 20 km of the trough is one of tectonic erosion or, south of ~39°30', an area of accretion. These latter regions, directly adjacent to the Hikurangi Trough, are not included within our model; their detailed structure is discussed in Collot et al. (1996). Here we outline the evidence for each of the three vertical tectonic zones we have delineated, and the vertical tectonic processes operating within them.

7.4.1 Coseismic uplift zone

Deformation within this zone is characterised by permanent deformation of the upper plate with locally high rates of uplift along margin-parallel compressional structures – these are probably dominantly short (< 50 km length) listric, reverse faults. The plate interface lies at a depth of 0-18 km (Fig. 6). The primary evidence for this zone is the well-documented Holocene coseismic uplift in the Pakarae region and at Mahia Peninsula (Ota et al., 1991; Berryman, 1993a; Wilson, Ch. 4.). These regions are located at the most southeasterly promontories of the Raukumara Peninsula and are the closest land to the Hikurangi Trough. Mahia Peninsula is ~80 km from the trough and the 15 km stretch of coastline of the Pakarae region is approximately 70 – 75 km from the trough.

Figure 5 (A) Topography, major geomorphic elements and offshore structures of the Raukumara Peninsula. Coloured circles show postglacial fluvial incision rates, which are used as a proxy for rock uplift rates, after Litchfield and Berryman (2006). Offshore structures after Lewis et al. (1997). NIDFB: North Island dextral fault belt. Red arrows and numbers measure the margin-normal distance of the coastal regions from the Hikurangi Trough. **(B)** A model of Raukumara sector forearc uplift mechanism zones. Area within the grey dotted line represents the deformation front of the Hikurangi Trough; structures within this zone are not included within this model.

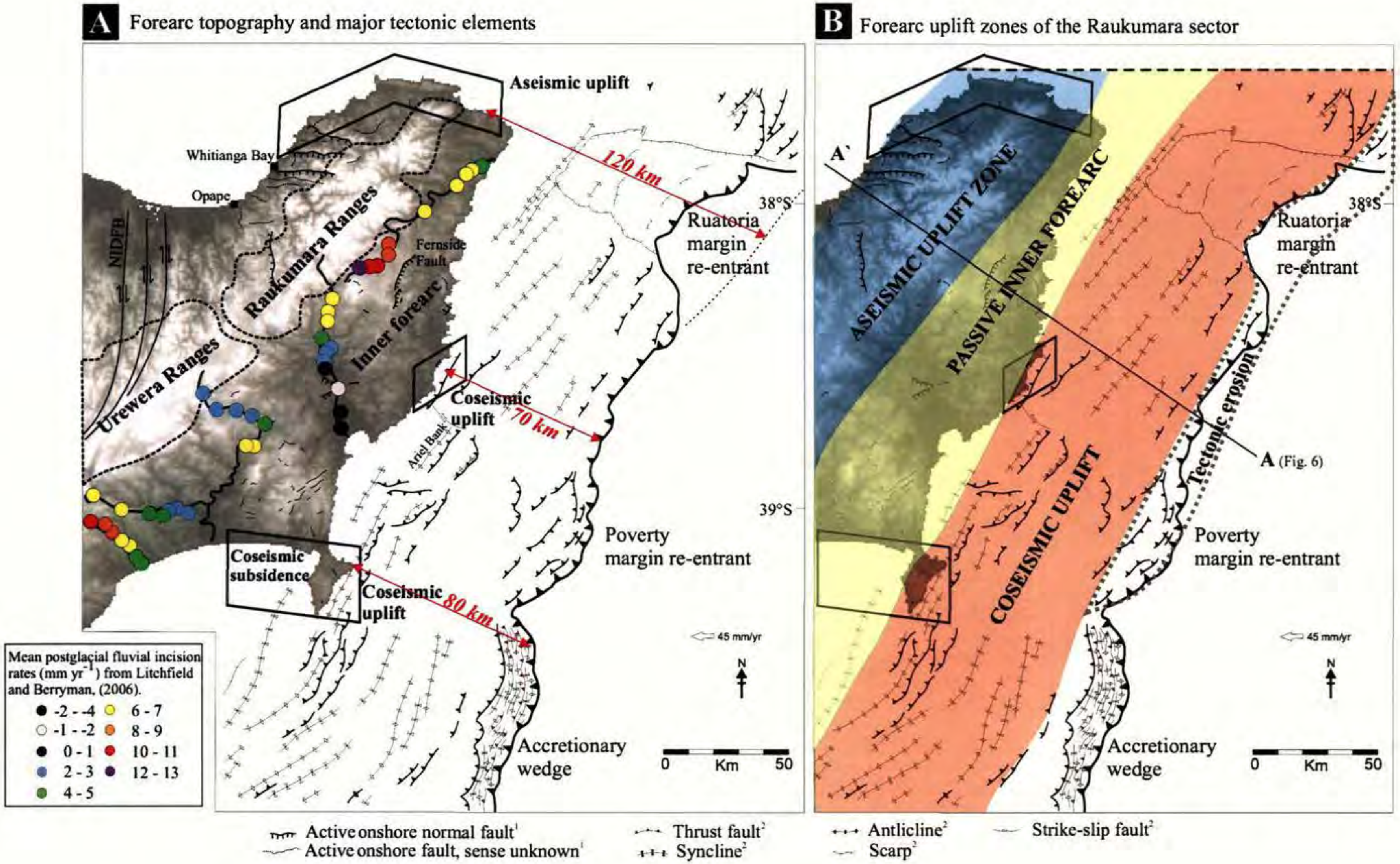
A
Forearc topography and major tectonic elements
Aseismic uplift
Whitianga Bay
Opape
NIDFB
Raukumara Ranges
Fernside Fault
Inner forearc
Urewera Ranges
120 km
Ruatoria margin re-entrant
38°S
Coseismic uplift
70 km
Ariel Bank
39°S
Poverty margin re-entrant
Coseismic subsidence
Coseismic uplift
80 km
45 mm/yr
N
Accretionary wedge
0 Km 50
Mean postglacial fluvial incision rates (mm yr-1) from Litchfield and Berryman, (2006).
-2 - -4
-1 - -2
0 - 1
2 - 3
4 - 5
6 - 7
8 - 9
10 - 11
12 - 13
B
Forearc uplift zones of the Raukumara sector
A'
ASEISMIC UPLIFT ZONE
PASSIVE INNER FOREARC
COSEISMIC UPLIFT
Tectonic erosion
A (Fig. 6)
Active onshore normal fault[1]
Active onshore fault, sense unknown[1]
Thrust fault[2]
Syncline[2]
Antlicline[2]
Scarp[2]
Strike-slip fault[2]

Estimates of the interseismic locked portion of the plate interface based on seismicity data place the trenchward edge of the locked zone directly below the Pakarae region and directly below Opoutama (Reyners, 1998). By implication, if the faults driving coastal uplift are listric to the plate interface, they intersect it within the interseismic locked portion. Current knowledge of structures offshore of the Raukumara sector indicate there are margin parallel reverse faults, synclines and anticlines (Fig. 5B, Lewis et al., 1997). These structures appear to form a zone with an arcward edge approximately in line with Mahia Peninsula and the Pakarae region. The nature and age of these structures are currently poorly known. We have made some preliminary interpretations of structure on a recently collected seismic line from the continental shelf approximately 20 km northeast of the Pakarae River mouth (Fig. 7). We presently have no age control on the units imaged in this seismic line but a nearshore fault offsets the seafloor, suggesting it has been active recently. Additional faults on the mid and outer shelf attest to the presence of numerous structures offshore of the Raukumara Peninsula, consistent with our suggestion of a compressional deformation zone. However, we emphasize these are preliminary interpretations and further interpretations of the 05CM 2D Seismic Survey collected in 2005 will provide a test of our model (Ministry of Economic Development Petroleum Report Series PR3136, 2005).

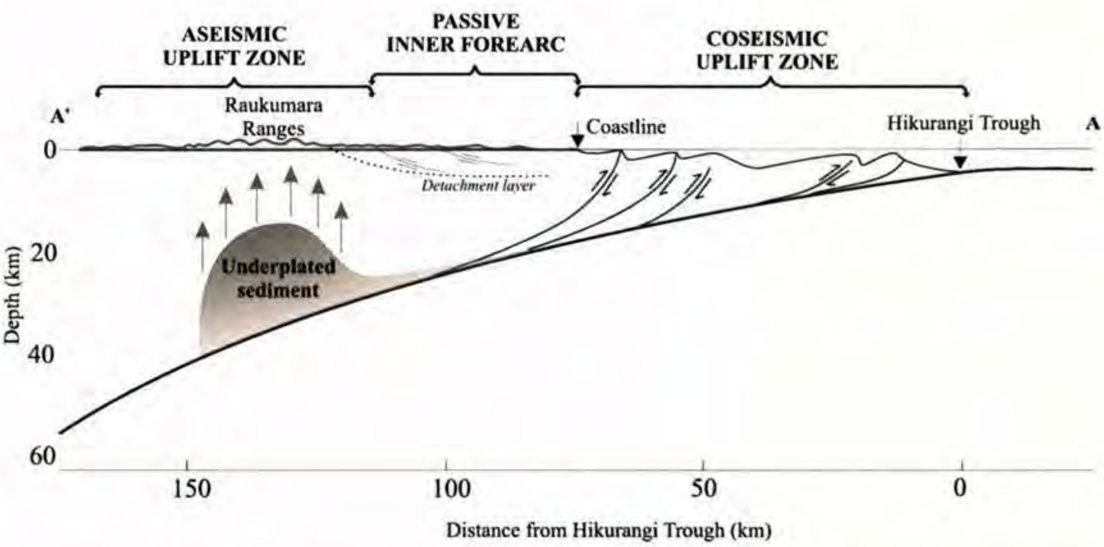

Figure 6. Schematic cross-section of the structures accommodating uplift across the Raukumara Peninsula. Geometry of the plate interface and ponded sediment body after Reyners et al. (1999). The nature of the offshore faults and the position of the detachment layer is an approximation and not based upon any seismic data. The forearc uplift zones from our model are shown above for reference.

7.4.2 *Passive inner forearc*

This zone encompasses most of the eastern Raukumara Peninsula, excluding the southeastern coastal promontories of the Pakarae region and Mahia Peninsula. The zone consists dominantly of Neogene forearc basin sedimentary rocks and parts of the East Coast Allochthon. The plate interface lies at a depth of ~18 – 25 km (Fig. 5B, Fig. 6). This zone encompasses most of the onland portion of the inner forearc and approximately 20 – 30 km of the continental shelf north of ~38° 30' S. The distinguishing characteristics of the zone are a comparative lack of active faults, subdued topography and low to moderate vertical movement rates along the coast.

This zone is termed the passive inner forearc because we suggest vertical movements within the area occur in response to movement on distant structures. There are no structures within the upper plate of the passive inner forearc zone that drive vertical surface movements. Rather, uplift or subsidence is driven by structures either located trenchward in the coseismic uplift zone, in the arcward aseismic uplift zone, or by plate interface seismicity. An example is in the Mahia-Wairoa region where subsidence at Te Paeroa lagoon and Opoho has probably been driven by either the Lachlan Fault, ~ 45 km away, or by rupture of the underlying plate interface (Cochran et al., 2006). Likewise, moderate uplift rates have been recorded at several locations along the coastline between the Pakarae region and East Cape (Ota et al., 1988; 1992) though no faults have been mapped in this area (Fig. 5A, Lewis et al., 1997; Mazengarb and Speden, 2000). Along this portion of the coastline it is not well resolved whether these moderate uplift rates are achieved by coseismic or aseismic mechanisms. While two or three marine terraces were recorded at four locations by Ota et al. (1992, Fig. 1B) that study was undertaken at a reconnaissance level. The study of terraces at Waipapa and Horoera by Wilson (Ch. 5) demonstrated that terrace geomorphology does not unambiguously equate with coseismic coastal uplift. Therefore we suggest further work to resolve the uplift mechanism may be justified along this portion of the coast with moderate uplift rates.

7.4.3 *Aseismic uplift zone*

Uplift within this zone is caused by a zone of underplated buoyant sediment. The most easterly localities of the northern Raukumara Peninsula region where aseismic uplift is inferred, namely Te Araroa, Waipapa and Horoera, are >120 km from the Hikurangi Trough (or rather, from the trend of Hikurangi trough because at this location the margin is indented by the head scar of the Ruatoria debris avalanche (Fig. 5B, Collot et al., 2001; Lewis et al., 2004). The plate interface is at a depth of 25 – 50 km and is overlain by an estimated 20 km of ponded underplated sediment (Fig. 6, Reyners et al., 1999). The edges of this zone are poorly constrained and currently are placed at the extent of the well-preserved Pleistocene marine terraces fringing the northern Raukumara Peninsula (Fig. 5B, Yoshikawa et al., 1980; Wilson, Ch. 6). However, the western coastline of the Raukumara Peninsula is approximately parallel

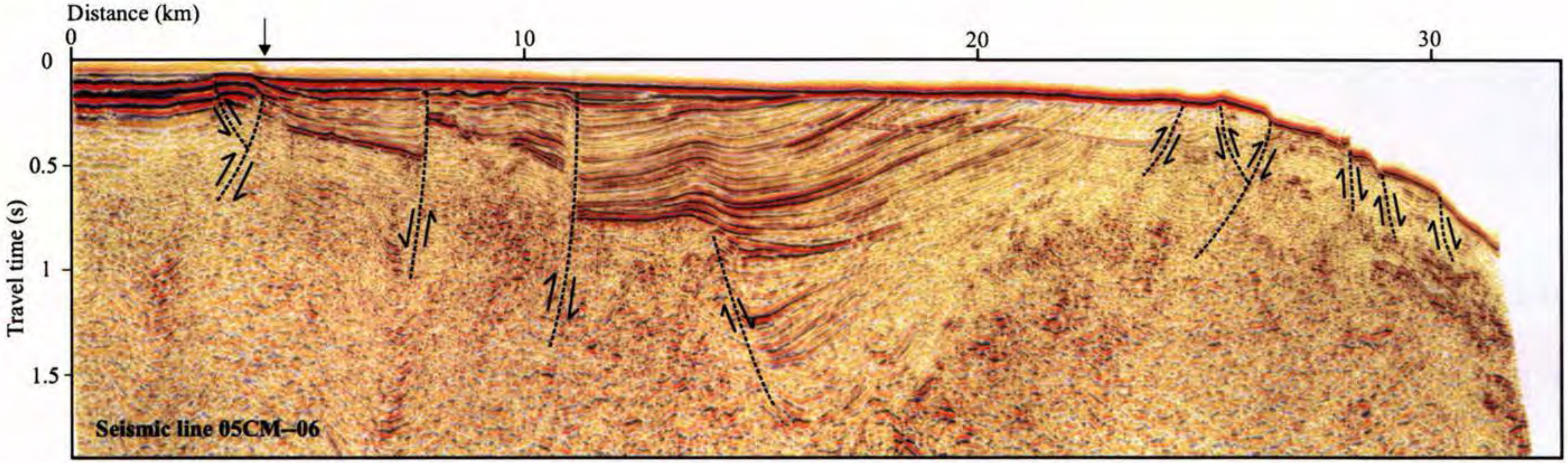

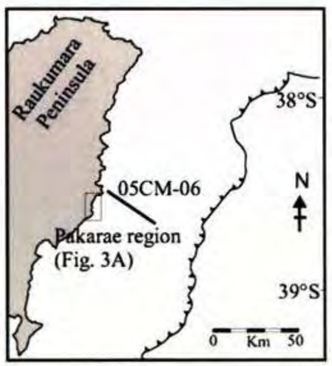

Figure 7. Migrated seismic profile 05CM-06 on the continental shelf off the Raukumara Peninsula continental shelf (Ministry of Economic Development Petroleum Report Series PR3136, 2005). Vertical exaggeration is approximately 1:5 based on a travel time of 2000 m/s. Inset shows the location of the seismic line relative to the Pakarae region. The arrow shows a probably bathymetric expression of active faulting. The overlay shows a preliminary interpretation of structure, though there is no age control on the offset units.

to the Hikurangi Trough, suggesting that subduction processes control the formation of this whole coastline. Westward from Opape, faulting associated with the boundary of the Taupo volcanic zone dominates the tectonic structure (Wright, 1990; Taylor et al., 2004).

The trenchward boundary of the aseismic zone is located at Waipapa, the most eastern location where Holocene coastal uplift has been unequivocally recorded (Yoshikawa et al., 1980, Wilson, Ch. 5). However, the boundary of this zone could be further east and, in fact, could encompass East Cape, but we have little control on uplift rates or mechanisms east of Waipapa. We locate the southwest boundary of the aseismic uplift zone at the edge of the Raukumara Ranges (Fig. 5B). This boundary coincides with an increase in uplift rates as determined from fluvial terrace incision rates (Litchfield and Berryman, 2006).

7.5 Discussion

7.5.1 Relationships between Pleistocene marine terrace geometry, sediment underplating, and Raukumara Ranges uplift within the aseismic uplift zone.

We have demonstrated that sediment underplating is probably the cause of aseismic uplift of the Pleistocene marine terraces of the northern Raukumara Peninsula. These terraces extend across the northern projection of the axis of the Raukumara Ranges. It is implicit in our interpretation that sediment underplating also drives uplift of the Raukumara Ranges (Fig. 5B), as suggested by Walcott (1987), Reyners et al. (1999), Upton et al. (2003) and Litchfield et al. (2007). These studies have generally assumed that the axis of the Raukumara Range is the zone of maximum uplift (for example, uplift maps by Walcott, 1987; Pillans, 1986 and Litchfield et al., 2007). However, differences between the geometry of the marine terraces and the Raukumara Ranges suggest this may not be the case (Fig. 8).

The point of maximum marine terrace uplift is offset ~13 km east of the approximate along-strike projection of the Raukumara Range axis (Fig. 8). Furthermore, the marine terraces, tilting uniformly northwest, do not display approximately symmetrical antiformal geometry like the Raukumara Ranges (Fig. 8). Do these dissimilarities imply that sediment underplating is not the only uplift process involved in marine terrace uplift? Or, given that the Pleistocene marine terraces are a younger landform than the Ranges, is there temporal variation in the zone of maximum uplift? Or, alternatively, are the crests of the Raukumara Ranges not actually the zone of maximum uplift?

Firstly, we are confident that both the Pleistocene marine terraces and the Raukumara Ranges have formed predominantly by the same uplift mechanism. Evidence to support this includes the absence of active onland faults or candidate offshore faults, imaging of ponded sediment beneath the ranges (Reyners et al., 1999) and modelling of sediment underplating (Upton et al., 2003; Litchfield et al., 2007).

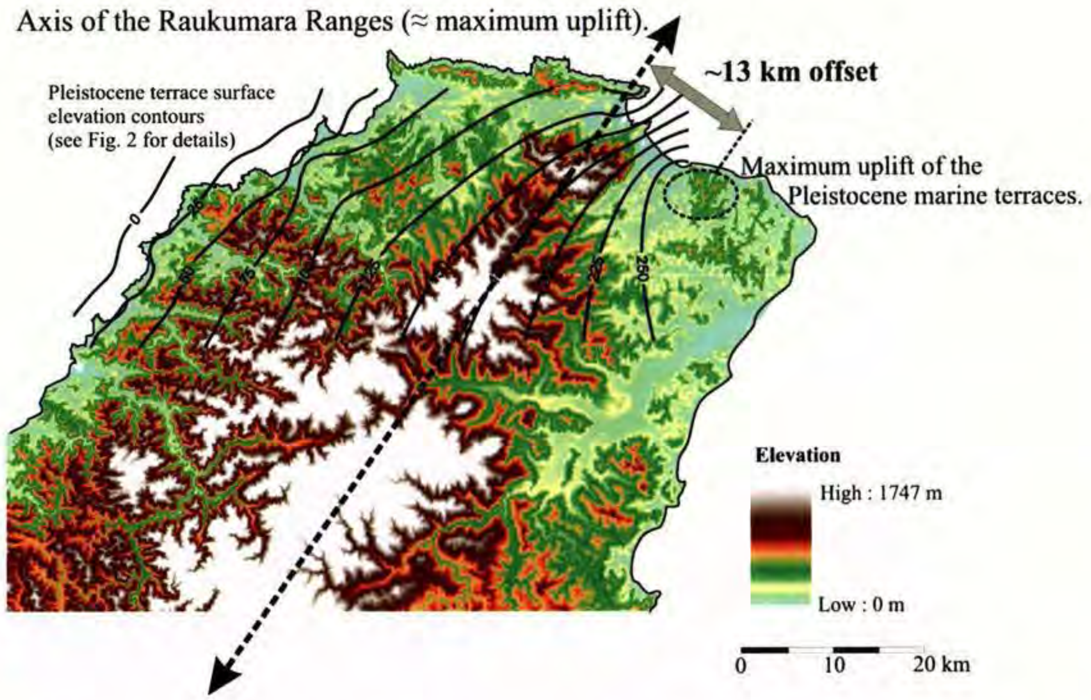

Figure 8. Map depicting the spatial offset between the zones of maximum aseismic uplift as estimated from the Raukumara Ranges and the Pleistocene marine terraces. Thick dashed line is an approximate trace of the crest of the Raukumara Ranges, inferred to represent the region of highest long-term uplift. 25 m contour lines on the Otamaroa Pleistocene marine terrace surface are shown for reference. The zone of highest Pleistocene terrace elevation is circled. The thick grey arrow indicates the spatial offset between the zones of highest uplift.

Regarding temporal variations in the uplift pattern, apatite fission track data from basement rocks of the Raukumara Ranges indicate that the present phase of uplift began in the mid-Miocene (Kamp, 1999). The Pleistocene terraces record uplift only since ~ 125 ka. It is possible that the region of high marine terrace uplift east of Te Araroa reflects a late Quaternary change or aberration to the uplift pattern of the Raukumara Peninsula. A candidate late Quaternary event that may have triggered accelerated uplift near Te Araroa is the subduction of a seamount. Collot et al. (2001) and Lewis et al. (2004) suggest that seamount subduction created the Ruatoria margin re-entrant at the Hikurangi Trough ~ 80 km southeast of Te Araroa (Fig. 5A) and that collapse of the margin occurred at 170 ± 40 ka based on offshore Quaternary unconformities and sedimentation rates from core samples. Lewis et al. (2004)

suggest that the seamount would currently be located near East Cape due to tentative correlation with the coastal uplift rates presented by Ota et al. (1992). Modelling of seamount subduction beneath the Hikurangi margin by Litchfield et al. (2007) suggests uplift over seamounts would occur in localised zones ~20 – 80 km diameter and would create uplift of ~0.7 mm yr^{-1}. This value is lower than the observed uplift rate at Te Araroa, implying seamount-related uplift would only contribute up to approximately one-third of the total uplift rate of the terraces east of Te Araroa.

An alternative explanation for the offset in maximum uplift between the marine terraces and the axial ranges is that the differential erosional resistance of the forearc rocks play a key role in Raukumara Ranges topography. The crests of the Raukumara Ranges, within Torlesse greywacke, may not represent maximum uplift; instead this zone could actually be further to the east within lower elevation hills composed of Miocene sedimentary rocks or the varied lithologies of the East Coast Allochthon. Topographic profiles across the Raukumara Peninsula indicate a strong correlation between elevation and lithology (Fig. 9). Average elevations sharply decrease over the transition from Torlesse greywacke, or Allochthon sediments to Neogene sedimentary rocks (Fig. 9). This correlation suggests that the locations of the crests of the Raukumara Ranges are controlled by a combination of uplift rate and bedrock erodibility. The less coherent Neogene sedimentary rocks may be uplifting at an equally fast or higher rate than the crest of the Torlesse ranges but comparable elevations are not achieved due to more rapid erosion of the neogene rocks. The eastern part of the Raukumara Peninsula may also have relatively low elevations as a result of trenchward sliding or slumping of its weak Neogene sedimentary cover, as suggested by Thornley (1996). The axis of maximum uplift may be located further east of the range crest and more in line with the maximum elevation of the Pleistocene marine terraces (Fig. 8). This scenario potentially aligns the regions of maximum aseismic uplift of the Raukumara Peninsula. However, it may be an over-simplification because the presence of allochthonous units or Neogene sedimentary sequences in itself may imply long-term uplift rates on the eastern Raukumara Peninsula are lower than within the Torlesse part of the Raukumara Ranges. This is because the East Coast Allochthon and the Neogene cover sequences probably formerly overlay the Torlesse greywacke (Kamp, 1999), thus exposure of the Torlesse testifies to higher uplift rates compared to regions where allochthonous and Neogene sedimentary sequences remain.

Finite element modelling of sediment underplating along the Hikurangi subduction zone by Upton et al. (2003) and Litchfield et al. (2007) suggests surface deformation above the ponded sediment would occur in a broad antiform. This deformation pattern contrasts with the broad northwest-tilting asymmetry of the Pleistocene marine terraces. These differences could be due to incomplete information on the geometry of the marine terraces, because there are no preserved terraces more than 5 km east of Te Araroa. However, the finite element models both assume the crust to be of uniform rheology, therefore they do not account for variable lithology and erosion rates at the surface, nor do they account for small-scale faults and folds in the upper plate. Furthermore, the constraints placed on the shape of the underplated sediment body in the models are weak. Upton et al. (2003) input an rectangular block of sediment directly on the plate interface spanning the approximate margin-normal width of the plate interface as inferred by Reyners et al. (1999). The Litchfield et al. (2007) model generates underplated sediment by imposing tectonic erosion at the trench. Without a upper plate backstop, however, the dimensions and position of the underplated sediment are unlikely to replicate the sediment body beneath the Raukumara Peninsula. The models of Raukumara Peninsula uplift produced to date are useful in demonstrating that sediment underplating is a likely mechanism of generating uplift of the Raukumara Ranges but they are too simplistic to be used to explain the surface geometry of the Pleistocene marine terraces. A model is needed that uses the Pleistocene terrace data to estimate the geometry of the underplated sediment beneath. This model could then be compared with the seismic velocity and attenuation models of the plate interface to better understand the relationships between the shape of the underplated sediment and surface geomorphology.

7.5.2 Uplift mechanism distribution in relation to geodynamic changes along the strike of the Raukumara Peninsula.

Our model of Raukumara Peninsula uplift mechanisms has focussed on changes normal to the subduction zone because distances from the subduction trench and depth to the plate interface are the most obvious parameters that change between regions with different uplift mechanisms. However, there are also some changes along the strike of the Raukumara Peninsula that should be considered when seeking to understand controls on uplift mechanisms. Firstly, there are changes in the thickness of the upper plate that, in turn are associated with differences in the thickness of underplated sediment (Reyners et al., 1999). Secondly, there are differences in the degree of plate coupling along the margin (Reyners, 1998; Wallace et al., 2004).

Reyners et al. (1999) infer that the thickness of the crust of the Australian Plate increases in the southern Raukumara Peninsula with an associated decrease in the volume of underplated sediment. If there is less or no ponded sediment southeast of the Tologa Bay-Opotiki line at ~ 38°30` S, our aseismic uplift zone, driven by sediment underplating, should not extend beyond this line. However, there is no significant change in axial range topography across this transition (Fig. 5A) nor is there any change in the occurrence of active faults within or adjacent to the ranges until 39°S where the faults of the North Island Dextral Fault Belt cut through the axial ranges (Fig. 5A). Uplift rate maps based on fluvial incision rates show an area of localised high uplift north of the Tologa Bay-Opotiki line (Litchfield and Berryman, 2006). Decreased fluvial incision rates within the axial ranges south of this line suggest the lesser thickness of underplated sediment southward has an influence on

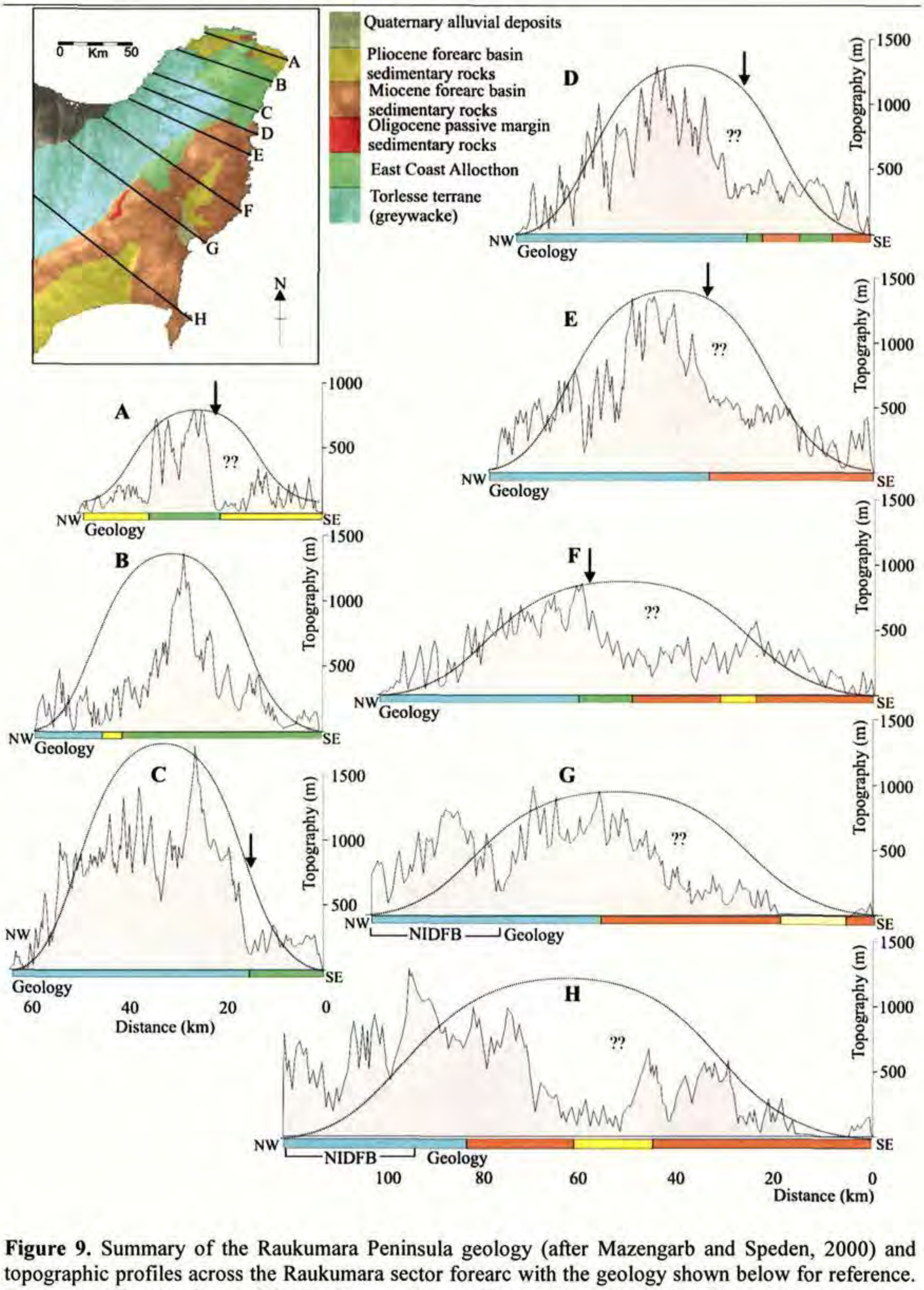

Figure 9. Summary of the Raukumara Peninsula geology (after Mazengarb and Speden, 2000) and topographic profiles across the Raukumara sector forearc with the geology shown below for reference. In most profiles the shape of the Raukumara Ranges departs from a typical antiformal shape. Regions of lower elevation correspond to Neogene sedimentary. The dashed lines represent a symmetrical antiformal shape. The small arrows highlight locations where there are sharp topographic changes across geologic contacts. The question marks highlight areas of lower elevations within Neogene sedimentary rocks. NIDFB: North Island dextral fault belt.

surface uplift (Fig. 5A). Even as far south as the Kaimanawa Ranges (Fig. 10C), accumulations of underplated sediment have been inferred from velocity models and are there suggested to be contributing the uplift the axial ranges (Reyners et al., 2006). Therefore, although there may be a change in uplift rates controlled by differences in crustal thickness southeastward along the Raukumara Peninsula, the mechanisms of uplift is not necessarily different.

The other notable change along the strike of the Raukumara Peninsula is in plate coupling. Reyners (1998) and Reyners and McGinty (1999) estimate a decrease in the width of the interseismically locked portion of the interface north of the Tologa Bay-Opotiki line (Fig. 1A). They relate this decrease to the change in crustal thickness and, as discussed above, there does not appear to be a change in uplift mechanisms. The Wallace et al. (2004) model of geodetically measured interseismic plate coupling shows a patch of slightly higher plate coupling beneath the Pakarae region (Fig. 10B). They suggest this patch may be due to an asperity on the plate interface related to seamount subduction. A similar patch of higher plate coupling is not evident in the Mahia region where coseismic uplift also occurs, suggesting a weak or no correlation between the contemporary plate interface slip rate deficit and coastal uplift mechanisms in the coseismic uplift zone. Notably, higher plate coupling has not been detected beneath the East Cape locality where a subducted seamount may be located (Lewis et al., 2004; Wallace et al., 2004).

7.5.3 Raukumara Peninsula forearc deformation and plate interface dynamics.

The risk of subduction earthquakes generated by rupture of the Hikurangi plate interface adjacent to and beneath the Raukumara Peninsula is poorly known (Stirling et al., 2002; Cochran et al., 2006). Paleoseismic records from coastal locations often provide the only records of subduction zone earthquakes (for example, Matsuda et al., 1978; Atwater, 1987; Nelson et al., 1996; Clague, 1997; Zachariasen et al., 1999; Ramirez-Herrera et al., 2004). We consider here the contribution that coastal tectonics discussed can make to resolving the subduction earthquake hazard along the Raukumara sector.

Firstly, coastal tectonic data within the aseismic uplift zone do not yield easily interpretable information about subduction earthquakes, as there is no evidence of coseismic events in that zone. The accumulation of ponded sediment beneath this zone is driving uplift in a gradual and continuous process, indicating that the plate interface directly below is moving in a state of stable sliding. Stable sliding of the plate interface is probably promoted by elevated fluid pressures in subducted sediment (Eberhart-Phillips and Reyners, 1999; Reyners et al., 1999).

Secondly, we have shown that coastal movements in the zone of coseismic coastal uplift occur primarily by slip on nearby reverse faults that may merge listrically with the plate interface. If these upper plate faults do intersect the plate interface, movement them does not necessarily require rupture of that interface. It is clear that coastal uplift at these locations represents permanent deformation of the upper plate. In contrast, elastic dislocation theory implies that coseismic vertical movement produced by subduction interface events will be recovered over time by elastic relaxation during the interseismic period (Savage, 1983; Okada, 1985; Thatcher, 1986). This theory has been supported by studies of postseismic deformation following historic earthquakes along the Nankai and Alaskan subduction zones (Thatcher, 1984; Savage, 1995; Savage et al., 1998). However, upper plate deformation related to subduction earthquakes is likely to be complex, and not all of the vertical deformation may be recovered after large earthquakes. Upper plate faults may accommodate a component of permanent coseismic deformation (McNeill et al., 1998; Kelsey et al., 2002). As there have been no historical subduction earthquakes off Raukumara Peninsula, it is unknown how the buoyancy of the Hikurangi Plateau may affect preservation of the subduction earthquake record along the Hikurangi margin.

It is unknown whether there has been interseismic relaxation and recovery of uplift at the Pakarae region or at Mahia Peninsula that would indicate plate interface involvement. The biostratigraphy of uplifted fluvio-estuarine sequences at the Pakarae River mouth is not of sufficiently high resolution, or within suitable fossiliferous sediments, to enable resolution of interseismic movement (Wilson, Ch. 4.). Similarly, the biostratigraphy of subsided coastal waterbody sequences at Te Paeroa lagoon and Opoho do not contain evidence of interseismic subsidence (Cochran et al., 2006). Nevertheless, it is reasonable to assume on the basis of the geological record of long-term uplift that most coseismic uplift at these locations is permanent and has not been recovered by interseismic relaxation. It is probable, therefore, that the uplift events of the Pakarae region and at Mahia Peninsula involved slip on upper plate faults. If so no events can be interpreted as the result of a simple subduction interface rupture. Geological evidence from the Pakarae and Mahia regions does not allow us to distinguish the effects of upper plate faulting from synchronous interface and upper plate faulting.

Figure 10. Major tectonic features of the Hikurangi margin. **(A)** Gravity map of the Hikurangi margin. Offshore data are the free air gravity anomaly derived from satellite altimetry data (Sandwell and Smith, 1997), onshore data are the gridded Bouguer gravity anomaly calculated from the GNS gravity database. **(B)** Current interseismic plate coupling coefficient along the Hikurangi margin as estimated from the GPS-determined plate motion slip rate deficit on the plate interface by Wallace et al. (2004). 1 = stronger coupling, 0 = weak coupling. **(C)** Significant geomorphic features and active faults of the Hikurangi margin. The boundaries of the Raukumara sector forearc uplift mechanism zones are shown for reference. Locations and numbers of Holocene marine terraces in the central and southern sectors are shown (after Berryman et al., 1989). Simplified offshore geology after Lewis and Pettinga (1993) and Barnes and Mercier de Lepinay (1997). Note the presence of the modern accretionary wedge south of the Raukumara sector. Major offshore features north and west of the Raukumara Peninsula are also indicated.

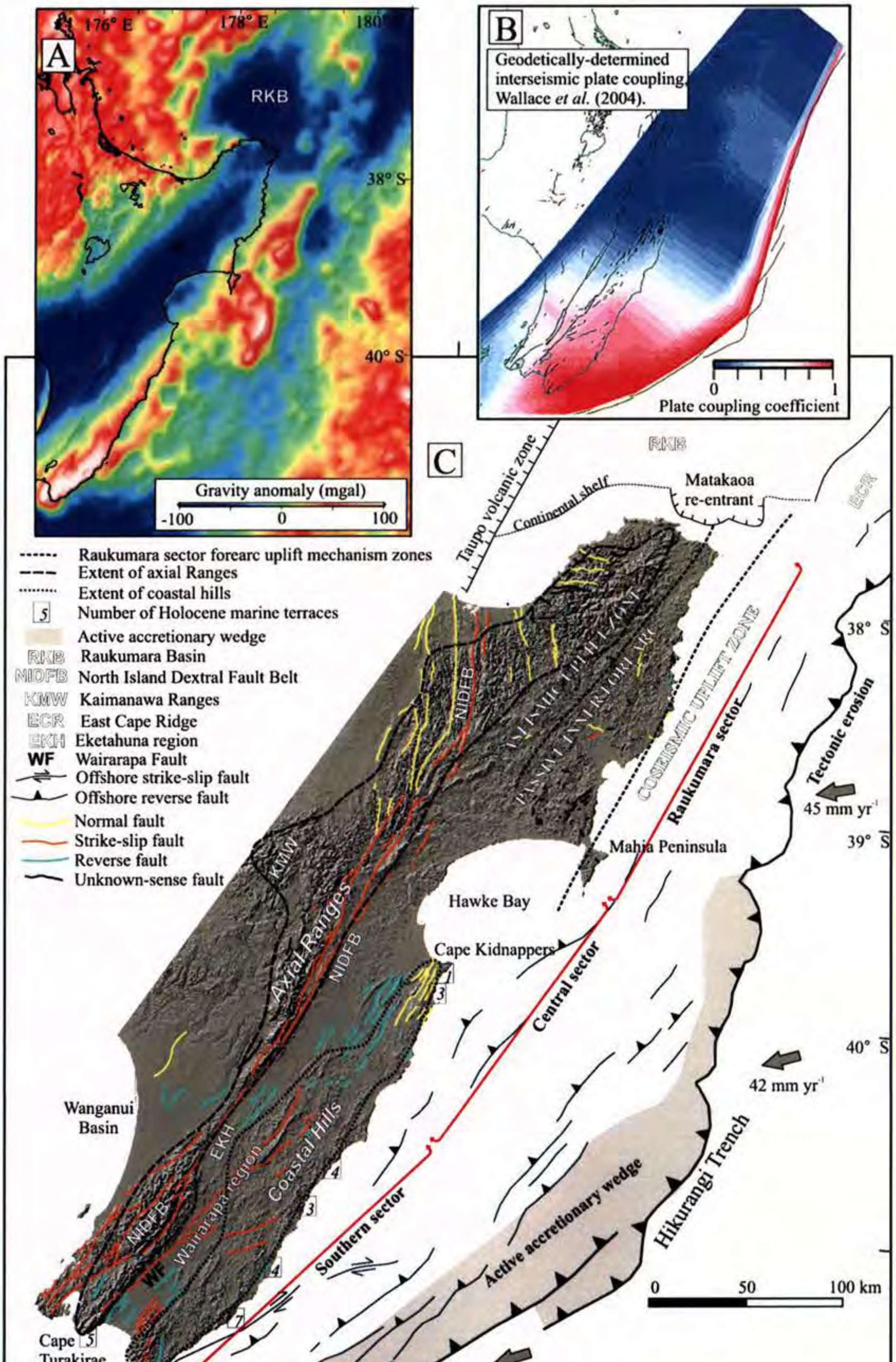
A
176° E
178° E
RKB
38° S
40° S
Gravity anomaly (mgal)
-100
0
100
B
Geodetically-determined interseismic plate coupling. Wallace et al. (2004).
0
1
Plate coupling coefficient
C
Taupo volcanic zone
Continental shelf
Matakaoa re-entrant
RKB
ECR
Raukumara sector forearc uplift mechanism zones
Extent of axial Ranges
Extent of coastal hills
5 Number of Holocene marine terraces
Active accretionary wedge
RKB Raukumara Basin
NIDFB North Island Dextral Fault Belt
KMW Kaimanawa Ranges
ECR East Cape Ridge
EKH Eketahuna region
WF Wairarapa Fault
Offshore strike-slip fault
Offshore reverse fault
Normal fault
Strike-slip fault
Reverse fault
Unknown-sense fault
NIDFB
KMW
Axial Ranges
COSEISMIC UPLIFT ZONE
Raukumara sector
Tectonic erosion
45 mm yr⁻¹
38° S
39° S
40° S
Mahia Peninsula
Hawke Bay
Cape Kidnappers
Central sector
42 mm yr⁻¹
Wanganui Basin
EKH
Coastal Hills
Wairarapa region
Southern sector
WF
Active accretionary wedge
Hikurangi Trench
0
50
100 km
Cape Turakirae
Cook Strait
38 mm yr⁻¹
176° E
178°

A possible method of detecting events involving plate interface rupture is to look for synchroneity of events along the margin. Scaling relationships of plate interface events by Abe (1975) imply that the length of a interface rupture for a large to great subduction earthquake would probably be longer than the rupture lengths of upper plate faults. Therefore interface rupture events could potentially be recorded at many widely separated sites along the margin, whereas deformation involving slip on upper plate reverse faults may be more localised and discontinuous. The 7 ka B.P. records of coseismic marine terraces at the Pakarae River mouth and Mahia Peninsula (involving 5 terraces at Mahia and 7 at the Pakarae River mouth, Berryman, 1993a and Wilson, Ch. 2) show different event ages that do not overlap at the 2-sigma uncertainty level, which suggests that plate interface rupture was not responsible for uplift at both sites. This analysis assumes that a plate interface rupture event would propagate across both locations, which are 65 km apart; with no available data to constrain rupture segments of the interface, this assumption is not necessarily correct.

Given the complication of upper plate faulting in the coseismic uplift zone, it is possible that coastal deformation within the passive inner forearc zone could potentially be a better indicator of subduction interface seismicity than deformation in the coseismic uplift region. The inner forearc zone has few or no active upper plate faults. However, the greater distance from the Hikurangi Trough and the greater depth to the interface may offset this benefit. As previously mentioned, further investigation of the mechanism of uplift within this zone is warranted, and searching for synchronous events could also be a research target.

An elastic dislocation model of surface deformation resulting from rupture of the current interseismically coupled portion of the interface along the entire length of the Hikurangi margin predicts that part of the coastal portion of the Raukumara Peninsula passive forearc zone will be uplifted and part will subside (Fig. 11, L. Wallace, *pers. comm.*). The dislocation model shown in Fig. 11 is based on current plate coupling estimated from GPS-measured plate motion slip rate deficits (Fig. 10B, Wallace et al., 2004) and assumes no significant spatial variation in coupling through time. A 100-year return time event is modelled. The predicted vertical displacements increase linearly with longer recurrence intervals. Interestingly, the model shows that for the coastline covered by our passive forearc zone the predicted deformation pattern is broadly similar to current information about coastal tectonics of this zone. For example, the model predicts subsidence in the Wairoa and western Poverty Bay regions, fitting with the subsidence documented by Brown (1995) and Cochran et al. (2006). Uplift is predicted for the coastline from the Pakarae region northward to Waipiro Bay at >0.1 m for a 100 year event (Fig. 11). Moderate uplift rates have been documented along this portion of the coast (Fig. 1B). No uplifted coastal features have yet been identified along the stretch of coastline from Waipiro Bay to East Cape where <0.1 m of uplift per 100 yrs is predicted by the model (Fig. 11), though fluvial terraces in this region indicate moderate rates of fluvial incision inland (Fig. 5A).

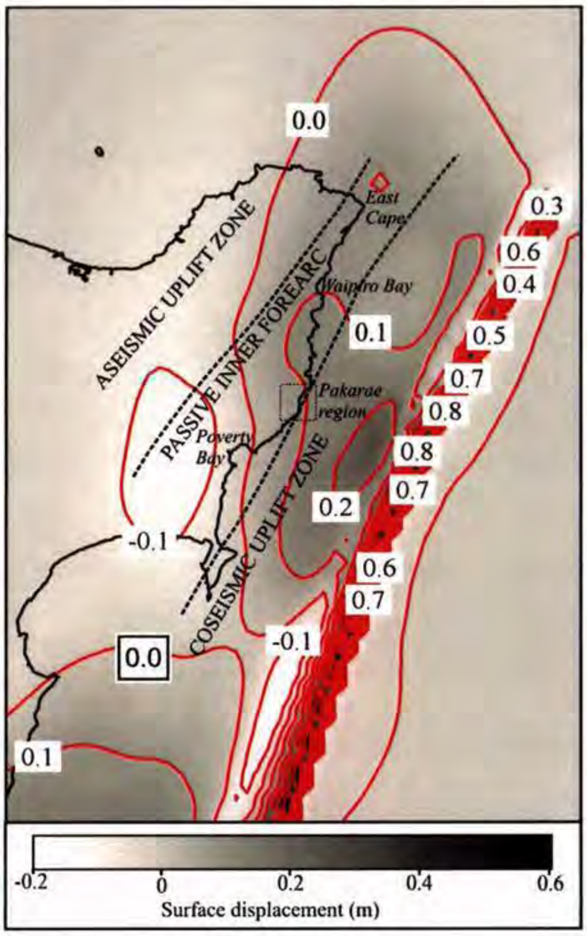

Figure 11. Elastic dislocation model of coseismic surface displacements during a 1 per 100-year plate interface rupture event (source: L. Wallace, pers. comm.). The model is based on rupture of the entire Hikurangi margin plate interface and uses GPS-derived estimates of interseismic plate coupling (Wallace et al., 2004). Surface displacements increase linearly with longer recurrence intervals. Also shown are some localities discussed in the text and the location of the forearc uplift mechanism zones for reference.

Areas where the dislocation model yields results inconsistent with the coastal geology are Mahia Peninsula and the northwestern coast of the Raukumara Peninsula; in both areas the model predicts minor subsidence while Pleistocene marine terraces clearly attest to uplift (Fig. 11). Also of note is that the regions with particularly high late Quaternary uplift rates – the Pakarae River mouth and Te Araroa – are not distinguishable by correlative high uplift patches in the elastic dislocation model. These areas of poor correspondence between the model and known coastal geology are within the coseismic uplift zone or the aseismic uplift zone. The general similarity between predicted coseismic displacement and coastal neotectonics within the passive forearc zone supports the suggestion that this zone may have more direct geodynamic relationship with the subduction interface and be a better recorder of subduction earthquakes than the neighbouring coseismic and aseismic uplift zones. However, elastic dislocation theory predicts that coseismic upper plate displacement caused by interface rupture modelled in Fig. 11 is recovered interseismically. Therefore, if the correlation between the model and the geology passive forearc zone is a true reflection of subduction earthquake deformation, not all of the coseismic displacement has been elastically recovered.

Wells et al. (2003) suggested that a correlation exists between the spatial distribution of gravity lows and plate interface rupture asperities. They found that most historical plate interface rupture events occurred beneath forearc basins, which were distinguishable as pronounced negative gravity anomalies. They suggested, therefore, that forearc basins could be indicators of long-term plate interface seismic moment release. There does not appear to be such a correlation on the Hikurangi margin. The present interseismically locked portion of the interface along the Hikurangi margin (Reyners, 1998) coincides with positive gravity anomalies from the Wairarapa to the Raukumara Peninsula (cf. Fig. 1A and Fig. 10A). However, there have been no historical earthquakes to test this theory along the Hikurangi margin.

To summarise, we cannot presently use the coastal neotectonic record of the Raukumara Peninsula to unequivocally constrain the nature, timing or extent of subduction earthquakes along this part of the Hikurangi margin. This remains a significant research target, particularly given the potentially widespread effects that could result from such an event. However, we can use our uplift mechanism model to identify priority areas of study. Priorities include: (1) attaining a better understanding of how upper plate faults within the coseismic uplift zone interact with the plate interface; (2) searching for evidence of interseismic recovery following coseismic events; (3) correlating events along the margin as a method of constraining the spatial extent of rupture; and (4) determining the mechanism of coastal uplift within the passive forearc region because it has a higher likelihood of being related to a subduction earthquake than records from the aseismic or coseismic uplift zones.

7.5.4 Seismic hazard implications for the Raukumara sector of the Hikurangi margin

Seismic hazard of the Raukumara Peninsula is currently poorly constrained, largely due to the absence of historical subduction interface events, a possibly incomplete historical seismicity catalogue and little paleoseismic data to estimate the frequencies and magnitudes of such events (Stirling et al., 2002; Cochran et al., 2006). We have shown that our model of Raukumara Peninsula forearc uplift mechanisms yields little new data regarding the subduction zone paleoseismology of this margin sector. However, the general correlation we identified between modelled forearc deformation from a subduction zone event (Fig. 11) and Holocene coastal uplift data does suggest that rupture of the subduction interface has previously occurred and may be responsible for some of the deformation observed in the forearc of the Raukumara Peninsula.

Our model of forearc uplift mechanisms justifies a reassessment of the hazard of the upper plate faults of the Raukumara Peninsula. Ota et al. (1992) suggested the Holocene marine terraces in the Hicks Bay to East Cape region were uplifted during earthquakes, thereby implying a significant hazard in this area from offshore earthquakes. Wilson (Ch. 5reinterpreted the marine terraces, presenting evidence of aseismic coastal uplift processes related to sediment underplating. Therefore, the hazard of earthquakes on nearshore upper plate faults in the northeastern Raukumara Peninsula is less than previously thought.

The identification of a 60 – 70 km wide zone of coseismic uplift off the eastern coast of the Raukumara Peninsula implies a significant hazard to coastal regions of the Peninsula. The paleoseismic record from Mahia Peninsula has been accounted for by including the Lachlan Fault in the New Zealand seismic hazard model by Stirling et al. (2002). The record from the Pakarae region, however, has not been included in the model. Our preliminary interpretation of a recently acquired seismic line from the Raukumara Peninsula continental shelf suggests there are active faults in the offshore region (Fig. 7). The active upper plate faults within the coseismic uplift zone appear to be relatively short (20 – 40 km long, Fig. 5A), therefore probably generate lesser magnitude earthquakes than the subduction interface. However, relatively short recurrence intervals are suggested for Mahia Peninsula (1060 ± 560 yrs, Berryman, 1993a) and the Pakarae River mouth (850 ± 450 yrs, Wilson, Ch. 2). By using the Lachlan fault as an analogy, a M_W 7.6 –8.0 earthquake is estimated to account for marine terrace uplift if a 60-70 km long upper plate fault ruptured to the depth of the plate interface (Berryman, 1993a; Barnes et al., 2002). Faults within the offshore coseismic uplift zone, therefore, present a significant and high frequency seismic hazard. Being of short length, they have a more localised effect than a subduction interface event. However, they could conceivably rupture at the same time as the plate interface (for example, slip on the upper plate Patton Bay Fault synchronous with the 1964 Alaska earthquake, Plafker, 1972). These offshore faults also represent a large tsunami hazard to the coastal communities of the eastern Raukumara Peninsula and warning times would be short, probably less than 30 minutes.

7.5.5 Onshore forearc deformation and offshore geology

Our model of Raukumara Peninsula uplift mechanisms includes the eastern offshore region out to the Hikurangi Trough. Here we examine how this model relates to offshore geology west and north of the Peninsula, where there are transitions into different geodynamic regimes.

There is a transition from the aseismic uplift zone across the northward extensions of the strike slip faults of the NIDFB and into the backarc extensional regime of the offshore extension of the Taupo volcanic zone (TVZ, Fig. 10C) west and northwest of the Raukumara Peninsula. Active normal faulting has been well-documented in the Bay of Plenty and occurs mainly within the Whakatane Graben, which is 35 – 50 km west off the western Raukumara Peninsula coastline (Fig. 10C, Wright, 1990; Taylor et al., 2004). Subsidence rates within the Whakatane graben average 2 – 2.5 mm yr^{-1} (Wright, 1990). We suggest there is a gradual westward transition between the aseismic uplift regime, which controls the position of the western Raukumara Peninsula coastline, across the NIDFB, and into the margins of the TVZ, where backarc coseismic extension and subsidence dominate.

The northern coast of the Raukumara Peninsula is flanked by a narrow section of continental shelf, a steep indented continental margin, and then the Raukumara Basin, which is a deep long-lived forearc basin developed on oceanic crust (Fig. 10A, C). Plate tectonic reconstructions by Davey et al. (1997) suggest that the northern Raukumara Peninsula continental margin was a subduction margin during the early Miocene. This former subduction zone, now identified as the Vening Meinesz fracture zone, was succeeded by the Hikurangi subduction zone in its present location during the mid-Miocene (Davey et al., 1997). The continental shelf is 15-20 km wide and is indented by the head scar of the Matakaoa Slide (Fig. 10C). While not yet fully understood (Carter, 1998; Joanne et al., 2005), the Matakaoa Slide may be related to strong northward tilt produced across the transition from the uplifting Raukumara Peninsula to the subsiding Raukumara Basin. The Raukumara Basin is a forearc basin lying at a depth of ~2.5 km, distinguished by a pronounced gravity low and infilled by 4 – 6.5 km of Cenozoic sediments (Gillies and Davey, 1986; Davey et al., 1997, Fig. 10A). The East Cape Ridge forms the eastern boundary of the basin (Fig. 10C). The western margin of the basin is formed by the offshore extension of the TVZ. The presence of the subsiding Raukumara Basin is clear evidence that forearc geodynamic processes abruptly change off the northern Raukumara Peninsula coastline. This change is probably related to the major crustal boundary of the Vening Meinesz fracture zone and the change to upper plate oceanic crust. Offshore structures closer to the Hikurangi Trough, such as the East Cape Ridge, have complex morphologies and tectonic histories involving transpression, uplift and extension (Collot et al., 1996; Collot and Davy, 1998). Perhaps our identified coseismic uplift zone extends further northeastward along the strike of the margin to encompass the region of the East Cape Ridge and trenchward structures. However, the aseismic uplift zone related to sediment underplating undoubtedly terminates at the present northern Raukumara Peninsula coastline.

7.5.6 Comparisons of the uplift mechanism model with results of other tectonic studies of the Raukumara Peninsula

This study has focussed on the use of coastal tectonics to infer the mechanisms of vertical forearc deformation in relation to subduction geodynamics. Here we discuss how our model of forearc uplift compares with and relates to previous studies of Raukumara Peninsula deformation using different methodologies.

Thornley (1996) suggested the Neogene sediments of the forearc are sliding trenchward on a detachment layer. This model is consistent with the coastal tectonics we see within the aseismic uplift zone and the passive forearc zone. Because this extension and sliding is essentially a surface process, it is largely geodynamically decoupled from the processes of forearc uplift that we discuss, which are more directly related to subduction zone processes. Regions that do not fit with the extensional and sliding model are those with high coastal uplift rates, excluding Mahia Peninsula which is not included in the Thornley (1996) study area. Thornley (1996) suggests areas of high coastal uplift, particularly Te Araroa and the Pakarae region, are the result of block rotation between active faults, primarily normal faults. We have shown that active faulting is unlikely in the Te Araroa area and that aseismic uplift is probably the dominant uplift mechanism in this region (Wilson, Ch. 5). Regarding the Pakarae region Thornley (1996) acknowledges the suggestion by Ota et al. (1991) that uplift is driven by a nearshore reverse fault, though figures produced by Thornley (1996) imply uplift at the Pakarae River mouth is driven by block rotation between onshore normal faults. Thus there is some disagreement between our model of uplift mechanisms in the Pakarae region and model of forearc deformation by Thornley (1996). Wilson (Ch. 2) shows that uplift at the Pakarae River mouth is unlikely to be related to uplift in the hanging wall of a normal fault. Other studies in the Pakarae region, building on the preliminary study by Litchfield and Wilson (2005) of fluvio-tectonic terraces along the Pakarae River, may assist in resolving the structure responsible for uplift.

Other significant studies of Raukumara Peninsula deformation have been based on geodesy (Walcott, 1978; Reilly, 1990; Darby and Meertens, 1995; Arnadottir et al., 1999) and seismicity (Webb and Anderson, 1998; Reyners et al., 1999; Reyners and McGinty, 1999; McGinty et al., 2000). Data from both sources support surficial trenchward extension of the Raukumara Peninsula. All studies agree that extension is probably related to gravitational collapse of the upper part of the forearc crust. Many of these studies mention the high coastal uplift rates along the Raukumara Peninsula coastline and reference the inference by Ota et al. (1991) that reverse faulting drives uplift of the Pakarae region. Few, however, provide discussions of how the uplift reconciles with the widespread extensional regime they document. Many of the studies appear to view the Pakarae region as an isolated and anomalous area. It is only by correlating coseismic uplift mechanisms between the Pakarae region and Mahia Peninsula and by examining the distribution of offshore structures that it becomes clear that a continuous and pervasive zone of compressional tectonics may exist trenchward of the eastern part of the onshore forearc. Because most of this zone lies offshore, it is not surprising that landbased techniques such as seismic deployments and GPS surveys have not documented deformation within the offshore area. One location where GPS data could test our uplift mechanism model is Matakaoa Point where a continuous GPS station has been installed. We predict that uplift is occurring continuously and aseismically at this location. Presently this station has only been in operation for 4 years and at least 5 years of data are required to obtain confident estimates of vertical deformation, longer if the deformation rates are low (Laura Wallace, *pers. comm.*).

7.5.7 Geodynamic changes along the strike of the Hikurangi margin

Significant changes are in onshore upper plate topography and neotectonics, and offshore structure and bathymetry occur along the strike of the Hikurangi margin (Fig. 10C). The Coastal Hills and NIDFB are significant tectonic geomorphic features of the central and southern Hikurangi margin sectors (Fig. 10C). The prevalence of active compressional faulting within the Coastal Hills indicates most, or all, of the uplift is achieved by coseismic upper plate deformation (Lamarche et al., 1995; Kelsey et al., 1998; Chanier et al., 1999; Nicol et al., 2002; Pettinga, 2004). Directly east of Mahia Peninsula, an active accretionary wedge begins to form. The wedge this increases in width southward offshore of the central and southern sector before pinching out near Cook Strait (Collot et al., 1996; Barnes et al., 1998). Uplifted marine terraces have been documented at many sites along the southern and eastern coastlines of Wairarapa and Wellington and near Hawke Bay (Fig. 10C, Wellman, 1971a, 1971b; Hull, 1987; Ota et al., 1988; Berryman et al., 1989; Miyauchi et al., 1989; Ota et al., 1990; Pillans and Huber, 1995). Historical coseismic coastal uplift events (M_W 7.6 1931 Napier earthquake, Hull, 1990; and the M_W 8.2 1855 Wairarapa earthquake, Grapes, 1989) and the prevalence of active nearshore reverse faults (Barnes and Mercier de Lepinay, 1997; Barnes et al., 1998; Barnes and Audru, 1999) suggest coastal uplift of the central and southern Hikurangi margin sectors occurs by coseismic mechanisms. These observations generally suggest the outer forearc uplift of the central and southern Hikurangi margin is mostly, or entirely, accommodated by permanent deformation on upper plate structures.

The characteristics of zones of forearc uplift mechanisms seen on the Raukumara Peninsula change in the central and southern sectors of the Hikurangi margin. We discuss how each uplift mechanism zone changes southward. Firstly, the aseismic uplift zone probably decreases in width southward. Sediment underplating may play a role in uplift of the central axial ranges (.eg., the Kaimanawas, Reyners et al., 2006) but mantle upwelling is also an important uplift process here (Pulford and Stern, 2004), and both the central and southern axial ranges are deformed by major upper plate strike slip faults. Secondly, the passive forearc zone is probably manifest in the southern Hawkes Bay and Wairarapa regions as the low-lying areas of the inner forearc, between the Coastal Hills and the axial ranges (Fig. 10C). These forearc basins have undergone relatively little deformation (Cashman et al., 1992), except in the Eketahuna region where there is a zone of strike slip and reverse faulting (Kelsey et al., 1995; Lamarche et al., 1995, Fig. 10C). Thirdly, the southward continuation of the Raukumara Peninsula coseismic uplift zone is probably manifest as the compressional faulting on the continental shelf and within the Coastal Hills.

Essentially the same coseismic uplift processes are operating in the central and southern sectors. However the zone appears to be much wider, extending up to 200 km from the Hikurangi Trough, and it probably accommodates a higher proportion of margin-normal deformation relative to the Raukumara Peninsula sector.

In summary, there are significant changes in forearc deformation along the strike of the margin. Like Litchfield et al. (submitted) we also ask the question why mechanisms of forearc deformation differ along strike of the Hikurangi margin and what parameters control or influence these changes.

Changes in the rate and obliquity of plate convergence along the margin affect the degree of slip partitioning (Beanland, 1995; Beanland and Haines, 1998; Nicol and Beavan, 2003). Several studies have inferred that margin-parallel motion is accommodated along the Raukumara sector by rotation of the Peninsula, rather than by strike slip faults as seen in the southern and central margin sectors (Beanland and Haines, 1998; Wallace et al., 2004). This change contributes to the absence of active faults in the Raukumara forearc. Margin-normal slip does not appear to significantly change along the margin; it is accommodated in all sectors by slip on the plate interface and on upper plate reverse faults (Reyners, 1998; Webb and Anderson, 1998). On the Raukumara Peninsula, however, the zone of reverse faulting is mainly offshore, whereas to the south it is wider and extends onshore.

An obvious factor that may have an effect on upper plate deformation is the character of the subducting plate and the Hikurangi Plateau. There are no significant changes in the thickness of the Hikurangi Plateau along the margin (Davy and Wood, 1994, Davy, *pers. comm.*), and recent seismicity does not show evidence of subducting slab segmentation (Ansell and Bannister, 1996; Reyners, 1998; Webb and Anderson, 1998). The only significant change appears to be an increase in the radius of subducted plate curvature along the southern Hikurangi margin (Ansell and Bannister, 1996). This increase arises because the subducted slab is slightly shallower with increasing distance from the trench in comparison to the northern Hikurangi margin. Several studies also indicate that the subducted slab extends to a greater depth in the northern Hikurangi margin relative to the south (Walcott, 1987; Beanland, 1995; Webb and Anderson, 1998). It is unknown how the geometry of the subducted slab affects the forearc deformation mechanisms, though Beanland (1995) suggests that the different depths of slab penetration along the margin have a major effect on the dynamic coupling between the plates. Dynamic coupling is a measurement of the forces acting pon the plate interface (Beanland, 1995, Scholz and Campos, 1995). Decreased dynamic coupling across the plate interface of the Raukumara sector means less margin-normal stress is transferred to the upper plate than is the case farther south. This difference helps to account for why the coseismic uplift zone of the Raukumara sector is narrower than farther south.

Alternative measurements of plate coupling also show strong differences along the strike of the margin. Current interseismic plate coupling, measured by the width of the plate interface locked zone as estimated from seismicity (Reyners, 1998, Fig. 1A) and measured by GPS-determined plate motion slip rate deficits (Wallace et al., 2004), decreases northward (Fig. 10B). We have discussed previously that the differences in plate coupling along the Raukumara sector do not appear to correlate with changing uplift mechanisms normal to the Hikurangi margin. However, the much greater amplitude changes in plate coupling along the whole margin does show a general correlation with the amount of coseismic compressional deformation, as reflected by the increasing margin-normal width of the coseismic uplift zone southwards.

Many other factors contribute to forearc deformation, aside from the morphology of the subducting plate. Two further factors that we consider are sediment thickness on the subducting plate and roughness of the subducting plate. There is less sediment infill of the Hikurangi Trough adjacent to the Raukumara Peninsula sector, mostly due to eastward deflection of the Hikurangi channel [*cf.* 2 – 4 km of sediment in the central and southern Hikurangi Trough (Lewis and Pettinga, 1993) and 1 – 1.5 km of sediment in the Raukumara sector trough (Collot et al., 1996)]. Less sediment thus is available for offscraping and construction of an accretionary wedge. Seamounts on the subducting Hikurangi Plateau increase northwards (Wood and Davy, 1994). Seamounts increase plate roughness, a factor elsewhere observed to increase forearc deformation (Fisher et al., 1998; Sak et al., 2004). Both the decrease in trench sediment and increase in seamounts contribute tectonic erosion at the Hikurangi Trough adjacent to the Raukumara sector. Tectonic erosion, in turn, causes offscraping of the base of the upper plate, entrained sediment is subducted beneath the margin and underplated at depth. However, as noted by Litchfield et al. (2007) diversion of the Hikurangi channel occurred relatively recently (2 – 0.5 Ma, Lewis et al., 1998), and their modelling suggests the effects of decreased sediment supply will take ~ 7 Ma to become manifest in the axial ranges. Therefore, seamount impacts are suggested as the more important cause of tectonic erosion.

In summary, significant changes in forearc uplift mechanisms occur along the strike of the margin. The causes of these changes are probably related to the geometry of the subducting plate, plate coupling, and sediment cover and seamount abundance on the Hikurangi Plateau. The Raukumara Peninsula sector and the southern Hikurangi margin sector probably represent two end members of a spectrum of plate coupling, and this is manifest by the along-strike changes in forearc uplift mechanisms.

7.5.8 Comparison of Raukumara Peninsula forearc uplift to global subduction zones

We question whether the Raukumara Peninsula sector of the Hikurangi margin is comparable to any global examples of forearc deformation in an effort to further understand the geodynamics of the Hikurangi subduction zone. In particular, are there any global analogies that possess subduction earthquake histories? Our dataset from the Raukumara Peninsula is unique because we are able to trace uplift mechanisms around the east, north and northwest coasts of the peninsula, a margin normal distance of almost 120 km. There are few subductions zones worldwide where such a setting exists. Most studies of spatial variation in forearc coastal uplift focus on changes in uplift rates along the strike of the margin, rather than normal to it (for example, Hsu, 1992; Kelsey and Bockheim, 1994; Personius, 1995). Studies of coastal uplift rates and mechanisms have been undertaken along margin-normal profiles at the Peninsula de Nicoya, Costa Rica, but only along a ~20 km distance (Marshall and Anderson, 1995; Gardner et al., 2001), and also in the Antofagasta region of northern Chile, across a width of ~ 50 km (Delouis et al., 1998).

Nakada et al. (2002) suggested that aseismic uplift associated with the buoyancy of a subducted oceanic ridge drives marine terrace uplift at ~1 mm yr^{-1} adjacent to the Nankai subduction zone. This setting is similar to the Raukumara Peninsula in that the marine terraces are located ~150 km from the trench and the subducted ridge is in some ways analogous to the Hikurangi Plateau beneath the Raukumara Peninsula. The estimated maximum magnitude of subduction earthquakes offshore of the Kyushu coastline is less than along the neighbouring segments that display coseismic uplifted coastal terraces (*cf.* M_W <7.5 for the Kyushu segment, M_W >8 for the neighbouring Shikoku segment). The decreased hazard of subduction earthquakes along the Kyushu segment is related to a decrease in plate coupling, probably caused by the subducted ridge (Nakada et al., 2002). The model is similar to that of Reyners (1998), indicating that the Raukumara sector has lesser magnitude subduction earthquakes than the southern margin. A trenchward zone of active faulting occurs offshore of Kyushu, a further similarity to the situation off the Raukumara Peninsula.

The northern Chilean forearc has perhaps the most similar forearc tectonics to the Raukumara Peninsula. Different faulting styles, inclusing extensional, transtensional, and compressional, occur in margin-parallel zones (Delouis et al., 1998; Adam and Reuther, 2000; Hartley et al., 2000). The outer forearc, extending from the trench ~120 km arcward and including the continental shelf and land, is undergoing synchronous uplift and trenchward extension. Uplift is thought to be driven by sediment underplating and forearc extension is related to gravitational collapse of the oversteepened forearc. The adjacent trench is sediment starved, and tectonic erosion is believed to be contributing to forearc oversteepening and is providing subducted sediment for arcward underplating (Adam and Reuther, 2000; Hartley et al., 2000). However, unlike the Raukumara Peninsula subduction zone, the northern Chilean subduction interface is believed to be strongly coupled and great earthquakes (> M_W 8.5) have occurred historically on neighbouring interface segments (Delouis et al., 1996). The forearc block above the underplated sediment zone is bounded by faults, and a M_W 8 subduction earthquake caused surficial extensional faulting in the Antofagasta region (Delouis et al., 1998). Therefore, while tectonic erosion, underplated sediment and forearc extension in Chile and New Zealand are similar, coseismic deformation above the underplated sediment zone is not. The dissimilarities may be related to the contrast between the typical oceanic crust of the Nazca plate and the overthickened oceanic crust of the Hikurangi Plateau.

Margin-parallel zones with different forearc deformation styles have also been documented along the Aleutian arc. Von Huene and Klaeschen (1999) documented a permanent strain zone within 30 km of the trench and an arcward elastic strain zone where subduction earthquake coseismic deformation was largely recovered interseismically. This situation differs from the Raukumara Peninsula, particularly as the forearc landmass is located > 200 km from the trench. Again these differences may reflect the subduction of normal oceanic crust at the strongly coupled interface of the Aleutian margin.

7.6 Conclusions

We have reviewed late Quaternary coastal uplift mechanisms of the Raukumara sector of the Hikurangi margin. The main factor controlling the spatial distribution of uplift mechanisms is the distance of the forearc from the trough and, by inference, the depth to the plate interface below. Three margin-parallel zones of forearc deformation are proposed: a trenchward coseismic uplift zone, an arcward aseismic uplift zone, and a passive inner forearc zone between the two. The boundary between the aseismic uplift zone and the passive forearc is the least well constrained though further study of the coastal geology of the Te Araroa to East Cape region may help to resolve this. The two onshore locations where coseismic uplift occurs, Mahia Peninsula and the Pakarae region, correlate along margin-strike with presently mapped offshore structures, though there is little data available regarding the nature and age of these structures. Preliminary interpretation of a recently acquired offshore seismic line supports our suggestion that this is a region dominated by active listric reverse faults, though more thorough investigation of more offshore data will provide a test of our interpretations.

Our model of forearc uplift mechanisms for the Raukumara Peninsula indicates that most of the upper plate deformation is not a direct consequence of plate interface seismicity. The coseismic uplift zone represents permanent strain on upper plate faults. These faults probably merge downwards with the plate interface, though we do not know if they rupture synchronously with, or independently of the plate interface. The passive forearc zone may have the greatest potential for preserving a record of subduction earthquakes due to the absence of nearby upper plate faults, Also the pattern of coastal uplift and subsidence within this zone best fits models of subduction earthquake displacements.

Previous models of seismic hazard have underestimated the potential for earthquake events on near- and offshore reverse faults, with major implications for tsunami hazard. Forearc deformation differs significantly along the Hikurangi margin, but the tripartite division of Raukumara sector forearc deformation appears to continue southward along the Hikurangi margin, although there is some change in the characteristics and widths of the deformation zones. Changes in forearc dynamics along the strike of the entire margin are probably due to changes in subducting plate geometry and morphology, and a related strong gradient in plate coupling.

While along-strike changes in forearc deformation of the Hikurangi margin are important for understanding the large scale tectonic evolution of the subduction zone and possible subduction earthquake segmentation boundaries, we have shown there are significant tectonic changes normal to subduction zones. On a regional scale these changes have important seismic hazard implications.

7.7 References

Abe, K. (1975). "Reliable estimation of the seismic moment of large earthquakes." Journal of the Physics of the Earth **23**: 381-390.

Adam, J. and C.-D. Reuther (2000). "Crustal dynamics and active fault mechanics during subduction erosion. Application of frictional wedge analysis on to the North Chilean Forearc." Tectonophysics **321**: 297-325.

Ansell, J., H. and S. C. Bannister (1996). "Shallow morphology of the subducted Pacific plate along the Hikurangi margin, New Zealand." Physics of the Earth and Planetary Interiors **93**: 3-20.

Arnadottir, T., S. Thornley, F. Pollitz, F. and D. J. Darby (1999). "Spatial and temporal strain rate variations at the northern Hikurangi margin, New Zealand." Journal of Geophysical Research **104**(B3): 4931-4944.

Atwater, B. F. (1987). "Evidence for great Holocene earthquakes along the outer coast of Washington State." Science **236**: 942-944.

Barnes, P. M. and J.-C. Audru (1999). "Quaternary faulting in the offshore Flaxbourne and Wairarapa Basins, southern Cook Strait, New Zealand." New Zealand Journal of Geology and Geophysics **42**: 349-367.

Barnes, P. M. and B. Mercier de Lepinay (1997). "Rates and mechanics of rapid frontal accretion along the very obliquely convergent southern Hikurangi margin, New Zealand." Journal of Geophysical Research **102**(B11): 24931-24952.

Barnes, P. M., B. Mercier de Lepinay, J.-Y. Collot, J. Delteil and J.-C. Audru (1998). "Strain partitioning in the transition area between oblique subduction and continental collision, Hikurangi margin, New Zealand." Tectonics **17**(4): 534 - 557.

Barnes, P. M., A. Nicol and T. Harrison (2002). "Late Cenozoic evolution and earthquake potential of an active listric thrust complex above the Hikurangi subduction zone, New Zealand." Geological Society of America Bulletin **114**(11): 1379-1405.

Beanland, S. (1995). The North Island Dextral Fault Belt, Hikurangi Subduction Margin, New Zealand. Unpublished PhD thesis, School of Earth Sciences, Victoria University of Wellington, New Zealand.

Beanland, S. and J. Haines (1998). "The kinematics of active deformation in the North Island, New Zealand, determined from geologic strain rates." New Zealand Journal of Geology and Geophysics **41**(311-323).

Berryman, K. R. (1993a). "Age, height, and deformation of Holocene terraces at Mahia Peninsula, Hikurangi subduction margin, New Zealand. 1." Tectonics **12**(6): 1347-1364.

Berryman, K. R. (1993b). "Distribution, age, and deformation of Late Pleistocene marine terraces at Mahia peninsula, Hikurangi subduction margin, New Zealand." Tectonics **12**(6): 1365-1379.

Berryman, K. R., Y. Ota and A. G. Hull (1989). "Holocene paleoseismicity in the fold and thrust belt of the Hikurangi subduction zone, eastern North Island, New Zealand." Tectonophysics **163**: 185-195.

Berryman, K. R., Y. Ota and A. G. Hull (1992). "Holocene evolution of an estuary on a tectonically rising coast: the Pakarae River locality, eastern North Island, New Zealand." Sedimentary Geology **80**: 151-162.

Brown, L. J. (1995). "Holocene shoreline processes at Poverty Bay, a tectonically active area, northeastern North Island, New Zealand." Quaternary International **26**: 21-33.

Carter, L. (1998). "Matakoa debris flow - a giant, Quaternary mass failure of the East Cape continental margin." Basset, K. N. and Nobes, D. C. (eds.) Programme and abstracts, Geological Society of New Zealand Annual Conference, Christchurch, New Zealand. Geological Society of New Zealand Miscellaneous Publication 101A: 63.

Cashman, S. M., H. M. Kelsey, C. F. Erdman, H. N. C. Cutten and K. R. Berryman (1992). "Strain partitioning between structural domains in the forearc of the Hikurangi subduction zone, New Zealand." Tectonics **11**(2): 242-257.

Chanier, F., J. Ferriere and J. Angelier (1999). "Extensional deformation across an active margin, relations with subsidence, uplift and rotations: the Hikurangi subduction, New Zealand." Tectonics **18**(5): 862-876.

Chapman-Smith, M. and J. A. Grant-Mackie (1971). "Geology of the Whangaparoa area, eastern Bay of Plenty." New Zealand Journal of Geology and Geophysics **14**(1): 3-38.

Clague, J. J. (1997). "Evidence for large earthquakes at the Cascadia subduction zone." Reviews of Geophysics **35**(4): 439-460.

Cochran, U., K. Berryman, D. Mildenhall, B. Hayward, K. Southall, C. Hollis, P. Barker, L. Wallace, B. Alloway and K. Wilson (2006). "Paleoecological insights into subduction zone earthquake occurrence, eastern North Island, New Zealand." Geological Society of America Bulletin, **118**(9/10): 1051-1074.

Collot, J.-Y. and B. Davy (1998). "Forearc structures and tectonic regimes at the oblique subduction zone between the Hikurangi Plateau and the southern Kermadec margin." Journal of Geophysical Research **103**(B1): 623-650.

Collot, J.-Y., J. Delteil, K. Lewis, B. Davy, G. Lamarche, J.-C. Andru, P. Barnes, F. Chanier, E. Chaumillon, S. Lallemand, B. M. De Lepinay, A. Orpin, B. Pelletier, M. Sosson, Toussaint and C. Uruski (1996). "From oblique subduction to intra-continental transpression: structures of the southern Kermadec-Hikurangi margin from multibeam bathymetry, side-scan sonar and seismic reflection." Marine Geophysical Researches **18**(2-4): 357-381.

Collot, J.-Y., K. Lewis, G. Lamarche and S. Lallemand (2001). "The giant Ruatoria debris avalanche on the northern Hikurangi margin, New Zealand; results of oblique seamount subduction." Journal of Geophysical Research **106B**(9): 19271-19297.

Darby, D. J. and C. M. Meertens (1995). "Terrestrial and GPS measurements across the taupo backarc and Hikurangi forearc in New Zealand." Journal of Geophysical Research **100**(B5): 8221-8232.

Davey, F. J., S. Henrys and E. Lodolo (1997). "A seismic crustal section across East Cape convergent margin, New Zealand." Tectonophysics **269**: 199-215.

Davy, B. and R. Wood (1994). "Gravity and megnetic modelling of the Hikurangu Plateau." Marine Geology **118**: 139-151.

De Mets, C., R. G. Gordon, D. F. Argus and S. Stein (1994). "Effect of recent revisions to the geomagnetic reversal timescale on estimates of current plate motions." Geophysical Research Letters **21**: 2191-2194.

Delouis, B., A. Cisternas, L. Dorbath, L. Rivera and E. Kausel (1996). "The Andean subduction zone between 22 and 25 degrees S (northern Chile): precise geometry and state of stress." Tectonophysics **259**: 81-100.

Delouis, B., H. Philip, L. Dorbath and A. Cisternas (1998). "Recent crustal deformation in the Antofagasta region (northern Chile) and the subduction process." Geophysical Journal International **132**: 302-338.

Eberhart-Phillips, D. and M. Chadwick (2002). "Three-dimensional attenuation model of the shallow Hikurangi subduction zone in the Raukumara Peninsula, New Zealand." Journal of Geophysical Research **107**(B2): ESE 3-1 - 3-15.

Eberhart-Phillips, D. and M. Reyners (1999). "Plate interface properties in the northeast Hikurangi subduction zone, New Zealand, from converted seismic waves." Geophysical Research Letters **26**(16): 2565-2568.

Fisher, D., T. Gardner, J. S. Marshall, P. Sak and M. Protti (1998). "Effect of subducting sea-floor roughness on fore-arc kinematics, Pacific coast, Costa Rica." Geology **26**(5): 467-470.

Gardner, T., J. S. Marshall, D. Merritts, B. Bee, R. Burgette, E. Burton, J. Cooke, N. Kehrwald, M. Protti, D. Fisher and P. Sak (2001). "Holocene forearc block rotation in response to seamount subduction, southeastern Peninsula de Nicoya, Costa Rica." Geology **29**(2): 151-154.

Garrick, R. A. (1979). "Late Holocene uplift at Te Araroa, East Cape, North Island, New Zealand." New Zealand Journal of Geology and Geophysics **22**(1): 131-139.

Gibb, J. G. (1986). A New Zealand regional Holocene eustatic sea-level curve and its application to determination of vertical tectonic movements, A contribution to IGCP-Project 200. Recent Crustal Movements of the pacific Region., Bulletin of the Royal Society of New Zealand. **24:** 377-395.

Gillies, P. N. and F. J. Davey (1986). "Seiemic reflection and refraction studies of the Raukumara forearc basin, New Zealand." New Zealand Journal of Geology and Geophysics **29**: 391-403.

Grapes, R. (1989). "The Wairarapa Fault: displacements and paleoseismicity." Bulletin of the New Zealand National Society for Earthquake Engineering **22**(1): 13-16.

Hartley, A. J., G. May, G. Chong, P. Turner, S. J. Kape and E. J. Jolley (2000). "Development of a continental forearc: A Cenozioc example from the Central Andes, northern Chile." Geology **28**(4): 331-334.

Hsu, J. T. (1992). "Quaternary uplift of the Peruvian coast related to the subduction of the Nazca Ridge: 13.5 to 15.6 degrees latitude." Quaternary International **15/16**: 87-97.

Hull, A. G. (1987). "A late Holocene marine terrace on the Kidnappers Coast, North Island, New Zealand: some implications for shore platform development processes and uplift mechanisms." Quaternary Research **28**: 183-195.

Hull, A. G. (1990). "Tectonics of the 1931 Hawke's Bay earthquake." New Zealand Journal of Geology and Geophysics **33**: 309-320.

Jackson, J. A., N. J. White, Z. Garfunkel and H. Anderson (1988). "Relations between normal-fault geometry, tilting and vertical motions in extensional terrains: an example from the southern Gulf of Suez." Journal of Structural Geology **10**(2): 155-170.

Joanne, C., T. Lebourg, G. Lamarche, J.-Y. Collot and S. Migeon (2005). "Mechanical parameters and sediment rheology in the submarine Matakoa avalanches, East Cape region." Pettinga, J. R. and Wandres, A. M. (eds.) Programme and abstracts, Geological Society of New Zealand 50th Annual Conference, Kaikoura, New Zealand. **Geological Society of New Zealand Miscellaneous Publication 119A**: 39.

Kamp, P. J. J. (1999). "Tracking crustal processes by FT thermochronology in a forearc high (Hikurangi margin, New Zealand) involving Cretaceous subduction termination and mid-Cenozoic subduction initiation." Tectonophysics **307**: 313-343.

Kelsey, H. M. and J. G. Bockheim (1994). "Coastal landscape evolution as a function of eustasy and surface uplift rate, Cascadia margin, southern Oregon." Geological Society of Americe Bulletin **106**: 840-854.

Kelsey, H. M., S. M. Cashman, S. Beanland and K. R. Berryman (1995). "Structural evolution along the inner forearc of the obliquely convergent Hikurangi margin." Tectonics **14**(1): 1-18.

Kelsey, H. M., A. G. Hull, S. M. Cashman, K. R. Berryman, P. Cashman, J. H. Trexler Jr and J. G. Begg (1998). "Paleoseismology of an active fault in a forearc setting: the Poukawa fault zone, Hikurangi forearc, New Zealand." Geological Society of America Bulletin **110**(9): 1123-1148.

Kelsey, H. M., R. C. Witter and E. Hemphill-Haley (2002). "Plate-boundary earthquakes and tsunamis of the past 5500 yr, Sixes River estuary, sothern Oregon." Geological Society of America Bulletin **114**(3): 298-314.

Lamarche, G., S. Beanland and J. Ravens (1995). "Deformation styles and history of the Eketahuna region, Hikurangi forearc, New Zealand, from shallow seismic reflection data." New Zealand Journal of Geology and Geophysics **38**: 105-115.

Lewis, K. (1980). "Quaternary sedimentation on the Hikurangi oblique subduction and transform margin, New Zealand." Special Publication of the Institute of Professional Sedimentologists **4**: 171-189.

Lewis, K. B. and J. R. Pettinga (1993). The emerging, imbricate frontal wedge of the Hikurangi Margin. Ballance, P. F. (Ed.). South Pacific Sedimentary Basins, Elsevier. Sedimentary Basins of the World 2: 225-250.

Lewis, K., J.-Y. Collot and S. Lallemand (1998). "The damned Hikurangi Trough: a channel-fed trench blocked by subducting seamounts and their wake avalanches (New Zealand-France GeodyNZ Project)." Basin Research **10**(4): 441-468.

Lewis, K., S. E. Lallemand and L. Carter (2004). "Collapse in a Quaternary shelf basin off East Cape, New Zealand: evidence for passage of a subducted seamount inboard of the Ruatoria giant avalanche." New Zealand Journal of Geology and Geophysics **47**: 415-429.

Lewis, K. B. and J. R. Pettinga (1993). The emerging, imbricate frontal wedge of the Hikurangi Margin. Ballance, P. F. (Eds). South Pacific Sedimentary Basins, Elsevier. **Sedimentary Basins of the World 2:** 225-250.

Lewis, K. B., J.-Y. Collot, B. Davy, J. Delteil, S. Lallemand and C. Uruski (1997). "North Hikurangi GeodyNZ swath maps: depths, texture and geological interpretation 1: 500 000." National Institute for Water and Atmospheric Research miscellaneous series chart 72. Wellington.

Litchfield, N. and K. Wilson (2005). "Holocene tectonic fluvial terraces at Pakarae River mouth, Gisborne region." Pettinga, J. R. and Wandres, A. M. (eds.) Programme and abstracts, Geological

Society of New Zealand 50th Annual Conference, Kaikoura, New Zealand. Geological Society of New Zealand Miscellaneous Publication 119A: 45-46.

Litchfield, N. J. and K. Berryman (2006). "Relations between postglacial fluvial incision rates and uplift rates in the North Island, New Zealand." Journal of Geophysical Research **111**(FO2007): doi:10.1029/2005JF000374.

Litchfield, N. J., S. Ellis, K. Berryman and A. Nicol (2007). "Subduction related uplift in the Hikurangi Margin, New Zealand." Journal of Geophysical Research, Earth Surface **112**, F02021, doi:10.1029/2006JF000535.

Marshall, J. S. and R. S. Anderson (1995). "Quaternary uplift and seismic cycle deformation, Peninsula de Nicoya, Costa Rica." Geological Society of America Bulletin **107**(4): 463-473.

Matsuda, T., Y. Ota, M. Ando and N. Yonekura (1978). "Fault mechanism and recurrence time of major earthquakes in southern Kanto district, Japan, as deduced from coastal terrace data." Geological Society of America Bulletin **89**: 1610 - 1618.

Mazengarb, C. (1984). "The Fernside Fault: an active normal fault, Raukumara Peninsula, New Zealand." New Zealand Geological Survey Record **3**: 98-103.

Mazengarb, C. and I. G. c. Speden (2000). Geology of the Raukumara area, Institute of Geological & Nuclear Sciences 1:250,000 Geological Map 6.

McGinty, P., M. Reyners and R. Robinson (2000). "Stress directions in the shallow part of the Hikurangi subduction zone, New Zealand, from the inversion of earthquake first motions." Geophysical Journal International **142**: 339-350.

McNeill, L. C., C. Goldfinger, R. Yeats and L. Kulm (1998). The effects of upper plate deformation on records of prehistoric Cascadia subduction zone earthquakes. Coastal Tectonics, Geological Society. **146:** 321-324.

Ministry of Economic Development Petroleum Report Series PR3136 (2005). 05CM 2D Seismic Survey, Offshore East Coast -North Island: 280 pp.

Miyauchi, T., Y. Ota and A. G. Hull (1989). "Holocene marine terraces and tectonic uplift in the Waimarama coastal plain, eastern North Island, New Zealand." New Zealand Journal of Geology and Geophysics **32**: 437-442.

Nakada, M., M. Tahara, H. Shimizu, S. Nagaoka, K. Uehira and S. Suzuki (2002). "Late Pleistocene crustal uplift and gravity anomaly in the eastern part of Kyushu, japan, and its geophysical implications." Tectonophysics **351**: 263-283.

Nelson, A. R., I. Shennan and A. J. Long (1996). " Identifying coseismic subsidence in tidal-wetland stratigraphic sequences at the Cascadia subduction zone of western North America." Journal of Geophysical Research **101**: 6115-6135.

Nicol, A. and J. Beavan (2003). "Shortening of an overriding plate and its implications for slip on a subduction thrust, central Hikurangi margin, New Zealand." Tectonics **22** (6): 1070, doi:10.1029/2003TC001521.

Nicol, A., R. Van Dissen, P. Vella, B. Alloway and A. Melhuish (2002). "Growth of contractional structures during the last 10 m.y. at the southern end of the emergent Hikurangi forearc basin, New Zealand." New Zealand Journal of Geology and Geophysics **45**: 365-385.

Okada, Y. (1985). "Surface deformation due to shear and tensile faults in a half-space." Bulletin of the Seismological Society of America **75**(4): 1135-1154.

Ota, Y., K. R. Berryman, A. G. Hull, T. Miyauchi and N. Iso (1988). "Age and height distribution of Holocene transgressive deposits in eastern North Island, New Zealand." Palaeogeography, Palaeoclimatology, Palaeoecology **68**: 135-151.

Ota, Y., K. R. Berryman, L. J. Brown and K. Kashima (1989). "Holocene sediments and vertical tectonic downwarping near Wairoa, Northern Hawkes Bay, New Zealand." New Zealand Journal of Geology and Geophysics **32**: 333-341.

Ota, Y., A. G. Hull and K. R. Berryman (1991). "Coseismic uplift of Holocene marine terraces in the Pakarae River area, eastern North Island, New Zealand." Quaternary Research **35**: 331-346.

Ota, Y., A. G. Hull, N. Iso, Y. Ikeda, I. Moriya and T. Yoshikawa (1992). "Holocene marine terraces on the northeast coast of North Island, New Zealand, and their tectonic significance." New Zealand Journal of Geology and Geophysics **35**: 273-288.

Ota, Y., T. Miyauchi and A. G. Hull (1990). "Holocene marine terraces at Aramoana and Pourerere." New Zealand Journal of Geology and Geophysics **33**: 541-546.

Personius, S. F. (1995). "Late Quaternary stream incision and uplift in the forearc of the Cascadia subduction zone, western Oregon." Journal of Geophysical Research **100**(B10): 20193-20210.

Pettinga, J. R. (2004). "Three-stage massive gravitational collapse of the emergent imbricate frontal wedge, Hikurangi Subduction Zone, New Zealand." New Zealand Journal of Geology and Geophysics **47**: 399-414.

Pillans, B. (1986). A late Quaternary uplift map for the North Island, New Zealand. Recent Crustal Movements of the Pacific Region., Bulletin of the Royal Society of New Zealand. **24:** 409-418.

Pillans, B. and P. Huber (1995). "Interpreting coseismic deformation using Holocene coastal deposits, Wellington, New Zealand." Quaternary International **26**: 87-95.

Plafker, G. (1972). "Alaskan earthquake of 1964 and Chilean earthquake of 1960: implications for arcc tectonics." Journal of Geophysical Research 77(901-925).

Pulford, A. and T. Stern (2004). "Pliocene exhumations and landscape evolution of central North Island, New Zealand: the role of the upper mantle." Journal of Geophysical Research **109**(FO1016): doi:10.1029/2003JF000046.

Ramirez-Herrera, M. T., V. Kostoglodov and J. Urrutia-Fucugauchi (2004). "Holocene-emerged notches and tectonic uplift along the Jalisco coast, Southwest Mexico." Geomorphology **58**: 291-304.

Reilly, W. I. (1990). "Horizontal crustal deformation on the Hikurangi margin." New Zealand Journal of Geology and Geophysics **33**(393-400).

Reyners, M. (1998). "Plate coupling and the hazard of large subduction thrust earthquakes at the Hikurangi subduction zone, New Zealand." New Zealand Journal of Geology and Geophysics **4**: 343-354.

Reyners, M., P. McGinty and K. Gledhill (1998). "The Ormond, New Zealand, earthquake of 1993 August 10: rupture in the mantle of the subducted Pacific plate." New Zealand Journal of Geology and Geophysics **41**(2): 179-185.

Reyners, M., D. Eberhart-Phillips and G. Stuart (1999). "A three-dimensional image of shallow subduction: crustal structure of the Raukumara Peninsula." Geophysical Journal International **137**: 873-890.

Reyners, M. and P. McGinty (1999). "Shallow subduction tectonics in the Raukumara Peninsula, New Zealand, as illuminated by earthquake focal mechanisms." Journal of Geophysical Research **104**(B2): 3025-3034.

Reyners, M. (2000). "Quantifying the hazard of large subduction thrust earthquakes in Hawke's Bay." Bulletin of the New Zealand Society for Earthquake Engineering **33**(4): 477-483.

Reyners, M., D. Eberhart-Phillips, G. Stuart and Y. Nishimura (2006). "Imaging subduction from the trench to 300 km depth beneath the central North Island, New Zealand, with Vp and Vp/Vs." Geophysical Journal International **165**: 565-583.

Sak, P., D. Fisher and T. Gardner (2004). "Effects of seafloor roughness on the upper plate vertical tectonism: Osa Peninsula, Costa Rica." Tectonics **23**(TC1017): doi:10.1029/2002TC001474.

Sandwell, D. T. and W. H. F. Smith (1997). "Marine gravity anomaly from Geosat and ERS 1 satellite altimetry." Journal of Geophysical Research **105**(B5): 10,039-10,054.

Savage, J. C. (1983). "A dislocation model of strain accumulation and release at a subduction zone." Journal of Geophysical Research **88**(B6): 4984-4996.

Savage, J. C. (1995). "Interseismic uplift at the Nankai subduction zone, southwest Japan, 1951-1990." Journal of Geophysical Research **100**(B4): 6339-6350.

Savage, J. C., J. L. Svarc, W. H. Prescott and W. K. Gross (1998). "Deformation across the rupture zone of the 1964 Alaska earthquake, 1993-1997." Journal of Geophysical Research **103**(B9): 21275-21283.

Scholz, C. H. and J. Campos (1995). "On the mechanisms of seismic decoupling and back arc spreading at subduction zones." Journal of Geophysical Research **100**(B11): 22103 - 22115.

Stirling, M. W., G. McVerry and K. R. Berryman (2002). "A new seismic hazard model for New Zealand." Bulletin of the Seismological Society of America **92**(5): 1878-1903.

Taylor, S. K., J. M. Bull, G. Lamarche and P. Barnes (2004). "Normal fault growth and linkage in the Whakatane Graben, new Zealand, during the last 1.3 Myr." Journal of Geophysical Research (Solid Earth) **109**(BO2408): doi:10.1029/2003JB002412.

Thatcher, W. (1984). "The earthquake deformation cycle at the Nankai Trough, Southwest Japan." Journal of Geophysical Research **89**(B5): 3087-3101.

Thatcher, W. (1986). "Cyclic deformation related to great earthquakes at plate boundaries." Royal Society of New Zealand Bulletin **24**: 245 - 273.

Thornley, S. (1996). "Neogene tectonics of Raukumara Peninsula, Northern Hikurangi margin, New Zealand." Victoria University of Wellington **Unpublished PhD thesis**.

Upton, P., P. Koons and D. Eberhart-Phillips (2003). "Extension and partitioning in an oblique subduction zone, New Zealand: constraints from three-dimensional numerical modeling." Tectonics **22**(6): doi:10.1029/2002TC001431.

von Huene, R. and D. Klaeschen (1999). "Opposing gradients of permanent strain in the aseismic zone and elastic strain across the seismogenic zone of the Kodiak shelf and slope, Alaska." Tectonics **18**(2): 248-262.

Walcott, R. I. (1978). "Geodetic strains and large earthquakes in the axial tectonic belt of North Island, New Zealand." Journal of Geophysical Research **85**(B9): 4419-4429.

Walcott, R. I. (1987). "Geodetic strain and the deformation history of the North Island, of New Zealand during the late Cainozoic." Philosophical Transactions of the Royal Society of London A **321**: 163-181.

Wallace, L. M., J. Beavan, R. McCaffrey and D. Darby (2004). "Subduction zone coupling and tectonic block rotations in the North Island, New Zealand." Journal of Geophysical Research **109**(B12406): doi:10.1029/2004JB003241.

Webb, T. and H. Anderson (1998). "Focal mechanisms of large earthquakes in the North Island of New Zealand: slip partitioning at an oblique active margin." Geophysical Journal International **134**: 40-86.

Wellman, H. W. (1971a). "Holocene tilting and uplift on the White Rocks Coast, Wairarapa, New Zealand." Recent Crustal Movements, Royal Society of New Zealand Bulletin **9**: 211-215.

Wellman, H. W. (1971b). "Holocene tilting and uplift on the Glenburn Coast, Wairarapa, New Zealand." Recent Crustal Movements, Royal Society of New Zealand Bulletin **9**: 221-223.

Wells, R. E., R. J. Blakely, Y. Sugiyama, D. W. Scholl and P. A. Dinterman (2003). "Basin-centered asperities in great subduction zone earthquakes: a link between slip, subsidence, and subduction erosion?" Journal of Geophysical Research **108**(B10): 2507, doi:10.1029/2002JB002072.

Wilson, K. J. (Ch. 2). "A revision of Mid to Late Holocene marine terrace distribution and chronology at New Zealand's most tectonically active coastal location, Pakarae River, North Island, New Zealand."

Wilson, K. J. (Ch. 3). "A facies architecture model for Holocene incised valley infill on a tectonically active coast: Pakarae River, New Zealand."

Wilson, K. J. (Ch. 4.). "Early Holocene paleoseismic history at the Pakarae locality, eastern North Island, New Zealand, inferred from transgressive marine sequence architecture and biostratigraphy."

Wilson, K. J. (Ch. 5). "Holocene coastal evolution and uplift mechanisms of the northeastern Raukumara Peninsula, North Island, New Zealand."

Wilson, K. J. (Ch. 6). "Distribution, age and uplift patterns of Pleistocene marine terraces of the northwaestern Raukumara Peninsula, North Island, New Zealand."

Wood, R. and B. Davy (1994). "The Hikurangi Plateau." Marine Geology **118**(153-173).

Wright, I. C. (1990). "Late Quaternary faulting of the offshore Whakatane Graben, Taupo Volcanic Zone, New Zealand." New Zealand Journal of Geology and Geophysics **33**: 245-256.

Yoshikawa, T. (1988). "Pattern and rate of tectonic movement and Late Quaternary geomorphic development in the Raukumara Peninsula, northeastern North Island, New Zealand." Bulletin of the Department of Geography University of Tokyo **20**: 1-28.

Yoshikawa, T., Y. Ota, N. Yonekura, A. Okada and N. Iso (1980). "Marine terraces and their tectonic deformation on the northeast coast of the North Island, New Zealand." Geographical Review of Japan **53**(4): 238-262.

Zachariasen, J., K. Sieh, F. W. Taylor, R. L. Edwards and W. S. Hantoro (1999). "Submergence and uplift associated with the giant 1833 Sumatran subduction zone earthquake: evidence from coral microatolls." Journal of Geophysical Research **104**(B1): 895-919.

CHAPTER EIGHT

CONCLUSIONS

The primary conclusion of this report is that forearc uplift mechanisms of the Raukumara Peninsula are spatially variable and the main parameter controlling the distribution of aseismic and coseismic uplift is distance from the Hikurangi trench and depth to the plate interface beneath the forearc. This outcome has been reached by using several methodologies applied to coastal geomorphic features, which represent deformation over varying late Quaternary time periods.

At the Pakarae River mouth the late Holocene terrace morphology and coverbed stratigraphy is consistent with coseismic uplift driven by slip on an offshore reverse fault cutting through the upper plate of the Hikurangi margin. Similar geomorphology occurs as terrace sequences at the Waipapa and Horoera localities on the northeastern Raukumara Peninsula. However, at these localities the coverbed sediments and strath elevations suggested a terrestrial origin for the terraces. Therefore, we found that different processes can produce quite similar terrace flights on active coasts. Despite the geomorphic similarities, different processes formed the Pakarae River mouth and Waipapa and Horoera locality terraces. Only the terraces at the Pakarae River mouth indicate a coseismic coastal uplift mechanism.

The fluvio-estuarine sequences exposed beneath the highest marine terrace at the Pakarae River mouth, and along the Wharekahika River bank at Hicks Bay are both superb examples of tectonically-modified valley infill sequences. Three early Holocene uplift events have been identified in the 10,000 – 7,000 cal. yrs B.P. sequence of the Pakarae River mouth. Paleoenvironmetal reconstructions using biostratigraphy suggest that these were sudden, coseismic events. The Hicks Bay sediments are characteristic of a typical valley infill sequence stratigraphy but consistent accommodation space deficits and the present elevation of the sequence above mean sea level imply tectonic uplift during and since deposition of the sediments. The similarity of paleoenvironmental facies transitions of the Hicks Bay sequence to stable coast models provides a stark contrast to the Pakarae sequence and implies there were no significant and sudden uplift events during infilling of the Hicks Bay paleo-valley. These two studies demonstrate that paleoenvironmental facies analysis of valley infill sequences can provide valuable data concerning paleoseismicity in the coastal zone. The infill sequence analysis technique requires knowledge of the regional eustatic sea level curve and benefits from good biostratigraphic control. However, we have shown that it can extend the record of coastal paleoseismicity well back into the early Holocene, and it has the potential to be applied to coastlines that are otherwise unfavourable to the preservation of marine terraces. The facies architecture model for actively uplifting coasts that we developed from the Pakarae River mouth valley infill sequence can be used as an analogue when further incised valley sequences are investigated along the Hikurangi margin. On a global scale this model provides a valuable comparison with stable coast models, which dominate the literature on valley infilling.

Holocene coseismic uplift of the Pakarae River mouth, on the southeastern Raukumara Peninsula, is well documented by the combined study of its marine terraces and transgressive valley infill sequence. An aseismic uplift mechanism of the northeastern Raukumara Peninsula coastal region through the Holocene is indicated by the gradually sloping beach ridge sequence at Te Araroa, the absence of marine terraces along the East Cape coastline and the gradually uplifted valley infill sequence of Hicks Bay. By integrating the Holocene aseismic uplift data from the northeastern Raukumara Peninsula region with the longer term, and more spatially extensive Pleistocene marine terraces, and with known tectonic data from the Raukumara Peninsula and offshore we can see that the structure accommodating uplift is not any discrete upper plate fault. Rather, a more deep-seated process of sediment underplating probably drives aseismic uplift of the northern Raukumara Peninsula region and the Raukumara Ranges. Correlation of coseismic uplift at the Pakarae region to a similar tectonic setting at Mahia Peninsula also allows the identification of a margin-parallel zone of coseismic uplift driven by offshore reverse faults. Although understanding the role that plate interface rupture plays in forearc deformation processes remains a significant challenge, the regional changes in uplift mechanisms we have identified have important implications for the seismic hazard of the Raukumara Peninsula.

Our initial proposition that similar coastal geomorphology along the Hikurangi margin should be controlled by the same tectonic processes has proven to be false. The detailed studies presented in this thesis have shown that there are significant and recognisable changes in coastal geomorphology and stratigraphy between different tectonic regimes. Somewhat surprising is that these changes in geomorphology and stratigraphy occur at regional scales within the confines of the Raukumara Peninsula itself, rather than at the scale of the entire Hikurangi margin. This is the first recognition of zones of different uplift mechanisms across the Hikurangi forearc and it has been achieved because the northern coastline of the Raukumara Peninsula uniquely provides a cross section through the forearc. The coseismic uplift and passive forearc zones appear to continue to along strike to the southern sectors of the margin although there are some changes in the width of the zones. We have shown that sediment underplating probably drives uplift of the Raukumara Ranges and an important implication of this study is that an aseismic process has evidently been capable of building an axial range with significant topography. This suggests that, although there are active faults within the axial ranges of the central and southern Hikurangi margin, uplift of these ranges may also be in part aseismic and therefore more closely linked with deep-seated subduction processes than previously appreciated.